e-ISSN 2149-6366

Cilt 11, Sayı 1, Mart 2022
Volume 11, Number 1, March 2022

TDFD
TÜRK DOĞA ve FEN DERGİSİ

TURKISH JOURNAL OF NATURE AND SCIENCE

TJNS

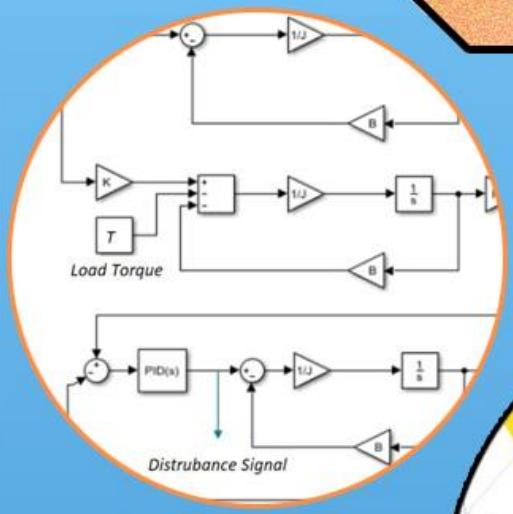

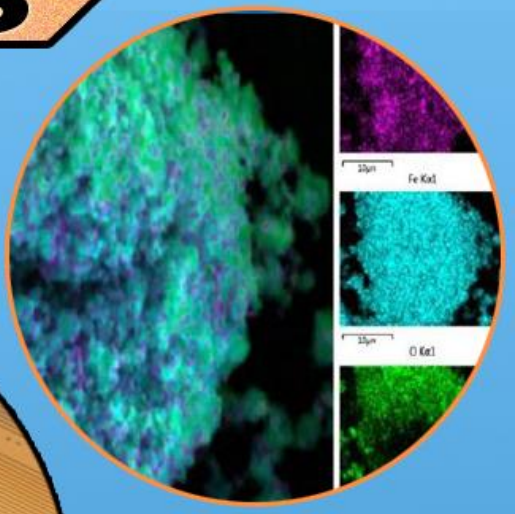

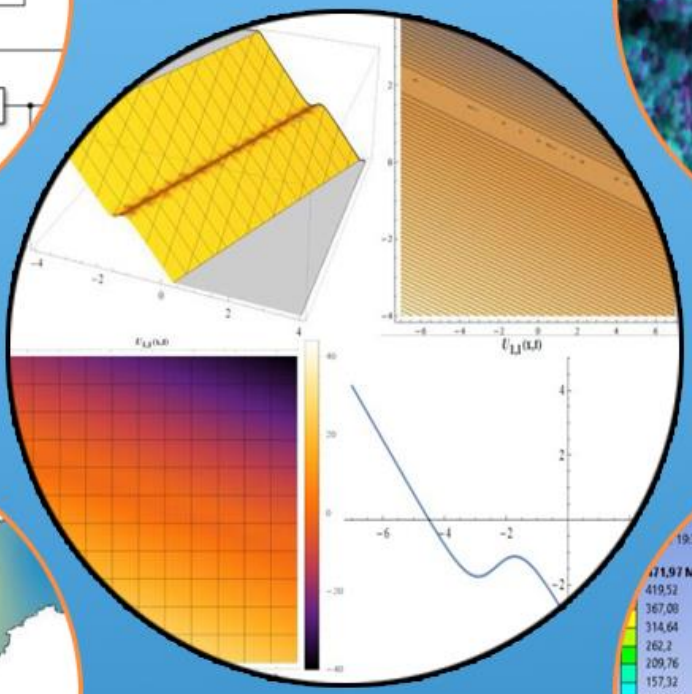

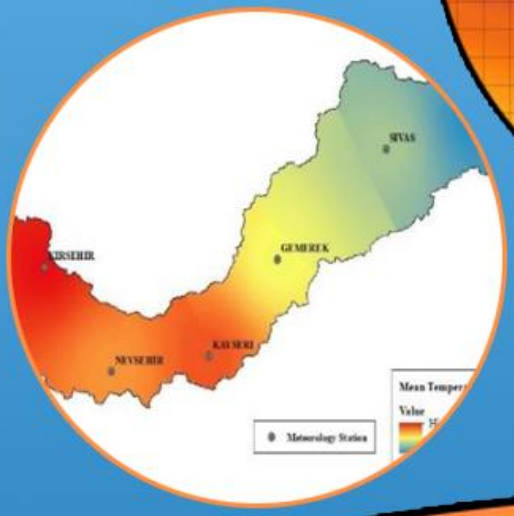

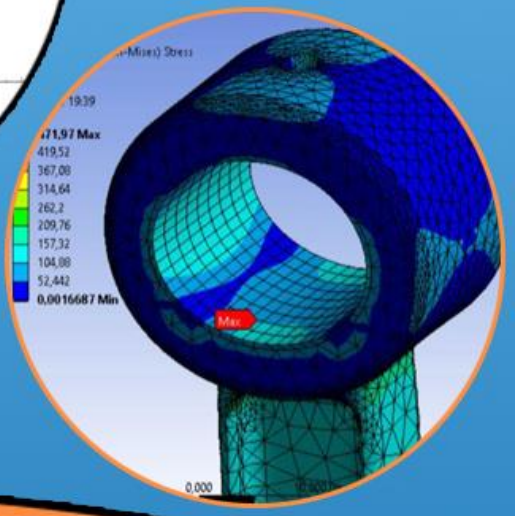

www.dergipark.gov.tr/tdfd

Bingöl Üniversitesi Fen Bilimleri Enstitüsü tarafından yayımlanmaktadır.
Published by Bingol University Institute of Science

TÜRK DOĞA VE FEN DERGİSİ

Amaç

Türk Doğa ve Fen Dergisi, Dergipark tarafından yayınlanan Bingöl Üniversitesi Fen Bilimleri Enstitüsüne ait ulusal ve hakemli bir dergidir. Türk Doğa ve Fen Dergisi, Türkiye ve dünyanın her yerinden gelen doğa ve fen bilimlerinin her alanında özgün, yayımlanmamış, yayımlanmak üzere başka yere gönderilmemiş makale, derleme ve sempozyum değerlendirmesi gibi çalışmaların bilim alemine sunulması amacıyla kurulmuştur.

Kapsam

Türk Doğa ve Fen Dergisinde Mühendislik, Ziraat, Veterinerlik, Fen ve Doğa Bilimleri alanlarından olmak üzere Türkçe ve İngilizce hazırlanmış orijinal makale, derleme ve sempozyum değerlendirmesi gibi çalışmalar yayımlanır. Türk Doğa ve Fen Dergisi sadece online sistemde yayınlanmakta olup ayrıca kağıt baskısı bulunmamaktadır.

Merhaba…

Türk Doğa ve Fen Dergisi, Dergipark tarafından yayınlanmakta olup Bingöl Üniversitesi Fen Bilimleri Enstitüsüne aittir. Bahar ve güz dönemi olmak üzere yılda iki defa çıkarılan ulusal hakemli bir dergi olarak ilk sayısını 2012 bahar döneminde yayımlamıştır. Türk Doğa ve Fen Dergisi, Türkiye ve dünyanın her yerinden gelen doğa ve fen bilimlerinin her alanında özgün, yayımlanmamış, yayımlanmak üzere başka yere gönderilmemiş makale, derleme ve sempozyum değerlendirmesi gibi çalışmaların bilim alemine sunulması amacıyla kurulmuştur. İlk sayısından bugüne kesintisiz olarak faaliyetlerini sürdürmektedir.

Türk Doğa ve Fen Dergisi sadece online sistemde yayınlanmakta olup ayrıca kağıt baskısı bulunmamaktadır. Dergimize gelen her çalışma öncelikle Turnitin intihal programında taranmaktadır. Dergimizde editörlerin, hakemlerin ve yazarların, uluslararası yayım etik kurallarına uyması ve makalelerin yazım kurallarına uyumlu olması zorunluluğu vardır.

Yazarlar yayımlanmak üzere dergimize gönderdikleri çalışmaları ile ilgili telif haklarını zorunlu olarak Bingöl Üniversitesi Türk Doğa ve Fen Dergisi'ne devretmiş sayılırlar. Yazarlardan herhangi bir ücret talep edilmemektedir. Yazarların değerlendirmeleri, dergimizin resmi görüşü olarak kabul edilemez. Çalışmaların her türlü sorumluluğu yazarlarına aittir. Araştırma ürünleri için etik kurul raporu gerekli ise, çalışma üzerinde bu raporun alınmış olduğu belirtilmeli ve kurul raporu sisteme kaydedilmelidir. Araştırma ile ilgili intihal, atıf manipülasyonu, sahte veri uydurma vb. suistimallerin tespit edilmesi halinde yayım ve etik ilkelerine göre davranılır. Bu durumda çalışmanın yayımlanmasını önlemek, yayımdan kaldırmak ya da başka işlemler yapmak için gerekli işlemler takip edilmektedir.

Dergimizde, kaynak gösteriminde uluslararası Vancouver sistemine geçilmiştir. Ayrıca dergimiz, Creative Commons ile lisanslanmak suretiyle dergimizde yayımlanan makalelerin paylaşımı, kaynak gösterimi ve yayımlanmasında dergi ve yazar haklarını korumaya almıştır. 2018 yılı güz döneminden itibaren makaleler, uluslararası yazar kimlik numarası ORCID No'su ile yayımlanmaktadır.

Dergi ekibi, dergimizin ulusal ve uluslararası indekslerce taranan bir dergi olması yönünde çalışmalarını titizlikle sürdürmektedir. Dergimize gösterilen ilgi bu yönde bizleri teşvik etmeye devam edecektir.

Bingöl Üniversitesi Fen Bilimleri Enstitüsü tarafından yayımlanmaktadır

EDİTÖRLER (YAYIN) KURULU

Prof. Dr. Zafer ŞİAR

Bingöl Üniversitesi, Fen-Edebiyat Fakültesi, Matematik Bölümü
E-Mail: zsiar@bingol.edu.tr

Prof. Dr. Uğur ÇAKILCIOĞLU

Munzur Üniversitesi, Pertek Sakine Genç Meslek Yüksekokulu, Bitki Morfolojisi ve Anatomisi Bölümü
E-Mail: ucakilcioglu@yahoo.com

Doç. Dr. Kamuran DİLSİZ

Bingöl Üniversitesi, Fen-Edebiyat Fakültesi, Fizik Bölümü
E-Mail: kdilsiz@bingol.edu.tr

Doç. Dr. Şükran KONCA

Bakırçay Üniversitesi, Mühendislik ve Mimarlık Fakültesi, Temel Bilimler, Matematik Bölümü
E-Mail: sukran.konca@bakircay.edu.tr

Doç. Dr. İdris YAZGAN

Kastamonu Üniversitesi, Fen Edebiyat Fakültesi, Biyoloji

E-Mail: idrisyazgan@gmail.com

Doç. Dr. Abdulcabbar YAVUZ

Gaziantep Üniversitesi, Mühendislik Fakültesi, Metalurji ve Malzeme Mühendisliği
E-Mail: ayavuz@gantep.edu.tr

Doç. Dr. Bünyamin ALIM

Bayburt Üniversitesi, Teknik Bilimler Meslek Yüksekokulu, Elektrik ve Enerji Bölümü
E-Mail: balim@bayburt.edu.tr

Dr. Öğr. Üyesi Mustafa Şükrü KURT

Erzurum Teknik Üniversitesi, Fen Fakültesi, Temel Bilimler
E-Mail: mustafa.kurt@erzurum.edu.tr

Dr. Öğr. Üyesi Sinan SAĞIR

Karamanoğlu Mehmetbey Üniversitesi, Fizik

E-Mail: sinansagir@kmu.edu.tr / sinan.sagir@cern.ch

Dr. Öğr. Üyesi Murat AYDEMİR

Erzurum Teknik Üniversitesi, Fen Fakültesi, Temel Bilimler

E-Mail: murat.aydemir@erzurum.edu.tr

Mühendislik Bilimleri

Doç. Dr. Özgür ÖZGÜN

Bingöl Üniversitesi, Sağlık Bilimleri Fakültesi, İş Sağlığı ve Güvenliği Bölümü
E-Mail: oozgun@bingol.edu.tr

Prof. Dr. Figen KOREL

İzmir Yüksek Teknoloji Enstitüsü, Gıda Mühendisliği Bölümü
E-Mail: figenkorel@iyte.edu.tr

Prof. Dr. Kubilay ASLANTAŞ

Afyon Kocatepe Üniversitesi, Teknoloji Fakültesi, Makine Mühendisliği Bölümü
E-Mail: aslantas@aku.edu.tr

Prof. Dr. Hamit Özkan GÜLSOY

Marmara Üniversitesi, Teknoloji Fakültesi, Metalurji ve Malzeme Mühendisliği Bölümü
E-Mail: ogulsoy@marmara.edu.tr

Prof. Dr. Ali Adnan HAYALOĞLU

İnönü Üniversitesi, Mühendislik Fakültesi, Gıda Mühendisliği Bölümü
E-Mail: adnan.hayaloglu@inonu.edu.tr

Prof. Dr. Barbara SAWICKA

University of Life Sciences in Lublin, Department of Plant Production Technology and Commodities Sciences
E-Mail: barbara.sawicka@gmail.com

Prof. Dr. İbrahim GÜNEŞ

Giresun Üniversitesi, Mühendislik Fakültesi, İnşaat Mühendisliği Bölümü
E-Mail: ibrahim.gunes@giresun.edu.tr

Doç. Dr. Sırma YEĞİN

Ege Üniversitesi, Mühendislik Fakültesi, Gıda Mühendisliği Bölümü
E-Mail: sirma.yegin@ege.edu.tr

Doç. Dr. Hasan OĞUL

Sinop Üniversitesi, Mimarlık ve Mühendislik Fakültesi, Nükleer Enerji Mühendisliği
E-Mail: hogul@sinop.edu.tr

Doç. Dr. Murat YILMAZTEKİN

İnönü Üniversitesi, Mühendislik Fakültesi, Gıda Mühendisliği Bölümü
E-Mail: murat.yilmaztekin@inonu.edu.tr

Doç. Dr. Ferhat AYDIN

Sakarya Uygulamalı Bilimler Üniversitesi, Teknoloji Fakültesi, İnşaat Mühendisliği Bölümü
E-Mail: ferhata@subu.edu.tr

Dr. Öğr. Üyesi Nurullah DEMİR

Bingöl Üniversitesi, Mühendislik ve Mimarlık Fakültesi, Gıda Mühendisliği Bölümü
E-Mail: ndemir@bingol.edu.tr

Dr. Öğr. Üyesi Ahmet GÜNER

Bingöl Üniversitesi, Mühendislik ve Mimarlık Fakültesi, Elektrik ve Elektronik Mühendisliği Bölümü
E-Mail: aguner@bingol.edu.tr

Dr. Öğr. Üyesi Tahir AKGÜL

Sakarya Uygulamalı Bilimler Üniversitesi, Teknoloji Fakültesi, İnşaat Mühendisliği Bölümü
E-Mail: tahirakgul@subu.edu.tr

Dr. Erhan Sulejmani

University of Tetova, Faculty of Food Technology and Nutrition
E-Mail: erhan.sulejmani@unite.edu.mk

Dr. Hacène Medjoudj

Larbi Ben M'Hidi University of Oum El Bouaghi, Food Science Department
E-Mail: medjoudjh@yahoo.com

Dr. Avinash Lakshmikanthan

Nitte Meenakshi Institute of Technology, Department of Mechanical Engineering, Karnataka, India
E-Mail: avinash.laks01@gmail.com

Dr. Manjunath Patel GC

PES Institute of Technology and Management, Department of Mechanical Engineering, Karnataka, India
E-Mail: manju09mpm05@gmail.com

Sağlık Bilimleri

Doç. Dr. Aydın Şükrü BENGÜ

Bingöl Üniversitesi, Sağlık Hizmetleri Meslek Yüksekokulu, Tıbbi Hizmetler ve Teknikler
E-Mail: abengu@bingol.edu.tr

Dr. Öğr. Üyesi Dilhun Keriman ARSERİM UÇAR

Bingöl Üniversitesi, Sağlık Bilimleri Fakültesi, Beslenme ve Diyetetik Bölümü
E-Mail: dkucar@bingol.edu.tr

Dr. Öğr. Üyesi Abdullah TUNÇ

Bingöl Üniversitesi, Sağlık Bilimleri Fakültesi, İş Sağlığı ve Güvenliği Bölümü
E-Mail: atunc@bingol.edu.tr

Dr. Öğr. Üyesi Ramazan GÜNDOĞDU

Bingöl Üniversitesi, Sağlık Hizmetleri Meslek Yüksekokulu, Eczane Hizmetleri
E-Mail: rgundogdu@bingol.edu.tr

Dr. Alexander HERGOVICH

UCL Cancer Institute, Faculty of Medical Sciences, Department of Cancer Biology, UCL, London, UK
E-Mail: a.hergovich@uc.ac.uk

Dr. Valenti GOMEZ

UCL Cancer Institute, Faculty of Medical Sciences, Department of Oncology, UCL, London, UK
E-Mail: valentin.gomez@ucl.ac.uk

Veterinerlik Bilimleri

Doç. Dr. Cüneyt ÇAĞLAYAN

Bingöl Üniversitesi, Veteriner Fakültesi, Temel Bilimler Bölümü
E-Mail: ccaglayan@bingol.edu.tr

Prof. Dr. Fatih Mehmet KANDEMİR

Atatürk Üniversitesi, Veteriner Fakültesi, Veteriner Hekimliği Temel Bilimler
E-Mail: fmehmet.kandemir@atauni.edu.tr

Doç. Dr. Akın KIRBAŞ

Bozok Üniversitesi, Veteriner Fakültesi, Klinik Bilimler Bölümü
E-Mail: akindahiliye55@yahoo.com

Doç. Dr. Emrah Hicazi AKSU

Atatürk Üniversitesi, Veteriner Fakültesi, Klinik Bilimler Bölümü
E-Mail: emrahaksu@atauni.edu.tr

Ziraat Bilimleri

Prof. Dr. Kağan KÖKTEN

Bingöl Üniversitesi, Ziraat Fakültesi, Tarla Bitkileri Bölümü
E-Mail: kahafe1974@yahoo.com

Prof. Dr. Mustafa SÜRMEN

Adnan Menderes Üniversitesi, Ziraat Fakültesi, Tarla Bitkileri Bölümü
E-Mail: mustafa.surmen@adu.edu.tr

Prof. Dr. Banu YÜCEL

Ege Üniversitesi, Ziraat Fakültesi, Hayvan Yetiştirme Anabilim Dalı, Zootekni Bölümü
E-Mail: banu.yucel@ege.edu.tr

Doç. Dr. Hakan İNCİ

Bingöl Üniversitesi, Ziraat Fakültesi, Zootekni Bölümü
E-Mail: hinci@bingol.edu.tr

TEKNİK EDİTÖRLER

Dr. Mücahit ÇALIŞAN

Bingöl Üniversitesi, Teknik Bilimler Meslek Yüksekokulu, Bilgisayar Teknolojileri
E-Mail: mcalisan@bingol.edu.tr

Dr. Ersin KARAKAYA

Bingöl Üniversitesi, Ziraat Fakültesi, Tarım Ekonomisi Bölümü
E-Mail: karakayaersin1982@gmail.com

Dr. Nimetullah KORKUT

Bingöl Üniversitesi, BİNUZEM, Bilgisayar Teknolojileri
E-Mail: nkorkut@bingol.edu.tr

DİL EDİTÖRÜ

Öğr. Gör. Ahmet KESMEZ
Bingöl Üniversitesi, Yabancı Diller Yüksekokulu, İngilizce Bölümü
E-Mail: akesmez@bingol.edu.tr

Türk Doğa ve Fen Dergisi
Turkish Journal of Nature and Science
www.dergipark.gov.tr/tdfd

İÇİNDEKİLER/CONTENTS

Cilt 11, Sayı 1, Sayfa 1-5, 2022 Volume 11, Issue 1, Page 1-5, 2022

Araştırma Makalesi https://doi.org/10.46810/tdfd.850555 Research Article

Türk Doğa ve Fen Dergisi
Turkish Journal of Nature and Science
www.dergipark.gov.tr/tdfd

Türkiye'nin Doğu ve Güneydoğu Bölgelerinde Abort Yapmış Sığır, Koyun ve Keçi Fötuslarında Pestivirus Enfeksiyonunun Araştırılması

Metin GÜRÇAY[1*]

[1]Bingöl Üniversitesi Veteriner Fakültesi, Klinik Öncesi Bilimler Bölümü, Bingöl, Türkiye
Metin GÜRÇAY ORCID No: 0000-0001-9160-7454

**Sorumlu yazar: mgurcay@bingol.edu.tr*

(Alınış: 30.12.2020, Kabul: 8.09.2021, Online Yayınlanma: 25.03.2022)

Anahtar Kelimeler
Pestivirus, Abort Yapmış Fötus, Doğu ve Güneydoğu Anadolu, Türkiye.

Öz: Bu çalışmada, Doğu ve Güneydoğu Anadolu bölgelerinde bulunan illerde yetiştirilen sığır, koyun ve keçilerin abort olmuş fötuslarında pestivirus antijen varlığının ticari bir ELISA (AgELISA,IDEXX Laboratories,Inc,Maine,USA) testi ile araştırılması amaçlanmıştır. Elâzığ, Malatya, Tunceli, Bingöl, Bitlis, Diyarbakır, Şırnak ve Hakkâri illerinden 2012 yılı, Ocak-Mayıs ayları arasında 245 sığır, 89 koyun, 36 keçi olmak üzere toplam 370 aborte olmuş fötus toplandı. Her bir fötus için, akciğer, karaciğer ve dalak doku numunelerini içeren, bir numune havuzu oluşturuldu. Her bir fötuse ait numune, Ag-ELISA testi ile test edildi. Test sonucunda, 245 sığır numunesinin 81'inde (%33), 89 koyun numunesinin 23'ünde (%25,8) ve 36 keçi numunesinin 8'inde (%22,2) pestivirus antijeni tespit edildi. Bu sonuçlara göre, araştırmanın yapıldığı bölgelerde sığır, koyun ve keçilerde abort yapma nedeni olarak önemli derecede pestivirus enfeksiyonunun sorumlu olduğu ortaya konulmuş oldu.

The Investigation of Pestivirus Infections in Bovine, Ovine and Caprine Foetuses in the East and Southeast Regions of Turkey

Keywords
Pestivirus, Aborted Foetuses, The East and Southeast Anatolia, Turkey.

Abstract: The present study was aimed to investigate the presence of pestiviruses in bovine, ovine and caprine foetuses in the East and Southeast regions of Turkey by antigen enzyme-linked immunosorbent assay (Ag-ELISA) method. For this purpose, 245 bovine foetuses, 89 ovine foetuses and caprine foetuses (in total 370 foetuses) were collected from Elazig, Malatya, Tunceli, Bingöl, Bitlis, Diyarbakır, Şırnak and Hakkâri provinces during January-May 2012. A pool of foetal tissues (lung, liver and spleen) was created for each foetus. The sample of each foetus was tested with the Ag- ELISA test. Pestivirus antigens were detected in 81 of 245 cattle samples (33%), 23 of 89 sheep samples (25.8%), and 8 of 36 goat samples (22.2%). According to these results, it has been revealed that pestivirus infection is responsible for abortion in cattle, sheep and goats in the investigated regions.

1. GİRİŞ

Flaviviridae ailesinde bulunan Pestivirus cinsi viruslar tek sarmallı, pozitif polariteli, RNA genomu taşıyan on bir tanınmış tür içerir. Daha önce tanımlanmış olan türlerden bovine viral diarrhoea virus -1 (BVDV-1), Pestivirus A, bovine viral diarrhoea virus-2 (BVDV-2) Pestivius B, classical swine fever virus (CSFV)

Pestivirus C ve border disease virus (BDV) Pestivirus D olarak yeniden adlandırılmaktadır. Bunlara ek olarak, *Pestivirus* cinsi içinde diğer 7 tür ise Pestivirus E-K olarak yeni sınıflandırmada yer almıştır. Bunlardan Pestivirus E, pronghorn antelope virüs, Pestivirus F, domuz pestivirusu, Pestivirus G giraffe pestivirusu, Pestivirus H, Hobi benzeri pestivirus aynı zamanda bovine viral diarrhoea virus-3 (BVDV-3) veya atipik ruminant pestivirusu olarak da bilinmektedir. Pestivirus I, Aydın benzeri pestivirus veya koyun pestivirusu, Pestivirus J, rat pestivirusu ve Pestivirus K atipik domuz pestivirusu olarak bilinmektedir [1]. Pestivirusların sınıflandırılması, genetik-antijenik ilişki ve orjin aldığı konakçıya göre yapılmaktadır [2]. Pestiviruslar konakçı tropizmi göstermediği, BVDV 'unun koyunları ve keçileri, BDV'unun ise sığırları enfekte edebildiği gösterilmiştir. Filogenetik analizlerde, 21 Pestivirus A alt tipi (BVDV-1a-u) ve 4 Pestivirus B alt tipi belirlenmiştir (BVDV-2a-d) [3]. Önceden atipik sığır pestivirusları olarak adlandırılan Pestivirus H (BVDV-

3), benzer değişkenliğe sahip olmasına rağmen ancak henüz tanımlanmış alt tipleri olmayan türdür [4]. Sığır pestivirusları koyun, keçi ve domuz gibi diğer evcil hayvan türlerini de enfekte eder [5]. Küçük ruminantların enfeksiyonu olarak bilinen Pestivirus D (sınır hastalığı virusu enfeksiyonunu boğalarda persiste bir enfeksiyon oluşturma yeteneği de dahil olmak üzere sığırlarda normal olarak enfeksiyona da neden olduğu göstermiştir [6]. Sığır pestivirusları, dünya çapında sığır yetiştiriciliğinde ciddi ekonomik kayıplara neden olan önemli enfeksiyöz ajan olarak bilinmektedir [7]. Sığır pestivirus enfeksiyonları genellikle sığırlarda persiste asemptomatik olarak görülür, persiste asemptomatik sığırların etkenin sitopatik effekt oluşturan biyotipi ile süper enfeksiyonu ile mukozal hastalık oluşur. Mukozal hastalığın mortalite oranı daha yüksektir. Sığır pestivirus enfeksiyonları sığırlarda genellikle asemptomatik olarak görülür, ancak tekrar citopatik effekt oluşturan biyotipi ile enfeksiyon sonucu akut hastalık olarak sığırların mortalite oranı yüksektir. Pestivirus ile enfekte hayvanlarda, transplasental enfeksiyonlar meydana gelebilir. Transplasental enfeksiyonlar embriyonik-fetal ölüm ve abort, embriyonun gelişimsel organ kusurları veya persiste enfeksiyon oluşumu bağışıklık toleransının gelişmesi ve buna bağlı olarak solunum yolu hastalıkları gibi çok faktörlü hastalıklara neden olabilir [8]. Sığırlarda gebeliğin 100-120 gününde meydana gelen fötal enfeksiyon, serebellar hipoplazi, mikroensefalopati, katarakt, mikrooftalmi ve timik aplazi gibi konjenital anormalliklere yol açabilir. Gebeliğin 150 ve 285. günleri arasında arasında enfekte olmuş föetuslar genellikle virustan arınabilir, normal şekilde gelişebilir ve pestivirusa karşı preklostral nötralize edici antikorlar oluşturabilir. Abortlar, deneysel enfeksiyonlarda gebeliğin 100. gününde virusla fötusun enfeksiyonu sonucu gerçekleşir [9].

Dünyada ve Türkiye'de çok değişik bölgelerde pestivirus enfeksiyonlarının sığır, koyun ve keçilerde varlığı ve yaygınlığı serolojik veya virolojik olarak yapılan birçok çalışma ile rapor edilmiştir [14,15,16,17,18,19,20]. Koyunlarda pestivirusa karşı oluşan seropozitifliğin Batı Avusturya'da %29,4 olduğu bildirilmiştir [20]. İran'da abort yapmış fötusler üzerine yapılan bir çalışmada sığırlarda (111/620) %17,90, koyunlarda (74/525) %14,09, keçilerde (71/442) %16,06, oranında antijen ELİSA testi ile pozitiflik bulmuşlardır [21]. Aynı zamanda Türkiye'de de atık yapmış hayvanlardan sağlanan fötuslerden pestivirus varlığı çalışılmış, abort etiyolojisindeki oranları belirlenmiştir. Albayrak ve ark. [22] Karadeniz Bölgesinde sığır ve koyunlarda abort yapmış fötuslarda pestivirus genom varlığını RT-PCR testi ile araştırmış ve sığır fötuslerinde (6/21) %28,57, koyun fötuslerinde (14/21) %66,66 oranlarında varlığını tespit etmişlerdir. Şevik [23], Türkiye'nin İç, Ege ve Akdeniz Bölgesinden sağladığı abort yapmış sığır, koyun ve keçi fötuslerinde pestivirus varlığını RT-PCR testi ile araştırmış, sığırlarda (61/553) %11, koyunlarda (124/1388) %8,9 ve keçilerde (3/88) %3,4 oranlarında abort etiyolojisinde pestivirus payını tespit etmiştir. Bu araştırma Doğu ve Güneydoğu Anadolu Bölgelerinde yetiştirilen sığır, koyun ve keçi sürülerinde abort yapmış fötuslada etiyolojideki pestivirus oranını tespit edildiği ilk çalışma olması nedeni ile önem arz etmektedir. Araştırmadan elde edilen sonuçlara göre, Doğu ve Güneydoğu Anadolu Bölgelerinde keçi fötusların %22,2'inde atık nedeni olarak pestivirus tespit edilmiştir. İç, Ege ve Akdeniz Bölgelerinde keçilerde tespit edilen %3,4 oranına göre daha yüksek oranda bulunmuştur. Bunun nedeni Bölgede yetiştirilen keçi ırklarının duyarlılığı ve yetiştirme farklılığı, abort vaka geçmişi, gebeliğin erken veya geç dönemi abort olması gibi nedenlerden kaynaklanmaktadır [13]. Albayrak ve ark. Karadeniz Bölgesinde sığır ve koyun fötuslarında sırası ile %28,57 ve %66,66 pestivirus oranları tespit etmiş, Şevik [23], İç, Ege ve Akdeniz Bölgelerinden sağladığı sığır ve koyun fötuslerinde sırası ile %11 ve %8,9 oranlarında pestivirus varlığı bulmuştur. Bu araştırmada ise sığır ve koyunlarda sırası ile %33 ve %25,8 oranları ile İç, Ege ve Akdeniz Bölgelerinin oranlarına göre yüksek oranlarda bulunmuştur. Karadeniz bölgesinde tespit edilen oranlara göre sığırlardaki görülme oranı paralel olmasına rağmen koyun pestivirus oranı düşük oranda tespit edilmiştir. Atık etiyolojisindeki sığır ve koyunlardaki pestivirus katkı oranlarının bölgelere göre farklılıklar göstermesinin nedenleri muhtemelen Bölgede yetiştirilen sürülerdeki klinik belirtiler, hayvan ırkları ve yetiştirmedeki bakım ve beslenme şartları ile ilgili yetiştiricilikteki değişikliklerdir [13].

Bu çalışmanın amacı, dünya çapında yaygı olarak enfeksiyonlara sebep olan pestivirusların Sığır, Koyun ve Keçi yetiştiriciliğinin yoğun olarak yapıldığı Elâzığ, Malatya, Tunceli, Bingöl, Bitlis, Diyarbakır, Şırnak ve Hakkâri illerinde yetiştirilen sığır, koyun ve keçi atıklarındaki rolünü ortaya çıkarmaktır.

2. MATERYAL VE METOT

2.1.Abort Yapmış Fötus Materyali

Elâzığ, Malatya, Tunceli, Bingöl, Bitlis, Diyarbakır, Şırnak ve Hakkâri illerinden buzağılama ve kuzulama mevsiminde, (Ocak- Mayıs) abort olgularının görüldüğü sığır (n=245), koyun (n=89), ve keçi (n=36), sürülerinden toplam 370 ölü fötus örneği araştırmanın materyalini oluşturdu (Tablo 1).

Bölgede çoğunlukla Holstein, Friesian ve Simmental ırkı ve/veya melezi sığır ırkları yetiştirilmektedir. Koyunların çoğu Akkaraman ve Morkaraman ırkı olup bölgede genelde yetiştirilen koyun ırklarıdır. Bölgenin keçi ırkı kıl keçisidir. Numune alınan işletmelerde koyun ve keçiler birlikte yetiştirilmekte, bazı işletmelerde sığır yetiştiriciliği de beraberinde yapılmaktadır. Sığır, koyun ve keçi yetiştiricileri tarafından ifade edilen anemnezler alındı Koyun ve keçi sürülerde ölü doğumlar, gelişmemiş zayıf ve zaman zaman anomalili oğlak ve kuzu doğumu şikayetleri çoğunlukla belirtildi.

Sığır, koyun ve keçi abort numunelerinde BVDV antijeninin aranması amacıyla abort yapmış fötusların otopsileri usulüne göre yapıldı. Açılan fötuslardan beyin, akciğer, dalak, böbrek ve karaciğerlerinden alınan doku parçaları 2 mL Phosphate-Buffered Saline ile (1/10) karıştırıldı. MagNa Lyser (Roche, Mannheim,

Germany)'da boncuklu tüplerde 3000 g'de 3 dakika homojenize edildi. Homojenat eppendorf tüplerde 3000 g'de 10 dakika santrifuj edildi. Alttaki katı maddeler ve boncuklar uzaklaştırıldı. Üstte kalan süpernatant inokulum olarak kullanılıncaya kadar –80 ºC de saklandı.

Tablo 1. Abort olgularının görüldüğü işletmelerinden alınan fötus örneklerinin sayıları, hayvan türleri ve alındığı iller.

İL	Sığır	Koyun	Keçi	Toplam
Elâzığ	55	2	5	62
Malatya	39	8	4	51
Tunceli	14	5	1	20
Bingöl	36	32	5	73
Bitlis	25	41	13	79
Diyarbakır	48	1	7	56
Şırnak	15	-	-	15
Hakkâri	13	-	1	14
TOPLAM	245	89	36	370

İnokulumlarda antijenin varlığı ticari BVDV antijen (Ag) ELISA (BVDV Ag Serum Plus HerdChek IDEXX Laboratories Westbrook, Maine 04092 USA) kiti ile araştırıldı. Test üretici firma protokolüne göre yapıldı.

3. BULGULAR

Toplamda 370 atık yapmış fötus numunesinin doku homojenatlarının Ag ELISA testi sonucunda, sığır sürülerine ait 245 örneğin 81'inde (%33), 89 koyun numunesinin 23'ünde (%25,8) ve 36 keçi numunesinin 8'inde (%22,2), pestivirus antijenlerinin varlığı tespit edildi. Atık Fetuslardan tespit edilen en yüksek pestivirus varlığı oranı sığırlarda Elazığ'dan sağlanan numunelerden (%38,18), koyun numunelerinde Bitlis'ten sağlanan numunelerde (%29,26), keçilerde ise yine Bitlis yöresinden sağlanan numunelerde (%30,76) tespit edildi (Tablo 2).

2.2. Metod

Tablo 2. Yavru atma olgularının görüldüğü işletmelerden alınan abort yapmış fötus örneklerinin Ag ELISA sonuçları

İl	Sığır (n)	(+)	%	Koyun (n)	(+)	%	Keçi (n)	(+)	%
Elâzığ	55	21	38,18	2	-	-	5	1	20,00
Malatya	39	14	35,89	8	2	25,00	4	-	-
Tunceli	14	3	21,42	5	1	20,00	1	-	-
Bingöl	36	11	30,55	32	8	25,00	5	1	20,00
Bitlis	25	9	36,00	41	12	29,26	13	4	30,76
Diyarbakır	48	16	33,33	1	-	-	7	2	28,57
Şırnak	15	4	26,66	-	-	-	-	-	-
Hakkâri	13	3	23,07	-	-	-	1	-	-
Toplam	**245**	**81**	**33,00**	**89**	**23**	**25,8**	**36**	**8**	**22,22**

4. SONUÇ

Çiftlik hayvanı yetiştiriciliğinde, önemli ekonomik kayıplara neden olan abortlar dünya çapında hayvancılığı etkileyen en önemli sorunlardan biridir [10]. Sığır, koyun ve keçilerde abort vakalarının bulaşıcı etiyolojik nedenini oluşturan ajanlar arasında virüsler en önemlisidir. Herpesviruslar ve pestiviruslar abort vakalarına neden olan ana patojenler arasında yer almaktadır [11,12,23]. Bu araştırmada, Elâzığ, Malatya, Tunceli, Bingöl, Bitlis, Diyarbakır, Şırnak ve Hakkâri illerinde yetiştirilen, gebeliğin farklı dönemlerinde abort yapmış toplam 370 adet Sığır, Koyun ve Keçi fötuslarında pestivirus antijenlerinin varlığı Ag- ELISA testi kullanılarak araştırılmıştır. Amaç atık fötuslardaki pestivirus etiyolojik rolünü ortaya koymaktır. Teşhis laboratuvarında, abort etiyolojisini adım adım araştırma yaklaşımı tavsiye edilir. Bu maksatla abort etiyolojisi tespitinde, abort vaka geçmişi, gebeliğin erken veya geç dönemi abort olması, mumyalanmış veya taze fetus elde edilmesi, gebe hayvan sayısına göre abort sayısı, ilk vakadan sonra geçen süre, sürülerdeki klinik belirtiler ve yetiştiricilikteki değişiklikler gibi anamnez bilgileri dikkate alınmalıdır [13]. Bu araştırmada çalışılan mataryal, hayvan yetiştiriciliğinde bakım ve besleme yönünden önemli değişikliğin olmadığı, yetiştiriciliğin geleneksel yöntemlere göre yapıldığı, hayvanlarda genel klinik belirtilerin zaman zaman görüldüğü, abort vakaları şekillenmiş sürülerden sağlanan fötuslardan oluştu. Örneklerin pestivirus enfeksiyonunun kanıtı için incelenmesinden önce, diğer abort etkenleri yönünden de incelemeleri yapıldı. Alpay ve ark. sürüde abort geçmişi olan 16 sürüden, abort vakası görülmeyen 6 sürüden sağladığı kan serumlarında koyunlarda %49,7 oranında, keçilerde %3,17 oranında pestivirus seropozitifliği tespit etmiştir [14]. Bu çalışmanın mataryalinin tamamını abort geçmişi olan sürülerden sağlanan fötuslar oluşturmaktadır. Pestivirus varlığı antijen-RLISA testi ile araştırıldı. Virüs izolasyonu, pestivirusların kan ve sütte tespiti için altın standart olarak kabul edilmektedir. Ancak günümüzde abort yapmış fötuslarda pestivirus varlığının tanısında, immünohistokimya ve antijen ELISA ile antijen tespiti yanında, polimeraz zincir reaksiyonu (PCR) tabanlı testlerle nükleik asit tespiti artık geniş bir şekilde uygulanmaktadır [1]. Bu çalışmada antijen-ELISA testi ile mataryalin tamamının atık tespit edilen sürülerden sağlanan fötuslarda koyunlarda %25,8, keçilerde %22,22 pestivirus varlığı ortaya konulmuştur.

Sonuç olarak abortlar, sığır, koyun ve keçi yetiştiriciliği yapılan işletmelerinde üretim kaybına neden olması ile ciddi ekonomik kayıplara neden olmasından dolayı sürü sağlığı, sürünün devamlılığı açısından ve hayvan yetiştiriciliğinde oldukça önemlidir. Abort nedenleri süt verimini de etkilediğinden özellikle süt üretimi yapılan hayvancılık işletmelerinde abortun etiyolojisi iyi bir şekilde tanımlanmalı ve gerekli koruma-kontrol önlemleri alınmalıdır. Hayvancılık işletmelerinde herhangi bir abort vakası görüldüğünde nedenin bakım ve beslenme şartları ile ilgili olması yanında enfeksiyöz bir etken de olabileceği unutulmamalıdır. Bu yüzden

abort materyalinin uygun bir şekilde alınıp, laboratuvar teşhisinin yapılması etiyolojinin belirlenmesi korunma ve kontrol açısından önemlidir. Viral hastalıkların hayvancılık işletmelerinde hızlı bir şekilde yayılabileceği ve sürü bazında ciddi kayıplara neden olabileceği düşüncesiyle özellikle primer viral abort etkenlerinin belirlenmesi gerekmektedir. Pestivirusun hayvanlarda persiste enfeksiyon oluşturması [24] ve aynı zamanda bölgede atık yapmış ruminant fötuslarında yaygın atık etkeni tespit edilmiş olması, sürü sağlığı ve devamlılığı yönünden enfeksiyonun hayvan yetiştiriciliğinde göz ardı edilmemesine bu araştırma ile vurgu yapılmaktadır. Bu nedenle bölgede viral etiyoloji yönünden sürüler düzenli kontrol altında tutulmalı, mücadelede sığırlar, koyun ve keçilerin bir arada yetiştirilmesi, enfeksiyonun yaygınlığına katkı sağlayacağından, bu durumun göz önünde bulundurularak, persiste enfekte hayvanların tespit edilmesi, korunma ve kontrol programlarının

KAYNAKLAR

[1] Smith DB, Meyers G, Bukh J, Gould EA, Monath T, Muerhoff, A.S, Pletnev A, Rico-Hesse R, Stapleton JT, Simmonds P, Becher P. Proposed revision to the taxonomy of the genus Pestivirus, family Flaviviridae. The Journal of general virology 2017; *98* (8), 2106.

[2] Simmonds P, Becher P, Bukh J, Gould EA, Meyers G, Monath T, Muerho S, Pletnev A, Rico-Hesse R, Smith DB et al. ICTV Virus Taxonomy Profile: Flaviviridae. J. Gen. Virol. 2017; 98: 2–3.

[3] Yesilbag K, Alpay G, Becher P. Variability and Global Distribution of Subgenotypes of Bovine Viral Diarrhea Virus. Viruses 2017; 9: 128.

[4] Bauermann FV, Ridpath JF, Weiblen R, Flores EF. HoBi-like viruses: An emerging group of pestiviruses. J. Veter. Diagn. Investig. 2013;25:6–15.

[5] Tao J, Liao J, Wang Y, Zhang X, Wang J, Zhu G. Bovine viral diarrhea virus (BVDV) infections in pigs. Veter. Microbiol. 2013; 165:185–189.

[6] Braun U, Hilbe M, Peterhans E, Schweizer M. Border disease in cattle. Veter. J. 2019;246: 12–20.

[7] Pinior B, Garcia S, Minviel JJ, Raboisson D. Epidemiological factors and mitigation measures influencing production losses in cattle due to bovine viral diarrhoea virus infection: A meta-analysis. Transboundary and emerging diseases, 2019; 66 (6): 2426-2439.

[8] Kelling CL. Viral diseases of the fetus. In: Youngquist RS, Threlfall WR, Editors. Current therapy in large animal therio-genology. 2nd ed. St. Louis: Elsevier 399–408. 2007.

[9] Givens MD, Marley MS, Infectious causes of embryonic and fetalmortality. Theriogenology. 2008; 70: 270–285.

[10] Adu-Addai B, Koney EB, Addo P, Kaneene J, Mackenzie C, Agnew DW, Importance of infectious bovine reproductive diseases: an example from Ghana. Veterinary record. 2012; 171: 47-48.

[11] Anderson ML. Infectious causes of bovine abortion during midto late-gestation. Theriogenology. 2007; 68: 474-86.

[12] Yang N, Cui X, Qian W, Yu S, Liu Q. Survey of nine abortifacient infectious agents in aborted bovine fetuses fromdairy farms in Beijing, China by PCR. Acta Veterinaria Hungarica. 2012; 60: 83-92.

[13] Borel N, Frey CF, Gottstein B, Hilbe M, Pospischil A, Franzoso F D, Waldvogel A. Laboratory diagnosis of ruminant abortion in Europe. The Veterinary Journal, 2014; 200 (2): 218-229.

[14] Alpay G, Öner EB, Yeşilbağ K. Seroepidemiology and molecular investigation of pestiviruses among sheep and goats in Northwest Anatolia. Turkish Journal of Veterinary and Animal Sciences, 2018; 42(3), 205-210.

[15] Radostits OM, Gay CC, Hinchcliff KW, Constable PD. Veterinary Medicine. Tenth Edition. Edinburgh, London, New York, Oxford, Philadelphia, St Louis, Sydney, Toronto: Saunders Elsevier, 1248-77, 2008.

[16] Burgu Ġ, Alkan F, Özkul A, ve ark. Türkiye'de süt sığırcılığı işletmelerinde bovine viral diarrhoea virus (BVDV) enfeksiyonunun epidemiyolojisi ve kontrolü. Ankara Üniv. Vet. Fak. Derg.2003; 50: 127-133.

[17] Tan MT, Karaoğlu MT, Erol N, et al. Serological and virological investigations of bovine viral diarrhoea virus (BVDV) infection in dairy cattle herds in Aydın province. Turkish Journal of Veterinary and Animal Sciences. 2006; 30(3): 299-304.

[18] Yildirim Y, Yilmaz V, Kalaycioglu AT et al. An investigation of a possible involvement of BVDV, BHV-1 and BHV-4 infections in abortion of dairy cattle in Kars district of Turkey. Kafkas Univ. Vet. Fak. Derg. 2011; 17: 879-883.

[19] Gürçay M, İssi M, Gül Y. Investigation of bovine viral diarrhoea virus in dairy cattle premises where aborts occur. Erciyes Üniversitesi Veteriner Fakültesi Dergisi. 2013; 10 (2) : 87-91.

[20] Krametter-Froetscher R, Duenser M, Preyler B,Theiner A, Benetka V, Moestl K, Baumgartner W. Pestivirus infection in sheep and goats in West Austria. Vet J. 2010; 186: 342-346.

[21] Dehkordi FS. Prevalence study of Bovine viral diarrhea virus by evaluation of antigen capture ELISA and RT-PCR assay in Bovine, Ovine, Caprine, Buffalo and Camel aborted fetuses in Iran. AMB express. 2011; 1(1): 1-6.

[22] Albayrak H, Gumusova SO, Ozan E, Yazici Z. Molecular detection of pestiviruses in aborted foetuses from provinces in northern Turkey. Tropical animal health and production. 2012; 44 (4): 677-680.

[23] Şevik M. Genomic characterization of pestiviruses isolated from bovine, ovine and caprine foetuses in Turkey: A potentially new genotype of pestivirus I species. Transboundary and Emerging Diseases. 2020;00:1-10.

[24] Gürçay M, Keçeci H, Öztürk M. Determination of presence and prevalence of Bovine Viral Diarrhea

Virus infection in cattle herds in Bingol province. Etlik Veteriner Mikrobiyoloji Dergisi, 31(1), 34-38.

Araştırma Makalesi https://doi.org/10.46810/tdfd.882078 Research Article

Türk Doğa ve Fen Dergisi
Turkish Journal of Nature and Science
www.dergipark.gov.tr/tdfd

The Effects of Valproic Acid on NO/cGMP in Pentylenetetrazole-Induced Acut Epilepsy Model in Rats

Arzuhan ÇETİNDAĞ ÇİLTAŞ[1*], Ayşegül ÖZTÜRK[2]

[1] Sivas Cumhuriyet Üniversitesi, Sağlık Hizmetleri Meslek Yüksekokulu, Tıbbı Hizmetler ve Teknikler Bölümü, Sivas, Türkiye

[2] Sivas Cumhuriyet Üniversitesi, Sağlık Hizmetleri Meslek Yüksekokulu, Tıbbı Hizmetler ve Teknikler Bölümü, Sivas, Türkiye

Arzuhan ÇETİNDAĞ ÇİLTAŞ ORCID No: 0000-0002-5420-3546

Ayşegül ÖZTÜRK ORCID No: 0000-0001-8130-7968

**Corresponding author: acetindag@cumhuriyet.edu.tr*

(Received: 17.02.2021, Accepted: 9.03.2022, Online Publication: 25.03.2022)

Keywords
Epilepsy, Pentylenetetrazole, Valproin Acid, NO/cGMP,

Absract: Epilepsy is a disease which causes neuronal damage and loss of consciousness in consequence of recurrent seizures. Nitric oxide as a neuromodulator in brain is a gas which can penetrate into cells. It has a significant role on physiological cases,pathology of many diseases such as inflammation and degenerative diseases. The purpose of this research is to search the activity of NO/cGMP pathway of valproic acid in an experimental acute epileptic model which is induced with pentylenetetrazol in rats.18 adult male Wistar Albino rats were used in the study. The rats were randomly divided into 3 groups (n=6) as control group, pentylenetetrazol (PTZ+salin) 45 mg kg-1, valproic acid (PTZ+VPA) 150 mg kg-1. After 24 hours of PTZ application, all rats brain tissues were removed and then cortex and hippocampus were separated. While PTZ increased the hippocampus and cortex NO/cGMP levels compared to control ($p < 0.01$), VPA decreased the hippocampus and cortex NO levels by comparison with PTZ ($p < 0.001$). On the other hand, while VPA decreased cortex cGMP levels ($p<0,05$) it did not change cGMP levels in hippocampus ($p> 0.05$). This study has suggested that VPA can show antiepileptic activity via NO/cGMP pathway.

Sıçanlarda Pentilentetrazol ile İndüklenen Akut Epilepsi Modelinde Valproik Asidin NO/cGMP Üzerindeki Etkileri

Anahtar Kelimeler
Epilepsi, Pentilentetrazol, Valproik Asit, NO/cGMP

Öz: Epilepsi, tekrarlayan nöbetlerle nöronal hasara, bilinç kaybına neden olan bir hastalıktır. Nitrik oksit (NO); beyinde nöromodülatör olarak ve hücreler arasında yayılabilen bir gazdır. Fizyolojik olaylarda, iltihaplanma ve dejeneratif hastalıklar gibi birçok hastalığın patolojisinde önemli rolü vardır. Bu araştırmanın amacı, sıçanlarda pentilentetrazol ile indüklenen deneysel akut epileptik modelde valproik asidin NO/cGMP yolağının aktivitesini araştırmaktır. Çalışmada 18 adet yetişkin erkek Wistar Albino sıçan kullanıldı. Sıçanlar rastgele kontrol grubu, pentilentetrazol (PTZ) 45 mg kg^{-1}, valproik asit (VPA) 150 mg kg^{-1} olarak 3 gruba (n=6) ayrıldı. PTZ uygulamasından 24 saat sonra tüm sıçanların beyin dokuları çıkarıldı, korteks ve hipokampus ayrıldı. PTZ hipokamp ve korteks NO/cGMP düzeylerini kontrole göre artırırken ($p <0,01$), VPA hipokamp ve korteks NO düzeylerini PTZ'ye göre düşürdü ($p<0,001$). Ancak VPA korteks cGMP düzeylerini düşürürken ($p <0,05$), hipokampus cGMP düzeylerini değiştirmedi ($p> 0,05$). Bu çalışma, VPA'nın antiepileptik aktivitesini NO/cGMP yolu ile gösterebileceğini düşündürmektedir.

1. INTRODUCTION

In the central nervous system, NO functions as an intercellular spreadable signalling molecule [1]. NO is produced from L-arginine in an NADPH-dependent reaction by NO synthase (NOS) in brain. [2]. NO is involved in many physiological and pathological events as a neurotransmitter/neuromodulator in the brain. These

events are involved in the pathology of many diseases such as depression, learning, memory, synaptic plasticity, inflammation, epilepsy, and long-term degenerative diseases [3]. Epilepsy, one of the neurodegenerative disorders, is reported to be caused by NO. Epilepsy is a neurodegenerative disease that affects 3% of the world population [4] and occurs with recurrent seizures [5].

Nitric oxide performs this function by activating the ryanodine receptors. Ryanodine receptors increase the release of intracellular calcium stores and thus neuronal damage occurs [6]. Nitric oxide is a potent stimulator of guanilyl cyclase and causes an increase in intracellular second messenger cyclic guanosine monophosphate (cGMP) levels [7]. Cyclic guanosine monophosphate levels are regulated by cyclic adenosine monophosphate (cAMP) and cyclic nucleotide phosphodiesterases (PDEs) that catalyze the hydrolysis of cGMP [8]. Nitric oxide (NO) is a seizure sensitivity modulator known for its dose-dependent anti-convulsant and pro-convulsant effects in epileptogenesis [9].

Although the mechanism of action of antiepileptic drugs is uncertain, GABA-A receptors are thought to be responsible. One of these drugs, valproic acid (VPA), increases GABA production, reduces GABA transaminase, and inhibits excitatory neurotransmission [10]. They reported that VPA has an anticonvulsive effect on the PTZ-kindled model [11].

It has been suggested that NO may also play a role in the antiepileptic effect mechanism of VPA [12].

In the central nervous system, NO can act as a second messenger, neuromodulator and neurotransmitter, suggesting that NO plays an important role in epilepsy and epileptogenesis. The aim of this study is to investigate the activity of the NO/ cGMP pathway on the antiepileptic efficiency of valproic acid in an experimental acute epileptic model induced by pentylenetetrazole in rats.

2. MATERYAL VE METOT

The research was conducted in Sivas Cumhuriyet University Faculty of Medicine Experimental Animals Laboratory. Not having been exposed to stress, 18 Wistar Albino rats, 4-5 months old (230±20 g), were kept in cages to able to use in the study. All rats in the study were kept at 22-24°C with a 12-hour light/dark cycle, isolated from sound, with %55±6 humidity, and they were fed at an appropriate rate. The experimental application was carried out between 09:00 and 16:00. The light and sound level of the experimental environment were kept under constant control. For experimental procedures, permission was obtained from Sivas Cumhuriyet University Animal Experiments Local Ethics Committee (license number 2020/327).

2.1. PTZ-Acute Epilepsy Protocol

A single dose of 45 mg kg^{-1} PTZ was applied to rats due to observe acute model epilepsy. After PTZ application, rats were placed in plexiglass cages (40 cmX40 cmX30 cm) and the seizures of each rat were observed within 30 mins. The seizure grade record was used to evaluate the seizures Modifies Racine's Convulsion Scale (RCS) as in the following, at initial phase there was no convulsion; at 1st phase there was twitching of vibrissae and pinnae; at 2nd phase there was a distinct twitching; at 3rd phase there were myoclonic jerks; at 4th phase there was tonic–clonic seizure while the animal remained on its feet; at 5th phase there was tonic–clonic seizure with loss of the righting reflex; at 6th phase there was tonic–clonic seizure with wild climbing and jumping; and 7th phase there was a lethal seizure [13].

2.2. Drugs

Pentylenetetrazole (PTZ) and valproic acid (VPA) were purchased from Sigma-Aldrich (St Louis, MO, USA). NO and cGMP Elisa kits were provided from Santa Cruz Biotechnology. PTZ and VPA were dissolved in saline and prepared in accordance with the doses stated below. PTZ and VPA were freshly dissolved before administering injections.

2.3. Experimental groups and Procedure

18 rats were randomly divided into 3 group (n=6). All injections were performed intraperitoneally.

Control group: Rats were administered 1 mg kg^{-1}ml single dose of saline and were applied another 1 mg kg^{-1}ml single dose of saline dose 30 min after the first injection. 24 hours after, white matter was removed, cortex and hippocampus were separated.

PTZ group: Rats in the PTZ group were applied 1ml/kg saline and administered a single dose of 45 mg kg^{-1} pentylenetetrazole 30 min after the saline injection. 24 hours after PTZ application, white matter was removed, cortex and hippocampus were separated.

VPA group: Rats were applied 150 mg kg^{-1} VPA and administered 45 mg kg^{-1} pentylenetetrazole 30 min after the VPA injection. 24 hours after PTZ application,white matter was removed, cortex and hippocampus were separated.

2.4. Preparation of Brain Tissue Homogenates

24 hours after the experimental protocol was completed, all experimental rats were euthanized. White matter of rats was removed immediately and the NO and cGMP levels in each sample were centrifuged after homogenization and frozen at -80° C to measure the NO and cGMP levels with Elisa kit.

2.5. Measurement of NO and cGMP

Rat ELISA commercial kits were used to determine the NO and cGMP levels in the supernatants of tissues taken from each group (YL Biont, Shanghai, China). Process protocols were done according to the manufacturer's instructions. Briefly, standard and tissue samples were added to the plate and incubated for 60 minutes at 37°C.

After the washing step, staining solutions were added and incubated for 15 minutes at 37° C. Stop solution was added and read at 450 nm. Standard curves were drawn to determine the value of the samples. The coefficients of variation within and between plates were found to be less than 10%.

2.6. Statistical Evaluation

All experimental results and biochemical analysis were converted into numerical values. Statistical analysis and graphing was used SPSS 25.0 for windows and GraphPad Prism 7. Results were presented as Mean ± SEM (standard error of mean). The results were evaluated by One-way ANOVA and followed by Tukey HSD (post-hoc test). $p<0.05$ values were defined.

3. BULGULAR

Hippocampus and Cortex NO Levels

As shown in Figure 1 of our research, a statistically important increase in hippocampus and cortex NO levels were observed in the PTZ administered group compared to the group control ($p<0.001$). However, a statistical decrease in hippocampus and cortex NO levels was found in the VPA administered group compared to the PTZ administered group ($p<0.001$).

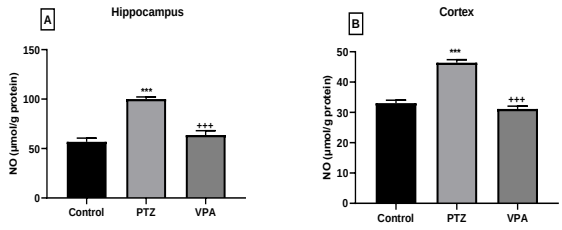

Figure 1. Effect of drugs on NO levels in the Hippocampus and Cortex after PTZ-induced seizure. * * * $p<0.001$ different from control; +++ $p<0.001$ different from PTZ.

3.2. Hippocampus and Cortex cGMP Levels

While a statistically important rise in hippocampus cGMP level was observed in the PTZ group compared to the control group ($p<0.001$), no significant difference was found between the VPA and PTZ group ($p>0.05$). However, a statistically significant increase in cortex cGMP level was observed in the VPA group compared to the PTZ group ($p<0.05$) (Figure 2).

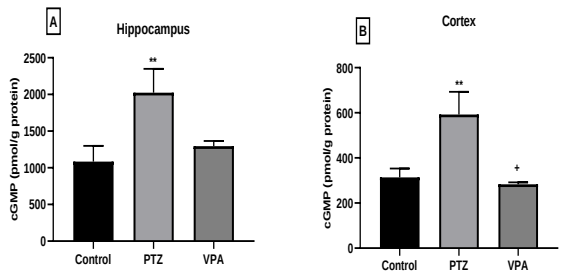

Figure 2. Effect of drugs on cGMP levels in the Hippocampus and Cortex after PTZ-induced seizure. * * $p<0.001$ different from control; + $p<0.001$ different from PTZ.

4. DISCUSSION

Epilepsy is a most common neurodegenerative disease that trigger progressive neuronal degeneration [14]. Over the past two decades, many studies have been conducted to discern the mechanisms underlying the epileptogenesis process and to treat epilepsy. Many events, such as apoptosis, inflammation, and oxidative stress play a role in the pathogenesis of epilepsy [15]. Nitric oxide, a known neurotransmitter/neuromodulator in the brain, plays a role in many physiological and pathological processes [16]. Nitric oxide is a potent stimulant of guanylyl cyclase, causing increased levels of cyclic GMP (cGMP) [7]. In the pathophysiology of epilepsy, NO shows anticonvulsant or a proconvulsant effects [17,18].

Han et al. [19] found that the 7-nitroindazole (7-NI) which is a NO inhibitor reduced hippocampus NO levels in the PTZ-induced rats, while PTZ caused seizures in rats as a result of an increase in hippocampus NO levels. This has been attributed to the increased density of PTZ's glutamate receptors as the activation of N-methyl-D-Aspartic acid (NMDA) receptors causes an increase in NO levels [20]. The hippocampus is activated after PTZ-induced seizure, as assessed by fos expression. But the mechanism of PTZ to increase NO production in the hippocampus is not clear [21]. PTZ can increase glutamate released by decrease GABA release, and thus stimulate NO production [22]. In our study, there was an important increase in both hippocampus and cortex NO levels in the PTZ group.

Nitric oxide triggers epileptic activity through cGMP formation. Glutamate activation stimulates NMDA receptors, activates nNOS by providing calcium flow to the cytosol, resulting in NO formation. Nitric oxide activates guanylate cyclase to synthesize cGMP, which is thought to initiate seizures [23]. Several studies on the role of NO in epileptic activity have mostly used proconvulsive drugs and NOS inhibitors. Some researchers have suggested that many factors, such as specific proconvulsive drugs, the type and concentrations of NOS inhibitor, method of administration, and employed specific strains or species, influence outcomes [24].

Another study researched the effect of Taurine on cortex NOS level in PTZ-induced rats and found that PTZ increased the cortex NOS level. The reason for this increase was explained by the stimulation of NMDA receptors by glutamate, catalyzing NO production and activating NOS, or by the fact that PTZ increases the NOS level by blocking GABA receptors. Taurine, on the other hand, has been found to significantly reduce the level of NOS [25]. We found that PTZ increased the level of cortex NO of rats, while VPA decreased it. The mechanism underlying this effect was demonstrated by PTZ, a GABA-A receptor antagonist, stimulating the NMDA receptor and activating neuronal nitric oxide synthase (nNOS) [26]. Therefore, in epileptic effect, it is suggested that nNOS increases NO as a result of stimulation with NMDA receptor [27]. Mülsch et al. [28] found that NO levels increased in the amygdala and cortex

during kainate-induced seizures in rats, and NO levels decreased in the group treated with 7-nitroindazole and diazepam. In our study, VPA, which was used as an antiepileptic, reduced NO levels in both the hippocampus and cortex, while decreased the cGMP levels in the cortex, but did not affect the hippocampus cGMP level. In another study, when looking at serum nitrite and nitrate levels in epileptic children using valproic acid or carbamazepine, nitrite and nitrate levels were found to be significantly higher in both valproic acid and carbamazepine groups compared to the control group. Based on these results, it has been suggested that valproic acid and carbamazepine may have an antiepileptic effect through nitric oxide [29]. It has been shown that 7-nitroindazole(7-NI) inhibitor improves the anticonvulsant effect of classic and second-generation antiepileptics, with the exception of tiagabin, felbamate and topiramate. However, the effect of NG-nitro-L-arginine methyl ester has not been clearly found. In the seizure models of pentylenetetrazole, pictotoxin and N-methyl-Daspartat, the inhibitor exhibited both convulsive and anticonvulsive effects depending on the dose. NG-nitro-L-arginine methyl ester enhanced the effectiveness of diazepam and clonazepam, decreased valproate and phenobarbital, but did not affect the anticonvulsant effect of phenytoin and ethosuximide [30].

The data of this research were consistent with previous works view that VPA caused a decrease in NO-cGMP levels in white matter, but an increase in NO-cGMP levels after PTZ-induced seizures.

5. SONUÇ

Our results show that NO plays an important role in acute epileptic model. However, VPA can demonstrate its antiepileptic effect by reducing the level of NO/cGMP, thus creating a protective effect against neuronal damage. Further research is needed to answer questions raised about possible involved mechanisms.

Acknowledgments

The researchers thank the institution for using the resources of the Sivas Cumhuriyet University.

Conflict of İnterest

The authors report no any conflict of interest

REFERENCES

[1] Dawson TM, Snyder SH. Gases as biological messengers: nitric oxide and carbon monoxide in the brain. *J Neurosci*. 1994;14(9):5147-5159.
[2] Moncada S, Palmer RM, Higg, EA. Nitric oxide: physiology, pathophysiology, and pharmacology. *Pharmacol Rev*. 1991;43(2):109-142.
[3] Bruckdorfer R. The basics about nitric oxide. Mol Aspects Med. 2005;26(1-2):3-31.
[4] Wyllie E. Wyllie's treatment of epilepsy: principles and practice. 6th ed. Philadelphia, PA: Wolters Kluwer Health; 2015.
[5] Tastemur Y, Gumus E, Ergul M, Ulu M, Akkaya R, Ozturk A, et al. Positive effects of angiotensin-converting enzyme (ACE) inhibitor, captopril, on pentylenetetrazole-induced epileptic seizures in mice. Trop J Pharm Res. 2020; 19(3):637–643.
[6] Mikami Y, Kanemaru K, Okubo Y, Nakaune T, Suzuki J, Shibata K, et al. Nitric Oxide-induced Activation of the Type 1 Ryanodine Receptor Is Critical for Epileptic Seizure-induced Neuronal Cell Death. EBio Medicine. 2016; 11:253-261.
[7] Snyder SH, Bredt DS. Nitric oxide as a neuronal messenger. *Trends Pharmacol Sci*. 1991;12(4):125-128.
[8] Kaster MP, Rosa AO, Santos AR, Rodrigues AL. Involvement of nitric oxide-cGMP pathway in the antidepressant-like effects of adenosine in the forced swimming test. *Int J Neuropsychopharmacol*. 2005;8(4):601-606.
[9] Buisson A, Lakhmeche N, Verrecchia C, Plotkine M, Boulu RG. Nitric oxide: an endogenous anticonvulsant substance. *Neuroreport*. 1993;4(4):444-446.
[10] Johannessen CU, Johannessen SI. Valproate: past, present, and future. *CNS Drug Rev*. 2003;9(2):199-216.
[11] Dziki M, Hönack D, Löscher W. Kindled rats are more sensitive than non-kindled rats to the behavioural effects of combined treatment with MK-801 and valproate. *Eur J Pharmacol*. 1992;222(2-3):273-278.
[12] Peker E, Oktar S, Ari M, Kozan R, Doğan M, Cağan E, et al. Nitric oxide, lipid peroxidation, and antioxidant enzyme levels in epileptic children using valproic acid. *Brain Res*. 2009; 1297:194-197.
[13] Erdogan MA, Yusuf D, Erdogan A, Erbas. Levodropropizine suppresses seizure activity in rats with pentylenetetrazol-induced epilepsy. Epilepsy Res.2019; 150:32–37.
[14] Zhu X, Dong J, Han B, Huang R, Zhang A, Xia Z, et al. Neuronal Nitric Oxide Synthase Contributes to PTZ Kindling Epilepsy-Induced Hippocampal Endoplasmic Reticulum Stress and Oxidative Damage. Front Cell Neurosci. 2017; 11:377.
[15] Kwon YS, Pineda E, Auvin S, Shin D, Mazarati A, Sankar R. Neuroprotective and antiepileptogenic effects of combination of anti-inflammatory drugs in the immature brain. J Neuroinflammation. 2013; 10:30.
[16] Akula KK, Dhir A, Kulkarni SK. Nitric oxide signaling pathway in the anti-convulsant effect of adenosine against pentylenetetrazol-induced seizure threshold in mice. Eur J Pharmacol. 2008;587(1-3):129-134.
[17] Nakamura TA, Yamada K, Hasegawa T, Nabeshima T. Possible involvement of nitric oxide in quinolinic acid-induced convulsion in mice. Pharmacol Biochem Behav. 1995;51(2-3):309-312.
[18] Lallement G, Shih TM Pernot-Marino, I, Baubichon D, Foquin A, McDonough JH. The role of nitric oxide in soman-induced seizures, neuropathology,

and lethality. Pharmacol Biochem Behav. 1996;54(4):731-737.
[19] Han D, Yamada K, Senzaki K, Xiong H, Nawa H, Nabeshima T. Involvement of nitric oxide in pentylenetetrazole-induced kindling in rats. J Neurochem. 2000;74(2):792-798.
[20] Royes LF, Fighera MR, Furian AF, Oliveria MS, Fiorenza NG, Myskiw JC, et al. Involvement of NO in the convulsive behavior and oxidative damage induced by the intrastriatal injection of methylmalonate. Neurosci Lett. 2005;376(2):116-120.
[21] Shehab S, Coffey P, Dean P, Redgrave P. Regional expression of fos-like immunoreactivity following seizures induced by pentylenetetrazole and maximal electroshock. Exp Neurol. 1992;118(3):261-274.
[22] Giorgi O, Orlandi M, Lecca D, Corda MG. MK-801 prevents chemical kindling induced by pentylenetetrazol in rats. Eur J Pharmacol. 1991;193(3):363-365.
[23] Garthwaite J. Glutamate, nitric oxide and cell-cell signalling in the nervous system. *Trends Neurosci*. 1991;14(2):60-67.
[24] Balter-Seri J, Yuhas Y, Weizman A, Nofech-Mozes Y, Kaminsky, E, Ashkenazi, S. Role of nitric oxide in the enhancement of pentylenetetrazole-induced seizures caused by Shigella dysenteriae. Infect Immun. 1999;67(12):6364-6368.
[25] El-Abhar HS, El Gawad HM. Modulation of cortical nitric oxide synthase, glutamate, and redox state by nifedipine and taurine in PTZ-kindled mice. Epilepsia. 2003;44(3):276-281.
[26] X. Zhu, J. Dong, K. Shen, Y. Bai, Y. Zhang, X. Lv, et al. NMDA receptor NR2B subunits contribute to PTZ-kindling-induced hippocampal astrocytosis and oxidative stress. Brain Res Bull. 2015;114: 70-78
[27] X. Zhu, J. Dong, K. Shen, Y. Bai, J. Chao, H. Yao Neuronal nitric oxide synthase contributes to pentylenetetrazole-kindling-induced hippocampal neurogenesis. Brain Res Bull. 2016;121:138-147
[28] Mülsch A, Busse R, Mordvintcev PI, et al. Nitric oxide promotes seizure activity in kainate-treated rats. *Neuroreport*. 1994;5(17):2325-2328.
[29] Karabiber H, Yakinci C, Durmaz Y, Temel I, Mehmet N. Serum nitrite and nitrate levels in epileptic children using valproic acid or carbamazepine. Brain Dev. 2004;26(1):15-8.
[30] Banach M, Piskorska B, Czuczwar SJ, Borowicz KK. Nitric oxide, epileptic seizures, and action of antiepileptic drugs. CNS Neurol Disord Drug Targets. 2011;10(7):808-19.

Cilt 11, Sayı 1, Sayfa 11-18, 2022 Volume 11, Issue 1, Page 11-18, 2022

Araştırma Makalesi https://doi.org/10.46810/tdfd.883218 Research Article

Türk Doğa ve Fen Dergisi
Turkish Journal of Nature and Science
www.dergipark.gov.tr/tdfd

Investigation of Nonlinear Wave Solutions for Fusion and Fission Phenomenas

Tolga AKTÜRK[1*], Volkan ÇAKMAK[2]

[1] Ordu University, Faculty of Education, Department of Mathematics and Science Education, Ordu, Turkey
[2] Ordu University, Faculty of Sciences , Department of Mathematics, Ordu, Turkey
Tolga AKTÜRK ORCID No: 0000-0002-8873-0424
Volkan ÇAKMAK ORCID No: 0000-0002-3262-9327

** Corresponding author: tolgaakturk@odu.edu.tr*

(Received: 19.02.2021, Accepted: 27.08.2021, Online Publication: 25.03.2022)

Keywords
Modified Exponential Function Method, The (3+1)-dimensional Jimbo-Miwa equation, Wave solutions

Abstract: In this study, wave solutions of the (3+1) dimensional Jimbo-Miwa equation and two different phenomena of the solution, fusion and fission, are obtained using the modified exponential function method. In order to get more possible solutions, two different cases are investigated due to the nature of the modified exponential function method. When the resulting solutions are analyzed, trigonometric, hyperbolic and rational functions are obtained. It was checked whether the solution functions found by the Wolfram Mathematica software provided the (3+1) dimensional potential Jimbo-Miwa equation. Two and three dimensional graphs, contour and density graphs of the solution function were get by determining the appropriate parameters.

Füzyon ve Fizyon Fenomenleri İçin Doğrusal Olmayan Dalga Çözümlerinin İncelenmesi

Anahtar Kelimeler
Geliştirilmiş Üstel Fonksiyon Metodu, (3+1)-boyutlu Jimbo-Miwa denklemi, Dalga çözümleri

Öz: Bu çalışmada, (3+1) boyutlu Jimbo-Miwa denkleminin dalga çözümleri ve buna bağlı olarak da çözümün füzyon ve fisyon olmak üzere iki farklı olgusu modifiye üstel fonksiyon yöntemi kullanılarak elde edilmiştir. Daha olası çözümler elde etmek için modifiye edilmiş üstel fonksiyon yönteminin doğası gereği iki farklı durum incelenmiştir. Ortaya çıkan çözümler incelendiğinde trigonometrik, hiperbolik ve rasyonel fonksiyonlar elde edilmiştir. Wolfram Mathematica yazılımı tarafından bulunan çözüm fonksiyonlarının (3+1) boyutlu potansiyel Jimbo-Miwa denklemini sağlayıp sağlamadığı kontrol edildi. Uygun parametreler belirlenerek çözüm fonksiyonunun iki ve üç boyutlu grafikleri, kontur ve hassasiyet grafikleri elde edildi.

1. INTRODUCTION

Physics, engineering, health, etc. all events encountered in natural and applied sciences are represented by mathematical models. These types of models are stated in nonlinear partial differential equations. Therefore, it is of great importance to obtain the solutions of such equations. In scientific studies in the literature, there are various methods to investigate the solutions of such equations. Some of these methods in the literature; generalized tanh function method [1], the modified extended tanh-function method [2-3], the generalized Bernoulli sub-equation function method [4-6], The trial equation method [7-11], the first integral method [12], the modified exponential function method [13-17] and many more methods.

In this study, we consider the (3+1) dimensional Jimbo-Miwa equation given following [18-24],

$$u_{xxxy} + 3u_y u_{xx} + 3u_x u_{xy} + 2u_{yt} - 3u_{xz} = 0. \quad (1)$$

Equation (1) given as a mathematical model has been encountered in fusion and fission phenomena which is a subject of nuclear physics. In the literature, there are

results obtained by using various methods regarding the solutions of equation (1) [18-24].

In the second part of this study, the modified exponential function method is introduced. To apply this method PDEs has been reduced to ordinary diferantial equations (ODEs). In the third chapter, the solutions obtained by applying the determined method (3+1)-dimensional Jimbo-Miwa equation and two- and three-dimensional graphs, contour graphs and density graphs of these results are presented for two cases. In the last part, the conclusion part is given.

2. ANALYSIS OF MODIFIED EXPONENTIAL FUNCTION METHOD

Let us consider the general form of the nonlinear partial differential equation for the modified exponential function method as follows;

$$P\left(U,U_x,U_y,U_z,U_t,U_{xx},U_{xt},U_{yy},U_{xxxz},\cdots\right)=0, \quad (2)$$

where $U=U(x,y,z,t)$ is unknown function.

Step 1. Taking the independent variables given in equation (1) into consideration, the wave transformation given below is considered,

$$U(x,y,z,t)=U(\xi),\ \xi=k\left(x+y+z-ct\right). \quad (3)$$

The terms k and c given here are constants in walking wave transformation. If the expression (3) is substituted by obtaining the derivative expressions in the equation (2) given as the general form of equation (1) by using the wave transformation,

$$N\left(U,U',\left(U'\right)^2,U'',U''',\cdots\right)=0, \quad (4)$$

the general form of the nonlinear ordinary differential equation is gotten.

Step 2: According to this method, the solution function of equation (1) is as follows.

$$U\left(\xi\right)=\frac{\sum_{i=0}^{n}A_i\left[\exp\left(-\Omega\left(\xi\right)\right)\right]^i}{\sum_{j=0}^{m}B_j\left[\exp\left(-\Omega\left(\xi\right)\right)\right]^j}= \quad (5)$$

$$=\frac{A_0+A_1\exp\left(-\Omega\right)+\cdots+A_n\exp\left(n\left(-\Omega\right)\right)}{B_0+B_1\exp\left(-\Omega\right)+\cdots+B_m\exp\left(m\left(-\Omega\right)\right)},$$

where $A_i,B_j,\left(0\le i\le n,0\le j\le m\right)$ are constants. The balancing procedure is applied to the nonlinear ordinary differential equation (4) obtained by applying the wave transformation. In other words, by equating the term with the highest order derivative in the equation (4) and the nonlinear term, the relation between m and n is obtained. Equality is found by giving value to the constants in this relation. Thus, the upper limits of the sum symbols in equation (5) are determined.

$$\Omega'\left(\xi\right)=\exp\left(-\Omega\left(\xi\right)\right)+\mu\exp\left(\Omega\left(\xi\right)\right)+\lambda. \quad (6)$$

The omega function given below is a function used as the power of the exponential function in the solution function. When we solve the Eq. (6), the following families are obtained by He et al [13]:

Family 1: When $\mu\neq0,\ \lambda^2-4\mu>0,$

$$\Omega\left(\xi\right)=\ln\left(\frac{-\sqrt{\lambda^2-4\mu}}{2\mu}\tanh\left(\frac{\sqrt{\lambda^2-4\mu}}{2}\left(\xi+E\right)\right)-\frac{\lambda}{2\mu}\right). \quad (7)$$

Family 2: When $\mu\neq0,\ \lambda^2-4\mu<0,$

$$\Omega\left(\xi\right)=\ln\left(\frac{\sqrt{-\lambda^2+4\mu}}{2\mu}\tan\left(\frac{\sqrt{-\lambda^2+4\mu}}{2}\left(\xi+E\right)\right)-\frac{\lambda}{2\mu}\right). \quad (8)$$

Family 3: When $\mu=0,\lambda\neq0$ and $\lambda^2-4\mu>0,$

$$\Omega\left(\xi\right)=-\ln\left(\frac{\lambda}{\exp\left(\lambda\left(\xi+E\right)\right)-1}\right). \quad (9)$$

Family 4: When $\mu\neq0,\lambda\neq0$ and $\lambda^2-4\mu=0,$

$$\Omega\left(\xi\right)=\ln\left(-\frac{2\lambda\left(\xi+E\right)+4}{\lambda^2\left(\xi+E\right)}\right). \quad (10)$$

Family 5: When $\mu=0,\ \lambda=0$ and $\lambda^2-4\mu=0,$

$$\Omega\left(\xi\right)=\ln\left(\xi+E\right). \quad (11)$$

where $A_0,A_1,\ldots,A_n,B_0,B_1,\ldots,B_m,E,\lambda,\mu$ are constants.

Step 3: After equation (6) is solved, when the equation (5) is written in its place, an algebraic equation system

consisting of coefficients is get. When this system of equations is solved with the help of the Mathematica program, the travelling wave solutions that provide the equation (1) are obtained.

3. APPLICATION

Using the traveling wave transformation (3) for equation (1), the following nonlinear ordinary differential equation is obtained,

$$k^2U''' + 3k\left(U'\right)^2 - (2c+3)U' = 0. \qquad (12)$$

If $U' = V$ transform is applied in equation (12), we obtain,

$$k^2V'' + 3kV^2 - (2c+3)V = 0. \qquad (13)$$

In equation (13), if the equalization term is applied between V'' and V^2 according to the balance procedure,

$$M + 2 = N. \qquad (14)$$

If $M = 1$ so as to satisfy the equation (14), $N = 3$ is obtained. In this case, the upper limits of the total symbols in the sought solution function in equation (5) are determined. Accordingly, the terms required in the equation (15) are given below.

$$V\left(\xi\right) = \frac{\psi}{\varphi} = \frac{A_0 + A_1e^{-\Omega(\xi)} + A_2e^{-2\Omega(\xi)} + A_3e^{-3\Omega(\xi)}}{B_0 + B_1e^{-\Omega(\xi)}},$$

$$V'\left(\xi\right) = \frac{\psi'\varphi - \psi\varphi'}{\varphi^2}, \qquad (15)$$

$$V''\left(\xi\right) = \frac{\psi''\varphi^3 - \varphi^2\psi'\varphi' - \left(\psi\varphi'' + \psi'\varphi'\right)\varphi^2 + 2\left(\psi'\right)^2\psi\varphi}{\varphi^4}.$$

Case 1:

$$A_0 = -\frac{1}{3}k(\lambda^2 + 2\,\mu)B_0,$$

$$A_1 = -\frac{1}{3}k(6\,\lambda B_0 + (\lambda^2 + 2\mu)B_1),$$

$$A_2 = -2\,k\,(B_0 + \lambda B_1),\ A_3 = -2\,k\,B_1,$$

$$c = \frac{1}{2}\left(k^2\left(-\left(\lambda^2 - 4\mu\right)\right) - 3\right).$$

By using the obtained coefficients, the traveling wave solutions of equation (1) have been analyzed considering the following family cases.

Family-1:

$$V_{1,1}(\xi) = -\frac{k\left(\lambda^2 - 4\mu\right)sech^2\left(\frac{1}{2}\phi\right)\left(\lambda\beta + \alpha - 4\mu\right)}{3\left(\sqrt{\lambda^2 - 4\mu}tanh\left(\frac{1}{2}\phi\right) + \lambda\right)^2}. \qquad (16)$$

Where $\alpha = \left(\lambda^2 - 2\mu\right)Cosh\left[\phi\right]$, $\beta = \sqrt{\lambda^2 - 4\mu}Sinh\left[\phi\right]$, $\phi = \sqrt{\lambda^2 - 4\mu}\left(EE + \xi\right)$.

Integrate ξ on both sides of the equation $U' = V$,

$$U_{1,1}(\xi) = \frac{1}{3}k\left(\lambda^2 - 4\mu\right)\left(\frac{3\lambda}{2\mu cosh\left(\phi\right) + \lambda^2 - 2\mu} - EE - \xi\right) + \frac{2k\mu\beta}{2\mu cosh\left(\phi\right) + \lambda^2 - 2\mu}. \qquad (17)$$

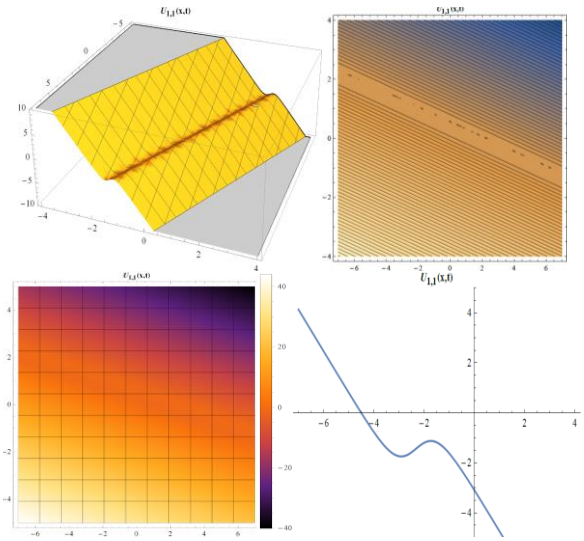

Figure 1. The three dimensional graph, contour graph, density graphs of Eq.(17) for the values $c = -4, A_3 = 2, B_1 = 1, \lambda = 3, \mu = 1, y = -1, z = 1, k = -1, \mathrm{EE} = 0.82$ and two-dimensional graph for $t = 1$.

Family 2:

$$V_{1,2}(\xi) = \frac{k\left(\lambda^2 - 4\mu\right)sec^2\left(\frac{1}{2}\tau\right)\left(\varsigma - \omega + 4\mu\right)}{3\left(\lambda - \sqrt{4\mu - \lambda^2}tan\left(\frac{1}{2}\tau\right)\right)^2}. \qquad (18)$$

Where $\varsigma = \lambda\sqrt{-\lambda^2 + 4\mu}Sin\left[\tau\right], \omega = \left(\lambda^2 - 2\mu\right)Cos\left[\tau\right]$, $\tau = \sqrt{-\lambda^2 + 4\mu}\left(EE + \xi\right)$.

$$U_{1,2}(\xi)=\frac{1}{3}k\left(\lambda^2-4\mu\right)\left(\frac{3\lambda}{2\mu cos\left(\tau\right)+\lambda^2-2\mu}-EE-\xi\right)-\frac{2k\mu\sqrt{4\mu-\lambda^2}sin\left(\tau\right)}{2\mu cos\left(\tau\right)+\lambda^2-2\mu}. \quad (19)$$

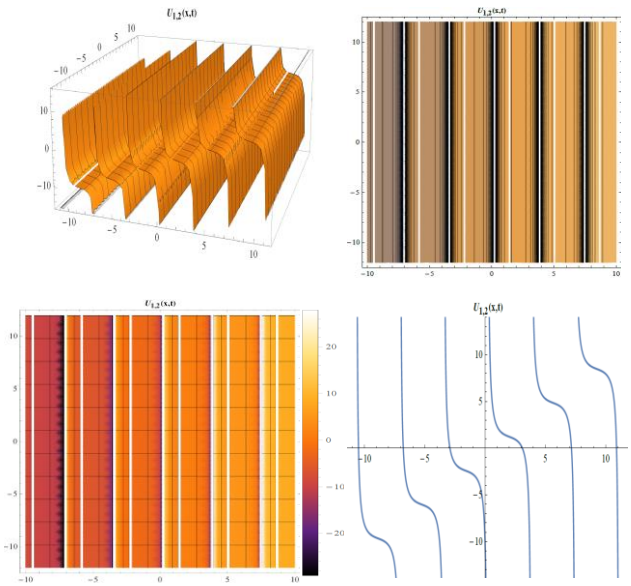

Figure 2. The three dimensional graph, contour graph, density graphs of Eq.(19) for the values $c=0, A_3=2, B_1=1, \lambda=1, \mu=1, y=-0.01, z=0.01, k=-1, \mathrm{EE}=0.82$ and two-dimensional graph for $t=1$.

Family 3:

$$V_{1,3}(\xi)=-\frac{1}{6}k\lambda^2(cosh(\lambda(EE+\xi))+2)\ csch^2\left(\frac{1}{2}\lambda(EE+\xi)\right). \quad (20)$$

Integrating equation (20) according to ξ,

$$U_{1,3}(\xi)=k\lambda coth\left(\frac{1}{2}\lambda(EE+\xi)\right)-\frac{1}{3}k\lambda^2(EE+\xi). \quad (21)$$

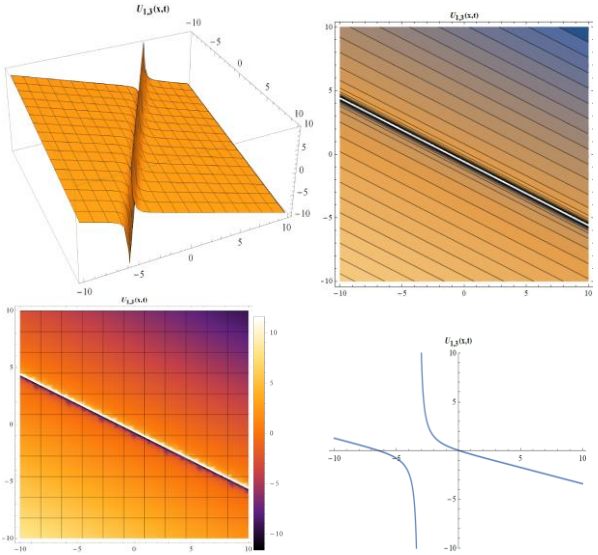

Figure 3. The three dimensional graph, contour graph, density graphs of Eq.(21) for the values $c=-2, \lambda=1, \mu=0, y=1, z=1, k=-1, \mathrm{EE}=0.82$ and two-dimensional graph for $t=1$.

Family 4:

$$V_{1,4}(\xi)=\frac{1}{6}k\left(\lambda^2\left(1-\frac{12}{(\lambda(EE+\xi)+2)^2}\right)-4\mu\right). \quad (22)$$

Integrating equation (22) according to ξ, we get,

$$U_{1,4}(\xi)=\frac{1}{6}k\left(\begin{array}{l}\lambda(\lambda(EE+\xi)+2)+\\ \frac{12\lambda}{\lambda(EE+\xi)+2}-4\mu\xi\end{array}\right). \quad (23)$$

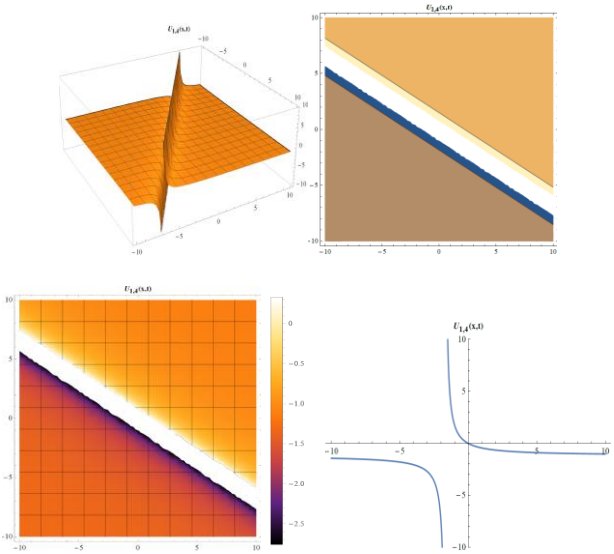

Figure 4. The three dimensional graph, contour graph, density graphs of Eq.(23) for the values $c=-1.5, \lambda=2, \mu=1, y=1, z=1, k=-1, \mathrm{EE}=0.82$ and two-dimensional graph for $t=1$.

Family 5:

$$V_{1,5}(\xi)=-\frac{2k}{(EE+\xi)^2}. \quad (24)$$

Integrating equation (24) according to ξ, we obtain,

$$U_{1,5}(\xi)=\frac{2k}{EE+\xi}. \tag{25}$$

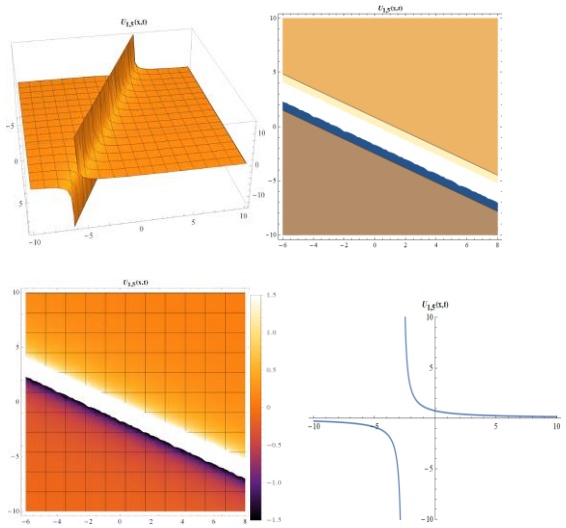

Figure 5. The three dimensional graph, contour graph, density graphs of Eq.(25) for the values $c=-1.5,\lambda=0,\mu=0,y=1,z=1,k=-1,\mathrm{EE}=0.82$ and two-dimensional graph for $t=1$.

Case 2:

$$A_0=-\frac{B_0\left(2c+3k^2\lambda^2+3\right)}{6k},$$

$$A_1=-\frac{B_1\left(2c+3k^2\lambda^2+3\right)}{6k}-2B_0k\lambda,$$

$$A_2=-2k\left(B_1\lambda+B_0\right),\quad A_3=-2B_1k,$$

$$\mu=\frac{2c+k^2\lambda^2+3}{4k^2}.$$

By using the obtained coefficients, the traveling wave solutions of the equation (1) are analyzed by considering the following family cases.

Family-1:

$$V_{2,1}(\xi)=-\frac{2c+3}{6k}-\frac{k\left(\lambda\beta+\lambda^2-4\mu\right)^2}{2\left(\beta+\lambda\right)^2}. \tag{26}$$

Where $\beta=\sqrt{\lambda^2-4\mu}\alpha$,$\alpha=tanh\left(\frac{1}{2}\phi\right)$,

$\phi=\sqrt{\lambda^2-4\mu}\left(EE+\xi\right)$.

Integrate ξ on both sides of the equation $U'=V$,

$$\beta\left(2(2c+3)\mu\xi+3\lambda k^2\left(\lambda^2-8\mu\right)\right)+$$
$$2(2c+3)\lambda\mu\xi++12k^2\mu tanh^{-1}\left(\alpha\right)$$
$$U_{2,1}(\xi)=-\frac{\left(\sqrt{\lambda^2-4\mu}(\beta+\lambda)\right)+3k^2\left(\lambda^2-4\mu\right)^2}{12k\mu\left(\beta+\lambda\right)}. \tag{27}$$

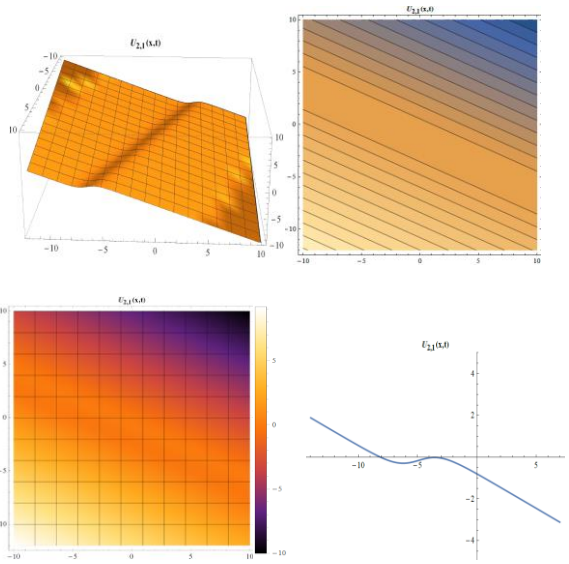

Figure 6. The three dimensional graph, contour graph, density graphs of Eq.(27) for the values $c=-2,\lambda=2,\mu=\frac{15}{16},y=1,z=1,k=2,\mathrm{EE}=0.75$ and two-dimensional graph for $t=1$.

Family 2:

$$V_{2,2}(\xi)=-\frac{2c+3}{6k}-\frac{k\left(-\lambda\varsigma+\lambda^2-4\mu\right)^2}{2\left(\lambda-\varsigma\right)^2}. \tag{28}$$

Where $\varsigma=\sqrt{\lambda^2-4\mu}tanh\left(\frac{1}{2}\tau\right)$, $\omega=\left(2\mu\right)Cos\left[\tau\right]$,

$\tau=\sqrt{-\lambda^2+4\mu}\left(EE+\xi\right)$.

$$U_{2,2}(\xi)=-\frac{(2c+3)\xi}{6k}-\frac{1}{2}k(EE+\xi)\left(\lambda^2-4\mu\right)+$$
$$\frac{k\lambda\left(\lambda^2-4\mu\right)}{\omega+\lambda^2-2\mu}-\frac{2k\mu\sqrt{4\mu-\lambda^2}sin\left(\tau\right)}{\omega+\lambda^2-2\mu}. \tag{29}$$

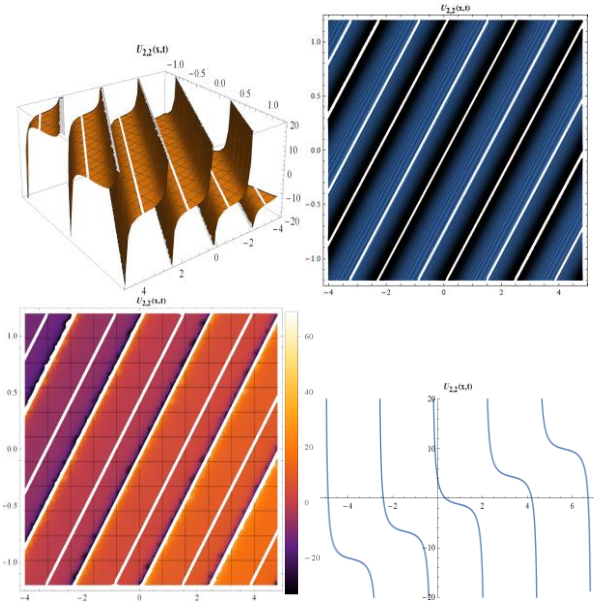

Figure 7. The three dimensional graph, contour graph, density graphs of Eq.(29) for the values $c = 2, \lambda = 1, \mu = \frac{11}{16}, y = -1, z = 1, k = 2, \mathrm{EE} = 0.75$ and two-dimensional graph for $t = 1$.

Family 3:

$$V_{2,3}(\xi) = \frac{2c + 3k^2\lambda^2 coth^2\left(\frac{1}{2}\lambda(EE+\xi)\right) + 3}{6k}. \quad (30)$$

Integrating equation (30) according to ξ,

$$U_{2,3}(\xi) = k\lambda\left(\begin{array}{l} coth\left(\frac{1}{2}\lambda(EE+\xi)\right) - \\ tanh^{-1}\left(tanh\left(\frac{1}{2}\lambda(EE+\xi)\right)\right)\end{array}\right) - \quad (31)$$

$$\frac{(2c+3)\xi}{6k}.$$

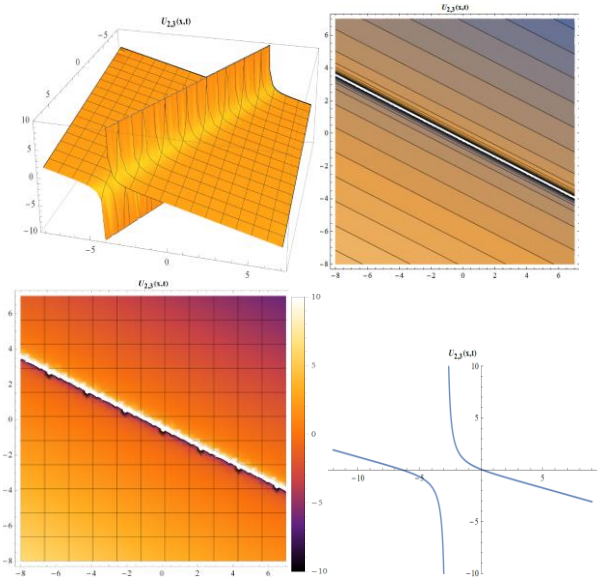

Figure 8. The three dimensional graph, contour graph, density graphs of Eq.(31) for the values $c = -2, \lambda = 1, \mu = 0, y = -1, z = 1, k = 1, \mathrm{EE} = 0.85$ and two-dimensional graph for $t = 1$.

Family 4:

$$V_{2,4}(\xi) = -\frac{2c+3}{6k} - \frac{2k\lambda^2}{(\lambda(EE+\xi)+2)^2}. \quad (32)$$

Integrating equation (32) according to ξ, we get,

$$U_{2,4}(\xi) = \frac{2k\lambda}{\lambda(EE+\xi)+2} - \frac{(2c+3)\xi}{6k}. \quad (33)$$

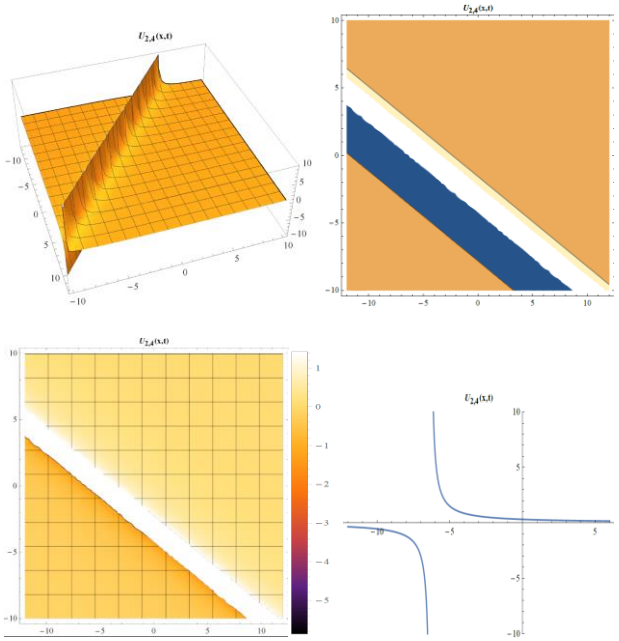

Figure 9. The three dimensional graph, contour graph, density graphs of Eq.(33) for the values $c = -1.5, \lambda = 1, \mu = 0.25, y = 1, z = 1, k = 1, \mathrm{EE} = 0.82$ and two-dimensional graph for $t = 1$.

Family 5:

$$V_{2,5}(\xi) = -\frac{2c+3}{6k} - \frac{2k}{(EE+\xi)^2}. \quad (34)$$

Integrating equation (34) according to ξ, we obtain,

$$U_{2,5}(\xi) = \frac{2k}{EE+\xi} - \frac{(2c+3)\xi}{6k}. \quad (35)$$

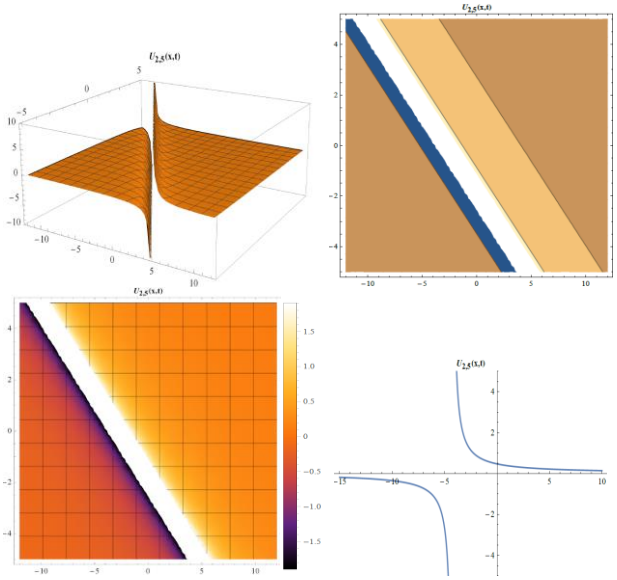

Figure 10. The three dimensional graph, contour graph, density graphs of Eq.(35) for the values $c = -1.5, \lambda = 0, \mu = 0, y = 1, z = 1, k = 1, \mathrm{EE} = 0.82$ and two-dimensional graph for $t = 1$.

4. CONCLUSION

In this article, MEFM was applied to the (3+1)-dimensional Jimbo-Miva equation considered as a nonlinear mathematical model. In this research, it was seen that the analytical solutions found under the conditions obtained according to the method provided the equation (1). When the analytical solution functions found are analyzed, it is seen that there are hyperbolic and trigonometric functions with periodic functions and rational functions. In particular, obtaining periodic functions is an advantage because such solution functions allow interpretation for an infinite range thanks to the understanding within a specific range of the behaviors represented by the mathematical model. All calculations and graphics were made using Mathematica software program. It has been observed that two and three dimensional graphs obtained by determining the appropriate parameters are suitable for the physical behavior of wave solutions. In addition, contour graphics and density graphics were found with the help of software program for wave solutions. Using this method, if more cases are investigated and different coefficient values are taken, different traveling wave solutions can be get. When the obtained solutions are analyzed, it can be stated that MEFM is effective and reliable in revealing analytical solutions of nonlinear partial differential equations. The obtaining results can help us learn more about the fusion and fission events.

REFERENCES

[1] Zheng X, Chen Y, Zhang H. Generalized extended tanh-function method and its application to (1+ 1)-dimensional dispersive long wave equation. Physics Letters A.2003; 311(2-3):145-157.

[2] Elwakil SA, El-Labany SK, Zahran MA, Sabry R. Modified extended tanh-function method for solving nonlinear partial differential equations. Physics Letters A.2002; 299(2-3):179-188.

[3] Fan E, Hon YC. Applications of extended tanh method to 'special' types of nonlinear equations. Applied Mathematics and Computation. 2003;141(2-3):351-358.

[4] Yang XF, Deng ZC , Wei YA. Riccati-Bernoulli sub-ODE method for nonlinear partial differential equations and its application. Advances in Difference equations.2015;2015(1):1-17.

[5] Baskonus HM , Bulut H. Regarding on the prototype solutions for the nonlinear fractional-order biological population model. In AIP Conference Proceedings AIP Publishing LLC.2016;1738:1.

[6] Abdelrahman MA. A note on Riccati-Bernoulli Sub-ODE method combined with complex transform method applied to fractional differential equations. Nonlinear Engineering.2018;7(4):279-285.

[7] Liu CS. Trial equation method and its applications to nonlinear evolution equations. Acta. Phys. Sin. 2005;54(6):2505-2509.

[8] Liu CS. Trial equation method to nonlinear evolution equations with rank inhomogeneous: mathematical discussions and its applications. CoTPh.2006;45(2): 219-223.

[9] Bulut H, Baskonus HM, Pandir Y. The modified trial equation method for fractional wave equation and time fractional generalized Burgers equation. In Abstract and Applied Analysis Hindawi.2013; Vol. 2013.

[10] Gurefe Y, Misirli E, Sonmezoglu A, Ekici M. Extended trial equation method to generalized nonlinear partial differential equations. Applied Mathematics and Computation.2013; 219(10): 5253-5260.

[11] Pandir Y, Gurefe Y, Misirli E. A multiple extended trial equation method for the fractional Sharma-Tasso-Olver equation. In AIP Conference Proceedings American Institute of Physics.2013; 1558(1): 1927-1930.

[12] Hosseini K, Gholamin P. Feng's first integral method for analytic treatment of two higher dimensional nonlinear partial differential equations. Differential Equations and Dynamical Systems.2015; 23(3): 317-325.

[13] He JH, Wu XH. Exp-function method for nonlinear wave equations, Chaos, Solitons & Fractals. 2006; 30(3):700-708.

[14] Baskonus HM, Askin M. Travelling wave simulations to the modified Zakharov-Kuzentsov model arising in plasma physics. In Litteris et Artibus, Lviv Polytechnic Publishing House. 2016.

[15] Gurefe Y, Misirli E. Exp-function method for solving nonlinear evolution equations with higher order nonlinearity.Computers & Mathematics with Applications.2011; 61(8): 2025-2030.

[16] Misirli E, Gurefe Y. The Exp-function method to

solve the generalized Burgers-Fisher equation. Nonlinear Sci. Lett. A. 2010;1: 323-328.
[17] Misirli E, Gurefe Y. Exact solutions of the Drinfel'd–Sokolov–Wilson equation using the exp-function method. Applied Mathematics and Computation.2010; 216(9): 2623-2627.
[18] Ma WX, Lee JH. A transformed rational function method and exact solutions to the 3+ 1 dimensional Jimbo–Miwa equation. Chaos, Solitons & Fractals.2009; 42(3): 1356-1363.
[19] Zhang Y , Sun S, Dong H. Hybrid solutions of (3+1)-dimensional Jimbo-Miwa equation. Mathematical Problems in Engineering. 2017.
[20] Tang Y, Ma WX, Xu W, Gao L. Wronskian determinant solutions of the (3+1)-dimensional Jimbo–Miwa equation. Applied Mathematics and Computation. 2011; 217(21): 8722-8730.
[21] Ma WX. Lump-type solutions to the (3+1)-dimensional Jimbo-Miwa equation. International Journal of Nonlinear Sciences and Numerical Simulation.2016; 17(7-8): 355-359.
[22] Yue Y, Huang L, Chen Y. Localized waves and interaction solutions to an extended (3+1)-dimensional Jimbo–Miwa equation. Applied Mathematics Letters.2019;89: 70-77.
[23] Zhang X, Chen Y. Rogue wave and a pair of resonance stripe solitons to a reduced (3+1)-dimensional Jimbo–Miwa equation. Communications in Nonlinear Science and Numerical Simulation.2017; 52: 24-31.
[24] Öziş T, Aslan I . Exact and explicit solutions to the (3+ 1)-dimensional Jimbo–Miwa equation via the Exp-function method. Physics Letters A, 2008;372(47): 7011-7015.

Cilt 11, Sayı 1, Sayfa 19-28, 2022 Volume 11, Issue 1, Page 19-28, 2022

Araştırma Makalesi https://doi.org/10.46810/tdfd.909817 Research Article

Türk Doğa ve Fen Dergisi
Turkish Journal of Nature and Science
www.dergipark.gov.tr/tdfd

3 Boyutlu Evrişimsel Sinir Ağı Kullanılarak Hiperspektral Görüntülerin Sınıflandırılması

Hüseyin FIRAT[1*], Davut HANBAY[2]

[1] Dicle Üniversitesi, Teknik Bilimler MYO, Bilgisayar Teknolojileri Bölümü, Diyarbakır, Türkiye
[2] İnönü Üniversitesi, Mühendislik Fakültesi, Bilgisayar Mühendisliği Bölümü, Malatya, Türkiye
Hüseyin FIRAT ORCID No: 0000-0002-1257-8518
Davut HANBAY ORCID No: 0000-0003-2271-7865

**Sorumlu yazar: huseyin.firat@dicle.edu.tr*

(Alınış: 5.04.2021 Kabul: 25.05.2021, Online Yayınlanma: 25.03.2022)

Anahtar Kelimeler
Hiperspektral görüntü sınıflandırma, Derin öğrenme, 2B ESA, 3B ESA

Öz: Hiperspektral görüntü sınıflandırma, uzaktan algılanan görüntülerin analizi için yaygın olarak kullanılmaktadır. Bir hiperspektral görüntü, uygulamalarda büyük potansiyele sahip olan yer nesnelerinin zengin spektral bilgilerini ve uzamsal bilgilerini içermektedir. Spektral uzamsal bilgi kullanımı hiperspektral görüntü sınıflandırmasının performansını önemli ölçüde arttırmaktadır. Hiperspektral görüntüler, 3B küpler biçiminde gösterilmektedir. Bu nedenle, 3B uzamsal filtreleme, bu tür görüntülerdeki spektral uzamsal özellikleri eşzamanlı olarak çıkarmak için doğal olarak basit ve etkili bir yöntem sunmaktadır. Bu çalışmada, hiperspektral görüntü sınıflandırması için bir 3B evrişimli sinir ağı (3B ESA) yöntemi önerilmiştir. Önerilen yöntem, derin spektral uzamsal birleştirilmiş özellikleri etkin bir şekilde çıkarmaktadır. Aynı zamanda herhangi bir ön işleme veya son işleme dayanmadan hiperspektral görüntü küpü verileri toplu olarak görüntülemektedir. Hiperspektral görüntü küpü önce küçük üst üste binen 3B parçalara bölünmektedir. Daha sonra bu parçalar, spektral bilgileri de koruyan birden çok bitişik bant üzerinde bir 3B çekirdek işlevi kullanarak 3B özellik haritaları oluşturmak için işlenmektedir. Önerilen yöntem Indian pines, Pavia üniversitesi ve Botswana veri setleri ile test edilmiştir. Deneysel çalışmalar sonucunda, Indian pines için %99,35, Pavia üniversitesi için %99,90 ve Botswana için ise %99,59 genel doğruluk sonuçları elde edilmiştir. Sonuçlar, 4 farklı derin öğrenme tabanlı yöntemle karşılaştırılmıştır. Deneysel sonuçlardan, önerilen 3B ESA yöntemimizin daha iyi performans gösterdiği görülmektedir.

Classification of Hyperspectral Images Using 3D Convolutional Neural Network

Keywords
Hyperspectral image classification, Deep learning, 2D CNN, 3D CNN

Abstract: Hyperspectral image classification is commonly used for the analysis of remotely sensed images. A hyperspectral image contains rich spectral and spatial information of ground objects that has great potential in applications. The use of spectral spatial information significantly improves the performance of hyperspectral image classification. Hyperspectral images are shown as 3D cubes. Therefore, 3D spatial filtering offers an inherently simple and effective method to simultaneously extract spectral spatial features in such images. In this study, a 3D convolutional neural network (3D CNN) method is proposed for hyperspectral image classification. The proposed method effectively extracts deep spectral spatially combined features. At the same time, the hyperspectral image cube displays data in aggregate without relying on any pre-processing or post-processing. The hyperspectral image cube is first divided into small overlapping 3D patches. Then these patches are processed to create 3D feature maps using a 3D kernel function on multiple adjacent bands that also preserve spectral information. The proposed method was tested with Indian pines, Pavia university and Botswana datasets. As a result of the experimental studies, the overall accuracy results were obtained 99.35% for Indian pines, 99.90% for the University Pavia, and 99.59% for Botswana. The results were compared with 4 different deep learning-based methods. From the experimental results, it is seen that our proposed 3D CNN method performs better.

1. GİRİŞ

Hiperspektral uzak sensörler, elektromanyetik spektrumun yüzlerce sürekli ve dar bant genişliğinde dijital görüntüler yakalayarak hem spektral hem de uzamsal bilgileri içeren 3 boyutlu hiperspektral görüntüler üretmektedir [1]. Hiperspektral görüntülerin zengin spektral bilgileri güçlüdür. Bu nedenle, tarım, astronomi, madencilik, nesne tespiti, askeri gözetim, çevre bilimleri, arazi yangın takibi ve biyolojik tehdit tespiti gibi bir dizi uygulamada yaygın olarak kullanılmaktadır [2, 3]. Hiperspektral görüntülerde, her pikselin sınıflandırılması bu uygulamalarda çok önemli rol oynamaktadır. Bu nedenle, son yıllarda çok sayıda hiperspektral görüntü sınıflandırma yöntemi önerilmiştir. Geleneksel hiperspektral görüntü sınıflandırma yöntemleri genellikle yalnızca spektral bilgilere dayanmaktadır. Bu sınıflandırıcılar arasında k-en yakın komşu [4], lojistik regresyon [5], destek vektör makinesi [6], rastgele orman [7] ve maksimum olabilirlik kriteri [8] temelli sınıflandırıcılar bulunmaktadır. Bu sınıflandırıcılar, spektral fazlalık ve spektral bantlar arasındaki yüksek korelasyon nedeniyle iyi performans gösterememektedir. Ayrıca, bu sınıflandırıcılar hiperspektral görüntülerin önemli uzamsal değişkenliğini korumada başarısız olmaktadır. Bu da düşük performansla sonuçlanmaktadır. Sınıflandırma performansını iyileştirmenin en basit yolu hem spektral hem de uzamsal bilgileri içeren bir sınıflandırıcı tasarlamaktır. Uzamsal bilgi, farklı yapıların şekli ve boyutu ile ilgili ek ayırt edici bilgiler sağlamaktadır. Bu durum uygun şekilde kullanılırsa daha doğru sınıflandırma haritalarına yol açmaktadır. Spektral uzamsal sınıflandırma yöntemleri genel olarak iki kategoriye ayrılabilmektedir. İlki, spektral ve uzamsal özellikleri ayrı ayrı incelemektedir. Başka bir deyişle, uzamsal özellikler, morfolojik işlemler [9], entropi [10], öznitelik profilleri [11] ve düşük dereceli temsil [12] gibi çeşitli uzamsal filtreler aracılığıyla önceden çıkarılmaktadır. Daha sonra bu uzamsal özellikler, piksel düzeyinde sınıflandırmayı gerçekleştirmek için spektral özelliklerle birleştirilmektedir. İkinci kategori, ortak özellikler üretmek için genellikle uzamsal özellikleri spektral özelliklerle birleştirmektedir. Örneğin, farklı ölçek ve frekanslarda üretilen bir dizi 3D dalgacık filtresi [13], 3D Gabor filtresi [14] ve 3D saçılım dalgacık filtreleri [15], ortak spektral-uzamsal özellikleri çıkarmak için hiperspektral görüntülere uygulanmaktadır. Hiperspektral görüntüler 3B küpler halinde gösterildiğinden dolayı, ikinci yaklaşım türü daha iyi performans için gerekli olan ortak uzamsal spektral korelasyonu koruyarak daha iyi sonuçlar üretebilmektedir. Bununla birlikte, geleneksel özellik çıkarma yöntemlerinin çoğu, el yapımı özelliklere ve derin olmayan öğrenme modellerine dayanmaktadır. Bu durum sınırlı özellik çıkarma ile sonuçlanmaktadır.

Derin öğrenme tekniklerindeki ilerleme, hiperspektral görüntü sınıflandırmasını yeni bir aşamaya taşımaktadır. Derin öğrenme yönteminin eğitim aşaması, özellikleri otomatik olarak çıkarmakta ve bunları sınıflandırma aşamasında kullanmaktadır. Destek vektör makinesi ve rastgele orman gibi geleneksel hiperspektral görüntü sınıflandırma yöntemleri, uzamsal özellikleri göz ardı ederken hiperspektral görüntülerin spektral özelliklerini çıkarmaya odaklanmıştır. Tipik bir derin öğrenme modeli olarak, yığınlı otokodlayıcı [16] ve derin inaç ağı [17] hem uzamsal hem de spektral bilgiyi çıkarabilmekte ve daha sonra bunları hiperspektral görüntü sınıflandırması için birleştirebilmektedir. Bununla birlikte, yukarıdaki derin öğrenme yöntemlerinin ikisi de girdi olarak tek boyutlu özellik vektörlerini kullanmaktadır. Bu durumda hiperspektral görüntülerdeki uzamsal özellikler tam olarak kullanılamamaktadır. Hiperspektral görüntü sınıflandırma için en sık kullanılan derin öğrenme yöntemlerinden biri de evrişimsel sinir ağlarıdır. Du, Mao ve ark. [18, 19], hiperspektral görüntü sınıflandırması için evrişimsel sinir ağını kullanmıştır. Bu çalışmalarda, uzamsal özellikler orijinal hiperspektral görüntülerinin ilk birkaç temel bileşen bantlarından yararlanılarak bir 2 boyutlu evrişimsel sinir ağı modeli ile elde edilmiştir. Evrişimsel sinir ağı tabanlı modeller, yığınlı otokodlayıcı ve derin inanç ağı modellerine göre gelişmiş sınıflandırma performansı elde edebildiği gösterilen yerel özellikleri tespit etme yeteneğine sahiptir. Ancak, 2 boyutlu evrişimsel sinir ağında (2B ESA), uzamsal ve spektral özellikler genellikle ayrı ayrı çıkarılmaktadır. Bu işlem spektrumdaki bazı ayrıntıları kaybedecek ve bu yöntemlerin farklı nesneleri ayırt etme kapasitesini azaltacaktır. Aynı zamanda, sınıflandırma için önemli olabilecek ortak uzamsal spektral korelasyon bilgilerinden tam olarak yararlanmayı geçersiz kılacaktır. Yani, 2B ESA, spektral boyutlardan iyi ayırt edici özellik haritalarını çıkaramamaktadır.

Bu çalışmada, hiperspektral görüntü sınıflandırması için 3 boyutlu evrişimsel sinir ağı (3B ESA) modeli önerilmektedir. 3B ESA, 3B hiperspektral görüntüye 3B çekirdek uygulayarak, özellik küplerinin hem uzamsal hem de spektral boyutlarındaki yerel sinyal değişikliklerini öğrenebilmektedir. Bu sayede, sınıflandırma için önemli ayırt edici bilgilerden faydalanılmaktadır. Spektral ve uzamsal özellikler eşzamanlı olarak çıkarıldığından, bu çalışma 3B hiperspektral görüntü verilerinin yapısal özelliklerinden tam olarak yararlanmaktadır. Önerilen 3B ESA yöntemi, girdi olarak tüm spektral bantları almaktadır. Herhangi bir ön işlem veya son işlem gerektirmemektedir. Ortaya çıkan derin sınıflandırıcı modeli, uçtan uca bir şekilde eğitilmektedir. Aynı ölçekte, önerilen 3B ESA diğer derin öğrenme tabanlı yöntemlerden daha az parametre içermektedir. Bu, tipik olarak eğitim örneklerine sınırlı erişimi olan hiperspektral görüntü sınıflandırma problemleri için daha uygundur. 3B ESA tabanlı yöntem ile farklı uzak sensörler tarafından yakalanan üç farklı hiperspektral görüntü veri seti üzerinde deneyler gerçekleştirilmiştir. Deneysel sonuçlar literatürdeki farklı derin öğrenme tabanlı tekniklerle karşılaştırılmıştır. Elde edilen deneysel sonuçlar ile önerilen 3B ESA yönteminin karşılaştırılan yöntemlerden daha iyi performans gösterdiği görülmektedir.

Bu çalışmada önerilen yöntemin teorik alt yapısını oluşturan evrişimsel sinir ağı modeli Bölüm 2'de ve

önerilen yöntem Bölüm 3'te anlatılmıştır. Bölüm 4'te kullanılan veri setleri ve deneysel sonuçlar verilmiştir. Bölüm 5'de ise sonuçlar tartışılmıştır.

2. EVRİŞİMSEL SİNİR AĞI (ESA)

Görüntü sınıflandırması için derin öğrenme teknikleri son zamanlarda yaygın olarak kullanılmaktadır. ESA, evrişim katmanı, havuzlama katmanı ve tamamen bağlı katmandan oluşan çok katmanlı bir sinir ağıdır. Evrişim katmanı, giriş verileri üzerinde evrişim işlemi gerçekleştiren ESA'nın temel parçasıdır. Evrişim, iki matris, yani alıcı alan (receptive field) ve çekirdek (kernel) arasındaki bir iç çarpım işlemidir. Genel olarak, çekirdek uzamsal olarak giriş verilerinden daha küçüktür. Çekirdek alıcı alan üzerinde kaymakta ve giriş verilerinin bir özellik haritasını oluşturmaktadır. Havuzlama katmanı, özellik haritasının uzamsal boyutunu azaltmaktadır. Bir dizi çıktıyı, yakındaki özellik değerlerinin istatistiklerine göre tek bir değerle değiştirmektedir. En yaygın kullanılan havuzlama tekniği maksimum havuzlamadır ve bir dizi özelliği maksimum değeriyle değiştirmektedir. Tamamen bağlı katman, tüm nöronların birbirini takip eden her katman nöronuna bağlandığı çok katmanlı bir algılayıcıdır. Bu katman, özellikleri çıktıya haritalamak için kullanılmaktadır [20]. x girdileri için tek nöronun çıktısı (y) Eşitlik 1.'deki gibi hesaplanmaktadır.

$$y = f(w * x + b) \tag{1}$$

Eşitlik 1.'de, w filtre ağırlığı ve b ise bias değeridir. $f(.)$, ağırlıklı bir girdi toplamına uygulanan doğrusal olmayan aktivasyonu ifade etmektedir. 2B ESA modeli, giriş verilerini etkinleştirmeden önce iki boyutlu bir çekirdek kullanarak evrişim işlemini gerçekleştirmektedir. Bu, giriş görüntüsünden uzamsal özellikleri çıkarmaya yardımcı olmaktadır. Her nöronun 2B evrişim çıktısı için Eşitlik 1. yeniden Eşitlik 2.'deki gibi formüle edilmektedir [20].

$$y_{mn} = f\left(\sum_{r}\sum_{i=0}^{h-1}\sum_{j=0}^{w-1} k_{ij}x_{(i+m)(j+n)} + bias_{mn}\right) \tag{2}$$

Eşitlik 2.'de y_{mn}, (m,n) konumunda çıkarılan özelliktir. k, $h \times w$ boyutundaki 2B evrişim çekirdeğidir. 2B görüntü olması durumunda, bu evrişim işlemi, alıcı alandaki tüm özellik haritalarını (r) üzerinde gerçekleştirilmekte ve doğrusal olmayan aktivasyon için tüm değerlerin toplamını almaktadır. Bu işlem, çok boyutlu veriler durumunda tüm katmanlar için tekrarlanmaktadır. Veriler üç boyutlu olduğunda (örneğin, video, renkli görüntüler, hiperspektral veya multispektral görüntüler), bunların hem uzamsal hem de spektral veya zamansal boyutları vardır. Bu giriş verileri için 2B evrişim başarısız olmaktadır. Çünkü, geleneksel 2B ESA'da, evrişim işlemleri yalnızca uzamsal boyuttaki özellikleri yakalayan 2B özellik haritalarına uygulanmaktadır. 3B ESA, 2B ESA'da 2B evrişim yerine üç boyutlu evrişim gerçekleştiren 2B ESA modellerinin değiştirilmiş şeklidir. Evrişim işlemleri, 3B verilere uygulandığında hem uzamsal hem de spektral boyutlardan özelliklerin yakalanması istenilmektedir. Bu amaçla, 3B giriş verilerinden ortak uzamsal spektral özellikleri hesaplamak için 3B evrişim işlemlerinin 3B özellik küplerine uygulandığı 3B ESA önerilmektedir. 3B evrişim, üç boyutlu spektral görüntülerden hem uzamsal hem de spektral özelliklerin çıkarılmasına yardımcı olmaktadır. 3B ESA modelinden çıkarılan özellik Eşitlik 3.'teki gibi formüle edilmektedir [20].

$$y_{mnp} = f\left(\sum_{r}\sum_{i=0}^{h-1}\sum_{j=0}^{w-1}\sum_{l=0}^{b-1} k_{ijl}x_{(i+m)(j+n)(l+p)} + bias_{mnp}\right) \tag{3}$$

Eşitlik 3.'te y_{mnp} , (m,n,p) konumunda çıkarılan özelliktir. b spektral boyut boyunca 3B çekirdeğin boyutudur. Çekirdek (k), üç boyutludur ve özellikler, 3B giriş verileri üzerinde 3B evrişim gerçekleştirilerek hesaplanmaktadır. Evrişimli sinir ağında en sık kullanılan aktivasyon fonksiyonu $f(.)$ ReLU'dur. ReLU, eğitim için gradyan iniş tekniklerini kullanırken diğer aktivasyon işlevlerinden daha hızlıdır. ReLU Eşitlik 4.'teki gibi formüle edilmektedir.

$$ReLU(y) = \max(0, y) \tag{4}$$

Softmax, sınıflandırma için bir derin öğrenme modelinin son katmanında genellikle kullanılan başka bir etkinleştirme işlevidir. Softmax, tüm örneklerin olasılık dağılımını üretmekte ve toplamı bire eşittir. Eğitim verilerini kullanarak ağırlıkları güncellemek için ESA'da farklı optimizasyon teknikleri kullanılmaktadır. En yaygın kullanılan optimizasyon gradyan iniş tekniğidir. Adam (uyarlanabilir momentum tahmini), genellikle konveks olmayan problemler için kullanılan başka bir optimize edicidir. Adam, birinci ve ikinci gradyan momentine bağlı olarak ağdaki her ağırlık değeri için ayrı bir öğrenme oranı sağlar. Adam optimizer'da kullanılan parametreler öğrenme hızı (lr), beta1 ve beta2'dir. beta1 ve beta2, sırasıyla birinci ve ikinci momentlerin üstel azalmasıdır [21]. Özetle, hiperspektral görüntü sınıflandırması için, 2B evrişim işlemi giriş verilerini uzamsal boyutta evrişim işlemine tabi tutarken, 3B evrişim işlemi giriş verilerini hem uzamsal hem de spektral boyutta eş zamanlı olarak evrişim işlemine tabi tutmaktadır. 2B evrişim işlemi ister 2B veriye ister 3B veriye uygulanıp uygulanmadığına bakılmaksızın, çıktısı 2B'dir. Hiperspektral görüntüye 2B evrişim işlemleri uygulandıysa, önemli spektral bilgiler kaybedilirken, 3B evrişim giriş hiperspektral görüntü verilerinin spektral bilgilerini koruyarak bir çıktı hacmi elde edebilmektedir. Bu, zengin spektral bilgi içeren hiperspektral görüntüler için çok önemlidir.

3. ÖNERİLEN YÖNTEM

Geleneksel bir 2B ESA, genellikle evrişimli katmanlardan, havuz katmanlarından ve tamamen bağlantılı katmanlardan oluşmaktadır. 2B ESA'dan farklı olarak, bu çalışmada, hiperspektral görüntü sınıflandırması için önerilen 3B ESA, yalnızca evrişim

katmanlarından, düzleştirme ve tamamen bağlantılı bir katmandan oluşmaktadır. Hiperspektral görüntülerde uzamsal çözünürlüğü azaltmasıyla bilinen havuzlama işlemleri önerilen yöntemde uygulanmamaktadır. Önerilen 3B ESA modeli piksel düzeyinde hiperspektral görüntü sınıflandırması için kullanılmaktadır. Spektral uzamsal özellikleri öğrenmek için 3B çekirdeklerle evrişim işlemine tabi tutulmak üzere girdi verileri olarak tüm spektral bantlar boyunca küçük bir uzamsal komşulukta (tüm görüntü değil) piksellerden oluşan görüntü küpleri çıkarılmaktadır. Hiperspektral görüntü $\boldsymbol{X}$, $\boldsymbol{M} \times \boldsymbol{N} \times \boldsymbol{D}$ boyutunda 3 boyutlu bir küp olarak belirtilmiştir. Burada $\boldsymbol{M}$ ve $\boldsymbol{N}$, görüntünün uzamsal genişliği ve yüksekliğidir. $\boldsymbol{D}$ ise, spektral bantların sayısını belirtir. Görüntü sınıflandırma tekniklerini kullanmak için, hiperspektral veri küpü, merkezi piksele dayalı gerçek etiketlerin oluşturulduğu küçük üst üste binen 3B uzamsal parçalara bölünmüştür. Uzamsal konumda (a,b) merkezlenmiş ve $\boldsymbol{SxS}$ penceresini veya uzamsal boyutu ve tüm $\boldsymbol{D}$ spektral bantlarını kapsayan hiperspektral veri küpünden 3B komşu parçaları $\boldsymbol{S\,X\,S\,X\,D}$ oluşturuldu. Hiperspektral veri küpünden üretilen toplam 3B parça sayısı $(\boldsymbol{n}), (\boldsymbol{M}-\boldsymbol{S}+\boldsymbol{1})\boldsymbol{x}(\boldsymbol{N}-\boldsymbol{S}+\boldsymbol{1})$ ile bulunur. 3B ESA, 3B evrişim çekirdeğini kullanarak her bir görüntü parçasını 3B evrişim işlemine tabi tutar. Hiperspektral görüntü verileri için önerilen modelde, evrişim katmanının özellik haritaları, giriş katmanındaki çoklu bitişik bantlar üzerinde 3B çekirdek kullanılarak oluşturulur. Böylelikle hem uzamsal hem de spektral özelliklere sahip özellikler çıkarılmış olur. Evrişim işlemi uygulanmış özelliklere doğrusal olmayan bir etkinleştirme işlevi olan ReLU uygulanmaktadır.

Önerilen 3B ESA modelinin akış diyagramı Şekil 1'de gösterilmektedir. Önerilen 3B ESA modelinde üç 3B evrişim katmanı, düzleştirme ve tam bağlantılı bir katman bulunmaktadır. Herhangi bir ön işlem aşaması gerçekleştirilmemektedir. Uygulanan 3B evrişim çekirdeklerinin boyutları ve kullanılan filtreler şu şekildedir. 1. evrişimli katmanda 3x3x7 (yani; iki uzamsal ve bir spektral boyut) boyutunda 16 filtre, 2. evrişim katmanında 3x3x5 boyutunda 32 filtre, 3. evrişim katmanında 3x3x3 boyutunda 64 filtre kullanılmaktadır. ReLU aktivasyon fonksiyonu tüm evrişim katmanlarında kullanılmaktadır. 3B Evrişim katmanlarından sonra çıkarılan özellikler düzleştirilmektedir. Daha sonra sınıflandırma için tam bağlı katmanlara girdi olarak verilmektedir. Bu modelde, 128 nöron bulunan bir tane tam bağlantılı katman kullanılmaktadır. Tam bağlantılı katmanının (FC) çıktısı, gerekli sınıflandırma sonucunu oluşturmak için basit softmax sınıflandırıcıya verilmektedir. Önerilen model için her katmanda kullanılan çıktı boyutu ve parametre sayısı Tablo 1'de gösterilmektedir. Önerilen modelde, 1.yoğun katmanda en fazla sayıda parametrenin mevcut olduğu görülebilmektedir. Son yoğun katmandaki düğüm sayısı, pavia üniversitesi veri setindeki sınıfların sayısı ile aynı olan 9'dur. Dolayısıyla, önerilen modeldeki toplam parametre sayısı, bir veri setindeki sınıfların sayısına bağlıdır. Pavia üniversitesi veriseti için önerilen yöntemdeki toplam eğitilebilir ağırlık parametresi sayısı 875,369'dur. 0,001 öğrenme oranına sahip kategorik çaprazentropi ve optimizasyon için kullanılan 1e-06 bozunma işlevine sahip Adam optimizer kullanılmıştır. Eğitim süreci, herhangi bir toplu normalleştirme (batch normalization) ve veri arttırma (data augmentation) olmaksızın 256 batch size 300 döngü (epochs) boyunca tekrar etmektedir.

Tablo 1. Pavia Üniversitesi veriseti için önerilen 3B ESA modelinin özeti

Katman (Tip)	Çıkış Boyutu	Parametre Sayısı
input_1 (Giriş katmanı)	(5,5,103,1)	0
conv3d_1 (Conv3d)	(5,5,103,16)	1024
conv3d_2 (Conv3d)	(3,3,99,32)	23072
conv3d_3 (Conv3d)	(1,1,97,64)	55360
flatten_1 (Flatten)	6208	0
dense_1 (Dense)	128	794752
dense_2 (Dense)	9	1161
Toplam Eğitilebilir Parametreler : 875,369		

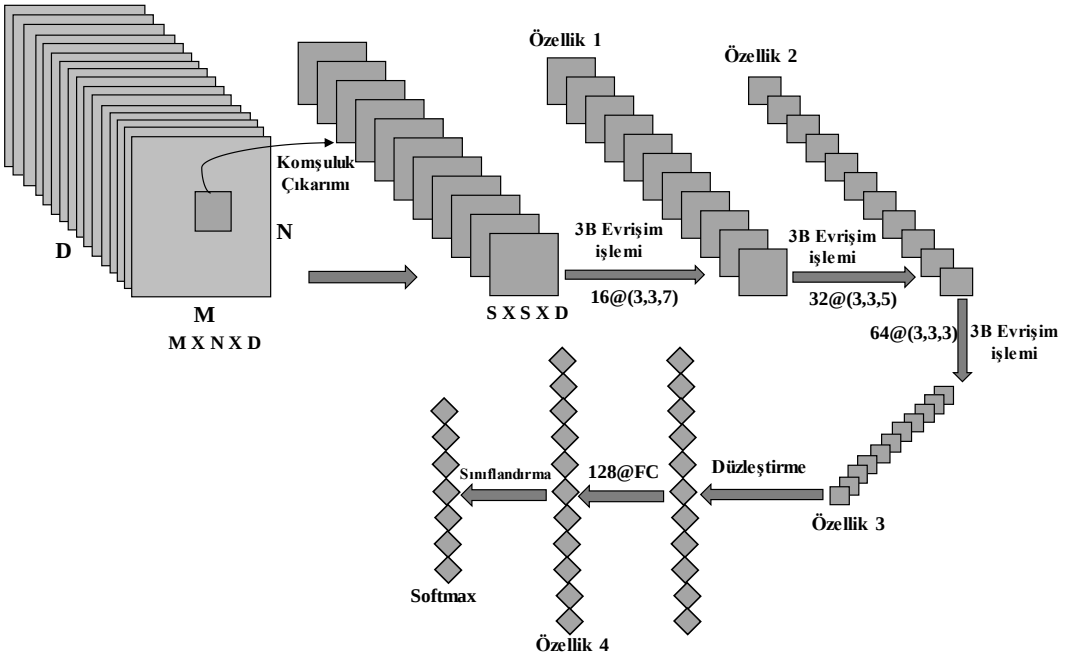

Şekil 1. Hiperspektral görüntü sınıflandırması için önerilen 3B ESA modeli

4. DENEYSEL VERİSETLERİ VE SONUÇLAR

4.1. Verisetleri

Önerilen yöntemin etkinliğini göstermek için Indian Pines (IP), Pavia Üniversitesi (PU) ve Botswana (B) veri setlerini içeren üç gerçek hiperspektral veri seti kullanılmıştır [22]. IP veriseti, Kuzeybatı Indiana'daki Indian Pines test alanında Havadan Görünür / Kızılötesi Görüntüleme Spektrometresi (Airborne Visible/Infrared Imaging Spectrometer-AVIRIS) sensörü tarafından elde edilmiştir. Bu verisetindeki her spektral görüntü 145 × 145 uzamsal boyutundadır. Sensör, 0.4-2.5 mikrometre dalga boyu aralığında toplam 224 spektral bant elde etmiştir. Bu 224 banttan, 24 bant tam su absorpsiyonu (emme) bölgesindedir ve bunlar sınıflandırma işlemi için yararlı değildir. 24 su emme bandı çıkarıldıktan sonra kalan 200 bant deneyler için kullanılmıştır. Şekil 2'de Indian pines verisetinin sahte-renkli görüntüsü ve temel gerçek (ground truth) haritası gösterilmektedir. Tablo 2'de ise IP veri setinin 16 tür arazi örtüsü ve 10249 örnek içerdiği gösterilmektedir.

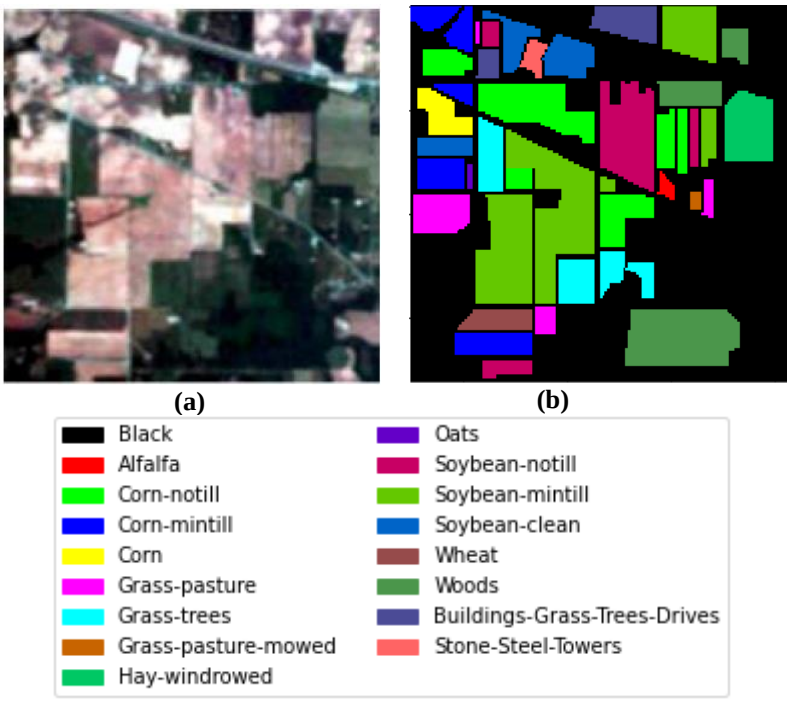

Şekil 2. Indian Pines veriseti. (a) Indian pines verisetinin sahte-renkli görüntüsü (b) Indian pines verisetinin temel gerçek (ground truth) haritası

Tablo 2. Indian pines veri seti için sınıflar ve örnek sayıları

Indian Pines (IP) Veriseti					
No.	**Sınıf**	**Örnek Sayısı**	**No.**	**Sınıf**	**Örnek Sayısı**
1	Alfalfa	46	**9**	Oats	20
2	Corn-notill	1428	**10**	Soybean-notill	972
3	Corn-mintill	830	**11**	Soybean-mintill	2455
4	Corn	237	**12**	Soybean-clean	593
5	Grass-pasture	483	**13**	Wheat	205
6	Grass-trees	730	**14**	Woods	1265
7	Grass-pasture-mowed	28	**15**	Buildings-Grass Trees-Drives	386
8	Hay-windrowed	478	**16**	Stone-Steel-Towers	93

PU veriseti, kuzeydoğu İtalya'daki Pavia Üniversitesi'nden Yansıtıcı Optik Sistem Görüntüleme Spektrometresi (Reflective Optics System Imaging Spectrometer - ROSIS) tarafından toplanan verilerdir. Veriseti, piksel başına 1.3 m uzamsal çözünürlükle 340 piksel genişliğinde ve 610 piksel yüksekliğindedir. 0.43 mikrometre ile 0.86 mikrometre arasında değişen 115 dalga boyuna sahiptir. 12 gürültü bandı çıkarıldıktan sonra, kalan 103 bant deneyde kullanılmıştır. PU veriseti 9 sınıfa ayrılmaktadır. Toplam 42776 örnek içermektedir. Şekil 3'de, PU verisetinin sahte-renkli görüntüsü ve temel gerçek (ground truth) haritası gösterilmektedir. Ayrıca, PU veriseti için sınıflar ve bu sınıfların içerdiği örnek sayıları Tablo 3'te gösterilmektedir.

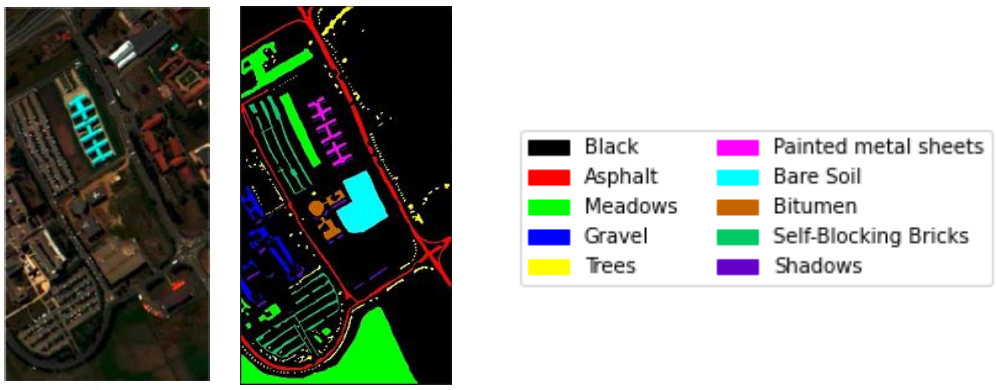

(a) **(b)**

Şekil 3. Pavia üniversitesi veriseti. (a) Pavia üniversitesi verisetinin sahte-renkli görüntüsü (b) Pavia üniversitesi verisetinin temel gerçek (ground truth) haritası

Tablo 3. Pavia üniversitesi veri seti için sınıflar ve örnek sayıları

Pavia Üniversitesi (PU) Veriseti					
No.	**Sınıf**	**Örnek Sayısı**	**No.**	**Sınıf**	**Örnek Sayısı**
1	Asphalt	6631	**6**	Bare Soil	5029
2	Meadows	18649	**7**	Bitumen	1330
3	Gravel	2099	**8**	Self-Blocking Bricks	3682
4	Trees	3064	**9**	Shadows	947
5	Painted Metal Sheets	1345			

B veriseti, 2001 yılında Botswana, Okavango Deltası üzerinde EO-1 üzerinde Hyperion sensörü tarafından toplandı. Elde edilen veriler orijinal olarak 30 m piksel çözünürlüklü 10 nm pencerelerde spektrumun 400–2500 nm bölümünü kapsayan 242 banttan oluşuyordu. Kalibre edilmemiş (Ayarlanmamış) ve su emilimini örten gürültülü bantlar [10-55, 82-97, 102-119, 134-164, 187-220] çıkarıldıktan sonra deneylerde sadece 145 bant kullanıldı. Kullanılan veriler, arazi örtüsü türlerini temsil eden 14 tanımlanmış sınıftan ve gözlemlerle 1476 x 256 pikselden oluşmaktadır. Toplam 3248 örnek içermektedir. Şekil 4'te, B verisetinin sahte-renkli görüntüsü ve temel gerçek (ground truth) haritası gösterilmektedir. B veriseti için sınıflar ve bu sınıfların içerdiği örnek sayıları ise Tablo 4'te gösterilmektedir.

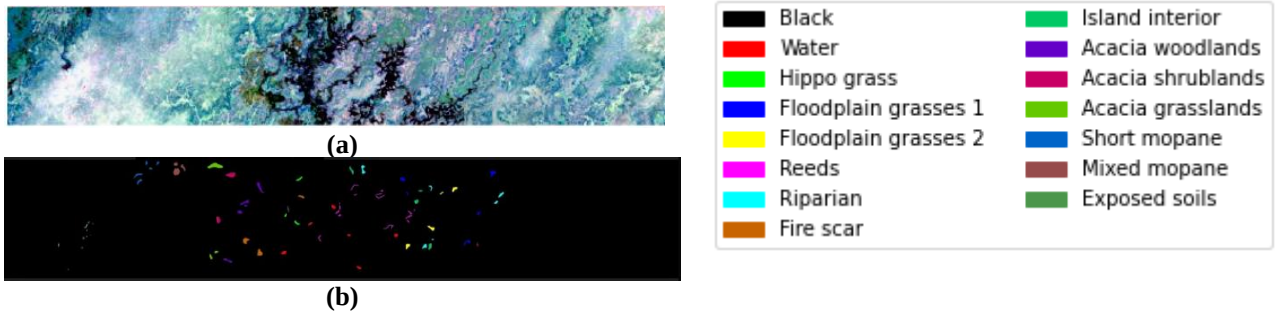

(a)

(b)

Şekil 4. Botswana veriseti. (a) Botswana verisetinin sahte-renkli görüntüsü (b) Botswana verisetinin temel gerçek (ground truth) haritası

Tablo 4. Botswana veri seti için sınıflar ve örnek sayıları

Botswana (B) Veriseti					
No.	**Sınıf**	**Örnek Sayısı**	**No.**	**Sınıf**	**Örnek Sayısı**
1	Water	270	**8**	Island interior	203
2	Hippo grass	101	**9**	Acacia woodlands	314
3	Floodplain grasses 1	251	**10**	Acacia shrublands	248
4	Floodplain grasses 2	215	**11**	Acacia grasslands	305
5	Reeds	269	**12**	Short mopane	181
6	Riparian	269	**13**	Mixed mopane	268
7	Fire scar	259	**14**	Exposed soils	95

4.2. Deneysel Kurulum

Tüm deneyler Google Colab olarak bilinen çevrimiçi bir platformda gerçekleştirilmiştir. Google Colab, herhangi bir ortamı çalıştırmak için iyi bir internet hızı gerektiren çevrimiçi bir platformdur. Google Colab, kodların Tensör İşlem Birimi (TPU), 35 GB Rasgele Erişim Belleği (RAM) ve veri hesaplaması için 107,77 GB depolama alanı içeren python 3 masaüstü bilgisayarda çalıştırılması için bir seçenek sunmaktadır. Tüm deneylerde, test-eğitim seti %30-70 oranına bölünmüştür. 0,001 öğrenme oranına sahip kategorik çaprazentropi ve optimizasyon için kullanılan 1e-06 bozunma işlevine sahip Adam optimizer kullanılmıştır. Eğitim süreci, 256 batch size ve 300 döngü (epochs) boyunca tekrar etmektedir. Softmax'ın kullanıldığı son katman hariç tüm katmanlar için bir aktivasyon işlevi olarak ReLU kullanılmaktadır. Üç verisetinin tümü,

evrişim için 5×5 komşuluk kullanmaktadır. Herhangi bir ön işlem ve son işlem gerektirmemektedir. Tüm spektral bant alınarak işlemler gerçekleştirilmektedir. Her modelin sınıflandırma performansını değerlendirmek için genel doğruluk (GD), ortalama doğruluk (OD) ve kappa istatistiği (K) kullanılmıştır. GD, test verilerindeki doğru sınıflandırılmış örnekler ile toplam test örneği sayısı arasındaki oranla hesaplanmıştır. OD her kategorinin doğruluğunun ortalama değeridir. K, temel gerçek (ground truth) haritası ile sınıflandırma haritası arasında güçlü bir anlaşma ile ilgili karşılıklı bilgi sağlayan bir istatistiksel ölçüm metriğidir. GD, OD ve K ölçümlerinin yanı sıra, f1 skoru (f1-score), hassasiyet (precision) ve geri çağırma (recall) gibi çeşitli istatistiksel testler de dikkate alınmaktadır.

4.3. Deneysel Sonuçlar

Önerilen 3B ESA yönteminin etkinliğini değerlendirmek için, dört derin öğrenme hiperspektral görüntü sınıflandırma yöntemiyle karşılaştırıldı: 3B ESA [1], DBN-LR [17], 2B ESA [19] ve SAE-LR [23]. 3B ESA, 2 tane 3B evrişim katmanı, tam bağlantılı katman ve sınıflandırma katmanından oluşmaktadır. 3B evrişim katmanlarının boyutları pavia üniversitesi için 2 adet 3x3x7 ve 4 adet 3x3x3 olarak alınmıştır. Pencere boyutu S=5 olarak ayarlanmıştır. Yani, orijinal spektral-uzamsal özellikleri hesaplamak için 5 × 5 × 103 küplerini çıkarılmıştır. Daha sonra bu küpler 3B ESA için girdi olarak kullanılmıştır. Botswana veri seti için, 2 adet 3x3x2 ardından 4 adet 3x3x2 evrişim katmanı kullanılmıştır. Indiana pines veri seti için 2 adet 3x3x7 ve 4 adet 3x3x3 evrişim katmanı kulllanılmıştır. SAE-LR, hiperspektral görüntülerin sınıflandırılması için yığınlı otokodlayıcı ile lojistik regresyonun birlikte kullanılmasını öneren yöntemdir.DBN-LR ise, derin inanç ağları ile lojistik regresyonun birlikte kullanılmasını öneren yöntemdir. SAE-LR ve DBN-LR için, orijinal hiperspektral görüntü, sırasıyla temel bileşen analizi yöntemiyle spektral boyut boyunca dört banda ve beş banda indirgenmiştir. Ardından, uzamsal özellikleri oluşturmak için 5 × 5 × 4 küp ve 5 × 5 × 5 küp kullanılmıştır. Son olarak, ortaya çıkan uzamsal özellikler spektral özellikler ile birleştirilmiştir. 2B ESA için, hiperspektral görüntü, temel bileşen analizi ile spektral boyut boyunca üç banda indirgenmiştir. Orijinal özellikleri oluşturmak için 42 × 42 × 3 küp çıkarılmıştır. Ağ, üç evrişim katmanı ve iki havuzlama katmanı içermektedir. Üç evrişim katmanı sırasıyla birinci, ikinci ve üçüncü katmanlar için 36 adet 5 × 5 çekirdek, 72 adet 6 × 6 çekirdek ve 72 adet 4 × 4 çekirdek içermektedir.

Tablo 5, Pavia üniversitesi verisetinden elde edilen farklı yöntemlerin GD, OD ve K olmak üzere üç değerlendirme göstergesine göre sınıflandırma sonuçlarını vermektedir. Önerilen yöntem ile tüm sınıflarda da en iyi sınıflandırma sonucu elde edilmiştir. Önerilen 3B ESA modeli %99,90 ile iki 3B evrişim katmanından oluşan 3B ESA modelinden %0,51, 2B ESA modelinden %0,87, DBN-LR modelinden %0,91 ve SAE-LR modelinden %1,44 daha iyi genel doğruluk sonucu elde etmektedir. Benzer şekilde önerilen model %99,78 ile sırasıyla, 3B ESA modelinden %0,93, 2B ESA modelinden %1,59, DBN-LR modelinden %1,4 ve SAE-LR modelinden %2,11 daha iyi ortalama doğruluk sonucu elde etmiştir. Kappa istatistiği değerlendirme ölçütünde ise yine önerilen yöntem %99,86 ile diğer tüm yöntemlerden en iyi sonucu elde ettiği görülmektedir. Tablo 5 göz önünde bulundurulduğunda, önerilen yöntemin sınıflandırma sonuçları temel gerçeğe (ground truth) çok benzerdir.

Tablo 5. PU verisetinde farklı yöntemlerle elde edilen sınıflandırma sonuçları

Sınıf	SAE-LR	DBN-LR	2B ESA	3B ESA	Önerilen 3B ESA
1	98,73	99,05	99,68	99,65	**99,90**
2	99,55	99,83	99,87	99,83	**99,96**
3	93,87	95,15	96,31	94,65	**99,36**
4	98,63	98,83	98,01	99,09	**99,89**
5	100	99,93	100	100	**100**
6	97,87	98,71	97,61	99,93	**100**
7	93,74	96,36	95,63	97,75	**99,25**
8	96,76	98,20	99,35	99,24	**100**
9	99,90	99,71	97,25	99,55	**99,65**
GD	98,46	98,99	99,03	99,39	**99,90**
OD	97,67	98,38	98,19	98,85	**99,78**
K	97,98	98,68	98,71	99,20	**99,86**

Tablo 6, Botswana verisetinden elde edilen çeşitli yöntemlerin GD, OD ve K olmak üzere üç değerlendirme göstergesine göre sınıflandırma sonuçlarını vermektedir. Tablo 6'dan, önerilen yöntemin 6 nolu sınıf için sınıflandırma doğruluğu 3B ESA yönteminden %1,19 daha düşük çıkmıştır. 8 nolu sınıf için sınıflandırma doğruluğu 3B ESA, 2B ESA ve SAE-LR yöntemlerinden %1,64 ve DBN-LR yönteminden ise %1,38 düşük çıkmıştır. 10 nolu sınıf için sınıflandırma doğruluğu DBN-LR ve 2B ESA yöntemlerinden %1,35, 3B ESA yönteminden %1,05 ve SAE-LR yönteminden %1,09 daha düşük çıkmıştır. Geri kalan diğer sınıfların tamamında önerilen yöntem ile başarılı sınıflandırma sonuçları elde edilmiştir. GD, OD ve K değerlendirme ölçütleri göz önüne alındığında önerilen yöntem ile diğer yöntemlerin tamamından yüksek sonuçlar elde edilmiştir. Önerilen yöntemin %99,59 GD sonucu, SAE-LR, DBN-LR, 2B ESA ve 3B ESA'dan sırasıyla, %1,1, %0,78, %0,71 ve %0,04 daha yüksek olduğu görülmektedir. Önerilen yöntem ayrıca, OD ve Kappa istatistiği açısından açısından sırasıyla, %99,61 ve %99,55 ile diğer yöntemlerin tamamından daha iyi performans gösterdiği görülmektedir. Tablo 6'dan, önerilen yöntemin sınıflandırma sonuçları temel gerçeğe (ground truth) çok benzer olduğu görülmektedir.

Tablo 6. B verisetinde farklı yöntemlerle elde edilen sınıflandırma sonuçları

Sınıf	SAE-LR	DBN-LR	2B ESA	3B ESA	Önerilen 3B ESA
1	**100**	**100**	99,18	99,64	**100**
2	**100**	**100**	**100**	**100**	**100**
3	**100**	**100**	**100**	**100**	**100**
4	99,58	**100**	99,16	99,45	**100**
5	94,70	94,84	99,54	98,60	**100**
6	92,96	95,33	97,36	**98,72**	97,53
7	99,88	**100**	**100**	99,68	**100**
8	**100**	99,74	**100**	**100**	98,36
9	96,68	96,98	94,99	99,67	**100**
10	99,74	**100**	**100**	99,70	98,65
11	99,47	99,67	100	99,87	**100**
12	100	100	96,63	99,63	**100**
13	99,52	99,82	100	99,43	**100**
14	99,26	100	97,44	100	**100**
GD	98,49	98,81	98,88	99,55	**99,59**
OD	98,70	99,03	98,88	99,60	**99,61**
K	98,36	98,72	98,78	99,51	**99,55**

Tablo 7, Indian pines verisetinden elde edilen çeşitli yöntemlerin GD, OD ve K olmak üzere üç değerlendirme göstergesine göre sınıflandırma sonuçlarını vermektedir. Tablo 7'den, önerilen yöntemin 12 nolu sınıf için sınıflandırma doğruluğu 3B ESA yönteminden %0,12 ve 14 nolu sınıf için sınıflandırma doğruluğu 3B ESA yönteminden %0,08, DBN-LR yönteminden daha % 0,27 daha düşük çıkmıştır. 12 ve 14 nolu sınıflar için sınıflandırma doğruluğu önerilen yöntemde düşük çıkmasına rağmen, GD, OD ve K değerlendirme ölçütleri göz önüne alındığında diğer yöntemlerin tamamından yüksek sonuçlar elde edilmiştir. Önerilen yöntemin %99,35 olan GD sonucu SAE-LR, DBN-LR, 2B ESA ve 3B ESA yöntemlerinden sırasıyla, %5,37, %3,44, %3,38 ve %0,28 daha yüksek olduğu görülmektedir. Önerilen yöntem ayrıca, OD ve Kappa istatistiği açısından açısından sırasıyla, %99,61 ve %99,21 ile diğer yöntemlerin tamamından daha iyi performans gösterdiği görülmektedir. Tablo 7 göz önünde bulundurulduğunda, önerilen yöntemin sınıflandırma sonuçları 9 sınıf için temel gerçek (ground truth) ile aynı geri kalan 7 sınıf için ise temel gerçeğe yakın sonuçlar elde edildiği görülmektedir.

Tablo 7. IP verisetinde farklı yöntemlerle elde edilen sınıflandırma sonuçları

Sınıf	SAE-LR	DBN-LR	2B ESA	3B ESA	Önerilen 3B ESA
1	85,56	80,90	86,11	95,89	**100**
2	90,72	93,97	91,37	98,46	**98,59**
3	91,58	95,13	95,37	98,99	**99,19**
4	89,81	85,14	98,54	99,14	**100**
5	96,16	98,05	91,40	99,29	**99,31**
6	98,98	100	98,05	99,92	**100**
7	95,29	94,92	97,73	100	**100**
8	98,75	100	98,44	100	**100**
9	100	100	50,87	92,31	**100**
10	94,52	97,37	93,53	98,12	**98,63**
11	94,79	97,70	97,62	98,96	**99,45**
12	86,43	84,72	94,89	**98,99**	98,87
13	99,80	99,35	100	99,82	**100**
14	97,48	**100**	99,29	99,81	99,73
15	84,35	84,64	99,59	99,56	**100**
16	96,76	95,33	98,88	99,38	**100**
GD	93,98	95,91	95,97	99,07	**99,35**
OD	93,81	94,20	93,23	98,66	**99,61**
K	93,13	95,34	95,40	98,93	**99,21**

Yukarıda sunulan deneysel sonuçlara göre, ilk olarak, ESA tabanlı yöntemler, SAE ve DBN tabanlı yöntemlerden daha iyi sınıflandırma sonuçları elde etmektedir. SAE-LR ve DBN-LR, derin öğrenme mimarisinin kullanımıyla derin özellikler çıkarabilse de, SAE ve DBN'nin girdi gereksinimini karşılamak için görüntü parçalarının tek boyuta düzleştirilmesi gerekmektedir. Düzleştirme işlemi, orijinal hiperspektral görüntüde bulunan uzamsal bilgiden yararlanmada başarısız olmaktadır. Bu durum da biraz daha kötü bir performansa yol açabilmektedir. Daha da önemlisi, SAE ve DBN, özellikleri denetimsiz bir şekilde öğrenmekte ve etiket bilgilerinden tam olarak yararlanamamaktadır. İkinci olarak, 3B ESA, 2B ESA'ya kıyasla spektral-uzamsal özellik öğrenimi için daha iyi çalışmaktadır. 3B ESA, 3B evrişim işlemleri ile daha ince spektral bilgileri modelleyebilmektedir. Ayrıca 3B hiperspektral görüntü üzerine 3B çekirdek uygulayarak, bir 3B ESA herhangi bir ön işleme dayanmazken, yöntemin uygulanması kolaydır. SAE-LR, DBN-LR ve 2B ESA'da ise spektral boyutluluğu kabul edilebilir bir düzeye indirmek için temel bileşen analizinin kullanılması gereklidir. Son olarak, SAE-LR, DBN-LR, 2B ESA ve 2 evrişim katmanına sahip 3B ESA ile karşılaştırıldığında, önerilen 3B ESA modeli üç veri kümesinin hepsinde daha iyi bir performans elde etti. Özellikle tüm verisetlerinde de, önerilen 3B ESA ile iki evrişim katmanından oluşan 3B ESA, 2B ESA'dan daha iyi genel doğruluk oranlarıyla en iyi sonuçları elde etti. Bu, 3B yaklaşımın geleneksel 2B evrişimlere kıyasla performansta bir artış sağlamaya

yardımcı olduğunu göstermektedir. Hiperspektral görüntü verilerindeki ortak spektral ve uzamsal bilgilerin 3B evrişim işlemleri yoluyla uygun modellenmesi, sınıflandırma işleminde ayırt edici özelliklerin yakalanması için önemlidir.

5. SONUÇ

Hiperspektral görüntü sınıflandırması için uygun bir derin öğrenme modelinin tasarımı büyük bir zorluktur. Uzamsal ve spektral özelliklerin birleşik kullanımı, sınıflandırma performansını arttırmaktadır. Bu çalışmada, hiperspektral görüntü sınıflandırmasını iyileştirmek amacıyla, hiperspektral görüntü verilerinde bulunan hem spektral hem de uzamsal bilgilerden tam olarak yararlanan yeni bir 3B ESA hiperspektral görüntü sınıflandırma modeli önerilmiştir. 3B ESA modelinin, sınıflandırma için hiperspektral görüntünün 3B yapısına uyacak şekilde uyarlanabileceği gösterilmiştir. Özellikle, önerilen 3B ESA modeli üç hiperspektral görüntü veri setinde, derin öğrenmeye dayalı dört hiperspektral görüntü sınıflandırma yöntemiyle karşılaştırılmıştır. Deneysel çalışmalar sonucunda sırasıyla genel doğruluk, ortalama doğruluk ve Kappa değerleri, Indian pines için %99,35, %99,61 ve %99,21, Pavia üniversitesi için %99,90, %99,78 ve %99,86 ve Botswana için ise %99,59, %99,61 ve %99,55 olarak elde edilmiştir. Sonuçlar, 4 farklı derin öğrenme tabanlı yöntemle karşılaştırılmıştır. Deneysel çalışmalar, önerilen 3B ESA tabanlı hiperspektral görüntü sınıflandırma yönteminin üç veri setinin tümünde en iyi genel doğruluğu, ortalama doğruluğu ve kappa değerini elde ettiğini göstermektedir.

KAYNAKLAR

[1] Li Y, Zhang H, Shen Q. Spectral-spatial classification of hyperspectral imagery with 3D convolutional neural network. Remote Sens. 2017;9(1). https://doi: 10.3390/rs9010067.

[2] Sun H, Ren J, Zhao H, Yan Y, Zabalza J, Marshall S. Superpixel based feature specific sparse representation for spectral-spatial classification of hyperspectral images. Remote Sens. 2019;11(5). https://doi: 10.3390/rs11050536.

[3] Dou P, Zeng C. Hyperspectral image classification using feature relations map learning. Remote Sens. 2020;12(18). https://doi: 10.3390/RS12182956.

[4] Ahmad M. Spatial prior fuzziness pool-based interactive classification of hyperspectral images. Remote Sens. 2019;11(9):1–19. https://doi: 10.3390/rs11091136.

[5] Ahmad M, Khan MA, Mazzara M, Distefano S, Ali M, Sarfraz MS. A Fast and Compact 3-D CNN for Hyperspectral Image Classification. IEEE Geosci. Remote Sens. Lett. 2020:1–5. https://doi: 10.1109/LGRS.2020.3043710.

[6] Wang Y, Yu W, Fang Z. Multiple Kernel-based SVM classification of hyperspectral images by combining spectral, spatial, and semantic information. Remote Sens. 2020;12(1). https://doi: 10.3390/RS12010120.

[7] Ham JS, Chen Y, Crawford MM, Ghosh J. Investigation of the random forest framework for classification of hyperspectral data. IEEE Trans. Geosci. Remote Sens. 2005;43(3):492–501. https://doi: 10.1109/TGRS.2004.842481.

[8] Alcolea A, Paoletti ME, Haut JM, Resano J, Plaza A. Inference in supervised spectral classifiers for on-board hyperspectral imaging: An overview. Remote Sens. 2020;12(3):1–29. https://doi: 10.3390/rs12030534.

[9] Ghamisi P, Dalla Mura M, Benediktsson JA. A survey on spectral-spatial classification techniques based on attribute profiles. IEEE Trans. Geosci. Remote Sens. 2015;53(5):2335–53. https://doi: 10.1109/TGRS.2014.2358934.

[10] Tuia D, Volpi M, Mura MD, Rakotomamonjy A, Flamary R. Automatic feature learning for spatio-spectral image classification with sparse SVM. IEEE Trans. Geosci. Remote Sens. 2014;52(10):6062–74. https://doi: 10.1109/TGRS.2013.2294724.

[11] Dalla Mura M, Villa A, Benediktsson JA, Chanussot J, Bruzzone L. Classification of hyperspectral images by using extended morphological attribute profiles and independent component analysis. IEEE Geosci. Remote Sens. Lett. 2011;8(3):542–46. https://doi: 10.1109/LGRS.2010.2091253.

[12] Jia S, Zhang X, Li Q. Spectral–spatial hyperspectral image classification using regularized low-rank representation and sparse representation-based graph cuts. IEEE J. Sel. Top. Appl. Earth Obs. Remote Sens. 2015;8(6):2473–84.

[13] Qian Y, Ye M, Zhou J. Hyperspectral image classification based on structured sparse logistic regression and three-dimensional wavelet texture features. IEEE Trans. Geosci. Remote Sens. 2013;51(4):2276–91. https://doi: 10.1109/TGRS.2012.2209657.

[14] Hanbay K. Hyperspectral image classification using convolutional neural network and two-dimensional complex Gabor transform. J. Fac. Eng. Archit. Gazi Univ. 2020;35(1): 443–56. https://doi: 10.17341/gazimmfd.479086.

[15] Tang YY, Lu Y, Yuan H. Hyperspectral image classification based on three-dimensional scattering wavelet transform. IEEE Trans. Geosci. Remote Sens. 2015;53(5):2467–80. https://doi: 10.1109/TGRS.2014.2360672.

[16] Zhang L, Kumar V. Deep learning for Remote Sensing Data. IEEE Geosci. Remote Sens. Mag. 2016;4(2):22–40.

[17] Chen Y, Zhao X, Jia X. Spectral-Spatial Classification of Hyperspectral Data Based on Deep Belief Network. IEEE J. Sel. Top. Appl. Earth Obs. Remote Sens. 2015;8(6): 2381–92. https://doi: 10.1109/JSTARS.2015.2388577.

[18] Zhao W, Du S. Spectral-Spatial Feature Extraction for Hyperspectral Image Classification: A Dimension Reduction and Deep Learning Approach. IEEE Trans. Geosci. Remote Sens. 2016;54(8):4544–54. https://doi: 10.1109/TGRS.2016.2543748.

[19] Yue J, Zhao W, Mao S, Liu H. Spectral-spatial

classification of hyperspectral images using deep convolutional neural networks. Remote Sens. Lett. 2015;6(6):468–77. https://doi: 10.1080/2150704X.2015.1047045.

[20] Mohan A, Venkatesan M. HybridCNN based hyperspectral image classification using multiscale spatiospectral features. Infrared Phys. Technol. 2020;108:103326 https://doi: 10.1016/j.infrared.2020.103326.

[21] Kingma DP, Ba JL. Adam: A method for stochastic optimization. 3rd International Conference for Learning Representations, ICLR 2015. San Diego: May; 2015. p. 1–15.

[22] Grana M, Veganzons MA, Ayerdi B. Hyperspectral Remote Sensing Scenes [Internet]. (Erişim tarihi: 17.03.2021). Available from: https://www.ehu.eus/ccwintco/index.php/Hyperspectral_Remote_Sensing_Scenes .

[23] Data H. Deep Learning-Based Classification of Hyperspectral Data. IEEE J. Sel. Top. Appl. Earth Obs. Remote Sens. 2014;7(6):2094–107.

Araştırma Makalesi https://doi.org/10.46810/tdfd.929840 Research Article

Türk Doğa ve Fen Dergisi
Turkish Journal of Nature and Science
www.dergipark.gov.tr/tdfd

Bazı İlaçların Koyun Dalak Dokusundan Saflaştırılan Glukoz-6-Fosfat Dehidrogenaz Enzimi Üzerine *İn Vitro* Etkileri

Çiğdem ÇOBAN[1], Mehmet ÇİFTCİ[2*]

[1] Bingöl Üniversitesi, Solhan Sağlık Hizmetleri Meslek Yüksek Okulu, Bingöl/Türkiye
[2*]Bingöl Üniversitesi, Veteriner Fakültesi, Bingöl/Turkiye
Çiğdem ÇOBAN ORCID No**:** 0000-0003-1141-544X
Mehmet ÇİFTCİ ORCID No: 0000-0002-1748-3729

** Sorumlu yazar: mciftci@bingol.edu.tr*

(Alınış: 29.04.2021, Kabul: 13.07.2021, Online Yayınlanma: 25.03.2022)

Anahtar Kelimeler
Glukoz 6-fosfat dehidrogenaz,
Saflaştırma,
İlaç,
İnhibisyon,
İveral,
Gentamisin

Öz: Bu çalışmada bazı ilaçların, koyun dalak dokusundan saflaştırılan glukoz-6-fosfat dehidrogenaz enzimi (G6PD; E.C. 1.1.1.49) üzerine *in vitro* etkileri araştırıldı. Çalışmanın ilk aşamasında G6PD enzimi koyun dalak dokusundan *salting out* (amonyum sülfat çöktürmesi) metodu ve 2', 5' ADP-Sepharose 4B afinite kromatografisi ile saflaştırıldı ve enzimin saflık derecesi SDS-PAGE metodu ile kontrol edildi. Çalışmanın ikinci aşamasında iveral, linkomisin, gentamisin, amoksisilin, ampisilin, streptomisin sülfat, novamizol, ketojezik, sefuroksim, sefazolin sodyum ve tylosin ilaçlarının enzim aktivitesi üzerindeki etkileri araştırıldı. Araştırma sonuçları; iveral, gentamisin, streptomisin sülfat ve linkomisin ilaçlarının G6PD enzimini sırasıyla 0,62 mM, 21,6 mM, 173,2 mM ve 231 mM, IC_{50} değerleri ile inhibe ettiğini, amoksisilin, ampisilin, novamizol, ketojezik, sefuroksim sodyum, sefazolin sodyum ve tylosin ilaçlarının ise enzim üzerinde önemli bir aktivasyon ya da inhibisyon etkisine sahip olmadıklarını gösterdi.

In Vitro Effects of Some Drugs on Glucose-6-Phosphate Dehydrogenase Enzyme Purified from Sheep Spleen Tissue

Keywords
Glucose 6-phosphate dehydrogenase,
Purification,
Drug,
Inhibition,
Iveral,
Gentamicin

Abstract: In this study, *in vitro* effects of some drugs on glucose-6-phosphate dehydrogenase enzyme (G6PD; E.C. 1.1.1.49) purified from sheep spleen tissue were investigated. In the first step of the study, G6PD enzyme was purified from sheep spleen tissue by *salting out* (ammonium sulfate precipitation) method and 2', 5' ADP-Sepharose 4B gel affinity chromatography and the purity of the enzyme was checked by SDS-PAGE method. In the second phase of the study, the effects of iveral, lincomycin, gentamicin, amoxicillin, ampicillin, streptomycin sulfate, novamizole, ketogesic, cefuroxime, cefazolin sodium and tylosin drugs on enzyme activity were investigated. Research results showed that iveral, gentamicin, streptomycin sulfate and lincomycin drugs inhibit the G6PD enzyme with IC_{50} values of 0.62 mM, 21.6 mM, 173.2 mM and 231 mM, respectively, amoxicillin, ampicillin, novamizole, ketogenic, cefuroxime sodium, cefazolin sodium and tylosin drugs did not have a significant activation or inhibition effect on the enzyme.

1. GİRİŞ

Glukoz-6-fosfat dehidrogenaz enzimi (G6PD; E.C. 1.1.1.49) pentoz fosfat yolunun birinci reaksiyonunu katalizleyerek $NADP^+$ varlığında NADPH üretimi ile birlikte, glukoz 6-fosfatın, 6-fosfoglukono laktona dönüşümünü gerçekleştiren kilit noktada bulunan bir enzimdir [1-3]. Reaksiyon ürünlerinden D-ribuloz 5-fosfat, ATP, CoA, NAD^+, FAD, RNA ve DNA gibi hayati öneme sahip biyomoleküllerin bileşeni olan riboz 5-fosfata izomerize olur. Reaksiyon sırasında oluşan NADPH ise yağ asitleri, steroidler ve bazı amino asitlerin sentezinde kullanılan önemli bir koenzimdir [4-6]. Glutatyon ve tiyoredoksin sistemleri hücre içi iki ana antioksidan sistemidir. Bir tripeptid olan glutatyonun yapısında bulunan sülfhidril grubu (-SH), hücreleri okside moleküllerin zararlı etkilerine karşı korur. Ayrıca, DNA ve protein sentezine, ksenobiyotiklerin detoksifikasyonuna, amino asit taşınmasına ve enzimatik reaksiyonlara katılır [7-9]. Tiyoredoksin sistemi, DNA sentezinde, hücresel büyümede, oksidatif stresin neden olduğu hücresel hasarın önlenmesinde, apoptozda, peroksitlerin olumsuz etkilerinden hücrelerin korunmasında ve transkripsiyon faktör aktivitesinin uyarılmasında önemli bir role sahiptir [10-12]. Hem glutatyonun hem de tiyoredoksinin indirgenmesinde NADPH koenzim olarak görev yapar. Bu nedenle NADPH üretimine sebebiyet veren G6PD enzimi aynı zamanda indirekt antioksidan enzim olarak da bilinir [2, 13].

Günümüzde insan ve hayvan tedavisinde birçok antibiyotik ve ilacın kullanıldığı bilinmektedir [14-16]. Kullanılan ilaçların birçoğunun hedefi metabolizmada önemli görevleri olan düzenleyici enzimlerdir. Metabolizmada kavşak noktalarda yer alan düzenleyici enzimlerin aktivitesinde meydana gelen bir inhibisyon bazı durumlarda bir patojenin ölümünü ya da metabolik bir bozukluğun düzeltilmesini sağlayabilir. İnhibitörler enzimlere dönüşümlü ya da dönüşümsüz olarak bağlanırlar. Bir inhibitörün bağlanması, bir substratın enzimin aktif bölgesine bağlanmasını durdurabilir veya enzimin reaksiyonunu katalize etmesini engelleyebilir. Hastalıkların tedavisinde kullanılan birçok ilaç molekülü enzim inhibitörleridir, bu nedenle keşifleri ve iyileştirmeleri biyokimya ve farmakolojide aktif bir araştırma alanıdır [17,18].

Ancak kullanılan bu kimyasal maddelerin organizmada bulunan enzimler üzerinde olabilecek muhtemel etkilerinin çoğu henüz çalışılamamıştır. Bugüne kadar G6PD enziminin birçok canlı dokusundan saflaştırıldığı, kinetik özelliklerinin belirlendiği ve birçok ilaç ve kimyasal maddenin enzim üzerine etkilerinin tespit edildiği bilinmektedir [2,19-23]. Ancak literatür kaynaklarından araştırdığımız kadarı ile şu ana kadar koyun dalak G6PD enzimi ile ilgili herhangi bir saflaştırma ve kinetik çalışma yapılmamıştır.

Bu çalışmada G6PD enziminin koyun dalak dokusundan saflaştırılması ve bazı ilaçların enzim aktivitesi üzerine etkilerinin araştırılması amaçlanmıştır.

2. MATERYAL VE METOT

2.1. Materyal

Bu çalışmada kullanılan ilaçlar piyasadan, G6P, $NADP^+$, Tris, elektroforez kimyasalları, protein standartları, amonyum sülfat, 2', 5' ADP-Sepharose 4B afinite jeli ve diğer kimyasallar Sigma–Aldrich Co. (St. Louis, MO) ve Merck (Darmstadt, Germany) den temin edildi.

2.2. Homojenatın Hazırlanması

Çalışmamızda kullanılan koyun dalak dokusu Bingöl ili Kombine Et ve Süt Kurumundan soğuk zincir kurallarına göre temin edildi. Alınan 15 gram dalak dokusu küçük parçalara ayrılarak 45 mL, 1 M Tris-HCI (pH= 8,0) tamponu içerisinde süspanse edildi. Elde edilen süspansiyon 10.000xg de 1 saat santrifüj edildikten sonra çökelti atılarak homojenat oluşturuldu [24].

2.3. Amonyum Sülfat Çöktürmesi ve Diyaliz

Koyun dalak dokusundan elde edilen homojenat için %0-%90 doygunluk konsantrasyonlarında amonyum sülfat çöktürmesi yapıldı ve G6PD enzimi için en uygun çöktürme aralığı % 40-60 olarak tespit edildi. Enzim bu doygunlukta amonyum sülfat tuzu ile salting out metoduna göre çöktürüldü. Elde edilen süspansiyon 10.000xg'de 15 dakika santrifüj edilerek süpernatant kısmı uzaklaştırıldı. Geriye kalan çökelek 1 M Tris-HCI tamponunda (pH= 8,0) çözüldü ve enzim için aktivite kontrolü yapıldı. Daha sonra enzim çözeltisi diyaliz torbalarına konarak 2 saat 50 mM K-asetat / 50 mM K-fosfat (pH= 7,0) tamponuna karşı diyaliz edildi [25].

2.4. Afinite Kolonunun Hazırlanması ve Koyun dalak G6PD Enziminin Saflaştırılması

Amonyum sülfat çöktürme ve diyaliz sonrası elde edilen enzim numunesi 2', 5' ADP Sepharose-4B afinite kromatografisi kullanılarak saflaştırıldı. Öncelikle 2', 5' ADP Sepharose-4B afinite kolonu hazırlandı. 10 mL'lik yatak hacmi için 2 g kuru 2', 5'-ADP sepharose 4B jeli tartılarak, 400 mL destile su ile katı maddelerin uzaklaştırılması için birkaç defa yıkandı. Yıkama esnasında jel şişirilmiş oldu. Şişirilmiş jelin havası su trompu kullanılarak vakum ile alındıktan sonra, dengeleme tamponu (0,1M KH_2PO_4 + 0.1M K-asetat pH= 6,0) ilave edilerek jel süspanse edildi. Süspanse edilmiş jel, 1x10 cm'lik kapalı sistemden oluşan soğutmalı kolona paketlendi. Jel çöktükten sonra peristaltik pompa yardımıyla yıkama ve dengeleme tamponu ile yıkandı. Kolonun dengelenmiş olduğu elüat ile tamponun 280 nm'de absorbanslarının ve pH'larının yaklaşık olarak eşitlenmesinden anlaşıldı. Böylece afinite kolonu hazırlanmış oldu. Daha önce hazırlanmış olan enzim numunesi hazırlanan 2', 5'- ADP- sepharose 4B afinite kolonuna tatbik edildi. Afinite kolonu sırası ile 25 mL 0,1M KH_2PO_4 + 0,1M K-asetat (pH= 6,0), 25 mL, 0,1 M KH_2PO_4 + 0,1M K-asetat (pH= 7,85) ve 25 mL 0,1M KH_2PO_4 + 0,1M KCI (pH= 7,85) çözeltileriyle yıkandı. Yıkama işlemi spektrofotometrik olarak takip edildi. Yıkama işlemine kolondan alınan numunenin absorbans

değeri ile kör arasındaki fark 0,05 olana kadar devam edildi. Kolon yıkandıktan sonra G6PD enzimi elüsyon tamponu (80 mM KH_2PO_4 + 80 mM KCI + 0,5 mM $NADP^+$ + 10 mM EDTA pH= 7,85) ile afinite kolonundan elüe edildi [26].

2.5. Glukoz 6-Fosfat Dehidrogenaz Enzimi Aktivitesi Ölçümü

G6PD enzimini aktivite ölçümü Beutler metoduna göre spektrofotometrik olarak ölçüldü. Bu metod, G6PD enziminin katalizlediği reaksiyonda $NADP^+$'nin indirgenmesi sonucu oluşan NADPH'ın 340 nm'de maksimum absorbans vermesi esasına dayanmaktadır [27].

2.6. Protein Tayini

Kantitatif protein miktarı spektrofotometrik olarak 595 nm'de Bradford metoduna göre yapıldı. Standart grafik sığır serum albümin proteini kullanılarak oluşturuldu [28].

2.7. SDS-PAGE ile Enzim Saflığının Kontrolü

Enzimin saflık kontrolü %3-8 kesikli sodyum dodesilsülfat poliakrilamid jel elektroforezi (SDS-PAGE) kullanılarak Laemmli metoduna göre gerçekleştirildi [29].

2.8. Kinetik Çalışmalar

Kinetik çalışmalarda iveral, linkomisin, gentamisin, amoksisilin, ampisilin, streptomisin sülfat, novamizol, ketojezik, sefuroksim, sefazolin sodyum ve tylosin ilaçlarının enzim aktivitesi üzerindeki etkileri araştırıldı. Aktivite ölçümleri sonucu inhibisyon etkisi gösteren iveral, lincocin, genta, streptomicin sülfat için farklı inhibitör konsantrasyonlarında % İnhibisyon – [I] grafikleri çizilerek IC_{50} değerleri hesaplandı [30].

3. BULGULAR

Bu çalışmada, koyun dalak dokusundan G6PD enzimi homojenatın hazırlanması, amonyum sülfat çöktürmesi ve 2', 5', ADP-Sepharose-4B afinite kromatografisi kullanılarak 13,68 EU/mg protein spesifik aktivite ile %33 verimle 1302,8 kat saflaştırıldı ve sonuçlar Tablo 1'de gösterildi.

Tablo 1. Koyun dalak dokusu G6PD enzimi saflaştırma basamakları.

Saflaştırma Basamağı	Toplam Hacim (mL)	Aktivite (EU/mL)	Protein (mg/mL)	Toplam Protein (mg)	Toplam Aktivite	Spesifik Aktivite (EU/mg protein)	%Verim	Saflaştırma Kat sayısı
Homojenat	25	1,128	106,62	2666	28,200	0,0105	100	1
Amonyum sülfat çöktürmesi (%40-70)	11	1,334	108,51	1193	14,674	0,0123	52,36	1,171
Afinite Kromatografisi	7,5	1,259	0,092	0,69	9,44	13,68	33,48	1302,8

Enzim saflık derecesinin tespiti için %3-8 kesikli sodyum SDS-PAGE yapıldı. Jel üzerinde tek bant elde edilmesi enzimin saf olarak elde edildiğini gösterdi (Şekil 1).

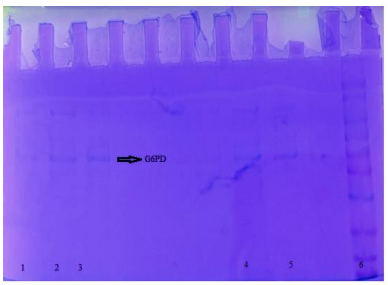

Şekil 1. Amonyum sülfat çöktürmesi ve afinite kromatografisi sonrası elde edilen koyun dalak dokusu G6PD enzimi (*1. 2. 3. 4. ve 5. kuyu: afinite kolonundan elüe edilen saf G6PD enzimi. 6. kuyu: standart proteinler (14 kDa - 175 kDa).

İn vitro kinetik çalışmalarda farklı konsantrasyonlarda iveral (0,057, 0,114, 0,224, 0,342, 0,448 ve 0,57 mM), linkomisin (3,7, 74, 111, 185, 296 mM), gentamisin (0,66, 1,32, 6,6, 13,2, 33, 39,6 ve 66 mM) streptomisin sülfat (4,29, 8,4, 16,8, 42, 84, 168 ve 210 mM) novamizol (3,2, 6,4, 9,6, 12,8 ve 16 mM), ketojezik (0,78, 1,56, 2,34, 3,1 ve 3,9 mM) amoksisilin (0,114, 0,228, 0,456, 1,14, 2,28, 3,42, 4,56, 5,7 ve 6,84 mM) ampisilin (0,095, 0,19, 0,38, 0,95, 1,9, 2,85, 3,8 ve 7,6 mM), sefuroksim sodyum (0,448, 0,896, 1,344, 1,790 ve 2,24 mM), sefazolin sodyum (0,83, 1,66, 2,49, 3,32 ve 4,15 mM) ve tylosin (0,095, 0,190, 0,285, 0,475 ve 0,95 mM) ilaçlarının enzim aktivitesi üzerindeki etkileri araştırıldı. Enzim üzerinde inhibisyon etkisi gösteren iveral, gentamisin, streptomicin sülfat ve linkomisin ilaçları için % Aktivite-[I] grafikleri çizilerek IC_{50} değerleri sırasıyla 0,62 mM, 21,6 mM, 173,2 mM ve 231 mM olarak hesaplandı (Şekil. 2, 3, 4 ve Tablo. 2). Amoksisilin, ampisilin, novamizol, ketojezik, sefuroksim sodyum, sefazolin sodyum ve tylosin ilaçlarının ise enzim üzerinde önemli bir aktivasyon ya da inhibisyon etkisine sahip olmadıkları belirlendi (Tablo. 2).

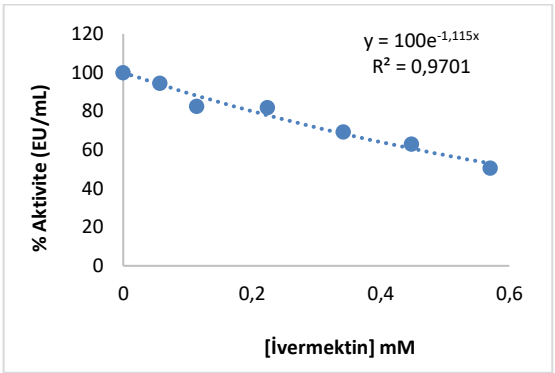

Şekil 2. İvermektinin koyun dalak G6PD enzimi üzerine etkisi.

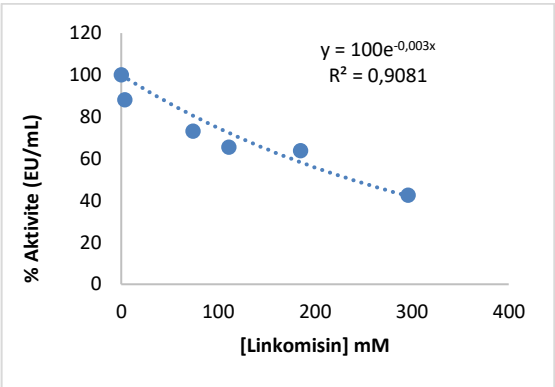

Şekil 3. Linkomisin'in koyun dalak G6PD enzimi üzerine etkisi.

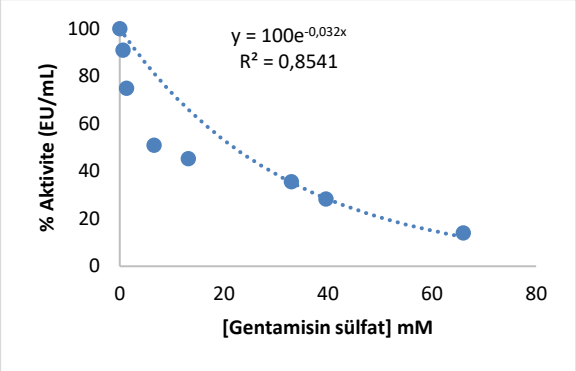

Şekil 4. Gentamisin sülfat'ın koyun dalak G6PD enzimi üzerine etkisi.

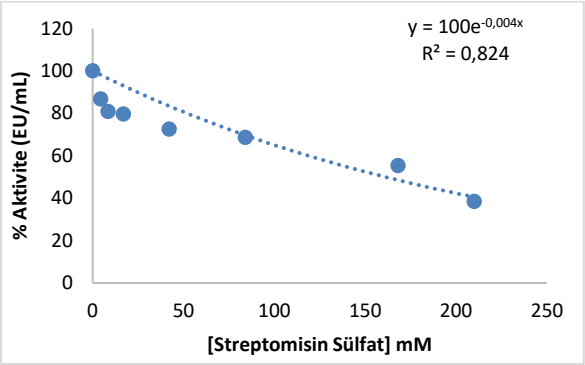

Şekil 5. Streptomisin sülfat'ın koyun dalak G6PD enzimi üzerine etkisi.

Tablo 2. Bazı ilaçları koyun dalak G6PD enzim aktivitesi üzerine etkileri.

İlaç	IC_{50} (mM)	R^2
iveral	0,62 mM	0,97
gentamisin	21,60 mM	0,85
streptomisin sülfat	173,2 mM	0,82
linkomisin	231 mM	0,91
amoksisilin	-	-
ampisilin	-	-
novamizol	-	-
ketojezik	-	-
sefuroksim sodyum	-	-
sefazolin sodyum	-	-
tylosin	-	-

4. SONUÇ

Pentoz fosfat metabolik yolu hücrelerin büyüme ve gelişiminde önemli rol oynar. Pentoz fosfat yolunun birinci basamak reaksiyonunu katalizleyen allosterik enzimi G6PD aktivitesinin işlevsiz bir durumu, normal hücre çoğalmasının yanı sıra embriyonik ve organizma gelişimini önler. G6PD'nin anormal aktivasyonu tümör oluşumu ile ilişkilidir [31]. Tümör oluşumu, tümör gelişiminin her durumunun yakından ilişkili olduğu dinamik ve karmaşık bir süreçtir. Hızlı büyüyen kanser hücreleri, NADPH üretimi ve nükleik asit sentezi talebini karşılamak için G6PD'yi uyarmak için çok sayıda mekanizma geliştirmiştir [32]. G6PD, lösemi, akciğer kanseri, yumurtalık kanseri, renal hücreli karsinom ve gliomada proliferasyonu, tümör hücrelerinin göçünü, glukoz alımını, NADPH üretimini arttırır ve reaktif oksijen türlerini (ROS) azaltır. Birçok çalışmaya göre, G6PD'nin yüksek ekspresyon seviyesi, mesane kanserinin kötü prognozu için bir risk faktörüdür ve G6PD aktivitesindeki artış farklı kanser türleri için kemoterapide ilaç direnci oluşturur. G6PD enzimi birçok hastalığın oluşum, tanı ve tedavisine aracılık ettiği ve etkilediği için G6PD inhibitörlerinin araştırılması ve geliştirilmesi önem arz etmektedir [33].

İvermektin, lakton grubu bir parazit ilacıdır ve Streptomyces avermitilis kültürlerinden elde edilir. İvermektin, parazitlerin sinir sisteminde Gama Amino Butirik Asit (GABA) salgısını artırarak klor kanallarını açık tutar ve impuls geçişini önleyerek parazitin felç olmasına ya da ölmesine neden olur [34]. Gentamisin, çoğunlukla *Pseudomonas, Proteus, Escherichia coli, Klebsiella pneumoniae, Enterobacter aerogenes, Serratia* ve Gram-pozitif *Staphylococcus* dahil olmak üzere çok çeşitli bakteriyel enfeksiyonlara karşı etkili bir antibiyotiktir [35]. Streptomisin aminoglikozid sınıfı, hem gram negatif hem de gram pozitif organizmalara ve Mycobacterium'a karşı aktif olan bakterisidal bir antibiyotiktir. Mikrobiyal hücrelerin protein sentezini inhibe ederek hücrenin ölümüne yol açar [36]. Linkozamidler gram pozitif koklar (özellikle stafilokoklar, streptokoklar ve enterokoklar), basil ve gram negatif koklara karşı etkilidirler [37] . Amoksisilin ve ampisilin beta laktam grubuna dahil aminopenisilinlerdendir. Bu antibiyotikler penisilin G gibi Gram pozitif bakterilere ve *H. influenza, E. coli, Proteus mirabilis, salmonella, shigella* gibi Gram negatif basillere karşı da etkilidirler [38]. Sefuroksim ve sefazolin üst solunum yolu enfeksiyonlarında kullanılan sefalosporin grubu antibiyotiklerdir [39]. Novamizol, metamizol sodyum içeren bir antienflamatuardır [40]. Ketojezik, ketoprofen içeren bir antienflamatuar ve analjeziktir [41]. Tylosin, *Streptomyces fradiae* suşları tarafından üretilen makrolid gurubu bir antibiyotiktir [42]. Bu çalışmanın birinci safhasında koyun dalak dokusundan G6PD enzimi amonyum sülfat çöktürmesi ve 2', 5' ADP-Sepharose-4B afinite kromatografisi ile saflaştırıldı. Afinite kromatografisi protein, DNA, RNA ve diğer makromoleküllerin saflaştırılmasında kullanılan ve spesifik etkileşimlere dayanan bir kromatografi yöntemidir. Bu yöntem günümüzde enzim saflaştırmalarında yaygın olarak kullanılmaktadır [12,43-45]. Bu çalışmada afinite kromatografisi kullanılarak kısa zamanda ve yüksek saflıkta enzim elde edildi. Çalışmanın ikinci safhasında insan hekimliğinde ve veteriner hekimlikte yaygın olarak kullanılan, iveral, gentamisin, streptomisin sülfat, linkomisin, amoksisilin, ampisilin, novamizol ketojezik, sefuroksim sodyum, sefazolin sodium ve tylosin ilaçlarının koyun dalak dokusundan saflaştırılan G6PD enzimi üzerine etkileri araştırıldı. Çalışma sonuçları, iveral, gentamisin, streptomisin sülfat ve linkomisin'in enzim aktivitesini inhibe ettiğini diğer ilaçların ise enzim aktivitesi üzerine herhangi bir etkileri olmadığını göstermektedir. Çalışma sonuçları analiz edildiğinde iveral'ın 0,62 mM IC_{50} değeriyle enzim üzerinde en etkili inhibitör olduğu, linkomisin'in ise 231 mM IC_{50} değeriyle enzim üzerine inhibisyon etkisi en düşük ilaç olduğu tespit edildi. Literatürde G6PD enzimi farklı dokulardan çeşitli kromatografik teknikler yardımıyla saflaştırılarak karakterize edilmiş ve bazı ilaç ve organik bileşiklerin enzim aktivitesi üzerine etkileri incelenmiştir [6,46,47]. Çiftci ve ark. insan eritrositlerinden afinite kromatografisi ile saflaştırdıkları G6PD enzim aktivitesi üzerine melatonin'in *in vitro* ve rat eritrosit G6PD enzimi üzerine *in vivo* etkisini incelemiştir.

Çalışma sonuçları melatonin'in G6PD enzim aktivitesini hem *in vitro* hem de *in vivo* olarak artırdığını göstermiştir [1]. Beydemir ve ark. yapmış oldukları çalışmada G6PD enzimini koyun eritrosit dokusundan afinite kromatografisi ile saflaştırmış ve gentamisin sülfat, penisilin G potasyum ve amicasin antibiyotiklerin enzim aktivitesi üzerine etkilerini incelemişlerdir. Araştırma sonuçları gentamisin sülfat'ın 10,01 mM, penisilin G potasyum'un 12,83 mM ve amicasin'in 41,88 mM, IC_{50} değerleriyle G6PD enzimini inhibe ettiğini göstermektedir [48]. Bu araştırmanın sonuçları ile bizim araştırmamızda elde ettiğimiz sonuçlar birbiri ile uyumludur. Temel ve ark. G6PD enzimini rat eritrositlerinden afinite kromatografisi ile saflaştırmış ve gentamisin, klindamisin ve furasemid antibiyotiklerinin enzim aktivitesi üzerine etkilerini araştırmıştır. Araştırma sonuçları gentimisin'in 1,75 mM, klindamisin'in 34,65 mM ve furosemid'in 0,526 mM IC_{50} değerleriyle G6PD enzimini inhibe ettiğini göstermiştir [16]. Çağlayan ve Gülçin yaptıkları çalışmada keçi karaciğerinden afinite kromatografisi ile saflaştırdıkları karbonik anhidraz (CA) enzimi üzerine bazı avermektin ilaçlarının inhibisyon etkilerini incelemiştir. Çalışma sonuçları abamectin, doramectin, eprinomectin, and moxidectin ilaçlarının sırasıyla 0.283, 0.153, 0.232, and 0.317 nM, *Ki* değerleriyle enzimi inhibe ettiğini göstermektedir (49).

Sonuç olarak, G6PD enziminin aşırı ekspresyonu bazı hastalıkların patofizyolojisi ile ilişkilidir. Hedefi enzim olan tedavi yaklaşımları için inhibitörler büyük önem arz etmektedir. Bu çalışmada iveral, gentamisin, streptomisin sülfat ve linkomisin'in koyun dalak dokusu G6PD enzimini inhibe ettiği belirlenmiştir. Bu çalışmada elde edilen sonuçlar hedefi G6PD enzimi olan tedavi yaklaşımları için yol gösterici olacaktır.

KAYNAKLAR

[1] Ciftci M, Bilici D, Kufrevioglu OI. Effects of metamizol and magnesium sulfate on enzyme activities of glucose-6-phosphate dehydrogenase from human erythrocytes in vitro and from rat erythrocytes in vivo. Pharmacol Res. 2001;44(1):7–11.

[2] Adem S, Ciftci M. Purification and biochemical characterization of glucose 6-phosphate dehydrogenase, 6-phosphogluconate dehydrogenase and glutathione reductase from rat lung and inhibition effects of some antibiotics. J Enzyme Inhib Med Chem. 2016; 31(6):1342-1348.

[3] Temel Y, Kocyigit UM. Purification of glucose-6-phosphate dehydrogenase from rat (Rattus norvegicus) erythrocytes and inhibition effects of some metal ions on enzyme activity. J Biochem Mol Toxicol. 2017;31(9): e21927.

[4] Gumustekin K, Ciftci M, Coban A, Altikat S, Aktas O, Gul M, et al. Effects of nicotine and vitamin E on glucose 6-phosphate dehydrogenase activity in some rat tissues in vivo and in vitro. J Enzyme Inhib Med Chem. 2005;20(5):497–502.

[5] Temel Y, Ayna A, Hamdi Shafeeq I, Ciftci M. In vitro effects of some antibiotics on glucose-6-phosphate dehydrogenase from rat (Rattus norvegicus) erythrocyte. Drug Chem Toxicol [Internet]. 2020;43(2):219–23.

[6] Temel Y, Bayındır S. The Synthesis of Thiosemicarbazone-Based Aza-Ylides as Inhibitors of Rat Erythrocyte Glucose 6-Phosphate Dehydrogenase Enzyme. J Inst Sci Technol. 2019;9(3):1503–12.

[7] Pljesa-Ercegovac M, Savic-Radojevic A, Matic M, Coric V, Djukic T, Radic T, et al. Glutathione transferases: Potential targets to overcome chemoresistance in solid tumors. Int J Mol Sci. 2018;19(12).

[8] Lu J, Holmgren A. Free Radical Biology and Medicine The thioredoxin antioxidant system. Free Radic Biol Med [Internet]. 2014;66:75–87. Available from:http://dx.doi.org/10.1016/j.freeradbiomed.2013.07.036

[9] Taysi MŞ, Temel Y. Glutathione S-transferase: Purification and Characterization from Quail (Coturnix coturnix japonica) Liver and the Impact of Some Metal Ions on Enzyme Activity. Bionanoscience. 2021;11(1):91–8.

[10] Arnér ESJ, Holmgren A. The thioredoxin system in cancer. Semin Cancer Biol. 2006;16(6):420–6.

[11] Carvalho CML, Chew E, Hashemy SI, Lu J, Holmgren A. Inhibition of the Human Thioredoxin System A Molecular Mechanısm Of Mercury Toxıcıty. 2008;283(18):11913–23.

[12] Temel Y, Kufrevioğlu ÖI, Çiftci M. Investigation of the effects of purification and characterization of turkey (Meleagris gallopavo) liver mitochondrial thioredoxin reductase enzyme and some metal ions on enzyme activity. Turkish J Chem. 2017;41(1).

[13] Akkemik E, Şentürk M, Özgeriş FB, Taşer P, Çiftci M. In vitro eff ects of some drugs on human erythrocyte glutathione reductase. 2011;41(2):235–41.

[14] Dilek EB, Ömer İ, Beydemir Ş. mpacts of some antibiotics on human serum paraoxonase 1 activity. 2013;28(February 2012):758–64.

[15] Zhang D, Liu Y, Luo Z, Chen Y, Xu A, Liang Y, et al. The novel thioredoxin reductase inhibitor A-Z2 triggers intrinsic apoptosis and shows efficacy in the treatment of acute myeloid leukemia. Free Radic Biol Med. 2020;146(November 2019):275–86.

[16] Temel Y, Ayna A, Hamdi Shafeeq I, Ciftci M. In vitro effects of some antibiotics on glucose-6-phosphate dehydrogenase from rat (Rattus norvegicus) erythrocyte . Drug Chem Toxicol. 2020;43(2):219-223.

[17] Shapiro R, Vallee BL. Interaction of Human Placental Ribonuclease with Placental Ribonuclease Inhibitor. Biochemistry. 1991;30(8):2246–55.

[18] Kose LP, Gülçin İ, Özdemir H, Atasever A, Alwasel SH, Supuran CT. The effects of some avermectins on bovine carbonic anhydrase enzyme. J Enzyme Inhib Med Chem [Internet]. 2015;6366(February 2017):1–6. Available from: http://www.ncbi.nlm.nih.gov/pubmed/26207514

[19] Adem S, Ciftci M. Purification of rat kidney glucose 6-phosphate dehydrogenase, 6-phosphogluconate dehydrogenase, and glutathione reductase enzymes using 2',5'-ADP Sepharose 4B affinity in a single

chromatography step. Protein Expr Purif. 2012;81(1):1–4.
[20] Özaslan MS, Balcı N, Demir Y, Gürbüz M, Küfrevioğlu Öİ. Inhibition effects of some antidepressant drugs on pentose phosphate pathway enzymes. Environ Toxicol Pharmacol. 2019;72(March).
[21] Temel Y, Ciftci M, Akkoyun HT, Akkoyun M. Effect of astaxanthin and aluminum chloride on erythrocyte G6PD and 6PGD enzyme activities in vivo and on erythrocyte G6PD in vitro in rats. 2017;31(10): e21954.
[22] Temel Y, Taysi MŞ. The Effect of Mercury Chloride and Boric Acid on Rat Erythrocyte Enzymes. Biol Trace Elem Res. 2019;191(1)172-187.
[23] Altikat S, Ciftci M, Buyukokuroglu ME. In vitro effects of some anesthetic drugs on enzymatic activity of human red blood cell glucose 6-phosphate dehydrogenase\r758. Pol J Pharmacol [Internet]. 2002;54(1):67–71.
[24] Temel Y, Bozkuş T, Karagözoğlu Y, Çİftcİ M. Glutatyon Redüktaz (GR) Enziminin Japon Bıldırcın (Coturnix coturnix japanica) Eritrositlerinden Saflaştırılması ve Karakterizasyonu Purification and Characterization of Glutathion Reductase Enzyme From Japanese Quail (Coturnix coturnix japanica) Er. 2017;7(3):143–50.
[25] Perosa F, Carbone R, Ferrone S, Dammacco F. Purification of human immunoglobulins by sequential precipitation with caprylic acid and ammonium sulphate. J Immunol Methods. 1990;128(1):9–16.
[26] Mannervik B, Jacobsson K, Boggaram V. Department of Biochemistry, Arrhenius Laboratory, University of Stockholm, Stockholm, Sweden. 1976;66(2):221–4.
[27] Buyukokuroglu ME. the Effects of Ethanol on Glucose 6-Phosphate Dehydrogenase Enzyme Activity From Human Erythrocytes in Vitro and Rat Erythrocytes in Vivo. Alcohol Alcohol. 2002;37(4):327–9.
[28] Bradford MM. Interactive effects of drought stress and chitosan application on physiological characteristics and essential oil yield of Thymus daenensis Celak. Crop J. 2017;5(5):407–15.
[29] Laemmli UK. 1970 Nature Publishing Group. Nat Publ Gr. 1970;228:1979.
[30] Lineweaver H, Burk D. The Determination of Enzyme Dissociation Constants. J Am Chem Soc. 1934;56(3):658–66.
[31] Jiang P, Du W, Wu M. Regulation of the pentose phosphate pathway in cancer. Protein Cell. 2014;5(8):1–11.
[32] Patra KC, Hay N. The pentose phosphate pathway and cancer. Trends Biochem Sci. 2014;39(8):347–54.
[33] Luo Z, Du D, Liu Y, Lu T, Liu L, Jiang H, et al. Discovery and characterization of a novel glucose-6-phosphate dehydrogenase (G6PD) inhibitor via high-throughput screening. Bioorg Med Chem Lett. 2021;40(February):127905.
[34] Goa Karen L, Donna McTavish, Stephen PC. Ivermectin: A review of its antifilarial activity, pharmacokinetic properties and clinical efficacy in onchocerciasis. Drugs. 1991;42(4):640–58.
[35] Sader HS, Farrell DJ, Flamm RK, Jones RN. Antimicrobial susceptibility of Gram-negative organisms isolated from patients hospitalized in intensive care units in United States and European hospitals (2009-2011). Diagn Microbiol Infect Dis. 2014;78(4):443–8.
[36] Kumar M, Kakkar V, Mishra AK, Chuttani K, Kaur IP. Intranasal delivery of streptomycin sulfate (STRS) loaded solid lipid nanoparticles to brain and blood. Int J Pharm. 2014;461(1–2):223–33.
[37] Leclercq R, Courvalin P. Erratum: Bacterial resistance to macrolide, lincosamide, and streptogramin antibiotics by target modification (Antimicrobial Agents and Chemotherapy 35 (1268)). Antimicrob Agents Chemother. 1991;35(10):2165.
[38] Poole K. Resistance to β-lactam antibiotics. Cell Mol Life Sci. 2004;61(17):2200–23.
[39] El-Shaboury SR, Saleh GA, Mohamed FA, Rageh AH. Analysis of cephalosporin antibiotics. J Pharm Biomed Anal. 2007;45(1):1–19.
[40] Gökçimen A, Özgüner M, Bayram D, Ural M, Sulak O. Metamizol sodyumun sıçan karaciğer, böbrek ve akciğer dokuları üzerine etkisi. SDÜ Tıp Fakültesi Derg. 2009;13(1):27–31.
[41] Alkimin GD, Soares AMVM, Barata C, Nunes B. Evaluation of ketoprofen toxicity in two freshwater species: Effects on biochemical, physiological and population endpoints. Environ Pollut. 2020;265:114993.
[42] Hendrickson OD, Zvereva EA, Zherdev A V., Godjevargova T, Xu C, Dzantiev BB. Development of a double immunochromatographic test system for simultaneous determination of lincomycin and tylosin antibiotics in foodstuffs. Food Chem. 2020;318(February):126510.
[43] Adem S, Ciftci M. Purification of rat kidney glucose 6-phosphate dehydrogenase, 6-phosphogluconate dehydrogenase, and glutathione reductase enzymes using 2???,5???-ADP Sepharose 4B affinity in a single chromatography step. Protein Expr Purif. 2012;81(1):1–4.
[44] Aksoy M, Ozaslan MS, Kufrevioglu OI. Purification of glutathione S-transferase from Van Lake fish (Chalcalburnus tarichii Pallas) muscle and investigation of some metal ions effect on enzyme activity. J Enzyme Inhib Med Chem. 2016;31(4):546–50.
[45] Ceylan M, Temel Y, Kocyigit UM, Alwasel SH, Gülçin I, Gürbüzlü B. Synthesis , carbonic anhydrase I and II isoenzymes inhibition properties , and antibacterial activities of novel tetralone-based 1 , 4-benzothiazepine derivatives. 2017; 31(4):e21872
[46] Bayindir S, Temel Y, Ayna A, Ciftci M. The synthesis of N-benzoylindoles as inhibitors of rat erythrocyte glucose-6-phosphate dehydrogenase and 6-phosphogluconate dehydrogenase. J Biochem Mol Toxicol. 2018;32(9):1–9.
[47] Bayindir S, Ayna A, Temel Y, Çiftci M. The synthesis of new oxindoles as analogs of natural product 3,3′-bis(indolyl)oxindole and in vitro evaluation of the enzyme activity of G6PD and 6PGD. Turkish J Chem. 2018;42(2):332-345.
[48] Beydemir S, Ciftçi M, Küfrevioğlu OI. Purification

and characterization of glucose 6-phosphate dehydrogenase from sheep erythrocytes and inhibitory effects of some antibiotics on enzyme activity. J Enzyme Inhib Med Chem. 2002;17(4):271–7.

[49] Caglayan C. The toxicological effects of some avermectins on goat liver carbonic anhydrase enzyme. 2018;32(1):e22010.

Araştırma Makalesi https://doi.org/10.46810/tdfd.933152 Research Article

Türk Doğa ve Fen Dergisi
Turkish Journal of Nature and Science
www.dergipark.gov.tr/tdfd

Investigation of Biogas Potential from Animal Waste in Bingöl Province

Üsame Demir[1], Perihan ÇULUN*[2]

[1]Bilecek Şeyh Edebali University, Engineering Faculty, Mechanical Engineering Department, Bilecik, Turkey
[2]Bingöl University, Engineering and Architecture Faculty, Department of Mechanical Engineering, Bingöl, Turkey
Üsame Demir ORCID No: 0000-0001-7383-1428
Perihan ÇULUN ORCID No: 0000-0021-7979-9695

**Corresponding author: pculun@bingol.edu.tr*

(Received: 5.05.2021, Accepted: 3.01.2022, Online Publication: 25.03.2022)

Key words: Energy, Biogas, Animal Waste, Bingöl

Abstract: In this study, biogas and energy potential of animal wastes belonging to Bingöl province was investigated. The study in question was based on data from the Bingöl Governorship Provincial Directorate of Agriculture and Forestry for the years 2002-2020. In the light of 18 years of data, it has been determined that annualy 741.452 tons of manure can be obtained from an average of 948.144 animals, and 34.225.934 m^3 of biogas can be obtained from this manure, also 161GWh of energy per year can be obtained from this biogas. If these animal wastes were evaluated in the said years, a total of 2898 GWh energy would have been obtained. In addition the evalueting data for 2020 it is understood that the biogas potential installation power of Bingöl province is 25.6 MW. Considering the distribution of biogas energy by districts, it is understood that Karlıova district plays an important role with a share of 31% in total power potantial. According to 2020 datas only it is seen that 73.8% of the 303.7 GWh electricity consumed can be met by biogas energy. In addition, according to turkey statistics institute data of 2020 total potential power of Bingöl and its neighboring provinces Diyarbakır, Elazığ, Erzurum, Erzincan, Muş and Tunceli is calculated as 298MW. However, it is understood that only 2.6% of this power (Equal to 7.63MW) is used currently.So it is obvious that the establishment of biogas facilities in related regions will decrease country's dependency on foreign energy.

Bingöl İli Hayvansal Atık Kaynaklı Biyogaz Potansiyelinin Araştırılması

Anahtar kelimeler Enerji, Biyogaz, Hayvansal atık, Bingöl

Öz: Bu çalışmada Bingöl iline ait hayvansal atıkların biyogaz ve enerji potansiyeli araştırılmıştır. Söz konusu çalışma, Bingöl Valiliği İl Tarım ve Orman Müdürlüğü'nün 2002-2020 yıllarına ait verilerine dayanmaktadır. 18 yıllık veriler ışığında, ortalama 948.144 hayvandan yıllık 741.452 ton gübre elde edilebileceği ve bu gübreden 34.225.934 m^3 biyogaz elde edilebileceği, ayrıca yıllık 161 GWh enerji üretilebileceği belirlenmiştir. Söz konusu yıllarda bu hayvan atıkları değerlendirilseydi toplam 2898 GWh enerji elde edilecekti. Ayrıca 2020 yılı verileri değerlendirildiğinde Bingöl ilinin biyogaz potansiyel kurulum gücünün 25.6 MW olduğu tespit edilmiştir. Biyogaz enerjisinin ilçelere göre dağılımına bakıldığında Karlıova ilçesinin% 31'lik pay ile önemli bir rol oynadığı anlaşılmıştır. Sadece 2020 verilerine göre tüketilen 303.7 GWh elektriğin %73.8'inin biyogaz enerjisi ile karşılanabileceği görülmektedir. Ayrıca türkiye istatistik enstitüsü verilerine göre 2020 yılı Bingöl ve komşu illeri Diyarbakır, Elazığ, Erzurum, Erzincan, Muş ve Tunceli'nin toplam potansiyel gücü 298 MW olarak hesaplanmıştır. Ancak şu anda bu gücün sadece %2.6'sının (7.63 MW'a eşit) kullanıldığı anlaşılmaktadır. Dolayısıyla ilgili bölgelerde biyogaz tesislerinin kurulmasının ülkenin dışa bağımlılığını azaltacağı aşikardır.

1. INTRODUCTION

With the increasing population and the development of technology, the need of energy increases day by day. At the same time with the population increase, environmental pollution increases, and it is generally known that fossil fuels are exhausted. In this sense, researches on alternative energy sources are increasing day by day. According to 2010 data, fuel and alternative energy sources used in the distribution of electricity generation in

the world are 28% nuclear, 25% solid fuels, 24% natural gas, 17% renewable energy sources excluding biomass, 4% biomass, 3% liquid fuel. By 2020, 23% of electricity production was met from nuclear, 23% ıf them from solid fuels, 17% of them from natural gas, 30% of them from renewable energy sources excluding biomass, 6% of them from biomass and 1% of them from liquid fuels. In the distribution of electricity generation, it is seen that there is a tendency towards renewable energy by abandoning fossil resources. A study is expected that by 2050 it will have a very high share of 92% of renewable energy including biomass in electrical energy production [1]. In Turkey according to 2010 sources 46.47% of electricity generation was obtained from natural gas, 26.22% of them from renewable energy sources excluding biomass, 18.05% of them from liquid fuels, 9.05% of them from solid fuels[2]. In 2020 26.8% of electricity generation was obtained from natural gas, 50.2% of them from renewable energy excluding biomass, 12.1% of them from liquid fuels, 9.4% of them from solid fuels, 1.5 of them from biomass [3]. Therefore, according to the sources of energy production it is seen that there is a high rate of turn to renewable energy in Turkey. On average 24% of the world's energy needs are met from nuclear energy and therefore, it is seen that investments are made in nuclear energy in our country too. By 2050 it is predicted that nuclear energy will not remain and 92% of energy will be met from renewable energy worldwide. In addition while 36% of energy in the world is met from renewable energy this rate is aproximately 51.7% in Turkey in 2020. This ratio shows that Turkey is above the world average in terms of transition to renewable energy. While energy production from biomass increased 1.5 times in the world from 2010 to 2020, it increased approximately 7 times in Turkey. There is a high tendency towards alternative energy sources in our country, especially to reduce foreign dependency. Biogas production from animal wastes should be prioritized as an alternative energy source considering the existence of animals in our country. When evaluated in terms of animal assets, it is known that there are 72 million 271 thousand total animals, including 18 million 158 thousand cattle and 54 million 113 thousand small cattle as of 2020 [4]. If this potential animal waste is evaluated, it is understood that the energy amount of 4.385.371 TEP/year can be met and it will make a great contribution to the country's economy, especially in terms of foreign dependency of energy [5]. Many studies have been carried out in terms of the biogas potential of Turkey. Biogas potential of Elazig province has been studied and an analysis of return figures of biogas to be produced in the biogas plant has also been conducted [6]. The amount of fertilizer that can be obtained from the wastes of all animal assets of Turkey and the maximum biogas production that can be produced depending on these fertilizer amounts have been evaluated. It has been understood that when this biogas is used for electricity generation, there will be a great decrease in the amount of electrical energy that we depend on. In this respect, it was emphasized that especially agricultural, domestic and animal wastes should be used for energy production [7]. Biomass potential of Eastern Anatolia Region was examined in another study. The amount of dry biomass in cultivated areas in all provinces in the Eastern Anatolia Region has been calculated. Average thermal values were calculated according to the amount of dry biomass and the amount of energy obtained from it. According to the values obtained, they suggested that necessary researches should be made especially in provinces for the utilization of biomass wastes or forest wastes and that necessary facility should be established and research centers should be established to close our energy deficit on a provincial basis [8]. In the study conducted to evaluate animal wastes in Tokat province, animal assets according to Tokat city center and districts were examined. According to these animal beings, the potential biogas production and the electrical energy to be obtained from it have been revealed. According to the data obtained, the amount of electrical energy produced from animal waste will meet approximately 32% of the electricity consumption of Tokat province in 2007 [9]. In the study carried out for Sivas province, the electrical energy that could potentially be produced according to the general animal number of the province was evaluated. In addition, in the study suggestions were given about the size of the biogas facility that they can establish on a small scale according to the number of animals for cattle, ovine and poultry breeders. In the data presented, the appropriate size of the facility for livestock holdings is suggested as 14, 21, 28 m^3 for 20, 30, 40 animals respectively; for 30 000, 40 000 cattles 356, 474 m^3 respectively. It was emphasized that for small ruminants it should be 16 m^3 for 500 animals and it is more important to establish small-scale biogas plants instead of a single large biogas plant [10]. In the study conducted for the province of Iğdır, the biogas potential from animal waste was evaluated according to the city center and districts. It has been determined that the district with the highest biogas potential is Tuzluca. In addition, they revealed that the biogas potential of Iğdır province constitutes 3.76% of the Eastern Anatolia Region and 0.679% of Turkey in general [11]. In the study conducted for the province of Ardahan, the amount of biogas that can be obtained from animal wastes and the amount of electrical energy that can be produced were determined for the city center and districts. According to the density of animal clusters, locations of the city center and districts to establish a biogas plant have been revealed. In addition, a guide has been prepared for the investments to be made for the biogas plant [12]. In the study conducted for the province of Malatya, the biogas potential that can be obtained from animal wastes was evaluated and the biogas potential of the province was revealed by comparing it with animal assets throughout Turkey [13]. In a statistical study conducted in Turkey, it was calculated that according to the number of chickens, the biogas potential that could be produced in Turkey in 2009 was 390 million m^3, which is equivalent to an energy of 8.853 million GJ. In addition, the provinces where more than 10 million m^3 of biogas will be obtained annually from chicken waste in Turkey are listed as Bolu, Balıkesir, Sakarya, Manisa, Afyon, Konya, İzmir, Ankara, Çorum and Bursa [14]. In the study conducted for Kahramanmaraş province, biogas production potentials from animal and plant wastes were determined. In this sense, it is predicted that the majority of production will consist of animal wastes. In addition, a mapping was made according to the production potential

of the districts and the places with the highest biogas potential were determined [15]. In the study conducted for Çanakkale province, situations related to electricity generation from biogas in the world and in Turkey have been presented. A comparison of biogas potential with Çanakkale province and other provinces has been made [16]. In the study conducted for Denizli province, biogas production potential from animal wastes and the amount of electrical energy that can be obtained from biogas were revealed according to their districts. In this sense, it is stated that it is important to have a facility made of animal wastes in Çivril district. In addition due to the high number of chickens in Honaz district, it was observed that a biogas production facility was suggested to be established here [17]. In the study conducted for the Thrace region, potential biogas production amounts from animal waste in all provinces and districts were evaluated. In this sense studies were carried out for the whole region with the numerical mapping method. It was stated that Edirne could be the province with the highest potential biogas production from animal wastes in the Thrace region [18]. Potential biogas production that can be obtained from animal wastes in Erzincan province has been determined. The use of potential biogas as an alternative to electricity generation and natural gas has been evaluated. In addition, it has been shown how

Erzincan province will benefit economically in the use of biogas to be produced annually [19]. Again, a study conducted for Erzincan determined where a biogas plant should be established in provincial and district centers [20]. In the study conducted for Kırşehir province, the amount of biogas obtained from animal wastes was determined and where the biogas facility should be established in the province [21]. In the study conducted for Bitlis, biogas production potential from animal wastes in the city center and districts was examined. In this sense, the amount of earning that can be obtained in case of utilizing this potential throughout the province has been presented [22]. In a study, the number of biogas facilities and production amounts in Turkey were examined. In 2017 it was determined that there are 122 licensed Renewable Waste Power Plants with 634.2MW power. It was emphasized that these facilities should increase as the demand for energy increases day by day [23].

Previous studies on biogas energy have been meticulously examined. Among the mentioned studies, there is no study on the biogas energy potential for the province of Bingöl. In this respect, this study will be both an original study and a guide for biogas studies to be carried out in Bingöl Province. And also it is aim to encourage the establishment of biogas facilities in the province of Bingöl and reduce foreign dependency by providing local energy production. Based on literature studies, the biogas potential and related energy data obtained from animal wastes were investigated for the province of Bingöl, which has a high livestock potential. So Animal waste data obtained from Governorship Provincial Directorate of Agriculture and Forestry for the years 2002-2020. Biogas potentials of province and districts were revealed separately. Electrical energy consumed by the region were compared with the electrical energy produced from biogas. In addition, the data of the provinces neighboring Bingöl for the year of 2020 were evaluated in terms of current installed power.

2. MATERIAL AND METHOD

Bingöl province is located in the Upper Euphrates Section of the Eastern Anatolia Region between 41º 20 ′ and 39º 56 ′ east longitudes and 39º 31 ′ and 36º 28 northern latitudes. The land within the provincial borders is quite hilly, and the city center was established on a plain bordered by mountains on all four sides. The majority of rural settlements are located in mountainous areas. In this respect, both bovine and ovine breeding constitute important sources of income in this city. Bingöl is adjacent to Erzincan and Erzurum in the north; Muş in the east; Tunceli and Elazig in the west and Diyarbakır in the south. There are 7 Districts of Bingöl, Yayladere, Kiğı, Yedisu, Adaklı, Karlıova Solhan and Genç. In the study in question, data belonging to the years 2002-2020 obtained from the Bingöl Governorship Provincial Directorate of Agriculture and Forestry were used. Within the scope of this study, Livestock data for the year 2020 published by Turkish Statistical Institute (TSI) was used [4]. Bovine, ovine and poultry data were used in biogas and energy calculations.

Table 1. Animal Presence of Bingöl Province in 2020 [4]

Districts	Bovines	Ovines	Poultry	Total
Adaklı	10.386	48.920	6.800	66.106
Genç	19.357	39.079	6.495	64.931
Karlıova	20.986	348.375	11.760	381.121
Kiğı	3.670	9.976	6.811	20.457
Merkez	60.050	101.398	723.600	885.048
Solhan	19.984	147.291	5.000	172.275
Yayladere	1.783	4.386	382	6.551
Yedisu	8.297	21.427	1.650	31.374
Total	144.513	720.852	762.498	1.627.863

According to 2020 data 60.050 of 144.513 cattle in Bingöl province belong to Bingöl center. The highest number of cattle belongs to Karlıova after the central district, followed by Solhan, Genç, Adaklı, Yedisu and Kiğı. The fertilizer used in the calculations was taken as 3,6 tons year-1 for cattle, 0.7 tons year^{-1} for small cattle and 0.022 tons year^{-1} for poultry [24]. The amount of biogas taken from the fertilizer on a ton basis is 33, 58, 78 m3 ton^{-1} for bovine, ovine and poultry respectively [24]. The electrical energy obtained from 1 m^3 of biogas is the same for all three animal species and is 4.7 kWh [25].

3. RESULTS

In this study, biogas and energy potential of animal wastes belonging to Bingöl province was investigated. In the study datas belonging to the years between 2002-2020 obtained from the Bingöl Governorship Provincial Directorate of Agriculture and Forestry were used. The land is quite hilly within the province of Bingöl and the city center was established on a plain bordered by mountains on four sides. The majority of rural settlements are located in mountainous areas. In this respect, both bovine and ovine breeding constitute important sources of

income in this city. Expecially small cattle breeding is the most common in the region. In Figure 1, the numbers of bovine, ovine and poultry animals belonging to the province of Bingol and theoretical biogas of them are given for 2002-2020 years. As seen in related figure the annual average bovine number is below 200000, while the average number of sheep and goats is around 500000. It is understood that potential of manure obtained from ovine animals is higher than that of bovine animals. As a matter of fact, while the potential biogas multiplier for ovines is 58, it is 33 for bovines. So the biogas potential of manure obtained from ovine animals is of higher quality than that of bovine animals. Considering ovines livestock has an important place due to its location, the importance of researching and evaluating potential biogas production can be better understood. In addition as seen from same figure (**Figure 1**) a significant increase is seen in the number of poultry animals in the last three years.

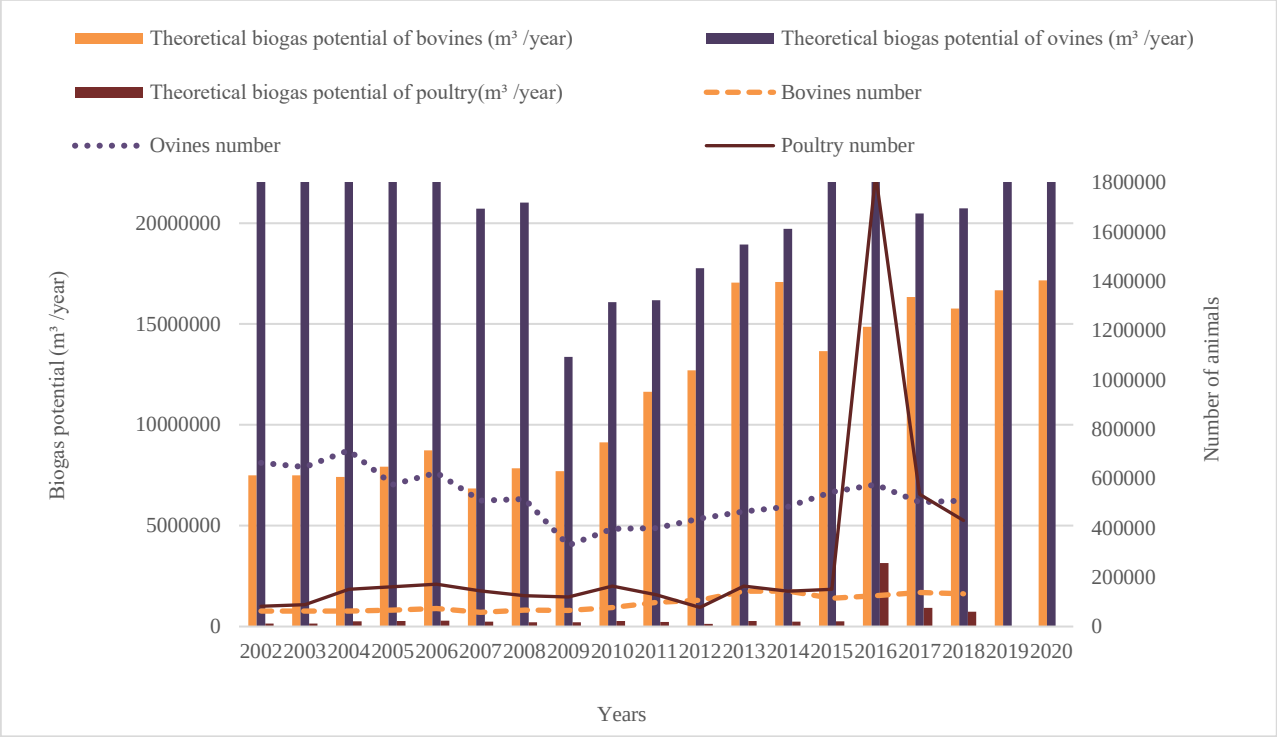

Figure 1. Number of animals and theoretical biogas potential of them for Bingöl province

According to annual average values data from Table 2, there is an annual total of 948.144 animals, including 99.047 bovines, 540.122 ovine, 308.975 poultry. From these animals, in totaly 741.452 tons/year of fertilizer is obtained from all animals, 356.569 tons/year of them obtained from cattles, 378.085 tons/year of them provided from ovine, 6.797 tons/year of them provided from poultry manure. And also 11.766.783 m^3/year of the total biogas produced annually is obtained by small animals, 21.928.953 m^3/year of them produced by cattle and 530.197 m^3/year of them produced by poultry. The relevant energy amounts were determined for bovines, ovines and poultry as 55.35 GWh / year, 103.1 GWh / year, 2.5 GWh / year respectively with an average annual total of 160.9 GWh/year (Table 2). In the light of these values, it was possible to establish a biogas plant with an installed power of 18.4MW in the 18 year period(from 2002 to 2020). If these animal wastes were evaluated in the said years, a total of 2898 GWh energy would have been obtained. But this energy became idle because the existing potential biogas energy was not utilized.

Table 2. Annual average data of 2002-2020

Animal breed	**Num. of animals per year**	**Theoretical Fertilizer Potential (tons / year)**	**Theoretical Biogas potential (m^3 /year)**	**Produced Energy (GWh /year)**
Bovines	99.047	356.569	11.766.783	55.3
Ovines	540.122	378.085	21.928.953	103.1
Poultry	308.975	6.797	530.197	2.5
Total	948.144	741.452	34.225.934	160.9

Table 3. Datas for 2020

Animal breed	Animal number	Theoretical Fertilizer Potential (tons / year)	Theoretical Biogas potential (m^3 /year)	Produced Energy (MWh /year)	Potantial power plant capacity(MW)
Bovines	144.513	520.247	17.168.144	80.700	9.2
Ovines	720.852	504.596	29.266.591	137.500	15.7
Poultry	762.498	16.775	1.308.447	6.100	0.7
Total	1.627.863	1.041.618	47.743.182	224.300	25.6

Table 3 shows the animal numbers, potential biogas and energy values for 2020 only. According to the result from Table 2 and Table 3 this is a sign that the number of animals will increase gradually for Bingöl. At the same time the increase in the energy produced by biogas in question will observed. The evalueting data of 2020 only it is understood that the biogas potential installation power of Bingöl province is 25.6 MW. In this regard, it is observed that there is an increase of approximately 40% in 2020 compared to the power of the facility that can be established for the other 18 years.

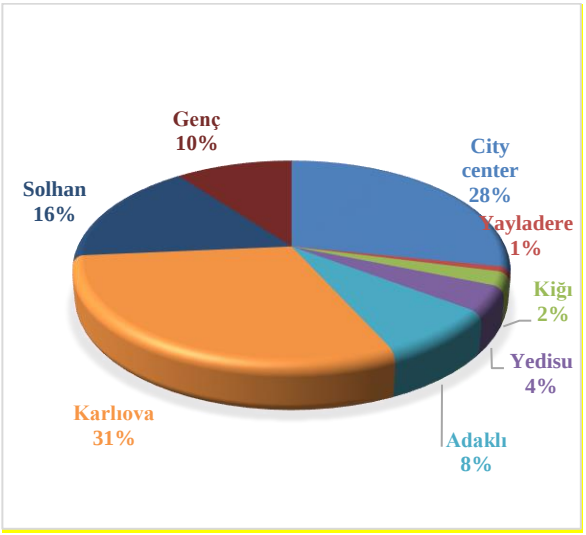

Figure 2. Distribution of biogas energy by districts

In Figure 2, the distribution of biogas energy by districts is shown in the pie chart. From the related graph, the distribution of total biogas energy in Bingöl province as 31% Karlıova, 28% city center, 16% Solhan, 10% Genç, 8% Adaklı, 4% Yedisu, 2% Kiğı, % 1 Yayladere respectively. It is understood that Karlıova has an important place in biogas production in Bingöl province.

Considering the distribution of biogas energy by districts, it is understood that Karlıova district plays an important role with 31% installed power potantial in this matter.

Table 4. Electricity Consumption Values in Bingöl Province by Years and Consumer Type (Obtained from board (EPDK)).

Bingöl	2020	2019	2018	2017
Lighting	16.126	14.633	12.469	10.403
Domicile	129.972	122.600	117.778	111.732
Industry	53.042	49.228	63.114	58.029
Agricultural watering	1.308	781	452	426
Business	103.293	118.748	111.723	114.144
Grand Total (MWh)	303.740	305.989	305.535	294.733

According to the electricity consumption values of Bingöl province obtained from EPDK (Table 4), it is seen that the annual consuption potential was in total approximately 294GWh in 2017; 305 GWh in 2018 and 2019 and 303.74 GWh in 2020. It is understood that by using the 224.3 GWh/year biogas potential energy obtained in 2020, 73.8% of the total consumption value of the relevant year,(Which is 303.7 GWh/year according to Table 4), will be met.

In Table 5, the number of animals in Bingöl province and its neighbors, the relevant biogas energy amounts and the current installed power are given for comparison purposes for 2020. The biogas facility established by Sütaş company in Bingöl for cattle manure, chicken manure and vegetable waste has a capacity of 2.1MW, whereas the biogas potential of Bingöl is much higher than this installed power. Similarly It is understood that the biogas potential in Diyarbakır is far above the installed power of 2.15MW.

Table 5 Biogas data of neighboring provinces of Bingöl for 2020 (Obtained from turkey statistics institute 02.12.2021)[4]

Data of 2020	Bingöl	Diyarbakır	Elazıg	Muş	Erzurum	Erzincan	Tunceli	Total
Ovine num.	720.852	2.091.344	854.456	1.235.552	904.587	501.027	432.565	6.740.383
Bovine num.	144.550	656.074	209.142	331.881	869.009	124.125	37.086	2.371.867
Biogas potantial(MWh/year)	218.264	765.396	279.825	421.077	657.833	164.911	103.249	2.610.555
Potantial installed biogas power (MW)	24.9	87.3	31.9	48	75	18.8	11.78	297.68
Installed biogas power(MW)	2.1	2.15	0	0	3.38	0	0	7.63

There are currently two biogas power plants with 3.38MW power in Erzurum named Erzurum and Akşehir biogas power plant. On the other hand, there is currently no biogas facility in Elazig, Erzincan, Muş and Tunceli that uses animal wastes. According to the relevant table, the total installed power potential of Bingöl and neighboring provinces is 297.68 MW, while all installed facilities are only 7.63MW.

4. DISCUSSION

In this study, the biogas potential of Bingöl province was evaluated. For this purpose, annual average results were obtained by using the data on animal waste between the years 2002-2020. Also using the data of 2020, the electricity rates that can be met with the biogas potential were examined. In addition, the data of the provinces

neighboring Bingöl for the year 2020 were evaluated. Considering the average values obtained according to 2020, it is understood that the potential biogas power of the province of Bingöl is approximately 25.6MW. It has been understood that 73.8% of the electricity consumed annually can be met if a 25.6MW biogas power plant is established. According to relevant data, the total installed power potential of Bingöl and neighboring provinces is 297.68 MW, while all installed facilities are only 7.63MW. Therefore, it is understood that only 2.5% of the potential of Bingöl and surrounding provinces is used. On the other hand, considering that approximately 27.4% of the electricity produced in Turkey is obtained from natural gas, 17% from ital coal and 2.2% from biogas [26], it is understood that sufficient attention should be given to biogas studies.

According to the February 2021 biogas production facility pre-feasibility report in Elazig province, although the biogas installed power of companies that have obtained a biogas license within the scope of Turkey increases every year, it is understood that the total installed power is currently 147MW[27]. Considering that the potential power of Bingöl and neighboring provinces is 297MW according to our own study. Therefore, it is understood that Turkey's total installed power corresponds to only 50% of the potential biogas energy of Bingöl and neighboring provinces. In other words, only the biogas potential of Bingöl and neighboring provinces is twice the current total installed power of Turkey. Therefore, when we consider this in terms of the eastern Anatolian region and Turkey, a large proportion of electrical energy can actually be met from these waste energies. Especially considering that biogas energy is not only caused by animal wastes, but also vegetable wastes and all organic wastes can be evaluated. In this sense, we believe that this issue will be even more important[7]. In this respect, it is clear that the evaluation of biogas energy produced both in the province of Bingöl and the other centers of Turkey will close a large energy deficit of country. With the use of this potential, it will be possible to get rid of the 50% energy dependence on abroad[26]. And also we are of the opinion that biogas energy should be re-evaluated not only throughout Bingöl but also in every region of Turkey.

REFERENCES

[1] Brugger H, Eichhammer W, Mikova N, Donitz E. Energy Efficiency Vision 2050: How will new societal trends influence future energy demand in the European countries? Energy Policy, 2021; 152:112216.

[2] Electricity Generation Inc., 2010 Annual Report[Internet], 2021[cited April 15]. Avoilable from: https://www.euas.gov.tr/tr-TR/yillik-raporlar Erişim tarihi:15.04.2021

[3] Chamber of Electrical Engineers, Turkish Electricity Statistics[Internet]. 2021[cited April [4] Turkish Statistical Institute Livestock Statistics[Internet], TÜİK - Data Portal (tuik.gov.tr) Available date:08.12.2021

[4] Biomass Energy Potential Atlas[Internet]. BEPA General Directorate of Energy Affairs; 2021[cited 2021 April 15]. Avoilable from: https://www.enerjiportali.com/biyokutle-enerjisi-atlasi-bepa-yenilendi/

[5] Akbulut A, Dikici A. Elazığ İlinin Biyogaz Potansiyeli ve Maliyet Analizi. Doğu Anadolu Bölgesi Araştırmaları Dergisi. 2004;2 (2): 36-41.

[6] Nacar Koçer N, Öner C, Sugözü İ. Türkiye'de Hayvancılık Potansiyeli ve Biyogaz Üretimi. Doğu Anadolu Bölgesi Araştırmaları Dergisi. 2006; 4(2):17-20.

[7] Nacar Koçer N., Ünlü A. Doğu Anadolu Bölgesinin Biyokütle Potansiyeli ve Enerji Üretimi. Doğu Anadolu Bölgesi Araştırmaları Dergisi. 2007; 5(2): 175-181.

[8] Kizilaslan H ve Onurlubas HE. Potential of Production of Biogas from Animal Origin Waste in Turkey (Tokat Provincial Example). Journal of Animal and Veterinary Advances. 2010; 9(6): 1083–1087.

[9] Yokuş İ. Sivas İlindeki Hayvansal Atıkların Biyogaz Potansiyeli. Ankara Üniversitesi Fen Bilimleri Enstitüsü, Yüksek Lisans Tezi, 2011.

[10] Altikat S, Çelik A. Iğdır İlinin Hayvansal Atık Kaynaklı Biyogaz Potansiyeli. Iğdır Üni. Fen Bilimleri Enst. Dergisi 2012;2(1): 61-66.

[11] Ardahan Belediyesi, Biyogaz ve Enerji Potansiyelinin Araştırılmasına Yönelik Fizibilite Çalışması, 2013.

[12] Nacar Koçer N, Kurt G. Malatya'da hayvancılık potansiyeli ve biyogaz üretimi. SAÜ. Fen Bil. Der. 2013; 17(1):1-8.

[13] Avcıoğlu AO, Çolak A, Türker U. Türkiye'nin Tavuk Atıklarından Biyogaz Potansiyeli. Namık Kemal Üniversitesi Tekirdağ Ziraat Fakültesi Dergisi, 2013 ; 10(1):21-28.

[14] Aybek A, Üçok S, Bilgili ME, İspir M A. Kahramanmaraş İlinde Bazı Tarımsal Atıkların Biyogaz Enerji Potansiyelinin Belirlenerek Sayısal Haritalarının Oluşturulması. Uludağ Üniversitesi Ziraat Fakültesi Dergisi, 2015; 29(2):25-37.

[15] Ilgar R. Hayvan Varlığına Göre Çanakkale Biyogaz Potansiyelinin Tespitine Yönelik Bir Çalışma. Eastern Geographical Review, 2016; 21(35):89-106

[16] Doruk İ. Bozdeveci A. Denizli İlinin Kırsal Kesimlerinde Hayvansal Kaynaklı Atıklardan Biyogaz Potansiyelinin Belirlenmesi. Iğdır Univ. J. Inst. Sci. & Tech. 2017; 7(3): 181-186.

[17] Tinmaz Köse E. Trakya bölgesinde hayvan gübrelerinin biyogaz enerji potansiyelinin belirlenmesi ve sayısal haritaların oluşturulması. Pamukkale Üniversitesi Mühendislik Bilimleri Dergisi, 2017; 23(6):762-772.

[18] Kurnuç Seyhan A, Badem A. Erzincan İlindeki Hayvansal Atıkların Biyogaz Potansiyelinin Araştırılması. Akademik Platform Mühendislik ve Fen Bilimleri Dergisi, 2018; 6(1):25-35.

[19] Kurnuç Seyhan A, Badem .Erzincan ili hayvansal atık kaynaklı biyogaz potansiyelinin değerlendirilmesine yönelik biyogaz tesisi senaryoları. Gümüşhane Üniversitesi Fen Bilimleri Enstitüsü Dergisi, 2021;111:245-256.

[20] Ahiler Development Agency, Field Study Report for Investigation of Biogas and Energy Potential from Animal Manure in Kırşehir Province, 2017.
[21] Demir Yetiş A, Gazigil L, Yetiş R., Çelikezen B. Hayvansal Atık Kaynaklı Biyogaz Potansiyeli: Bitlis Örneği. Akademik Platform Mühendislik ve Fen Bilimleri Dergisi, 2019;7(1):74-78.
[22] Yilmaz A. Türkiye'de Biyogaz Üretimi Ve Kurulu Santrallerin Ürettiği Elektrik Enerjisi. Ecological Life Sciences, 2019;14(1): 12-28.
[23] Deniz Y. Türkiye 'de Biyogaz Potansiyeli ve Biyogazın Sağlayacağı Yararlar. Ankara, 1987.
[24] Bilir M, Deniz Y, Karabay E. Biyogaz Üretimine Yönelik Değerlerin Saptanması. Toprak Su Araştırma Ana Projesi, Proje No: 872, Ankara, 1983.
[25] [cited 2021 December 08]. Avoilable from https://www.enerjiatlasi.com/elektrik-uretimi/, Available date: 03.12.2021
[26] 2021 Şubat ayı Elâzığ ili biyogaz üretim tesisi ön fizibilite raporu, 2021[cited 2021 December 8]. Avoilablefromhttps://www.yatirimadestek.gov.tr/pdf/assets/upload/fizibiliteler/elazig-ili-biyogaz-tesisi-on-fizibilite-raporu2021.pdf, Available date:08.12.2021

Araştırma Makalesi https://doi.org/10.46810/tdfd.935657 Research Article

Türk Doğa ve Fen Dergisi
Turkish Journal of Nature and Science
www.dergipark.gov.tr/tdfd

Mısır (*Zea mays* L.): Bir Bitki; İki veya Üç Farklı Ürün

Burhan KARA[1*]

[1]Isparta Uygulamalı Bilimler Üniversitesi Ziraat Fakültesi Tarla Bitkileri Bölümü, Isparta, Türkiye
Burhan KARA ORCID No: 0000-0002-4207-0539

**Sorumlu yazar: burhankara@isparta.edu.tr*

(Alınış: 10.05.2021, Kabul: 20.10.2021, Online Yayınlanma: 25.03.2022)

Anahtar Kelimeler
Zea mays L., Taze mısır, Körpe mısır, Tane özellikleri

Öz: Çalışma, mısırda bir bitkiden birden fazla farklı ürün elde etme imkânlarını araştırmak amacıyla yürütülmüştür. Bu amaçla, mısır bitkisi üzerindeki koçanlar tüketim amaçlarına göre körpe mısır (koçan püskülü çıkarma dönemi), haşlamalık/közlemelik (süt olum dönemi) ve tane verimi (tam olum dönemi) için farklı dönemlerde hasat edilmiştir. Deneme, "Karadeniz Yıldızı" sert mısır ve "Batem Tatlı" şeker mısır çeşitleri kullanılarak tesadüf blokları deneme desenine göre üç tekerrürlü olarak Isparta koşullarında iki ayrı deneme şeklinde 2019 yılında kurulmuştur. Her iki mısır alt türünde de dekara körpe ve taze koçan sayıları bakımından kontrol ile uygulamalar arasındaki farklılık istatistiksel olarak P≤0,01 düzeyinde önemli olurken, koçan özellikleri arasındaki farklar önemsiz çıkmıştır. Sert mısırda koçan koparılmayan uygulamada (kontrol) tane verimi bitki üzerinde tek koçan bırakılan uygulamaya göre daha yüksek olurken, koçan ve tane özellikleri bakımından bitki üzerinde tek koçan bırakılan uygulama kontrolden daha yüksek olmuştur. Sonuç olarak; bu uygulamaların başarısı mısır bitkisinin birden fazla koçan bağlama özelliğine bağlı olmakla birlikte, bir bitkiden iki veya üç farklı ürünün elde edilebileceği ve pratikte uygulanabilir bir yöntem olduğu sonucun varılmıştır.

Maize (*Zea mays* L.): Two or Three Different Products from One Plant

Keywords
Zea mays L., Fresh corn, Baby corn, Seed Characteristics

Abstract: The study was conducted to investigate the possibilities of obtaining more than one crop from one plant of maize. For this purpose, cops on the plant were harvested in different stages according to consumption aims for baby corn (ear silk-out time), boiling/roasting (milk maturity stage), and seed yield (full maturity). The experiment was set up as two separate trials according to randomized complete block design with three replications using "Karadeniz Yıldızı" flint corn and "Batem Tatlı" sweet corn in 2019 year in Isparta conditions. In both maize subspecies, the difference between the control and the treatments in terms of the number of baby and fresh ear per decare was statistically significant at the P≤0.01 level, while the difference between the ear characteristics was not significant. While the grain yield was higher in unremoved corn treatment (control) than the application with a single cob on the plant, the treatment with single cob on the plant was higher than the control in terms of the ear and grain characteristics. As a result; although the success of the treatments depends on the ear binding properties of more than one of the maize plants, it conclusion has been reached that two or three products can be obtained from one plant and it is a practically applicable method.

1. GİRİŞ

Mısır; dünyada ekim alanı, üretimi, kullanımı ve ticareti en fazla olan üç bitkiden biridir. Mısır hızlı gelişmesi, kısa sürede yüksek tane ve sap veriminden dolayı silaj, yeşil ve kesif yem olarak Dünyada ve Türkiye'de hayvansal üretimde yem açığının kapatılmasında önde gelen bitkilerden biridir. Mısırın yüksek melez gücünden dolayı son 20-25 yılda Türkiye'de verimi önemli ölçüde artmış ve silajı son yirmi yılda süt sığırlarının rasyonlarında temel yem bileşeni haline gelmiştir [1]. Mısırın tanesinden yemeklik yağ, biyoyakıt ve etanol, mısır şurubu, alkol üretimi ile sanayide kullanımı da hızla yükselmektedir. İnsan beslenmesinde haşlamalık/ közlemelk, popcorn, körpe mısır, çerez, un, sıvı yağ, nişasta, tatlandırıcı olarak geniş bir kullanım alanına sahiptir [2]. Mısır bu özellikleri ile gelişmiş ülke bitkisi olarak adlandırılabilir. Ülkelerin gelişmişlik düzeyi arttıkça hem üreticiler hem de tüketiciler bilinçlenmektedir. Böylece tarımda hibrit tohum

kullanımı artmakta, mısırın kullanıldığı sanayi kolları gelişmekte ve insan beslenmesinde tüketim tercihleri değişmektedir. Örneğin taze tüketim için atdişi ve sert mısır yerine şeker mısır tercihi, konserve ve körpe mısır tüketimi, şeker yerine tatlandırıcıların kullanımı ve diğer mısır ürünlerinin tüketimi artmaktadır.

Giderek artan dünya nüfusu ve azalan tarım alanları dikkate alındığında, insanların gıda ve hayvanların yem ihtiyacını karşılamak için tarım alanlarının birim alan verimini artırmak ve bu ürünlerden daha etkin faydalanmak gerekmektedir. Akdeniz iklimi dışında kalan bölgelerde ikinci ürün ve ara ürü tarımının yapılabilme olanaklarının araştırılması ve yaygınlaştırılması ile tarım alanları daha etkin kullanılabilir. Son yıllarda mısır tarımında hibrit tohum kullanımı önemli oranda artmıştır. Mısırda iri koçan oluşumu ve yüksek tohum verimi için her bitkinin tek koçan bağlaması istenmektedir. Ancak hibrit tohumlar ekildiklerinde çeşide, iklime ve yetiştirme koşullarına göre 3-4 koçan bağlayabilmektedirler. Bu durumda mısırdan daha etkin faydalanmak için hasat amacına göre (taze tüketim ve tohum) bir koçan ana üretim hedefi için ayrılıp, diğer koçanlar farklı tüketim amacıyla hasat edilebilir. Örneğin şeker mısırda bir koçan taze tüketim amacıyla bırakılıp bitkideki diğer koçanlar körpe mısır amacıyla koçan püskülü çıkarma devresinde, sert mısırda çok koçan bağlayan bitkilerde bir koçan tane hasadı için bitki üzerinde bırakılıp, bir koçan taze tüketim için süt olum döneminde ve diğer koçanlar körpe mısır olarak hasat edilebilir. Türkiye'de şeker mısırın fazla tanınmaması ve koçanının biraz küçük olması nedeniyle daha iri koçan yapısına sahip olan sert mısır taze tüketim amacıyla kullanılmaktadır. Mısırın yanı sıra fasulye bitkisinin bir kısmı taze tüketim, bir kısmı kuru tane amaçlı, patates bitkisinin bir kısmı erkenden turfanda şekilde, bir kısmı normal hasat zamanda hasat edilerek daha etkin kullanılabilir. Ancak fasulye ve patates gibi bitkilerde bu hasat şekli nihai ürünün verimini azaltabilir. Mısırda hibrit bitki ıslahında tek koçanlılık istenen bir özelliktir. Bu nedenle mısır bitkisi üzerinde tek koçan bırakılarak diğer koçanların farklı tüketim amacıyla hasat edilmesi ile hem istenen tek koçanlılığı sağlamış, hem de bitkiden daha etkin faydalanılmış olacaktır. Kara ve ark. [3] şeker mısırda ikinci koçanın koparılarak körpe mısır olarak değerlendirmesi ve bunun taze koçan özelliklerine etkisini araştırdıkları çalışmada, koparılan ikinci koçanların birinci koçan boyutlarına azda olsa pozitif katkı yaptığı, elde edilen koçanların körpe mısır olarak değerlendirebileceğini bildirmişlerdir. Kara [4] birim alandan daha fazla körpe mısır elde etmek amacıyla ocakta tohum sayısını artırarak yürüttüğü çalışmada en yüksek körpe koçan verimi ve koçan sayısını ocağa 5-6 tohum ekilmesi ile elde etmiştir. Yıldırkan ve Kara [5,6] karasal iklimin hüküm sürdüğü Burdur il merkezinde sulanabilen tarım arazilerde buğday hasadından sonra ikinci ürün koşullarında taze tüketim amaçlı 84-90. günde ve körpe mısır amacıyla 50-76. günde hasadının başarıyla yapılabildiğini ve kullanılan tarım arazisi üzerinde sonraki ürünün ekim zamanını etkilemeden üretim yapılabildiğini bildirmişlerdir.

Bu çalışma; şeker ve sert mısırda bitki üzerinde tek koçan bırakılıp, diğerlerinin kullanım amacına göre değişik olum dönemlerinde hasat edilerek bir bitkiden birden fazla ürün elde etme olanaklarını araştırmak amacıyla yürütülmüştür.

2. MATERYAL VE YÖNTEM

Araştırma, Isparta merkez ekolojik koşullarında "Batem tatlı" şeker mısır ve "Karadeniz yıldızı" sert mısır çeşitleri kullanılarak 2019 yılında yürütülmüştür. Denemede yer verilen çeşitler, önceki yıllarda farklı amaçlarla yürütülen çalışmalarda bir bitkide birden fazla koçan bağladığı gözlenen çeşitlerden seçilmiştir [20].

2.1. İklim Özellikleri

Isparta ili İç Anadolu, Akdeniz ve Ege bölgeleri arasında geçiş iklimi özelliğine sahiptir. Yıllık yağışın büyük bir bölümü kış aylarında yağmur ve kar şeklinde olup, uzun yıllar ortalama yağış miktarı 526,0 mm'dir. Denemenin yürütüldüğü yılın Mayıs-Eylül aylarına ilişkin toplam yağış miktarı 133,8 mm ve 204,7 mm, aynı döneminde aylık ortalama sıcaklık 19,4 ºC ve 19,6 ºC olmuştur (Tablo 1). Vejetasyon süresindeki gece sıcaklıklarının bir miktar düşmesinden kaynaklanan aylık ortalama sıcaklık değerleri mısır tarımı için düşük görünse de gündüz sıcaklıkları yüksek olması mısırı yetiştiriciliği için uygun koşulları oluşturmaktadır.

Tablo 1. Deneme yılına ve uzun yıllara ait iklim verileri*

İklim verileri	Yıllar	Aylar						Toplam veya Ort.
		Mayıs	Haziran	Temmuz	Ağustos	Eylül	Ekim	
Ortalama sıcaklık (ºC)	2019	17,0	20,6	23,4	24,4	18,9	12,6	19,4
	Uzun yıllar	15,6	20,2	23,6	25,8	18,3	13,4	19,5
Toplam yağış (mm)	2019	62,9	29,4	4,1	10,2	1,6	25,6	133,8
	Uzun yıllar	51,4	29,8	14,6	0,3	15,4	38,4	

*Isparta meteoroloji istasyonu kayıtları

2.2. Toprak Özellikleri

Deneme alanı toprağı hafif bazik (pH: 7,6), kireç oranı düşük (%13,6), organik madde içeriği orta (%2,2) ve kumlu-tınlı bir yapıdadır.

2.3. Denemenin Kurulması

Şeker ve sert mısır tohumları ayrı iki deneme şeklinde tesadüf blokları deneme desenine göre 3 tekerrürlü olarak parsel sıra uzunluğu 5 m ve 4 sıra, bloklar arasında 2 m, her parsel arasında bir sıra aralık bırakılarak 26 Nisan 2019'da kurulmuştur. Ekim işlemi; sıra arası 70 cm ve sıra üzeri 18 cm mesafede (70 cm x 18 cm) olacak şekilde elle

her ocağa iki tohum gelecek şekilde 4-5 cm derinliğinde ekilmiştir. Ekimden sonra parsellere damla sulama boruları döşenerek çıkıştan sonra her ocakta bir bitki kalacak şekilde tekleme yapılmıştır.

Uygulamalar: 1. Kontrol, her iki mısır türü için herhangi bir uygulama yapılmayıp geleneksel mısır yetiştiriciliği uygulanmıştır. 2. Uygulama I (U1): Her iki alt türde de bitki üzerinde birden fazla olan koçanlardan en üst koçan süt olum döneminde hasat edilmek üzere bırakılmış ve diğer koçanlar koçan püskülü çıkarma aşamasında körpe mısır (baby corn) olarak hasat edilmiştir. 3. Uygulama II (U2): Sert mısırda ikiden fazla olan koçanlardan en üst koçan tam olum döneminde tane mısır amaçlı, hemen altındaki koçan süt olum döneminde taze haşlamalık mısır olarak ve diğer koçanlar koçan püskülü çıkarma aşamasında körpe mısır olarak hasat edilmiştir. Bu uygulamada iki koçan bağlayan bitkilerde ikinci koçan süt olum döneminde, tek koçan bağlayan bitkilerin koçanları ise tam olum döneminde hasat edilmiştir.

Toprak analiz sonuçları esas alınarak her iki denemede de saf olarak 20 kg da^{-1} azot ve 8 kg da^{-1} P_2O_5 uygulanmıştır [7]. Azotun yarısı (amonyum sülfat formunda %21) ekimle, kalan yarısı boğaz doldurmadan sonra bitki diz boyuna (35-40 cm) ulaştığında, fosforun ise tamamı ekimle birlikte verilmiştir.

Ekimden sonra çıkış yapana kadar ve çıkıştan sonra toprak nem düzeyi kontrol edilerek sulama yapılmıştır. Hasat, her parselde uçlardan 50 cm ve kenarlardan 1'er sıra kenar tesirleri atıldıktan sonra her iki mısır alt türünde de körpe mısır için koçan püskülü çıkışının 2. gününde, haşlamalık veya közlemelik için süt olum döneminin sonuna doğru ve sert mısırda tane hasadı için tam olum döneminde tane nemi %12-13 iken hasat edilmiştir.

Körpe mısırda; körpe koçan boyu (cm), körpe koçan çapı (mm), körpe koçan ağırlığı (g) ve körpe koçan sayısı (adet da^{-1}) [8], taze mısırlarda; koçan boyu (cm), koçan çapı (mm), koçanda tane sayısı (adet) ve tek koçan ağırlığı (g) [9] ve sert mısırda; koçan boyu (cm), çapı (mm), ağırlığı (g), koçanda tane sayısı (adet), 1000 tohum ağırlığı (g), hektolitre ağırlıkları (kg^{100L}) ve tane verimi (kg da^{-1}) [23] değerleri belirlenmiştir.

2.4. Verilerin İstatistiki Olarak Değerlendirilmesi

Çalışmadan elde edilen verilerin varyans analizleri SAS istatistik paket programından faydalanılarak ayrı ayrı yapılmış ve istatistik açıdan önemli olduğu ortaya çıkan ortalamalar arasındaki farklılıklar LSD testine ($P<0.05$, $P<0.01$) göre karşılaştırılmıştır.

3. SONUÇLAR VE TARTIŞMA

3.1. Körpe Koçan Özellikleri

Her iki mısır alt türünde de dekara körpe koçan sayıları bakımından kontrol (12390,5 ve 12462,7 adet/da) ile U1 (4420,0 ve 845,3 adet/da) arasındaki farklılık istatistiksel olarak $P\leq0,01$ düzeyinde önemli olurken, koçan özellikleri arasındaki farklar önemsiz bulunmuştur (Tablo 2). TAS 1504-2007 standartlarına göre, her iki mısır alt türüne ait körpe mısır koçanları pazarlanabilir özellikler taşımaktadır. Kontrol uygulamasının körpe koçan sayısının yüksek çıkması; koçanların koparılmamasından kaynaklanırken, körpe koçan özellikleri arasında farkın çıkmaması; hem kontrolde hem de U1'de körpe mısır hasadının bitkide koçan püskülünün çıkışının ikinci gününde yapılması ve koçanların gelişimini tamamlamaması ile açıklanabilir. Sert mısırın körpe koçan özellikleri şeker mısırdan daha yüksek olmuştur. Bu farklılık sert mısırın genetik olarak hem bitki morfolojisi olarak hem de koçan özellikleri bakımından şeker mısırdan daha büyük yapıda olması ve bu özelliğin körpe koçanda da kendini göstermiş olmasından kaynaklanmaktadır. Kara ve ark. [10] sert mısırın körpe koçan özelliklerinin şeker ve cin mısırdan daha yüksek olduğunu bildirmişlerdir. Körpe mısırın koçan özelliklerinin mısır alt türlerine, çeşitlerin erkenci ve geçci olmalarına, koçan bağlama sayısı gibi özeliklerine bağlı olarak önemli ölçüde değişmektedir. Almeida ve ark. [11] ortalama körpe mısır koçan çapının 13,6 mm, boyunun 9,36 cm ve koçan sayısının 6814,6 adet da^{-1} olduğunu, Castro ve ark. [12] ortalama körpe mısır koçan çapının 16,5 mm, koçan boyunun 11,4 cm ve Kara ve ark [10] körpe mısır koçan çapının 12,7-13,5 mm arasında, koçan boyunun 9,4-10,4 cm arasında olduğunu tespit etmişlerdir. Çalışmamızda elde edilen körpe koçan özellikleri araştırmalarda belirtilen sınırlar içerisinde yer almıştır. Gözübenli ve Konuşkan [13] ile Lopes ve ark. [14] körpe mısır verim ve koçan özeliklerinin cinslere ve hatta aynı cinse ait mısır çeşitleri arasında da farklılıklar gösterdiğini bildirmişlerdir.

Tablo 2. Şeker ve sert mısırda alt koçanların körpe mısır özellikleri

Şeker mısır				
Uygulamalar	Körpe koçan sayısı (da^{adet})	Körpe koçan boyu (cm)	Körpe koçan çapı (mm)	Körpe koçan ağırlığı (g)
Kontrol	12390,5 a	11,3	9,10	12,5
UI	4420,0 b	11,7	9,33	12,3
F değeri	358,85**	1,07	0,49	0,18
LSD (%)	417,5	öd	öd	öd
CV(%)	6,13	2,05	1,44	3,17
Sert mısır				
Uygulamalar	Körpe koçan sayısı (da^{adet})	Körpe koçan boyu (cm)	Körpe koçan çapı (mm)	Körpe koçan ağırlığı (g)
Kontrol	12462,7 a	15,5	13,9	14,2
UI	845,3 b	15,3	14,3	14,8
F değeri	191,3**	0,17	0,63	0,99
LSD (%)	263,9	öd	öd	öd
CV(%)	4,88	4,40	2,17	3,06

**: $P\leq0.01$ düzeyinde önemli, öd: Önemli değil
UI: Bitki üzerinde birden fazla olan koçanlardan en üst koçan taze mısır olarak bırakılmış ve diğer koçanlar körpe mısır olarak hasat edilmiştir.

3.2. Taze Koçan Özellikleri

Her iki mısır alt türünde de (şeker ve sert mısır) en üst koçanlar taze mısır olarak hasat edilmiştir. Kontrol uygulamasının dekara koçan sayıları (12021,3 ve 12229,0 adet/da) U1 den (6015,7 ve 4890,3 adet/da) ve sert mısırda U2 den (5524,7 adet/da) daha yüksek olurken, taze koçan özellikleri bakımından istatistiksel olarak fark çıkmamıştır (Tablo 3). Araştırmada sert mısırda U1 ile U2 uygulamasının dekara koçan sayıları arasında istatiksel olarak fark çıkmamıştır. Kontrol uygulamasında taze koçan sayısının yüksek çıkması; koçanların tamamının sayılmasından kaynaklanırken, taze koçan özellikleri arasında farkın çıkmaması; süt olum dönemi sonunda hasat edilen taze mısırlarda nişasta dolum döneminin başlamamış olmasından kaynaklandığı düşünülmektedir. Çünkü nişasta dolum dönemi (sarı olum) verim ve verimle ilişkili komponentleri doğrudan etkilemektedir [15]. Taze tüketim amaçlı mısırın pazarlanmasında etkili olan en önemli iki koçan özelliği boyu ve çapıdır. Amerikan (US) tüketici standartları sınıflandırmasına (US Fancy, US No. 1 ve US No. 2) göre şeker mısırdan elde edilen taze koçanların %65'i, sert mısırdan elde edilen koçanların ise %80'i pazarlanabilir koçan sınıfına girmiştir. Şeker mısır kardeşlenme özelliğine sahiptir, bu nedenle kardeşlerden ve aynı bitkiden çıkan ikinci koçanlar pazarlanabilir koçan sınıfı dışında kalmıştır. Sert mısırın taze koçan özellikleri şeker mısırdan daha yüksek olmuştur. Bu farklılığın iki alt türün genetik özelliklerinden kaynaklandığı düşünülmektedir. Kara ve ark. [3] şeker mısırda koparılan ikinci koçanların taze mısır boyu, çapı ve ağırlıklarını pozitif etkilediğini bildirmiştir.

Kara ve Akman [16] Isparta koşullarında şeker mısırın koçan boyunun 19,2-20,9 cm, koçan çapının 45,6-47,5 mm, koçandaki tane sayısının 713-720 adet, tek koçan ağırlığının 320,3-329,7 g, Sakin ve Azapoğlu [17] Tokat koşullarında şeker mısırın koçan boyunun 19,6-20,8 cm ve tek koçan ağırlığının 181,0-260,5 g ve Yıldırkan ve Kara [5] Burdur koşullarında şeker mısırın koçan boyunun 17,5- 22,0 mm, çapının 43,6-50,3 mm, koçanda tane sayısının 515,6-750,4 adet, ağırlığının 201,1-315,4 g ve taze koçan sayısının 10384,5-10732,0 da^{adet} arasında değiştiğini bildirmişlerdir. Mısırda koçan özelliklerinin ekolojik koşullara, çeşitlere, kardeşlenme özelliklerine, bakım işlemlerine ve koçan bağlama sayısı gibi özeliklere bağlı olarak değişebileceği pek çok araştırıcı tarafından bildirilmiştir [18, 19].

Tablo 3. Şeker ve sert mısırda taze koçan özellikleri

Şeker mısır					
Uygulamalar	Koçan sayısı (da^{adet})	Koçan boyu (cm)	Koçan çapı (mm)	Koçan ağırlığı (g)	Koçanda tane sayısı (adet)
Kontrol	12021,3 a	15,3	38,6	184,7	499,3
UI	6015,7 b	15,9	39,3	187,6	527,6
F değeri	156,06**	1,00	0,57	0,22	3,75
LSD (%)	477,1	öd	öd	öd	öd
CV(%)	6,52	4,44	2,63	4,35	6,07
Sert mısır					
Uygulamalar	Koçan sayısı (da^{adet})	Koçan boyu (cm)	Koçan çapı (mm)	Koçan ağırlığı (g)	Koçanda tane sayısı (adet)
Kontrol	12229,0 a	18,1	39,0 b	198,6	579,5
UI	4890,3 b	18,6	41,6 a	203,3	576,3
UII	5524,7 b	18,3	40,3 ab	200,1	569,8
F değeri	153,5**	1,29	1,21	2,49	1,54
LSD (%)	675,0	öd	1,53	öd	öd
CV(%)	2,38	3,34	2,05	3,48	4,06

**: P≤0.01 düzeyinde önemli, öd: Önemli değil
UI: Bitki üzerinde birden fazla olan koçanlardan en üst koçan taze mısır olarak bırakılmış ve diğer koçanlar körpe mısır olarak hasat edilmiştir.
UII: Sert mısırda bitki üzerinde ikiden fazla olan koçanlardan en üst koçan tane mısır, hemen altındaki koçan taze mısır ve diğer koçanlar körpe mısır olarak hasat edilmiştir.

3.3. Sert Mısırda Verim, Koçan ve Tane Özellikleri

Sert mısırda birden fazla koçan bağlayan bitkilerde koçan koparılmasının koçan boyu, çapı, ağırlığı, koçanda tane sayısı, tane verimi, bin tane ağırlığı, hektolitre ağırlığı, tane genişliği ve tane boyuna etkisi istatistiksel olarak önemli olmuştur (Tablo 4). Araştırmada koçan koparılmayan kontrol uygulamasında tane verimi bitki üzerinde tek koçan bırakılan uygulamalara göre daha yüksek olurken, incelenen koçan ve tane özellikler bakımından bitki üzerinde tek koçan bırakılan uygulamalarda kontrole göre daha yüksek değerler belirlenmiştir. Kontrol uygulamasında tane veriminin yüksek olması birden fazla koçan bağlayan bitkilerdeki koçanların koparılmamasına ve dolayısıyla daha fazla koçan sayısına bağlanabilir. U2 uygulamasında koçan ve tane iriliği özelliklerinin yüksek olması, bitki üzerinde en üst koçanın bırakılması ve bir C_4 bitkisi olan mısırın üst yapraklarındaki fotosentez ürünlerinin daha kısa yoldan tek bir koçana taşınması ile ilişkili olduğu ve bunun koçan ve tane iriliğine yansıması ile açıklanabilir. Akdoğan ve Kara [20] sert mısırda ortalama tane genişliğini 4,86-5,19 mm, tane boyunu 9,24-9,64 mm, koçanda tane sayısını 622,2-631,5 adet, bin tane ağırlığını 384,3-397,1 g, hektolitre ağırlığını 72,8-73,2 kg ve tane verimini 1202,1-1263,2 kg da^{-1} arasında, Öztürk ve Büyükgöz [21] Trabzon ili yerel mısır popülasyonlarında koçan uzunluğunu 10,85-21,95 cm, koçan çapını 3,34-4,71 cm, koçanda tane sayısını 193.1-534.5, bin tane ağırlığını 270,6-397,0 g ve tane verimini 319,3-1167,1 kg da^{-1} arasında belirlemişlerdir. Bu çalışmada belirlenen sonuçlar araştırıcıların bildirdiği sınırlar içerisinde yer almaktadır. Mısırda tane verimi, koçan ve tane özellikleri gibi parametreler çeşitlere, iklim faktörlerine, agronomik işlemlere ve bitki üzerinde yürütülen farklı uygulamalara göre değişebilir [21, 22, 23].

Tablo 4. Sert mısırda tane özellikleri ve verim

Uygulamalar	Koçan boyu (cm)	Koçan çapı (mm)	Koçan ağırlığı (g)	Koçanda tane sayısı (adet/koçan)	Tane verimi (kg da^{-1})
Kontrol	20,6 b	46,3 b	236,3 b	547,3 b	1160,3 a
UII	22,3 a	48,0 a	248,1 a	558,4 a	895,0 b
F değeri	4,10*	4,57*	5,90*	7,99*	19,62**
LSD (%)	1,21	0,96	6,24	8,06	226,83
CV(%)	2,70	6,02	6,50	2,58	6,11

Uygulamalar	1000 tane ağırlığı (g)	Hektolitre ağırlığı (kg$^{100\ L}$)	Tane genişliği (mm)	Tane boyu (mm)
Kontrol	320,4 b	63,9 b	8,75 b	8,85 b
UII	338,0 a	65,6 a	9,36 a	9,01 a
F değeri	7,62*	6,20*	5,19*	4,43*
LSD (%)	12,30	1,23	0,51	0,12
CV(%)	7,29	3,71	4,57	6,90

*, **: Sırsıyla P≤0.05 ve P≤0.01 düzeyinde önemli, öd: Önemli değil
UII: Sert mısırda bitki üzerinde ikiden fazla olan koçanlardan en üst koçan tane mısır, hemen altındaki koçan taze mısır ve diğer koçanlar körpe mısır olarak hasat edilmiştir.

4. SONUÇ

Mısırın birden fazla koçan bağlayan bitkilerinde farklı tüketim amaçlarına göre değişim olum dönemlerinde hasat edilmiş ve dekara koçan sayısı dışında hem körpe mısır hem de taze mısır koçan özelliklerini etkilememiştir. Çeşitlere göre ekimden itibaren 55-70. günlerde körpe mısır, 81-102. günlerde taze mısır hasadı yapılmıştır. TAS 1504-2007 standartlarına göre, her iki mısır alt türüne ait körpe mısır koçanları pazarlanabilir özelliklere sahip olmuş ve US Fancy, US No. 1 ve US No. 2'ye göre taze koçanların %65 (şeker mısır) ile %80'i (sert mısır) pazarlanabilir koçan sınıfına girmiştir. Tane amaçlı mısır üretiminde bitki üzerinde tek koçan bırakılması koçan ve tane özeliklerini pozitif etkilemiştir.

Sonuç olarak; i. Her iki mısır alt türünde de birden fazla koçan bağlayan bitkilerde tek koçan bırakılarak diğer koçanların farklı tüketim amacıyla erken dönemlerde koparılmasının, körpe ve taze koçan özellikleri üzerine olumsuz bir etkisinin olmadığı, bununla birlikte sert mısırda tam olum döneminde tane ve koçan özelliklerini olumlu etkilediği belirlenmiştir. ii. Tek koçak bırakılarak diğer koçanların koparılmasının sert mısırın tane veriminde bir düşüşe neden olmasına rağmen tane boyutlarına pozitif yansıması nedeniyle tohumluk mısır üretiminde bu yöntem uygulanabilir. iii. Mısırda bu uygulamaların başarısı bitkilerin birden fazla koçan bağlama özelliklerine bağlı olmakla birlikte, bir bitkiden iki veya üç farklı ürünün elde edilebileceği ve pratikte uygulanabilirliğinin olduğu soncuna varılmıştır.

KAYNAKLAR

[1] Korkmaz Y, Ayasan T, Aykanat S, Avcı M. Çukurova ikinci ürün koşullarında yetiştirilen silajlık mısır (*Zea mays* L.) çeşitlerinin verim ve silaj kalite performanslarının değerlendirilmesi. Türk Tarım-Gıda Bilim ve Tek Der. 2019; 7: 13-19.

[2] Özcan S. Modern dünyanın vazgeçilmez bitkisi mısır: Genetiği değiştirilmiş (Transgenik) mısırın tarımsal üretime katkısı. Türk Bilimsel Derlemeler Der. 2009; 2(2): 1-34.

[3] Kara B, Gül H, Dizlek H. Şeker mısırda kardeş ve ikinci koçanın koparılmasının taze/körpe koçanın verimine ve bazı özelliklerine etkisi. Mediterranean Agric Sci. 2018; 31(2): 137-140, https://doi.org/10.29136/mediterranean.379093.

[4] Kara B. Ocakta tohum sayısının körpe mısır verimine ve bazı özelliklerine etkisi *Akademik Ziraat Der.* 2019; 8(1): 93-96, http://dx.doi.org/10.29278/azd.593820.

[5] Yıldırkan Ü, Kara B. Burdur ikinci ürün koşullarında bazı şeker mısır (*Zea mays* L. *var. saccharata*) çeşitlerinin taze koçan özellikleri. Türk Bilim ve Müh Der, 2020a; 2(1): 30-33.

[6] Yıldırkan Ü, Kara B. Burdur koşullarında ikinci ürün körpe mısır yetiştirme olanaklar. Türk Doğa ve Fen Der. 2020b; 9: 114-117.

[7] Özkan A, Ülger AC. Çukurova ekolojik koşullarında değişik azot dozu uygulamalarının iki cin mısırı (*Zea mays* L. *everta* Sturt.) çeşidinde tane verimi ve bazı tarımsal özelliklere etkisi. Yüzüncü Yıl Üniv Tarım Bilim Der. 2011; 21(3): 198-208.

[8] Bar-Zur A, Saadi H. 1990. Prolific maize hybrids for baby corn. J of Horti Sci. 1990; 65: 97-100.

[9] Lizaso JI, Boote KJ, Cherr CM, Scholberg JMS, Casanova JJ, Judge J, Jones JW, Hoogenboom G. Developing a sweet corn simulation model to predict fresh market yield and quality of ears. J American Society.Horti Sci. 2017; 132(3): 415-422.

[10] Kara B, Şener A, Işık C, Gündüz A. 2017. Farklı mısır (*Zea mays* L.) alt türlerinin körpe mısır özelliklerinin karşılaştırılması. Uluslararası Tarım ve Yaban Hayatı Bilim Der. 2017; 3(2): 95-99.

[11] Almeida IPC, Silva PSL, Negreiros MZ, Barbosa Z. Baby corn, green ear, and grain yield of corn cultivars. Horticulture Brasilia, 2005; 23: 960-964.

[12] Castro RS, Silva PSL, Cardoso MJ. Baby corn, green corn, and dry corn yield of corn cultivars. Horticultura Brasileira, 2013; 31: 100-105.

[13] Gözübenli H, Konuşkan Ö. Farklı bitki sıklıklarının bazı mısır genotiplerinde körpe koçan (baby corn) verimi ve özelliklerine etkisi. Türkiye VIII. Tarla Bitkileri Kongresi, 19-22 Ekim, Hatay, Poster Bil., 2009, s. 573-576.

[14] Lopes AP, Nobrega LHP, Pacheco FP, Cruz-Silva CTA. Maize varieties for baby corn yield and post-harvest quality under organic cropping. Bioscience J. 2016; 32: 298-307.

[15] Kün E. Serin İklim Tahılları. Ders Kitabı No: 299, AÜ Ziraat Fakültesi Yayın No: 032, 1998, Ankara

[16] Kara B, Akman Z. Şeker mısırında (*Zea mays saccharata* Sturt.) koltuk ve uç alma ile yaprak sıyırmanın verim ve koçan özelliklerine etkisi.

Akdeniz Üniv Ziraat Fakültesi Der. 2002; 15(2): 9-18.

[17] Sakin MA, Azapoğlu Ö. Tokat-Kazova koşullarında şeker mısırın (*Zea mays saccharata* Sturt.) taze koçan ve tane verimi ile bazı verim ve kalite özelliklerine azot ve fosforun etkileri. Gaziosmanpaşa Üniv Ziraat Fakültesi Der. 2017; 34(3): 46-55, doi:10.13002/jafag4275.

[18] Özata E, Geçit HH, Ünver İS. Orta Karadeniz ekolojik koşullarında şeker mısırda (*Zea mays saccharata* Sturt.) değişik ekim sıklıkları ve azot dozlarının verim öğelerine etkisi. Tarla Bitkileri Merkez Araş Ens Der. 2016; 25(1): 74-80.

[19] Stansluos AAL, Öztürk A, Kodaz S. Agronomic performance of different sweet corn varieties in the highest plain of Turkey: Quality characteristics. Atatürk Üniv Ziraat Fakültesi Der. 2020; 51(3): 249-257.

[20] Akdoğan M, Kara B. Atdişi ve sert mısırda yaprak sıyırma ve uç almanın verim ve bazı tane özelliklerine etkisi. Adnan Menderes Üniv Ziraat Fakültesi Der. 2020; 17: 215-219.

[21] Öztürk A, Büyükgöz A. Trabzon iline ait bazı yerel mısır populasyonlarının agronomik performansları. Atatürk Üniv Ziraat Fakültesi Der. 2021; 52(1): 67-80. https://doi.org/10.17097/ataunizfd.768620.

[22] Pamukçu M, Erdal G, Savur O, Toros A, Özata E. Beyaz hibrit mısır aday çeşitlerinin Antalya ve Samsun koşullarında performanslarının değerlendirilmesi. Türkiye 9. Tarla Bitkileri Kongresi, 21-15 Eylül 2011, Bursa.

[23] Konuşkan Ö, Atış İ, Gözübenli H. Yield and yield components of some dent maize genotypes grown as main-crop in Amik plain conditions. Mustafa Kemal Univ J of Agric Fac. 2015; 20: 1-6.

Araştırma Makalesi https://doi.org/10.46810/tdfd.955393 Research Article

Türk Doğa ve Fen Dergisi
Turkish Journal of Nature and Science
www.dergipark.gov.tr/tdfd

Homogeneity and Trend Analysis of Temperature Series in Hirfanli Dam Basin

Utku ZEYBEKOĞLU[1*], Gaye AKTÜRK[2]

[1] Sinop University, Boyabat Vocational School of Higher Education, Construction Department, Boyabat, Sinop, Turkey
[2] Kirikkale University, Faculty of Engineering and Architecture, Department of Civil Engineering, Kirikkale, Turkey
Utku Zeybekoğlu ORCID No: 0000-0001-5307-8563
Gaye AKTÜRK ORCID No: 0000-0002-9477-7827

**Corresponding author: utkuz@sinop.edu.tr*

(Received: 21.06.2021, Accepted: 23.02.2022, Online Publication: 25.03.2022)

Keyywords
Trend analysis, Homogeneity analysis, Spearman's Rho Test, Mann Kendall Test, Hirfanli Dam basin

Abstract: Climates are constantly changing on a temporal and spatial scale, so they are not static. In recent years, global warming and changes in climate have shown more and more effects on the hydrological cycle and water resources, and their effects have become so noticeable that they hinder sustainable life. For this reason, the studies on the investigation of the main causes of the observed changes in the climate, the evaluation of climate change as a process and the determination of the effects that will emerge, have increased over time. In the present study, the homogeneity of annual and seasonal temperature series in Hirfanli Dam basin were examined by using the Pettitt Test (PT), and the trends were examined with the Spearman's Rho (SR) test and Mann Kendall (MK) test. Hirfanli Dam basin, which is located in the semi-arid climate region where climate change can be seen due to its location, was chosen as the study area. The temperature data of the Gemerek, Kayseri, Kirsehir, Nevsehir, Sivas and Zara meteorological stations in the basin between 1965 and 2017 were analyzed. It was noted that summer temperatures increased throughout the basin. Significant trends to increase were also detected in spring and autumn. The trend to increase was statistically significant at a 95% confidence level in all stations except for the Zara in terms of annual temperatures. Trend maps were prepared for the basin by using the results obtained here and the Geographical Information Systems. It was reported that the tendency to increase in annual temperature series was because of the increase in summer temperatures at intense levels throughout the basin.

Hirfanlı Baraj Havzasında Sıcaklık Serilerinin Homojenlik ve Eğilim Analizleri

Anahtar Kelimeler
Trend analizi, Homojenlik analizi, Spearman's Rho Test, Mann Kendall Test, Hirfanlı Baraj havzası

Öz: İklimler durağan olmamakla beraber zamansal ve mekânsal ölçekte sürekli değişim halindedir. Son yıllarda küresel ısınma ve iklimde gözlenen değişimler, hidrolojik çevrim ve su kaynakları üzerinde gün geçtikçe daha fazla etkisini göstererek, günümüzde sürdürülebilir yaşamı engelleyecek boyutlarda hissedilebilir hale gelmiştir. Bu sebeple, iklimde gözlenen değişimlerin temel sebeplerinin araştırılması, iklim değişikliğinin süreç olarak değerlendirilmesi ve ortaya çıkacak etkilerin belirlenmesine yönelik yapılan çalışmaların sayısı zamanla artmaktadır. Çalışmada, Hirfanlı baraj havzasındaki yıllık ve mevsimlik sıcaklık serilerinin homojenlikleri Pettitt Testi (PT), eğilimleri ise Spearman's Rho (SR) ve Mann Kendall (MK) testleri kullanılarak araştırılmıştır. Yarı kurak iklim bölgesinde yer alan ve konumu gereği iklim değişiminin görülebileceği Hirfanlı Baraj havzası çalışma alanı olarak seçilmiştir. Havzada içerisinde bulunan Gemerek, Kayseri, Kırşehir, Nevşehir, Sivas ve Zara meteoroloji gözlem istasyonlarına ait 1965-2017 yılları arasındaki sıcaklık verileri analiz edilmiştir. Havza genelindeki yaz sıcaklıklarının arttığı dikkat çekmektedir. İlkbahar ve sonbahar mevsimlerinde de anlamlı artma eğilimleri belirlenmiştir. Yıllık ortalama sıcaklıklarda ise Zara dışındaki bütün istasyonlardaki artma eğilimleri istatistiki olarak %95 güven düzeyinde anlamlıdır. Elde edilen sonuçlar ve coğrafi bilgi sistemleri kullanılarak havzaya ait trend haritaları hazırlanmıştır. Yıllık sıcaklık serilerindeki artma eğiliminin havza genelinde yoğun bir şekilde yaz sıcaklıklarından artmasında kaynaklandığı ifade edilmiştir.

1. INTRODUCTION

Different climatic conditions occurred in Turkey due to global warming, as it is the case in other countries in the world. Due to being surrounded by seas on three sides, has a fragmented topography and orographic features, the effects of global climate change occur differently in various regions of our country [1]. Climate parameters need to be analyzed in order to determine the effects of climate change and to take necessary measures [2, 3]. Hydro-meteorological parameters were investigated during the observation periods in order to investigate the effects of global climate change on our country [4-20]. Partal and Kahya [21] examined the trends of precipitation from 1929 to 1993 of 96 stations. Ucgun [22] conducted trend analysis of precipitation, temperature, evaporation and flow data obtained from stations in the Kızılırmak basin. Yerdelen [23] investigated the trends of Susuruluk basin flows using the Sequential MK. It is stated that there is a downward trend in river flows in the basin. Simsek et al. [24] investigated the seasonal and annual trends of temperature, humidity, wind speed and precipitation data of Hatay. In Antakya, they determined an increase in temperature, a decrease in wind speed, an increase in temperature and precipitation and a decrease in humidity values for the Iskenderun. Zeybekoglu and Karahan [25] investigated the trends of annual maximum rainfall intensity series for 206 stations using the MK, SR and Innovative Trend Analysis.

Southeast, Central Anatolia, Aegean and Mediterranean Regions, which have the characteristics of arid and semi-arid climates under the threat of desertification and which are expressed as semi-humid regions due to their lack of sufficient water resources, are expected to be affected more by the increase in temperature [26, 27]. From the past to the present, research has been carried out for seven geographical regions using temperature data, which is the subject of this study also. Toros [28] evaluated low and high temperature data and precipitation data of 18 stations. When daytime and nighttime temperatures are compared, they determined that there are significant increases in night temperature. Kadioglu [29] used temperature data measured at 18 stations between 1929 and 1990 and investigated local and regional trend analysis with the MK. Altin et al. [30] conducted trend analysis using rainfall and temperature series of 33 stations in the Central Anatolia region between 1975 and 2007 using the MK test in the analysis, and observed that the precipitation decreases in the winter and spring months and tends to increase in the summer and autumn months. Kizilelma et al. [31] determined that there were significant increases in the maximum and minimum temperature trends for the central Anatolia region, and that there were increases in the values of the mean temperatures at all stations, except the Ürgüp. Dogan et al. [32] reported in their study that the trends achieved a milestone in the 1950-2006 period based on the analysis of trends in temperature series in Turkey. Ulke and Ozkoca [33] investigated the changes in temperature series of Sinop Ordu and Samsun provinces located in the central Black Sea Region over time using the MK Test and Sen's Trend Slope Test. As a result of their findings, they stated that the temperatures in the region are in an increasing trend. Gumus [34] investigated precipitation and temperatures in the Seyhan-Ceyhan river basin. As a result of annual and seasonal scale evaluations, it has been determined that temperatures tend to increase throughout the basin.

In this study, Hirfanli Dam basin, which is located in the semi-arid climate region where climate change can be seen due to its location, was chosen as the study area. Seasonal and annual temperature series analyzes were made by using PT, SR and MK Tests.

2. MATERIALS AND METHHOD

2.1. Study Area

The Hirfanli Dam basin, which is a sub-basin of the Kizilirmak River basin, is about 27,092 km^2 in areal size (Fig.1.) and located between 33.3-38.7ºE longitudes and 38.3-40.1ºN latitudes. The Hirfanli Dam, which was built on the Kizilirmak River in 1959 for flood control and hydropower purposes, has a surface area of 263 km^2 and reservoir volume of 5,980 hm^3 at normal water surface level. The Hirfanli Dam basin has a high and mountainous plateau with the altitude varying between 799-3880 m. The east part of the basin is the hilliest region of the basin, which consists of high peaks and is bordered by mountainous areas. Plateaus, wide plains, and meadows are more common in the west part of the basin. Agriculture is a major economic sector in the study area where wheat, barley, potato and sugar beet are the main agricultural products [35, 36].

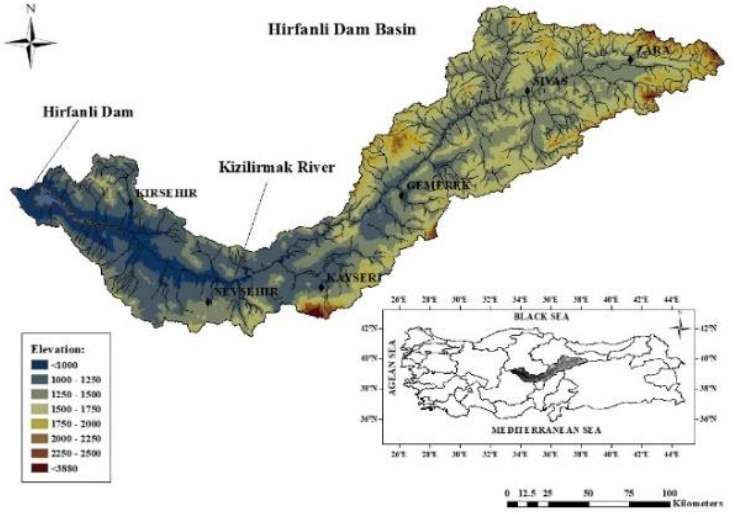

Figure 1. Hirfanli Dam basin

Annual and seasonal mean temperature data between 1965 and 2017 were obtained from the Turkish State Meteorological Service. Table 1 gives the geographical details of the six meteorological stations used in the study. Statistical characteristics of annual and seasonal mean temperature (minimum, maximum and mean) are shown in Table 2.

Table 1. Geographical information of the meteorological stations in the Hirfanli Dam basin

Station Name	Station ID	Latitude (N)	Longitude (E)	Elevation (m)
Gemerek	17162	39.11	36.04	1173
Kayseri	17196	38.44	35.29	1093
Kirsehir	17160	39.09	34.10	1007
Nevsehir	17193	38.35	34.40	1260
Sivas	17090	39.45	37.01	1285
Zara	17716	39.54	37.45	1348

Table 2. Statistical information of temperature series in the Hirfanli Dam basin (°C)

		Gemerek	Kayseri	Kirsehir	Nevsehir	Sivas	Zara	Basin
Annual	Min.	6.94	8.41	9.43	8.49	6.64	5.94	7.64
	Max.	11.77	13.23	13.78	13.64	11.99	11.27	12.61
	Mean	9.63	10.52	11.46	10.69	9.17	8.63	10.02
Winter	Min.	-7.63	-6.87	-3.80	-4.73	-7.93	-9.03	-6.39
	Max.	2.47	4.13	4.70	5.40	2.87	2.60	3.67
	Mean	-1.66	-0.46	0.93	0.71	-1.89	-2.30	-0.78
Spring	Min.	6.80	8.17	7.70	7.13	6.37	5.23	7.38
	Max.	11.63	13.07	12.73	12.40	11.10	10.83	13.36
	Mean	9.20	10.23	10.52	9.83	8.67	7.96	9.40
Summer	Min.	17.90	18.73	19.83	17.73	16.90	16.03	17.86
	Max.	22.20	23.70	24.30	23.03	21.93	20.90	22.59
	Mean	20.15	21.07	21.95	20.50	19.29	18.61	20.26
Autumn	Min.	8.30	8.87	10.37	9.37	8.33	7.73	8.94
	Max.	13.63	13.67	15.00	14.63	12.90	12.30	13.36
	Mean	10.81	11.24	12.44	11.70	10.60	10.26	11.18

The basin is dominated by convective and frontal precipitation in general. The mean temperature is around 10.02ºC and also the annual temperature decreases from the upstream to the downstream due to the increase in altitude. In the basin the hottest months are July and August, and the coldest months are January and February, and the difference between the highest temperature value and the lowest temperature value is over 10ºC. While the temperature is around 21~22ºC in July and August, the temperature drops to around -2~-1ºC in January and February. As can be seen, the mean temperature drops below 0ºC in winter months.

According to Table 2, the maximum temperature is during the summer at 20.26ºC; the minimum temperature is seen in the winter at -0.78ºC. In addition, the mean temperature values of basin in autumn and spring were 11.18ºC and 9.40ºC, respectively. The spatial distribution of seasonal and annual temperature in the basin was given in Figure 2.

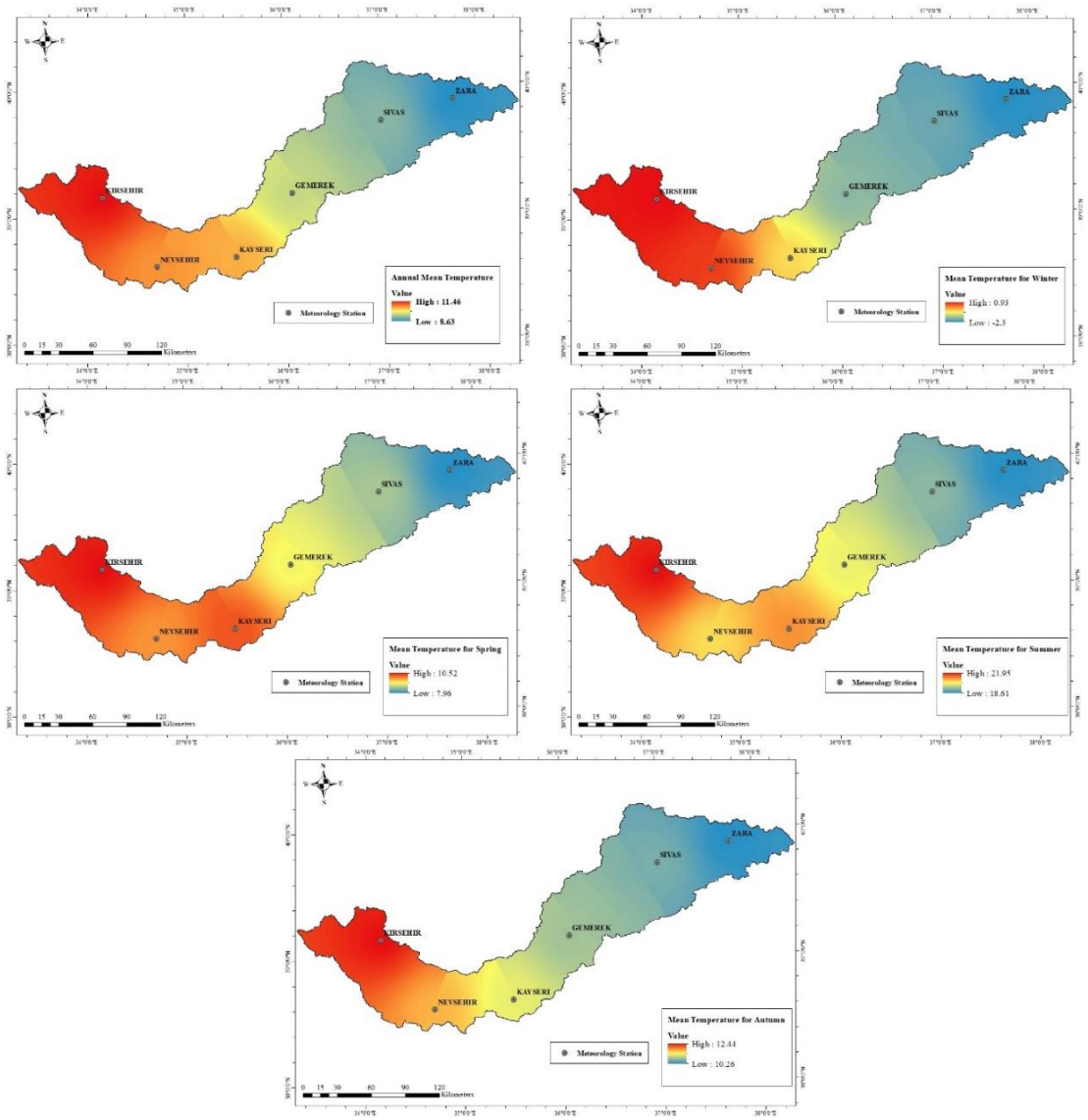

Figure 2. Spatial distribution of annual and seasonal temperature series

2.2. Pettitt Test (PT)

This non-parametric method developed by Pettitt [37] to determine the change point in a time series can find the change point on a monthly or annual scale [37]. The null hypothesis (H_0) states that the series has an independent and random distribution, the alternative hypothesis states that there is a sudden change. The test statistic is associated with the Mann-Whitney statistic [38]. The critical values of this test are given in Table 3 [37].

Table 3. Critical values of X_E

N	20	30	40	50	70	100
%95	57	107	167	235	393	677
%99	71	133	208	293	488	841

Observation values Y_1, ..., Y_n values are listed as r_1, ..., r_n.

$$X_k = 2\sum_{i=1}^{k} r_i - k(n+1)\,; k = 1,\ldots\ldots,n \qquad (1)$$

Xk values are plotted graphically by means of Equation 1. In Equation 2, the absolute maximum value of X_k determines the change point.

$$X_E = max_{1\le k\le n}^{|X_k|} \qquad (2)$$

If the result of the homogeneity test is smaller than the value determined as the critical value, that data set is called homogeneous. The confidence level was chosen as 95% in the study. The critical value at this level of confidence was calculated as 256.

2.3. Spearman's Rho (SR) Trend Test

SR method is a simple and fast method used to investigate whether a linear trend exists. The purpose of the SR test is to investigate the existence of a linear relationship between the two observation series [39, 40]. Using Equation 3, the r_s value for the SR test statistic is calculated [41, 42].

$$r_s = 1 - \frac{6[\sum_{i=1}^{n}(R(x_i) - i)^2]}{(n^3 - n)} \qquad (3)$$

If the observation period (n) exceeds 30 years, the Z value is calculated using Equation 4.

$$Z = r_s\sqrt{n-1} \quad (4)$$

If the Z value at a selected α significance level is greater than the Z_α value determined from the standard normal distribution table, the H_0 (No trend) hypothesis based on the fact that the observation values do not change over time is rejected and it is concluded that there is a certain trend.

2.4. Mann Kendall (MK) Trend Test

The MK test is independent of the distribution of variables [43, 44]. Whether there is a tendency in the time series is tested by the null hypothesis (H_0: no trend) [21, 45, 46]. The pairs x_i, x_j in the series x_1, x_2, …, x_n are divided into two groups. The test statistic (S) is expressed by Equation 5, where for i <j the number of pairs with $x_i < x_j$ is P and the number of pairs with $x_i > x_j$ is M. Kendall correlation coefficient with Equation 5; variance is calculated by Equation 7. If there are equal values in observations in the series, the variance value is calculated using Equation 8.

$$S = P - M \quad (5)$$

$$\tau = \frac{S}{\left[n(n-1)/_2\right]} \quad (6)$$

$$\sigma_s = \sqrt{\frac{n(n-1)(2n+5)}{18}} \quad (7)$$

$$\sigma_s = \sqrt{\frac{n(n-1)(2n+5) - \sum t_i(t_i-1)(2t_i+5)}{18}} \quad (8)$$

Standardized MK test statistics are calculated by Equation 9.

$$\begin{cases} \frac{(S-1)}{\sigma_s} & ; \quad S > 0 \\ 0 & ; \quad S = 0 \\ \frac{(S+1)}{\sigma_s} & ; \quad S < 0 \end{cases} \quad (9)$$

If the absolute Z obtained by Equation 5 is less than the critical Z of the normal distribution corresponding to the selected α significance level, the H_0 is accepted; otherwise, the existence of the trend is determined. Positive values indicate the presence of an increasing trend, while negative values indicate a decreasing tendency [47].

3. RESULTS AND DISCUSSION

The homogeneity of annual and seasonal temperature series was tested by the PT at the significance level of 0.05 across the Hirfanli Dam basin. Six meteorological stations for the period 1965-2017 were analyzed, with the test results and break years given in Table 4.

Table 4. Results of PT

	Annual	Winter	Spring	Summer	Autumn
Gemerek	**358 (1994)**	124	**310 (1994)**	**394 (1985)**	172
Kayseri	**466 (1998)**	222	**384 (1999)**	**596 (1995)**	**462 (1988)**
Kirsehir	**424 (1992)**	104	252	**494 (1995)**	**360 (1991)**
Nevsehir	**456 (1996)**	146	**294 (1993)**	**598 (1989)**	**336 (2000)**
Sivas	**408 (1993)**	166	**286 (1998)**	**448 (1991)**	**328 (1986)**
Zara	**276 (1994)**	164	172	**358 (1994)**	150

According to Table 4, it was determined that the annual, spring and summer temperatures of Gemerek were not homogeneous. The years when the break occurred were determined as 1994, 1994 and 1985, respectively. For Kayseri, annual, spring, summer and autumn temperature values are not homogeneous and the breaking years are 1998, 1999, 1995 and 1988, respectively. In the Kirsehir temperature data, non-homogeneous values belong to the annual, summer and autumn temperature results. While the deterioration in the annual temperature values started in 1992, the deteriorations in the mean temperature values of summer and autumn began in 1995 and 1991. It was seen that the annual, spring, summer and autumn temperature values for Nevsehir were not homogeneous and the breaking years were 1996, 1993, 1989 and 2000, respectively. In the Sivas mean temperature data, non-homogeneous values belong to the annual, spring, summer and autumn mean temperature results. While the deterioration in the annual temperature values started in 1993, the deteriorations in the mean temperature values of spring, summer and autumn began in 1998, 1991 and 1986. It is concluded that the annual and summer temperatures of Zara are not homogeneous. Breakings in the annual and summer temperature values occurred in 1994.

Annual and seasonal temperature results of SR and MK of the Hirfanli Dam basin are shown in Table 5. In this study, the critical Z value was chosen as 1.96, which corresponds to 0.05 significance level.

Table 5. Results of SR and MK Trend Tests

		Annual		Winter		Spring		Summer		Autumn	
		Z	**Trend**	**Z**	**Trend**	**Z**	**Trend**	**Z**	**Trend**	**Z**	**Trend**
Gemerek	SR	**2.42**	**Δ**	0.68	-	**2.18**	**Δ**	**3.91**	**Δ**	0.68	-
	MK	**2.43**	**Δ**	0.69	-	1.91	-	**3.90**	**Δ**	0.63	-
Kayseri	SR	**4.13**	**Δ**	1.46	-	**2.78**	**Δ**	**5.41**	**Δ**	**3.81**	**Δ**
	MK	**4.48**	**Δ**	1.53	-	**2.70**	**Δ**	**5.64**	**Δ**	**3.93**	**Δ**
Kirsehir	SR	**3.12**	**Δ**	0.50	-	1.83	-	**4.71**	**Δ**	**2.96**	**Δ**
	MK	**3.18**	**Δ**	0.47	-	1.62	-	**4.86**	**Δ**	**3.14**	**Δ**
Nevsehir	SR	**3.72**	**Δ**	0.74	-	**2.43**	**Δ**	**4.94**	**Δ**	**2.47**	**Δ**
	MK	**3.82**	**Δ**	0.83	-	**2.45**	**Δ**	**4.92**	**Δ**	**2.45**	**Δ**
Sivas	SR	**3.21**	**Δ**	1.23	-	**2.39**	**Δ**	**4.52**	**Δ**	**2.68**	**Δ**
	MK	**3.32**	**Δ**	1.16	-	**2.31**	**Δ**	**4.62**	**Δ**	**2.62**	**Δ**
Zara	SR	1.88	-	0.82	-	1.15	-	**3.18**	**Δ**	0.64	-
	MK	1.90	-	0.75	-	1.03	-	**3.14**	**Δ**	0.63	-

According to Table 5, significant increasing trends in annual, spring, summer and autumn temperatures were determined at Kayseri, Nevsehir and Sivas. Statistically significant trends of increase in annual, spring and summer temperatures in the Gemerek temperature series. On the other hand the MK result of the Spring for Gemerek, a significant trend could not be determined. Significant positive trends were found in the annual, summer and autumn temperature series in the results of Kirsehir. In Zara, a significant increasing trend was identified for just summer temperatures.

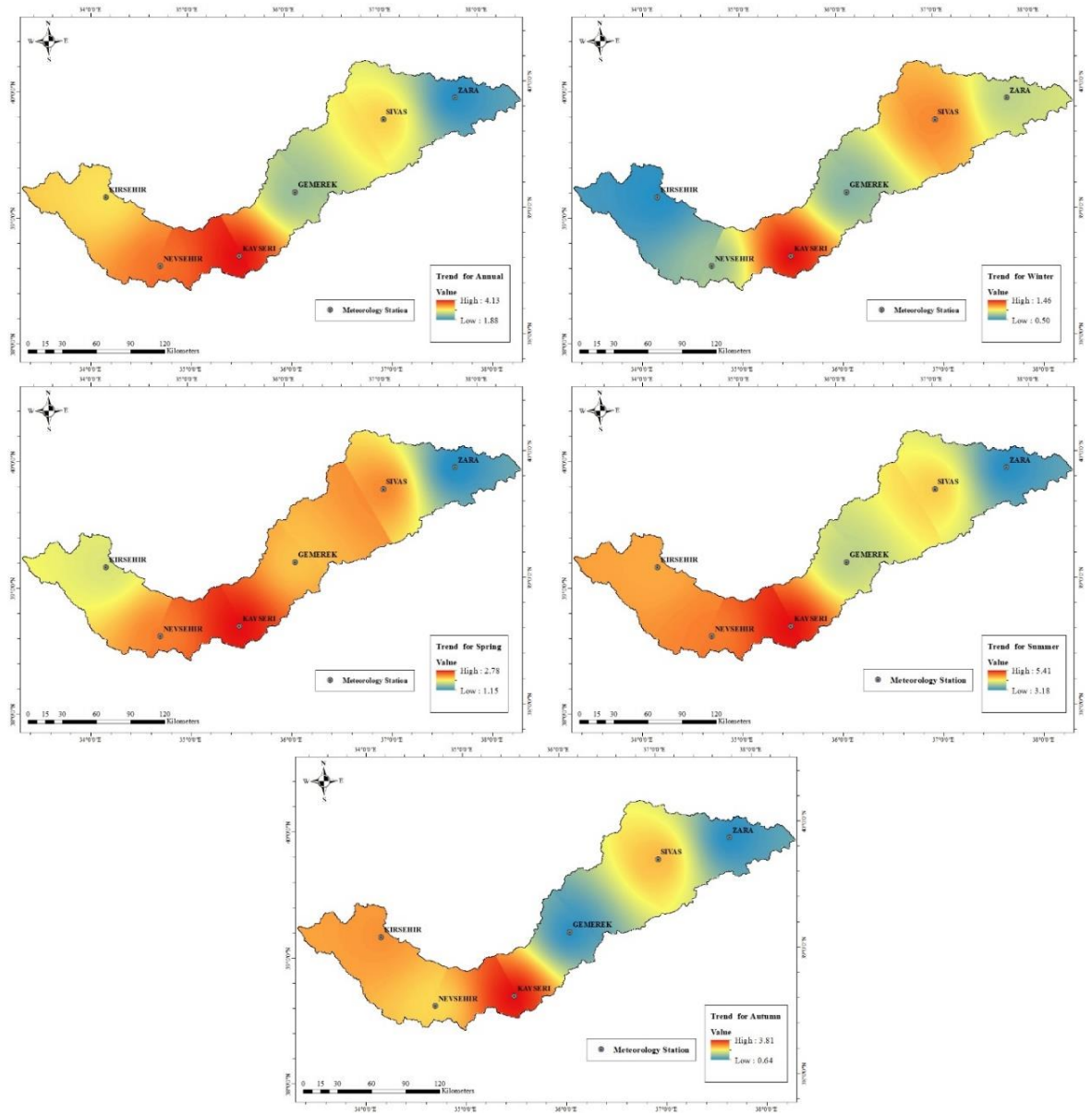

Figure 3. Annual and seasonal trend maps for SR Results.

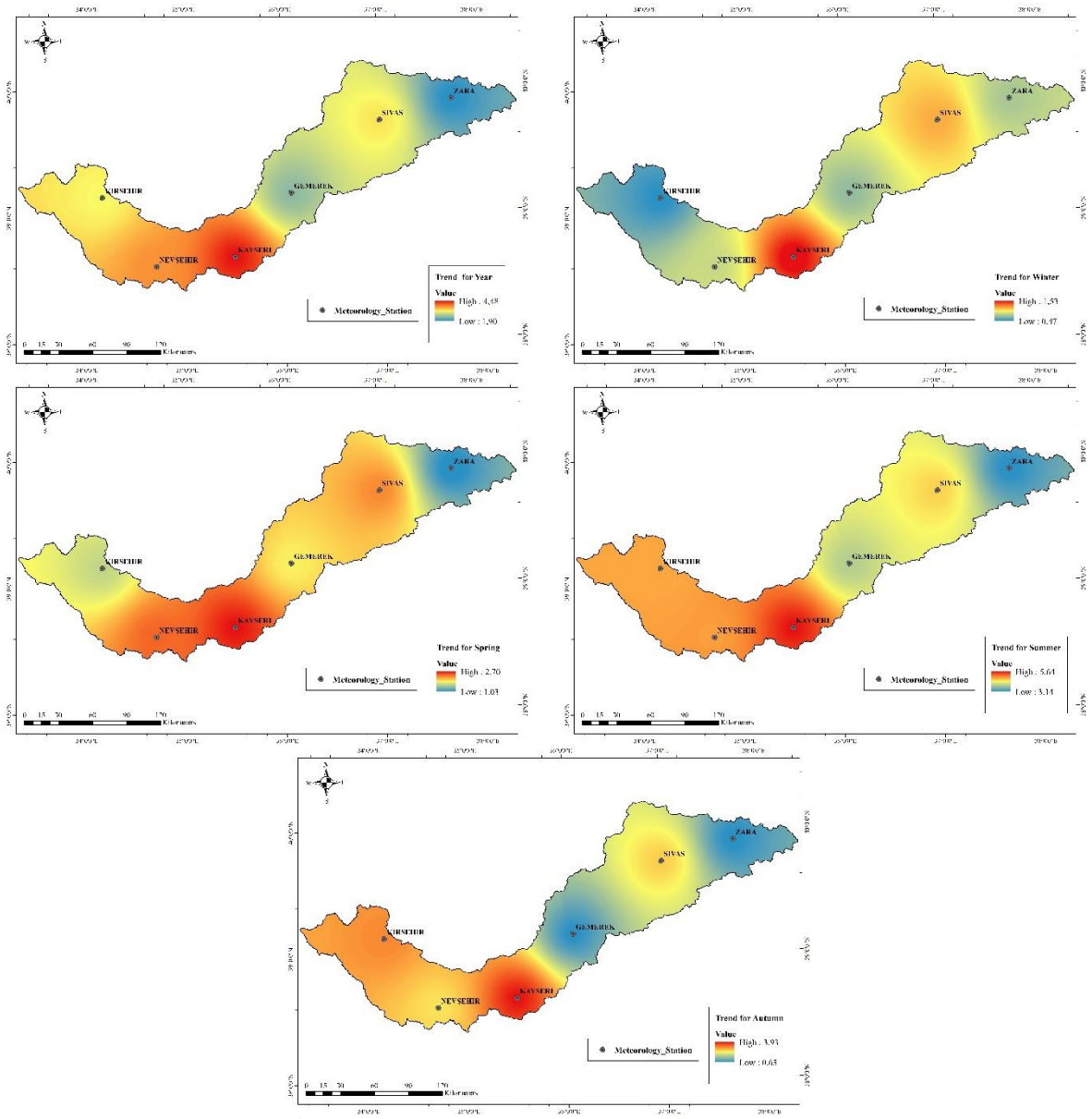

Figure 4. Annual and seasonal trend maps for MK Results.

The increasing trend in spring and summer temperatures determined in Gemerek will cause an increase in the annual temperatures. The increasing trend in annual temperatures in Kirsehir is due to the increasing trend in summer and autumn. In addition, the reason for the increase in annual temperatures of Kayseri, Nevsehir and Sivas is due to the significant increases in spring, summer and autumn temperatures.

In the studies carried out for Turkey, an increasing trend was reported in the temperature series [48-51]. The existence of an increasing trend in annual and seasonal temperature series has been revealed by various trend analysis methods in the Central Anatolia region and the Kizilirmak River basin [31, 52-55]. The findings of this study, obtained by SR and MK methods for the Hirfanli dam basin, show parallelism with the studies carried out for the Kizilirmak River basin, of which it is a sub-basin, and the Central Anatolian region. In addition, annual and seasonal trend maps of the basin were prepared using geographic information systems and Z scores of SR and MK (Figs. 3-4).

4. CONCLUSION

In this study, the annual and seasonal temperature series of the Hirfanli Dam basin in the period 1965-2017 were investigated using the PT, SR and MK. According to the homogeneity test results, deterioration was detected in the annual and summer mean temperatures of all stations in the basin. All stations in the basin showed homogeneous characteristics in the winter temperature series. In the trend analysis results, the significant increase trend in the annual temperature series, except for Zara, is remarkable in the basin. Another remarkable point is that significant increase trends were detected in all stations in summer temperatures throughout the basin. Also, significant increases were determined in the spring and autumn temperature series at the several stations in the basin. There is no significant trend in winter temperature series for all stations. In addition, the results of trend analysis methods (SR and MK) are generally compatible with each other.

Homogeneity analysis and trend analysis results support each other at all stations, other than the Zara. In other words, the reason for the deterioration of homogeneity may be the increasing trend. However, it is thought that this situation determined at the Zara is due to its highest altitude in the basin and being under the influence of the climate of the Eastern Anatolian region.

In the Hirfanli Dam basin, which has a semi-arid feature, it is possible that severe drought events will be seen as a result of the temperature increase caused by global climate change. For this reason, it is of great importance to evaluate the basin in terms of climatic parameters, drought and water resources.

REFERENCES

[1] Turkes M. İklimsel Değişebilirlik Açısından Türkiye'de Çölleşmeye Eğilimli Alanlar. II. Hidrometeoroloji Sempozyumu, T.C. Başbakanlık Devlet Meteoroloji İşleri Genel Müdürlüğü, Ankara; 1998.

[2] Buken ME. Adana İlinde İklim Değişikliği Etkileri Değerlendirmesi [Yüksek Lisans Tezi]. Adana: Çukurova Üniversitesi; 2016.

[3] Ceribasi G. Batı Karadeniz Havzasının Yağış Verilerinin Yenilikçi Şen Yöntemi ile Analizi. Academic Platform Journal of Engineering and Science, 2018; 6(3):168-173. https://doi.org/10.21541/apjes.431965.

[4] Icaga Y, Harmancioğlu N. Yeşilırmak Havzasında Su Kalitesi Eğilimlerinin Belirlenmesi. Türkiye İnşaat Mühendisliği XIII. Teknik Kongresi, Ankara; 1995.

[5] Bayazit M, Cigizoglu HK, Onoz B. Türkiye Akarsularında Trend Analizi. Türkiye Mühendislik Haberleri, 2002; 420-421-422: 8-10.

[6] Buyukyildiz M, Berktay A. Parametrik Olmayan Testler Kullanılarak Sakarya Havzası Yağışlarının Trend Analizi. Selçuk Üniversitesi Mühendislik, Bilim ve Teknoloji Dergisi. 2004; 19(2): 23-38.

[7] Turkes M. Orta Kızılırmak Bölümü Güney Kesiminin (Kapadokya yöresi) İklimi ve Çölleşmeden Etkilenebilirliği. Ege Coğrafya Dergisi. 2005; 14(1-2): 73-97.

[8] Gumus V, Yenigun K. Evaluation of Lower Fırat Basin Streamflow by Trend Analysis. 7th International Advances in Civil Engineering Conference, Yildiz Technical University, Istanbul, Turkey; 2006.

[9] Ozfidaner M. Türkiye Yağış Verilerinin Trend Analizi ve Nehir Akımları Üzerine Etkisi [Yüksek Lisans Tezi]. Adana: Çukurova Üniversitesi; 2007.

[10] Karabulut M, Cosun F. Kahramanmaraş İlinde Yağışların Trend Analizi. Coğrafi Bilimler Dergisi. 2009; 7(1): 65-83. https://doi.org/10.1501/Cogbil_0000000095.

[11] Sen Z. Innovative trend analysis methodology. J. Hydrol. Eng. 2012; 17(9): 1042-1046. https://doi.org/10.1061/(ASCE)HE.1943-5584.0000556.

[12] Haktanir T, Citakoglu H. Trend Independence Stationarity and Homogeneity Tests on Maximum Rainfall Series of Standard Durations Recorded in Turkey. Journal of Hydrologic Engineering. 2014; 19(9): 1-13. https://doi.org/10.1061/(ASCE)HE.1943-5584.0000973.

[13] Ceribasi G, Dogan E. Karadeniz ve Sakarya Havzalarında Yıllık Ortalama Yağışların Trend Analizi. SDU International Technologic Science. 2015; 7(1), 1-7.

[14] Ay M, Kisi O. Kızılırmak Nehrinde Bazı İstasyonlardaki Akımların Trend Analizi. Teknik Dergi. 2017; 28(2): 7779-7794. https://doi.org/10.18400/tekderg.304034.

[15] Arslan O. Niğde İlindeki Potansiyel Evapotranspirasyon Tahminlerinin Trend Analizi. Niğde Ömer Halisdemir Üniversitesi Mühendislik Bilimleri Dergisi. 2017; 6(2): 602–608. https://doi.org/10.28948/ngumuh.341813.

[16] Bacanli UG, Tanrikulu A. Ege Bölgesinde Buharlaşma Verilerinin Trend Analizi. Afyon Kocatepe Üniversitesi Fen ve Mühendislik Bilimleri Dergisi. 2017; 17(3):980-987.

[17] Ceribasi G. Analysis of Meteorological and Hydrological Data of Iznik Lake Basin by Using Innovative Sen Method. Journal of Environmental Protection and Ecology. 2018; 19(1): 15–24.

[18] Zeybekoglu U, Partal T. Sinop İline Ait Aylık ve Yıllık Yağış Yükseklikleri ile Standart Süreli Yağış Şiddetlerinin Farklı Trend Analizi Yöntemleriyle Değerlendirilmesi. İklim Değişikliği ve Çevre. 2018; 3(1): 1-8.

[19] Dalkilic HY. Yağışların Trend Analizi. Erzincan Üniversitesi Fen Bilimleri Enstitüsü Dergisi. 2019; 12(3): 1537–1549. https://doi.org/10.18185/erzifbed.587610.

[20] Sen K, Aksu H. İstanbul İçin Standart Süreli Gözlenen En Büyük Yağışların Eğilimleri. Teknik Dergi. 2021; 32(1), 10495-10514. https://doi.org/10.18400/tekderg.647558.

[21] Partal T, Kahya E. Trend Analysis in Turkish Precipitation Data. Hydrological Processes. 2006; 20(9): 2011-2026. http://doi.org/10.1002/hyp.5993.

[22] Ucgun E. Kızılırmak Havzası'ndaki Hidrometeorolojik Verilerin Trend Analizi. [Yüksek Lisans Tezi]. Kırıkkale: Kırıkkale Üniversitesi; 2010.

[23] Yerdelen C. Susurluk Havzası Yıllık Akımların Trend Analizi ve Değişim Noktasının Araştırılması. DEÜ Mühendislik Fakültesi Mühendislik Bilimleri Dergisi. 2013; 15(44): 77-87.

[24] Simsek O, Gumus V, Soydan NG, Yenigun K, Kavsut ME, Topcu E. Hatay İlinde Bazı Meteorolojik Verilerin Gidiş Analizi. SDÜ Uluslararası Teknolojik Bilimler Dergisi. 2013, 5(2): 132-144.

[25] Zeybekoglu U, Karahan H. Standart süreli yağış şiddetlerinin eğilim analizi yöntemleriyle incelenmesi. Pamukkale Üniversitesi Mühendislik Bilimleri Dergisi. 2018; 24(6): 974-1004. http://doi.org/10.5505/pajes.2017.54265.

[26] Turkes M, Koc T, Saris F. Spatiotemporal Variability of Precipitation Total Series over

Turkey. International Journal of Climatology. 2008; 29(8): 1056-1074. https://doi.org/10.1002/joc.1768.
[27] Turkes M, Erlat E. Influence of the Arctic Oscillation on Variability of Winter Mean Temperatures in Turkey. Theoretical and Applied Climatology. 2008; 92(1-2): 75-85. https://doi.org/10.1007/s00704-007-0310-8.
[28] Toros H. Klimatolojik Serilerden Türkiye İkliminde Trend Analizi [Yüksek Lisans Tezi]. İstanbul: İstanbul Teknik Üniversitesi; 1993.
[29] Kadioglu M. Trends In Surface Air Temperature Data Over Turkey. International Journal of Climatology. 1997; 17(5): 511-520. https://doi.org/10.1002/(SICI)1097-0088(199704)17:5<511::AID-JOC130>3.0.CO;2-0.
[30] Altin TB, Barak B, Altin BN. Change in Precipitation and Temperature Amounts over Three Decades in Central Anatolia Turkey. Atmospheric and Climate Sciences. 2012; 2(1), 107–125. https://doi.org/10.4236/acs.2012.21013.
[31] Kizilelma Y, Celik MA, Karabulut M. İç Anadolu Bölgesinde sıcaklık ve yağışların trend analizi. Türk Coğrafya Dergisi. 2015; 64: 1-10. https://doi.org/10.17211/tcd.90494.
[32] Dogan M, Ulke A, Cigizoglu, HK. Trend direction changes of Turkish temperature series in the first half of 1990s. Theor. Appl. Clim. 2015; 121(1 -2): 23-39. https://doi.org/10.1007/s00704-014-1209-9.
[33] Ulke A, Ozkoca T. Sinop, Ordu ve Samsun İllerinin Sıcaklık Verilerinde Trend Analizi. Gümüşhane Üniversitesi Fen Bilimleri Enstitüsü Dergisi. 2018; 8(2): 455-463. https://doi.org/10.17714/gumusfenbil.351294.
[34] Gumus V. Spatio-temporal precipitation and temperature trend analysis of the Seyhan–Ceyhan River Basins, Turkey. Meteorological Applications. 2020; 26(3): 369-384. https://doi.org/10.1002/met.1768.
[35] Yildiz O. Assessing Temporal and Spatial Characteristics of Droughts in the Hirfanli Dam Basin Turkey. Scientific Research and Essays. 2009; 4(4): 249–255. https://doi.org/10.5897/SRE.9000212.
[36] Yildiz O. Spatiotemporal Analysis of Historical Droughts in the Central Anatolia, Turkey. Gazi University Journal of Science. 2014; 27(4): 1177-1184.
[37] Pettitt AN. A Non-Parametric Approach to the Change-Point Detection. Applied Statistic. 1979; 28(2): 26-135. https://doi.org/10.2307/2346729.
[38] Wijngaard JB, Tank AMGK, Können GP. Homogenity of 20th Century European Daily Temperature and Precipitation Series. International Journal of Climatololgy. 2003; 23(6): 679-692. https://doi.org/10.1002/joc.906.
[39] Yue S, Pilon P, Cavadias G. Power of the Mann–Kendall and Spearman's rho tests for detecting monotonic trends in hydrological series. Journal of Hydrology. 2002; 259(1–4): 254–271. https://doi.org/10.1016/S0022-1694(01)00594-7.
[40] Yenigun K, Gumus V, Bulut H. Trends in Streamflow of Euphrates Basin Turkey. ICE Water Management. 2008; 161(4): 189–198. https://doi.org/10.1680/wama.2008.161.4.189.
[41] Sneyers R. On the Statistical Analysis of Series of Observations. World Meteorological Organization, Geneva, Switzerland, Technical Note no. 143, WMO-no. 415; 1990.
[42] Kalayci S, Kahya E. Susurluk havzası nehirlerinde su kalitesi trendlerinin belirlenmesi. Turkish Journal of Engineering and Environmental Sciences. 1998; 22(6): 503-514.
[43] Mann HB. Non-parametric test against trend. Econometrika. 1945; 13: 245-259. https://doi.org/10.2307/1907187.
[44] Kendall, MG. Rank Correlation Method. London: Charles Griffin; 1975.
[45] Bayazit, M. İnşaat Mühendisliğinde Olasılık Yöntemleri. İstanbul: İTÜ İnşaat Fakültesi Matbaası; 1996.
[46] Onoz B, Bayazit M. The power of statistical tests for trend detection. Turkish J. Eng. Env. Sci. 2003; 27(4): 247-251.
[47] Yu S, Zou S, Whittemore D. Non-parametric trend analysis of water quality data of Rivers in Kansas. Journal of Hydrology. 1993; 150(1): 61-80. https://doi.org/10.1016/0022-1694(93)90156-4.
[48] Acar-Deniz Z, Gonencgil B. Variations in Temperature Extremes in Turkey. Journal of Geography. 2017; 35:41-54.
[49] Kuyucu H, Demir V, Geyikli MS, Citakoglu H. Trend Analysis of Turkey Temperatures. 1st International Symposium on Multidisciplinary Studies and Innovative Technologies Proceedings. Tokat; 2017. p.157-159.
[50] Hadi SJ, Tombul M. Long-term spatiotemporal trend analysis of precipitation and temperature over Turkey. Meteorological Applications. 2018; 25(3): 445-455. https://doi.org/10.1002/met.1712.
[51] Celebioglu T, Tayanc M, Oruc HN. Determination of Temperature Variabilities and Trends in Turkey. Bursa Uludağ University Journal of The Faculty of Engineering. 2021; 26(3): 1003-1020. https://doi.org/10.17482/uumfd.881416.
[52] Altin TB. Observed Changes in Annual and Seasonal Temperatures in Nevşehir (Central Anatolia, Turkey) for Period 1960-2016. Eurasian Journal of Agricultural Research. 2017; 1(2): 4-12.
[53] Ercan B, Yuce MI. Trend Analysis of Hydro-Meteorological Variables of Kızılırmak Basin. Nevşehir Bilim ve Teknoloji Dergisi. 2017; 6: 333-340. https://doi.org/10.17100/nevbiltek.323640.
[54] Terzi O, Ilker A. Trend Analysis of Temperature Values in Kızılırmak Basin. Süleyman Demirel University Journal of Natural and Applied Sciences. 2020; 24(3): 626-634. https://doi.org/10.19113/sdufenbed.686484.
[55] Koycegiz C, Buyukyildiz M. Determination of Change Points and Trend Analysis of Annual Temperature Data in Konya Closed Basın (Turkey).

Nigde Omer Halisdemir University Journal of Engineering Sciences. 2020; 9(1): 393-404. https://doi.org/10.28948/ngumuh.598289.

Cilt 11, Sayı 1, Sayfa 59-65, 2022 Volume 11, Issue 1, Page 59-65, 2022

Araştırma Makalesi https://doi.org/10.46810/tdfd.956778 Research Article

Türk Doğa ve Fen Dergisi
Turkish Journal of Nature and Science
www.dergipark.gov.tr/tdfd

Traditional Uses of Some Food Plants in Suruç (Şanlıurfa, Turkey)

Serhan YALÇIN[1], Hasan AKAN[2], Uğur ÇAKILCIOĞLU[3*]

[1,2] Harran Üniversitesi, Fen Edebiyat Fakültesi, Biyoloji Bölümü, Şanlıurfa, Türkiye
[3] Munzur Üniversitesi, Pertek Sakine Genç MYO, Tunceli, Türkiye
Serhan YALÇIN ORCID No: 0000-0002-6379-8748
Hasan AKAN ORCID No: 0000-0002-3033-4349
Uğur ÇAKILCIOĞLU ORCID No: 0000-0002-3627-3604

** Corresponding author: ucakilcioglu@yahoo.com*

(Received: 24.06.2021, Accepted: 14.03.2022, Online Publication: 25.03.2022)

Keywords
Suruç, Food plants, Traditional use, Ethnobotany, Şanlıurfa, Turkey

Abstract: This research was carried out throughout a period of approximately two years between 2019-2020 and aimed to identify wild food plants frequently used by people living in Suruç district (Şanlıurfa) and some of its surrounding villages. 64 taxa belonging to 27 families were identified through these interviews that we conducted with 44 people. The demographic information of the interviewees, both the local and scientific names of the plants they use for food purposes, the parts of the plants used and the methods of preparing the plants were recorded. The plants used by the habitants of the region were scientifically diagnosed at Harran University herbarium and were recorded as herbarium material. The families of the plant taxa, their scientific and local names, their patterns of use and use value (UV) of the plants were calculated and presented in a table. The families with the widest taxa discovered in our research throughout the region are Asteraceae with 10 taxa (16%), Lamiaceae with 10 taxa (16%), Malvaceae with 5 taxa (8%), Brassicaceae with 4 taxa (6%), Fabaceae with 4 taxa (6%), Apiaceae with 3 taxa (5%) and Rosaceae with 3 taxa (5%); while genus discovered to have the widest taxa are *Mentha* L. with 3 taxa, *Crocus* L., *Euphorbia* L., *Malva* L., *Papaver* L., *Salvia* L. with 2 taxa. Food plants are usually consumed as food after their stems are peeled, their leaves are used to make salads; they are cooked by adding tomato paste, rice or egg, used as a spice and brewed like tea. Most common plant parts used for food purposes are above ground, leaf, stem, root and fruit. Some cultivated and natural plants in Suruç district are used for food purposes. Our literature review has revealed that the food plants used in Suruç district are also used both for food and medicinal purposes in different regions of our country.

Suruç'ta (Şanlıurfa-Türkiye) Bazı Gıda Bitkilerin Geleneksel Kullanımları

Anahtar Kelimeler
Suruç, Gıda bitkileri, Geleneksel kullanım, Etnobotanik, Şanlıurfa, Türkiye

Öz: Bu araştırma 2019-2020 yılları arasında yaklaşık iki yıllık bir sürede, Suruç ilçesi (Şanlıurfa) ve çevresindeki bazı köylerinde yaşayan insanların kullandığı yabani gıda bitkilerin tespit edilmesi için yapılmıştır. 44 kaynak kişi ile yapılan görüşmelerde 27 familyaya ait 64 takson tespit edilmiştir. Görüşme yapılan kişilerin demografik bilgileri, gıda amaçlı kullandıkları bitkilerin yerel adları ve bilimsel adları, kullanılan bitki kısımları ve bitkileri hazırlama yöntemleri kayıt edilmiştir. Bölge halkının kullandığı bitkilerin Harran Üniversitesi herbaryumunda teşhisleri yapılmış ve herbaryum materyali haline getirilmiştir. Bitki taksonların familya, bilimsel ve yöresel adları, bitkilerin kullanım şekilleri ve kullanım değerleri (UV) hesaplanarak tablo halinde sunulmuştur. Bölgede yaptığımız araştırmada en çok takson içeren familyalar şöyledir; Asteraceae 10 takson (% 16), Lamiaceae 10 takson (% 16), Malvaceae 5 takson (% 8), Brassicaceae 4 takson (% 6), Fabaceae 4 takson (% 6), Apiaceae 3 takson (% 5), Rosaceae 3 takson (% 5), en çok takson içeren cinsler ise; *Mentha* L. 3 takson, *Crocus* L., *Euphorbia* L., *Malva* L., *Papaver* L., *Salvia* L. ise 2 takson içermektedir. Gıda bitkileri en çok gövdesi soyulduktan sonra yenilir, yaprakları salata yapımında kullanılır, salçalı, pirinçli, yumurtalı yemeği yapılır, baharat olarak kullanılır ve çay olarak demlenip içilir. Gıda amaçlı en çok kullanılan bitki parçaları; toprak üstü, yaprak, gövde, kök ve meyve gibi organlardır. Suruç ilçesinde bazı kültür ve doğal yetişen bitkiler gıda amaçlı kullanılmaktadır. Literatür araştırmamızda, Suruç ilçesinde kullanılan gıda bitkileri ülkemizin farklı bölgelerinde gıda ve tıbbi amaçlı kullanıldığı görülmüştür.

1. INTRODUCTION

Our plants, which naturally grow in spring, are widely used in many regions of our country, particularly in Eastern Anatolia and the Aegean region for food purposes besides being a source of medication. Wild plants used for food purposes may either be consumed raw, or by adding eggs or yogurt, may be boiled or cooked by adding rice; they are also widely used in salads [1-4]. Wild food plants were also essential in ancient times for human survival. For example, people in besieged settlements during the war in Bosnia and Herzegovina benefited from plants to survive. The World Health Organization (WHO) has specified that wild plants consumed for food purposes will meet the daily vitamins (particularly A and C) and mineral needs of individuals [5].

Ethnobotany refers to the relationships of people in human societies with plants. In this context, "ethno" is used for human studies whereas "botany" refers to plant research or plant science. Ethnobotanical information has been compiled by trial and error methods over a long period of time and has reached the present day. It is inevitable that the culture of benefiting from plants will eventually disappear before it can be transferred to the younger generations due to the increase in migration to cities and the development of technology. Therefore, it is an extremely important requirement to record this knowledge before it is completely lost [6-7].

When our country is examined in terms of plant existence, it is possible to mention that it is among the richest countries in the world. According to the information included in the book titled ’Türkiye Bitkileri Listesi’’ there are 167 plant families, 1320 genera and 11707 taxa of plants in Turkey. Among the 11707 taxa in our country, 3649 are endemic [8-11]. This study aimed to record the use of wild plants for food purposes in Suruç district and its surrounding villages and to shed light on future research on wild food plants.

2. MATERIALS AND METHODS

Our research was carried out by interviews held with local people living in Suruç district of Şanlıurfa province (Figure 1) and some of its surrounding villages (Aybastı, Bahçe, Yalınca, Zeyrek and Ziyaret) over a period of about two years (2019-2020). The villages we researched were further transformed into neighborhoods by law [12].

2.1. Study of Area

Suruç, a district of Şanlıurfa province, is located in the southwest of the province and is 45 km from the city center. Surrounded by the Güvercik, Devres and Cudi mountains, the altitude of the district is 537 m. Syria is located to the south of the district. The population of the district has approached 103.000 and its surface area is 706 km2. The region is located in a semi-arid climate zone. The annual average temperature is 18 °C and the average precipitation is 457 mm. The summer months are hot and dry while winter months are warm. The hottest period of the region is experienced in July and August [13-15].

90% of the total surface area of the district comprises of agricultural lands whereas remaining10% is meadow, pasture, forest and non-agricultural areas. Cotton, wheat, barley, legumes and corn are grown in the district. In addition, although not much, olives, pistachios, sesame, chickpeas, vegetables, fruits, especially pomegranates are grown in the district [16].

2.2. Plants Materials

For the purpose of this study we have interviewed 44 people using food plants in the region. Personal information such as age, educational background, profession of these people were recorded. In addition to Kurdish, limited Arabic and Zazaki are spoken around the Suruç district. During our trips in the region, we asked local people to show us the plants they used for food purposes; we recorded the local names of the plants they used, the parts of the plant they used and how they prepared it for food. We collected the plants used in the region and took photographs of some of them. The plants we diagnosed were scientifically named and were recorded as herbarium material at Harran University. The plants are currently preserved in the Herbarium of Harran University (HUH). The plants we recorded at the end of the research are exhibited in the table on the basis of family names (Table 1). Family names, scientific and local names of plants, plant parts used for food, patterns of use and use value (UV) each plant are exhibited respectively in the table 1. The book titled “Flora of Turkey and the East Aegean Islands” were used for scientific naming of the plants we recorded [17-20].

2.3. Calculations

Use value indicating the degree of relative importance of native species is a quantitative method [21]. and is calculated according to the formula below and exhibited in the table accordingly (Table 1).

Use Value (UV) = T / K
T: The number of citations to each taxon
K: Indicates the number of people providing information

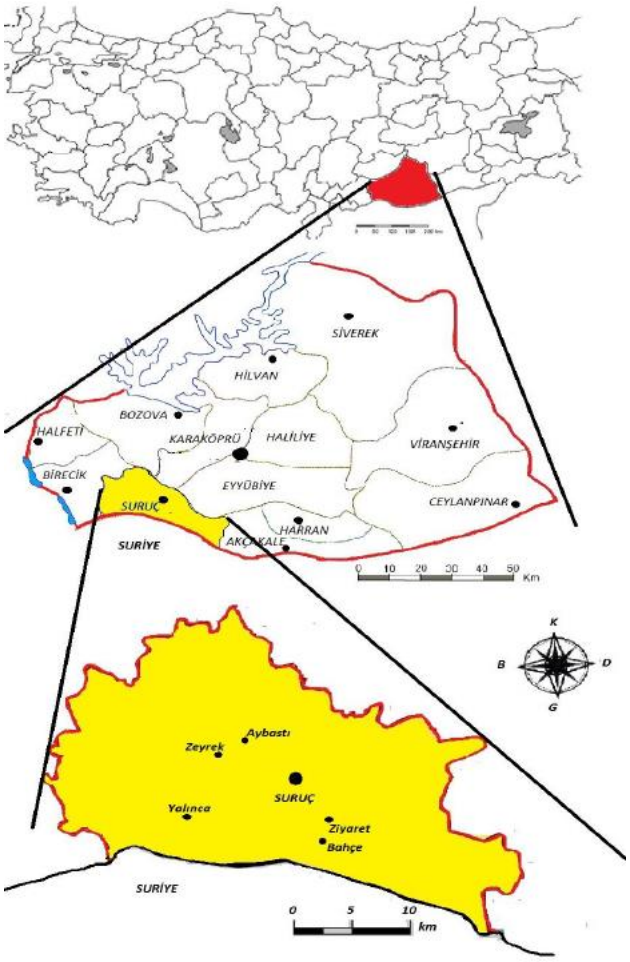

Figure 1. Maps of the study area

3. RESULTS AND DISCUSSION

Our interviews, held within the scope of our research in Suruç district, were conducted face-to-face with the people providing information (Figure 2).

3.1. Demographic Characteristics of Study Participants

Mean age of the people who provided us information was 49. Examining the educational background of 44 people who provided us information, 10 were found out (23%) to have received no education at all, 19 (43%) were found out to be primary school graduates, 2 (4%) were secondary school graduates, 3 (7%) were high school graduates and 10 (23%) were university graduates. Elder people have been observed to be more experienced and acquainted about plants.

Figure 2. Interviews with local people (Suruç)

3.2. Interviews with Locals and Literature Review

Examining the profession of 44 people who provided us information, 30% were found out to be farmers, 19% were tradesmen, 17% were workers, 9% were housewives and 25% were from other professions.

For the purpose of the ethno-botanical study we conducted around Suruç district, it was recorded that local people of the region used 64 taxa belonging to 27 families of plants for food purposes (Table 1). No study have been conducted specific to wild food plants within the scope of our research area, however there are a few studies conducted in the immediate vicinity [22-23]. We have concluded in our study that the plant families with the widest taxa were Asteraceae (16%) and Lamiaceae (16%) with 10 taxa each. Among other plant species available in the research area, Malvaceae has 5 taxa (8%), Brassicaceae has 4 taxa (6%), Fabaceae has 4 taxa (6%), Apiaceae has 3 taxa (5%) and Rosaceae has 3 taxa (5%) (Figure 3). The genera of plants with the widest taxa discovered in our research area are *Mentha* L. with 3 taxa, *Crocus* L., *Euphorbia* L., *Malva* L., *Papaver* L., *Salvia* L. with 2 taxa each (Figure 3).

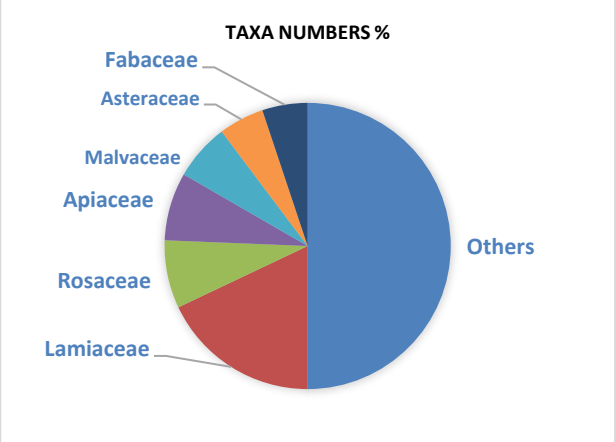

Figure 3. Plant families with the widest taxa

Most common food plants that we have identified throughout our research are; *Allium sativum* L., *Mentha longifolia* (L.) L. subsp. *typhoides* (Briq.) Harley, *Mentha* x *piperita* L. *Glycyrrhiza glabra* L., *Gundelia tournefortii* L., *Juglans regia* L., *Nigella sativa* L., *Thymus fallax* Fisch. & C.A. Mey. *Portulaca oleracea*

L., *Thymbra spicata* L., *Urtica dioica* L. and *Vitis vinifera* L.

Local people have been determined to either peel the stems of the food plants and consume them raw (7 use-report), use the leaves to make salads (6 use-report), cook them by adding tomato paste (7 use-report), rice or eggs (7 use-report), use them as a spice to flavor their meals (3 use-report) or brew them to serve as tea (18 use-report). The above-ground, leaves, stems, roots and fruits of some cultivated and naturally grown plants in Suruç district are used for food purposes. Plants are generally consumed fresh, however there are also examples where they are either dried and/or frozen for further consumption in the winter season.

Some plants that are traditionally used for food purposes in Suruç district have been reported to show different activities in studies carried out in the laboratory environment. For instance; *Rosa canina* is recorded to have antidiabetic, antioxidant, anti-inflammatory and antinociceptive activity; *Rhus coriaria* and *Salvia* species are recorded to have antioxidant activity and gastrointestinal diseaces, *Malva* species are recorded to have antioxidant and antiulcerogenic activity; *Urtica dioica* are recorded to have anti fungal, anti analgesic, immunomodulatory, antimicrobial, antidiabetic, anti ulcer activity, depurative, diuretic and *Helichrysum* is reported to have antinociceptive and anti-inflammatory activity [24-34]. Local names of plants available in Turkey vary according to dialect and local languages [35]. As the local people around Suruç speak Kurdish, the plants are also known by their Kurdish names.

Literature review revealed that food plants used throughout the district are used for therapeutic purposes in many different parts of our country [36-39]. “Use value” (UV) has been calculated in many ethnobotanical studies [40-42]. The plants with the highest use value (UV) identified in the research area are as follows (Table 1); *Mentha* x *piperita* (0.44), *Allium sativum* (0.43), *Thymus fallax* (0.43), *Glycyrrhiza glabra* (0.39), Urtica dioica (0.39), Nigella sativa L. (0.38), *Mentha longifolia* subsp. *typhoides* (0.37), *Gundelia tournefortii* (0.36), *Juglans regia* (0.36), and *Polygonum cognatum* (0.36).

It has been determined in studies that Euphorbia and Equisetum taxa, which are used by the people of the region, show toxic effects [43-44]. People do not know about the toxic effects of these plants.

4. CONCLUSION

64 wild and cultivated plant taxa belonging to 27 families determined as a result of face-to-face interviews held with local people in and around Suruç district are used for food purposes.

Most common plant parts used in the region for food purposes are above ground, leaves, stem, root and fruits. Food plants are usually consumed as food after their stems are peeled, their leaves are used to make salads, their above-ground parts are cooked by adding tomato paste, rice or egg or used as a spice and brewed like tea.

Some cultivated and natural plants in Suruç district are used for food purposes. Our literature review has revealed that the food plants used in Suruç district are also used both for food and medicinal purposes in different regions of our country.

The studies carried out in the Eastern and Southeastern Anatolia Regions revealed that the local names of the plants used in this region for food purposes are similar to the local names of the plants used in Suruç.

It was recorded that the food plant with the highest calculated use value was *Mentha* x *piperita* with 0.44. Other plants with the highest use value are It was recorded that the food plant with the highest calculated use value was *Mentha* x *piperita* with 0.44. Other plants with the highest use value are *Allium sativum*, *Thymus fallax*, *Glycyrrhiza glabra*, *Urtica dioica*, *Nigella sativa*, *Mentha longifolia*, *Gundelia tournefortii* (0.36), *Juglans regia* (0.36), and *Polygonum cognatum* respectively.

The traditional use of plants in the region is decreasing day by day due to migration. In addition, the vegetation of the region is being destroyed due to agricultural activities and herding. Plant protection measures should be implemented urgently in the region.

Consumption of food plants by human raises the question of whether these plants are safe. We think that the wild plants that we have reported will be a resource for those working on food safety. We believe that ethnobotanical studies carried out in provinces and districts of the region where this kind of research has not yet been carried out will be rather beneficial.

Acknowledgment

This article was reproduced from the master's thesis (Serhan Yalçın) financially supported by Harran University Coordination Unit for Scientific Research Projects (HÜBAP) (Project No: 19110). We are grateful to HÜBAP for their valuable support.

REFERENCES

[1] Arslan N. Doğal ekonomik bitkilerin korunması. Tarım Köy Der. 1992;74:17-9.
[2] Kaval İ, Behçet L, Çakılcıoğlu U. Survey of wild food plants for human consumption in Geçitli (Hakkari, Turkey). Indian J Tradit Knowled. 2015;14:183-90.
[3] Polat R, Güner B, Yüce-Babacan E, Çakılcıoğlu U. Survey of wild food plants for human consumption in Bingöl (Turkey). Indian J Tradit Knowled. 2017;16:378-84.
[4] Çakılcıoğlu U. An ethnobotanical field study; Traditional foods production and medicinal utilization of *Gundelia* L. species in Tunceli (Turkey). Indian J Traditional Knowled. 2020;19(4):714-8.

[5] Redzic S. Wild edible plants and their traditional use in the human nutrition in Bosnia-Herzegovina. Ecol Food Nutr. 2006;45(3):189-232.
[6] Ertuğ F. Etnobotanik. Güner A., Ekim T. (Editörler) Resimli Türkiye Florası (Cilt 1). İstanbul: ANG Vakfı, Flora Araştırmaları Derneği ve Türkiye İş Bankası Kültür Yayınları; 2014;319-420.
[7] Heinrich M, Barnes J, Gibbons S, Williamson EM. Fundamentals of pharmacognosy and phytotherapy. Edinburgh; Churchill Livingstone, 2004.
[8] Öztürk M, Özçelik H. Doğu Anadolu'nun faydalı bitkileri (Useful plants of East Anatolia). SİSKAV (Siirt, İlim, Spor, Kültür ve Araştırma Vakfı). Ankara: Semih Ofset; 1991.
[9] Baytop T. Türkiye'de bitkiler ile tedavi. İstanbul Eczacılık Fakültesi, No: 40, İstanbul: İstanbul Üniversitesi Yayınları; 1984.
[10] Baytop T. Therapy With Medicinal Plants in Turkey (Past and Present). Istanbul: Nobel Medicine Publication; 1999.
[11] Güner A, Aslan S, Ekim T, Vural M, Babaç MT. Türkiye bitkileri listesi (Damarlı Bitkiler). İstanbul: Nezahat Gökyiğit Botanik Bahçesi ve Flora Araştırmalar Derneği Yayınları; 2012.
[12] Muratoğlu T. Mahalli idareler mevzuatında 6360 sayılı kanunla yapılan değişiklikler. Dicle Üniv Hukuk Fak Der. 2015;20(32):59-96.
[13] Akman Y. İklim ve biyoiklim. Ankara: Palme Yayınları; 2011.
[14] T.C. Suruç Kaymakamlığı; www.suruc.gov.tr/tarih
[15] www.urfafx.mekan360.com/iys_ilceçiler
[16] Şahinalp MS. Fonksiyonları ve arazi kullanım problemleri açısından Suruç şehri. J Int Social Res. 2019;12(68):461-78.
[17] Davis PH. Flora of Turkey and the East Aegean Islands. Vol 1-9, UK. Edinburgh: Edinburg University Press; 1965–1985.
[18] Davis PH, Mill RR, Tan K. Flora of Turkey and the East Aegean Islands. Vol 10, UK. Edinburgh: Edinburg University Press; 1988.
[19] Güner A, Ekim T. Resimli Türkiye Florası. Cilt: 1, NGBB yayınları flora dizisi 2, İstanbul: Flora Araştırmaları Derneği ve Türkiye İş Bankası kültür yayınları; 2014.
[20] Güner A, Özhatay N, Ekim T, Başer KHC. Flora of Turkey and the East Aegean Islands. (Supplement 2). UK. Edinburgh: Edinburg Univ. Press; 2000.
[21] Trotter RT, Logan MH. Informant consensus: a new approach for identifying potentially effective medicinal plants, In: Plants in indigenous medicine and diet, behavioural approaches, edited by Etkin NL, Bredford Hills, NY: Redgrave Publishing Company; 1986.
[22] Akan H, Aslan M, Balos MM. Şanlıurfa semt pazarlarında satılan doğal bitkilerin etnobotaniği. Ot Sist Bot Der. 2005;12(2):43-58.
[23] Akan H, Balos MM, Tel AZ. Birecik (Şanlıurfa) yöresindeki bazı baklagil bitkilerin etnobotanik özellikleri. Adıyaman Üniv Tarım Araşt Uyg Merk Uluslararası Der. 2013;1(1):32-40.
[24] Akbay P, Basaran AA, Undeger U, Basaran N. In vitro immunomodulatory activity of flavonoid glycosides from *Urtica dioica* L. Phytotherapy Res. 2003;17:34-7.
[25] Bnouham M, Merhfour FM, Ziyyat A, Mekhfi H, Aziz M, Legssyer A. Antihyperglycemic activity of the aqueous extract of Urtica dioica. Fitoterapia 2003;74:677-81.
[26] Özcan M. Antioxidant activities of rosemary, sage, and sumac extracts and their combinations on stability of natural peanut oil. J Med Foods. 2003;6:267-70.
[27] Gülçin İ, Küfrevioğlu OI, Oktay M. Büyükokuroğlu ME. Antioxidant, antimicrobial, antiulcer and analgesic activities of nettle (*Urtica dioica* L.). J Ethnopharmacol. 2004;90:205-15.
[28] Küpeli E, Tosun A, Bahadır Ö. Evaluation of anti-inflammatory and antinociceptive activities of Helichrysum Gaertner species (Asteraceae). Turk J Pharmaceutical Sci. 2006;3:141-9.
[29] Deliorman DO, Hartevioğlu A, Küpeli E, Yeşilada E. In vivo anti-inflammatory and antinociceptive activity of the crude extract and fractions from *Rosa canina* L. fruits. J Ethnopharmacol. 2007;112:394-400.
[30] Hadizadeh I, Peivastegan B, Kolahi M. Antifungal activity of nettle (*Urtica dioica* L.), colocynth (*Citrullus colocynthis* L. Schrad), oleander (*Nerium oleander* L.) and konar (*Ziziphus spina-christi* L.) extracts on plants pathogenic fungi. Pakistan J Biological Sci. 2009;12:58-63.
[31] Orhan N, Aslan M, Hosbas S, Deliorman OD. Antidiabetic effect and antioxidant potential of Rosa canina fruits. Pharmacog Mag. 2009;5:309-15.
[32] Güner Ö, Selvi S. Wild medicinal plants sold in Balıkesir/Turkey herbal markets and their using properties. Biological Diversity and Conservation, 2016;9;96-101.
[33] Korkmaz M, Karakuş S, Özçelik H, Selvi S. An ethnobotanical study on medicinal plants in Erzincan, Turkey. Indian J Tradit Knowled. 2016;15:192-202.
[34] Sargın SA. Akçiçek E, Selvi S. An ethnobotanical study of medicinal plants used by the local people of Alaşehir (Manisa) in Turkey. J Ethnopharmacol. 2013;150:860-74.
[35] Mükemre M, Behçet L, Çakılcıoğlu U. Survey of wild food plants for human consumption in villages of Çatak (Van-Turkey). Indian J Tradit Knowled. 2016;15:183-91.
[36] Mükemre M, Behçet L, Çakılcıoğlu U. Ethnobotanical study on medicinal plants in villages of Çatak (Van-Turkey). J Ethnopharmacol. 2015;166:361-74.
[37] Bulut G, Korkmaz A, Tuzlacı E. The ethnobotanical notes from Nizip (Gaziantep-Turkey). İstanbul J Pharm. 2017; 47(2):57-62.
[38] Güneş S, Savran A, Paksoy MY, Koşar M, Çakılcıoğlu U. Ethnopharmacological survey of medicinal plants in Karaisalı and its surrounding (Adana-Turkey). J Herbal Med. 2017;8,68-75.
[39] Şahin-Fidan E, Akan H. Tek Tek Dağları Milli Parkı (Şanlıurfa-Türkiye) eteklerindeki bazı

köylerde etnobotanik bir çalışma. Bağbahçe Bilim Der. 2019;62:64-94.
[40] Paksoy MY, Selvi S, Savran A. Ethnopharmacological survey of medicinal plants in Ulukışla (Niğde-Turkey). J Herbal Med. 2015;6:42-8.
[41] Nadiroğlu M, Behçet L, Çakılcıoğlu U. An ethnobotanical survey of medicinal plants in Karlıova (Bingöl-Turkey). Indian J Tradit Knowled. 2019;18(1):76-87.
[42] Kawarty AMAMA, Behçet L, Çakılcıoğlu U. An ethnobotanical survey of medicinal plants in Ballakayati (Erbil, North Iraq). Turk J Bot. 2020;44:345-57. doi.org/10.3906/bot-1910-39
[43] Bangayan, JMB., Palattao, JRM, Chua, JMT, Capili, JT, Ramirez Jr. RB, Evaluation of Equisetum hyemale and *Euphorbia hirta* leaf extracts in increasing platelet count of sprague dawley rats. Int J Biosci. 2020;17(2):58-65.
[44] Müller J, Puttich PM, Beuerle T. Variation of the main alkaloid content in *Equisetum palustre* L. in the light of its ontogeny. Toxins. 2020;12(11):710. doi.org/10.3390/toxins12110710

Table 1. Food plants used in the region

Familya	Scientific name / voucher specimen	Vernacular name(s)	Use parts	Place and form of use	UV
Amaryllidaceae	**Allium sativum* L. SY-	Sarımsak	Fruit	Used to flavor food	0.43
Anacardiaceae	*Rhus coriaria* L. SY -	Sumak	Fruit	Used as a spice	0.22
Apiaceae	*Eryngium creticum* Lam. SY 1099	Çistok	Leaves, Stem	The stem is consumed after peeling; the leaves are used to make salads	0.04
Apiaceae	*Ferula orientalis* L. SY 1051	Kingor	Root	It is cooked by adding tomato paste; it is brewed and served like tea	0.23
Apiaceae	*Malabaila secacul* (Mill.) Boiss. SY 1100	Harık	Aerial parts	The plant is boiled and cooked by adding rice and consumed with yoğurt; the leaves are used in salads	0.02
Asparagaceae	*Ornithogalum narbonense* L. SY 1096	Akbandır	Leaves	Cooked with eggs	0.02
Asteraceae	*Achillea oligocephala* DC. SY 1088	Civanperçemi	Aerial parts	Brewed and served like tea	0.02
Asteraceae	*Carduus pycnocephalus* L. SY 1101	Kerbeş	Stem	The stem is consumed raw after peeling	0.02
Asteraceae	*Carthamus tinctorius* L. SY 1020	Aspir, Diken, Zafur	Flower	Added to soups and local rice pudding called "zerde"	0.04
Asteraceae	*Centaurea iberica* Trevir. ex Spreng. SY 1118	Hesteriyezer, Çakırdiken	Aerial parts	It is cooked by adding tomato paste	0.03
Asteraceae	*Echinops orientalis* Trautv SY 1010	Şekerok	Stem	The stem is consumed raw after peeling	0.04
Asteraceae	*Gundelia tournefortii* L. var. *armata* Freyn & Sint. SY 1119	Kereng, kenger	Stem	The stem is consumed raw after peeling; cooked with eggs	0.36
Asteraceae	*Helichrysum orientale* (L.) Vaill. SY 1041	Ölmez çiçek	Aerial parts	Brewed and served like tea	0.05
Asteraceae	*Matricaria chamomilla* L. SY 1009	Papatya	Aerial parts	Brewed and served like tea	0.04
Asteraceae	*Notobasis syriaca* (L.) Cass. SY 1120	Kerbeş, Kırbeş	Stem	The stem is consumed raw after peeling	0.02
Asteraceae	*Onopordum carduchorum* Bornm. & Beauverd SY 1125	Kulındor, Qulındor	Stem	The stem is consumed raw after peeling	0.07
Boraginaceae	*Alkanna orientalis* (L.) Boiss. SY 1140	Mıtmıtok, Fısfıso	Flower	Its flowers are absorbed by children	0.05
Boraginaceae	*Anchusa azurea* Mill. SY 1139	Guriz	Leaves, Stem	Cooked with eggs; consumed by adding it to rice	0.28
Brassicaceae	*Alyssum strictum* Willd. SY 1137	Nanieçuçuka	Aerial parts	Consumed by adding it to rice	0.09
Brassicaceae	*Capsella bursa-pastoris* (L.) Medik. SY 1049	Çobançantası, Kuş otu, Kuşkuş otu	Aerial parts	Brewed and served like tea	0.06
Brassicaceae	*Lepidium draba* L. SY 1126	Kıniberk	Aerial parts	It is cooked by adding tomato paste	0.02
Brassicaceae	*Thlaspi perfoliatum* L. SY 1121	Nanieçuçuka	Aerial parts	Used in salads	0.02
Cannabaceae	*Celtis australis* L. SY 1124	Dağdağan	Fruit	Consumed as a fruit	0.14
Equisetaceae	*Equisetum arvense* L. SY 1061	Atkuyruğu, Kırkkilitotu	Aerial parts	Brewed and served like tea	0.02
Ericaceae	*Erica vulgaris* L. SY 1076	Taşakcılotu	Leaves, Flower	Brewed and served like tea	0.02
Euphorbiaceae	*Euphorbia cheiradenia* Boiss. & Hohen. SY 1098	Heşül	Branch, Flower	Used to add a pleasant smell and taste to molasses	0.05
Euphorbiaceae	*Euphorbia falcata* L. SY 1097	Heşül	Branch, Flower	Used to add a pleasant smell and taste to molasses	0.02
Fabaceae	*Astragalus aleppicus* Boiss. SY 1130	Gunpisik	Fruit	Consumed as a fruit	0.08
Fabaceae	*Glycyrrhiza glabra* L. SY 1019	Meyan, Biyan, Biyam balı	Roots	The roots are boiled and drunk as juice	0.39

Fabaceae	*Prosopis farcta* (Banks & Sol.) J.F.Macbr. SY 1134	Hurnif, Çeti	Fruit	Consumed as a fruit	0.02
Fabaceae	*Pisum sativum* L. SY 1111	Bezelye	Seed	Fresh seeds are consumed raw	0.04
Iridaceae	*Crocus cancellatus* Herb. subsp. *damascenus* (Herb.) B.Mathew SY 1103	Pivok	Bulb	Eaten raw	0.03
Iridaceae	**Crocus sativus* L. SY 1032	Zahferan, Safran	Stylus	Sprinkled on top of the local pudding named "zerde" to add a pleasant smell and color	0.06
Juglandaceae	**Juglans regia* L. SY -	Ceviz, Koz, Goz	Seed	Consumed as an appetizer; used in making cakes and desserts	0.36
Lamiaceae	*Clinopodium congestum* (Boiss. & Hausskn.) Kuntz SY 1107	Pungietehta	Aerial parts	Used in salads	0.05
Lamiaceae	*Melissa officinalis* L. SY 1085	Melisa, oğulotu, Acem otu	Leaves	Brewed and served like tea	0.04
Lamiaceae	*Mentha longifolia* (L.) L. subsp. *typhoides* (Briq.) Harley SY 1117	Nane, Pung	Aerial parts	Brewed and served like tea	0.37
Lamiaceae	**Mentha x piperita* L. SY 1028	Nane, Pung	Aerial parts	Brewed and served like tea	0.44
Lamiaceae	*Mentha pulegium* L. SY 1064	Kaya yarpuzu, Punge tahte, Tüylü nane	Aerial parts	Brewed and served like tea	0.21
Lamiaceae	*Rosmarinus officinalis* L. SY 1006	Kuşdili, Biberiye	Leaves	Brewed and served like tea	0.11
Lamiaceae	*Salvia fruticosa* Mill. SY 1026	Adaçayı	Leaves	Brewed and served like tea	0.19
Lamiaceae	*Salvia multicaulis* Vahl SY 1104	Rehan	Aerial parts	Brewed and served like tea	0.20
Lamiaceae	*Thymbra spicata* L. SY 1033	Zahter, Yalancı kekik	Aerial parts	Used as a spice; brewed and served like tea	0.35
Lamiaceae	*Thymus fallax* Fisch. & C.A. Mey. SY 1046	Kekik	Aerial parts	Used as a spice	0.41
Malvaceae	**Abelmoschus esculentus* (L.) Moench SY -	Bami	Fruit	The fruits are consumed by boiling	0.02
Malvaceae	*Althaea officinalis* L. SY 1069	Hatmi, Hiro	Flower, Leaves	Brewed and served like tea	0.10
Malvaceae	**Hibiscus sabdariffa* L. SY -	Narçiçeği	Flower	Brewed and served like tea	0.12
Malvaceae	*Malva parviflora* L. SY 1116	Tollik	Aerial parts	Cooked with adding tomato paste and eggs	0.14
Malvaceae	*Malva sylvestris* L. SY 1067	Kömeç, Tollik, Ebegümeci	Aerial parts	Cooked with adding tomato paste and eggs	0.19
Moraceae	*Morus nigra* L. SY 1082	Karadut	Fruit	Consumed as a fruit; used in making fruit juice and molasses	0.27
Oleaceae	**Olea europaea* L. SY-	Zeytin	Fruit	Fruit is eaten	0.24
Papaveraceae	*Papaver dubium* L. SY 1141	Zingılzava	Whole plant	Cooked with adding tomato paste and eggs	0.16
Papaveraceae	*Papaver somniferum* L. SY 1081	Haşhaş	Leaves, Seed	Sprinkled on the cake	0.12
Pedaliaceae	**Sesamum indicum* L. SY -	Susam, Küncü	Seed	Sprinkled on cakes, breads and pastries	0.29
Poaceae	*Triticum aestivum* L. SY 1144	Gennim	Seed	Used as flour	0.25
Poaceae	**Zea mays* L. SY -	Mısır	Seed	Consumed as an appetizer; used in making cakes and desserts	0.32
Polygonaceae	*Polygonum cognatum* Meisn. SY 1142	Tırşok	Aerial parts	Used in salads	0.36
Portulacaceae	*Portulaca oleracea* L. SY 1024	Semizotu, Parpar	Leaves	Used in salads	0.28
Ranunculaceae	*Nigella sativa* L. SY 1030	Çörekotu, Kara çörek	Seed	Sprinkled on cakes, breads and pastries	0.38
Rosaceae	*Amygdalus communis* L. SY 1147	Beivf	Fruit, Seed	Consumed as a fruit; consumed as an appetizer	0.32
Rosaceae	*Crataegus monogyna* Jacq. SY 1047	Alıç, Guviç	Flower, Fruit	Consumed as a fruit; brewed and served like tea; used for producing vinegar	0.37
Rosaceae	*Rosa canina* L. SY 1008	Kuşburnu	Fruit	Consumed as a fruit; jam is made	0.29
Urticaceae	*Urtica dioica* L. SY 1021	Isırgan	Leaves	Cooked with adding tomato paste and eggs	0.39
Vitaceae	**Vitis vinifera* L. SY -	Üzüm, Tiri	Fruit	Consumed as a fruit; used for producing vinegar	0.35

*Cultivated plants

Cilt 11, Sayı 1, Sayfa 66-70, 2022 Volume 11, Issue 1, Page 66-70, 2022

Araştırma Makalesi https://doi.org/10.46810/tdfd.982316 Research Article

Türk Doğa ve Fen Dergisi
Turkish Journal of Nature and Science
www.dergipark.gov.tr/tdfd

Dergimiz yazarlarından Ramazan Şadet GÜVERCİN'in vefat haberini almış bulunmaktayız. Merhuma Allah'tan rahmet, sevdiklerine başsağlığı diliyoruz.

Vegetative Propagation of Cotton (Gossypium spp.) By Rooting

Ramazan Şadet GÜVERCİN[1*]

[1] Kahramanmaraş Sütçü İmam University, Turkoglu Vocational High School, Kahramanmaraş, Turkey
Ramazan Şadet GÜVERCİN ORCID No: 0000-0002-6195-5762

**Corresponding author: rguvercin@ksu.edu.tr*

(Received: 13.08.2021, Accepted: 16.09.2021, Online Publication: 25.03.2022)

Keywords
Clone production, Cotton, Hybrid vigor, Rooting

Abstract: Cotton plant is produced with seeds. However, its genetic structure is suitable for vegetative production. In this study, rooting method used to propagate cotton plant as vegetative. Experiment was conducted in climate chamber at East Mediterranean Transitional Zone Agricultural Research Institute in 2020. Stems of Askabat 100 (*G. barbadense* L.), Stoneville 468 (*G. hirsutum* L.) cultivars and their F_1 hybrid were used as plant materials while 2000 ppm IBA (Indole butyric acid) concentration used as chemical materials. As a result of the study, it was determined that cotton genotypes rooted and formed shoots in different rates. Moreover, F_1 hybrid produced more clones than their parents, followed by Askabat 100 and Stoneville 468. Also, F_1 hybrid were showed that superior heterotic effects as heterosis and heterobeltiosis in term of investigated properties. This result showed that cotton cultivars and hybrids can be propagation as clone using by rooting, and these clones could be used as rootstocks again in clone production.

Pamuk (Gossypium spp.) Bitkisinin Köklendirme Yöntemiyle Vejetatif Çoğaltılması

Anahtar Kelimeler
Klon üretimi, Pamuk, Hibrit gücü, Köklendirme

Öz: Pamuk bitkisi tohumlarla üretilir. Ancak genetik yapısı vejetatif üretime uygundur. Bu çalışmada, pamuk bitkisinin vejetatif olarak çoğaltılması amacıyla köklendirme yöntemi kullanılmıştır. Deneme, 2020 yılında Doğu Akdeniz Geçit Kuşağı Tarımsal Araştırma Enstitüsü Müdürlüğü'nün iklim odasında yürütülmüştür. Bitki materyali olarak Askabat 100 (*G. barbadense* L.), Stoneville 468 (*G. hirsutum* L.) çeşitleri ile bunların F_1 hibritlerine ait gövde parçaları, kimyasal material olarak ise 2000 ppm IBA (Indol butirik asit) konsantrasyonu kullanılmıştır. Çalışma sonucunda pamuk genotiplerinin sürgün oluşturduğu ancak farklı oranlarda köklendiği belirlenmiştir. Ayrıca F_1 melezi, ebeveynlerinden daha fazla kök üretmiş, bunu Askabat 100 ve Stoneville 468 çeşitleri izlemiştir. Dahası F_1 melezleri incelenen özellikler yönünden önemli heterotik etki (heterosis ve heterobeltiosis) göstermiştir. Bu sonuç, pamuk çeşitlerinin ve hibritlerinin köklendirme yoluyla klon olarak çoğaltılabileceğini ve bu klonların klon üretiminde tekrar anaç olarak kullanılabileceğini göstermiştir.

1. INTRODUCTION

The Gossypium L. genus contains more than 50 species in the world. One of them is G. hirsutum L. (Upland cotton) which different varieties of it were cultivated in Turkey. Turkey is major G. hirsutum L. producers with Greece and Spain in Europe. Moreover, Bulgaria has been producing some amount of cotton. Farming of cotton starts with its seed planting, and quality seeds are bases of modern farming of cotton. But, preparing of quality seeds starts with breeder seeds, and takes minimum five years to serve for farmers with systematic and its expensive methods after breeding studies that takes 8-12 years.

Cotton is having sexual reproduction system, but it can rapidly propagation by vegetative methods too such as T or Shield budding method [1]. However, because of easy sowing of cotton seeds with machine, in traditional, grafting, transplantation and pruning practices are not widely used in cotton farming. Whereas, vegetative propagation of cotton is get some advantages. For example, because of every new individual (clone) has the same genetic constitute with its parent, breeders will can save their important hybrids or genotypes along with years in the greenhouse. Moreover, cotton farming will can be done with clones some areas having problems such as salty, droughty and contaminated with Verticillium dahliae Kleb. In this areas, if varieties have strong root development, tolerant to disease with high

yield and fiber quality, can be propagated with rooting, furthermore because have strong root system these cultivars can be used as rootstock plant in grafting methods.

On the other hand, for production of cotton seed, rooting, grafting or combination of rooting with grafting can be used in greenhouse. This production is very important. When breeders use this method, will can offer seeds having same genetic potential which produced from lots of clone plants to farmers. So, farmers will know about yield and quality potential of their field before harvest. There are a lot of studies on propagation of cotton by vegetative. Numerous cotton clones have been produced via micro-propagation from shoot [2], cotyledon explants [3] and hypocotyl of cotton seedlings [4]. Moreover, cotton was propagation as vegetative by grafting method in Turkey [1, 5]. The aim of this work is to search possibility of vegetative propagation on cotton (Gossypium spp) by rooting.

2. MATERIALS AND METHODS

2.1. Plant Materials

Stoneville 468 (G. hirsutum L.), Askabat 100 (G. barbadense L.) and their F1 hybrid were used as plant material in this experiment. Askabat 100 needs longer vegetation period for productions cotton, but produced lower seed cotton yield, lint yield and ginning out-turn in Turkey. On the other hand, Stoneville 468 is an upland cultivar having extra seed cotton yield; lint yield and ginning out-turn than Askabat 100, but lower fiber qualities.

2.2. Field Experiment and Climate Chamber Applications

This experiment was conducted at East Mediterranean Transitional Zone Agricultural Research Institute in 2020 (37o 38' N; 36o 37' E, altitude: 568 m), in climate chamber between 15 October 2020 and 30 November 2020, according to Randomized Complete Block Design (RCBD) with three replications. Plant stems of 22 weeks were used in study. The stems are divided into pieces with at least 4 nodes. Genotypes were represented by 100 plant stem parts in replications. Plant pieces were kept in indole butyric acid (2000 ppm) for 5 minutes and then transferred to perlite medium prepared before in the climate chamber. Then the climatic room conditions were fixed at 28+/-2 oC temperature and 70-80% humidity. With the counts made on 30 November 2020, the number of rooting plants, root number, root length, shoot number and shoot length were determined. Data were analyzed for number of rooting plant, root number per plant, root length per plant (cm), shoot number per plant, shoot length per plant (cm). Then, means of investigated properties were compared by Least Significant Degree at 0.05 (LSD0.05). In addition, hybrid vigor (heterosis and heterobeltiosis) values were determined by the following Eq.1 and Eq.2 formulas at below.

Heterosis (%)	Ht = ((F_1-MP)/MP)*100, MP=(Line parent+Tester parent)/2	(1)
Heterobeltiosis (%)	Htb = (F_1-Better Parent)/Better Parent)*100	(2)

3. RESULTS

3.1. Rooting Stages

In the study, the visuals about rooting can be seen in Figures 1, 2, 3, 4, 5 and 6. Plant parts with or without wood (bark) texture developed callus and rooted (Figure 1 and Figure 2).

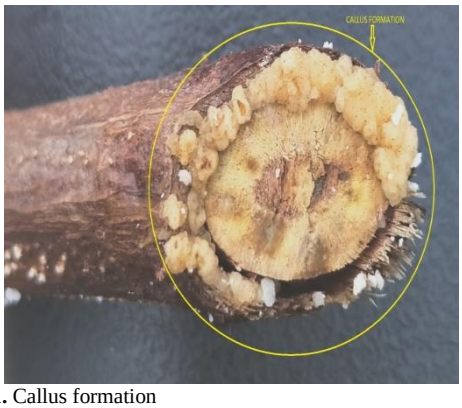

Figure 1. Callus formation

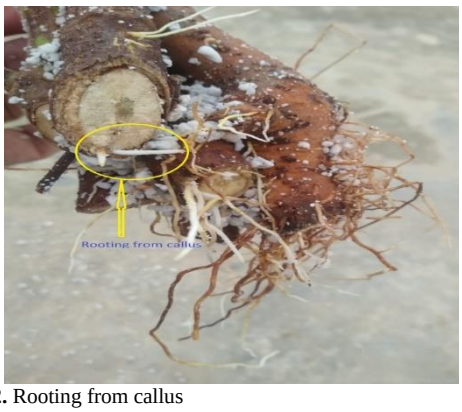

Figure 2. Rooting from callus

Thick plant parts formed mostly roots and long shoot (Figures 3 and 4). IBA 2000 dose and duration were sufficient for callus formation (Figures 1 and Figure 2). Furthermore, plant parts forming roots and shoots adapted to pots filled with 1/2 peat + 1/2 soil (Figure 6).

Figure 3. Rooting from green and non-green cuttings

Figure 4. Advanced roots

Figure 5. Clone plant with developed roots and shoots

Figure 6. Clone plant in pots

3.2. Number of Rooting Plant

The variance analysis regarding the number of rooting plants is shown from According to Table 1, the number of rooting plants differed according to their genotypes. The F1 hybrid was the most rooted genotype with 54.88%, and it was followed by Askabat 100 with 49.22% and Stoneville 468 with 26.88% (Table 2). According to Ouma et al. [4], cotyledon node explants of Stoneville 474 have rooted on sucrose based medium + IBA and +/- activated charcoal after a 25, 39 and 65 cumulative days in culture. It is a plant that can reproduce by cotton grafting and micro propagation methods. This study showed that the stem of cotton plant can be rooted and reproduced vegetative. This finding is very important. Wood texture or green plant body parts did not differ and were rooted.

The method will help breeders easily reproduce the plants they want to use for many years in seed production. In addition, they will be able to reproduce and protect important breeding materials in a short time. Moreover, seeds of commercial varieties will be propagated from clones of a plant and given to farmers. Thus, efficiency and quality losses will be reduced. On the other hand, triploid genotypes developed by interspecies hybridization will be easily reproduced by the method and can be used for many years in polyploidy studies.

3.3. Root Number Per Plant

Differences of cultivars were found important for average root number per plant (Table 1). The root number per plant has changed from 19.22 (Stoneville 468) to 37.56 (F1 hybrid).

Table 1. Variance analysis for the rooting application

Sources	Degree of freedom	Number of rooting plant	Root number per plant (cm)	Root length per plant	Shoot number per plant	Shoot length per plant (cm)
Replication	2	93.78	14.77	1.77	1.33 *	0.45
Cultivars	2	657.44 *	253.45 *	40.78 *	1.33 *	70.78 *
Error	4	23.61	18.44	3.11	0.17	3.61
Total	8	199.61	76.28	12.19	0.75	19.61

Table 2. Values of investigated properties in term of rooting applications

Cultivars	Number of rooting plant (number)	Number of root per plant (number)	Root length per plant (cm)	Shoot number per plant	Shoot length per plant (cm)
Stoneville 468	26.88 b	19.22 b	9.89 b	4.00 b	7.11 b
Askabat 100	49.22 a	27.22 b	12.89 b	4.66 b	11.10 b
F_1 hybrid	54.88 a	37.56 a	17.22 a	5.33 a	16.77 a
CV (%)	9.70	15.65	12.80	10.20	15.98
$LSD_{0.05}$	11.01	9.74	3.99	0.93	1.53

CV (%):*Coefficient of variation*, LSD: *Least significant degree*

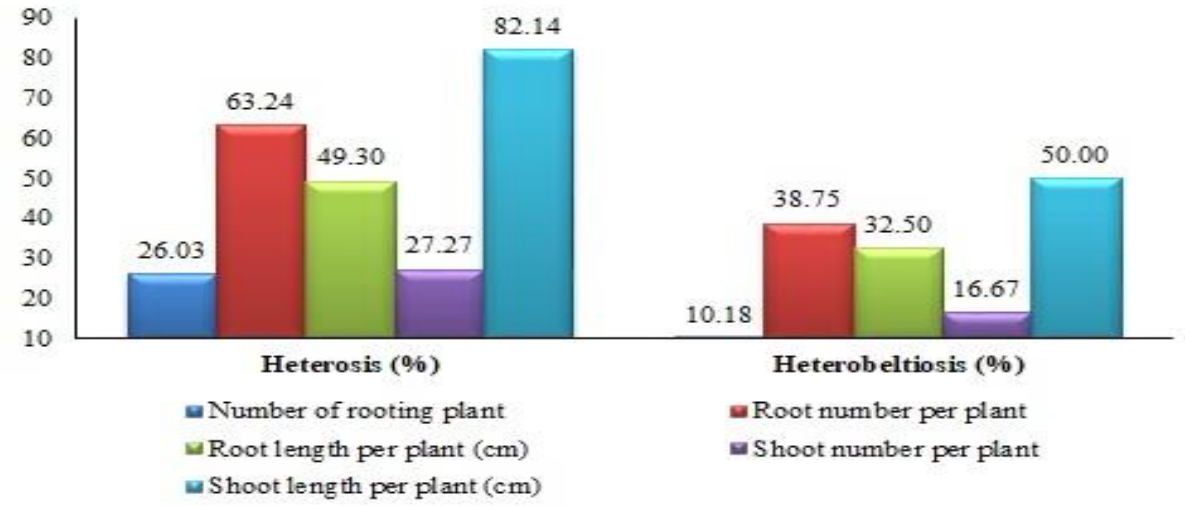

Figure 7. Hybrid vigor (Heterosis and heterobeltiosis) values of F_1 hybrid

Also, Askabat 100 has produced 12.89 roots per plant. The F1 hybrid has most number of roots than Askabat 100 and Stoneville 468 having minimum numbers of root (Table 2). Cotton has a rapidly growing taproot and the seedling can reach 20-25 cm deep without even growing above the ground. The final depth of the root system depends on soil moisture, aeration, temperature and variety, but is usually about 180-200 cm. Although cotton stem pieces are rooted, they cannot taproot form like a normal cotton plant.

3.4. Root Length in Plant

Differences of mean of root length of cultivars were found very important (Table 1). According to Table 2, means of root length of cultivars were differed. F1 hybrid has development very long roots than Stoneville 468 and Askabat 100. While F1 hybrids getting 17.22 cm root length, the Askabat 100 and Stoneville 468 cultivars had 12.89 cm and 9.89 cm root length, respectively. Root length is very important to reach water and nutrients in the soil. Furthermore, the number of roots is also important in terms of the plants holding in the soil and resisting wind effects.

3.5. Shoot Number Per Plant

In the study, where the average number of shoots varied between 4.0 and 5.33 (Table 2), and difference among genotypes was found to be significant (Table 1). While the F1 hybrid is produce 5.33 shoot, Askabat 100 and Stoneville 468 have produced 4.66 and 4.00 shoots, respectively. The high numbers of shoots were found important in terms of photosynthesis. Özyiğit [2] reported that shoot development was maximum 74.2 % in cotyledon nodes.

3.6. Shoot Length per Plant

Plant shoot lengths of genotypes were found to be significant (Table 1). The F1 hybrid had the longest shoots, followed by Askabat 100 and Stoneville 468. This situation may have occurred due to genetic difference. Shoot length of F1 cross was 16.77 cm, while shoot length of Askabat 100 and Stoneville 468 were 11.10 cm and 7.11 cm, respectively. Plant shoot length was found to be related to shoot number. Those with more plant shoots formed shorter shoots.

3.7. Hybrid Vigor (Heterosis and Heterobeltiosis)

The hybrid vigor of the F1 hybrid for the traits examined is monitored from Figure 7. According to Figure 7, high heterosis and heterobeltiosis values were found to be significant. The highest heterosis and heterobeltiosis were observed in plant shoot length. It was followed by plant root number and plant root length. The importance of hybrid power of root number and length was found to be important in terms of clone production in cotton plant. The F1 hybrid produced 50% more shoots, 38.75% more root count, 32.50% more root length and 10.18% more clones than its superior parent.

4. CONCLUSIONS

Cotton plant is produced with seeds. Lots of studies have shown that cotton can also be produced by vegetative propagation methods. While cotton is propagated by grafting method [1, 6-7], Özyiğit [2] produced vegetative from internodes under in vitro conditions. In addition, Karaca et al. [5] had been successful in seedling with grafting. In addition, Karaca et al. [5] had been successful in seedling with grafting. In this study, another vegetative reproduction method has been experiment, which rooting. At the end of study, it was determined that not only cultivars belonging to G. hirsutum L but also G. barbadense L with their F1 hybrid had been produced by rooting. Moreover, F1 hybrid was found more important than their parents in tern of investigated properties, showed more important heterotic effects (heterosis and heterobeltiosis). This may be due to heterozygous genetic makeup of the F1 hybrid. The results of study showed that rooting can be done on cotton in advanced plant form. On the other hand, the fact that F1 hybrid is superior to its parents in terms of root number and root length has shown that F1 crosses can be used as rootstock for clone production. Thus, quality seeds will be provided to farmers by producing clones of productive and high quality varieties on clone rootstock.

Acknowledgement

I would like to express my gratitude to Dr Remzi UĞUR who supported me in this study.

REFERENCES

[1] Güvercin RŞ. Clonal production of cotton (Gossypium spp.) by T-budding method. J Agr Fac Gazi Osman Pasa Univ. 2016;34(3):100-104.
[2] Özyiğit İİ. In vitro shoot development from three different nodes of cotton (G. hirsutum L.). Notulae Botanicae Horti Agrobotanici Cluj-Napoca. 2009;37(1):74-78.
[3] Ouma JP, Young MM, Reichert NA. Rooting of in vitro regenerated cotton (G. hirsutum L.) is influenced by genotype, medium composition, explant type and age. African J Bio. 2004;3 (6):313-318.
[4] Hayta-Smedley S, Özbek O, Ansız A, Bayraktar M, Gürel A. The effect of different plant growth regulators on callus induction from hypocotyl explants and plantlet regeneration through somatic embryo in cotton (G. hirsutum L.) genotype Nazilli-143. Anadolu J Aegean Agr Res Ins. 2018;28(2):55-61.
[5] Karaca M, İnce AG, Reddy UK. Interspecific grafting between G. hirsutum, G. barbadense and G. herbaceum lines. Sci Reports. 2020;10:18649.
[6] Rea HE. Asexual reproduction of cotton. J Heredity. 1928;19: 357.
[7] Rea HE. Callusing cotton stem cuttings. Plant Phy. 1930;5:575-586.

Araştırma Makalesi https://doi.org/10.46810/tdfd.994714 Research Article

Türk Doğa ve Fen Dergisi
Turkish Journal of Nature and Science
www.dergipark.gov.tr/tdfd

Çift Silindirli Su Soğutmalı Bir Motorun Biyel Kolu Yapısal Analizi

Eda ŞAHİN[1], İdris CESUR[1], Hüseyin KAHRAMAN[1,*]

[1] Sakarya Uygulamalı Bilimler Üniversitesi, Teknoloji Fakültesi, Makine Mühendisliği Bölümü, Sakarya, Türkiye
Eda ŞAHİN ORCID No: 0000-0003-2060-2191
İdris CESUR ORCID No: 0000-0001-7487-5676
Hüseyin KAHRAMAN ORCID No: 0000-0003-3322-9904

**Sorumlu yazar: huseyink@subu.edu.tr*

(Alınış: 13.09.2021, Kabul: 03.03.2022, Online Yayınlanma: 25.03.2022)

Anahtar Kelimeler
Biyel kolu, Dizel motor, Yapısal analiz, Ansys

Öz: Biyel kolu, taşıtlarda pistonun doğrusal hareketini krank milinin dairesel hareketine iletmek için kullanılır. Bu hareket iletimi sırasında çeşitli gerilme türlerine maruz kalan biyel kolunun malzeme seçimi ve tasarımı, biyel kolunun mukavemet değerlerini etkileyen önemli faktörlerdendir. Bu çalışmada, çift silindirli dizel bir motor olan TR-ERB modelinin biyel kolu için yapısal analiz testleri yapılmış ve bu modele alternatif bir tasarım geliştirilmiştir. İlk aşamada TR-ERB modeli için beş faklı malzeme üzerinden analizler gerçekleştirilmiş ve daha sonra en uygun bulunan malzeme için alternatif model tasarımı üzerinden analizler tekrarlanmıştır. Yapısal analiz sonucunda en iyi sonucu veren malzeme 42CrMo4 olup gerilme değeri 425 MPa'dır. Malzemedeki deformasyon değerleri incelendiğinde ise en az deformasyon değeri 42CrMo4 malzemesinde olup miktarı 0,0609'dır. Maksimum deformasyon değeri dökme demir malzemesinde 0,107'dir. Eşdeğer elastik gerilim miktarında en iyi değer AISI1050 malzemesinde elde edilmiştir.

Structural Analysis of a Two-cylinder, Water-Cooled Engine

Keywords
Connecting rod, Diesel engine, Structural analysis, Ansys

Abstract: The connecting rod is used in vehicles to transmit the linear motion of the piston rod to the circular motion of the crankshaft. The selection and design of the connecting rod, which is subjected to various types of tension in this movement transfer, is one of the important factors affecting the strength of the connecting rod. With this study, analysis tests of the connecting rod of the TR-ERB model, which is a twin cylinder diesel engine, have been made and then an alternative design has been made for this model. In the first stage, analyses were made on five different materials for the TR-ERB model, then the analyses were repeated over the alternative model design for the material with the highest strength. As a result of the structural analysis, the material that gives the best result is 42CrMo4 and its stress value is 425 MPa. In terms of deformation values in the material, the least deformation value is in 42CrMo4 material and its amount is 0.0609. Its value at maximum deformation is 0.107 in cast iron material. The best value was obtained for the AISI1050 material in the equivalent amount of elastic tension.

1. GİRİŞ

Motor teknolojisinin gelişmesindeki en büyük etken şüphesiz ki Otto ve Dizel çevrimlerinin bulunmasıdır. Dizel motorları, silindir içerine alınan havanın sıkıştırılıp, sıcaklığı ve basıncı artan yanma odası içeresindeki havanın üzerine yakıt püskürtülmesi ve yakıtın alev alması ve patlaması prensibiyle çalışır [1]. Yanma odasına gelen hava ve yakıtın yakılabilmesi için pistonun doğrusal bir ileri geri hareketi yapması gerekmektedir. Biyel kolunun motordaki ana fonksiyonu ise pistondan aldığı doğrusal hareketi krank miline dairesel hareket olarak iletmektir [2]. Biyel kolu bu hareketi sırasında; piston başındaki gaz basıncından kaynaklı basma yüküne, piston hızındaki değişiklikler nedeniyle karşılıklı çekme ve basma kuvvetlerine, salınım hareketinden dolayı biyel gövdesinde eğilmeye ve büyük basma kuvvetlerinden dolayı burkulmaya maruz kalır. Biyel kolu eksenel çekme ve basma yüklerine ek olarak çok yönlü genlikli eğilme yüklemeleri, atalet kuvvetleri ve burkulma yüklerine de maruz kalır. Motorun normal çalışması durumunda 2000-3000 devir yapan biyel kolunun motor içerisinde hareket ederken oluşacak gerilmelere karşı da yeterince dayanıklı olması gerekmektedir [3].

İçten yanmalı motorlarda, motor parçalarının tasarım ve hesaplamalarında sonlu elemanlar metodu kullanılmaktadır. Sonlu elemanlar metodu, karmaşık mühendislik ve matematiksel modellerde kullanılan bir sayısal analiz yöntemidir [4]. İlk olarak uçak gövdelerinin analizlerinde kullanılan bu metot daha sonra yaygınlaşarak mühendislik problemleri ve uygulamaları için de kullanılmaya başlanmıştır. Sonlu elemanlar yöntemi özellikle kütle aktarımı, yapı statiği, ısı aktarımı ve elektriksel potansiyel problemlerinde kullanılır [5]. Sistem analiz edilmesi gereken parçayı sonlu eleman denilen küçük parçalara ayırarak problemin çözüleceği uzayı ayrıklaştırır [6]. Sınır değerlerinin bu formülasyonu sonucu cebirsel bir denklem sistemi elde edilmektedir. Bu denklemler daha sonra çeşitli metotlarla çözülmektedir [7].

Literatüre baktığımızda; Ali ve ark., biyel kolu üzerine farklı miktarda değişken yükler uygulanmasını etkilerini sonlu elemanlar yöntemiyle incelemişlerdir. Analiz sonuçlarını biyel kolu üzerindeki basma be çekme yük dağılımlarını göre yapmışlardır [8]. Mohankumar ver ark., Ansys programında biyel koluna gelen yanma basıncının oluşturduğu kuvvetleri analiz etmişlerdir. Çalışmalarında, farklı malzemelerden yapılmış biyel kolunun analizleri yapılmıştır. Analizde emniyet faktörü, yorulma analizi ve deformasyon miktarları irdelenmiştir [9]. Al Hasan, Biyel kolu ve pimleri üzerine etkileyen kuvvetlerin analizi sonlu elemanlar yöntemi ile gerçekleştirmiştir. Çalışma sonucunda; biyel kolunun küçük ve büyük başında farklı malzemeler ile takviye edilmesi ile olumlu sonuçlar elde etmiştir [10]. Shenoy, deneysel çalışma sonucunda elde ettikleri yanma basıncına göre biyel kolu ve pimleri üzerine etkileyen kuvvetlerin etkilerini sonlu elemanlar analizi yapmıştır. Analizler iki aşamada gerçekleşmiştir. İlk bölümde statik yük altında FEA ve quasi-dinamik yük altında FEA analizleridir. Analizler sonucunda; biyel kolu üzerine etkileyen kuvvetler belirlenmiştir. İkinci kısımda ise biyel kolunun yorulma ömrü incelenmiştir. Sonuçta is eC-70 çeliği diğer malzemeye göre %10 daha hafiftir [11]. Dale, toz metal teknolojisi, dövme ve dökme yönetimine göre imal edilen biyel kolunun mekanik analizi yapmıştır. Çalışma sonucunda; dövme yöntemi döküm yöntemine göre %25–33 daha fazla yorulma dayanımına sahip olduğunu saptamıştır. Malzeme özellikleri ve imalat tekniğinin biyel optimizasyonunda önemli olduğunu belirlemiştir [12]. Webster ve ark., biyel kolunun sonlu elemanlar yöntemi ile analiz yapmışlardır. Biyel kolunun üzerine etkileyen kuvvet miktarı deneysel çalışma ile belirlemişlerdir. Biyelin büyük ve küçük başlarındaki etkileyen kuvvet dağılımlarını incelemişlerdir [13].

Literatürdeki çalışmalar incelendiğinde, farklı malzemelerden üretilmiş ve farklı yükler altındaki biyel kolunun yapısal analizi incelenmiştir. Bu çalışmada ise farklı malzeme ve yüklere ek olarak, yeni bir biyel tasarımı yapılmıştır. Bu çalışmada; çift silindirli dizel bir motor olan TR-ERB modelinin biyel kolu için yapısal analiz testleri yapılmış ve bu modele alternatif bir tasarım geliştirilmiştir. İlk aşamada TR-ERB modeli için beş faklı malzeme üzerinden analizler gerçekleştirilmiş ve daha sonra en uygun bulunan malzeme için alternatif model tasarımı üzerinden analizler tekrarlanmıştır.

2. MATERYAL VE METOT

Biyel kolunun yapısal analizlerinin yapılabilmesi için öncelikle bir tasarım modeli belirlenmiştir. Bu çalışma kapsamında TR-ERB modelli biyel kolu ana tasarım modeli olarak kabul edilmiştir. Bu model üzerine beş farklı malzeme tanımı yapılarak, biyel kolunun statik analizleri yaptırılmıştır. Yapılan analiz sonuçlarına göre bu malzemeler içerisinde biyel kolu için en uygun olan malzeme belirlenmiştir.

2.1. Malzemeler

Piston ile krank milini birbirine bağlayan biyel kolu, piston kuvvetini kranka ileterek krankın dönüşünü sağlar. Bu hareket sırasında biyel kolu basma, çekme ve burkulma kuvvetlerine maruz kalır. Biyel kolu malzemesi seçilirken de tüm bu kuvvetler göz önüne alınmalı ve bu zorlamalara karşı dirençli malzemeler seçilmelidir. Bu özellikleri karşılaması amacıyla biyel kolu için aşağıdaki malzemelerin analizler yapılmıştır.

- 42CrMo4
- C70S6 Çelik
- 36MnVS4
- AISI 1050 Çeliği
- Gri Dökme Demir

Bu malzemelerin biyel kolunun istenilen özelliklerine göre değerlendirilmesini yaparak, biyel kolu için en uygun malzemeyi tanımlayabiliriz [13].

Tablo 1'de analizler için belirlenmiş olan beş farklı malzemenin özellikleri belirlenmiştir. Bu özelliklerin kendi aralarında kıyaslamaları yapılmıştır. En iyi sonuç AISI 4140 çeliği hem mukavemet değerleri açısından hem de maliyet açısından diğer malzemelere göre daha uygun bulunmuştur. Ancak değerlendirme için sadece bu tablo baz alınmamış ve analizlerden elde edilen sonuçlara da bakılmıştır.

Tablo 1. Analizi Yaptırılacak Malzemelerin Özellikleri Tablosu [15,16]

Özellik/ Malzeme	42CrMo4	C70S6 Çelik	36MnVS4	AISI 1050 Çeliği	Gri Dökme Demir
Yoğunluk	7850	7817	7800	7850	7200
Çekme-Akma Dayanımı	750 MPa	550 MPa	742 MPa	580 MPa	551.49 MPa
Basma-Akma Dayanımı	750 MPa	550 MPa	742 MPa	580 MPa	551.49 MPa
Çekme-Kopma Dayanımı	1110 MPa	900 MPa	998 MPa	460 MPa	861.7 MPa
Birim Hacim Fiyatı	0,639 Usd /kg	0,8 Usd/kg	0,9 Usd/kg	0,438 Usd/kg	0,648 Usd/kg

2.2. Mühendislik Hesapları ve Analizler

Biyel kolu tasarımında referans alınan TR-ERB markalı biyel kolunun ölçüleri baz alınarak Solidworks üzerinden tasarım tamamlanmıştır. Solidworks üzerinden modellenmiş olan biyel kolları ANSYS programına aktarılarak malzeme bilgileri ve uygulanan kuvvetler programda tanımlanarak statik analizleri yaptırılmıştır.

Analizler biyel kolunun maksimum yük ve basınç altındaki durumu yani 20º'lik konumu baz alınarak yapılmıştır.

Bu çalışmada kullanılan dizel motorun maksimum basıncı katalog değerlerinden elde edilmiştir. Silindir içi basınç değeri 2,26 MPa' dır. Bu basınçtan yola çıkarak kuvvet hesabı yapılırsa;

Piston Çapı = 77 mm
$F = P^* A = 2{,}26 * (\pi * 38{,}5\ ^2)$ (1)
F = 10518,64 N

olarak bulunur. Pistona dik olarak etkiyen bu kuvvet biyel koluna 20º 'lik açı ile vurduğundan biyel üzerinden işlem yaparken bu kuvvetin bileşenleri dikkate alınır (Şekil 1).

$F = F^1 * Cos20$ (2)
$10518{,}64 = F^1 * Cos20$
$F^1 = 11194{,}80$ N

olarak hesaplanır. Bu kuvvet biyel kolu 20º'lik konumdayken biyele etkiyen dik kuvveti bize gösterir. Biyel kolu için statik analiz yaptırılırken biyele etkiyen kuvvet olarak denklem ikiden elde edilen kuvvet esas alınmıştır [17].

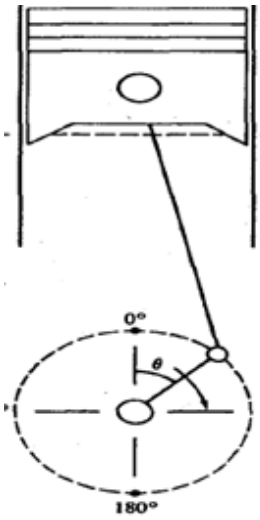

Şekil 1. Biyel Kolunun geometrisi

Analizi yaptırılacak biyel kolu Tablo 2'de verilen ölçüler doğrultusunda Solidworks üzerinden Şekil 2'de gözüktüğü gibi modellenmiştir.

Tablo 2. Biyel Kolu Ölçüleri

Strok	68 mm
Küçük Biyel Başı İç Çapı	20 mm
Küçük Biyel Başı Dış Çapı	30 mm
Büyük Biyel Başı İç Çapı	40 mm
Büyük Biyel Başı Dış Çapı	52 mm
Burç İç Çapı	19 mm
Yatak İç Çapı	37 mm
Yağlama Deliği Çapı	4 mm
Profil Kesiti	16 mm
Profil Derinliği	3,6 mm

Şekil 2. Biyel Kolunun 3D Modellenmesi

Solidworks üzerinden çizilmiş olan model-1 datası Ansys workbench ortamına alınmış ve gerekli analizlerin yapılabilmesi için ağ modeli (mesh) örülmüştür. Programda default olarak tanımlı mesh modeli kullanıldığı zaman biyel kolu üzerine 7803 nodes ve 4242 eleman tanımlanmaktadır. Ancak biyel kolu gibi karmaşık bir geometri için bu düğüm ve eleman sayısı oldukça yetersizdir. Bu nedenle mesh modeli oluşturulurken ''default mesh'' modülü yerine "fine mesh" modülü kullanılmıştır. Bu modül üzerinde de iyileştirmeler yapılarak toplamda 555088 düğüm ve 390245 eleman elde edilmiştir. Bu eleman sayısı analizler için yeterli bulunmuştur.

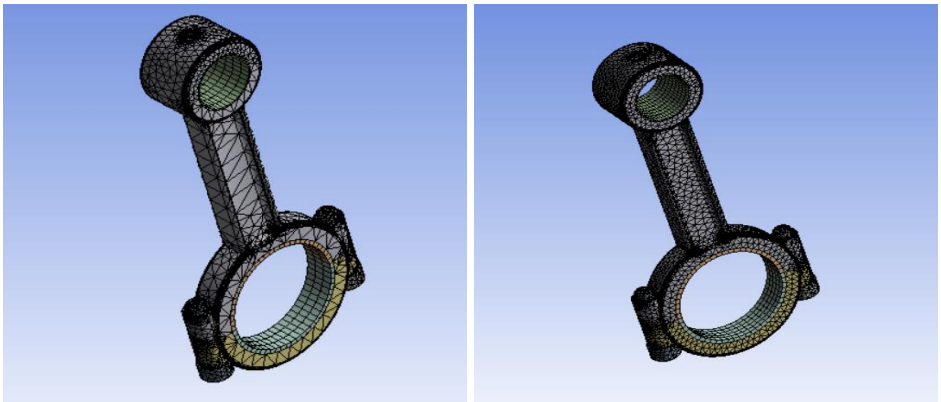

Şekil 3. Model-1'in Default ve Fine Olarak Tanımlı Mesh Görünümleri

Biyel kolunun statik analizini yaptırılırken, biyelin krank miline bağlandığı yataklardan model sabitlenmiştir. Biyel kolu 20°'lik konumundayken yanma basıncı maksimumu durumda olduğu bilindiği için pistona etkiyen kuvvetin düşey bileşeni hesaplanmış ve bu kuvvet biyele etki ettirilerek analiz yaptırılmıştır. Kuvvetin etki noktası biyel kolunun pistona bağlandığı gajin piminin bulunduğu küçük biyel başı olarak seçilmiştir. Böylece biyel kolu dik konumdaymış gibi kabul edilerek analizler bu konumda yaptırılmıştır (Şekil 3).

2.2.1. 42CrMo4 Malzemesi Analizleri

Model-1'de biyel malzemesi olarak 42CrMo4 çelik, yataklar için AISI 4340 tavlı çelik ve burç için 1023 karbon çeliği kullanılmıştır. Yatak ve burçların sürtünme etkisine karşı daha dayanıklı olması gerektiğinden sert malzemelerden seçilmiştir. Seçilen malzemelerin özellikleri Solidworks üzerinden belirlenip Ansys programına aktarılmıştır. Daha sonra her bir parça üzerine kendi malzemesinin tanımlaması yapılmıştır. Analiz sonuçları Şekil 4 ve Şekil 5'te verilmiştir. Bu sonuçlara göre maksimum deformasyon bölgesi biyelin üst yağlama deliği ve çevresinde bulunmuştur. Maksimum eşdeğer gerilme ise biyel küçük başı ve kol uzunluğu arasında meydana gelmiştir.

2.2.2 C70S6 Çeliği Analizleri

Analizlerde kullanılacak olan ikinci model için C70S6 çeliği kullanılmıştır. Yataklar için AISI 4340 tavlı çelik ve burç için 1023 karbon çeliği kullanılmıştır. Malzemelerin mekanik özellikleri Ansys üzerine aktarılmış ve model üzerinde gerekli tanımlamalar yapılmıştır. Malzeme özellikleri ve tanımlamalar yapıldıktan sonra parça model-1'de olduğu gibi alt başından sabitleniş ve biyelin küçük başından kuvvet etki ettirilmiştir. Analiz sonuçları Şekil 6 ve Şekil 7'de verilmiştir. Bu sonuçlara göre maksimum deformasyon bölgesi biyelin üst yağlama deliği ve çevresinde bulunmuştur. Maksimum eşdeğer gerilme ise biyel küçük başında meydana gelmiştir. Maksimum gerilme enerjisi biyel kol uzunluğunda görülmüştür.

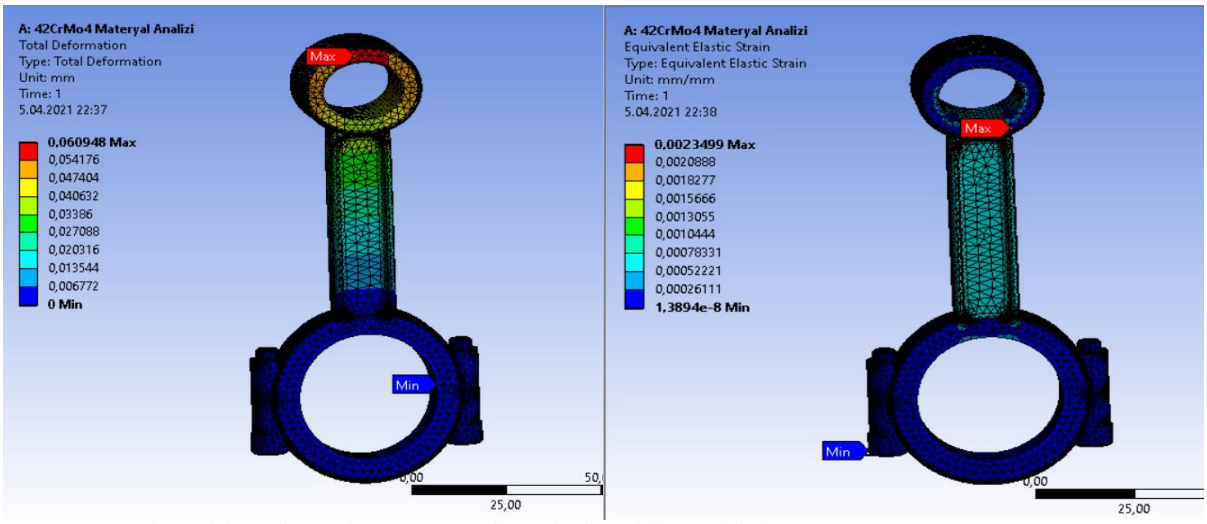

Şekil 4. 42CrMo4 Malzemesinin Toplam Deformasyon ve Eşdeğer Elastik Gerinim Analizleri

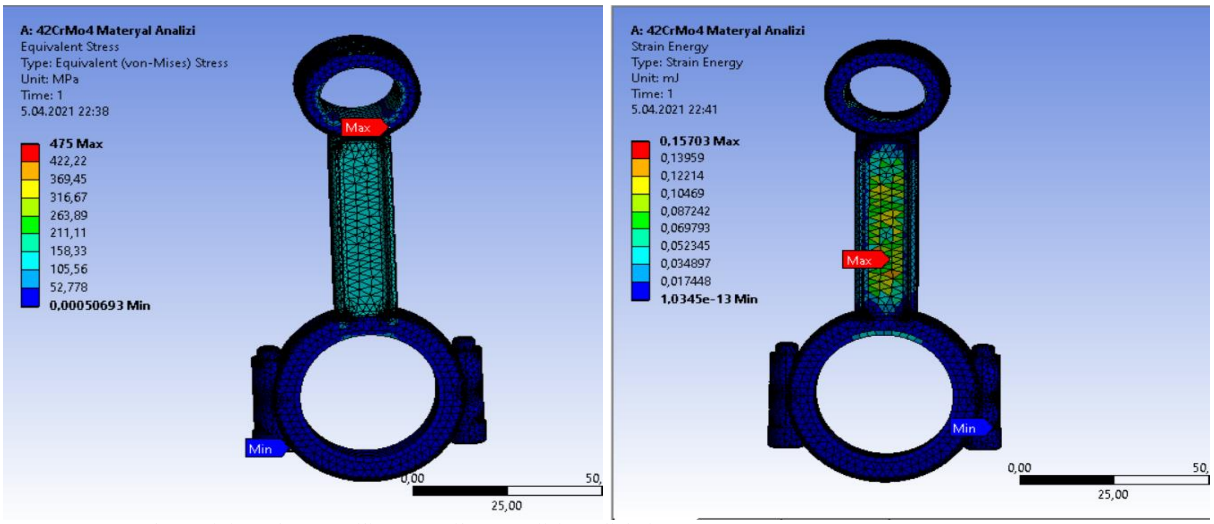

Şekil 5. 42CrMo4 Malzemesinin Eşdeğer Gerilim ve Gerilme Enerjisi Analizleri

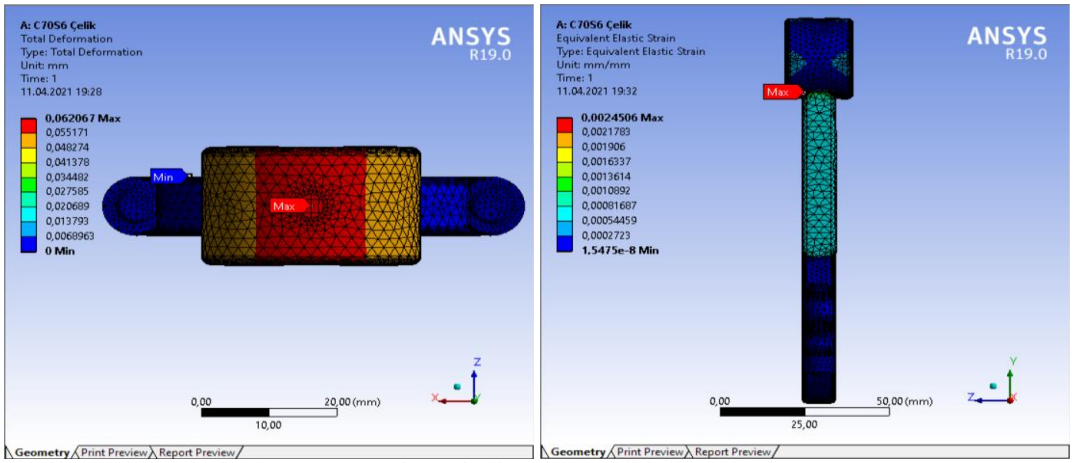

Şekil 6. C70S6 Malzemesinin Toplam Deformasyon ve Eşdeğer Elastik Gerinim Analizleri

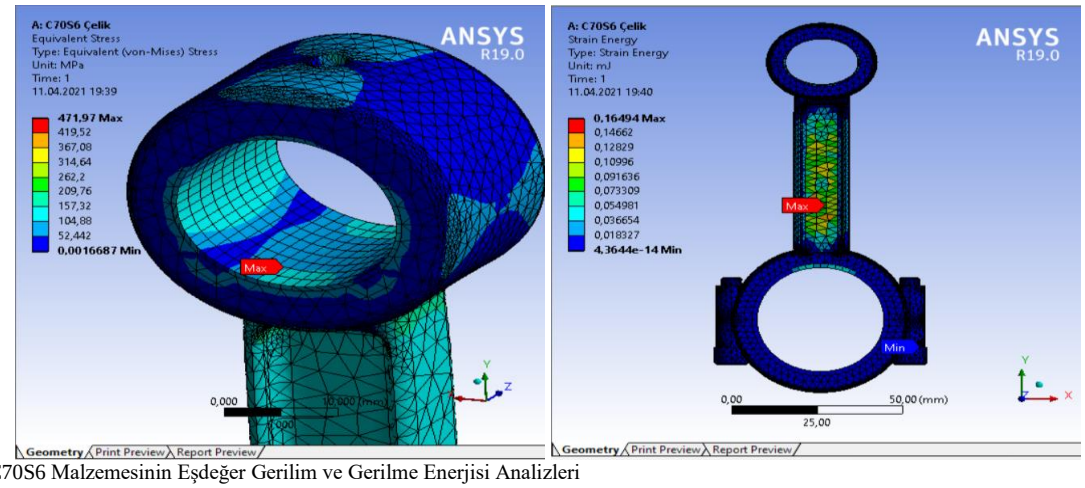

Şekil 7. 4C70S6 Malzemesinin Eşdeğer Gerilim ve Gerilme Enerjisi Analizleri

2.2.3 36MnVS4 Malzemesi Analizleri

Model III malzemesi olarak 36MnVS4 malzemesi seçilmiştir. Analiz sonuçlarında biyelin ana malzemesinin önemini ayırt edebilmek için biyel burç ve yataklarında tüm modellerde aynı malzemeler kullanılmıştır. Malzemenin özellikleri Ansys ortamına girildikten sonra malzeme tanımlamaları yapılmıştır. Model üzerinde yeniden mesh oluşturulup işlem yüzeyleri elde edildikten sonra analiz sonucunda görülmek istenen sonuçlar programa tanımlanmıştır. Analiz sonuçları Şekil 8 ve Şekil 9'da gösterilmektedir. Analizler sonucunda maksimum deformasyon biyel üst yağlama deliği ve çevresinde görülmüştür. Maksimum gerilme enerjisi biyel kol uzunluğu bölgesinde görülmektedir.

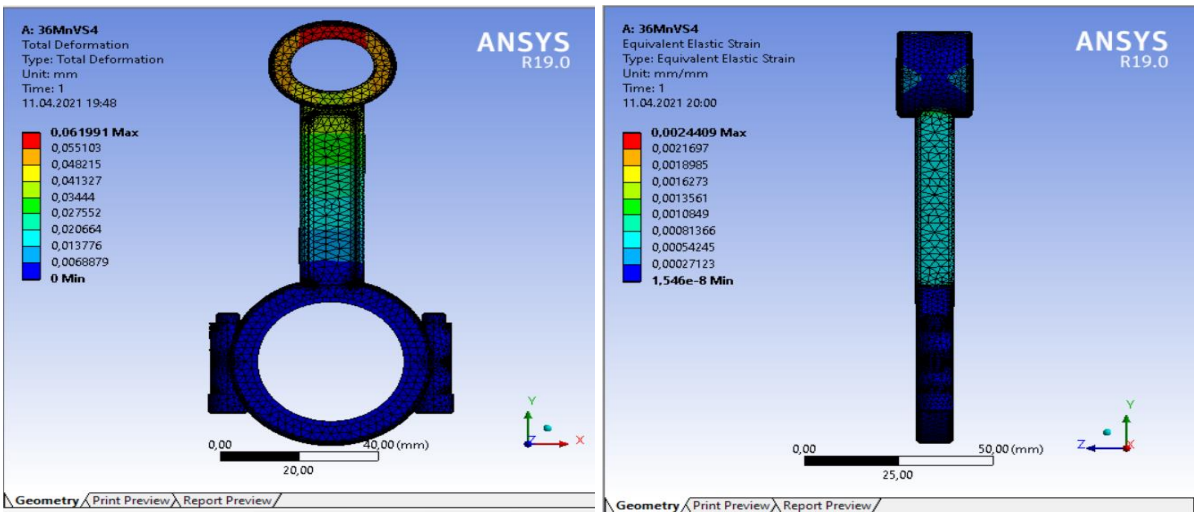

Şekil 8. 36MnVS4 Malzemesinin Toplam Deformasyon ve Eşdeğer Elastik Gerinim Analizleri

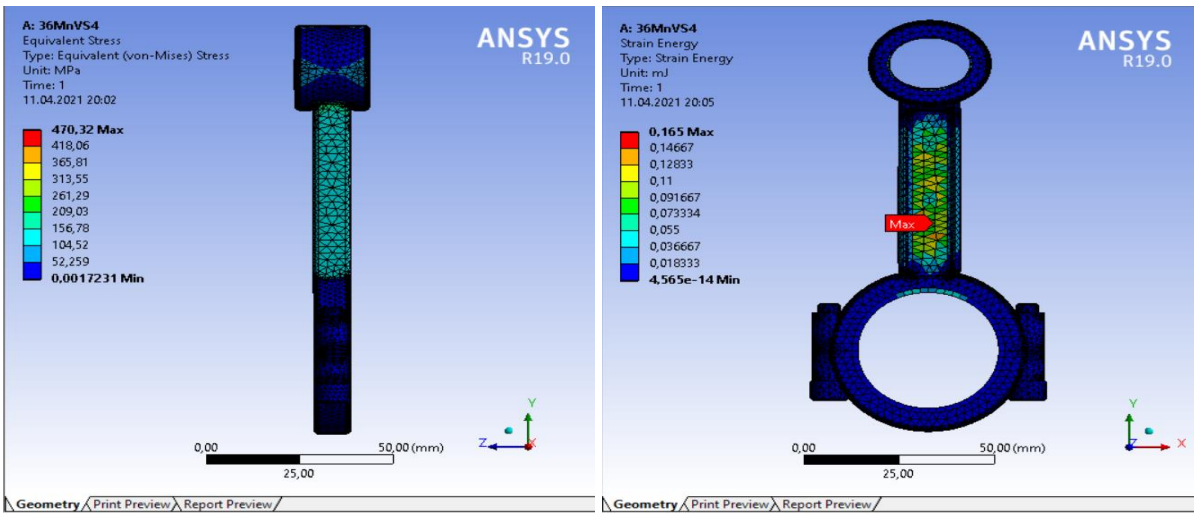

Şekil 9. 36MnVS4 Malzemesinin Eşdeğer Gerilim ve Gerilme Enerjisi Analizleri

2.2.4. AISI 1050 Çeliği Analizleri

Model IV'de ölçüleri tanımlanmış olan biyel kolunun yatak, burç ve cıvata malzemeleri aynı kalırken biyelin malzemesi AISI 1050 çeliği olarak değiştirilmiştir. Ansys ortamına alınan tasarım modeline malzeme atamaları gerçekleştirilmiş ve default olarak tanımlı olan mesh modeli fine olarak değiştirilmiş ve analizler yaptırılmıştır. Analizler sonucunda maksimum deformasyon biyel üst yağlama deliği ve çevresinde görülmektedir. Maksimum gerilme değeri ise biyel küçük başının bağlantı noktasında görülmektedir. Analiz sonuçları Şekil 10 ve 11'de görülmektedir.

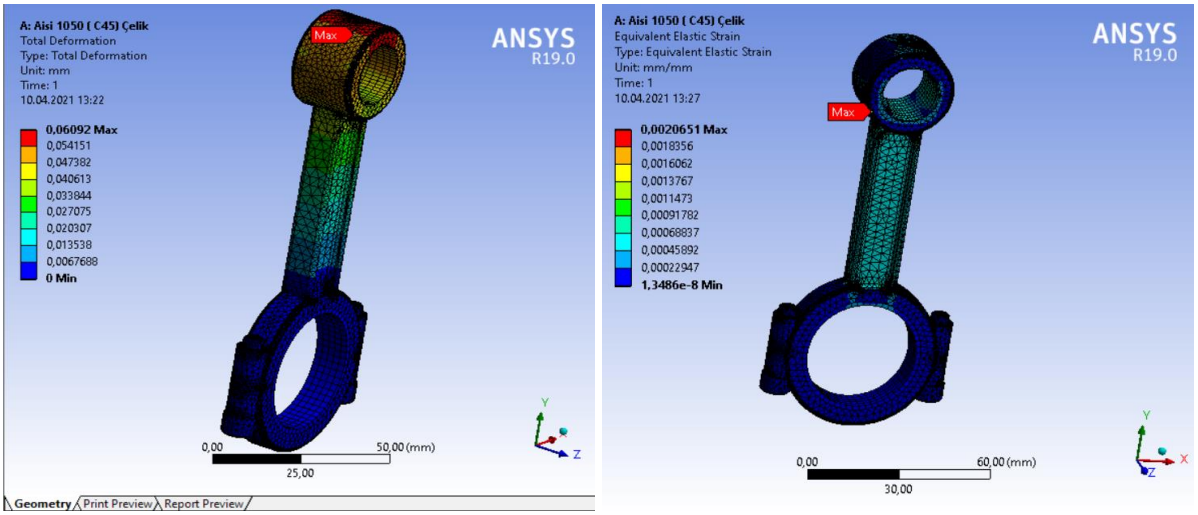

Şekil 10. AISI 1050 Malzemesinin Toplam Deformasyon ve Eşdeğer Elastik Gerinim Analizleri

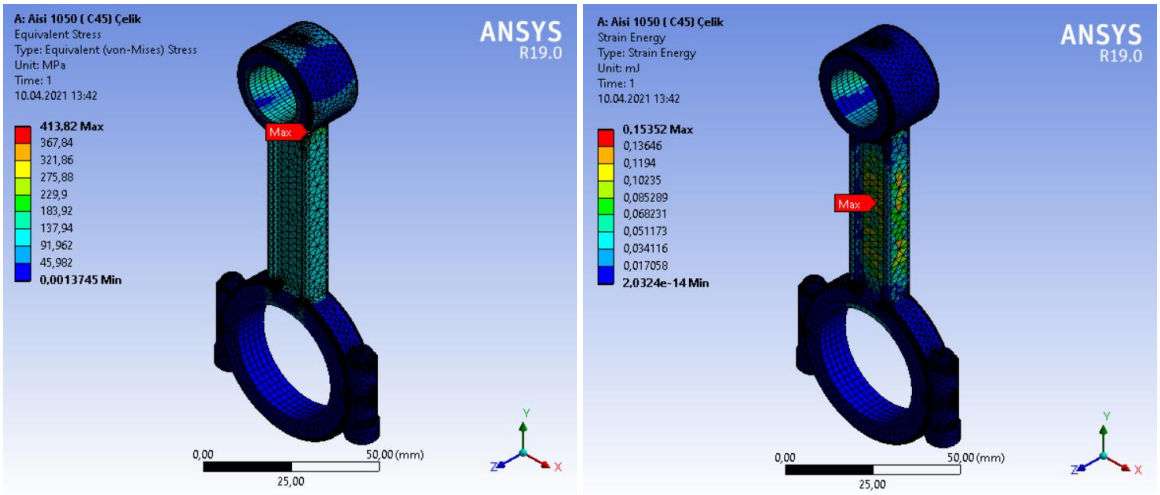

Şekil 11. AISI 1050 Malzemesinin Eşdeğer Gerilim ve Gerilme Enerjisi Analizleri

2.2.5. Gri Dökme Demir Malzeme Analizleri

Bu model için biyel malzemesi gri dökme demir olarak seçilmiştir. Biyel burç ve yatakları diğer modellerle aynı olacak şekilde yataklar için AISI 4340 tavlı çelik ve burç için 1023 karbon çeliği kullanılmıştır. Analiz sonuçları Şekil 12. ve Şekil 13.'te gösterilmiştir. Analiz sonuçlarına göre maksimum gerinim biyel küçük başının bağlantı noktasında görülürken maksimum uzama enerjisi biyel kol uzunluğunda görülmüştür. Maksimum deformasyon diğer analizlerde de olduğu gibi biyelin üst yağlama deliği ve çevresinde görülmektedir.

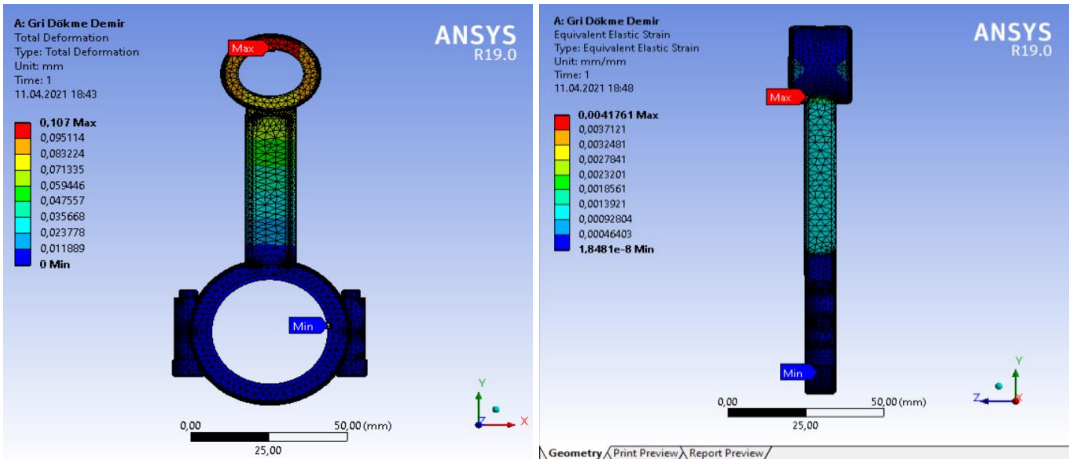

Şekil 12. Gri Dökme Demir Malzemesinin Toplam Deformasyon ve Eşdeğer Elastik Gerinim Analizleri

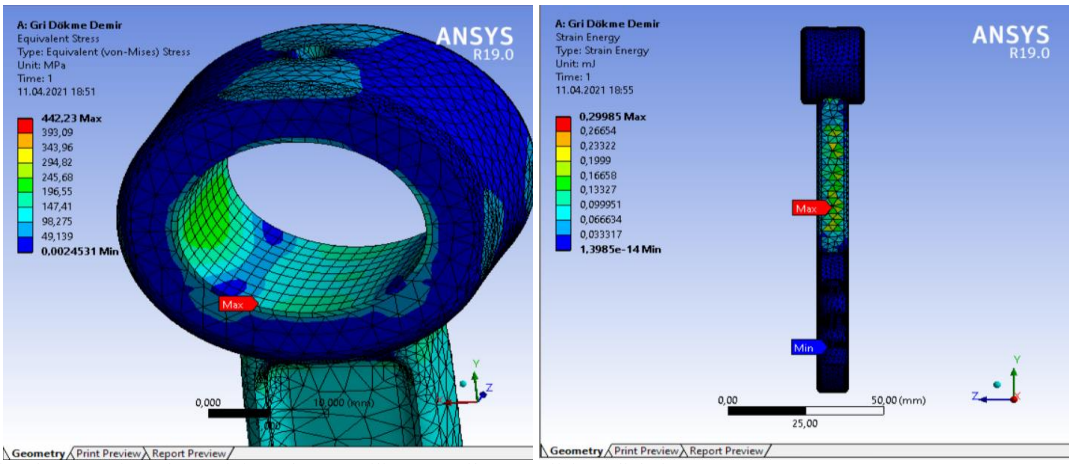

Şekil 13. Gri Dökme Demir Malzemesinin Eşdeğer Gerilim ve Gerilme Enerjisi Analizleri

3. BULGULAR

Bu çalışmada, iki silindirli bir dizel motora ait olan biyel kolunu beş farklı malzemesi için statik analizi Ansys programında yapılmıştır. Yapılan bu analiz sonucunda biyel kolu için en uygun biyel kol malzemesi tespit edilmiştir. Çalışma sonucunda tüm malzemeler için maksimum gerilme değerleri hesaplanmıştır. Şekil 14'te farklı malzemeler için analiz sonucunda elde edilmiş maksimum gerilme değerleri görülmektedir. Şekil incelendiğinde maksimum gerilme değeri 42CrMo4 malzemesinde elde edilmiştir. 42CrMo4 malzemesi için gerilme değeri 475 MPa'dır.

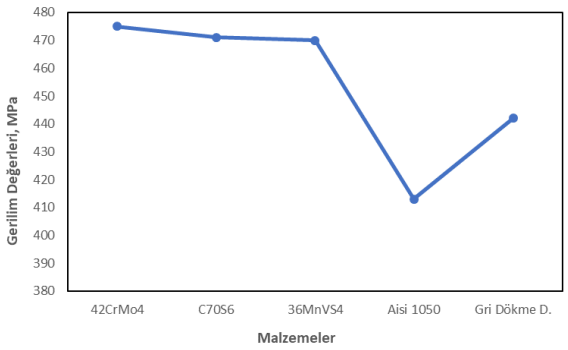

Şekil 14. Farklı malzemeler için analiz sonucu elde edilen maksimum gerilme değerleri

Şekil 15'te beş farklı malzeme için toplam deformasyon değerlerini gösteren grafik verilmiştir. Şekil incelendiğinde en düşük deformasyon değeri 42CrMo4 malzemesinde, en büyük deformasyon değeri ise gri dökme demir malzemesinde elde edilmiştir. Toplam

deformasyon maksimum ve minimum değerleri sırasıyla 0,107 ve 0,0609'dır.

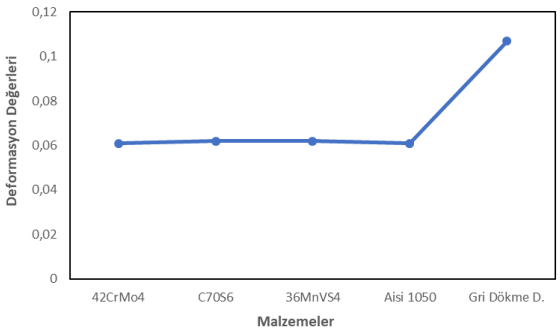

Şekil 15. Farklı malzemeler için analiz sonucu elde edilen toplam deformasyon değerleri

Şekil 16'da beş farklı malzeme için eş değer elastik gerinim değerleri verilmiştir. Şekil incelendiğinde en düşük deformasyon değeri AISI1050 malzemesinde, en büyük deformasyon değeri ise gri dökme demir malzemesinde elde edilmiştir. Toplam deformasyon maksimum ve minimum değerleri sırasıyla 0,0041 ve 0,002'dır.

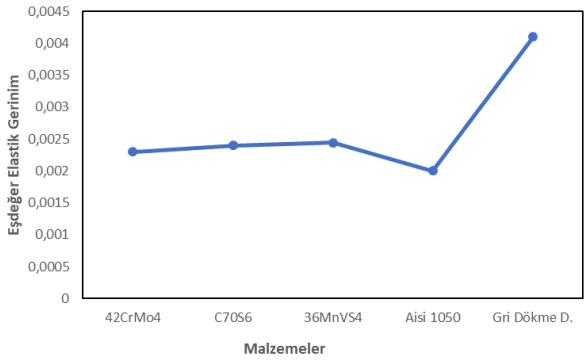

Şekil 16. Farklı malzemeler için analiz sonucu elde edilen eş değer elastik gerinim

Çalışma sonucunda elde edilen beş farklı malzeme maksimum gerilme değerleri malzemelerin çekme değerlerine göre karşılaştırılmıştır. Tüm malzemelerin çekme değerleri analiz sonuçları ile elde edilen gerilme değerlerinden daha yüksektir (Şekil 17). Bu sonuçlara göre tüm malzemeler silindir içi basıncın etkilediği değeri taşıyabilmektedir. Fakat motorun farklı çalışma şartları esnasında kuvvetin statik olmaması dinamik kuvvetlerin olmasın biyel koluna gelene gerilme değerlerini yükseltmektedir. Bu nedenle kullanılan malzemeler için bir emniyet katsayı gerekmektedir. Analizi yapılan malzemelerin emniyet katsayıları; 42CrMo4 çeliği için akma dayanımı 750 MPa ve analizden elde edilen oluşabilecek maksimum gerilme değeri 475 MPa olarak bulunmuştur. Bu durumda malzemenin emniyet katsayısı 1,57 olarak bulunur. C70S6 çeliği için akma dayanımı 742 MPa olarak bulunmuş olup, analizde elde edilen maksimum gerilme değeri 471 MPa'dır. Bu durumda C70S6 çeliği için hesaplanan emniyet katsayısı 1,06 olmaktadır. 36MnVS4 alaşımı için akma dayanımı 742 MPa olarak bulunmuştur. Analizlerden elde edilen maksimum gerilme değeri ise 470 MPa'dır. Bu durumda malzemenin emniyet katsayısı 1,57 olarak bulunur. AISI 1050 çeliği için akma dayanımı 580 MPa olarak bulunmuştur. Analizlerden elde edilen maksimum gerilme ise 413 MPa 'dır. Bu durumda malzemenin emniyet katsayısı 1,40 olarak bulunur. Gri dökme demir için akma gerilmesi 551 MPa olarak bulunmuştur. Malzemenin analiz sonuçlarına göre elde edilen maksimum gerilme ise 442 MPa'dır. Bu durumda elde edilen emniyet katsayısı 1,24'tür.

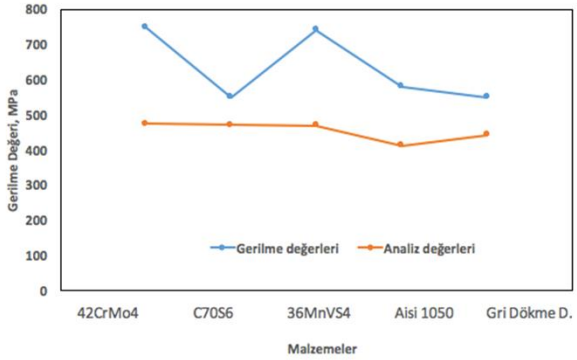

Şekil 17. Farklı malzemeler için çekme değerleri ve analiz değerlerini karşılaştırılması

Bu durumda gerilme değerleri üzerinden bir karşılaştırma yaparsak; 36MnVS4 alaşımı ve AISI 4140 çeliği emniyet katsayısı en yüksek olan malzeme olarak bulunurken, C70S6 çeliği en düşük emniyet katsayısına sahip malzeme olarak bulunmuştur.

Von-mises gerilme analizlerine göre değerlendirme yapacak olursak 42CrMo4 çeliğinin dayanım değerleri diğer malzemelere oranla daha yüksek çıkmıştır. Gri dökme demir ve AISI 1050 çeliğinin dayanım değerleri 413-442 MPa aralıklarındayken diğer malzemeler 470-475 MPa aralıklarına kadar mukavemetli bulunmaktadır. 42CrMo4 çelik, C70S6 çeliği ve 36MnVS4 çeliğinin değerleri birbirine çok yakın olarak çıkarken; AISI 1050 çeliği değerleri nispeten diğerlerinden daha düşük, gri dökme demirin değerleri ise daha yüksek çıkmıştır. Alaşım çelikleri olan malzemeler birbirlerine benzer özellikler göstermişlerdir.

4. SONUÇLAR

Bu çalışmada, iki silindirli bir dizel motora ait olan biyel kolunu beş farklı malzemesi için yapısal analizi Ansys programında yapılmıştır. Çalışma sonucunda biyel kolu için en uygun biyel kol malzemesi tespit edilmiştir. Analiz sonuçları malzemelerin von-mises gerilme değerleri ve sahip oldukları emniyet katsayılarına göre değerlendirilmiştir. Bu sonuçlara göre 42CrMo4 çeliği biyel tasarımımız için en uygun malzeme olarak bulunmuştur. Analiz sonuçlarına göre maksimum gerilme değeri 475 MPa ve emniyet katsayısı ise 1,57 olarak tespit edilmiştir. Biyelin üst kısmında bulunan yağlama deliği ve çevresi tüm analizlerde maksimum deformasyona uğrayan bölge olarak belirlenmiştir. Yağlama deliğinin varlığı biyel başının mukavemet açısından değer kaybetmesine neden olmuştur. Analizler biyel kolunun alt yataklarından sabit olarak

düşünülüp yapılmasından dolayı biyelin kranka bağlandığı alt yataklar tüm analizlerde mukavemetli çıkmıştır. Daha sağlıklı bir analiz çalışması yürütmek için biyele dinamik analiz yaptırılıp, çeşitli yük şartları altında elde edilen mukavemet değerleri incelenerek daha verimli sonuçlar elde edilebilir.

KAYNAKLAR

[1] Celin R, Arzen B ve Kmeti, D. A Metallographıc examination of a fractured connectıng rod. Materials Tech 2008;42(2):93–95.

[2] Cesur İ, Akgündüz M. Krom-nikel kaplı segmanların segman silindir çifti arasındaki sürtünme ve aşınma özelliklerinin incelenmesi. Türk Doğa Fen Derg. 2021;10(1):75-82.

[3] Vinet L. Zhedanov A. A "missing" family of classical orthogonal polynomials. J Physic A: Mathematical and Theoretical. 2011;44(8):1689–1699.

[4] Gu Z, Yang S, Ku S, Zhao Y, Dai X. Fracture splitting technology of automobile engine connecting rod. Int J Adv Manuf Tech. 2005;25:883-887.

[5] Özdemir T. Motor Biyel Kolunun Baş Kısmının Kırılmasının Sonlu Elemanlar Yöntemi ile Nümerik Analizi Üzerine Bir Çalışma, Doktora Tezi, Balıkesir Üniversitesi – Fen Bilimleri Enstitüsü, Balıkesir, 2013.

[6] Topçu M ve Taşgetiren S. Mühendisler İçin Sonlu Elemanlar Metodu, Pamukkale Üniversitesi Mühendislik Fakültesi, Denizli, 1998.

[7] Afzal A and Fatemi AA. Comparative Study of Fatigue Behavior and Life Predictions of Forged Steel and PM Connecting Rods. SAE International. 2004.

[8] Ali MM, Haneef M. Finite element analysis of connecting rod. World Academy Sci Eng Tech Int J Mech Mechatronic Eng. 2016;10(7):1271-1276.

[9] Mohankumar D, Rakesh L, Bıher B. Design and analysis of a connecting rod. Int J Pure Appl Math. 2017;116(15):105-109.

[10] Al Hasan NHJ. Simulation of connecting rod using finite element analysis. Int J Innov Res Comp Sci Tech. 2018;6(5):113-116.

[11] Shenoy PS. Dynamic Load Analysis and Optimization of Connecting Rod. The University of Toledo. May. ABD. 2004.

[12] Dale JR. Connecting Rod Evaluation Metal Powder Industries Federation. January 2005.

[13] Webster WD, Coffel R Alfaro D. A Three Dimensional Finite Element Analysis of a High Speed Diesel Engine Connecting Rod. SAE Technical Paper Series. 1983.

[14] Fındık F, Okumuş CS, Çolak M. Malzeme Seçimi ve Uygulamaları. Ankara: Seçkin Yayıncılık. 2018.

[15] Avner SH. Introduction to Physical Metallurgy. McGraw Hill Book Company. 2.ed. New York. 1986.

[16] Choo S-H, Lee S, Golkovsky MG. Effects of accelerated electron beam irradiation on surface hardening and fatigue properties in an AISI 4140 steel used for automotive crankshaft. Mater Sci Eng A-Structural Mater Prop Microstruc Process. 2000;293:56-70.

[17] Heywood JB. Internal Combustion Engine Fundamentals. McGraw-Hill, New York. 1988.

Araştırma Makalesi https://doi.org/10.46810/tdfd.995786 Research Article

Türk Doğa ve Fen Dergisi
Turkish Journal of Nature and Science
www.dergipark.gov.tr/tdfd

Genetic Diversity Analysis of Some Upland Cotton (*Gossypium hirsutum* L.) Genotypes Using SSR Markers

Sadettin ÇELİK[1*]

[1]Bingöl University, Genç Vocational School, Department of Forestry, Bingöl, Turkey
Sadettin ÇELİK ORCID No: 0000-0002-0588-1391

**Corresponding author: sadettincelik@bingol.edu.tr*

(Received: 15.09.2021, Accepted: 30.11.2021, Online Publication: 25.03.2022)

Keywords

Genetic diversity, MAS, PIC, SSR, Upland cotton

Abstract: Cotton plant is an important crop cultivated under biotic and abiotic stress conditions worldwide. The best way to avoid the harmful effects of chemicals used to combat these stresses is to develop tolerant or resistant varieties in plant breeding programs. In the present study, some of Upland cotton varieties were screened with 20 polymorphic SSR primers, and their population structure and genetic diversity analysis were examined. 17 SSR primers amplified 99 alleles with a 5.82 allele per locus. The mean PIC value of the markers was 0.312. The highest PIC value (0.491) belongs to the Nau3736 SSR marker while Bnl1611 and Bnl3449 markers had the lowest PIC value (0.105). The Genetic Distance (GD) values of the markers varied between 0.26 and 1.09. The highest GD values were between Sure Grow 96 and Carmen, Sealand-542 and Siokra ¼, and between Sphinx V and Stoneville-453 cultivars. As a result, the genetically distant cultivars (Acala maxxa, Carmen, Aleppo 40, Siokra ¼, and Tex) can be recommended to use as parents in Marker-assisted selection (MAS) technology to develop new cotton varieties which are resistant or tolerant to stress factors.

SSR Markörleri Kullanılarak Bazı Upland Pamuk *(Gossypium hirsutum* L.) Genotiplerinin Genetik Çeşitlilik Analizlerinin Yapılması

Anahtar Kelimeler

Genetik çeşitlilik, MAS, PIC, SSR, Upland pamuk

Öz: Pamuk bitkisi dünya genelinde biyotik ve abiyotik stres koşullarında yetiştirilen çok önemli bir tarla bitkisidir. Bu stres koşullarıyla mücadelede kimyasal ilaçlarının olumsuz etkilerinden kaçınmanın en etkili yolu, bitki ıslah metodlarıyla biyotik ve abiyotik stres faktörlerine dayanıklı/tolerant yeni bitki çeşitlerini geliştirmektir. Bu çalışmamızda bazı upland pamuk genotipleri 20 adet polimorfik SSR primerleriyle taranmış, populasyon yapıları ve genetik çeşitlilik analizleri yapılmıştır. 17 SSR primeri lokus başına 5.82 allel olmak üzere totalde 99 allel üretmiştir. Markörlerin ortalama PIC değerleri 0.312 olmuştur. En yüksek PIC değeri (0.491)'ni Nau3736 SSR marköründe elde edilirken, en düşük PIC değeri (0.105) Bnl1611, Bnl3449 markörlerinde elde edilmiştir. Markörlerin genetik mesafe değerleri 0.26 ile 1.09 arasında değişmiştir. En yüksek genetik mesafe Sure Grow 96 ve Carmen, Sealand-542 ve Siokra ¼ ile Sphinx V ve Stoneville-453 arasında ölçülmüştür. Sonuç olarak, genetik olarak birbirinden uzak olan çeşitler (Acala maxxa, Carmen, Aleppo 40, Siokra ¼, and Tex), stres faktörlerine karşı dirençli çeşit geliştirme teknolojisi olan Markör Destekli Seleksiyon (MAS) ıslah programına ebeveyn olarak kullanılabileceği güçlü bir şekilde önerilmektedir.

1. INTRODUCTION

Cotton (*Gossypium spp.*) is an important crop as a source of natural fiber and oil. It covers 35% of the fiber used worldwide. There are about 50 species of cotton, and 45 of these are known to be diploids (2n = 2x = 26), and 5 are allotetraploid (2n = 4x = 52) [1]. The most common diploid ones are *G. arboreum* L. and *G. herbaceum* L. with AA (2n = 2x = 26) genome group, and the tetraploid ones are *G. hirsutum* L. and *G. barbadense* L. with AADD (2n = 4x = 52) genome group [2].

Approximately there are 20 diseases, pests, and harmful stress factors that reduce the yield, quality, and restrict cotton cultivation worldwide. Particularly, more than 41% of the yield loss is due to biotic factors such as insects (15%), weeds (13%), and other harmful pathogens [3]. To

combat such stress factors, Cook. [4]. has proposed four possibilities: (i) breeding new tolerant or resistant varieties, (ii) developing a healthy root environment, (iii), increasing the quality of water, and (iv) protecting the plants from airborne threats. Developing tolerant/resistant genotypes against biotic and abiotic stress conditions are more environmentally safe compared to chemicals that pollute the atmosphere.

Corresponding to recent climate changes, the identification of desired alleles at QTL underlying tolerance/resistance to biotic and abiotic stresses is a primary breeding strategy for improving crop productivity and production under stress conditions [2;5]. The strategy involves germplasm screening, QTL mapping, and the development of DNA markers linked to QTL. Marker-assisted selection (MAS) in breeding programs has been applied to introduce the desired alleles into the genetic backgrounds of elite varieties [6].

Fundamental studies on quantitative traits associated with stress tolerance/resistance are necessarily required to apply marker-assisted selection to practical crop breeding. On the other hand, diversity studies may contribute to screening desired genotypes as parents for crossing but cannot directly contribute to breeding through marker-assisted selection. When a broad range of diverse germplasm and genome-wide DNA markers are used for the analysis, genome-wide association mapping using genotypic and phenotypic data is applicable to identify chromosomal regions involving QTL/genes conferring target traits [7; 8; 5; 9].

Genetic diversity comes from the allelic variation in the genome (insertion, deletions in DNA) and constitutes the basis of Marker-assisted breeding. Genetic diversity and the selection of parents play important roles in terms of the level of variation, and heterosis (hybrid vigor), hybrid strength, molecular breeding, and in obtaining cotton genotypes tolerant or resistant to diseases and pests, early with high efficiency. To achieve this, molecular markers that measure the genetic diversity at the DNA level must be employed [5; 9]. DNA markers can be classified as sequence-based (SNP, Single Nukliotit polymorphism), hybridization-based (RFLP, Restriction Fragment Lenght Polymorphism), and PCR-based markers (RAPD, Randomly Amplified Polymorphic DNA; AFLP, Amplified Fragment Lenght Polymorphism; SSR, Simple Sequences Repeats) [10]. Genetic markers are used for predicting the genetic diversity in wild and designed populations [11; 12; 13], Quantitative Trait Loci (QTL) and association mapping [7; 8; 14; 15; 16], pedigree analyses [17], heterotic group classification [18; 19], and for the protection of genotype rights [20].

The Simple Sequence Repeat (SSR) (Microsatellites or Short tandem repeat) molecular markers were used in the genetic diversity analyses because they have a high ability to show genetic differences between cotton genotypes, they are present in all eukaryotic cells, show uniform distribution throughout the genome, provide the opportunity to determine genetic diversity, are repeatable, allow working on low DNA samples amount, are cheap and co-dominant, and give reliable results. SSR markers are in 1-4 to 1-6 nucleotide length [21; 22; 23; 24; 25]. Bertini et al. [26] reported that they obtained 66 alleles in total, with an average of 2.13 alleles per locus in her genetic diversity with 53 cotton varieties using 31 SSR markers. Liu et al. [27] reported that they obtained 165 polymorphic DNA fragments in a study using SSR markers on Asian cotton (*Gossypium arboreum* L.), and the genetic similarities of the accessions were between 0.58 and 0.87. The development of new varieties against biotic and abiotic stress factors increased the quality, germination, emergence, seedling, growing, and yield of cotton [28; 29; 30; 31].

Some important parameters must be known about the individuals that will be used as parents in developing new varieties with the breeding method. Genetic differences and the degree of these differences among the genetic materials that will be used in the breeding program have critical importance in variety breeding. Islam et al. [32] reported that a high rate of stability was observed in yield in some regions because of the use of germplasm sources as breeding materials, where genetic diversity is very small. Therefore, genotypes to be used in plant breeding should be analyzed to determine their kinship degrees and those have close kinship degree is not recommended to use in plant breeding program.

The present study was conducted to determine the genetic diversity between upland cotton (*Gossypium hirsutum* L.) germplasm and examine population structure using 20 SSR markers.

2. MATERIALS AND METHOD

2.1. Plant Materials

A total of seventeen upland (*G. hirsutum* L.) cotton genotypes belong to the AD_1 genome group collected from different countries (The USA, Syria, Turkey, Australia, Albania) used for genetic diversity analysis, in Kahramanmaras Sutcu Imam University, Faculty of Agriculture, Department of Agricultural Biotechnology, in Kahramanmaraş City-Turkey.

2.2. DNA Extraction, and Visualization Genomic DNA

From the young leaves, 0.5 g amount picked up at the 3-4-leaf stage, from each genotype with sterile scissors. The samples were then washed with distilled water (dH_2O) and ethanol and placed in plastic tissue bags in thermally insulated containers with -80ºC dry ice during transport to the laboratory and were kept in the -80ºC freezer until DNA isolation. The Genomic DNA isolation protocol Centyltrimeyhtlaminiumbromide (CTAB) was developed by Doyle and Doyle. [33] was modified and used in this study.

2.3. SSR Amplification

Amplification with PCR and gel electrophoresis stage was performed according to Zhang and Stewart. [34]. The PCR protocol consisted of incubating at 94ºC for 5 min, then 34

cycles of at 94ºC for 1 min, at 60ºC for 1 min and 72ºC for 2 min; later at 72ºC for 7 min. A reaction volume of 15 µL was used for each PCR process. In PCR reaction mixture, there were 0.75 µL dNTP (Conc.10 mM), 1.5 µL 10X PCR buffer, 1 µL forward primer, 1 µL reverse primer, 0.5 µL Taq DNA polymerase enzyme (Conc.5 µL, 2 µL template DNA (Conc. 25ng/µL), 8.25 µL ddH_2O (double-distilled) components [35].

Table 1. Information about Simple sequence repeat (SSR) used in this study

Primer Name	Species, Germplasm	Chromosome	Repeat motif	Publication
BNL1079	*G. hirsutum* L, Deltapine 90	AD_chr.18	(CA)11 (GT)11	Mei et al. [36].
BNL1604	*G. hirsutum* L, Deltapine 90	AD_chr.7-16	(AG)25	Mei et al. [36].
BNL3449	*G. hirsutum* L, Deltapine 90	AD_chr.18	(AC)15, (TC)6T (AC)15G(CA)2	Yu et al. [37].
BNL3479	*G. hirsutum* L, Deltapine 90	AD_chr.18	(AC)15(TC)6T(AC)15 G(CA)2	Yu et al. [37].
BNL2571	*G. hirsutum* L, Deltapine 90	AD_chr. 13-18	(AG)13, (TC)13	Yu et al. [37].
BNL1611	*G. hirsutum* L, Deltapine 90	AD_chr.19	(AG)12	Yu et al. [37].
CIR 0141	*G. hirsutum* L Guazuncho-2	AD_chr.07-16	(TG)30	Nguyen et al.[38].
CIR0253	*G. hirsutum* L, Guazuncho-2	AD_chr.5-19-22	(TC)15, (N)8(A C)5(N)7(CA)8	Nguyen et al. [38].
CIR0099	*G. hirsutum* L, Guazuncho-2	AD_chr.18-25	(GT)8	Nguyen et al. [38].
NAU3736	*Gossypium raimondii*	AD_chr.01-15	(GTA)6	Guo et al. [39].
NAU2714	*Gossypium raimondii*	AD_chr.6-25	(TTA)7	Guo et al. [39].
NAU4024	*Gossypium raimondii*	AD_chr.14	(GTC)6	Guo et al. [39].
NAU2761	*Gossypium raimondii*	AD_chr.02-17	(TTAA)6	Guo et al. [39].
NAU2173	*G. hirsutum* L, Xuzhou 142	AD_chr.14	AAG (17)	Han et al. [40].
JESPR0065	*G. hirsutum* L, Tamcot Sphinx	AD_chr.04-12	(GAA)25	Reddy et al. [41].
JESPR0153	*G. hirsutum* L, Tamcot Sphinx	AD_chr.13,18,20	(CTA)18	Reddy et al. [41].
JESPR0114	*G. hirsutum* L, Tamcot Sphinx	AD_chr.09-23	(GT)12	Reddy et al. [41].
MGHES16	*G. hirsutum* L, Acala Maxxa	AD_chr.11-21	(CT)10, (TCT)4	Qureshi et al. [42].
MGHES31	*G. hirsutum* L, Acala Maxxa	AD_chr.12-26	(CAT)9	Qureshi et al. [42].
NAU2251	*G. hirsutum* L, Xuzhou 142	AD_chr.12-26	AGA (8)	Han et al. [40].

In table 1., it is indicated the SSR markers properties were obtained from the varieties of *G. hirsutum* L. and *Gossypium raimondii* cotton species. Bnl1079, Bnl1604, Bnl3449, Bnl3479, Bnl2571, Bnl1611 SSR markers were obtained from *G. hirsutum* L. species's Deltapine 90 variety; Cır0141, Cır0253, Cır0099 from Guazuncho-2; Nau2173, Xuzhou 142, Jespr0065, Jespr00654, JesprR00654 from Tamcot Sphinx; Mghes16 and Mghes31 were obtained from Acala Maxxa variety. Nau3736, Nau2714, Nau4024, Nau2761, Nau2173 SSR markers were obtained from the cotton species, *Gossypium Raimond*. Besides, in table 1, the references, repeat motifs, and chromosomes that SSR markers used in this study were also displayed [43].

2.4. Genetic diversity and phylogenetic analyses

Each SSR marker locus, amplified alleles were scored as either '1' (present) or '0' (absent). Each amplified allele of SSR was indicated with A, B, C and so on… letters. Analysis of genetic distance (GD) to obtain genetic dissimilarity matrix PopGENE 1.32 ver. software was used [44].

Genetic diversity was conducted for all SSR locus across germplasm individuals based on the number of alleles, polymorphic alleles numbers, percent of polymorphism, gene diversity [45], and the polymorphic information content (PCI) [46] was determined with PowrMarker 3.25 version program [47]. Genetic distances (GD) [48] were calculated, and the phylogenetic tree was built with the distance matrix using UPGMA (Unweighted pair group method with arithmetic) data panel provided in PowerMarker 3.25 [47]. The phylogenetic tree was created in MEGA-X 10.1.7 version. PIC values show the number of alleles at each locus and the distinctive features of the markers through the relative frequencies of alleles in the population [49]. PIC calculation was made based on the formula given below.

$$PIC=1-\Sigma(Pi)^2 \quad (1)$$

In equation 1, the P-value is the frequency of the i^{th} allele of the total Upland cotton genotypes subjected to the analysis [50].

2.5. Population Structure Analysis

The genetic structure of the subpopulation (*Q-matrix*) was analyzed with Bayesian Model-Based (MBB) analysis model provided in Structure 2.3.4 version software [51]. To calculate the Q matrix, the software was set up to run under 10,000 (Leng of burning periods)-100,000 (Number of reps after burning) Markov Chain Monte Carlo iteration after the burn-in and Number of the population (K) from 1 to 10 and number of iterations was 5. The average likelihood value L(K) was calculated for each K cross of all the runs. The number of populations is estimated by estimating ΔK [52]. The results were transferred to the web-based "Structure Harvester" (http://taylor0.biology.ucla.edu/structureHarvester/) program.

3. RESULTS and DISCUSSIONS

As a result of the amplification made using 20 polymorphic SSR primers, 99 alleles were produced. There was an average of 5.82 alleles per locus. Zhang et al. [53] and Lacape et al. [54] obtained 5.5 alleles per average locus that ranged between 2 and 26 per locus, which was similar to the results of the present study. Besides, Lacape et al. [54] also reported that the number of the alleles obtained per marker did not only stem from the diversity in germplasm, but also depended on the marker type, the fragment separation technique used, and the resolution.

As given in figure 1, after scanning with 20 SSR markers [43] the cotton varieties belong to *G. hirsutum* L. 17 SSR markers were found as polymorphic. Polymorphic information content (PIC) ranged from 0.0-0.5 with an average of 0.312; Each SSR marker amplified at least 2 loci and Jespr SSR produced the most alleles. Genetic diversity among SSR markers differed from 0.0 to 0.6 (Figure 1).

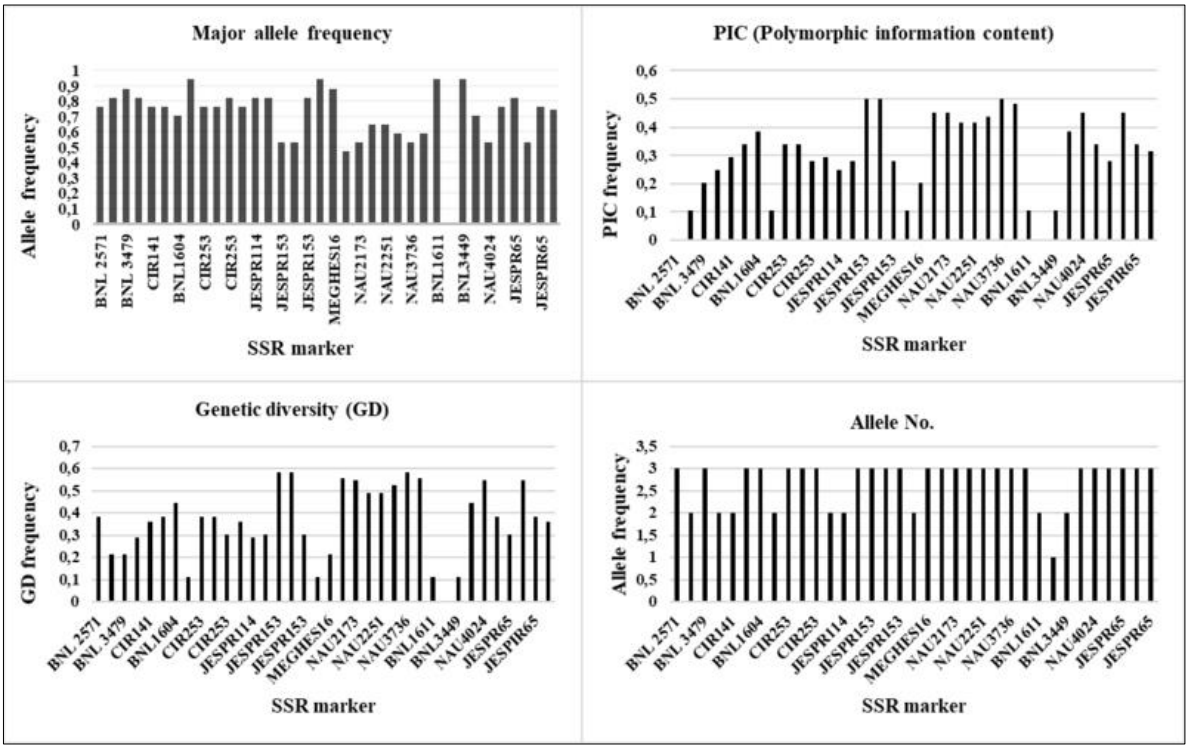

Figure 1. Major allele frequency (MAF), Polymorphic information content (PIC), Genetic Diversity (GD), and Number of Alleles per SSR locus

Table 2. Analysis results of SSR primers used in this study

Primer Name	Forward Primer (5'-3')	Reverse Primer (3'-5')	Alleles Band size (bp)	Allele no.	PIC
BNL1604	AGAGGGAGTAAAGATTTGGGG	TCCAGTTCTTTTTGCCTTGG	120-50	6	0.362
BNL3449	AAGCTGTGGCTATGATGCCT	AGAGCAAAAAACAATTACAAAAGC	180-150	2	0.105
BNL3479	AGTGGGTTGGACTTTCATGC	CACGGGCTTTTTTTTTTTCA	350-200	5	0.216
BNL2571	TCGCTATCGCTCTGAAATCA	ATGCCACGGAATTAGCAAAC	400-320	3	0.345
CIR 0141	CGCACAAGGAATAGAAG	ACCCAACATAAGGACTAAA	300-200	4	0.271
CIR0253	CCAACCAAGAAACCAG	GTAAGCATGGGCATTT	150-50	11	0.256
NAU3736	CATGTGCATTTCATCCTGTC	CCAAGTGAGAGGCATTTTCT	200-80	6	0.491
NAU2714	GCAGCCATTACAGAACATCA	TCATTGATCCATTGCTTCTG	300-200	6	0.384
NAU4024	ACAAGCATCTTCATGGACCT	AGAAGGATGATGCAAAGAGG	200-150	3	0.449
NAU2751	GACAAGTTTTTGGACCCACT	TTCATAGAGGGGTTTTGCAT	350-50	2	0.345
NAU2173	GCCAAATAGGTCACACACAA	AGCGAGAAGGAGACAGAAAA	350-320	6	0.450
JESPR0065	CCACCCAATTTAAGAAGAAATTG	GGTTAGTTGTATTAGGGTCGTTG	300-200	12	0.325
JESPR0153	GATTACCTTCATAGGCCACTG	GAAAACATGAGCATCCTGTG	300-100	12	0.390
JESPR0114	GATTTAAGGTCTTTGATCCG	CAAGGGTTAGTAGGTGTGTATAC	300-100	4	0.248
MGHES16	ACCCCAATACAACCCCATTT	GCAGAGAAAAGGGACAGAGG	400-50	5	0.154
NAU2251	TTCTCCAGTAACCAACAAAGG	AAAATATCATCCCCGTCAAA	400-200	9	0.422
BNL1611	CAATGAACAAAAAATGTAAGGG	TGGGCATTTAGCCATTTACC	100-50	3	0.105
				Mean= 5.82	Mean= 0.312

As indicated in table 2. the average Polymorphic Information Content (PIC) of the markers was 0.312. The PIC values of the markers changed between 0.105 and 0.491. The Nau3736 marker had the highest value with a PIC value of 0.491, and the Bnl1611 and Bnl3449 markers had the lowest value of 0.105. While the mean of alleles is 5.82, each of Jespr0065 and Jespr0153 SSR markers has amplified 12 loci (The highest alleles number) and both Bnl3449 and Nau2751 amplified 2 loci (2 alleles) markers. As a result of the amplification with 31 pairs of SSR primers, Bertini et al. [26] reported similar results with 2.13 alleles per average SSR locus, with PIC values ranging from 0.18-0.62 to 0-0.41 in 66 alleles. Seyoum et al. [35] propounded also close results such as PIC value ranged from 0.319 to 0.019 with 0.279 mean value, the number of alleles per locus ranged from 2 to 12 with 4.53 average.

Liu et al. [55] made amplification with 62 SSR primers and identified 139 alleles in 69 SSR locus as 2 alleles per locus, as well as 325 alleles as 5 alleles per locus; Lacape et al. [54] reported that they identified a total of 1128 alleles including an average of 5.61 alleles per locus because of 201 SSR markers using 47 wild *Gossypium* genotypes. The reason that Lacape et al. [54] had more alleles and higher average alleles per locus than us could be depended on their SSR amount and wild Cotton genotypes. Iqbal et al. [56] reported that they obtained 349 alleles with 50 primers, and detected polymorphism in 23 cotton genotypes using 49 primers. In these studies, it is considered that the reason for producing more alleles than in the present study is related to the excessive SSR primers used.

In figure 2, the Bnl1611 SSR marker produced 3 alleles with 100, 75, 50 bp between 100-50 bp fragment size. The Bnl1611marker amplified the target locus in all genotypes except Gloria and produced at least 2 maximum 3 alleles in genotypes except the Nazilli 84s. The reason for not being able to produce bands in the Gloria genotype may be due to pipetting errors or absences of template DNA.

The gel image taken under UV light after Bnl1611 running through 1% agarose was given in Figure 2. Scoring fragments were performed in all genotypes except the Gloria variety.

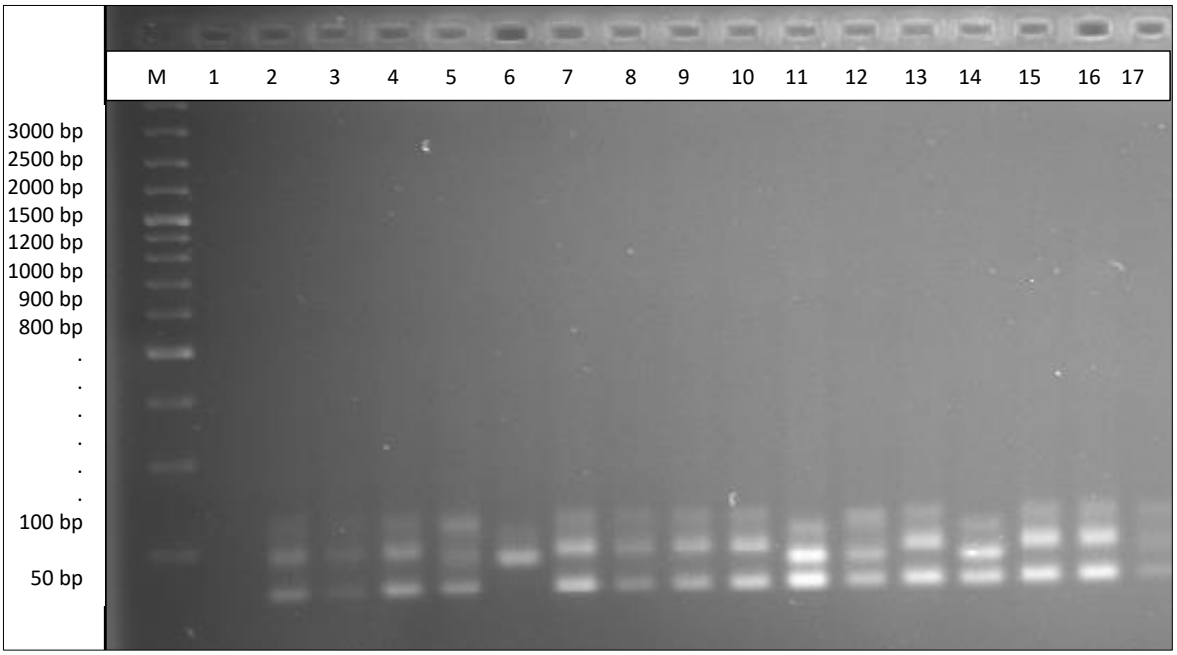

Figure 2. PCR gel image of BNL1611 (Locus) SSR primer. **M**=Marker, DNA ladder= Vivantis 10 bp (1% agarose 1 X TBE). **1**=Gloria, **2**=Aleppo-40, **3**=Carmen, **4**=Cukurova 1518,5=Albania-6172, **6**=Nazilli 84S, **7**=Siokra 1/4, **8**=Sphinx V, **9**=Stoneville-453, **10**=Sure grow 96, **11**=TamcotSP37, **12**=Tex, **13**=Sealand-542, **14**=Acala 1517-95, **15**=Acala Maxxa, **16**=TMS 108/2, **17**=Candia

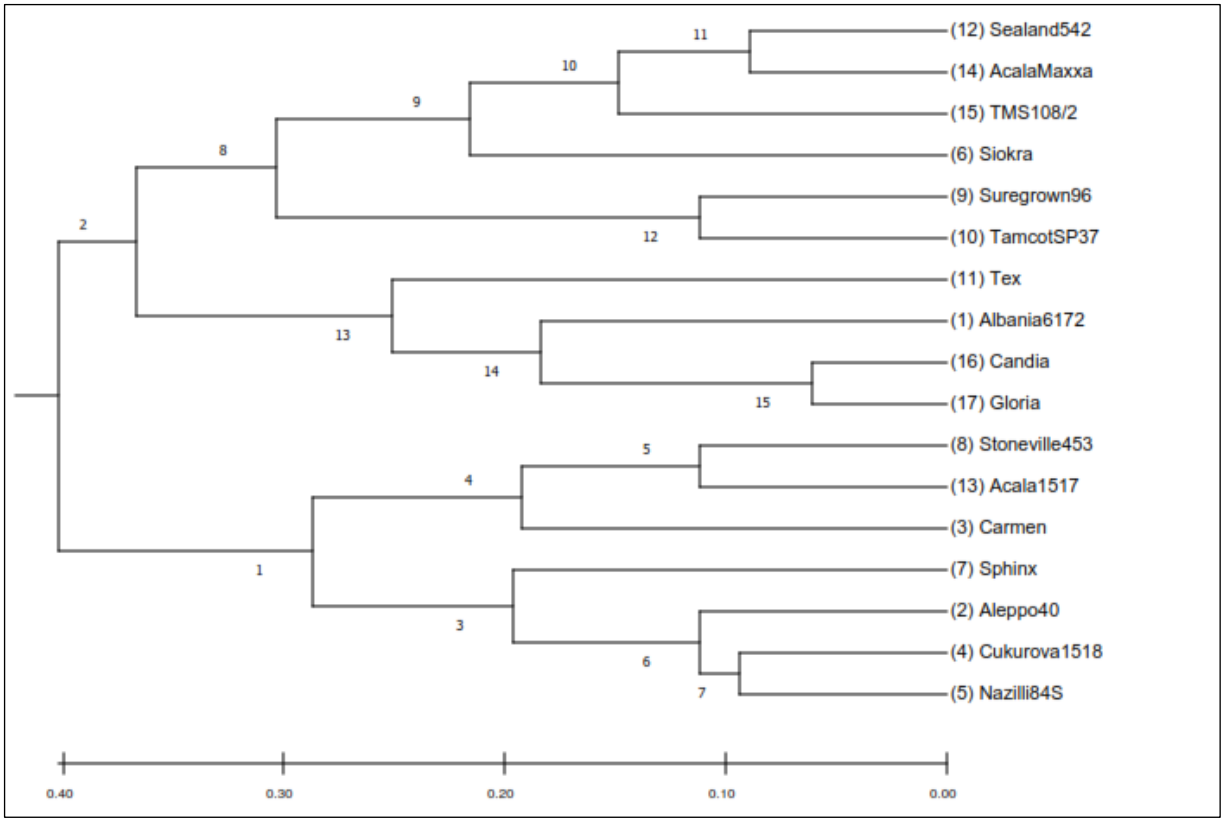

Figure 3. Dendrogram based on Nei's [45] genetic distance: Method = UPGMA of *G. hirsutum* L. genotypes based on 20 Genome-Wide SSR markers

The results of UPGMA (Unweighted pair group method with arithmetic) analysis were shown in Figure 3. The genotypes are divided into two main clusters. 1st main cluster consists of 7 genotypes (Nazilli 84S, Çukurova 1518, Aleppo 40, Sphinx, Carmen, Acala 1517, Stonville 453), the 2nd cluster consists of 10 genotypes (Sealand 542, Acala maxxa, TMS 108/2, Siokra, Sure grow 96, Tamcot SP 37, Tex, Albania 6172, Candia, Gloria). The 1st main cluster is divided into two subclusters and 2nd main cluster is also divided into two subclusters. Accordingly, 15 different subclusters emerged in total. In this respect, Sealand-542, Acala maxxa, TMS 108/2, Siokra ¼, Suregrow96, Tamcot, Tex, Albania-6172, Candia and Gloria were classified in a different cluster, in other words, they have pedigree relations, Stonville-453, Acala-1517, Carmen, Sphinx V, Aleppo-40, Çukurova 1518 and Nazilli 84S genotypes were classified in a different cluster. The first cluster was also divided into further subclusters, and Sealand-542, Acala maxxa, TMS 108/2, Siokra ¼, Sure grow 96, and Tamcot, were included in the first subcluster of this cluster while Albania-6172, Candia, Gloria, and Tex were included in the second subcluster.

Although Stoneville-453, Acala-1517, and Carmen varieties in Group 4 were collected from different geographical areas, there was a unity of origin among them. The Sphinx V, Aleppo-40, Çukurova 1518, and Nazilli 84S were classified in Group 3. Again, it was seen that the second subcluster of the second main cluster also may have common parents even though they were the genotypes obtained from different regions, as was the case in the first subcluster. Eminenur and Hancer. [57] conducted genetic diversity analysis with *G. hirsutum* L. genotypes (Flash, BA119, ST506, Tamcot Sp21, Tamcot 22, Tamcot 94, Tamcot Camd-eS and Tamcot Sp23, Sphinx v, Stn468), and *G. barbadance* L. (Giza 70) variety, and reported that Giza 70 was included in a separate cluster and the remaining genotypes were included in a separate cluster.

In Figure 3, some genotypes classified in the same cluster have some similar characteristics. This may be clarified that they come from a common pedigree. For instance, Sealand-542 which is an interspecies hybrid (*G. hirsutum* L X *G. barbadance* L.), and Acala maxxa were classified in the same cluster. Nazilli 84S, which is a hybrid of Carolina Queen X 153-F and Çukurova 1518 are also among the closest relatives. It was seen that Sure Grow 96 and Tamcot SP37 genotypes, which were clustered in Group 12 that originated from the USA, and Candia and Gloria, two Australian originating varieties, were in Group 15.

SSR markers were distributed on 20 different chromosomes, and produced a total of 99 alleles ranging from 2-12 with a 5.82 average. Tyagi et al. [58] reported similar results in that they produced 546 alleles in 141 loci in genetic diversity study with 381 cotton accessions using 120 Genome-wide SSR markers. Bardak and Bolek. [59] reported similar results with the present study as they obtained a total of 173 alleles, including 3.93 alleles per locus, as a result of their study with 39 SSRs and 5 ISSRs using for screening 25 cotton genotypes.

According to Nei's [45] pair-wise comparison on the genetic distance between genotypes, and according to the

results of the Genetic Distance matrix, the highest GD (1.09) was measured at the highest score between Carmen and Sure Grow 96, Sealand-542 and Siokra ¼, and Sphinx V and Stoneville-453 genotypes. The lowest GD (0.26) was measured between Gloria and Carmen, and Tex and Stoneville-453 genotypes. The GD between the genotypes varied between 0.26 and 1.09, in this respect, it was seen that the GD between Cukurova 1518 and Gloria, Nazilli 84S and Siokra ¼, Tamcot SP37 and Cukurova 1518, TMS 108/2 and Çukurova 1518, Sure Grow 96 and Tex, Acala Maxxa and Tamcot SP37 and Acala-1517 and TMS 108/2 were the same. Bardak and Bolek. [59] also reported close results to this study that the lowest GD (0.04) was detected between Siokra ¼ and Nazilli 84S, and the highest GD (0.58) was between Erşan 92 cotton variety of the AD genome and *G. sturtianum* of the C genome group *Nandewarense* variety.

In the present study, the Genetic Distance (GD) between upland cotton genotypes ranged from 0.26 to 1.09. The previous studies were reported Genetic distance between 0.06-0.34 [60], 0.06-0.38 [61]; 0.82-0.93 [56] and 0.19-0.36, [62] in upland cotton genotypes. These results are on the line with the previous genetic diversity studies.

Zhao et al. [63] have reported the highest genetic diversity in cotton from the USA followed by China; Chen and Du. [64] indicated the higher genetic diversity of introduced genotypes particularly obtained from China and USA countries than the domesticated genotypes.

The Structure analysis of population results revealed the highest population numbers took place at K:5 and this can be evaluated as cotton germplasm can be grouped into five subpopulations (figure 4). Five (5) different colors in Figure 4, and each color represents a population or genotype collected from the same geographical area.

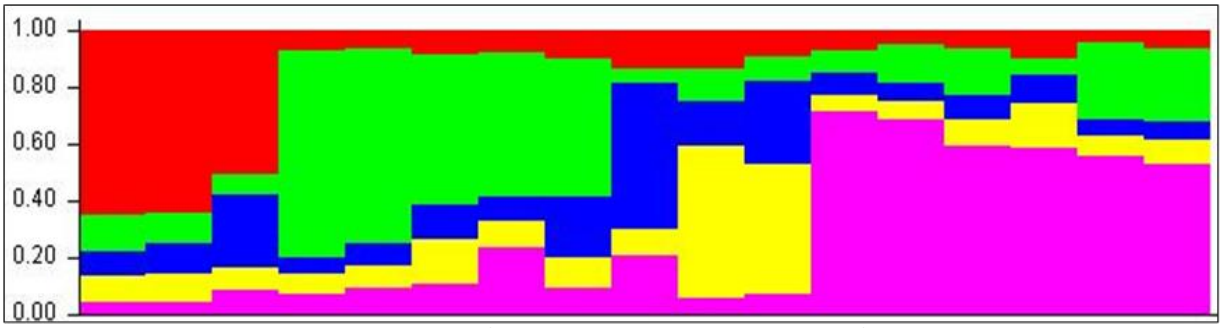

Figure 4. Plot Q-Matrix shows the genotypic data analysis of cotton genotypes in Structure 2.3.3 ver. software. Each colored subsection bar represents the cotton genotypes group origin

These genotypes were obtained from the United States (Acala maxa, Sure Grow 96, Stoneville-453, Tamcot SP 37, Teks, Sealand-542, Acala-1517, Siokra ¼, Sphinx V), Turkey (Çukurova 1518, TMS 108/2, Nazilli 84S), Albania (Albania-6172), Syria (Aleppo-40) and Australia (Carmen, Candia, Gloria). Abdurakhmonov et al. [65] reported that the germplasm materials they used were divided into three categories as native, Mexican, and African origin. Bardak et al. [66] reported that 48 cotton genotypes they used were divided into 3 different groups. Tyagi et al. [58] reported similar results as their 381 cotton genotypes were divided into 5 different groups. Genetically distant genotypes should be selected as parents as much as possible when breeding programs are carried out.

4. CONCLUSIONS

As it is already known, the success of breeding depends on the selection of the right parents, which is the first and most important step in the strength and success of this process. Genetic distance between parents in a breeding program brings the possibility of allelic diversity and improved phenotypic values as well as a higher chance of hybrid vigor.

Therefore, exploring the genetic diversity, in other words, determining the genetic distance between genotypes plays a key role in the development of a new variety.

In the study, most SSR primers produced polymorphic bands. Some of them didn't produce.

The cotton varieties with far distance from each other such as Acala maxxa, Carmen, Aleppo 40, Siokra ¼, and Tex, (onsidering the high yield and quality) are highly rCecommended to use as parents in Marker-assisted selection (MAS) to develop new varieties.

Acknowledgments

I am grateful to Associate Prof. Dr. Adem BARDAK for providing cotton germplasm materials, and Dr. Halil TEKEREK and Osman YİĞİT for the assistance on laboratory analysis in Kahramanmaraş Sutçu Imam University, Agricultural Biotechnology Lab.

REFERENCES

[1] Zhang J, Fang H, Zhou H, Sanogo S, Ma Z. Genetics, Breeding, and Marker-Assisted Selection for Verticillium Wilt Resistance in Cotton. *Crop Science*. 2014; 54(4):1289-1303.

[2] Hui-Fang BS. Development of Molecular Markers and Mapping of Quantitative Trait Locf for Resistance to Verticillium Wilt Disease Using Two Inbred Line Populations in Tetraploid Cotton. [P.H.D Thesis]: New Mexico State University Las Cruces, *New Mexico*; 2013.

[3] Pimentel D. Techniques for reducing pesticide use. Wiley, *Hoboken*; 1997.

[4]. Cook JR. Advances in plant health management in the twentieth century. *Annu Rev Phytopathol; 2000*: (38):95–116.

[5] Jia JZ. Molecular germplasm diagnostics and molecular marker assisted breeding. *Scientia Agricultura* Sinica. 1996; 29(4): 1-10.

[6] Varshney R, Hoisington D, Nayak S, Graner A. Molecular Plant Breeding: Methodology and Achievements. In: Gustafson J., Langridge P., Somers D. (eds) *Plant Genomics*. Methods in Molecular Biology™ (Methods and Protocols). *Humana Press*. 2009; 513.

[7] Young ND. A Cautiously Optimistic Vision for Marker-Assisted Breeding. *Molecular Breeding*. 1999;5: 505-510

[8] Kohel RJ, Yu J, Park YH, Lazo GR. Molecular Mapping and Characterization of Traits Controlling Fiber Quality in Cotton. *Euphytica*. 2001; 121: 163-172.

[9] Xie J, Cai Z, Liu XH, Li FH, Cao HL, Luan YC. Application of biotechnology on evaluation of genetic diversity of germplasm. *CROPS (Supplement*). 1998; 71-76.

[10] Meena KK, Sorty AM, Bitla UM, Choudhary K, Gupta P, Pareek A. Abiotic Stress Responses and Microbe-Mediated Mitigation in Plants: The Omics Strategies. Front. *Plant Scientist*. 2017; 8:172.

[11] Manjarrez-Sandoval P, Carter TE, Webb DM, Burton JW. Heterosis in Soybean and Its Prediction by Genetic Similarity Measures. *Crop Science*. 1997; 37(5):1443-1452.

[12] Tatineni V, Cantrell RG, Davis DD. Genetic Diversity in Elite Cotton Germplasm Determined by Morphological Characteristics and RAPDs. *Crop Science*. 1996; 36(1):186-192.

[13] Wendel JF, Brubaker CL, Percival AE. Genetic diversity in *Gossypium hirsutum* and the origin of upland cotton. *American Journal of Botany*. 1992; 79:1291-1310.

[14] Schuster EW, Kumar S, Sarma SE, Willers JL, Milliken GA. Infrastructure for Data-Driven Agriculture: Identifying Management Zones for Cotton Using Statistical Modeling and Machine Learning Techniques. In Emerging Technologies for A Smarter World (Cewıt). *8th International Conference & Expo*, 2013. Ieee. P.1-6.

[15] Lacape JM, Nguyen TB, Thibivilliers S, Courtois B, Bojinov BM, Cantrell RG, et al. A combined RFLP, SSR-AFLP map of tetraploide cotton based on a *G. hirsutum* x *G. barbadense* backcross population. *Genome*. 2003; 46: 612-626.

[16] Ulloa M, Saha S, Jenkins JN, Meredith WR, McCarty JC, Stelly MD. Chromosomal Assignment of RFLP Linkage Groups Harboring Important QTLs on an Intraspecific Cotton (*Gossypium hirsutum* L.) *Joinmap. J. Hered*. 2005; 96: 132-144.

[17] Smith JSC, Chin ECL, Shu HO, Smith S, Wall SJ, Senior ML, et al. An evaluation of the utility of SSR loci as molecular markers in maize (*Zea Mays* L.) comparisons with data from RFLPs and pedigree. *Theor Appl Genet*. 1997; 95:163-173.

[18] Dudley JW, Maroof MAS, Rufener GK. Molecular Markers and Grouping of Parents in Maize Breeding Programs. *Crop Science*. 1991; 31: 718-723.

[19] Senior ML, Murphy JP, Goodman MM, Stuber CW. Utility of SSRs for Determining Genetic Similarities and Relationships in Maize using an Agarose Gel System. *Crop Science*. 1998; 38: 1088-1098.

[20] Smith JSC, Smith OS. Fingerprinting crop varieties. Adv. *Agron*. 1992; 47:85-140.

[21] Chaters YM, Robertson A, Wilkinson MJ, Ramsay G. PCR analysis of oil seed rape cultivars (*Brassica napus* L. sp. oleifera) using 50-anchored simple sequence repeat (SSR) primers. *Theor. Appl. Genet*. 196; 92: 442-447.

[22] Powell W, Machray GC, Provan J. Polymorphism revealed by simple sequence repeats. *Trends in Plant Sciences*. 1996; 1:215-222.

[23] Abdalla AM, Reddy OUK, El-Zik K Man, d Pepper AE. Genetic diversity and relationships of diploid and tetraploid cottons revealed using AFLP. *Theoretical and Applied Genetics.* 2001; 102:222-229.

[24] Iqbal MJ, Reddy OUK, El-Zik KM, Pepper AE. A genetic bottleneck in the evolution under domestication' of upland cotton *Gossypium hirsutum* L. examined using DNA fingerprinting. *Theoretical and Applied Genetics*. 2001; 103:547-554.

[25] Lu HJ, Myers GO. Genetic relationships and discrimination of ten influential upland cotton varieties using RAPD markers. *Theoretical and Applied Genetics*. 2002; 105:325-331.

[26] Bertini CH, Schuster I, Sediyama T, Barros E, Moreira MA. Characterization and genetic diversity analysis of cotton cultivars using microsatellites. *Genetics and Molecular Biology*. 2006; *29*(2): 321-329.

[27] Liu D, Guo X, Lin Z, Nie Y, Zhang X. Genetic diversity of Asian cotton (*Gossypium arboreum* L.) in China evaluated by microsatellite analysis. *Genetic Resources and Crop Evolution*. 2006; *53*(6): 1145-1152.

[28] Nachimuthu G, Webb AA. Closing the Biotic and Abiotic Stress-Mediated Yield Gap in Cotton by Improving Soil Management and Agronomic Practices. In: Senthil-Kumar M. (eds) Plant Tolerance to Individual and Concurrent Stresses. *Springer*. 2017.

[29] Liu HS, Li FM. Root respiration, photosynthesis and grain yield of two spring wheat in response to soil drying, *Plant Growth Regul*. 2005; 46, 233–240.

[30] Bange M. The impact of temperature extremes on cotton performance. *CSIRO Plant Industry*. 2004.

[31] Farooq M, Wahid A, Kobayashi N, Fujita D, Basra SMA. Plant drought stress: effects, mechanisms and management. Agronomy for Sustainable Development, Springer Verlag/EDP *Sciences*/INRA. 2009; 29 (1): 185-212.

[32] Islam S, Haque MS, Emon RM, Islam MM, Begum SN. Molecular characterization of wheat (*Triticum aestivum* L.) genotypes through SSR markers. *Bangladesh Journal of Agricultural Research*. 2012; *37*(3): 389-398.

[33] Doyle and Doyle. A rapid DNA isolation procedure from small quantities of fresh leaf tissue. *Phytochem Bull*. 1997; 19: 11-5.
[34] Zhang J, Stewart JM. Economical and rapid method for extracting cotton genomic DNA. *J Cotton Sci*. 2000; *4*(3): 193-201.
[35] Seyoum M, Du X, He SP, Jia YH, Pan Z, Sun JL. Analysis of genetic diversity and population structure in upland cotton (*Gossypium hirsutum* L.) germplasm using simple sequence repeats. *Journal of genetics*. 2018; *97*(2): 513-522.
[36] Mei M, Syed N, Gao W, Thaxton P, Smith C, Stelly D, et al. Genetic mapping and QTL analysis of fiber-related traits in cotton (Gossypium). *Theoretical and applied genetics*. 2004; 108(2):280-291.
[37] Yu J, Yu S, Lu C, Wan W, Fan S, Song M, Zhang J. High-density linkage map of cultivated allotetraploid cotton based on SSR, TRAP, SRAP and AFLP markers. *Journal of Integrative Plant Biology*. 2007; *49*(5): 716-724.
[38] Nguyen TB, Gigel M, Brottier P, Risterucci AM, Lacape JM. Wide coverage of the tetraploid cotton genome using newly developed microsatellite markers. *Theoretical and applied genetics.* 2004; 109(1):167-75.
[39] Guo W, Cai C, Wang C, Han Z, Song X, Wang K, Niu X, Wang C, Lu K, Shi B. A microsatellite-based, gene-rich linkage map reveals genom structure, function and evolution in Gossypium. *Genetics*. 2007; 176(1):527-541.
[40] Han Z, Wang C, Song X, Guo W, Gou J, Li C, Chen X, Zhang T. Characteristics, development and mapping of Gossypium hirsutum derived EST-SSRs in allotetraploid cotton. *Theoretical and applied genetics.* 2006; 112(3):430-439.
[41] Reddy O, Pepper A, Abdurakhmonov I, Saha S, Jenkins J, Brooks T, et al. new dinucleotide and trinucleotide microsatellite marker resources for cotton genome research. *Journal of cotton science*. 2011; 5(2):103-113.
[42] Qureshi SN, Saha S, Kantety RV, Jenkins JN. EST-SSR: a new class of genetic markers in cotton. 2004.
[43] Yu J, Jung S, Cheng CH, Ficklin SP, Lee T, Zheng P, et al. CottonGen: a genomics, genetics and breeding database for cotton research. *Nucleic acids research*. 2014; *42*(D1), D1229-D1236.
[44] Yeh, F.C., Yang, R. C., Boyle, T., Ye, Z. H., & Mao, J.X. (1999). POPGENE, version 1.32: the user friendly software for population genetic analysis.
[45] Nei M. Genetic distance between populations. *The American Naturalist*. 1972; *106*(949): 283-292.
[46] Botstein D, White RL, Skolnick M, Davis RW. Construction of a genetic linkage map in man using restriction fragment length polymorphisms. *Am. J. Hum. Genet.1980*; 32: 314–331.
[47] Liu J, Muse SV. Powermarker: an integrated analysis environment for genetic marker analysis. *Bioinformatics*. 2005; 21:2128-2129.
[48] Nei M, Tajima FA, Tateno Y. Accuracy of estimated phylogenetic trees from molecular data. *J. Mol. Evol*. 1983; 19: 153–170.
[49] Pei Z, Gao JQ, Chen J, Wie Z, Li F, Luo L, et al. Genetic diversity of elite sweet sorghum genotypes assessed by SSR markers. *Biologia Plantarum*. 2010; 54 (4): 653-658.
[50] Weir BS. Genetic Data Analysis II: Methods for Discrete Population Genetic Data. 2nd ed. Sunderland, MA, USA: *Sinauer Associates Inc*. 1996.
[51] Pritchard JK, Wena X, Falush D. Documentation for structure software: Version 2.3. Department of Human *Genetics, University of Chicago*.http://pritch.bsd.uchicago.edu/structure_software/release_versions/v2.3.3/structure_doc.pdf; 2010.
[52] Evanno G, Regnaut S, Goudet J. Detecting the number of clusters of individuals using the software STRUCTURE: a simulation study. *Mol. Ecol*. 2005; 14(8):2611-2620.
[53] Zhang Y, Wang XF, Li ZK, Zhang GY, Ma ZY. Assessing genetic diversity of cotton cultivars using genomic and newly developed expressed sequence tag-derived microsatellite markers. *Genetics and Molecular research*. 2011; 10(3): 1462-1470.
[54] Lacape JM, Dessauw DM, Rajab JL, Noyer B, Hau B. Microsatellite diversity in tetraploid *Gossypium* germplasm: assembling a highly informative genotyping set of cotton SSRs. *Mol. Breed*. 2007; 19:45–58.
[55] Liu S, Cantrell RG, Mccarty JCJR, Stewart JMcD. Simple Sequence Repeat based assessment of genetic diversity in cotton race stock accessions. *Crop Sci*. 2000; 40:1459-1469.
[56] Iqbal MJ, Aziz N, Saeed NA, Zafar Y, Malik KA. Genetic diversity evaluation of some elite cotton varieties by RAPD analysis. *Theoretical and Applied Genetics*. 1997; *94*(1):139-144.
[57] Eminur E, Hançer T. Cotton (*Gossypium hirsutum* L.) Germination Analysis and Molecular Characterization of Genotypes in Constrained Irrigation Conditions. *Turkey Agricultural Research Journal*. 2016; *3*(2): 122-129.
[58] Tyagi P, Gore MA, Bowman DT, Campbell BT, Udall JA, Kuraparthy V. Genetic diversity and population structure in the US Upland cotton (*Gossypium hirsutum* L.). *Theoretical and Applied Genetics*. 2014; *127*(2): 283-295.
[59] Bardak A, Bolek Y. Genetic diversity of diploid and tetraploid cottons determined by SSR and ISSR markers. *Turk. J. Field Crops*. 2012; *17*(2): 139-144.
[60] Gutierrez OS, Basu S, Saha JN, Jenkins DB, Shoemaker CL, Cheatham JC, et al. Genetic distance among selected cotton genotypes and its relationship with F_2 performance. *Crop Sci*. 2002; 42:1841-1847.
[61] Zhang JF, Lu Y, Adragna H, Hughs E. Genetic improvement of New Mexico Acala cotton germplasm and their genetic diversity. *Crop Sci*. 2005; 45:2363-2373.
[62] Khan AI, Fu YB, Khan IA. Genetic diversity of Pakistani cotton cultivars as revealed by simple sequence repeat markers. *Communications in Biometry and Crop Sci.* 2009; 4(1): 21-30.
[63] Zhao YL, Wang HM, Chen W, Li YH, Gong HY, Sang X, H et al. Genetic diversity and population structure of elite cotton (*Gossypium hirsutum* L.) germplasm revealed by SSR markers. *Plant Syst. Evol*. 2015; 301; 327–336.

[64] Chen G, Du XM. Genetic diversity of source germplasm of upland cotton in China as determined by SSR marker. *Acta Genet. Sinica*. 2006; 33: 1–10.
[65] Abdurakhmonov IY, Kohel RJ, Yu JZ, Pepper AE, Abdullaev AA, Kushanov FN, Jenkins JN. Molecular diversity and association mapping of fiber quality traits in exotic G. hirsutum L. germplasm. *Genomics*. 2008; *92*(6): 478-487.
[66] Bardak A, Fidan Ms, Dağgeçen E, Tekerek H, Çelik S, Parlak D, Hayat K. Pamukta İlişkilendirme Haritalaması Yöntemiyle Gossypol ile İlişkili Markörlerin Belirlenmesi (Determination of Gossypol-Related Markers with the Association of Cotton Mapping Method). *Journal of agricultural and nature*. 2017; *20*: 236.

Araştırma Makalesi https://doi.org/10.46810/tdfd.1000424 Research Article

Türk Doğa ve Fen Dergisi
Turkish Journal of Nature and Science
www.dergipark.gov.tr/tdfd

Bingöl Yöresi Arıcılık İşletmelerinde (*Apis mellifera L.*) Nosema Hastalığının Araştırılması

Halil ŞİMŞEK[1*], Zeynep AYAN[2]

[1] Bingöl Üniversitesi, Sağlık Hizmetleri Meslek Yüksekokulu, Bingöl, Türkiye
[2] Bingöl Üniversitesi, Fen Bilimleri Enstitüsü, Arı ve Arı Ürünleri Anabilim Dalı, Bingöl, Türkiye
Halil ŞİMŞEK ORCID No: 0000-0002-9637-1265
Zeynep AYAN ORCID No: 0000-0002-5854-1040

**Sorumlu yazar: hsimsek@bingol.edu.tr*

(Alınış: 06.10.2021, Kabul: 27.12.2021, Online Yayınlanma: 25.03.2022)

Anahtar Kelimeler
Bingöl,
Bal Arısı,
Nosema
Hastalığı

Öz: Bu araştırmada Bingöl ili arı işletmelerinde Nosema hastalığı yaygınlığının belirlenmesi amaçlandı. Araştırmada Bingöl merkez ve diğer ilçelerde arıcılık yapan 123 adet arı işletmesi ziyaret edilerek toplam 1245 adet arı örneği toplandı. Örneklerin laboratuvar incelemeleri sonrası işletmelerden 26 (%21,13)'sı ve örneklerden 98 (%7,87)'i Nosema hastalığı yönünden pozitif bulundu. Araştırmada işletme bazında hastalık oranı en yüksek oranda merkez ilçedeki işletmelerde %24,52 görülürken en düşük oranın ise Karlıova ilçesindeki işletmelerde %13,33 tespit edildi. İşletmelerden alınan ve incelenen örneklerden ise en yüksek oran merkez ilçede %15,11 tespit edilirken en düşük oranın ise Karlıova %2,80 ve Yayladere %2,85 ilçelerinde saptandı.

Investigation of Nosema Disease in Beekeeping Establishments (*Apis mellifera L.*) In Bingöl Region

Keywords
Bingöl,
Honeybee,
Nosema
Disease

Abstract: In this study, it is aimed to determine the prevalence of Nosema disease in bee establishments in Bingöl province. In the research, 1245 bee sample was collected by visiting 123 beekeeping establishments in the center of Bingöl and other towns. After laboratory examinations of the samples, 26 (21.13%) of the establishments and 98 (7.87%) of the samples were found to be positive for Nosema disease. In the study, the highest rate of the disease was found in the establishments in the central town (24.52%), while the lowest rate was found in the establishments in Karlıova town 13.33%. Among the samples taken from the establishments and examined, the highest rate was found in the central town 15.11%, while the lowest rate was found in Karlıova 2.8% and Yayladere 2.85%.

1. GİRİŞ

Arıcılık, dünyanın neredeyse her bölgesinde yapılan önemli tarımsal bir faaliyettir [1,2]. Yapılan arıcılık aktiviteleriyle bal, polen, arı zehri, arı sütü, bal mumu ve propolis gibi arı ürünleri ile gıda, eczacılık ve kozmetik sektörü gibi alanlarda kullanılan hammadde üretilmektedir [3,4]. Bunun yanında arılar meyve ağaçlarından ve bitkilerden nektar ve polen toplayarak besinsel ihtiyaçları tedarik ederken, diğer yandan da polinasyon ile ürün miktarını ve niteliğini arttırarak tarımsal üretime önemli düzeyde katkı sağlamaktadır. Ayrıca yabani floranın devamlılığını tozlaşma ile sağlamak sureti ile önemli katkıları olmaktadır [5,6]. Ülkemiz yüz ölçümü, topoğrafik yapısı, iklim ve bitki örtüsü açısından arıcılık için uygun bir coğrafyadır. Bu özelliğine rağmen diğer ülkelere oranla ülkemizde kovan başına bal üretimi ise düşük düzeyde kalmakta olup bunda; teknik bilgi yetersizliği, bakım ve besleme noksanlığı, ana arı üretiminin istenilen seviyede olmaması, arı kışlatmalarındaki bilgisizlik ve en önemlisi de hastalık ve zararlarının bilinmemesi, zamanında teşhis ve tedavinin yapılamaması gibi nedenlerin büyük payı vardır [7].

Arıcılık faaliyetlerinin daha verimli hale gelmesi, kovan başına elde edilen yıllık bal miktarında artışın sağlanması ve dünya çapında daha üst sıralara ulaşabilmesi için arıcılara bilimsel ve teknik yöntemlerle daha fazla bilgilendirmeler yapılması gerekmektedir. Ayrıca eş zamanlı olarak arı hastalıkları ile mücadele ve koloninin güçlendirilmesinde uygun yöntemlerin kullanılması sağlanmalıdır [8,9,10]. Son dönemlerde arıcılık faaliyetleri dünya genelinde olduğu gibi ülkemizde de tercih edilen üretim faaliyetleri arasına

girmiş olup her geçen gün arıcılığa olan ilgi artarak devam etmektedir [8].

Ülkemizin arıcılık için çok önemli bir potansiyele sahip olmasına rağmen beklenilen verimin alınamamasında hastalıkların önemli bir yeri vardır [11]. Arıcılıkta kovanlarda bal verimini önemli düzeyde düşüren ve ayrıca kolonilerde büyük kayıplara neden olan birçok hastalık bulunmaktadır. Bu hastalıklar gerek yavru ve gerekse ergin arılarda görülmekte ve arı işletmelerine önemli düzeyde ekonomik açıdan zarar vermektedir [12,13]. Arılarda, bakteri, virüs, parazit ve mantarların sebep olduğu birçok hastalık bulunmaktadır. Bunlar; Amerikan Yavru Çürüklüğü, Avrupa Yavru Çürüklüğü, Arı Felci, Varroa, Nosema, Trake Akarı, Kireç Hastalığı, Taş Hastalığı, Tulumsu Yavru Çürüklüğü hastalıkları gibi kolonilerde önemli kayıplara neden olan hastalıklardır [11]. Nosema sporları, arıların bağırsak ve midelerinde hareket ederek gelişmeye devam eden ve arılarda ölümlere neden olan etkenler arasında en önemlileri olarak bilinmektedir. Hastalığın etkenleri *Nosema apis* ve *Nosema ceranae*'dir. Bu faktörler yetişkin arıların sindirim sistemine yerleşir ve burada Nosema hastalığının meydana gelmesine neden olur [14]. Nosema hastalığının teşhisi klinik bulgulara göre tespit edilebilse de kesin teşhis ancak laboratuvar yöntemleri ile yapılmaktadır [11,14,15].

Bingöl ve yöresi iklim ve bitki örtüsü, zengin endemik bitkileri içeren florası ile arıcılık için önemli bir merkez olarak bilinmektedir. İşletme sayısı ve arılı kovan sayısı bakımından önemli bir düzeyde olmasına rağmen bal üretimi bakımından beklenen başarı elde edilememektedir. Bunda birçok nedenin yanında arı hastalıklarının önemli bir etken olduğu gerçeğinden hareketle bu çalışmada, kolonilerde önemli kayıplara neden olan, bal verimi oranının düşmesinin de önemli bir etkeni olduğu düşünülen Nosema hastalığının araştırılması, düzeyinin belirlenmesi ve ortaya konulması amaçlanmıştır.

2. MATERYAL VE METOT

2.1. Materyal

Bu çalışmada Bingöl Merkez ve ilçelerinde arıcılık yapan ve Bingöl Arıcılar Birliğine kayıtlı bulunan 802 arı işletmesinin 123'ünden alınan 1245 arı örneği materyal olarak kullanıldı.

Çalışmada kullanılmak üzere arı örneklerini toplamak için Bingöl Merkez ve ilçelerindeki arı işletmelerine 2020 yılı ilkbahar, yaz ve sonbahar aylarında periyodik olarak gidildi. Gidilen işletmeler rastgele toplam işletmenin yaklaşık %10'nunu oluşturacak şekilde belirlendi. İşletmelerden örnek alınan kovanlar işletmedeki toplam kovanın yaklaşık %5'ini oluşturacak şekilde olmasına dikkat edildi. Örnekler içerisinde %70'lik etil alkol bulunan 50 ml'lik falkon tüplere alındı. Alınan örneklerde ortalama 35-40 adet ergin arı olmasına dikkat edildi. Çalışma boyunca Merkez İlçe 53, Adaklı 5, Genç 15, Karlıova 15, Kiğı 10, Solhan 15, Yayladere 5 ve Yedisu 5 olmak üzere toplam 123 işletmeye gidildi ve bu işletmelerden toplam 1245 örnek toplandı.

2.2. Metot

İşletmelerden alınan örnekler Bingöl Üniversitesi Sağlık Hizmetleri Meslek Yüksek Okulu laboratuvarına getirildi. Tüplerdeki arı örnekler 24 saat sonra havlu peçete üzerine konuldu ve arılardan alkolün uzaklaşması sağlandı. Arılardan alkol uzaklaştırıldıktan hemen sonra bisturi ve pens yardımı ile abdomenleri ayrıldı ve porselen havan içerisine konuldu ve üzerine 10-15 ml serum fizyolojik su ilave edilip tokmakla ezilerek homojen bir karışımın oluşması sağlandı [11].

2.2.1. Natif İnceleme

Alınan örneklerden hazırlanan homojen karışımdan içerisinde herhangi bir partikül bulunmayan kısmından bir miktar lam üzerine alındı ve üzerine lamel kapatılarak ışık mikroskobunda 40 objektif ile incelendi ve *Nosema* sporları arandı [11].

2.2.2. Boyama Yöntemi İle İnceleme

Alınan örneklerden hazırlanan homojen karşımdan temiz bir lam üzerine 2-3 damla alındı, başka bir lamla yüzeye yayılması sağlandı ve kurutuldu. Kuruma işleminden sonra lamlar hafif alevden geçirilerek tespit edildi. Lamların üzerine %1'lik safranin boyasından 2-3 damla damlatıldı ve alevde lamların üzerindeki boyaların kaynayarak lam yüzeyine yayılması sağlandı. Soğuma işleminden sonra lamlar musluk suyunda yıkandı. Daha sonra lam üzerine pipetle metilen mavisi boyası döküldü 20 dakika beklendi. Boya döküldü ve musluk suyunda yıkandı. Lamlar kurutuldu ve mikroskopta incelemeye hazır hale getirildi. Lamlar mikroskopta 100'lük immersiyon objektifi ile incelendi safranin ile boyanan Nosema sporları gözlendi. İncelemede *Malpighamoeba mellificae* kistleri ve mantar sporları metilen mavisi boyası ile boyandıklarından Nosema sporlarından ayırımları sağlandı. Yapılan mikroskobik incelemede Nosema sporları gözlenen örnekler pozitif olarak değerlendirildi [11,16,17].

2.2.3. İstatistiksel Değerlendirme

Bu çalışmada toplanan örneklerde incelemeler sonrası pozitif olan örneklerin oranı yüzde olarak değerlendirildi ve tabloda gösterildi [18].

3. BULGULAR

Çalışmada işletmelerden toplanan örneklerden Bingöl merkezde 13, Adaklı ilçesinde 1, Genç ilçesinde 3, Karlıova ilçesinde 2, Kiğı ilçesinde 2, Solhan ilçesinde 3, Yayladere ilçesinde 1 ve Yedisu ilçesinde ise 1 işletme olmak üzere toplamda 26 arı işletmesi Nosema hastalığı yönünden pozitif olarak gözlendi (Tablo 1, Şekil 1). İlçelerdeki arı işletmelerinden alınan örneklerde ise; Merkez ilçede 68, Adaklı ilçesinde 2, Genç ilçesinde 9, Karlıova ilçesinde 7, Kiğı ilçesinde 5, Solhan ilçesinde 5, Yayladere ilçesinde 1 ve Yedisu ilçesinde 1

olmak üzere toplamda 98 örnek pozitif olarak tespit edildi (Tablo 1, Şekil 2).

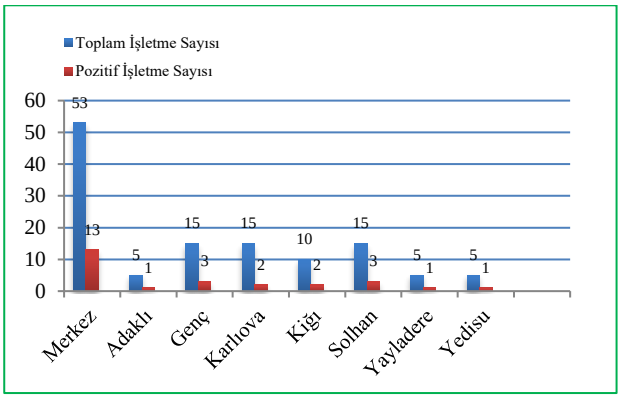

Şekil 1. Arı işletmelerinin pozitiflik oranları

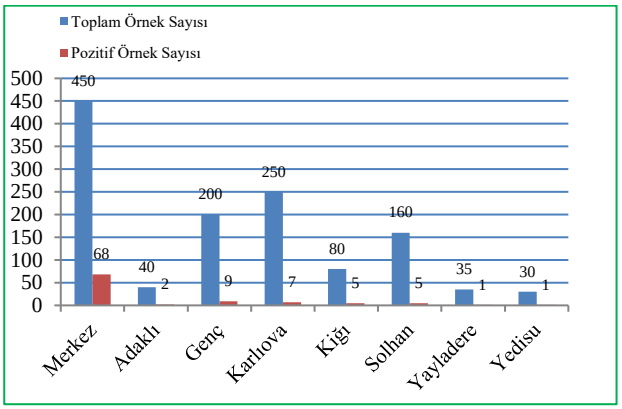

Şekil 2. Arı örneklerinin pozitiflik oranları

Tablo 1. Arı örneği alınan işletmelerin Nosema hastalığı yönünden pozitiflik düzeyi

Yerleşim Yeri	Toplam İşletme Sayısı	Örnek Alınan İşletme Sayısı	Pozitif İşletme Sayısı	%	Alınan Örnek Sayısı	Pozitif Örnek Sayısı	%
Merkez	356	53	13	24,52	450	68	15,11
Adaklı	39	5	1	20,00	40	2	5,00
Genç	99	15	3	20,00	200	9	4,50
Karlıova	75	15	2	13,33	250	7	2,8
Kiğı	79	10	2	20,00	80	5	6,25
Solhan	91	15	3	20,00	160	5	3,12
Yayladere	25	5	1	20,00	35	1	2,85
Yedisu	38	5	1	20,00	30	1	3,33
Toplam	**802**	**123**	**26**	**21,13**	**1245**	**98**	**7,87**

4. SONUÇ

Dünya çapında geniş bir dağılıma sahip olan Nosema hastalığı ilk defa Zander tarafından 1909 yılında adlandırılmıştır [19]. *N. apis*, Nosema hastalığının tek etkeni olarak görülmekteyken, *N. ceranae*'nın 1996 yılında Asya bal arısı *Apis ceranae*'da hastalık oluşturduğu ortaya konulmuştur [20,21]. *N. ceranae*'nın Avrupa'da *A. mellifera*'da enfeksiyon oluşturduğu ve aynı zamanda uyum sağladığı bildirmiştir. Böylelikle *N. ceranae*'nın dünyanın çoğu yerinde, batı bal arısı ırkları arasında geniş bir yayılıma sebep olduğu ve *N. apis*'in yerini aldığı belirtilmektedir [22].

Kısa bir süre sonra, *N. ceranae*'nın varlığına Amerika ve Asya'da rastlanıldığı doğrulanmıştır [23,24]. Öncelikle, Nosema hastalığına neden olan etmenin *N. apis* olduğu ve dünyanın her yerinde yayılım gösterdiği düşünülürken, *N. ceranae*'nın ise yalnızca Asya bal arısı ırkı olan *Apis ceranae*'yı etkilediği söylenmekteydi [25,26]. Ancak son yıllardaki çalışmalar, *N. ceranae*'nın *Apis mellifera*' ya da bulaştığı ve böylece tüm Avrupa'dan Avusturalya, Tayvan ve Kuzey Amerika'ya kadar yayıldığı bildirilmektedir [21,27,28].

Kanada'da yapılan bir araştırmada 2008, 2010 ve 2012 yıllarında toplanan bal arısı örneklerinde *Nosema* sporları saptanmış olup oransal olarak bakıldığında; 2008'de toplanan örneklerin %39'unda, 2010'da örneklerin %60'ında ve 2012'de ise örneklerin %45'inde karışık olarak *N. apis* ve *N. ceranae* sporları olduğu belirlenmiştir [29]. Bollan ve ark. [30] tarafından İskoçya'da yapılan bir çalışmada kolonilerde %70,4 oranında *N. ceranae* ve *N. apis* görüldüğü bildirilmektedir. Fries [22] tarafından İsveç'te yapılan bir çalışmada kolonilerin %17'inde *N. ceranae* ve *N. apis* birlikte görülürken %83'ünde ise sadece *N. apis*'e rastlanıldığı belirtilmektedir. Taric ve ark. [31] tarafında yapılan bir araştırmada Yugoslavya'nın kuzey bölgesinden toplanan 2439 arı örneğinin 630'u (%25,83) nosema sporları bakımından pozitif bulunmuştur. Ansari ve ark. [32] tarafından Suudi Arabistan'da yapılan bir çalışmada nosema hastalığının oranını %20,59 düzeyinde olduğu ve bu oranın ise %58'inin *N.ceranae* olduğu bildirilmiştir. Lotfi ve ark. [33] tarafında yapılan bir çalışmada İran'ın kuzeybatısındaki 294 arı kovanının 72'sinde Nosemotosis tespit edilmiştir.

Ülkemizde nosema hastalığının ilk teşhisi 1986 yılında Uygur ve Girişgin [34] tarafından Türkiye Kalkınma Vakfı Arı Hastalıkları Laboratuvarında teşhisi yapılmıştır. Aydın ve ark. [12] yaptıkları çalışmada nosema sporlarının varlığını Balıkesir, Bursa ve Çanakkale illerinde araştırmışlar ve sonuçları sırasıyla Balıkesir %30, Bursa %25,8 ve Çanakkale'de %25 düzeyinde tespit ettiklerini bildirmişlerdir. Çakmak ve ark. [35] yaptıkları bir araştırmada Bursa'da 22 ayrı bölgedeki 217 arı kovanından alınan arı örneklerinde nosema sporlarının yaygınlık düzeyini %24 düzeyinde olduğunu saptamışlardır. Topçu ve Arslan [16] tarafında Kars ilinde yaptıkları çalışmada 8 lokasyon bölgesindeki toplam 50 arılıkta yürüttükleri çalışmada 8 bölgenin 7 yerleşim yerinde %87,50 seviyesinde ve 50 örneklenen arılığın 20'sinde ise %40 düzeyinde *N. apis* sporlarına rastlamışlardır. Şimşek [36] tarafından yapılan araştırmada Elâzığ'daki arı işletmelerinden alınan örneklerde nosema hastalığının yaygınlığının %8,7 oranında olduğunu tespit edilmiştir. Doğaroğlu ve Sıralı [37] yaptıkları araştırmada Trakya'da nosema hastalığı yaygınlığının %6,5 düzeyinde olduğunu saptamışlardır. Ütük ve ark. [38] tarafından 2006-2010 yılları arasında Türkiye'nin 36 şehirlerinde Merkez Veteriner Kontrol ve Araştırma Enstitüsü, Arı hastalıkları Laboratuvarına gelen toplam 140 adet numune üzerinde yapılan araştırmada %4,28'inde nosema hastalığı, %2,85'inde hem varroa hem de nosema hastalığı, %56,42'sinde ise yalnızca varroa zararlısı tespit etmişlerdir. Büyük ve ark. [39] yaptıkları çalışmada Kırşehir ilinde 5 lokasyondan Merkez, Mucur, Akpınar, Boztepe ve Kaman olarak tanımlanan 5100 bal arı örneği incelenmişler çalışmada hastalığın görülme sıklığının Merkez bölgesinde %25, Boztepe ilçesinde %60, Mucur bölgesinde %23,07 ve

Akpınar bölgesinde %12,5 olduğunu tespit etmişlerdir. Zerek [40] Hatay yöresinde yaptıkları çalışmada İşletmelerin %45'inde ve kovanlarında %20'sinde *N. ceranae* enfeksiyonu saptanmıştır.

Yaptığımız bu araştırmada Bingöl merkez ve diğer ilçelerde Bingöl Arıcılar Birliğine kayıtlı arı işletmelerinden alınan örneklerde Nosema hastalığının %7,8 oranında olduğu tespit edildi. Sonucun [36-38] araştırmacıların bulgularıyla uyumlu iken, [12,16,22,29-33,35,39,40] araştırmacıların bulgularından ise düşük oranda olduğu gözlendi. Bu durumun merkez ilçede diğer ilçelere nazaran daha yüksek oranda gözlenmesinde; merkez ilçe arıcılarının çoğunluğunun gezginci arıcılık yapmaları ve dışarıdan gelen gezginci arıcıların çoğunlukla merkez ilçe meralarında konaklamalarının sebep olabileceği düşünülmektedir.

Yaptığımız bu araştırmada Bingöl merkez ve tüm ilçelerinde nosema hastalığına rastlanılmış olup nosema hastalığının en yüksek oranda Bingöl merkez ilçede rastlanılmıştır. Hastalığın yayılmasında gezginci arıcılığın önemli bir etken olduğu da dikkate alınılarak gezginci arıcıların merkez ve diğer ilçe meralarında konaklamaları kontrollü bir şekilde sağlanmalıdır. Hastalık yönünden şüpheli işletmeler ile diğer arı işletmelerinin temasının engellenmesi, arıcıların bilgilendirilmesi ve koruyucu önlemlerin alınması noktasında çalışmalar yapılmalıdır.

Arıcılığın önemli problemlerinden olan arı hastalık ve zararlıları eğer zamanında fark edilip gerekli önlemler alınmazsa, arıcılığın gelişmesi için yapılan tüm gayret ve çabaları olumsuz yönde etkilemeye devam edecektir. Diğer yandan arıcıların kullandıkları ortak su kaynaklarında bölgede hastalığın yayılmasının önemli bir etkeni olabileceği düşünülmektedir. Bundan dolayı nosema hastalığının yaygınlığı üzerine yapılan çalışmalar yalnızca kolonilerdeki arılarda ve arılıkta değil aynı zamanda arı kolonilerinin kullandıkları su kaynaklarında da olmalıdır. Böylelikle hastalıkta olası tüm etkenlerin tespiti ve ortaya konması ile daha kalıcı önlemlerin alınmasına imkân sağlayacağından önemli görülmektedir.

Teşekkür

Bu çalışma Zeynep AYAN'ın BAP-FBE.2020.00.003 numaralı Bingöl Üniversitesi Bilimsel Araştırma Projeleri (BAP) tarafından desteklenen yüksek lisans tezinden özetlenmiş olup desteklerinden dolayı BÜBAP birimine teşekkür ederiz.

KAYNAKLAR

[1] Fıratlı Ç, Gençer HV. Dünya arıcılığı ve Türkiye'nin yeri. TC Ziraat Bankası Kültür Yayınları, 1995; (28): 20-28.
[2] Bingöl M, Erkan C. Van ili arı hastalıkları ve zararlılarının belirlenmesine yönelik bir araştırma. YYÜ Tar Bil Derg, 2014; 24(2): 168-174.
[3] Kence A. Türkiye balarılarında genetik çeşitlilik ve korunmasının önemi. U Arı D, 2006; 6(1): 25-32.
[4] Tunca Rİ, Taşkın A, Karadavut U. Türkiye'de arı ürünlerinin bazı illerdeki tüketim alışkanlıklarının ve farkındalık düzeylerinin belirlenmesi. Türk Tarım-Gıda Bilim ve Teknoloji Dergisi, 2015; 3(7): 556-561.
[5] Tunca Rİ, Çimrin T. Kırşehir ilinde bal arısı yetiştiricilik aktiviteleri üzerine anket çalışması. Iğdır Üniv Fen Bil Ens Derg, 2012; 2(2): 99-108.
[6] Büyük M, Tunca Rİ, Taşkın A. Türkiye'de Nosema spp. varlığına yönelik yapılmış çalışmalar. Türk Tarım ve Doğa Bilimleri Derg, 2014; 1(2): 234-238.
[7] Doğanay A. Arı hastalıkları 1. Bal arısı hakkında genel bilgi. Türk Vet Hek Der Derg, 1993; 5: 29-35.
[8] Fıratlı Ç, Karacaoğlu M, Gençer HV, Koç A. Türkiye arıcılığına ilişkin değerlendirmeler ve öneriler. TMMOB Ziraat Mühendisleri Odası. Türkiye Ziraat Mühendisliği VI. Teknik Kongresi, 2005; Ocak, 03-07, Ankara, 3-7.
[9] Kekeçoğlu M, Gürcan EK, Soysal Mİ. Türkiye arı yetiştiriciliğinin bal üretimi bakımından durumu. Tekirdağ Ziraat Fak Derg, 2007; 4(2): 227-236.
[10] Sezgin A, Kara M. Arıcılıkta verim artışı üzerinde etkili olan faktörlerin belirlenmesine yönelik bir araştırma: Tra2 Bölgesi Örneği. Harran Ünv Ziraat Fak Derg, 2011; 15(4): 31-38
[11] Zeybek H. Arı hastalıkları ve zararlıları. Tarım Köyişleri Bak. Etlik Hay Hast Araş Enst Müd Yayınları, Ankara, 1991; 1-96.
[12] Aydın L, Güleğen E, Çetinbaş H. Prevalence of nosemaapis in southern marmara region. XVII. Apimondia 28. October. 1 November Durban, South Africa 2001.
[13] Çakmak I, Aydin, L, Camazine S, Wells H. Pollen traps and walnut-leaf smoke for Varroa control. Am Bee J, 2002; 142(5): 367-370.
[14] Furgala B, Mussan EC. Protozoa. In: Morse R, Nowogrodzki R. (Editors). Honey Bee Pests, Predators and Diseases. Second Edition. Ithaca and London: Comstock Publishing Associates, Cornell Univ. Press 1990; 1-474.
[15] Girişgin AO. Mantar hastalıkları. Nosemosis. In: Doğanay A, Aydın L, (Editörler). Bal Arısı Yetiştiriciliği Ürünleri Hastalıkları. 1. Baskı: Dora Basım Yayın Dağıtım Ltd. Şti. Bursa, 2017; 381-389.
[16] Topçu B, Arslan MÖ. Kars yöresindeki balarılarında nosemosis'in yaygınlığı. Uludağ Arıcılık Derg, 2004; 4: 164-170.
[17] Aydın L, Doğanay A, Oruç HH, Yeşilbağ, K, Bakırcı S, Girişkin O. Bal arısı yetiştiriciliği ürünleri hastalıkları. Dora Yayın Evi, Bursa, 2017; 155-90.
[18] Sümbüloğlu K, Sümbüloğlu V. Biyoistatistik. 6. Baskı. Özdemir Yayıncılık. Ankara. 1995; 1-184.
[19] Matheson, A. World bee health update. Bee World, 1996; 77: 45-51.
[20] Fries I, Feng F, Da Silva A, Slemenda SB, Pieniazek NJ. Nosema ceranae N. Sp. (Microspora,

Nosematidae), Morphological and Molecular characterization of a microsporidian parasite of the Asian honeybee *Apis cerana* (Hymenoptera, Apidae). Europ J Protistol, 1996; 32(3): 356-365.
[21] Higes M, Martin R, Meana A. Nosema ceranae, a new microsporidian parasite in honey bees in Europe. J Invertebr Pathol, 2006; 92: 93-95.
[22] Fries I. Nosema ceranae in European honey bees (*Apis mellifera*). J Invertebr Pathol, 2010; 103: 73-79.
[23] Sarlo E, Medici SK, Braunstein M, Eguaras M. Presencia Y distribucion de Nosema ceranae en la region sudeste de la provincial de Buenos Arires. In Actas del Segundo Congreso Argentino de Apicultura, Mar del Plata, Argentina, 2008; p. 26.
[24] Williams GR, Shafer ABA, Rogers REL, Shutler D, Stewart DT. First detection of Nosema ceranae, a microsporidian parasite of European honeybees (*Apis mellifera*), in Canada and central USA. J Invertebr Pathol, 2008; 97:189-192.
[25] Somerville D, Hornitzky M. Nosema disease, Primefacts 2007; 699: 3.
[26] Higes M, Martín-Hernández R, Meana A. Nosema Ceranae in Europe: an Emergent Type C Nosemosis, Apidologie, 2010; 41(10): 375-392.
[27] Huang WF, Jiang JH, Chen YW, Wang CH. A nosema ceranae isolate from the honeybees *Apis mellifera*. Apidologie, 2007; 38: 30-37.
[28] Whitaker J, Szalanski AL, Kence M. Molecular Detection of N. ceranaeband N. Apis brom Turkish Honey Bees. Apidologie, 2010; 42(2): 174-180.
[29] Emsen B, Guzman-Novoa E, Hamiduzzaman M, Eccles L, Lacey B, Ruiz-Pérez RA, Nasr M. Higher prevalence and levels of Nosema ceranae than Nosema apis infections in Canadian honey bee colonies. Parasitol Res, 2016; 115(1): 175-181
[30] Bollan KA, Hothersall JD, Moffat C, Durkacz J, Saranzewa N, Wright GA, et al. The microsporidian parasites Nosema ceranae and Nosema apis are widespread in honeybee (*Apis mellifera*) colonies across Scotland. Parasitol Res, 2013; 112(2): 751-759.
[31] Taric E, Glavinic U, Stevanovic J, Vejnovic B, Aleksic N, Dimitrijevic V, et al. Occurrence of honey bee (*Apis mellifera L.*) pathogens in commercial and traditional hives. J Apicult Res, 2019; 58(3): 433-443.
[32] Ansari MJ, Al-Ghamdi A, Nuru A, Khan KA, Alattal Y. Geographical distribution and molecular detection of Nosema ceranae from indigenous honey bees of Saudi Arabia. Saudi J Biolog Sci, 2017; 24(5): 983-991
[33] Lotfi A, Jamshidi R, Aghdam Shahryar H, Yousefkhani M. The prevalence of nosemosis in honey bee colonies in Arasbaran region (Northwestern Iran). American-Eurasian J Agric & Environ Sci, 2009; 5(2): 255-257.
[34] Uygur ŞÖ, Girişgin AO. Bal arısı hastalık ve zararlıları. Uludağ Arıcılık Derg, 2008; 8(4):130-142.
[35] Çakmak İ, Aydın L, Gülegen AE. Güney marmara bölgesinde balarısı zararlıları ve hastalıkları. Uludağ Arıcılık Derg, 2003; 3(2): 33-35.
[36] Şimşek H. Elazığ yöresi bal arılarında bazı parazit ve mantar hastalıklarının araştırılması. Ankara Üniv Vet Fak Derg, 2005; 52: 123-126.
[37] Doğaroğlu M, Sıralı R. Survey results on honeybee pests and diseases in Thracian region of Turkey. Uludag Bee Journal, 2005; 5: 71-78.
[38] Ütük AE, Pişkin FÇ, Deniz A, Balkaya I. A retrospective study on varroosis and nosemosis. Etlik Vet. Mikrobiyoloji Derg, 2011; 22(1): 11-15.
[39] Büyük M, Tunca Rİ, Taşkın A. Kırşehir ilindeki arılıklarda nosema hastalığının belirlenmesi. Türk Tarım-Gıda Bilim ve Teknoloji Derg, 2017; 5(1): 1-5.
[40] Zerek A. Hatay yöresi bal arılarında (*Apıs Mellıfera* L. 1758) nosemosisin yaygınlığı. Doktora Tezi, Sağlık Bilimleri Enstitüsü Parazitoloji (Vet) Anabilim Dalı, Hatay Mustafa Kemal Üniversitesi, Hatay. 2020; 1-73.

Cilt 11, Sayı 1, Sayfa 95-101, 2022 Volume 11, Issue 1, Page 95-101, 2022

Araştırma Makalesi https://doi.org/10.46810/tdfd.1011220 Research Article

Türk Doğa ve Fen Dergisi
Turkish Journal of Nature and Science
www.dergipark.gov.tr/tdfd

Synthesis and Characterization of ZnO@Fe3O4 Composite Nanostructures by Using Hydrothermal Synthesis Method

Naim ASLAN[1*]

[1]Munzur University, Faculty of Engineering, Department of Metallurgical and Materials Engineering, Tunceli, Turkey
Naim ASLAN ORCID No: 0000-0002-1159-1673

**Corresponding author: aslan.naim@gmail.com; naimaslan@munzur.edu.tr*

(Received: 18.10.2021, Accepted: 08.03.2022, Online Publication: 25.03.2022)

Keywords
Nanocomposite, $ZnO@Fe_3O_4$, Morpho-structural characteriza-tion, Medical imaging, Magnetic and optical properties

Abstract: In this study, $ZnO@Fe_3O_4$ composite nanostructures were synthesized using the hydrothermal method. X-ray diffraction analysis was performed for the structural characterization of nanostructures obtained with the addition of Fe_3O_4 at different ratios, and no impurity peaks were found. Scanning electron microscope (SEM) and transmission electron microscope (TEM) were used for morphological imaging. It was understood that ZnO nanoparticles were decorated around Fe_3O_4 in the morphology of nanostructures. Fe, Zn, and O peaks were detected in elemental analysis. Energy band gaps of $ZnO@Fe_3O_4$ nanocomposite structures were obtained from absorbance data collected by use of UV-VIS spectrometer. The band gap values of nanostructures were calculated to be in the range of 2-2.1 eV. Magnetic properties were determined using a vibrating sample magnetometer (VSM), and the values of 3.76 emu/g and 7.96 emu/g were found depending on the Fe_3O_4 content. Although these values show a limited ferromagnetic property, they are important in optoelectronic and medical imaging applications due to the advanced optical and electronic properties of ZnO.

Hidrotermal yöntem kullanılarak ZnO@Fe3O4 kompozit nanoyapıların sentezi ve karakterizasyonu

Anahtar Kelimeler
Nanokompozit $ZnO@Fe_3O_4$, Morfo-yapısal karakterizas-yon, Medikal görüntüleme, Manyetik ve optik özellikler

Öz: Bu çalışmada, $ZnO@Fe_3O_4$ kompozit nanoyapılar hidrotermal yöntem kullanılarak sentezlenmiştir. Farklı oranlarda Fe_3O_4 katkısıyla elde edilen nanoyapıların yapısal karakterizasyonu için X-ışını kırınım analizi gerçekleştirildi ve herhangi bir safsızlık pikine rastlanmadı. Morfolojik görüntülemede taramalı elektron mikroskobu (SEM) ve geçirimli elektron mikroskobu (TEM) kullanıldı. Nanoyapıların morfolojisinde Fe_3O_4 etrafında ZnO nano taneciklerinin dekore edildiği anlaşılmıştır. Elemental analizde ise Fe, Zn ve O pikleri kaydedilmiştir. $ZnO@Fe_3O_4$ nanokompozit yapıların bant aralığı enerjileri Uv-Vis spektromotresi aracığılıyla elde edilen absorbans datalarından elde edilmiştir. Nanoyapıların bant gap değerleri yaklaşık olarak 2-2.1 eV aralığında hesaplanmıştır. Manyetik özellikler ise Vibrating Sample Magnetometer (VSM) kullanılarak tespit edildi ve Fe_3O_4 katkı oranına bağlı olarak 3.76 emu/g ile 7.96 emu/g değerleri bulundu. Bu değerler sınırlı bir ferromanyetik özellik göstermesine rağmen ZnO'nun sahip olduğu gelişmiş optik, elektronik özelliklerinden dolayı optoelektronik ve medikal görüntüleme uygulamalarında önem arz etmektedir.

1. INTRODUCTION

Nanostructures, which are the basic elements of nanoscience and nanotechnology, have come to the fore as important engineering materials in composite, semiconductor, photocatalytic, magnetic, metal oxide, and biomedical applications with their structural, physical, chemical, and biological properties. Metallic-based nanostructures have received intense attention from both scientific and industrial community [1]. As a matter of fact, magnetic information storage has gained a place in a wide range of areas from industrial applications such as biomedicine and catalysis to new applications in photonics, imaging, and biomedical field [2]. Metallic or metal oxide nanostructures have been extensively studied in recent years due to their specific surface area and crystallinity. Metallic nanostructures stand out in technological product developments with their tunable and improvable properties such as melting

points, electrical and thermal conductivity, light absorption and scattering properties, optical sensitivity, photocatalytic activity, and wettability. Zinc oxide (ZnO), which is a metal oxide, is a biocompatible metal oxide resistant to corrosion and oxidation with its cheap raw material, high crystallinity, synthesis at low temperatures, high optical transmittance, and electrical conductivity. With these significant properties, it has become an important engineering material for optoelectronics, solar cells, detectors, biosensors, drug delivery, and biomedical applications [3]. Iron-based magnetic nanoparticles, especially Fe_3O_4 as another important metal oxide, are important materials used in ceramics, catalysis, magnetic information storage, medical imaging, drug delivery, biomedical applications, and various electronic applications with their natural magnetic properties. Thus, thanks to the unique and compatible properties of their structures, Fe_3O_4 and ZnO allow the production of a higher performance hybrid or composite nanostructure in future applications. In previous studies, sol-gel [4, 5], co-precipitation [6], deposition [7], wet milling [8], microwave assisted [9], and wet chemical [10] methods were used for the synthesis of ZnO/Fe_3O_4 nanocomposites.

ZnO based nanostructures show good electric, optoelectronic, and catalytic properties [11-13]. Fe_3O_4 nanoparticles illustrates superparamagnetic and/or ferromagnetic properties depending on their size [14]. Decorating ZnO nanoparticles with Fe_3O_4 give them magnetic characteristics which enhance the application range of the ZnO nanoparticles [6,10]. Therefore, particles electrical and electronically active ZnO nanoparticles with good magnetic properties can be used in different applications such as magnetic filtering, magnetic catalysis materials, etc [15]. Recently, the hydrothermal method has started to be used for producing nanosized hybrid materials. This method allows the synthesis of different hybrid structures under suitable pressure and temperature conditions without disturbing the chemical structure of the materials [16]. In the present study, the structural, morphological, optoelectronic, and magnetic properties of ZnO@Fe_3O_4 nanostructures obtained in different ratios (1:1 and 1:2) using the hydrothermal method were investigated in detail. SEM (scanning electron microscopy) and TEM (transmission electron microscopy) were used in the structural analysis. EDS (energy dispersive spectra) and X-ray diffraction methods were used in the analysis of chemical composition. UV-vis spectroscopy was used to assess the energy band gaps. Vibrational sample magnetometry was used in the investigation of the magnetic characteristics.

2. MATERIALS AND METHODS

2.1. Materials and Measurements

Iron(II) sulfate ($FeSO_4 \cdot 7H_2O$, Sigma-Aldrich), zinc acetate ($Zn(CH_3CO_2)_2.2H_2O$, Sigma-Aldrich) salts, and urea ($CO(NH_2)_2$, Sigma-Aldrich, PEG (polyethylene glycol; MW=4,000), NaOH (sodium hydroxide) were used for the synthesis of ZnO@Fe_3O_4 nanostructures. X-ray diffraction (XRD) patterns (RIGAKU miniflex600), scanning electron microscope (SEM-HitachiSU3500), high resolution transmission electron microscopy (HR-TEM, Joel 2100 F), energy dispersive x-ray spectroscopy (EDS, Oxford), UV-Vis spectrum (UV-1800 ENG240V), and vibrating sample magnetometer (Cryogenic Limited PPMS) were used for structural, morphological, elemental, optical, and magnetic characterizations, respectively.

2.2. Synthesis of ZnO Nanoparticles

After 1 g of PEG was dissolved in 20 mL of water, 2.19 g of $Zn(CH_3CO_2)_2.2H_2O$ salt was added. After dissolution, 0.5 M 20 mL urea solution was added dropwise. The resulting mixture was transferred to 50 mL capacity Teflon lined stainless steel autoclaves and then heated in an oven at 150 ºC for 12 hours. After spontaneous cooling to room temperature, the precipitate was rinsed with distilled water and ethanol and dried at 80 ºC for 12 hours. The resulting solid was annealed in a muffle furnace at 350 ºC for 2 hours (with a temperature increase of 2 ºC/min).

2.3. Synthesis of Magnetic ZnO@Fe_3O_4 Composite Nanostructures

0.2 g of ZnO was dispersed in 20 mL of deionized water in an ultrasonic bath. In a separate beaker, 0.328 g of $FeSO_4.7H_2O$ was dissolved in 20 mL of deionized water. 1.6 g of NaOH was added to it, and it was mixed for 10 minutes. Then the prepared solution was poured onto ZnO. It was mixed in the ultrasonic bath for 5 more minutes, taken to 50 mL capacity Teflon autoclave coated with stainless steel, and kept at 150 ºC for 12 hours. The resulting black precipitate was collected by centrifugation at 8000 rpm for 20 minutes by use of a centrifuge and washed with deionized water and absolute ethanol several times. The precipitate was kept at 80 ºC for 12 hours (ZnO@Fe_3O_4-1:1). The same procedures were repeated for 0.656 g of $Fe_3O_4.7H_2O$ and 3.2 g of NaOH (ZnO@Fe_3O_4-1:2) [17-19]. Also, such process are illustrated schematically in Fig. 1.

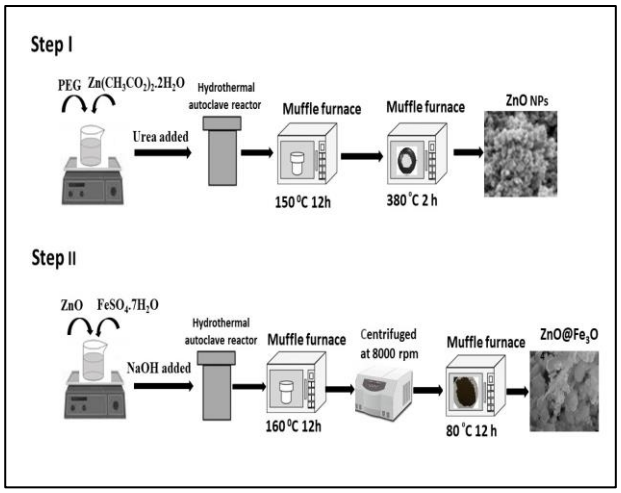

Figure 1. Schematic representation of synthesized ZnO@Fe_3O_4 nanostructures using hydrothermal method

3. RESULTS AND DISCUSSION

3.1. Morpho-structural Characteristic of Nanostructures

The XRD graph of ZnO, Fe_3O_4, ZnO@Fe_3O_4 (1:1), and ZnO@Fe_3O_4 (1:2) nanostructures synthesized by the hydrothermal method is given in Figure 2. As can be understood from the XRD diffraction patterns obtained, peaks characteristic to the ZnO and Fe_3O_4 structures were also observed in ZnO@Fe_3O_4 nanostructures with 1:1 and 1:2 weight ratios. In the ZnO@Fe_3O_4 (1:2) diffraction, the characteristic peaks became more evident with the increase of Fe_3O_4 content. However, the ZnO peak intensity decreased. In addition, the lack of any impurity peak in the XRD diffraction patterns in these structures indicates that they have high crystallinity. The resulting XRD patterns were seen to be consistent with the ZnO@Fe_3O_4 nanostructures obtained by different methods in the literature, but they gave better results in terms of impurity [5,6], [20-22].

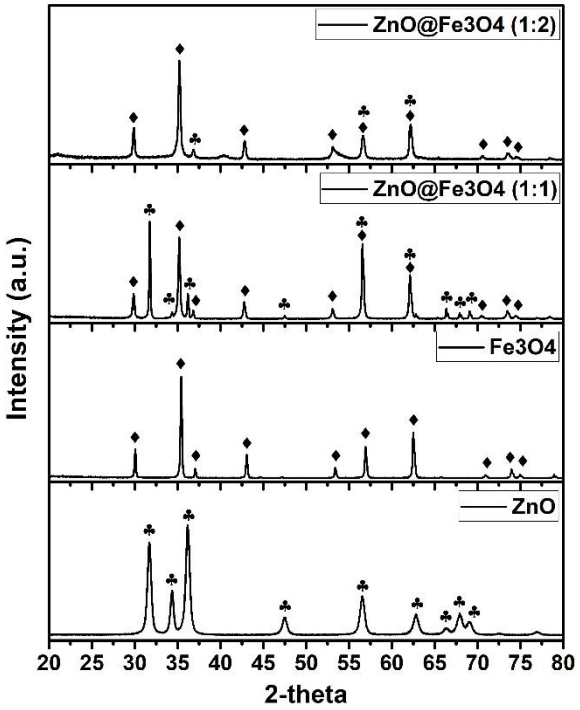

Figure 2. XRD spectra of ZnO, Fe_3O_4, and ZnO@Fe_3O_4 nanostructures

The synthesized SEM images of the ZnO nanostructures containing different weight ratios of Fe_3O_4 are shown in Figure 3a and Figure 3b. As shown in the SEM images, the ZnO and Fe_3O_4 structures were detected to have composite character. In addition, TEM analysis was carried out to check the nano dimensions of the composite structures. The presence of different types of structures was observed in the TEM analysis, as shown in Figure 4a and Figure 4b. It was understood that 10-20 nm irregular spherical ZnO NPs accumulated around Fe_3O_4 structures with 50-100 nm amorphous branches [22].

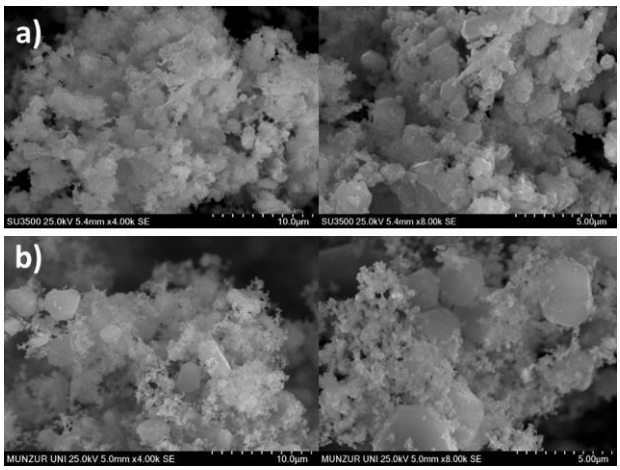

Figure 3. SEM photos of ZnO@Fe3O4 (1:1), ZnO@Fe3O4 (1:2)

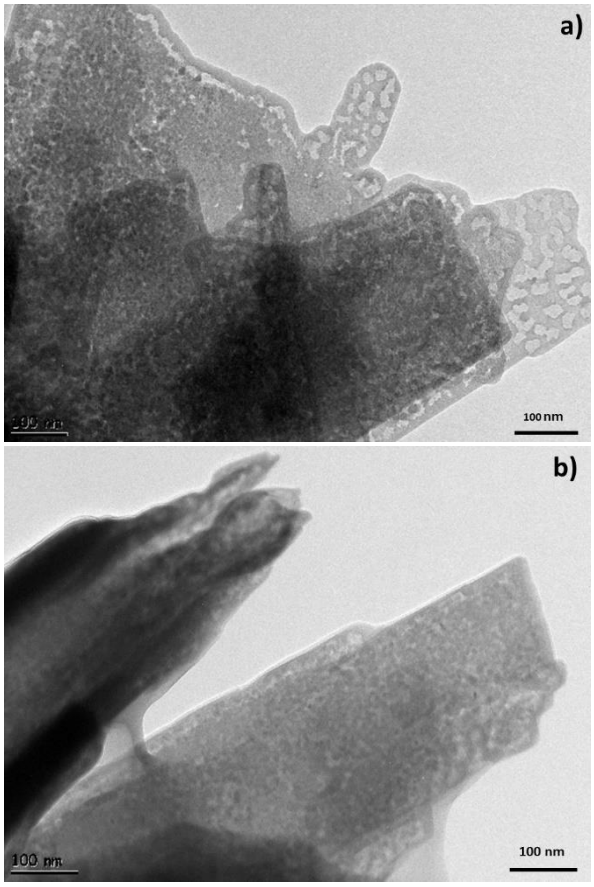

Figure 4. TEM photos of (a)-ZnO@Fe_3O_4(1:1), (b)-ZnO@Fe_3O_4 (1:2)

The EDS-spot and EDS-mapping results of the hydrothermally synthesized ZnO@Fe_3O_4 nanostructures are shown in Fig. 5 and Fig. 6, respectively. Fe, Zn, O were observed in the obtained EDS spectrum as shown in Figure 5a and Figure 5b. Before the SEM investigations Au sputtering was applied to the samples which is a standard procedure used to enhance the performance of the SEM. This is procedure cause a visible Au peak in the EDS spectra. Such a peak is not related to the structure of the nanoparticles. While the percentages of the Fe, Zn, and O elements in the ZnO@Fe_3O_4 (1:1) nanostructure were 38.9, 35.4, and 23.5, respectively, they were observed as 62.7, 16.8, and 19.4 in the ZnO@Fe_3O_4 (1:2) nanostructure. Addition of Fe_3O_4 at different weight ratios nearly doubled the Fe

ratio in the structure. Moreover, in the EDS-mapping images given in Figure 6a and 6b, color intensities are presented based on the presence and content of the Fe, Zn, and O phases in the ZnO@Fe_3O_4 composite structure.

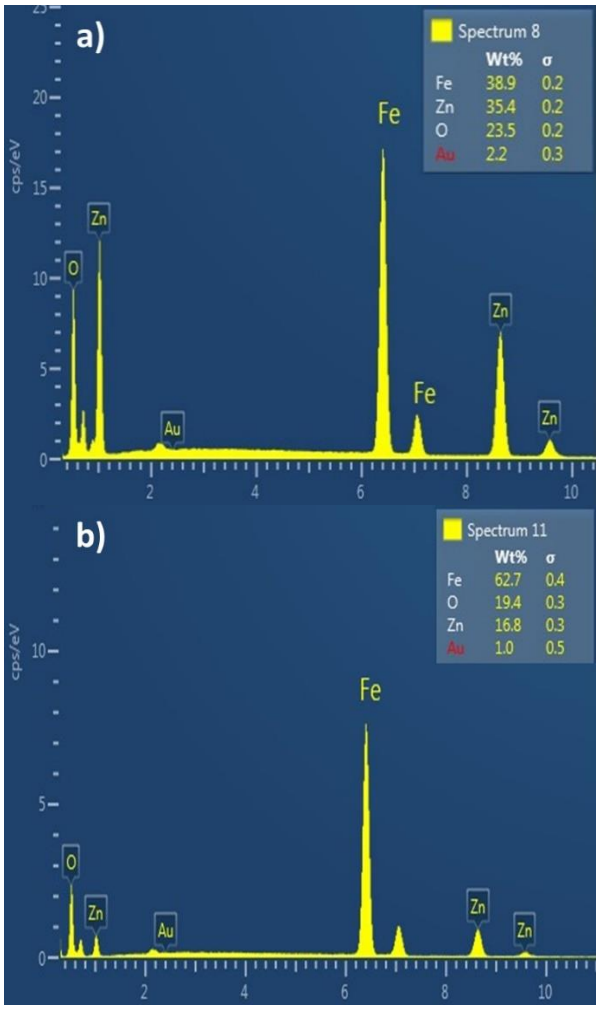

Figure 5. EDS spectrum of (a)-ZnO@Fe_3O_4 (1:1), (b)-ZnO@Fe_3O_4 (1:2)

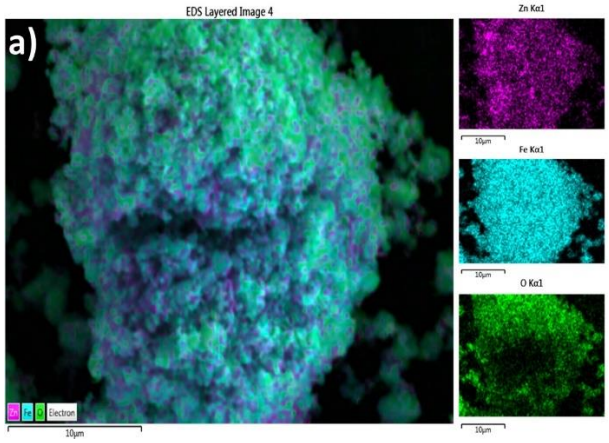

Figure 6. (a) EDS-mapping spectrum of (a)-ZnO@Fe_3O_4(1:1) nanostructure

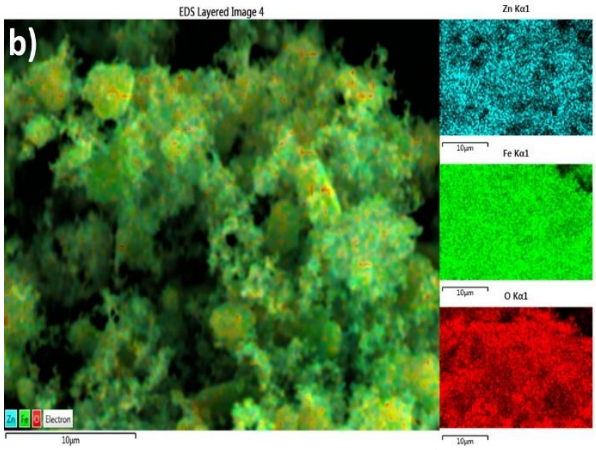

Figure 6. (b) EDS-mapping spectrum of) ZnO@Fe_3O_4(1:2) nanostructure

3.2. Optical Properties of ZnO@Fe_3O_4 Nanostructures

The optical absorbance data of the hydrothermally produced ZnO, Fe_3O_4, and ZnO@Fe_3O_4 nanostructures scanned in the range of 200 nm-800 nm are shown in Figure 7a,b,c,d. When the absorbance spectrum of the ZnO nanostructure was examined, no significant difference was observed. This can be attributed to the very small nanosize of ZnO nanoparticles [23]. In Figure 7b, the absorbance peak of the Fe_3O_4 nanostructure is recorded as approximately 436 nm. These peaks are consistent with those obtained in the literature [17],[24]. The absorbance peaks of ZnO@Fe_3O_4 nanostructures were detected to be 235 nm, 325 nm, and 380 nm, respectively (Figure 7c-d). Furthermore, optical band gaps of the nanostructures were estimated from Einstein's energy equation (1) [17, 25-27].

$$E_g^{nano} = {hc}/{\lambda} \quad (1)$$

where E_g^{nano} is the energy band gap of the nanoparticles, c is the speed of light, h is Planck's constant, and λ is the cut off wavelength obtained from the absorption spectra. The direct energy band gap of the ZnO nanostructure in Figure 6a was obtained as 2.3 eV. In general, single crystal ZnO band gap is accepted as 3.34 eV. The value obtained in the present study was considerably lower than the value of 3.34 eV. The low values obtained in similar studies in the literature were attributed to the defects in the nanostructure [28]. The optical energy band gap of the Fe_3O_4 nanostructure was found to be 2 eV, which is consistent with the literature [17, 29]. Moreover, as shown in Figure 7c-d, the energy band gap of ZnO@Fe_3O_4 nanostructures was determined around 2.1 eV.

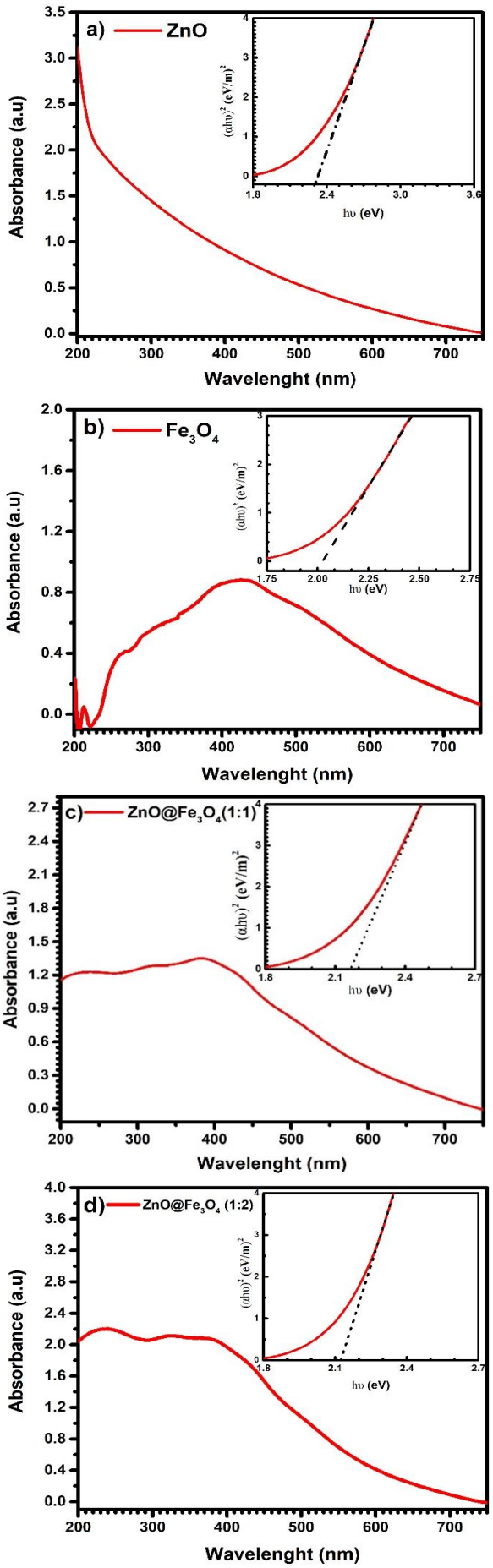

Figure 7. Absorbance and band gap characteristics of ZnO (a), Fe_3O_4 (b), ZnO@Fe_3O_4 -1:1 (c) and ZnO@Fe_3O_4 -1:2 (d) nanostructures

3.3. Magnetic Properties of ZnO@Fe_3O_4 Nanostructures

Magnetic hysteresis curves of ZnO@Fe_3O_4 (1:1) and ZnO@Fe_3O_4 (1:2) nanocomposite structures are shown in Figure 8a and Figure 8b. While the magnetic saturation value of the nanostructure synthesized at a ratio of 1:1 was obtained as 3.76 emu/g, as shown in Figure 8a, that of the nanostructure synthesized at a ratio of 1:2 was obtained as 7.97 emu/g, as shown in Figure 8b. With the doubling of the Fe_3O_4 content by weight ratio, that value approximately doubled as well. However, these values are lower than those found just for the Fe_3O_4 nanostructures in the literature. In their magnetic saturation measurements of Fe_3O_4@Bi2S3 nanoflowers synthesized by the hydrothermal method, Yetim et al., found a value of 89.8 emu/g for the Fe_3O_4 nanostructure [17]. In a similar study, Karacam et al. reported the magnetic saturation values of the Fe_3O_4 nanostructures as 87.7 emu/g and 90.7 emu/g [18]. The magnetic value of the ZnO additive obtained in this study decreased considerably. Sin et al. found the magnetic saturation value as 2.81 emu/g in the ZnO@ Fe_3O_4 nanostructure they synthesized with a facile surfactant-free method [30]. Długosz et al., reported the magnetic saturation value of the Fe_3O_4/ZnO nanostructure they synthesized with a microwave reactor as 9.5 emu/g [22]. This study is consistent with the values obtained in the literature. It is also known that the ZnO structure does not have good magnetic properties. However, it was revealed that a ferromagnetic property was shown through the addition of ZnO to the Fe_3O_4 structure. These results are important especially in terms of the use of ZnO@Fe_3O_4 nanostructures as contrast agents in medical imaging applications [31, 32].

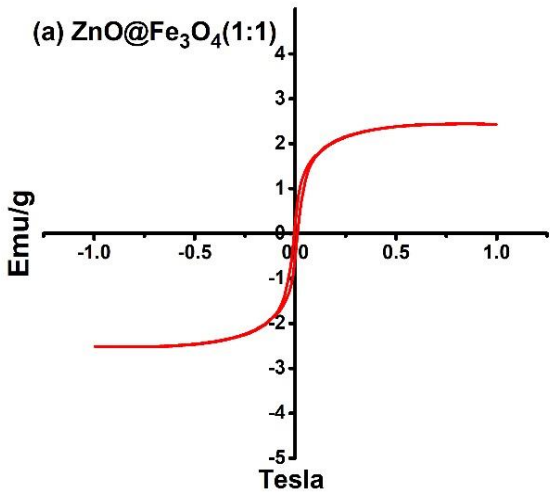

Figure 8. (a) Magnetic hysteresis of ZnO@Fe_3O_4 -1:1 nanostructure

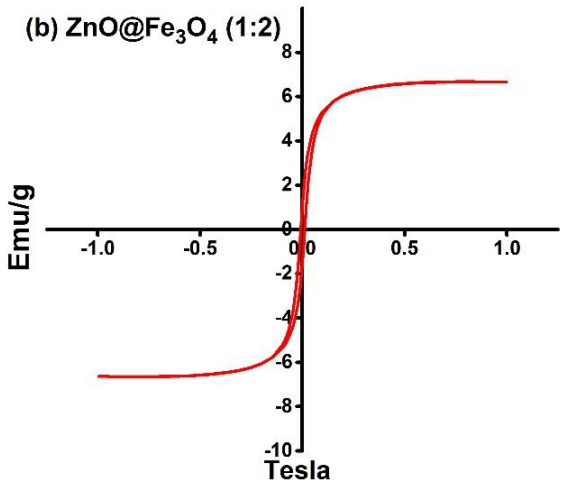

Figure 8. (b) Magnetic hysteresis of ZnO@Fe_3O_4 -1:2 nanostructure

4. CONCLUSIONS

This study investigated the structural, morphological, elemental, optical, and magnetic properties of ZnO@Fe_3O_4 nanostructures synthesized by the hydrothermal method. ZnO@Fe_3O_4 nanostructures were successfully produced by the hydrothermal method. The ZnO and Fe_3O_4 structures were defined in the structural characterization, and no impurity peaks were found. In the morphological images, the presence of composite nanostructures was revealed by both SEM and TEM microscopy. The energy band gaps of the synthesized ZnO@Fe_3O_4 nanostructures were calculated as approximately 2.1 eV. This value is important in terms of being a potential nanomaterial in solar cell, photodetector, photocatalysis, sensor, supercapacitor, and optoelectronic applications, especially with its use in semiconductor technology. In the magnetic susceptibility measurements, the values of 3.76 emu/g and 7.97 emu/g were calculated for ZnO@Fe_3O_4 nanostructures. Although these values show a limited ferromagnetic property, they may contribute to the medical imaging applications of ZnO additive with advanced optical properties.

REFERENCES

[1] Nasrollahzadeh M, Issaabadi Z, Sajjadi M, Sajadi SM, Atarod M. Chapter 2 - Types of Nanostructures. In: Nasrollahzadeh M, Sajadi SM, Sajjadi M, Issaabadi Z, Atarod MBT-IS and T, editors. An Introduction to Green Nanotechnology. Elsevier; 2019. p. 29–80. Available from:https://www.sciencedirect.com/science/article/pii/B978012813586000002X

[2] Pascariu P, Koudoumas E, Dinca V, Rusen L, Suchea MP. Chapter 14 - Applications of metallic nanostructures in biomedical field. In: Dinca V, Suchea MPBT-FNI for E and BA, editors. Micro and Nano Technologies. Elsevier; 2019. p. 341–61. Available from: https://www.sciencedirect.com/science/article/pii/B9780128144015000141

[3] Tripathy N, Kim D-H. Metal oxide modified ZnO nanomaterials for biosensor applications. Nano Converg. 2018;5(1):27. Available from: https://doi.org/10.1186/s40580-018-0159-9

[4] Bahari A, Roeinfard M, Ramzannezhad A. Characteristics of Fe3O4/ZnO nanocomposite as a possible gate dielectric of nanoscale transistors in the field of cyborg. J Mater Sci Mater Electron. 2016;27(9):9363–9. Available from: https://doi.org/10.1007/s10854-016-4978-3

[5] Nurul Ulya H, Taufiq A, Sunaryono. Comparative Structural Properties of Nanosized ZnO/Fe3O4 Composites Prepared by Sonochemical and Sol-Gel Methods. IOP Conf Ser Earth Environ Sci. 2019;276:12059. Available from: http://dx.doi.org/10.1088/1755-1315/276/1/012059

[6] Hong RY, Zhang SZ, Di GQ, Li HZ, Zheng Y, Ding J, et al. Preparation, characterization and application of Fe3O4/ZnO core/shell magnetic nanoparticles. Mater Res Bull. 2008;43(8):2457–68. Available from: https://www.sciencedirect.com/science/article/pii/S0025540807003352

[7] Atla SB, Lin W-R, Chien T-C, Tseng M-J, Shu J-C, Chen C-C, et al. Fabrication of Fe3O4/ZnO magnetite core shell and its application in photocatalysis using sunlight. Mater Chem Phys. 2018;216:380–6. Available from: https://www.sciencedirect.com/science/article/pii/S0254058418305194

[8] Winatapura, D. S., Dewi, S. H., & Adi WA. Synthesis, characterization, and photocatalytic activity of Fe3O4@ZnO nanocomposite. Int J Technol. 2016;7(3):408–16.

[9] Machovsky M, Kuritka I, Kozakova Z. Microwave assisted synthesis of nanostructured Fe3O4/ZnO microparticles. Mater Lett. 2012;86:136–8. Available from: https://www.sciencedirect.com/science/article/pii/S0167577X12010099

[10] Roychowdhury A, Pati SP, Mishra AK, Kumar S, Das D. Magnetically addressable fluorescent Fe3O4/ZnO nanocomposites: Structural, optical and magnetization studies. J Phys Chem Solids. 2013;74(6):811–8. Available from: https://www.sciencedirect.com/science/article/pii/S0022369713000231

[11] Chandekar K V., Shkir M, Khan A, Al-Shehri BM, Hamdy MS, AlFaify S, et al. A facile one-pot flash combustion synthesis of La@ZnO nanoparticles and their characterizations for optoelectronic and photocatalysis applications. J Photochem Photobiol A Chem. 2020;395(3):112465. Available from: https://doi.org/10.1016/j.jphotochem.2020.112465

[12] Senol SD, Ozugurlu E, Arda L. The effect of cobalt and boron on the structural, microstructural, and optoelectronic properties of ZnO nanoparticles. Ceram Int. 2020;46(6):7033–44. Available from: https://doi.org/10.1016/j.ceramint.2019.11.193

[13] Polat S. Production of ZnFe 2 O 4 Doped Carbon Cloth-Based Flexible Composite Electrodes for Supercapacitors. Turk. J. Natur. Sci. 2021;10(2):199–205.

[14] Hasanoğlu Özkan E, Aslan N, Koç MM, Kurnaz Yetim N, Sarı N. Fe3O4 nanoparticle decorated novel magnetic metal oxide microcomposites for the catalytic degradation of 4-nitrophenol for wastewater cleaning applications. J Mater Sci Mater Electron. 2022;33(2):1039–53.

[15] Alula MT, Lemmens P, Madingwane ML. Determination of cysteine via its inhibition of catalytic activity of silver coated ZnO/Fe3O4 composites used for conversion of 4-nitrophenol into 4-aminophenol. Microchem J. 2020;156(2):104976. Available from: https://doi.org/10.1016/j.microc.2020.104976

[16] Kurnaz Yetim N, Kurşun Baysak F, Koç MM, Nartop D. Synthesis and characterization of Au and Bi2O3 decorated Fe3O4@PAMAM dendrimer nanocomposites for medical applications. J Nanostructure Chem. 2021; Available from: https://doi.org/10.1007/s40097-021-00386-w

[17] Kurnaz Yetim N, Aslan N, Koç MM. Structural and catalytic properties of Fe3O4 doped Bi2S3 novel magnetic nanocomposites: p-Nitrophenol case. J Environ Chem Eng. 2020;8(5):104258. Available from:https://www.sciencedirect.com/science/article/pii/S2213343720306072

[18] Karaçam R, Yetim NK, Koç MM. Structural and Magnetic Investigation of Bi2S3@Fe3O4 Nanocomposites for Medical Applications. J Supercond Nov Magn. 2020;33(9):2715–25. Available from: https://doi.org/10.1007/s10948-020-05518-x

[19] Kurnaz Yetim N. Catalytic Properties of Hydrothermally Synthesized Flower-like NiO@Fe3O4. Düzce Univ J Sci Technol. 2020;(8):1964–74.

[20] Bahtiar S, Taufiq A, Utomo J, Hidayat N, Sunaryono. Structural Characterizations of Magnetite/Zinc Oxide Nanocomposites Prepared by Co-precipitation Method. IOP Conf Ser Mater Sci Eng. 2019;515:12076. Available from: http://dx.doi.org/10.1088/1757-899X/515/1/012076

[21] Siregar J, Sebayang K, Yuliarto B, Humaidi S. XRD characterization of Fe3O4-ZnO nanocomposite material by the hydrothermal method. AIP Conf Proc. 2020;2221(3):1–5.

[22] Długosz O, Szostak K, Krupiński M, Banach M. Synthesis of Fe3O4/ZnO nanoparticles and their application for the photodegradation of anionic and cationic dyes. Int J Environ Sci Technol. 2021;18(3):561–74. Available from: https://doi.org/10.1007/s13762-020-02852-4

[23] Goh EG, Xu X, McCormick PG. Effect of particle size on the UV absorbance of zinc oxide nanoparticles. Scr Mater. 2014;78–79:49–52. Available from: https://www.sciencedirect.com/science/article/pii/S1359646214000372

[24] Wang X, Chen X, Gao L, Zheng H, Zhang Z, Qian Y. One-Dimensional Arrays of Co3O4 Nanoparticles: Synthesis, Characterization, and Optical and Electrochemical Properties. J Phys Chem B. 2004 Oct 1;108(42):16401–4. Available from: https://doi.org/10.1021/jp048016p

[25] Bhadwal AS, Tripathi RM, Gupta RK, Kumar N, Singh RP, Shrivastav A. Biogenic synthesis and photocatalytic activity of CdS nanoparticles. RSC Adv. 2014;4(19):9484–90. Available from: http://dx.doi.org/10.1039/C3RA46221H

[26] Yetim NK, Aslan N, Sarıoğlu A, Sarı N, Koç MM. Structural, electrochemical and optical properties of hydrothermally synthesized transition metal oxide (Co3O4, NiO, CuO) nanoflowers. J Mater Sci Mater Electron. 2020;31(15):12238–48. Available from: https://doi.org/10.1007/s10854-020-03769-x

[27] Yetim NK, Kurş F. Magnetic and Structural Characterization of Inorganic/Organic coated. J Mater Electron Devices. 2021;2:12–8.

[28] Hu Y, Chen H-J. Preparation and characterization of nanocrystalline ZnO particles from a hydrothermal process. J Nanoparticle Res. 2008;10(3):401–7. Available from: https://doi.org/10.1007/s11051-007-9264-0

[29] Kulkarni SA, Sawadh PS, Palei PK, Kokate KK. Effect of synthesis route on the structural, optical and magnetic properties of Fe3O4 nanoparticles. Ceram Int. 2014;40(1, Part B):1945–9. Available from:https://www.sciencedirect.com/science/article/pii/S0272884213008973

[30] Sin J-C, Tan S-Q, Quek J-A, Lam S-M, Mohamed AR. Facile fabrication of hierarchical porous ZnO/Fe3O4 composites with enhanced magnetic, photocatalytic and antibacterial properties. Mater Lett. 2018;228:207–11. Available from: https://www.sciencedirect.com/science/article/pii/S0167577X18309340

[31] Koç MM, Aslan N, Kao AP, Barber AH. Evaluation of X-ray tomography contrast agents: A review of production, protocols, and biological applications. Microsc Res Tech. 2019;82(6):812–48.

[32] Aslan N, Ceylan B, Koç MM, Findik F. Metallic nanoparticles as X-Ray computed tomography (CT) contrast agents: A review. J Mol Struct. 2020;1219:128599. Available from: https://www.sciencedirect.com/science/article/pii/S0022286020309248

Araştırma Makalesi https://doi.org/10.46810/tdfd.1013782 Research Article

Türk Doğa ve Fen Dergisi
Turkish Journal of Nature and Science
www.dergipark.gov.tr/tdfd

A Macroanatomic Study on Coronary Arteries and its Branches in Southern Karaman Sheep: Corrosion Casting Technique and Latex Method

Hülya KARA[1*], Zekeriya ÖZÜDOĞRU[2]

[1] Atatürk University, Faculty of Veterinary Medicine, Department of Anatomy, Erzurum, Turkey
[2] Aksaray University, Faculty of Veterinary Medicine, Department of Anatomy, Aksaray, Turkey
Hülya KARA ORCID No: 0000-0002-7678-6471
Zekeriya ÖZÜDOĞRU ORCID No: 0000-0002-0789-3628

**Corresponding author: h.goktas@atauni.edu.tr*

(Received: 23.10.2021, Accepted: 10.02.2022, Online Publication: 25.03.2022)

Keywords
Anatomy, Southern Karaman sheep, Coronary artery, Corrosion casting, Latex

Abstract: This study was carried out to reveal the coronary arteries and their branches that provide vascularization of the heart in Southern Karaman sheep. Eight Southern Karaman sheep were used in the study. The coronary arteries and their branches providing arterial vascularization of the heart were determined using latex injection and corrosion casting technique. Arteria coronaria sinistra and its branches were observed to be more dominant than arteria coronaria dextra. It was determined that after the origin of arteria coronaria sinistra, it splits into two main branches as ramus interventricularis paraconalis and ramus circumflexus sinister. It was determined that arteria coronaria dextra continued on its way as ramus circumflexus dexter after reaching the sulcus coronarius and gave branches to ensure the vascularization of the region tissues. This study aimed to reveal the coronary arteries and their branches in Southern Karaman of Turkey's domestic sheep breeds, and it is thought that it will contribute to new studies on this breed.

Güney Karaman Koyunlarında Koroner Arterler ve Dalları Üzerine Makroanatomik Bir Çalişma: Korozyon Kast Tekniği ve Lateks Yöntemi

Anahtar Kelimeler
Anatomi, Güney Karaman koyunu, Koroner arter, Korozyon kast, Lateks

Öz: Bu çalışma Güney Karaman koyununda kalbin vaskularizasyonunu sağlayan koroner arterler ve dallarının ortaya çıkarılması amacıyla yapıldı. Çalışmada 8 adet Güney Karaman ırkı koyun kullanıldı. Lateks enjeksiyon ve korozyon kast teknikleri kullanılarak kalbin arteriyel vaskularizasyonunu sağlayan koroner arterler ve dalları belirlendi. Arteria coronaria sinistra ve dallarının arteria coronaria dextra'ya göre daha dominant olduğu gözlendi. Arteria coronaria sinistra'nın orijininden sonra ramus interventricularis paraconalis ve ramus circumflexus sinister olarak 2 ana dala ayrıldığı belirlendi. Arteria coronaria dextra'nın ise sulcus coronarius'a vardıktan sonra yoluna ramus circumflexus dexter olarak devam ettiği ve seyri esnasında bölge vaskularizasyonunu sağlamak üzere dallar verdiği tespit edildi. Bu çalışmada Türkiye'nin yerli koyun ırklarından biri olan Güney Karaman koyununda koroner arterler ve dalları ortaya konulmaya çalışılmış olup, çalışmanın bu ırk üzerine yapılacak olan yeni çalışmalara katkı sağlayacağı düşünülmektedir.

1. INTRODUCTION

The Southern Karaman sheep is a separate breed formed as a result of crossbreeding Karagül rams with Akkaraman and Dağlıç sheep brought by the nomads (Türkmen) who migrated from Türkistan to the Mediterranean during the Ottoman period. Southern Karaman Sheep is highly productive in terms of meat and milk and is a frequently preferred breed inbreeding [1,2].

The heart is vascularized by the arteria (a) coronaria dextra and arteria coronaria sinistra, which originate from the sinus aorta portion of the ascending aorta [3-7]. Arteria coronaria sinistra is more dominant in cattle [8], buffalo [9], sheep [10], and dog [11]. Arteria coronaria dextra is more dominant in goats [12], pigs [13], donkeys [14], and 90% of humans [15].

After arteria coronaria sinistra originates from the aorta, it reaches the sulcus coronarius by going downwards and slightly to the left between the truncus pulmonalis and

auricula sinistra [16,17,18]. At the level of this sulcus, it divides into two main branches: ramus circumflexus sinister and ramus interventricularis paraconalis [19,20]. The branches given by ramus interventricularis paraconalis are ramus coni arteriosi, ramus collateralis sinister proximalis, ramus collateralis sinister distalis, and rami septales during its course [21]. Ramus circumflexus sinister gives to feed atrium sinistrum ramus proximalis atrii sinistri, ramus intermedius atrii sinistri and ramus distalis atrii sinistri [7] to feed ventriculus sinister ramus proximalis ventriculi sinistri, ramus marginis ventricularis sinistri and ramus distalis venticuli sinistri [22].

Arteria coronaria dextra originates from the beginning of the aorta at the level of the valvula semilunaris dextra [7]. After reaching the sulcus coronarius, it continues as ramus circumflexus dexter [7,10,11]. During the course of the arteria coronaria dextra, it is also divided into branches as ramus proximalis atrii dextri, ramus intermedius atrii dextri, ramus distalis atrii dextri, ramus coni arteriosi, ramus proximalis ventriculi dextri, ramus marginis ventricularis dextri, and ramus distalis ventriculi [6,7]. This study aimed to reveal the coronary arteries and their branches that provide arterial vascularization of the heart in Southern Karaman of Turkey's domestic sheep breeds.

2. MATERIAL AND METHOD

The present study was admitted by Atatürk University Local Ethics Committee (2021-23). In the study, eight Southern Karaman sheep were obtained from Konya Bahri Dağdaş International Agricultural Institute to be used in the study. The arteria carotis communis in the neck region of the sheep [23] were cut under xylazine HCl (0.2 mg/kg/IV) and ketamine HCl (2.2 mg/kg/IV) anesthetized. Then, their blood was drained, and coronary arteries and their branches were washed with 0.9% physiological saline. Afterward, a latex mixture colored with red acrylic dye was applied to the coronary arteries from the ascending aorta by the latex injection method [24]. They were kept in 10% formaldehyde solution for 72 hours for fixation. The dissected coronary arteries and their branches were named based on Nomina Anatomica Veterinaria [25] and photographed to illustrate vessels.

To create cast models of the coronary arteries, an acrylic solution prepared as 80% liquid (polymethylmetachrylate) and 20% powder (monomethylmetachrylate) was colored with red dye, which was injected from the ascending aorta. The tissues were kept in water overnight and then incubated in a 20% potassium hydroxide solution (KOH) solution at 37ºC for 24 hours. The coronary arteries and their branches, which were cast and dissected, were photographed and named based on Nomina Anatomica Veterineria [25].

3. RESULTS

The ascending aorta started from the ventriculus sinister. According to the study, it gave arteria coronaria dextra and arteria coronaria sinistra from the sinus aorta section to provide arterial vascularization of the heart immediately after its origin. It was observed that both main branches were partially intramyocardial (Figure 1, Figure 2a,c, and Figure 3a,b,c).

Compared to the arteria coronaria dextra, the arteria coronaria sinistra separated from the aorta ascendens in the section that overlaps the valvula semilunaris sinistra as a thicker root in all animals used in the study. The ramus proximalis atrii sinistri of arteria coronaria sinistra fed the atrium sinistrum shortly after its formation from the aorta ascendens. After that, the arteria coronaria sinistra split into two more main branches, the ramus interventricularis paraconalis, and the ramus circumflexus sinister (Figure 1, Figure 2a, and Figure 3a,b,c).

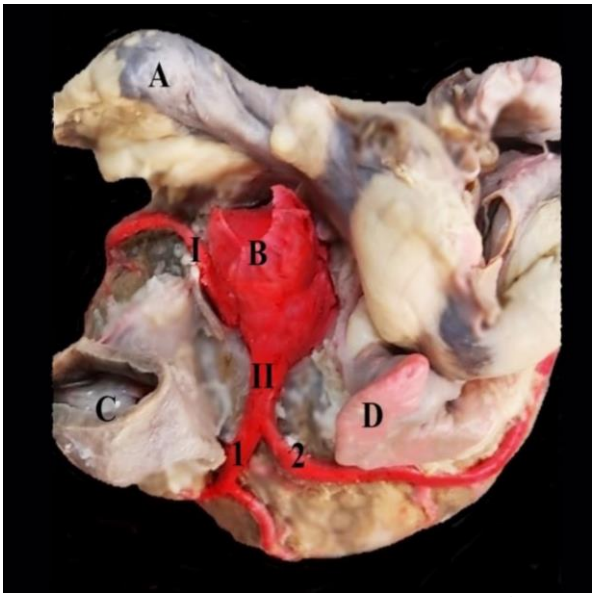

Figure 1. Aorta ascendens and its branches in the heart of the South Karaman sheep, A: auricula dextra, B: aorta ascendens, C: truncus pulmonalis, D: auricula sinistra I: arteria coronaria dextra, II: arteria coronaria sinistra, 1: ramus interventricularis paraconalis, 2: ramus circumflexus sinister.

The ramus interventricularis paraconalis first proceeded subepicardially in the sulcus interventricularis paraconalis, caudoventrally towards the apex cordis, with the vena cordis magna. It was seen that it gave branches to facies atrialis before reaching incisura apicis cordis along its path. Ramus interventricularis paraconalis gives branches towards facies auricularis. These branches are from proximal to distal; proximal branch to ventriculus sinister, ramus collateralis proximalis, distal branch to ventriculus sinister and ramus collateralis distalis. After feeding the ventriculus sinister, the ramus collateralis proximalis spread to the proximal 1/3 of the ventriculus sinister. The ramus collateralis distalis was found to be dispersed, supplying the ventriculus sinister's middle and distal 1/3. Ramus septalis, the branch it gave to feed ramus coni arteriosi, and ventriculus dexter, the branch it gave to feed the

conus arteriosus region, were the branches that ramus interventricularis paraconalis gave respectively from proximal to distal from proximal to facies atrialis after its origin. In addition to these, it was determined that ramus interventricularis paraconalis gave many rami septales branches to feed the septum interventriculare during its course (Figure 2a and Figure 3a).

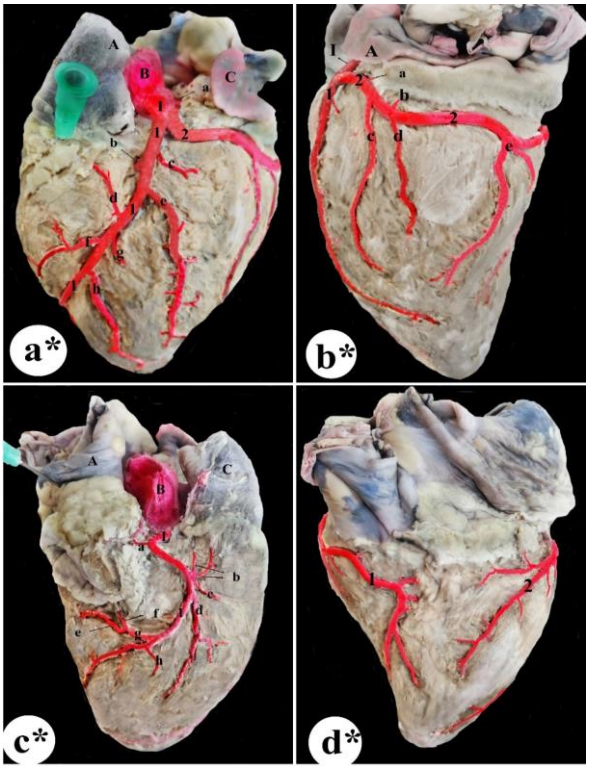

Figure 2. Branches of arteria coronaria sinistra and arteria coronaria dextra in the heart of South Karaman sheep with the latex method, a*: ramus interventricularis paraconalis and its branches; A: truncus pulmonalis, B: aorta ascendens C: auricula sinistra I: arteria coronaria sinistra, a: ramus proximalis atrii sinistri, b: ramus septalis, c: proximal branch of ramus interventricularis paraconalis for ventriculus sinister, d: ramus coni arterio , e: ramus collateralis proximalis, f: branch of ramus interventricularis paraconalis to ventriculus dexter, g: distal branch of ramus interventricularis paraconalis to ventriculus sinister h: ramus collateralis distalis, 1: ramus interventricularis paraconalis, 2: ramus circumflexus. b* ramus circumflexus sinister and its branches; A: auricula sinistra, I: arteria coronaria sinistra. a: ramus intermedius atrii sinistri, b: ramus distalis atrii sinistri, c: ramus proximalis ventriculi sinistri d: ramus marginis ventricularis sinistri,, e: ramus distalis ventriculi sinistri, 1: ramus interventricularis paraconalis, 2: ramus circumflexus sinister. c*: arteria coronaria dextra and its branches; A: auricula dextra, B: aorta ascendens, C: truncus pulmonalis, I: arteria coronaria dextra, a: ramus proximalis atrii dextri, b: ramus coni arteriosi, c: ramus proximalis ventriculi dextri, d: ramus marginis ventricularis dextri, e: ramus distalis atrii dextri, f: ramus intermedius atrii dextri, g: ramus intermedius atrii dextri ve ramus distalis atrii dextri'nin ortak kökü, h: ramus proximalis ventriculi dextri. d*: ramus interventricularis subsinuosus and ramus circumflexus dexter; 1: ramus interventricularis subsinuosus, 2: ramus circumflexus dexter.

Arteria circumflexus sinister, the other of the two main branches of the arteria coronaria sinistra, proceeded laterally on the heart's facies auricularis within the sulcus coronarius. It was observed that it provided ramus intermedius atrii sinistri to vascularize the atrium sinistrum along its dorsal surface during its course. It was discovered that it gave rise to the ramus proximalis ventriculi sinistri, a thicker branch that feeds the ventriculus sinister from the caudoventral direction. After continuing its course for a while, it was determined that one of them originated from its dorsal side and gave ramus distalis atrium sinistri to feed the atrium sinistrum. The other one, which was thicker and separated from the ventral face, proceeded in the caudoventral direction and gave ramus marginis ventricularis sinistri to feed the ventriculus sinistri. The ramus marginis ventricularis sinistri originated shortly after the margo ventricularis and spread to the proximal 1/3 of the ventriculus sinister, according to research. The ramus circumflexus sinister was observed to continue its route for a bit of time before splitting into two more branches that came from a single root on its ventral surface and proceeded in a caudoventral direction. These branches, which gradually spread up to the distal 1/3 of the ventriculus sinister, were found to be ramus distalis ventriculi sinistri. After giving all these branches, ramus circumflexus sinister tended towards caudoventrally and continued on its way as ramus interventricularis subsinuosus in sulcus interventricularis subsinuosus. In the meantime, it was observed that it gave thin side branches to feed the tissues of the region (Figure 2b,d and Figure 3b,d).

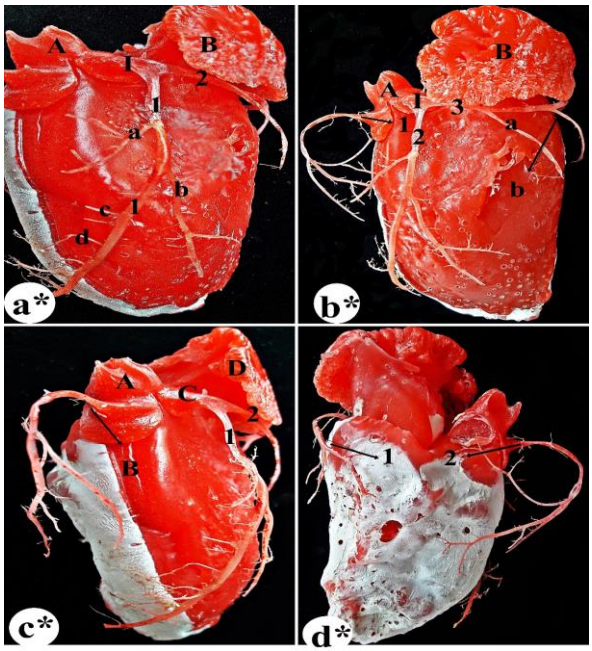

Figure 3. Branches of arteria coronaria sinistra and arteria coronaria dextra in the heart of South Karaman sheep with Corrosion Casting Technique, a*: ramus interventricularis paraconalis and its branches; A: aorta ascendens, B: auricula sinistra, I: arteria coronaria sinistra, a: ramus septalis, b: ramus collateralis proximalis, c: ramus coni arteriosi, d: branch of ramus interventricularis paraconalis to ventriculus dexter, 1: ramus interventricularis paraconalis, 2: ramus circumflexus sinister. b* ramus circumflexus sinister and its branches; A: aorta ascendens, B: auricula sinistra, I:arteria coronaria sinistra., a: ramus proximalis ventriculi sinistri, b: ramus marginis ventricularis sinistri, 1: arteria coronaria dextra, 2: ramus interventricularis paraconalis, 3: ramus circumflexus sinister. c*: arteria coronaria dextra and arteria coronaria sinistra; A: aorta ascendens, B: arteria coronaria dextra, C:arteria coronaria sinistra D: auricula sinistra 1: ramus interventricularis paraconalis, 2: ramus circumflexus sinister. d*: ramus interventricularis subsinuosus and ramus circumflexus dexter; 1: ramus interventricularis subsinuosus, 2: ramus circumflexus dexter.Şekil, grafik, resim açıklamasında numaradan sonra nokta kullanılmalı ve bu noktaya kadar olan kısım (nokta dâhil) koyu yazılmalıdır. Açıklama kısımlarında metin Times New Roman, 8 punto, sola hizalı olarak yazılmalı ve görsel ile açıklama satırı arasında boşluk olmamalıdır. Görsel ile önceki paragraf arasında bir satır boşluk olmalıdır.

It was found that arteria coronaria dextra moved between the truncus pulmonalis and the auricula dextra, originating from the aorta ascendens at the level of the valvula semilunaris dextra. It was discovered that it inclined towards the facies atrialis and passed through the sulcus coronarius, under the subepicardial adipose tissue. It continued as ramus circumflexus dexter after reaching the sulcus coronarius. The ramus proximalis atri dextri was discovered to be the thin branch that arteria coronaria dextra gave towards the dorsocranial to feed the atrium dextrum. It continued over the ventral aspect of the arteria coronaria dextra. It continued towards the facies auricularis, showing ramus coni arteriosus, which is responsible for the arterial vascularization of the conus arteriosus region and separated with ramus proximalis ventriculi dextri in two branches in five of the materials used in the study. Three branches are separated from a single root as two branches. The ventriculus dexter was fed over the caudoventral side of the arteria coronaria dextra after the ramus proximalis ventriculi dextri was separated. This branch proceeded intramyocardially in the middle levels of the ventriculus dexter, parallel to the sulcus interventricularis paraconalis. The ramus marginis ventricularis dextri was found as the branch that separated from the caudoventral of the arteria coronaria dextra and proceeded parallel to the sulcus interventricularis subsinosus to feed the ventriculus dexter. This branch proceeded across the middle 1/3 of the ventriculus dexter and had branching along the way. Ramus intermedius atrii dextri and ramus distalis atrii dextri were discovered at the level of margo ventricularis dexter to be branches that ramus circumflexus dexter gave towards dorsocranial to feed the atrium dextrum. From a common root, these two branches were split off. It was found that ramus distalis ventriculi dextri, which proceeds towards caudoventral on the ventral surface of ramus circumflexus dexter, is involved in the arterial vascularization of ventriculus dexter. Various numbers of thin lateral branches were separated from this branch in order to ensure the vascularization of the region during its course (Figure 2c,d and Figure 3c,d).

4. DISCUSSION

The study was similar to the literature findings [6,7,10,17,26]. As a result, it was discovered that arteria coronaria dextra et sinistra originating from the aorta ascendens provides arterial vascularization of the heart in Southern Karaman sheep. Unlike our findings, Aksoy et al. [27] found that a separate third coronary artery accompanied the arterial vascularization of the heart.

In contrast to research on buffalo, donkey, Malakan horse, and goat [9,14,28,29], arteria coronaria sinistra had a thicker layer than arteria coronaria dextra in our study. Similar to us in the most investigations in goat [30], Roe deer [19], and sheep [6,7], arteria coronaria sinistra was found to be thicker than arteria coronaria dextra. In the literature, it was observed that nine out of ten Awassi sheep [27], Hasak sheep [7], nine out of 14 Kıvırcık sheep [10], five out of ten Hemşin and Tuj sheep each [6], ramus proximalis atrii sinistri was separated from arteria coronaria sinistra. In this study, the literature findings of arteria coronaria sinistra [7,8,9,14,20,26,31,32] were similarly divided into ramus interventricularis paraconalis and ramus circumflexus sinister. Monfared et al. [18], on the other hand, found that, unlike our study findings, arteria coronaria sinistra was divided into three branches in 18.5% of cats.

Unlike our study findings, Doğruer and Özmen [10] reported that ramus interventricularis paraconalis terminated in 10 of the materials in Kıvırcık sheep, and Gürbüz and Aksoy [6] reported that it was terminated in facies auricularis in 6 of 10 Tuj and 7 of 10 Hemşin sheep. Similar to the literature [7,8], it was observed in the study that ramus interventricularis paraconalis ends by turning to facies atrialis before reaching incisura apicis cordis. Teke et al. [7] reported that, in accordance with our study findings, ramus collateralis sinister proximalis originates from the caudoventral of ramus interventricularis paraconalis and distributes to the upper 1/3 of the ventriculus sinister, while ramus collateralis sinister distalis originates from ramus interventricularis paraconalis in the caudoventral direction and it provides nutrition to the middle and distal 1/3 of the ventriculus sinister by taking it. Unlike the Hasak sheep [7], it was seen that a distal branch was separated from the ramus interventricularis paraconalis in the caudolateral direction to the ventriculus sinister after giving the ramus collateralis proximalis branch in the study. Despite the conclusions of the study, Aksoy ve Karadağ [17], Christensen and Campeti [31], and Gürbüz and Aksoy [6] revealed that in 5 Tuj and 4 Hemşin sheep, the ramus septalis was separated from the arteria coronaria sinistra. In contrast to the literature [7], the ramus coni arteriosi was identified as the second branch of the ramus interventricularis paraconalis, giving way to the facies atrialis after the ramus septalis.

In contrast to our findings, Gürbüz and Aksoy [6] found that ramus intermedius atrii sinistri was lacking in one of the materials and two of the Hemşin sheep in his study on Tuj sheep, and that ramus distalis atrii sinistri was responsible for vascularization of the region. Parallel to our study findings, in the literature [8,17], it was found that ramus proximalis ventriculi sinistri originates from the ventral aspect of the ramus circumflexus sinister. In addition, contrary to our findings, this artery sometimes originates from the angle between the ramus interventricularis paraconalis and the ramus circumflexus sinister in Kıvırcık sheep [10], in Tuj sheep [6] and Hemşin sheep [6]. According to Aksoy et al. [33], r. proximalis vetriculi sinistri was not found in two of five fox hearts. According to Doğruer and Özmen [10], the ramus marginis ventriculi sinistri is the second branch that separates from the ramus circumflexus sinister in the caudoventral direction, originates alone in 14 sheep, which is similar to our findings. Together with ramus distalis ventriculi sinistri in six sheep, which is contrary to our results. In addition to this, Gürbüz and Aksoy [6] stated that this artery started with ramus proximalis ventriculi sinistri in four Tuj and three Hemşin sheep, ramus distalis ventriculi sinistri in one Tuj and three Hemşin sheep, and in other materials the artery started from ramus circumflexus sinister as a

single root. Unlike the findings of the study on Hasak sheep [7], it was observed that ramus distalis ventriculi sinistri started in two branches. Similar to the study findings, it has been reported that ramus circumflexus sinister continues on its way as ramus interventricularis subsinuosus in sulcus interventricularis subsinuosus in cattle [8], sheep [10] and Hasak sheep after giving all these branches.

As reported in studies on alpaca [26], Hasak sheep [7] and Tuj and Hemşin breed sheep [6], arteria coronaria dextra originates from the aorta ascendens and proceeded between the truncus pulmonalis and auricula dextra, after reaching the sulcus coronarius, it continued on its way as ramus circumflexus dexter. Unlike our study findings, it has been reported in the literature [14,17] that arteria coronaria dextra is more dominant. Similar to the findings of the study [6,7,8], it has been reported in the literature that ramus proximalis atrii dextri, ramus coni arteriosi, ramus proximalis ventriculi dextri, ramus marginis ventricularis dextri orginated from arteria coronaria dextra. Unlike the findings in the literature [6-8], Özüdoğru [7] and our study revealed that ramus intermedius atrii dextri originated from ramus circumflexus dexter instead of arteria coronaria dextra. Contrary to the study findings, ramus coni arteriosi originates from the aorta ascendens in Kıvırcık sheep [10] and dog [34], and in Zavot cattle [35] and Malakan horse [28], it has been reported to originate as a single branch from arteria coronaria dextra. In 5 of the materials studied, ramus coni arterosi, ramus proximalis ventriculi dextri, and ramus proximalis ventriculi dextri came from a common root, similar to what was found in 3 Hasak sheep [7], 6 Hemşin sheep, and 4 Tuj sheep [6]. In Hasak breed sheep [7], Zavot breed cattle [35], and Malakan horses [28], it has been discovered that it originates in two branches from a single root separate from arteria coronaria dextra.

5. CONCLUSION

In the study, arterial vascularization of the heart was also provided by arteria coronaria dextra et sinistra and its branches in South Karaman sheep, but unlike arteria coronaria dextra et sinistra and its branches reported in the literature, in South Karaman sheep, it has been revealed that;

-Arteria coronaria sinistra is more dominant than arteria coronaria dextra,

-Ramus coni arteriosi is the second branch that separates from ramus interventricularis paraconalis,

-Ramus distalis ventriculi sinistri originates from ramus circumflexus sinister in two branches,

-Ramus intermedius atrii dextri originates from ramus circumflexus dexter.

REFERENCES

[1] Ertuğrul M, Dellal G, Soysal İ, Elmacı C, Akın O, Arat S, et al. Türkiye yerli koyun ırklarının korunması, Bursa Uludag Üniv. Ziraat Fak. Derg. 2009;23(2):97-119.

[2] Kaymakçı M, Taşkın T. Türkiye koyunculuğunda melezleme çalışmaları. Hayvansal Üretim. 2008;49(2):43-51.

[3] Vladova D. Ventricular coronary pattern in the cat, Trakia J Sci. 2005;3(2):44-49.

[4] Bhimalli S, Dixit D, Siddibhavi M, Shirol VS. A studuy of variations in coronary arterial system in cadaveric human heart, World j sci technol. 2011;1(5):30-35.

[5] Yoldaş A, Gezici M. Devekuşunun (Struthio camelus) koroner arterleri üzerinde makroanatomik bir araştırma, Adana Veteriner Kontrol ve Araştırma Enstitüsü Müdürlüğü Dergisi. 2011;1:1-7.

[6] Gürbüz İ, Aksoy G. Macroanatomical investigation of arteria coronaria and myocardial bridges in Tuj and Hemshin sheep, Indian J Anim Res. 2019;54(8):962-967.

[7] Teke BE, Özüdoğru Ö, Özdemir D, Balkaya H. Hasak Koyunlarında kalp kas köprüleri ve koroner arterler, Bahri Dağdaş Hayvancılık Araştırma Dergisi. 2017;6 (1):1-12.

[8] Karadağ H, Soygüder Z. Doğu Anadolu Kırmızısı sığırında kalp ve kalp arteria'ları üzerinde anatomik bir araştırma, Ankara Univ Vet Fak Derg. 1989;36(2):482-495.

[9] Gupta A, Bansal N. Braching pattern of coronary arteries in prenatal heart of buffalo (Bubalus bubalis), Indian Journal of Veterinary Anatomy. 2012;24(1):41-42.

[10] Doğruer A ve Özmen E: Kıvırcık koyunlarında koroner arterler üzerine makroanatomik bir çalışma, Atatürk Üniversitesi Vet Bil Derg. 2012;7(1):35-45,.

[11] Oliveira CL, Dornelas D, Carvalho MO, Wafae GC, David GS, et al. Anatomical study on coronary arteries in dogs, Eur J of Anat. 14 (1), 2010;1-4.

[12] Pinto Neto JL, Leão CES, Vieira THM, Lopes AKMS, Vieira, SRC, et al. Anatomical indicators of dominance among the coronary arteries in goats, Braz J Vet Res Anim Sci. 2009;46:48–53.

[13] Vieira THM, Moura PCJr, Vieira SRC, Moura PR, Silva NC, et al. Anatomical indicators of dominance between the coronary arteries in swine, Morphologie. 2008;92:3–6.

[14] Özgel Ö, Çengelci Halıgür A, Dursun N, Karakum E: Macroanatomy of coronary arteries in donkeys (Equus asinus L.), Anat Histol Embryol. 2004;33(5):278-283.

[15] Gebhard C, Fuchs TA, Stehli J, Gransar H, Berman DS, et al. Coronary dominance and prognosis in patients undergoing coronary computed tomographic angiography: Results from the confirm (coronary ct angiography evaluation for clinical outcomes: An international multicenter) registry, Eur Heart J Cardiovasc Imaging. 2015;16:853–862.

[16] Karami H, Tooloei M, Hasanzadeh B, Hasan M, Khani M. Architecture of Buffalo's (Bubalus bubalis) coronary arteries. J Anim Vet Adv. 2008;7(12):1635-1639.
[17] Aksoy G, Karadağ H. Evcil kedi ve Beyaz Yeni Zelanda tavşanlarında kalp ve kalp arteria'ları üzerinde anatomik bir araştırma, Veteriner Bilimleri Dergisi. 2002;18:33-40.
[18] Monfared AL, Moosavi S, Bazdar A. The macroanatomy of coronary arteries in the Irinian native cats, Global Veterinaria. 2013;10(4):413-416.
[19] Frackowiak H, Jasiczak K, Pluta K. Coronary arteries of the Roe Deer (Capreolus capreolus, Linnaeus 1758), Pol J Vet Sci. 2007;10(2):105-108.
[20] Gómez FA, Ballesteros LE, Estupiñan HY. Morphological characterization of the left coronary artery in horses. Comparative analysis with humans, pigs, and other animal species, Ital J of Anat Embryol. 2017;122:137-146.
[21] Dursun N, Türkmenoğlu İ. Kangal köpeklerinde septum interventriculare'nin arterial vascularizasyonu, Veteriner Bilimleri Dergisi. 1996;141-144.
[22] Bull ML, Martins MRFB. Study of the arterial coronary circulation in the dog (Canis familiaris), Revista Chilena de Anatomia. 2002;20:117–123.
[23] Özüdoğru Z, Aksoy G. Tuj koyununun ön bacak venaları üzerine makroanatomik bir çalışma, Kafkas Univ Vet Fak Derg. 2009;15(5):771-778.
[24] Aycan K, Bilge A. Investigation of vascular system anatomy by plastic injection and corrosion method, Erciyes Medical Journal. 1984;545-552.
[25] NAV, Nomina Anatomica Veterinaria. "The International Committee on Veterinary Gross Anatomical Nomenclature." Published by the Editorial Committee Hannover (Germany), Columbia, MO (USA), Ghent (Belgium), Sapporo (Japan), 6th edition (Revised version) 2017.
[26] Pérez W, Méndez V, Vazquez N, Navarrete M, König HE. Gross anatomy of the heart of the alpaca (Vicugna pacos, Linnaeus 1758). Anat Histol Embryol, 2017;47(2):110-118.
[27] Aksoy G, Özüdoğru Z, Özdemir D. A macroanatomic investigation of the coronary arteries and myocardial bridges in Awassi sheep, Eurasian J Vet Sci. 2018;34 (3):171-177.
[28] Gürbüz İ, Demiraslan Y, Aslan K. A macroanatomic investigation on the arterial vascularization of the Malakan Horses's heart, Atatürk University J Vet Sci. 2016;11(3):288-295.
[29] Barszcz K, Jordanow OS, Czopowicz M, Mickiewicz M, Moroz A, et al. Topography of coronary arteries and their ramifications in the goat, Biologia. 2019;74(6): 683-689.
[30] Yang KQ, Zhang GP, Chen HQ, Zhang LR, Xue ZN. Observation and measurement of the coronry arteries of goat, Hua Xi Yi, Ke DA Xue Xue Bao. 1989;20(2):175-177.
[31] Christensen GC, Campeti FL. Anatomic and functional studies of the coronary circulation in the dog and pig, Am J Vet Res. 1959;20:18-26.
[32] Akbulut Y, Kırbaş Doğan G, Takcı İ, Dalga S, Erkılıç E.E, Uzlu E. Venous drainage of the heart of the red fox (Vulpes vulpes), Folia Morphologica. 2021. Doi: 10.5603/FM.a2021.0035.
[33] Aksoy G, Özüdoğru Z, Gürbüz İ. Tilkide koroner arterlerin makroanatomik özellikleri. VII. Ulusal Veteriner Anatomi Kongresi, Selçuk Üniversitesi, Side/Antalya, 2011;69-70.
[34] Türkmenoğlu İ. Köpekte r. coni arteriosi'nin farklı orijin olgusu, Veteriner Bilimler Dergisi. 1996;12(2):121-123.
[35] Akbulut Y, Demiraslan Y, Aslan K, Gürbüz İ, Koral Taşçı S. Zavot ırkı sığırlarda arterler ve kalp kası köprüleri, Kafkas Univ Vet Fak Derg. 2014;20(2):287-293.

Cilt 11, Sayı 1, Sayfa 108-115, 2022 Volume 11, Issue 1, Page 108-115, 2022

Araştırma Makalesi https://doi.org/10.46810/tdfd.1026437 Research Article

Türk Doğa ve Fen Dergisi
Turkish Journal of Nature and Science
www.dergipark.gov.tr/tdfd

Power Generation Variation Analysis of Solar Panels Coated With TiO_2

Dursun ÖZTÜRK[1*], Aydın DENER[2]

[1] Bingöl University, Faculty of Engineering and Architecture, Department of Electrical-Electronics Engineering, Bingöl, Turkey
[2] Bingöl Vocational and Technical Anatolian High School, Bingöl, Turkey
Dursun ÖZTÜRK ORCID No: 0000-0002- 0335-8118
Aydın DENER ORCID No: 0000-0001- 8124-9411

**Corresponding author: dozturk@bingol.edu.tr*

(Received: 20.11.2021, Accepted: 20.12.2021, Online Publication: 25.03.2022)

Anahtar Kelimeler
Renewable energy, Solar panels, Pollution, Photocatalytic materials, Titanium dioxide

Abstract: Solar energy, which is an inexhaustible, clean and easily accessible energy source, can be converted into electrical energy with the help of photovoltaic (PV) panels. Environmental factors such as dust and dirt cause pollution of PV panels and decrease the efficiency of energy conversion. One of the methods used to reduce the negative effect of dirt on panel efficiency is to coat the surface of the panels with photocatalytic materials. Oxygen and nanoparticles are formed on photocatalytic surfaces with the help of ultraviolet rays in sunlight. These particles form a chemical reaction between the coating and the surface, breaking down and destroying the dirt on the surface. In this study, the effect of titanium dioxide (TiO_2) as a photocatalytic material on the efficiency of solar panels was investigated. Experimental studies were carried out in Bingöl city using two 285 W polycrystalline solar panels. One of the panel surfaces is coated with TiO_2 and no treatment has been applied to the surface of the other panel. When the measured data were analyzed, it was seen that while the powers of the two panels were almost the same at the beginning, with the contamination of the panels, the power obtained from the TiO_2 coated panel was up to 19% higher. In addition, it was observed that the excess power produced as a result of cleaning the PV panels after rainy days decreased again.

TiO_2 ile Kaplanan Güneş Panellerinin Güç Üretim Değişimi Analizi

Keywords
Yenilenebilir enerji, Güneş panelleri, Kirlenme, Fotokatalitik malzemeler, Titanyum dioksit

Öz: Tükenmeyen, temiz ve kolay erişilebilen bir enerji kaynağı olan güneş enerjisi fotovoltaik (PV) paneller yardımıyla elektrik enerjisine dönüştürülebilmektedir. Toz ve kir gibi çevresel faktörler PV panellerin kirlenmesine ve enerji dönüşüm verimlerinin düşmesine neden olmaktadır. Kirin panel verimi üzerindeki olumsuz etkisini azaltmak için kullanılan yöntemlerden biri panellerin yüzeyini fotokatalitik malzemelerle kaplamaktır. Fotokatalitik yüzeylerde güneş ışığındaki ultraviyole ışınları yardımıyla oksijen ve nano partiküller oluşur. Bu partiküller, kaplama ile yüzey arasında kimyasal bir reaksiyon oluşturarak yüzeydeki kirleri parçalar ve yok eder. Bu çalışmada, fotokatalitik malzeme olarak titanyum dioksitin (TiO_2) güneş panellerinin verimi üzerine etkisi incelenmiştir. Deneysel çalışmalar Bingöl İlinde iki adet 285 W polikristal güneş paneli kullanılarak yapılmıştır. Panel yüzeylerinden biri TiO_2 ile kaplanmış ve diğer panelin yüzeyine herhangi bir işlem uygulanmamıştır. Ölçülen veriler incelediğinde, başlangıçta iki panelin güçleri hemen hemen aynıyken panellerin kirlenmesiyle birlikte TiO_2 kaplanmış panelden elde edilen gücün %19 a kadar daha fazla olduğu görülmüştür. Ayrıca yağmurlu günlerden sonra PV panellerin temizlenmesi sonucunda üretilen fazla gücün tekrar azaldığı görülmüştür.

1. INTRODUCTION

Population growth, industrialization, and the increase in electric powered devices raise the energy demand of countries. As a result of the use of fossil fuels, carbon dioxide is released into the atmosphere. The increasing amount of carbon dioxide causes the greenhouse effect in the atmosphere and thus the average temperature of the world rises. An increase of 1 °C in temperature may lead to visible changes in the world's climate zones. Increases up to 3 °C may cause melting of polar ice caps,

rising of seas, drying up of lakes and agricultural drought [1,2]. In addition, many negative factors such as limited fossil energy resources, sudden price changes, foreign dependency in energy causing various political and economic problems make it necessary to turn to renewable energy resources. When the data of the rates of electricity generation from renewable energy sources of the Organization for Economic Cooperation and Development (OECD) countries between 1991 and 2017 are examined, it is observed that there is a continuous increase [3]. In Turkey, the amount of energy production from renewable energy sources has increased every year and today, half of the total installed power is renewable energy sources. As of the end of September 2019, the distribution of installed power by resources; 31.4 percent hydraulic energy, 28.6 percent natural gas, 22.4 percent coal, 8.1 percent wind, 6.2 percent solar, 1.6 percent geothermal and 1.7 percent is other sources [4].

In order to meet the increasing energy demand, the use of solar energy, which is eternal and clean energy, is becoming widespread. Compared to the damage done to the environment while producing electricity from fossil fuels, the production of electricity from solar energy with photovoltaic panels is an extremely clean and environmentally friendly method.

The panels absorb the sunlight falling on them and generate direct current depending on the efficiency of the cells. There are solar cells on solar panels proportional to the power of the panel. Panel efficiency is the ratio of the amount of electrical energy produced to the solar energy coming to the panel surface. There are many factors that affect the efficiency of the panel. Cell type, quality and design, and the quality of glass and other components affect the efficiency of the panel. In addition, factors such as temperature, amount of radiation, shading, angle of incidence of light also determine the amount of power to be produced in the panel.

The installation cost of photovoltaic systems is higher than other electricity generation systems. With the long-term use of the system, this cost can be compensated by spreading over the years. In addition, high efficiency of the system is also important for tolerating the cost.

Due to being outdoors, the surface of the panels is contaminated with particles such as dust, chemical dirt, leaves and bird droppings over time. Due to these dirt accumulated on the panel surface, less sunlight falls on the solar cells inside the panels. Depending on the decrease in the amount of light falling on the cells, the electrical energy produced by the panels also decreases [5]. There have been many studies examining the effect of dirt on panel efficiency [6-9].

The surfaces of the panels in the regions with low rainfall are dustier. Where there is excessive dust, a yield loss of 14% occurs. If the angle of the panels with the horizontal axis is greater than 16 degrees, it can be assumed that the panel surface has been cleaned with rain water. Contamination under these conditions is assumed to cause a yield loss of 6%. However, if the angle of inclination is less than 16 degrees or if there is little rainfall in the region, and if more dirt accumulates on the panel surfaces due to dusting caused by agricultural and industrial activities in the region, this rate is greater than 6%. In a PV system whose surface is cleaned periodically, dust losses are around 5% [10,11].

In this study, the change of panel efficiency in the case of application of photocatalytic materials to solar panels under the conditions of climate, air pollution level, etc. of Bingöl has been revealed. There is no such study in the literature for this region before. In addition, the data obtained sets a precedent for other settlements with similar conditions.

2. MATERIALS AND METHOD

Wind is one of the factors affecting panel efficiency. Wind speed and intensity change the power produced by the panel. The temperature of the panel cells is taken into account in examining the efficiency of solar panels. The formula used for the relationship between temperature and wind is given in Eq.-1 [12].

$$T_c=T_a+\omega\times\left(\frac{0,32}{8,91+2\times V_f}\right)\times I_T \quad (1)$$

Here, T_c is the panel cell temperature, T_a is the atmosphere temperature, ω is the assembly coefficient, V_f is the wind speed, and I_T is the instantaneous radiation.

Another factor affecting panel efficiency is temperature. As the temperature increases, the output voltage of the panel decreases and the current increases a little. The output power of PV panels varies directly with the amount of radiation and inversely with the panel temperature. In other words, if the panel temperature increases, the panel power decreases. Many studies [13-17] and postgraduate theses [18-20] have been carried out both to examine the negative effects of temperature on panel efficiency and to eliminate these negative effects. The variation of panel power depending on temperature is given in Eq.-2 and Eq.-3 [21].

$$T_C=T_{ORT}+0,0256\times G \quad (2)$$

$$P_{PV\text{-}OUT}=P_{N\text{-}PV}\times\left(\frac{G}{G_{REF}}\right)\times[1+K_T(T_C-T_{REF})] \quad (3)$$

Here; $P_{PV\text{-}OUT}$ PV cell output power (W), $P_{N\text{-}PV}$ nominal power (W) of PV cell under reference conditions, G solar radiation (W/m2), G_{REF} solar radiation (G_{REF}=1000 W/m^2) under reference conditions, K_T maximum power temperature coefficient (K_T=-3.7x10-3(1/^{o}C) for mono and poly-crystalline Si), T_C PV cell temperature (^{o}C), T_{ORT} ambient temperature (^{o}C), T_{REF} PV cell temperature under reference conditions (T_{REF}=25 ^{o}C)) represents.

Equation-2 and Equation-3 show that temperature has a direct effect on panel power. If calculations are made using these equations, it will be seen that the panel output power will be 221.695 W at 30 ^{o}C ambient

temperature and 226.32 W at 25 ºC ambient temperature. This difference for each panel will reach a significant value in large power solar power plants.

2.1. Photocatalysis Phenomenon and Photocatalytic Materials

Photocatalysis and photosynthesis can be compared to each other. By absorbing the sun's rays falling on chlorophyll in plants, it converts water and CO_2 into oxygen and glucose. Similarly, the photocatalyst absorbs the sun's rays by forming radicals (oxide, peroxide and hydroxyl radicals), which are strongly oxidizing species on its surface, and allows the formation of harmless species such as water and CO_2 by breaking down harmful organic molecules. Photocatalysis and photosynthesis events, which are compared in this way, are simply shown in Figure 1 [22].

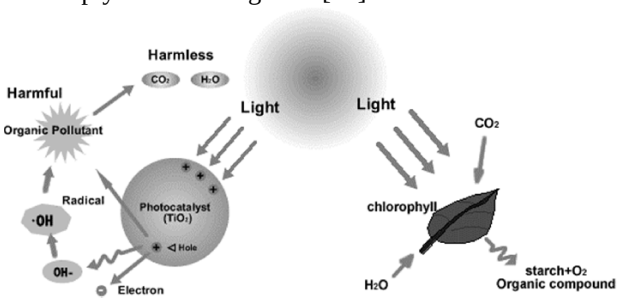

Figure 1. Photocatalysis process as compared to photosynthesis [23]

Recently, panels are coated with nano coating method. With this method, the panel surface is covered with a layer containing particles such as nano-sized titanium dioxide (TiO_2), silicon dioxide (SiO_2), etc. Thus, many different superior properties such as self-cleaning, easy-to-clean, antimicrobial, non-abrasive, scratch-proof and corrosion-proof are given to the material [24,25].

Coating methods are implemented by dipping, spinning, spray, plasma and chemical vapor precipitation methods [24]. Surfaces coated with these methods are called hydrophobic (water-repelling), hydrophilic (water-attracting) or photocatalytic surfaces. The water droplet falling on the surface does not spread on hydrophobic surfaces, but takes the shape of a sphere, while it spreads on hydrophilic surfaces.

TiO_2 is a semiconductor material and has three crystal structures: brookite, anatase and rutile. In photocatalytic applications, TiO_2 in the anatase crystal structure is mostly used.

Thin films containing TiO_2 have many advanced features such as self-cleaning at nanoscale, enabling the creation of antibacterial surfaces, preventing odors, non-fogging, etc., due to their photocatalytic properties and very good hydrophilic surface. Thanks to these superior properties, the use of TiO_2 films has become quite common recently. On the surfaces on which these films are coated, organic dirt adhered to the surface is broken down with the help of UV light, and thanks to the hydrophilic feature, water molecules flow on the surface in the form of a thin film and the fragmented dirt is easily removed from the surface. This allows the surface to be self-cleaning.

2.2. Experimental Study

In experimental system, two polycrystalline solar panels of the same power (285 W) were placed in the construction at the same angle and an experimental application was made in the Central District of Bingöl (Latitude: 38,8851578 Longitude: 40,5072665 Altitude: 1.126 m). Photocatalytic surface consisting of titanium dioxide (TiO_2) material is coated on one of the panels. No treatment has been applied to the surface of the other panel. As of 19.09.2021, the short circuit current and open circuit voltages of the panels were measured at approximately the same time every day, and the measurement results were recorded (Figure 2 and Figure 3). With the help of these measurements, the power produced by the solar panel covered with self-cleaning material (TiO_2) and the power produced by the normal panel were compared.

Figure 2. Experimental system

Figure 3. Measurement of short circuit current and open circuit voltage

The short-circuit current and open-circuit voltages of the panels were measured with a measuring instrument every day and the measurement results were recorded (Annex: 1).

When the first measured data on 19.09.2021 are analyzed, it is seen that the power difference between the two panels is 6.64 watts and the percentage difference is 2.26%. However, in the measurements made on 22.09.2021, it is seen that the difference increases up to 10.2 watts and up to 19.74% as a percentage, depending on the contamination of the panels. After it rained on September 24, 2021, it was determined that the power produced on September 25 was close to each other again. With the rain, the power difference produced as a result

of cleaning the panels decreased. Again, when the data in the table is examined, it is seen that the power produced on cloudy days and in shady conditions decreases considerably. Based on the measurements made, the average power difference produced between the two panels in the measurements made on September 19-31 was calculated as 5.39%, 4.09% on October 1-31 and 3.18% on November 1-30.

3. RESULTS AND DISCUSSION

Panel powers for each month are shown in Annex-1 as a table and in Figure 4 graphically. When the measured data are examined, the power difference of the two panels was very close to each other at first, but in the following days, the difference approached 20% due to the pollution of the panels. In addition, it was observed that the power difference produced as a result of cleaning the panels after rainy days decreased again.

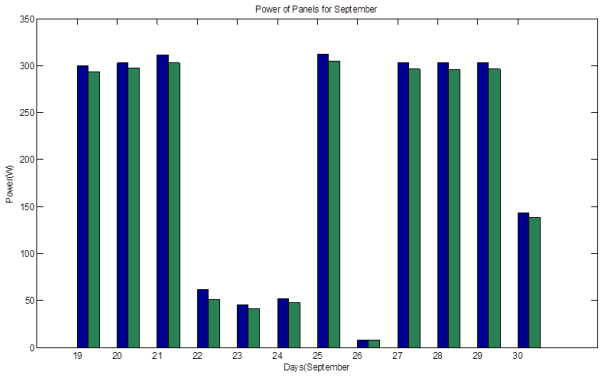

(a)

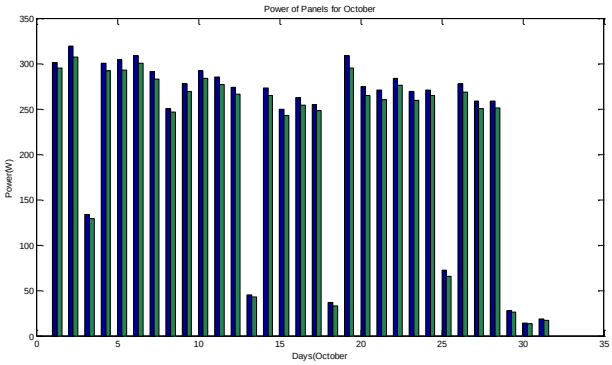

(b)

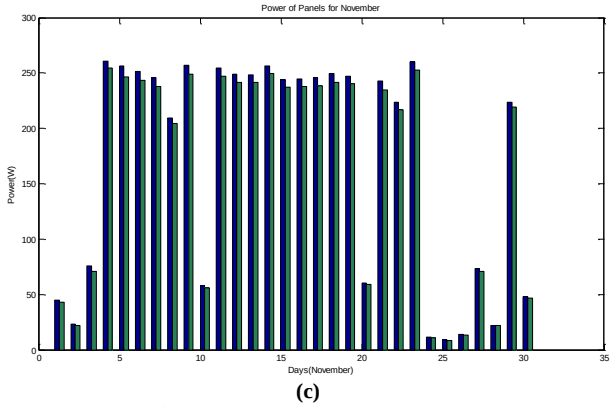

(c)

Figure 4. Power of panels (a) September (b) October (c) November

The power produced by the photocatalytic coated panel is greater than the power of the other panel under all conditions. In other words, it is seen in the measurements that the power produced by the photocatalytic coated panel is slightly higher than the power produced by the normal panel, both in sunny days, rainy weather and shady conditions, whether there is dirt or not. Because the light falling on the panel is less reflected and absorbed better thanks to the photocatalytic coating.

In addition, in September and October, panel powers were measured over 300 W on sunny days, but a maximum of 260 W was recorded in November. Although there is less pollution in November, the measurement of less power value can be explained by the temperature and wind factor.

Considering all the measured values, it is seen that the panels coated with photocatalytic material in the autumn season in Bingöl show a better efficiency than the normal panels. Although the percentage difference in yield increases to larger values on a daily basis, the seasonal average is around 4%. When the yield amount is compared on a monthly basis, the highest yield rate was 5.39% in September, while it decreased gradually in other months.

4. CONCLUSION

The obtained results show the effects of pollution, temperature and wind on panel efficiency. In addition, when the panel surface is covered with TiO_2, it is seen that the efficiency of the panels increases to a certain extent. The amount of change in yield was presented as daily, monthly and autumn season averages. Considering that the pollination is less in the fall and more in the summer, it is estimated that the production difference between the two panels will be higher in the summer months. In addition, Bingöl is a relatively underdeveloped city in terms of population and industrial development. It is predicted that in similar cities with this feature, the yield increase in TiO_2 coated panels will be the same, while this difference will be higher in crowded and industrially developed cities.

Acknowledgment

This study was supported by Bingöl University Scientific Research Projects Unit (BÜBAP) (Project No: BAP-FBE-2021.001).

REFERENCES

[1] Varınca KB, Varank G. Güneş kaynaklı farklı enerji üretim sistemlerinde çevresel etkilerin kıyaslanması ve çözüm önerileri. Güneş Enerjisi Sistemleri Sempozyumu ve Sergisi, 2005. İçel, 24-25.

[2] Ültanır MÖ. 21. Yüzyılın eşiğinde güneş enerjisi. Bilim ve Teknik. 1996;340:50-55.

[3] Altun Y, İşleyen Ş. Bazı OECD ülkelerinde yenilenebilir enerji kaynaklarından elektrik

üretimine yönelim üzerine ampirik bir çalışma. Atatürk Üniversitesi Sosyal Bilimler Enstitüsü Dergisi. 2018;22(3):1577-1590

[4] Gürel B. Türkiye'deki güncel biyokütle potansiyelinin belirlenmesi ve yakılmasıyla enerji üretimi iyi bir alternatif olan biyokütle atıklar için sektörel açıdan ve toplam yanma enerji değerlerinin hesaplanması. Mühendislik Bilimleri ve Tasarım Dergisi. 2020;8(2):407-416.

[5] An-Bo Nano Teknolojik Ürünler ve Ekolojik Çözümler [Internet] 2021 [cited 2021 Nov. 15] http://www.an-bonano.com.tr/solarpanelkoruma.html

[6] Lu H, Cai R, Zhang LZ, Lu L, Zhang L. Experimental investigation on deposition reduction of different types of dust on solar PV cells by self-cleaning coatings. Solar Energy. 2020;206:365-373.

[7] Mohammad AA, Zakariya D, Firas A, Christina B. Class, Modeling and quantifying dust accumulation impact on PV module performance, Solar Energy. 2019;194:86-102

[8] Xueqing L, Song Y, Luyi L, Jianlan L. Investigation of the dust scaling behaviour on solar photovoltaic panels. Journal of Cleaner Production. 2021;295:126391.

[9] Mamadou SD, Dialo D, Kharouna T, Moussa D, Balla DN, Bado N. Structural and physicochemical properties of dust collected on PV panels surfaces and their potential influence on these solar modules efficiency in Dakar, Senegal, West Africa. Scientific African. 2021;Volume 12:e00810

[10] Rüstemli S, Dinçer F. Modeling of photovoltaic panel and examining effects of temperature in MATLAB/Simulink. Elektronika Ir Elektrotechnika (Journal of Electronics and Electrical Engineering). 2011;3(109):35–40.

[11] Yıldırım Ö. Güneş santrallerinde verim arttırma teknikleri [Master Thesis]. Malatya: İnönü Üniversitesi; 2016.

[12] Skoplaki, E., Boudouvis, AG., Palyvos, JA. A simple correlation for the operating temperature of photovoltaic modules of arbitrary mounting. Solar Energy Materials and Solar Cells. 2008;92:1393-1402.

[13] Rezvan T, Shahdad K, Hossein E, Seyed HV, Ali RS, Barat G, et al. A new cooling method for photovoltaic panels using brine from reverse osmosis units to increase efficiency and improve productivity. Energy Conversion and Management. 2022;251:115031

[14] Reda MN, Spinnler M, Al-Kayiem HH, Sattelmayer T. Assessment of condensation and thermal control in a photovoltaic panel by PV/T and ground heat exchanger. Solar Energy. 2021;221:502-511.

[15] Senthil Kumar K, Ashwin Kumar H, Gowtham P, Hari Selva Kumar S, Hari Sudhan R. Experimental analysis and increasing the energy efficiency of PV cell with nano-PCM (calcium carbonate, silicon carbide, copper). Materials Today: Proceedings. 2021;37:1221-1225.

[16] Bigorajski J, Chwieduk D. Analysis of a micro photovoltaic/thermal-PV/T system operation in moderate climate. Renewable Energy. 2019;137:127-136.

[17] Adak S, Cangi H, Yılmaz AS. Fotovoltaik Sistemin Çıkış Gücünün Sıcaklık ve Işımaya Bağlı Matematiksel Modellemesi ve Simülasyonu. International Journal of Engineering Research and Development, 2019, 11 (1), 316-327.

[18] Umut Ö. Yoğunlaştırıcı Fotovoltaik (CPV) Sistemlerde Fotovoltaik (PV) Yüzey Sıcaklığının Sistem Performansına Etkisinin İncelenmesi [Master Thesis]. Bartın: Bartın Üniversitesi; 2018.

[19] Muhammet B. Fotovoltaik Panellerin Verimine Panel yüzey sıcaklığı Etkisinin İncelenmesi [Master Thesis]. İstanbul: Marmara Üniversitesi; 2013.

[20] Buket SE. Güneş Panelleri İçin Optimum Eğim Açısının Belirlenmesi, Rüzgârın Soğutma Etkisinin Verime Etkilerinin İncelenmesi [Master Thesis]. Bursa: Bursa Uludağ Üniversitesi; 2019.

[21] Azaza M, Wallin F. Multi objective particle swarm optimization of hybrid micro-grid system: A case study in Sweden. Energy. 2017;123:108–118.

[22] Funda S. Nano-TiO2 fotokatalizör sentezi ve fotokatalitik aktivitesinin belirlenmesi [PhD Thesis]. Malatya: İnönü Üniversitesi; 2007.

[23] Tang GL. Converting Volatile Organic Compounds to CO2 and Water. American Journal of Chemical Engineering. 2016;4(2):62-67.

[24] Osman Ç. Fotovoltaik (Pv) paneller için fotokatalitik, antibakteriyel ve yansıma önleyici yüzey kaplamaların geliştirilmesi ve karakterizasyonu [Master Thesis]. Afyon: Afyon Kocatepe Üniversitesi; 2020.

[25] Elvin G. Nanobilim ve nanoteknoloji. ODTÜ Yayıncılık. 2. Baskı. Ankara: 2007. s. 124

ANNEX: POWER MEASUREMENT RESULTS OF PANELS

Table 1. Panel power values measured in September

No	Date	Hour	Photocatalytic Panel			Normal Panel			Power Diff. (W)	Per (%)	Explanation
			Current (A)	Voltage (V)	Power (W)	Current (A)	Voltage (V)	Power (W)			
1	19.09.2021	12:41	9.04	33.2	300.1	8.84	33.2	293.49	6.64	2.26	Sunny-27 ºC
2	20.09.2021	11:42	8.82	34.3	302.5	8.65	34.4	297.56	4.97	1.67	Sunny-27 ºC
3	21.09.2021	12:40	9.19	33.9	311.5	8.92	33.9	302.39	9.15	3.03	Sunny-29 ºC
4	22.09.2021	12:40	1.82	34	61.88	1.52	34	51.68	10.20	19.74	Cloudy-28 ºC
5	23.09.2021	12:25	1.35	34	45.9	1.21	34	41.14	4.76	11.57	Cloudy-24 ºC
6	24.09.2021	12:55	1.47	35.6	52.33	1.35	35.6	48.06	4.27	8.89	Rainy-13 ºC
7	25.09.2021	11:45	9.08	34.4	312.4	8.87	34.4	305.13	7.22	2.37	Sunny-18 ºC
8	26.09.2021	16:50	0.26	32.5	8.45	0.25	32.5	8.125	0.33	4.00	Sunny-20 ºC
9	27.09.2021	12:55	9.04	33.6	303.7	8.82	33.6	296.35	7.39	2.49	Sunny-26 ºC
10	28.09.2021	12:30	8.92	34	303.3	8.69	34	295.46	7.82	2.65	Sunny-26 ºC
11	29.09.2021	12:55	8.71	34.8	303.1	8.47	35	296.45	6.66	2.25	Sunny-25 ºC
12	30.09.2021	12:15	4.11	34.9	143.4	3.96	34.9	138.2	5.24	3.79	Cloudy-22 ºC
Average Difference										**5.39**	

Table 2. Panel power values measured in October

No	Date	Hour	Photocatalytic Panel			Normal Panel			Power Diff. (W)	Per (%)	Explanation
			Current (A)	Voltage (V)	Power (W)	Current (A)	Voltage (V)	Power (W)			
1	01.10.2021	12:10	8.70	34.60	301.02	8.48	34.80	295.10	5.92	2.00	Sunny-23 ºC
2	02.10.2021	12:55	9.20	34.70	319.24	8.81	34.90	307.47	11.77	3.83	Sunny-22 ºC
3	03.10.2021	14:02	4.12	32.50	133.90	3.97	32.50	129.03	4.88	3.78	Cloudy-20 ºC
4	04.10.2021	12:00	8.68	34.60	300.33	8.44	34.60	292.02	8.30	2.84	Sunny-19 ºC
5	05.10.2021	12:40	8.82	34.50	304.29	8.49	34.50	292.91	11.39	3.89	Sunny-18 ºC
6	06.10.2021	12:30	8.83	35.00	309.05	8.56	35.10	300.46	8.59	2.86	Sunny-16 ºC
7	07.10.2021	12:55	8.50	34.30	291.55	8.22	34.40	282.77	8.78	3.11	Sunny-17 ºC
8	08.10.2021	10:00	7.26	34.50	250.47	7.13	34.60	246.70	3.77	1.53	Sunny-17 ºC
9	09.10.2021	13:25	8.15	34.10	277.92	7.88	34.20	269.50	8.42	3.12	Sunny-21 ºC
10	10.10.2021	12:40	8.56	34.10	291.90	8.29	34.20	283.52	8.38	2.96	Sunny-22 ºC
11	11.10.2021	12:30	8.55	33.40	285.57	8.29	33.40	276.89	8.68	3.14	Sunny-22 ºC
12	12.10.2021	12:50	8.16	33.60	274.18	7.90	33.70	266.23	7.95	2.98	Sunny-22 ºC
13	13.10.2021	12:00	1.32	33.90	44.75	1.25	34.00	42.50	2.25	5.29	Cloudy-24 ºC
14	14.10.2021	12:00	8.12	33.60	272.83	7.85	33.70	264.55	8.29	3.13	Sunny-24 ºC
15	15.10.2021	11:45	7.27	34.30	249.36	7.05	34.40	242.52	6.84	2.82	Sunny-25 ºC
16	16.10.2021	12:00	7.72	34.00	262.48	7.46	34.10	254.39	8.09	3.18	Sunny-23 ºC
17	17.10.2021	11:00	7.36	34.60	254.66	7.16	34.70	248.45	6.20	2.50	Sunny-21 ºC
18	18.10.2021	11:45	1.06	34.50	36.57	0.96	34.60	33.22	3.35	10.10	Cloudy-16 ºC
19	19.10.2021	12:30	8.77	35.20	308.70	8.36	35.30	295.11	13.60	4.61	Sunny-18 ºC
20	20.10.2021	12:50	8.03	34.20	274.63	7.75	34.20	265.05	9.58	3.61	Sunny-19 ºC
21	21.10.2021	13:10	7.87	34.40	270.73	7.57	34.40	260.41	10.32	3.96	Sunny-20 ºC
22	22.10.2021	11:50	8.30	34.20	283.86	8.05	34.30	276.12	7.75	2.80	Sunny-19 ºC
23	23.10.2021	13:00	7.73	34.80	269.00	7.44	34.90	259.66	9.35	3.60	Sunny-21 ºC
24	24.10.2021	11:00	7.78	34.80	270.74	7.58	34.90	264.54	6.20	2.34	Sunny-19 ºC
25	25.10.2021	12:35	2.02	35.70	72.11	1.82	35.80	65.16	6.96	10.68	Cloudy-14 ºC
26	26.10.2021	13:00	7.72	36.00	277.92	7.44	36.10	268.58	9.34	3.48	Sunny-17 ºC
27	27.10.2021	12:40	7.43	34.80	258.56	7.18	34.90	250.58	7.98	3.19	Sunny-16 ºC
28	28.10.2021	12:30	7.40	35.00	259.00	7.15	35.10	250.97	8.03	3.20	Sunny-15 ºC
29	29.10.2021	11:50	0.79	35.30	27.89	0.74	35.30	26.12	1.77	6.76	Rainy-10 ºC
30	30.10.2021	12:40	0.41	34.60	14.19	0.38	34.70	13.19	1.00	7.58	Rainy-8 ºC
31	31.10.2021	13:40	0.53	34.60	18.34	0.49	34.70	17.00	1.34	7.85	Rainy-11 ºC
Average Difference										**4.09**	

Table 3. Panel power values measured in November

No	Date	Hour	Photocatalytic Panel			Normal Panel			Power Diff. (W)	Per (%)	Explanation
			Current (A)	Voltage (V)	Power (W)	Current (A)	Voltage (V)	Power (W)			
1	01.11.2021	16:15	1.28	34.80	44.54	1.23	34.80	42.80	1.74	4.07	Cloudy-13 ºC
2	02.11.2021	12:40	0.67	35.00	23.45	0.62	35.10	21.76	1.69	7.76	Rainy-11 ° C
3	03.11.2021	11:20	2.14	35.40	75.76	2.00	35.50	71.00	4.76	6.70	Cloudy-13 ° C
4	04.11.2021	12:20	7.52	34.70	260.94	7.33	34.70	254.35	6.59	2.59	Sunny-21 ° C
5	05.11.2021	11:10	7.32	35.00	256.20	7.02	35.10	246.40	9.80	3.98	Sunny-16 ° C
6	06.11.2021	13:25	7.18	35.00	251.30	6.95	35.00	243.25	8.05	3.31	Sunny-20 ° C
7	07.11.2021	13:00	7.03	35.00	246.05	6.80	35.00	238.00	8.05	3.38	Sunny-19 ° C
8	08.11.2021	13:40	6.02	34.80	209.50	5.88	34.80	204.62	4.87	2.38	Sunny-19 ° C
9	09.11.2021	12:30	7.41	34.70	257.13	7.17	34.70	248.80	8.33	3.35	Sunny-15 ° C
10	10.11.2021	12:10	1.63	35.60	58.03	1.56	35.70	55.69	2.34	4.19	Cloudy-11 ° C
11	11.11.2021	12:30	7.07	36.00	254.52	6.85	36.10	247.29	7.24	2.93	Sunny-13 ° C
12	12.11.2021	11:15	7.01	35.50	248.86	6.79	35.60	241.72	7.13	2.95	Sunny-12 ° C
13	13.11.2021	12:00	7.03	35.30	248.16	6.82	35.40	241.43	6.73	2.79	Sunny-14 ° C
14	14.11.2021	12:00	7.29	35.20	256.61	7.07	35.30	249.57	7.04	2.82	Sunny-14 ° C
15	15.11.2021	11:50	6.72	36.30	243.94	6.51	36.40	236.96	6.97	2.94	Sunny-13 ° C
16	16.11.2021	11:30	6.95	35.20	244.64	6.73	35.30	237.57	7.07	2.98	Sunny-13 ° C
17	17.11.2021	11:40	6.97	35.30	246.04	6.74	35.40	238.60	7.44	3.12	Sunny-13 ° C
18	18.11.2021	12:15	7.05	35.40	249.57	6.83	35.40	241.78	7.79	3.22	Sunny-13ºC
19	19.11.2021	11:35	7.02	35.20	247.10	6.81	35.30	240.39	6.71	2.79	Sunny-12ºC
20	20.11.2021	12:35	1.64	36.70	60.19	1.61	36.80	59.25	0.94	1.59	Rainy-6 ° C
21	21.11.2021	11:40	6.79	35.80	243.08	6.54	35.90	234.79	8.30	3.53	Sunny -12^0 C
22	22.11.2021	13:30	6.26	35.70	223.48	6.07	35.70	216.70	6.78	3.13	Sunny -13^0 C
23	23.11.2021	12:30	7.30	35.60	259.88	7.08	35.70	252.76	7.12	2.82	Sunny -14^0 C
24	24.11.2021	11:20	0.32	34.80	11.14	0.31	34.90	10.82	0.32	2.93	Cloudy -6^0 C
25	25.11.2021	12:10	0.26	34.40	8.88	0.25	34.50	8.63	0.25	2.90	Rainy -7^0 C
26	26.11.2021	11:30	0.39	35.10	13.62	0.38	35.20	13.38	0.24	1.82	Rainy -6^{0}C
27	27.11.2021	12:30	2.01	36.39	73.14	1.95	36.43	71.04	2.11	2.96	Cloudy -8^0 C
28	28.11.2021	12:35	0.62	35.50	22.01	0.61	35.60	21.72	0.29	1.35	Cloudy -8^0 C
29	29.11.2021	12:40	6.20	36.10	223.82	6.06	36.20	219.37	4.45	2.03	Sunny -13^0 C
30	30.11.2021	12:40	1.32	36.10	47.65	1.29	36.20	46.70	0.95	2.04	Cloudy-11^0 C
Average Difference										**3.18**	

Araştırma Makalesi https://doi.org/10.46810/tdfd.1031911 Research Article

Türk Doğa ve Fen Dergisi
Turkish Journal of Nature and Science
www.dergipark.gov.tr/tdfd

Investigation of Biogas Production Potential from Livestock Manure by Anaerobic Digestion in Bingöl Province

Sinem IŞIK[1*], Sıraç YAVUZ[2]

[1] Bingöl Üniversitesi, Mühendislik ve Mimarlık Fakültesi, Makine Mühendisliği Bölümü, Bingöl, Türkiye
[2] Bingöl Üniversitesi, Ziraat Fakültesi, Zootekni Bölümü, Bingöl, Türkiye
Sinem IŞIK ORCID No: 0000-0002-1044-5092
Sıraç YAVUZ ORCID No: 0000-0001-5878-8994

**Corresponding author: sinemisik@bingol.edu.tr*

(Received: 03.12.2021, Accepted: 07.01.2022, Online Publication: 25.03.2022)

Keywords
Alternative energy, Anaerobic digestion, Organic waste, Animal feces, Energy of household appliances

Abstract: Biogas is one of the sustained alternative energy sources. The annual biogas potential of Bingöl province was calculated according to the data of bovine, ovine and poultry animals between 2015-2020 years which were obtained from the Turkish Statistical Institute (TSI). In addition, liquid and available manure amount, biogas potential, electrical energy and heat energy amounts were determined according to the animal data of the districts in Bingöl province for 2020. It is estimated that the biogas energy potential between 2015-2020 years with 39.02 million m^3 will be the most in 2018, with 36.1 m^3 the least in 2019 and 36.5 million m^3 in 2020. In 2020, the biogas energy potential of the districts were found among; 263 thousand m^3-12.65 million m^3. It is clear that in Bingöl province in 2020 from a total number of 5694302 livestock, 865202 of which are bovine and ovine that approximately 754 thousand tons of utilizable manure, 36.5 million m^3 biogas, 171.4 GWh electrical energy and 171449*10^6 kcal m^{-3} heat energy can be obtained. A facility to be established in Bingöl will enable to increase the use of renewable energy sources, decrease methane gas emissions and meet energy needs of farmers or householders.

Bingöl İli Hayvancılık Gübresinden Anaerobik Çürütme ile Biyogaz Üretim Potansiyelinin Araştırılması

Anahtar Kelimeler
Alternatif enerji, Anaerobik çürüme, Organik atık, Hayvan gübresi, Ev aletleri enerjisi

Öz: Biyogaz, sürekliliği olan alternatif enerji kaynaklarından biridir. Türkiye İstatistik Kurumu (TÜİK)'ndan alınan Bingöl iline ait 2015-2020 yılları arasındaki büyükbaş, küçükbaş ve kanatlı hayvan sayıları verilerine göre yıllık biyogaz potansiyeli hesaplanmıştır. Ayrıca, Bingöl ilinde bulunan ilçelerin 2020 yılı hayvan verilerine göre yaş ve kullanılabilir gübre miktarı, biyogaz potansiyeli, elektrik enerjisi ve ısı enerjisi miktarları belirlenmiştir. Elde edilen verilere göre, 2015-2020 yılları arasında biyogaz enerjisi potansiyelinin 39.02 milyon m^3 ile en fazla 2018 yılında, 36.1 m^3 ile en az 2019 yılında, 2020 yılında ise 36.5 milyon m^3 olabileceği görülmüştür. 2020 yılında Bingöl ilçelerindeki biyogaz enerjisi potansiyeli 263 bin m^3 - 12.65 milyon m^3 arasında değişmiştir. 2020 yılı içerisinde Bingöl ilindeki 865202'si büyükbaş ve küçükbaş olmak üzere toplam 5694302 hayvandan, yaklaşık 754 bin ton kullanılabilir gübre, 36.5 milyon m^3 biyogaz, 171.4 GWh elektrik enerjisi ve 171449*10^6 kcal m^{-3} ısı enerjisi elde edilebilecektir. Bingöl'de kurulacak biyogaz enerji üretim tesisleri, yenilenebilir enerji kaynaklarının kullanımının artırılmasına, metan gazı emisyonlarının azaltılmasına, çiftçilerin veya hanelerin bazı enerji ihtiyaçlarının karşılanmasına olanak sağlayacaktır.

1. INTRODUCTION

Depending on population growth and industrial development, energy demand is constantly increasing. The current amount of energy has become unable to meet this demand. This situation causes a continuous increase in energy prices. In addition, due to limited fossil fuel reserves, there will be difficulties in meeting energy needs in the coming years. Therefore, the demand for new and renewable energy sources has been increasing rapidly in the world as well as in Turkey in recent years, and many studies have been carried out seriously. Since using of renewable energy sources, there has been less damage to the nature and the use of fossil fuels is reduced [1, 2].

Global warming, which is one of the serious problems of nowadays, will have negative effects on our world in the future. Global warming and climate change occur with the increase of greenhouse gases (carbon dioxide (CO_2), methane (CH_4), nitrogen oxide (NO) and water vapor (H_2O)). The most serious reason for climate change is the uncontrolled increase in the amount of CO_2 in nature. Population growth have led to, the decrease in green areas, the increase in fossil fuel-powered motor vehicles and consequently increase in the amount of CO_2 released into the nature. This problem make policies eager to take an action against CO_2 amount globally. Renewable energy sources play the most important role in reducing the CO_2 emissions [3, 4]. The energy obtained from organic wastes is more advantageous than renewable energy sources such as solar, wind and geothermal. Because these wastes has continuity. Therefore, this energy source will be one of the most common renewable energy sources in the future. Biogas production from organic solid wastes is obtained by anaerobic digestion (AD), which is one of the most widely used and traditional biochemical methods, as shown in Figure 1. In addition, the conversion of AD organic wastes to biogas is the most preferred biotechnological method [5, 6, 7].

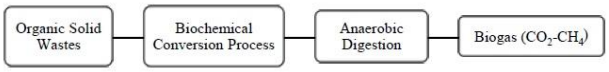

Figure 1. Waste recycling technologies [7].

Anaerobic digestion is a biological process in which anaerobic bacteria decompose organic matter and produce biogas in conditions with little or no oxygen. During the AD, nutrients are retained and digestion residues are made suitable to become an organic fertilizer that can replace mineral fertilizers that require fossil energy [8]. The main by-product of AD is the digested solid fraction, which is rich in nitrogen (N) content and can be used as fertilizer. As a result of AD process, the significant methane emission caused by the uncontrolled decomposition of organic waste into the atmosphere will be stopped and the emission of methane gas, which is 25 times more effective in retaining heat in the atmosphere than carbon dioxide, will be trapped [9, 10]. Anaerobic digestion is possible in principle at temperatures between 3 °C and about 70 °C. The differentiation generally varies between three temperature ranges respectively: the psychrophilic temperature is below 20 °C, the mesophilic temperature is between 20 °C and 40 °C, and the thermophilic temperature is above 40 °C [11-13].

Since the interest in biogas potential obtained from animal manure has increased in recent years, biogas potential has been investigated for many provinces in Turkey as well. These provinces and studies are following as; Adana [14, 15], Ankara [16], Bitlis [17], Burdur [18], Bursa [19], Elazig [20], Erzincan [21], Hatay [22], Isparta [23], Kahramanmaraş [24], Kayseri [25], Muş [26], Tekirdağ [27], Yozgat [28]. Organic matter which is consisted in animal manure are fermented and digested by microorganisms (bacteria, protozoa and archaea) under anaerobic conditions and produce CH_4 in 3 stages. Organic wastes (carbohydrates, proteins and fats) undergo fermentation by micro-organisms and decompose into hydrogen, carbon dioxide, acetic acid, butyric acid, propionic acid, various alcohols and other compounds. In the second stage H_2, CO_2 and acetic acid are reacted by acetogenic bacteria. And in the final stage, methane and carbon dioxide gases are formed by methanogenic bacteria [12].

Biogas energy is a variable renewable that can be used to replace fossil fuels in energy and heat generation and can also be converted into transportation fuel after its purification. It is rich in methane and carbon dioxide can replace natural gas as a raw material for the production of other biochemicals [29, 30]. In addition, it has been preferred as one of the most energy productive and environmentally advantageous technologies for bioenergy production [31].

Biogas is a fuel gas which containing 50-70% methane (CH_4), 25-50% carbon dioxide (CO_2), 1-5% hydrogen (H_2), 0.3-3% nitrogen (N_2), traces of ammonia (NH_3) and hydrogen sulfide (H_2S) [32-34]. It can be produced from raw materials such as agricultural wastes, animal manure, municipal wastes, plant materials, sewages, green wastes or food wastes. And it is a renewable energy source and in mostly exerts a very small carbon footprint. It can be also used as a fuel to generate heat and electricity, or it can be injected into the gas grid as biomethane. This energy production creates more employment and livelihood in rural areas. It also plays a major role in reducing important greenhouse gases such as CO_2 and CH_4 [35]. By converting these two gases into biogas production instead of dispersing them into the atmosphere, the energy we need will be met without harming the environment, thus contributing to the reduction of global warming. The use of biogas energy may become advantageous when designing sustainable energy solutions in industrial applications, farms and households as seen in developing countries [31, 36].

The production of biogas is a process of gas formation as a result of biological decomposition of organic materials in anaerobic conditions. In a biogas production facility, livestock manure is diluted with water and transferred to an on–off tank. AD is carried out by bacteria, protozoa and archaea (microbiological flora) which are in different amount and in the structure of animal manure. Biogas is formed 10-15 days after the filling of the tank and this

production continues for about 60 days and then decreases. As a result of AD, gases accumulate in the upper part of the tank and organic fertilizers in the lower parts [12, 16].

In this study, the biogas potential that can be obtained from livestock manure in Bingöl province and its districts according to 2020 datas were determined. In addition, the biogas potential of Bingöl province the years between 2015-2020 was also calculated. The data of this study were obtained from Bingöl Provincial Directorate of Agriculture Forestry and Turkish Statistical Institute [38, 39]. By determining the number of animals in the provinces and districts, the amount of livestock manure that can be obtained according to the animal type was calculated. Hence the annual biogas and electricity potential of Bingöl province and energy savings were calculated theoretically.

2. MATERIALS AND METHODS

2.1. Geographical Characteristics of Bingöl Province

This study includes the borders of Bingöl province, which is located between 41-20° and 39-56° east longitudes and 39-31° and 36-28° north latitudes. Bingöl province, is located in the Eastern Anatolia Region of Turkey, has a total population of 281768, 165867 of which are in the central district, according to 2020 TSI datas. And that means 67.7% of the population lives in central district [40]. It has an area of 8004 km^2 , of which 3 million 137 thousand 710 decares (approximately 42% of the surface area) covers pastureland and 300 thousand decares of agricultural land [39]. As seen in Figure 2, Bingöl province consists of 8 districts in total namely; Adaklı, Genç, Karlıova, Kiğı, Center, Solhan, Yayladere and Yedisu. Livelihood of the province is animal husbandry. Locals earn a good income from the beekeeping sector with the sale of livestock and dairy products.

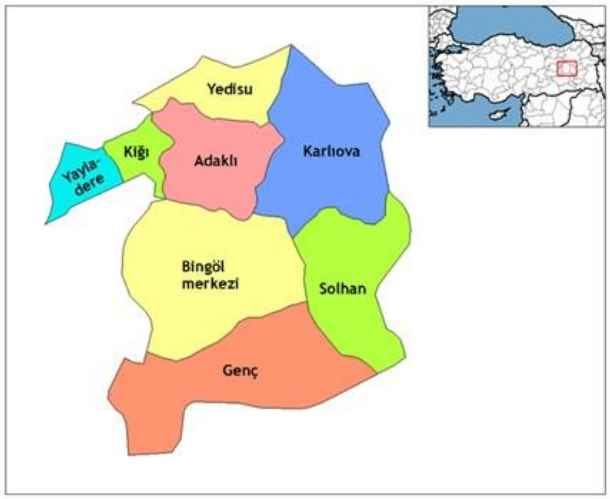

Figure 2. Geographic map of Bingöl province [40].

2.2. Animal Data

The animal data of Bingöl province for the year 2020 which is obtained from the Ministry of Agriculture and Forestry are given in Table 1. The number of animals was determined, based on this informations. The total number of ovine make up sheep with 73.4% and cattle make up with 99.95% of bovine. According to TSI datas, in 2020 when animal husbandry was the highest numbers, the number of bovine decreased compared to the previous year, while the number of ovine and poultry increased compared to the previous years (Table 1). As it is clear that in Table 1, poultry constitute the majority of the number of animals in the province [39].

Table 1. The total number of livestocks in Bingöl province between 2015–2020 [38, 39].

Years	Bovine	Ovine	Poultry	Total
2015	166695	817548	904404	1888647
2016	165849	859668	1832055	2857572
2017	182892	783043	2624772	3590707
2018	184670	792160	2582922	3559752
2019	197689	635603	2847660	3680952
2020	144550	720652	4829100	5694302

The district where sheep and goats breeding is carried out the most in 2020 is Karlıova with 348375 ovine numbers as mentioned in Figure 3. Karlıova is followed by Solhan with 147291 sheep and then Central districts with 101198 sheep and goats. The majority of bovine breeding is carried out in Bingöl central (60087), Karlıova (20986) and Solhan (19984) districts, respectively (Figure 3). Since the majority of poultry are in the Central district, it is considered the place where animal husbandry is most engaged in terms of the total number of bovine, ovine and poultry, with approximately 4.7 million animals [38]. Poultry breeding is more preferred in areas close to transit centers where transportation is easy, rather than rural areas [41]. Therefore, the number of poultry in the central district of Bingöl has a considerably higher number than other districts. It is also reported that the reason for the huge differences in the number of total animals by years is due to the grants given by the Ministry of Agriculture and Forestry in the relevant years [39]. Animal husbandry is carried out the least in Yayladere district with a total number of 8845 animals, including bovine, ovine and poultry. It is considered that the reason Kiğı, Yayladere and Yedisu total animal assets are less than other districts is to be proportional to the number of populations they have. In addition, the fact that there is such a great number of sheep and goats in Karlıova district can be shown among the results that the geographical structure of the district is more suitable for these type of animal breeding and the improvement projects carried out by the public [42].

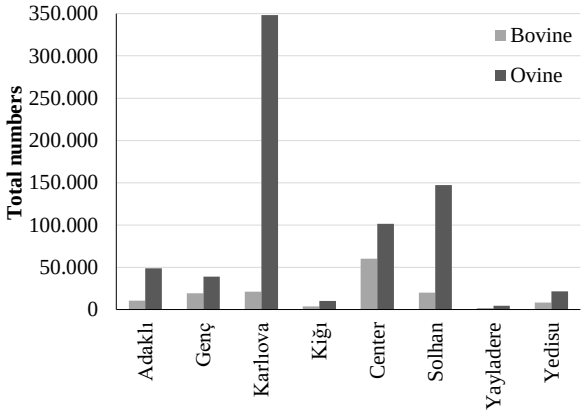

Figure 3. Ruminants distribution by districts in 2020.

The average accepted values of calculation the biogas energy potential are given in Table 2 below [20, 43]. It is accepted that approximately 1:3 of the manure obtained from animal wastes are destroyed by mixing with nature in the pastures, and only 2:3 is usable [20]. In the calculation; equations given in between Eq. 1-11 below are used [14-28].

Table 2. Acceptances for biogas energy potential [16, 37, 43, 44].

Animal Species	Annual Manure (tons an^{-1})	Biogas obtained from 1 tons of manure (m^3)
Bovine	3.6 t	33 m^3
Ovine	0.7 t	58 m^3
Poultry	0.022 t	78 m^3

Annual amount of liquid manure that animals can produce;

$$M_b = n*3.6 \text{ tons an.}^{-1} \quad (1)$$

$$M_o = n*0.7 \text{ tons an.}^{-1} \quad (2)$$

$$M_p = n*0.022 \text{ tons an.}^{-1} \quad (3)$$

$$M_t = M_b + M_o + M_p \text{ tons an.}^{-1} \quad (4)$$

In the equations; *n:* Number of animals, M_b : Amount of liquid manure obtained from bovine animals, M_o : Amount of liquid manure obtained from ovine animals, M_p : Amount of liquid manure obtained from poultry, M_t : It expresses the total amount of liquid manure. Usable amount of liquid manure. *(M_u)*;

$$M_u = M_t*2*3^{-1} \text{ tons an.}^{-1} \quad (5)$$

Potential biogas energy *(PB_e)*;

$$PB_{eb} = M_b *2*3^{-1}*33 \text{ m}^3 \text{ an.}^{-1} \quad (6)$$

$$PB_{eo} = M_o*2*3^{-1}*58 \text{ m}^3 \text{ an.}^{-1} \quad (7)$$

$$PB_{ep} = M_p*2*3^{-1}*78 \text{ m}^3 \text{ an.}^{-1} \quad (8)$$

$$PB_{et} = PB_{eb} + PB_{eo} + PB_{ep} \text{ m}^3 \text{ an.}^{-1} \quad (9)$$

In the equations given above; PB_{eb}*:* Biogas energy obtained from bovine, PB_{eo}*:* Biogas energy obtained from ovine, PB_{ep}*:* It refers to biogas energy obtained from poultry and PB_{et}*:* Total potential biogas energy.

Total potential electrical energy (PEE_t);

$$PEE_t = PB_{et} *4.70 \text{ kWh an.}^{-1} \quad (10)$$

Total potential thermal energy (TPT_e) is between values given below [14-28];

$$TPT_e = PB_{et} *4700 \text{ kcal } m^{-3} - 5700 \text{ kcal } m^{-3} \text{ (approximately)} \quad (11)$$

3. RESULTS AND DISCUSSION

3.1. Biogas Energy

The biogas potential according to the amount of manure that can be obtained from bovine, ovine and poultry between 2015-2020 in Bingöl province is given in Figure 4. It is seen in Figure 4 that the biogas production potential between these years could be at most in 2018 with 39.02 million m^3 and at least in 2019 with 36.1 million m^3.

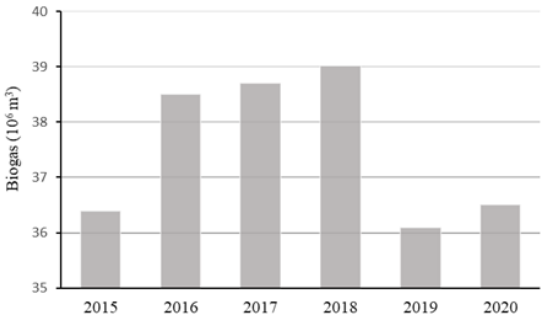

Figure 4. Distribution of biogas production potential of Bingöl province by years.

In 2020, approximately 36.5 million m^3 of biogas will be obtained from a total of 5694302 animal population. In Figure 5 below is given, the percentage (%) potential distribution of biogas that can be produced in the central and the other districts of Bingöl province in 2020. The majority of biogas energy in Bingöl province, 34.68% can be obtained from the Central, 30.73% Karlıova and 15.39% Solhan districts (Figure 5). The minimum biogas production potential in the province can be obtained in Yayladere district with 0.72% (Figure 5).

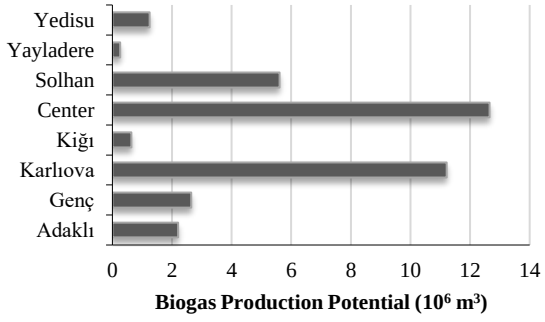

Figure 5. Distribution of biogas production potential by districts in 2020.

The Central district with a total number of 4665425 animals, including 60087 bovine, 101198 ovine and 4504140 poultry is the highest in number of animals. According to datas $12650.7*10^3$ m^3 of biogas energy is generated from $257.5*10^3$ tons of usable manure per year that can be obtained from the central district. In addition, the obtained biogas energy is equivalent to $59458.4*10^3$ kWh electrical energy or $59.5*10^9$ kcal thermal energy (Table 3).

Table 3. Theoretical biogas potential produced by animal species in the province and districts of Bingöl in 2020.

Districs	Num. of Animals	Usable Manure Amount	Biogas Potential	Electrical Energy	Heat Energy
	Head	10^3 t an^{-1}	10^3 m^3 an^{-1}	10^3 kWh an^{-1}	10^9 kcal m^{-3}
Adaklı	111356	48.5	2206.2	10369.2	10.4
Genç	107918	65.4	2647.4	12442.8	12.4
Karlıova	473047	214.5	11210	52687.3	52.7
Kiğı	80516	14.4	637.1	2994.7	2.9
Center	4665425	257.5	12650.7	59458.4	59.5
Solhan	204877	117.2	5612.4	26378.4	26.4
Yayladere	8845	6.4	262.9	1236	1.2
Yedisu	42318	30.1	1251.4	5881.9	5.9
Total	**5694302**	**754**	**36478.1**	**171448.7**	**171.4**

3.2. Energy Conversions

Bingöl with its all districts have a potential of 754051.1 tons liquid manure production per year from bovine, ovine and poultry. The comparison with other fuel types of 36478.5*10^3 m^3 biogas which can be obtained from liquid manure in 2020 was made based on the following assumptions. According to the assumptions stated below, approximately 171.4 GWh of electrical energy and 171449-207927.4 x106 kcal m^{-3} of heat energy are revealed from 36478.5*10^3 m^3 of biogas (Figure 6). The energy equivalents obtained from 1 m^3 biogas are given in Table 4 below.

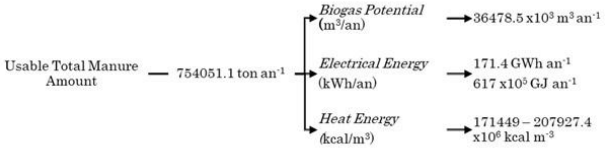

Figure 6. Energy conversions according to the total amount of biogas in 2020.

Table 4. The energy equivalents obtained from 1 m^3 of biogas [16, 20, 37, 43-46]:

1 m^3 biogas	4.70 kWh electrical energy
	4.700 – 5.700 kcal m^{-3} heat energy
	0.43 kg butane gas
	12.3 kg turd
	3.47 kg wood
	0.8 L gasoline
	0.63 L gas oil
	1.46 kg charcoal energy

3.3. Electrical Energy

According to our calcultions a house of 4 people consumes approximately 21.3 kWh electrical energy per day and 72.4 kWh per week, as shown in Table 5 below. And this consumption reaches about 7774.5 kWh per year. The electrical energy that can be obtained from animal manure in Bingöl province is 171448.7*10^3 kWh $year^{-1}$ according to 2020 datas. This amount of electrical energy that can be obtained annually from biogas energy in Bingöl, has the power to meet the electricity approximate of 22052 households.

According to the January 2021 residential tariffs, 1 kWh of electricity is 0.7102 TL (Turkish lira) taxes included [47]. Accordingly, the annual electricity bill of a household is approximately 5521.4 TL. Thanks to biogas energy, Bingöl province has the potential to meet 121.7 million TL the electricity bill of per year.

Table 5. Electricity consumption of a household per week.

Household Appliances	P	Num.	DWT	DC	NWU	WC
	Watt-hour	1-10	Hours	Watt-hour	1-10	Watt-hour
Refrigerator (A+)	46	1	24	1104	7	7728
Dishwasher (A+)	1800	1	2	3600	5	18000
Wash. Machine (A+)	800	1	2	1600	3	4800
LCD TV (A+)	65	1	5	325	7	2275
Iron	2600	1	2	5200	2	10400
Vacumm Cleaner	2000	1	2	4000	3	12000
Bakery	2500	1	1.5	3750	2	7500
Led Lamp	12	5	5	300	7	2100
Kettle	2200	1	0.2	440	7	3080
Toast Machine	2000	1	0.2	400	3	1200
Microwave Oven	800	1	0.1	80	7	560
Laptop	90	1	3	270	7	1890
Hair Dryer	1300	1	0.2	260	3	780
Other (Charging etc.)	10	1	2	20	7	140
Total				**21349**		**72453**

P: Power, DWT: Daily working time, DC:Daily consumption, NWU: Number of weekly use, WC: Weekly consumption

4. CONCLUSIONS

Global warming, which has been caused by the accumulation of greenhouse gases in the atmosphere in recent years, has become the biggest problem of nowadays [48, 49]. This will cause serious drought and water problems in the future. In order to meet the needs of the increasing the world population, the demand for agriculture and industry will increase and the number of animals will need to increase as well. This will accelerate global warming by increasing the amount of methane and carbon dioxide gas day by day. In order to reduce global warming, the use of alternative energy sources should be risen. In particular, studies on biogas energy should be focused. Moreover, continuity should be ensured in the source of raw materials in biogas plants.

Biogas is an alternative energy source to meet the increasing energy needs in the world as well as in Turkey. Biogas production will reduce the use of fossil fuels and reduce CO_2 emissions. Biogas is a combustible gas that is produced from waste materials under anaerobic conditions by AD method, similar to natural gas and mostly consisting of CH_4 and CO_2.

In this study, the amount of manure that can be obtained from bovine, ovine and poultry in Bingöl province and accordingly the biogas production potential was determined. According to 2015-2020 year data, depending on the total number of animals in Bingöl province, the highest biogas production was obtained in 2018 with 39.02 million m^3. As can be seen in 2020 data, the amount of manure that can be obtained from total of 5694302 animals (bovine, ovine and poultry) in Bingöl has the potential to produce approximately 36.5 million m^3 of biogas energy. The total biogas production potential of the province is max. as following respectively; Central district (12.6 million m^3), Karlıova (11.2 million m^3) and Solhan (5.6 million m^3). The min. biogas production potential has been determined in Yayladere with approximately 263 thousand m^3. According to 2020 data (bovine, ovine and poultry) in Bingöl province, 36.5 million m^3 of biogas can be produced with 754051.1 tons of annually usable manure. In addition, this 36.5 million m^3 of biogas has been determined that it is equivalent to 171.4 GWh of electrical energy, 171449 million kcal m^{-3} of heat energy, 126.6 kg of wood and 29.2 million liters of gasoline.

REFERENCES

[1] Türkeş, M. What is climate change? basic definition, causes, observed and predicted results of climate change. Climate Change and Enviroment 2008;1(1):26-37.

[2] Kılıçkap, S., El, E., Yıldız, C. Investigation of the effect on the efficiency of phase change material placed in solar collector tank. Thermal Science and Engineering Progress 2018;5:25-31.

[3] Cudjoe, D., Han, M.S., Nandiwardhana, A.P. Electricity generation using biogas from organic fraction of municipal solid waste generated in provinces of china: techno-economic and environmental impact analysis. Fuel Processing Technology 2020;203:106381.

[4] Jelínek, M., Mazancová, J., Van Dung, D., Banout, J., Roubík, H. Quantification of the impact of partial replacement of traditional cooking fuels by biogas on global warming: evidence from vietnam. Journal of Cleaner Production 2021;292:126007.

[5] Ni, M., Leung, D.Y., Leung, M.K., Sumathy, K. An overview of hydrogen production from biomass. Fuel Processing Technology 2006;87(5):461-472.

[6] Zhang, L., Xu, C.C., Champagne, P. Overview of recent advances in thermo-chemical conversion of biomass. Energy Conversion and Management 2010;51(5):969-982.

[7] Appels, L., Lauwers, J., Degrève, J., Helsen, L., Lievens, B., Willems, K. Anaerobic digestion in global bio-energy production: potential and research challenges. Renewable and Sustainable Energy Reviews 2011;15(9):4295-4301.

[8] Nkoa, R. Agricultural benefits and environmental risks of soil fertilization with anaerobic digestates: a review. Agron Sustain Dev 2014;34:473-492.

[9] Bharathiraja, B., Sudharsana, T., Jayamuthunagai, J., Praveenkumar, R., Chozhavendhan, S., Iyyappan, J. Biogas production–a review on composition, fuel properties, feed stock and principles of anaerobic digestion. Renewable and Sustainable Energy reviews 2018;90(April):570-582.

[10] Anonymous [Internet]. U.S. Environmental protection agency; 2021 [cited 2021 April 21]. Available from: www.epa.gov/methane

[11] Kossman, W., Pönitz, U., Habermehl, S., Hoerz, T., Kramer, P., Klingler, B. Information and advisory service on appropriate technology (ISAT). GATE in Deutsche Gesellschaft für Technische Zusammenarbeit (GTZ) 1; 1996.

[12] Öztürk, M. Biogas production from animal manure. Republic of Turkey Ministry of Environment and Urbanisation, Ankara 2005;5:8-18.

[13] Náthia-Neves, G., Berni, M., Dragone, G., Mussatto, S.I., Forster-Carneiro, T. Anaerobic digestion process: technological aspects and recent developments. International Journal of Environmental Science and Technology 2018;15(9):2033-2046.

[14] Dağtekin, M., Aybek, A., Bilgili, M.E. Evaluation of biogas and electricity production potential of fertilizer in broiler poultry houses in Adana and Mersin. Çukurova University Journal of the Faculty of Engineering and Architecture 2019;34(2):9-22.

[15] Yağlı, H., Koç, Y. Determination of biogas production potential from animal manure: a case calculation for Adana province. Çukurova University Journal of the Faculty of Engineering and Architecture 2019;34(3):35-48.

[16] Şenol, H., Elibol, E.A., Açıkel, Ü., Şenol, M. Primary biomass sources for biogas production in Turkey. BEU Journal of Science 2017a;6(2):81-92.

[17] Yetiş, A.D., Gazigil, L., Yetiş, R., Çelikezen, B. Biogas potential from animal waste: a case study for Bitlis province. Academic Platform Journal of Engineering and Science 2019;7(1):74-78.

[18] Akyürek, Z. Energy recovery from animal manure: biogas potential of Burdur, Turkey. Eskişehir Technical University Journal of Science and

Technology A-Applied Sciences and Engineering 2019;20(2):161-170.
[19] Ulusoy, Y., Arslan, R., Ulukardeşler, A.H., Kaplan, C., Kul, B., Arslan. R. Biogas potential of agricultural organic waste in Bursa and investigation of use of biogas as a fuel in diesel engines. Journal of Agricultural Faculty of Uludag University 2015;29(2).
[20] Akbulut, A., Dikici, A. Biogas potential and cost analysis of Elazig province. Fırat University Research of Eastern Anatolia Region 2004;2(2):36-41.
[21] Seyhan, A.K., Badem, A. Investigation of biogas potential of animal wastes in Erzincan province. Academic Platform Journal of Engineering and Science 2018;6(1):25-35.
[22] Karaca, C. Determination of biogas production potential from animal manure in Hatay province. Journal of Agricultural Faculty of Mustafa Kemal University 2017;22(1):34-39.
[23] Gökdoğan, O. Greenhouse heating with the energy that can be acquired from Isparta province's animal waste. Academia Journal of Nature and Human Sciences 2019;5(1):27-34.
[24] Ay, Ö.F., Kaya, A. Biogas potential from animal waste of Kahramanmaraş province. Journal of the Institute of Science and Technology 2020;10(4):2822-2830.
[25] Poyraz, H.N., Elden, G., Genç, G. Investigation of the biogas and electric production potential and cost from the cattle waste in Kayseri. Dicle University Journal of Engineering 2020;11(3):1175-1185.
[26] Çağlayan, G., Koçer, N. Evaluation of the potential of livestock breeding in the city of Muş for the research of biogas production. Muş Alparslan University Journal of Science 2014;2(1):215-220.
[27] Aktaş, T., Özer, B., Soyak, G., Ertürk, M.C. Determination of the electricity generation potential from animal biogas in Tekirdag city. Journal of Agricultural Machinery Science 2015;11(1):69-74.
[28] Taşova, M., Yazarel, S. Determination of biogas and energy potential of animal wastes in Yozgat province. International Journal of Life Sciences and Biotechnology 2019;2(1):16-24.
[29] Weiland, P. Biogas production: current state and perspectives. Appl Microbiol Biotechnol 2010;85:849–860.
[30] Vanholme, B., Desmet, T., Ronsse, F., Rabaey, K., Breusegem, F., De Mey, M. Towards a carbon-negative sustainable bio-based economy. Front Plant Sci. 2013;4:174.
[31] Lozanovski, A., Lindner, J.P., Bos, U. Environmental evaluation and comparison of selected industrial scale biomethane production facilities across europe. The International Journal of Life Cycle Assessment 2014;19(11):1823-1832.
[32] McKendry, P. Energy production from biomass (part 2): conversion technologies. Bioresource Technology 2002;83(1):47-54.
[33] Abuşoğlu, A., Demir, S., Kanoğlu, M. thermoeconomic analysis of a biogas engine powered cogeneration system. J. Of Thermal Science and Technology 2013;33(2):9-21.
[34] Kayişoğlu, B., Göncü, S. Determination of commercially available biogas production capacity and effects on methane capture in Tekirdağ province. Tekirdağ Ziraat Fakültesi Dergisi, 2020;17(3),445-455.
[35] Cebula, J., Chygryn, O., Chayen, S.V., Pimonenko, T. Biogas as an alternative energy source in Ukraine and Israel: current issues and benefits. Int. J. Environmental Technology and Management 2018;21(5/6):421–438.
[36] Rajendran, K., Aslanzadeh, S., Taherzadeh, M.J. Household biogas digesters– a review. Energies 2012;5:2911-2942.
[37] Şenol, H., Elibol, E.A., Açıkel, Ü., Şenol, M. Major organic waste sources in Ankara for biogas production. BEU Journal of Science 2017b;6(2):15-28.
[38] Anonymous [Internet]. Turkish statistic institution; 2021 [cited 2021 April 16]. Available from: https://www.tuik.gov.tr/
[39] Anonymous [Internet]. Republic of Turkey ministry of agriculture and forestry, bingöl animal data report; 2021 [cited 2021 April 12]. Available from: https://www.tarimorman.gov.tr/SGB/TARYAT/Belgeler/il_yatirim_rehberleri/Bingöl.pdf
[40] Anonymous [Internet]. Bingöl districts; 2021 [cited 2021 April 16]. Available from: https://tr.wikipedia.org/wiki/Dosya:Bing%C3%B6l_districts.png
[41] Avcıoğlu, A. O., Çolak, A., Türker, U. Biogas potential from chicken waste in Turkey. Journal of Tekirdag Faculty of Agriculture, 2013;10(1),21-28.
[42] Koca, H., Sever, R. Cow and sheep husbandry in Karlıova (Upper Göynük Village Area). Eastern Geographical Review 2006;11(16):165-192.
[43] Deniz, Y. Biogas potential and its benefits in Turkey. Ankara; 1987.
[44] Türkmenler, H., Varınca, K., Can, R. Final report of biogas workshop, Adıyaman University Faculty of Engineering; 2021 [cited 2021 April 27] Available from: https://biyoenerjidergisi.com/50-milyon-liralik-biyogaz-tesisi/.
[45] Salihoğlu, N.K., Teksoy, A., Altan, K. Determination of biogas production potential from cattle and sheep wastes: Balikesir case study. Omer Halisdemir University Journal of Engineering Sciences 2019;8(1):31-47.
[46] Lan, W., Chen, G., Zhu, X., Wang, X., Xu, B. Progress in techniques of biomass conversion into syngas. J Energy Inst 2015;88:151-156.
[47] Anonymous [Internet]. Calculation of 1 kWh electricity price; 2021 [cited 2021 May 1]. Available from: https://gazelektrik.com/faydali-bilgiler/1-kwh-elektrik-kac-tl
[48] Işık, S., Yıldız, C. Improving thermal energy storage efficiency of solar collector tanks by placing phase change materials in novel finned-type cells. Thermal Science and Engineering Progress, 2020;19,100618.
[49] Kılıçkap, S., Yıldız, C., Çakmak, G. Elazığ iklim koşullarında sıcak sulu güneş kolektörlerine ilişkin verimlerin araştırılması. Dicle Üniversitesi Mühendislik Fakültesi Mühendislik Dergisi, 2015;6(2),103-110.

Araştırma Makalesi https://doi.org/10.46810/tdfd.1036416 Research Article

Türk Doğa ve Fen Dergisi
Turkish Journal of Nature and Science
www.dergipark.gov.tr/tdfd

Investigation of *In Vivo* Effects of Carbon Tetrachloride (CCl_4) and Quercetin on Some Metabolic Enzyme Activities in Rat Erythrocyte

Yusuf YEMEL[1], Mahire BAYRAMOĞLU AKKOYUN[2], H.Turan AKKOYUN[3*], A.Şükrü BENGÜ[4], Fatma KARAGÖZOĞLU[5]

[1] Bingöl University, Solhan Vocational School, Medical Servıces and Technıques, Bingöl, Turkey
[2] Siirt University, Faculty of Veterinary Science, Department of Biochemistry, Siirt, Turkey
[3] Siirt University, Faculty of Veterinary Science, Department of Physiology, Siirt, Turkey
[4] Bingöl University, Vocational School of Health Services, Bingöl, Turkey
[5] Bingöl University, Faculty of Veterinary Science, Department of Zootechnıque And Anımal Nutrıtıon, Bingöl, Turkey
Yusuf TEMEL, ORCID No: 0000-0001-8148-3718
Mahire BAYRAMOĞLU AKKOYUN ORCID No: 0000-0001-5150-5402
H.Turan AKKOYUN ORCID No: 0000-0002-4547-8003
A.Şükrü BENGÜ ORCID No: 0000-0002-7635-4855
Fatma KARAGÖZOĞLU ORCID No:0000-0001-7970-0306

**Corresponding author: turanakkoyun@siirt.edu.tr*

(Received: 14.12.2021, Accepted: 18.02.2022, Online Publication: 25.03.2022)

Keywords
Carbon tetrachloride, Quercetin, Glucose 6-phosphate dehydrogenase, 6-phosphogluconate dehydrogenase, Glutathione reductase, Glutatyon S-transferaz.

Abstract: In the study; the purpose was to investigate the *in vivo* impact of carbon tetrachloride (CCl_4) and quercetin (Qu) on activities of important metabolic enzymes such as Glucose 6-phosphate dehydrogenase (G6PD), 6-phosphogluconate dehydrogenase (6PGD), glutathione reductase (GR) and glutathione S-transferase (GST) in rat erythrocytes. At the experimental stage, rats were divided into 4 groups. 1.Group (Control): Pure olive oil at a dose determined according to their body weight (1mL/kg) was given to the rats in this group, 2.Group (CCl4: 1.0 mL/kg (ip)(1:1), 3.Group (Ku: 25) mg/kg (ip), 4.Group (CCl4(1.0 ml/kg (ip)+ Ku (25 mg/kg (ip) was injected. The study was continued for 3 days. The results revealed that the activities of; G6PD ($p<0.01$), 6PGD ($p<0.01$), GR($p<0.001$) and GST ($p>0.05$) enzyme activities were decreased in the CCl_4 group compared to the control group. It was determined that enzyme activities were higher in CCl_4+Qu applied groups compared to CCl_4 group. The application of Qu caused an increase in the enzyme activity value. This can be accepted as an indication that the inhibition caused by CCI_4 has disappeared. Consequently; It is thought that Qu may be effective in preventing oxidative damage due to CCl_4 administration.

Sıçan Eritrositlerinde Karbon Tetraklorürün(CCl_4) ve Kuersetinin Bazı Metabolik Enzim Aktiviteleri Üzerine *İn Vivo* Etkisinin İncelenmesi

Anahtar Kelimeler
Karbon tetraklorür, Kuersetin, Glukoz 6-Fosfat Dehidrogenaz, 6-fosfoglukonat dehidrogenaz, Glutatyon redüktaz, Glutatyon S-transferaz.

Öz: Çalışmada; Sıçan eritrositlerinde karbon tetraklorür (CCl_4) ve Kuersetinin(Ku)'in, Glukoz 6-fosfat dehidrogenaz (G6PD), 6-fosfoglukonat dehidrogenaz (6PGD), glutatyon redüktaz (GR) ve glutatyon S-transferaz (GST) gibi önemli metabolik enzim aktiviteleri üzerine *in vivo* etkilerinin incelenmesi hedeflendi. Deneysel aşamada sıçanlar 4 gruba ayrıldı. 1.Grup(Kontrol): Bu gruptaki ratlara vücut ağırlıklarına göre belirlenen dozda(1 mL/kg)saf zeytin yağı, 2.Grup(CCl_4: 1.0 mL/kg (i.p.)(1:1), 3.Grup(Ku: 25 mg/kg (i.p),4.Grup(CCl_4(1.0 ml/kg (i.p.)+ Ku (25 mg/kg (i.p.) enjekte edildi.Çalışma 3 gün sürdürüldü. Sonuçlar değerlendirildiğinde; G6PD ($p<0,01$), 6PGD ($p<0,01$) GR ($p<0,001$) ve GST ($p>0,05$) enzim aktiviteleri kontrol grubuna oranla CCl_4 grubunda azalmıştır. CCl_4+Ku uygulanan gruplarda ise enzim aktivitelerinin CCl_4 grubuna oranla yüksek olduğu belirlenmiştir. Ku uygulanması, enzim aktivite değerinin yükselmesine neden olmuştur. Buda CCI_4'ün neden olduğu inhibisyonun ortadan kalktığının göstergesi olarak kabul edilebilir. Sonuç olarak, CCl_4 uygulamasına bağlı olarak ortaya çıkan oksidatif hasarı önlemede Ku'nın etkili olabileceği düşünülmektedir.

1. INTRODUCTION

Carbon tetrachloride (CCl_4) is a colorless, non-flammable, quickly evaporating, fragrant dense liquid, and is widely used in the production of petroleum products, varnishes, lacquers, resin solvents and organic compounds [1]. It is frequently used in dry cleaning, firefighting, grain disinfection and insect control [2]. Biologically inactive CCl_4 is transformed into reactive toxic metabolites for their activation and takes part in target cells [3,4,5]. CCl_4 exerts its toxic effect with the formation of a free radical, the trichloromethyl radical. The peroxyl radical, which is formed as a result of the combination of this radical with oxygen, is a strong lipid peroxidation initiator that plays a role as the primary mechanism in the formation of cell damage by disrupting the cell membrane structure [3,6,7,8]. Malondialdehyde (MDA), which is formed as the end product of lipid peroxidation, is frequently used in the determination of oxidative damage [9]. In CCl_4 poisoning; analogous to oxidative damage as an experimental model [10] (Figure 1).

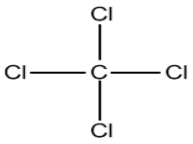

Figure 1. Molecular structure of carbon tetrachloride (CCl_4) [11].

Quercetin (Qu) is one of the most widely studied bioflavonoids in the flavonols class [12] and is one of the most common flavonoids found and many dietary sources [13]. Qu, occurs mainly in the leaves and other parts of the plant in the form of glycosides or aglycones formed by the attachment of one or more sugar groups to phenolic groups by glycosidic bonds. Qu has powerful anti-oxidative and cytoprotective impact on oxidant-induced endothelial cell apoptosis due to its chemical structure [12]. Qu, which is included in various herbal teas today; It is used in biochemistry, food chemistry, paint chemistry, medical chemistry, paint industry and cosmetics[14,15]. Qu, prevents oxidative damage and cell death by prohibit lipid peroxidation and scavenging free oxygen radicals [16,17]. Qu, exerts its possible biological properties through its antioxidant activity [18] (Figure 2).

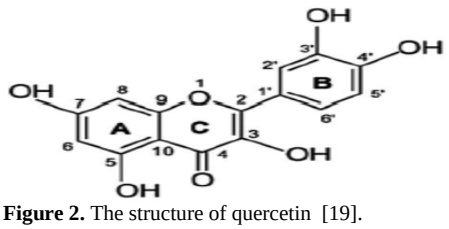

Figure 2. The structure of quercetin [19].

G6PD and 6PGD are known as metabolic enzymes that catalyze the first and third steps of the pentose phosphate pathway. As an agent that protects cells against oxidative stress, NADPH is known as an important molecule for biochemical processes such as reducing biosynthesis reactions [20,21]. NADPH is the most important molecule that reduces the disulfide form of glutathione, as well as being considered as a cellular reducer, which is significant for nitric oxide biosynthesis, detoxification of xenobiotics and pharmaceuticals [22-24]. GR preserve the cell counter the harmful effects of these molecules by reducing oxidized molecules thanks to the –SH groups in its construction. In addition, membrane proteins such as GSH, the reduced form of GR, hemoglobin and spectrin, and the preserve of thiol groups of various enzymes, DNA and protein synthesis, detoxification of xenobiotics and some metabolic end products, and transport of amino acids [25,26]. The GR enzyme catalyzes the regeneration reaction of glutathione in the presence of NADPH, thereby maintaining the intracellular redox balance [27]. The binding reactions of GSH to endogenous and exogenous hydrophobic electrophiles are carried out by GST isoenzymes. GSTs can non-catalytically bind many exogenous and endogenous compounds such as fatty acids, hormones, flavonoids, bilirubin and xenobiotics [28,29].The purpose of the presented study was to investigate the *in vivo* effects of CCl_4 and Qu treatments on some metabolic enzymes G6PD, 6PGD, GR and GST activities in rat erythrocytes.

2.MATERIALS AND METHODS

2.1.Chemicals

The chemicals used in the study were purchased from Sigma and Merck.

2.2. Experimental Design

Twenty-eight Wistar albino male rats weighing 200-300 g were used.They were fed ad-libitum with standard laboratory chow and water at a constant temperature of 20 ± 2ºC and twelve (12 hours) light-dark cycle (light; 07:00-19:00, dark 19:00-07:00). The rats were randomly divided into 4 groups of 7 in each group. The study was approved by the Bingol University Experimental Animal Ethics Committee. (BUHADEK: 4.10.2018-2018/08-08/01).

1. Group (Control): Pure olive oil i.p. given through in a dose determined according to the body weight of the rats (1 mL/kg) was given to the rats in this group [30].
2.Group (CCl_4): The rats in this group were mixed with 1 mL/kg of CCl4 in olive oil at a ratio of 1:1 and administered i.p. was applied as. [31].
3.Group (Qu): The rats in this group were administered i.p. at a dose of 25 mg/kg by using the stock solution prepared in dimethyl sulfoxide (DMSO) [32].
4.Group (CCl_4 + Qu): The rats in this group were administered 1 mL/kg CCl4 (1:1 in olive oil) + 25 mg/kg Qu (using the stock solution prepared in DMSO) i.p. At the end of the 3rd day, blood samples were taken from the rats under anesthesia.

2.3. Preparation of Hemolysate

Blood samples were taken into EDTA tubes. Fresh blood samples were taken into EDTA tubes. Afterwards, plasma and leukocytes were eliminated by centrifugation for 15 minutes (2500 xg). Red cells packed with KCl solution (0.16 M) were washed three times. Blood

samples were centrifuged at (2500 xg) and supernatants were discarded. Erythrocytes were hemolyzed using 5-fold distilled water. Samples were centrifuged at +4°C (10000 xg) for 30 minutes to eliminated cell membranes and insoluble molecules. The supernatant was saved for analysis [33].

2.4. Determination of Enzyme Activities

G6PD and 6PGD enzyme activity was measured spectrophotometrically according to the Beutler method at 340 nm. This method is based on the principle that NADPHs in the reaction medium absorb light at 340 nm. In reactions catalyzed by both G6PD and 6PGD, enzymes react with $NADP^+$ as a co-substrate and convert to NADPH. This increase is followed spectrophotometrically, the amount of absorption per minute is found and converted into enzyme units [34-36]. The method proposed by Carlberg and Mannervik was used for the measurement of GR enzyme activity. This method depends on the reduction of NADPH in the reaction catalyzed by the GR enzyme. This decrease was monitored by spectrophotometry at 340 nm to determine enzyme activity [37] and the activity of the GST enzyme was determined according to the Habig method. This method is based on the conversion of 1-chloro-2,4-dinitrobenzene (CDNB) to S-glutathione dinitrobenzene (DNB-SG). The product of this reaction, DNB-SG, shows maximum absorbance at 340 nm [38].

3. STATİSTİCAL ANALYSİS

Statistical evaluation was made using the SPSS 20 program. Data were expressed as mean ± SD. The Kruskal Wallis test followed by the Mann Whitney U test was used to define the diverse among the groups. The diverse among the groups was remerkable important when $p< 0.05$.

4. RESULTS AND DISCUSSION

According to the results of the current study; G6PD enzyme activity was statistically lower in the CCl_4 group compared to the control group ($p<0.01$). Qu applied group; G6PD enzyme activity was found close to the control group.In the CCl_4+Qu group, the G6PD enzyme activity was discover to be higher than the CCl_4-treated group (Figure 3)

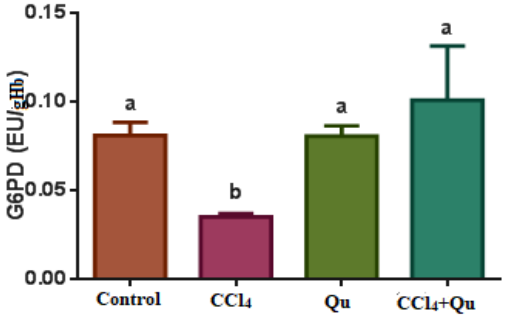

Figure 3. The in vivo effect of CCl_4 and Qu on rat erythrocyte G6PD enzyme activity (a,b differs between groups with different letters) ($p<0.01$).

When the 6PGD enzyme activity was assessed, a statistically significant reduction was observed in the CCl_4 treated group compared to the control group ($p<0.01$). The 6PGD enzyme activity was found to be higher in the Qu-treated group than in the CCl_4 group. Enzyme activity rised in CCl_4+Qu group compared to CCl_4 group. These results show that Qu reduces the inhibitory effects of CCl_4 on 6PGD enzyme activity(Figure 4).

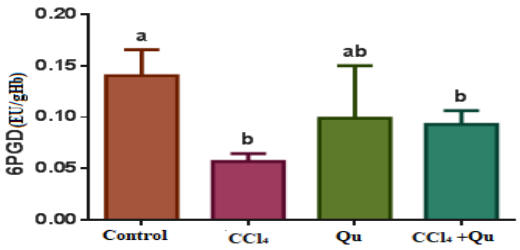

Figure 4. In vivo effect of CCl_4 and Qu on rat erythrocyte 6PGD enzyme activity (a,b, difference between groups with different letters) ($p<0,01$).

When the GR enzyme activity is evaluated; it was observed that the enzyme activity was reduced in the CCl_4 applied group compared to the control group($p<0,001$). In the CCl_4 +Qu applied group, it was identified that the GR enzyme activity was increased compared to the CCl_4 group (Figure 5).

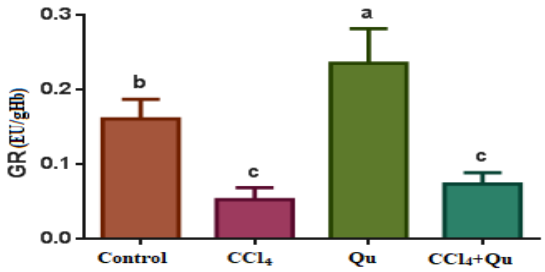

Figure 5. In vivo effect of CCl_4 and Qu on rat erythrocyte GR enzyme activity (a,b,c there is difference between groups with different letters) ($p<0,001$).

When the GST enzyme activity was assessed; it was determined that there was a decrease in the CCl_4 group compared to the control group, and a partial increase was observed in the CCl_4+Qu group compared to the CCl_4 group. No statistical differences were discovered between the groups ($p>0,05$) (Figure 6).

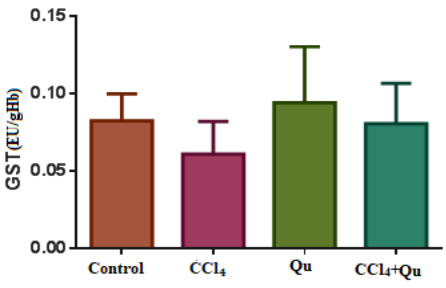

Figure 6. In vivo effect of CCl_4 and Qu on rat erythrocyte GST enzyme activity ($p>0,05$).

When the results of this study are evaluated in general; G6PD, 6PGD and GR enzyme activities are inhibited by CCl_4. As a result of prevention of G6PD and 6PGD enzyme activities, cells cannot produce enough NADPH in the pentose phosphate pathway to detoxify endogenous and exogenous oxidized molecules. At the same time, inhibition of GR and GST enzyme activities may cause disruption in intracellular GSH metabolism, thus rendering cells vulnerable to oxidative stress. In the study; G6PD enzyme activity was decreased in CCl_4 group compared to control group ($p<0.01$). Enzyme activity in the Qu group was discover to be close to the control group. In the CCl_4+Qu group, the enzyme activity was discover to be higher than in the CCl_4 group. This suggests that quercetin may have a decreasing effect on the inhibition of CCl_4 in G6PD enzyme activity. When 6PGD enzyme activity is evaluated; The decrease in enzyme activity ($p<0.01$) in the group treated with CCl_4 compared to the control group can be considered as an indicator of inhibition of the 6PGD enzyme by CCl_4 application. The rise in the enzyme activity value in the CCl_4+Qu applied group can be considered as an indication that the inhibition effect is partially eliminated. While it was observed that GR enzyme activity reduction statistically important ($p<0.001$) in the carbon tetrachloride group compared to the control group, it was concluded that the enzyme activity increased partially in the CCl_4 +Qu administered group. When the GST enzyme activity was assesment, a partial reduction was determined in the CCl_4 group compared to the control group. It was seen that the increases or decreases between the groups were not statistically significant. In the literature review, no study was found that examined the effects of CCl_4 and Qu on metabolic enzymes in rat erythrocytes. In a different study, it was determined that carbon tetrachloride (CCl_4) intoxication caused a decrease in enzyme activities such as NADPH-cytochrome c reductase, NADH-cytochrome reductase, coumarin hydroxylase, 7-ethoxy coumarin-O-deethylase, UDP-glucuronyl transferase and glutathione-S-transferase [39]. In a different study by Sheweita et al., it was determined that CCl_4 application caused inhibition of GST enzyme activity [40]. In a study by Elbe et al., the antioxidative effects of Qu in CCl_4-caused cardiac detriment were histologically and biochemically investigated. While SOD activity were remarkably declined in CCl_4 administered group, Qu administration caused considerable rise in SOD activity. In CCl_4 toxicity, it was concluded that the use of Qu could provide beneficial effects owing to its antioxidative properties [41]. In a different study investigating the antioxidant defense system in tissue damage caused by CCl_4 and ethyl alcohol in goose liver and kidneys, which are among the important antioxidant and metabolic enzymes due to damage to the liver and kidneys, glutation peroxidase(GSH-Px), catalase (CAT),glucose-6-phosphate dehydrogenase (G6PD) activities were decreased [42]. In a different study by Jeon et al., it was reported that carbon tetra chloride administration caused a decrease in the activities of important metabolic enzymes glutathione S-transferase and glutathione reductase in the rat liver [43]. In a different study researchers evaluated teh effects of CCl_4 and Qu treatment. They demonstrated that Qu isolated from *Delonix elata* L. plant has significant prophylactic effects on liver function markers AST, ALT, ALP, serum bilirubin and total protein, as well as antioxidant enzymes SOD, CAT, GPx and GST [44]. Literature also stated that after CCl_4 exposure, antioxidant enzyme activities such as SOD, CAT and GPx decreased significantly in the rat kidney, CCl_4 exposure caused oxidative stress by inhibiting antioxidant enzyme activities [45]. There are many other studies revealing various drugs and substances inhibit activities of metabolic enzymes [46-48].

5. CONCLUSION

When the results of this study are evaluated in general; G6PD, 6PGD and GR enzyme activities are inhibited by CCl4. In the CCl_4+Qu applied groups, the enzyme activities were higher than the CCl_4 group. While the GST enzyme activity decreased in the CCI4-administered group, it partially increased in the Qu-treated group. These results indicated that Qu reduces the inhibition impact of CCl_4 on G6PD, 6PGD and GR enzyme activities. Accordingly, it is thought that Qu may be effective in preventing oxidative damage due to CCl_4 administration. At the same time, there is a need for further studies in which different Quercetin dosages will be used.

CONFLICTS OF INTEREST

There is no conflict between the authors.

REFERENCES

[1] Vural DF. Karbontetraklorür (CCl_4) Uygulanmış Sıçanların Gastrocnemius Kasına Melatoninin Etkisi. Ankara Üniversitesi Fen Bilimleri Enstitüsü. Yüksek Lİsans Tezi.2015.

[2] Akkoyun-Bayraoğlu M**,** Akkoyun HT. Effect Of Carbon Tetrachlorıde (CCl_4) And Ellagıc Acıd On Rat Erythrocyte G6PD, 6PGD, GR, GST AND TrxR Enzyme Actıvıtıes. Fresenius Environmental Bulletin. 2019;28(9), 6779-6785

[3] Akkuş İ. Serbest Radikaller ve Fizyopatolojik Etkileri. Mimoza Yayınları, Konya.1995.

[4] Murray RK, Mayes PA, Granner DK, and Rodwell VW. Harper'ın Biyokimyası. Barış Kitapevi. 1993.

[5] Kayaalp O. Rasyonel Tedavi Yönünden Tıbbi Farmakoloji. 10. Baskı, Hacettepe Taş. 2002.

[6] Kurt H, Başaran A, Musmul A. Sıçanlarda Karbon Tetraklorit (CCl_4)'in Oluşturduğu Oksidatif Stresin Kateşin ile Önlenmesi. Kocatepe Tıp Dergisi. 2004; 5(2),29-34.

[7] León OS, Menéndez S, Merino N, Castillo R, Sam S, Pérez L, Cruz E, Bocci V. Ozone oxidative preconditioning: a protection against cellular damage by free radicals. Mediators Inflamm. 1998;7(4),289-94.

[8] Süha-Yalçin A, Koçak-Toker N, Uysal M, Aykaç G, Sivas A, Oz H. Stimulation of lipid peroxidation and impairment of glutathione-dependent defence system in the liver of rats repeatedly treated with

carbon tetrachloride. J Appl Toxicol. 1986; 6(4),303-6.
[9] Tekeli H,Bildik A. Karbon Tetraklorür İle Oluşturulan Karaciğer Hasarında Glutatyon (GSH) Ve Glutatyon S-Transferaz (GST) Aktivitesi Üzerine N-Asetil Sisteinin Etkisi. Balikesir Saglik Bil Derg. 2016; 5(2).
[10] Akkoyun HT, Bengü AŞ,Ulucan A,Bayramoğlu-Akkoyun M,Arihan O. Protectıve Effect Of Ellagıc Acıd Agaınst Carbon Tetrachlorıde (CCl_4) Induced Oxıdatıve Braın Injury In Rats. Fresenius Environmental Bulletin. 2018; 27(5),3148-3155.
[11] Demiralp T. Sıçanlarda Karbon Tetraklorürün (CCl_4) Böbrekte Oluşturduğu Hasara Karşı Dekspantenolün (Provitamin B5) Koruyucu Etkisinin Biyokimyasal Açıdan Araştırılması. Yüksek Lisans Tezi-2021. T.C. İnönü Üniversitesi. Sağlık Bilimleri Enstitüsü.
[12] Choi YJ, Kang JS, Park JH, Lee YJ, Choi JS, Kang YH. Polyphenolic flavonoids differ in their antiapoptotic efficacy in hydrogen peroxide treated human vascular endothelial cells. J Nutr. 2003;133,985–991.
[13] Pavanato A, Tunon MJ, Sanchez-Campos S, Marroni CA, Llesuy S, Gonzalez- Gallego J, Marroni N. Effects of quercetin on liver damage in rats with carbon tetrachloride-induced cirrhosis. Digestive Diseases and Sciences. 2003;48(4), 824-829.
[14] Ergüzel ET. Quercetin (3, 3', 4', 5, 7-pentahidroksiflavon)'in Bakır (II) ve Çinko (II) Komplekslerin Kararlılık Sabitlerinin Tayini. Yüksek Lisans. İstanbul: Marmara Üniversitesi. 2006.
[15] Emek H. Dönmez Burukoğlu D. Bayçu C, Musmul A. Erişkin erkek sıçanlarda karbon tetraklorür ile oluşturulan testis hasarı üzerine kuersetinin etkisi, Osmangazi Tıp Dergisi. 2017;39(65-73).
[16] Cho JY, Kim IS, Jang YH, Kim AR, Lee SR. Protective effect of quercetin, a natural flavonoid against neuronal damage after transient global cerebral ischemia. Neurosci Lett. 2006;404(3),330–335
[17] Schültke E, Kamencic H, Zhao M, Tian GF, Baker AJ, Griebel RW, Juurlink BH. Neuroprotection following fluid percussion brain trauma: a pilot study using quercetin. J Neurotrauma. 2005;22(12),1475–1484
[18] Terao J,Piskula M. Flavonoids as inhibitors of lipid peroxidation in membranes. In: Flavonoids in Health and Disease. Rice-Evans, C. and Packer, L., eds. Marcel Dekker: New York. 1998; 277–93.
[19] Mitchell LJ. Spectrophotometry of Molybdenum, Tungsten and Chromium chelates of quercetin. PhD Thesis, Oregeon State University: USA. 1965.
[20] Temel Y, Ayna A, Hamdi Shafeeq I, Ciftci M. *In vitro* effects of some antibiotics on glucose-6-phosphate dehydrogenase from rat (*Rattus norvegicus*) erythrocyte. Drug Chem Toxicol. 2020;43(2),219-223.
[21] Temel Y, and Kocyigit U M. Purification of glucose-6-phosphate dehydrogenase from rat (Rattus norvegicus) erythrocytes and inhibition effects of some metal ions on enzyme activity, Journal of biochemical and molecular toxicology. 2017; 31(9),e21927.
[22] Krebs HA. and Eggleston LV. The regulation of the pentosephosphate cycle in rat liver. In: G. Weber, ed. Advances in Enzyme Regulation. Oxford: Pergamon Press Ltd. 1978; 12, 421–433.
[23] Nelson DL and Cox MM. Lehninger Principles of Biochemistry. 4th ed. New York: WH. Freeman & Co, ABD. 2005; 558–561.
[24] Stanton RC. Glucose-6-phosphate dehydrogenase, NADPH, and cell survival. IUBMB Life. 2012; 64 (5), 362–369
[25] Temel Y, Bozkuş T, Karagözoğlu Y, Çiftci M. "Glutatyon Redüktaz (GR) Enziminin Japon Bıldırcın (Coturnix coturnix japanica) Eritrositlerinden Saflaştırılması ve Karakterizasyonu." Iğdır Univ. J. Inst. Sci. Tech. 2017; 7(3),143-150.
[26] Ballatori N, Krance SM, Notenboom S, Shi S, Tieu K, Hammond CL. Glutathione dysregulation and the etiology and progression of human diseases. Biol. Chem. 2009;390, 191–214,
[27] Couto N, Wood J, Jill B. "The role of glutathione reductase and related enzymes on cellular redox homoeostasis network." Free radical biology and medicine. 2016; 95, 27-42.
[28] Işık M, Demir Y, Kırıcı M, Demir R, Şimşek F, Beydemir Ş. Changes in the anti-oxidant system in adult epilepsy patients receiving anti-epileptic drugs. Archives of physiology and biochemistry. 2015; 121(3), 97-102.
[29] Temel Y, Koçyigit UM, Taysı MŞ, Gökalp F, Gürdere MB, Budak Y, Çiftci M. Purification of glutathione S-transferase enzyme from quail liver tissue and inhibition effects of (3aR, 4S, 7R, 7aS)-2-(4-((E)-3-(aryl) acryloyl) phenyl)-3a, 4, 7, 7a-tetrahydro-1H-4, 7-methanoisoindole-1, 3 (2H)-dione derivatives on the enzyme activity. Journal of biochemical and molecular toxicology. 2018; 32(3), e22034.
[30] Karaca Ö, Pekmez H, Kuş MA, Akpolat N, Ögetürk M, Kuş İ. Deneysel Karbon Tetraklorür Toksisitesi Sonucu Karaciğerdeki IŞP70 İmmunoreaksiyon Artışı Üzerine Melatonin Hormonunun Etkisi. F.Ü.Sağ.Bil.Tıp Derg. 2011; 25 (2): 73 - 76.
[31] Makni M, Chtourou Y, Garoui EM, BoudawaraT, Fetoui H. Carbon tetrachloride- induced nephrotoxicity and DNA damagein rats: Protective role of vanillin. Human and Experimental Toxicology. 2012; 31, 844-852.
[32] Yuan Y, Ma S, Qi Y, Wei X, Cai H, Dong L, Guo Q. Quercetin inhibitedcadmium-induced autophagy in the mouse kidneyvia inhibition of oxidative stress. Journalof Toxicologic Pathology. 2016; 29(4), 247-252.
[33] Bayramoğlu-Akkoyun M, Bengü AŞ, Temel Y, Akkoyun HT, Ekin S, Ciftci M. The effect of astaxanthin and cadmium on rat erythrocyte G6PD, 6PGD, GR, and TrxR enzymes activities in vivo and on rat erythrocyte 6PGD enzyme activity in vitro. J Biochem Mol Toxicol. 2018;32(8),e22170.

[34] Beutler E. Redcell metabolism. Manual of biochemical methods Acad Pres London. 1971;12,68–70.
[35] Bayindir S, Temel Y, Ayna A, Ciftci M. The synthesis of N-benzoylindoles as inhibitors of rat erythrocyte glucose-6-phosphate dehydrogenase and 6-phosphogluconate dehydrogenase. Journal of biochemical and molecular toxicology. 2018; 32(9), e22193.
[36] Bayindir S, Ayna A, Temel Y, Ciftci M. The synthesis of new oxindoles as analogs of natural product 3,3-bis(indolyl) oxindole and *in vitro* evaluation of the enzyme activity of G6PD and 6PGD. Turkish Journal of Chemistry. 2018b;42(2),332-345.
[37] Carlberg I, Mannervik B.Purification and characterization of glutathione reductase from calf liver. Glutathione reductase assays. Methods Enzymol. 1981;113,484-4.
[38] Habig WH, Pabst MJ, Jakoby WB. Glutathione S-transferases the first enzymatic step in mercapturic acid formation. Journal of Biological Chemistry. 1974; 249(22), 7130-719.
[39] Kumaravelu, P, Dakshinamoorthy DP, Subramaniam S, Devaraj H, Devaraj NS. Effect of eugenol on drug-metabolizing enzymes of carbon tetrachloride-intoxicated rat liver. Biochemical pharmacology. 1995; 49(11), 1703-1707.
[40] Sheweita SA, Abd El-Gabar M, Bastawy M. Carbon tetrachloride-induced changes in the activity of phase II drug-metabolizing enzyme in the liver of male rats: role of antioxidants. Toxicology. 2001; 165(2-3), 217-224.
[41] Elbe H, Eşrefoğlu M, Taslidere A, Taşlıdere E, Ateş B. Sıçanlarda karbon tetraklorür ile indüklenen kardiyak hasar üzerine melatonin ve quercetin'in tedavi edici etkileri. İnönü Üniversitesi Turgut Özal Tıp Merkezi Dergisi. 2016; 23(2), 171-176.
[42] Güven A. and Yılmaz S. The effect of carbon tetrachloride (CCl_4) and ethanol (C_2H_5OH) on the determination of levels glutathione peroxidase, catalase, glucose-6-phosphate dehidrogenase and lipid peroxidation liver and kidney in the goose. Kafkas Üniversitesi Veteriner Fakültesi Dergisi. 2005; 11(2), 113-117.
[43] Jeon TI, Hwang SG, Park NG, Jung YR, Im Shin S, Choi SD, Park DK. Antioxidative effect of chitosan on chronic carbon tetrachloride induced hepatic injury in rats. Toxicology. 2003; 187(1), 67-73.
[44] Krishnappa P, Venkatarangaiah K, Rajanna S, Kumar S, Kashi Prakash Gupta R. Antioxidant and prophylactic effects of Delonix elata L., stem bark extracts, and flavonoid isolated quercetin against carbon tetrachloride-induced hepatotoxicity in rats. BioMed Research International. 2014;1155-507851
[45] Akkoyun HT. Karbontetraklorür'ün Neden Olduğu Sıçan Böbrek Dokusu Hasarlarına Karşı Kuersetin'in Koruyucu Etkisi. Journal of the Institute of Science and Technology.2019;9(2),708-716.
[46] Ayna A, Khosnaw L, Temel Y, Ciftci M. Antibiotics as Inhibitor of Glutathione S-transferase: Biological Evaluation and Molecular Structure Studies. Current drug metabolism.2021; 22(4), 308-314.
[47] Ayna A, Moody PC. Crystal structures of a dual coenzyme specific glyceraldehyde-3-phosphate dehydrogenase from the enteric pathogen Campylobacter jejuni. Journal of Molecular Structure.2021;1242, 130820.
[48] Ayna A, Moody PC. Activity of fructose-1, 6-bisphosphatase from Campylobacter jejuni. Biochemistry and Cell Biology.2020; 98(4), 518-524.

Araştırma Makalesi https://doi.org/10.46810/tdfd.1038341 Research Article

Türk Doğa ve Fen Dergisi
Turkish Journal of Nature and Science
www.dergipark.gov.tr/tdfd

Determination of Some Yield Features of Foreign-Origin Alfalfa Cultivars (*Medicago sativa* L.) in Bingöl Conditions

Sanaz YARYAB [1*], Erdal ÇAÇAN [2]

[1] Bingöl University, Institue of Science, Departmen of Field Crops, Bingöl, Türkiye
[2] Bingöl University, Vocational School of Food, Agriculture and Livestock, Department of Crop and Animal Production, Bingöl, Türkiye
Sanaz YARYAB ORCID No: 0000-0002-7139-3900
Erdal ÇAÇAN ORCID No: 0000-0002-9469-2495

**Corresponding author: 1811042002@bingol.edu.tr*

(Received: 18.12.2021, Accepted: 28.12.2021, Online Publication: 25.03.2022)

Keywords
Alfalfa,
Stems number,
Stem thickness,
Green forage yield,
Dry matter yield

Abstract: This study was carried out to determine the some yield features of foreign origin alfalfa cultivars in Bingöl ecological conditions. In the research, a total of 15 alfalfa cultivars,12 of them are from foreign-origin (Iside, Osjecka 99, Ezzelina, Diane, Prosementi, Queen, Emiliana, Rivierea Vicentina, Banat vs, La Torre, Sabrina and Escorial) and 3 of them are standard (Elci, Bilensoy 80 and Basbag) cultivars were used as plant material. In the research; plant height, number of stems, stem thickness, green forage yield and dry matter yield were investigated. Average plant height was 97.6 cm, number of stems was 15.8, stem thickness was 2.80 mm, forage yield was 11018 kg da^{-1} and dry matter yield was 3228 kg da^{-1}. In line with these parameters examined, it has concluded that Ezzelina and Emiliana cultivars showed superior characteristics in Bingöl province.

Bingöl Koşullarında Yurtdışı Kaynaklı Yonca Çeşitlerinin (*Medicago sativa* L.) Bazı Verim Özelliklerinin Belirlenmesi

Anahtar Kelimeler
Yonca,
Sap sayısı,
Sap çapı,
Yeşil ot verimi,
Kuru ot verimi

Öz: Bu çalışma, Bingöl ekolojik koşullarında bazı yabancı orijinli yonca çeşitlerinin ot verimini belirlemek amacıyla yürütülmüştür. Araştırmada 12'si yabancı-orijinli (Iside, Osjecka 99, Ezzelina, Diane, Prosementi, Queen, Emiliana, Rivierea Vicentina, Banat vs, La Torre, Sabrina ve Escorial) ve 3'ü de standart çeşit (Elçi, Bilensoy 80 ve Başbağ) olmak üzere toplam 15 yonca çeşidi bitkisel materyal olarak kullanılmıştır. Araştırmada; bitki boyu, sap sayısı, sap çapı, yeşil ot verimi ve kuru ot verimi incelenmiştir. Ortalama bitki boyu 97,6 cm, sap sayısı 15,8, sap çapı 2,80 mm, yeşil ot verimi 11018 kg da^{-1} ve kuru ot verimi 3228 kg da^{-1} olarak tespit edilmiştir. İncelenen bu parametreler doğrultusunda Bingöl ilinde Ezzelina ve Emiliana çeşitlerinin üstün özellikler gösterdiği sonucuna varılmıştır.

1. INTRODUCTION

Fodder (forage) crops farming has great importance in developed countries, and these countries allocate a significant portion of their agricultural land to forage crop farming. For example, the ratio allocated to forage crops in the total field land are 49.8% in Australia, 36.5% in Germany, 31.4% in the Netherlands; 25.8% in France, 25.4% in England and 23.0% in the USA [1].

Alfalfa has large cultivation areas in many countries of the world and is defined as the queen of forage crops because have a high adaptability, long life, can be cut many times in a vegetation period, high yield, high nutritional value, so alfalfa is distinguished from other forage crops. Alfalfa is rich in protein, as well as vitamins such as carotene (provitamin A) and tocopherol (vitamin E). With the help of deep root, alfalfa easily benefits from water and plant nutrients found in deep areas that other plants could not use. Alfalfa leaves a nitrogen-rich soil for the next plant in its root nodosities [2].

Alfalfa naturally found in almost every region of Turkey. Cultivation of alfalfa has become increasingly common in recent years. This situation makes it necessary to research and adapt new varieties for our country besides existing alfalfa varieties. In forage

crops and especially alfalfa because mentioned reasons, it has become compulsory to develop new varieties. To increase the number of registered varieties by conducting regional adaptation studies especially after the enactment of the Pasture Law No. 4342, in Turkey important developments have taken place in terms of agriculture and forage crops [3].

In the previous studies; plant height was 59.8-76.3 cm in the first year and 90.0-121.3 cm in the second year of the Elci cultivar of alfalfa. In the first and second years of the study, the ztotal green forage yield was 6284-9159 kg da^{-1} and 7538-10715 kg da^{-1} [4].

In a three-year study examining the yield characteristics of 8 alfalfa cultivars in Ankara conditions; it has been reported that the green forage yield was determined as 7907-11140 kg da^{-1} and dry matter yield was determined as 2619-3615 kg da^{-1} [5].

In order to determine the suitable alfalfa varieties for the Eastern Anatolia region, 16 different alfalfa varieties have compared from aspect of yield and quality features in Bingöl conditions. The study has conducted in randomized block design with three replications during three years between 2014 and 2016. According to the results of the research, plant height values of alfalfa cultivars were 41.9-54.7 cm, forage yields were 2735-3591 kg da^{-1} and dry matter yields were 924-1227 kg da^{-1} [6].

The study has conducted in Bornova and Odemiş ecological conditions 2006 and 2007 years with four different alfalfa genotypes, it has found that there were significant differences from the aspect of genotypes between locations. The researchers determined that the forage yield was 9769-12235 kg da^{-1}, dry matter yield was 2078-2862 kg da^{-1}, plant height was 77.1-86.8 cm, main stem was 13.14-15.57, the main stem thickness was 3.57-3.99 mm in Odemiş condition and the forage yield was 9260-11832 kg da^{-1}, dry matter yield was 1984-2601 kg da^{-1}, plant height was 70.8-76.1 cm, main stem was 12.74-14.22 and main stem thickness was 2.84-3.12 mm in Bornova conditions [7].

The research conducted in order to determine the yield and quality characteristics of some perennial warm season legume forage crops in Adana region in the irrigated conditions the Nimet variety of alfalfa was used, the average plant height was 69.2 cm, the green forage yield was 5094.5 kg da^{-1} and dry matter yield was 1135 kg da^{-1} [8].

The aim of this study is to determine some yield features of foreign-origin alfalfa cultivars in Bingöl ecological conditions.

2. MATERIAL AND METHOD

2.1. Material

This research has conducted in Bingöl University Genc Vocational School's Application and Research Area between 2019 and 2021, under watery conditions and for two years. Genc is a town and district of Bingöl Province in the Eastern Anatolia Region of Turkey. Totally 15 alfalfa cultivars have been used in the study, 12 of which were of foreign origin (Iside, Osjecka 99, Ezzelina, Diane, Prosementi, Queen, Emiliana, Riviera vicentina, Banat vs, La Torre, Sabrina and Escorial) and the remaining 3 were used as standard (Elci, Bilensoy 80 and Basbag) and native ones.

When look at the data of climate, monthly average temperature value was 13.8-14.2 ^{0}C, total precipitation was 839.2-668 mm and relative humidity was 51.9-48.5% for 2020 and 2021. It has observed that the average temperature values for the years 2021 and 2022 are above the long-years average, while the precipitation amounts and relative humidity values are below the long-years averages.

Analysis of soil samples taken from 10 different points and 0-30 cm depth of the research location has carried out in "Bingöl University Faculty of Agriculture, Soil Science and Nutrition Department Laboratory". The soil structure of the research location was found to be sandy, clayey and loamy (clay rate 19.11%, silt rate 16.71% and sand rate 64.18%), pH level neutral (7.10), salt-free, less limy, organic matter and available phosphorus ratios low, potassium content sufficient determined.

2.2. Method

The field experiment has carried out in August 2019 following the soil preparation made in July. The research will be set up with 3 replications according to the randomized blocks trial pattern. In the experiment, parcel lengths were 5 m, the distance between rows was 20 cm and 6 rows were planted in each parcel. 3 kg of seed has be used per decare in planting. Fertilizer was given directly to the decare on the basis of pure substance before planting. Irrigation of the experiment has done by sprinkler irrigation.

The plant height (cm), the distance between the first bud until the soil surface was measured with a ruler. The stem thickness (cm) of the first plants that form flower bud has measured with a caliper between the second and third node in 10 plants. For determining the number of main stems, 10 plants have selected in each parcel. The stems emerging of the determined 10 plant roots have counted, the average number of stems was determined by taking the average per cultivar.

Green forage yield (kg da^{-1}) located 1 row further from the top of the parcel and 1 row from the bottom of the parcel, and 0.5 m from the edges has removed from the

parcel. The remaining area was harvested by cutting and the green forage yield obtained from each parcel was weighed and the values were obtained were converted to yield per decare. A sample of 0.5 kg of forage obtained from each parcel have randomly taken and dried in a drying chamber at 70 ^{0}C for 48 hours in drying chamber. Then it has been kept in drying chamber for 24 hours and then weighed so the dry herbage weight has been found then the obtained dry matter has been converted to yield per decare.

The data that have been obtained have been evaluated by variance analysis with the help of the JMP statistical package program (a software belonging to the SAS program), and the differences of the groups have been compared with the Tukey test.

3. RESULTS AND DISCUSSION

3.1. Plant Height (cm)

Two-year averages of plant heights of foreign origin alfalfa cultivars and groupings of these averages have given in Table 1. As seen in Table 1, the difference between the plant heights of alfalfa cultivars was significant in terms of years and cultivars (P≤0.01), in terms of year x cultivar interaction was determined to be insignificant. In terms of cultivars, the highest plant height cultivar is Emiliana (106.2 cm), it has seen that other cultivars except Basbag and Sabrina cultivars are in the same group statistically. The lowest plant height was determined in Basbag (87.6 cm) and Sabrina (90.8 cm) cultivars. In terms of years, the average plant height (100.9 cm) determined in 2021 higher than the average plant height determined in 2020 (94.4 cm).

Table 1. Plant heights of alfalfa cultivars (cm)

Cultivars Name	2020	2021	Mean
Banat vs	98.7^{ns}	99.3	99.0 abc**
Basbag	86.6	88.7	87.6 c
Bilensoy 80	96.7	103.3	100.0 abc
Diane	92.1	101.9	97.0 abc
Elci	93.8	106.2	100.0 abc
Emiliana	108.8	103.5	106.2 a
Escorial	87.4	98.6	93.0 abc
Ezzelina	97.4	109.8	103.6 ab
Iside	87.4	105.7	96.6 abc
La Torre	91.2	97.4	94.3 abc
Osjecka 99	90.8	97.4	94.1 abc
Prosementi	99.9	103.9	101.9 abc
Queen	93.5	102.3	97.9 abc
Riviera vicentina	104.7	100.7	102.7 ab
Sabrina	86.2	95.3	90.8 bc
Mean	94.4 B**	100.9 A	97.6

CV(%): 7.50%, **(P≤0.01), ns: none significant

When look at the previous studies on the plant height in alfalfa; it has been reported that it is detected between 79-100 cm in Bornova conditions [9], 57.70-79.40 cm in Northern Cyprus conditions [10], 74.8-86.8 cm in Izmir conditions [11], 85.10-93.20 cm in Tokat-Kazova conditions [12], 66.61-101.28 cm in Antalya conditions [13], 80.33-103.22 cm in Goller Region [14], 76.3-90 cm in Yozgat ecological conditions [15] and 59.3-109.3 cm in Bingöl conditions [16]. It is seen that the 87.6-106.2 cm alfalfa height obtained in this study is close and similar to the plant heights obtained in these studies.

3.2. Stem Number

Two-year averages of plant heights of foreign origin alfalfa cultivars and groupings of these averages have given in Table 2. As seen in Table 2, the difference between the stem number of alfalfa cultivars was determined to be insignificant in terms of year, cultivar and year x cultivar interaction. The average number of stems of the cultivars is between 14.9-18.3 and the average is 16.1 in the first year, between 12.3-17.9 and the average is 15.4 in the second year. As the average of two years, it changed between 13.8-18.1 and the average two years were obtained as 15.8.

Table 2. The stem number of alfalfa cultivar (number)

Cultivars	2020	2021	Mean
Banat vs	15.3^{ns}	16.4	15.8^{ns}
Basbag	17.2	16.0	16.6
Bilensoy 80	16.3	14.1	15.2
Diane	16.2	16.2	16.2
Elci	15.1	15.0	15.1
Emiliana	14.9	14.5	14.7
Escorial	16.7	17.7	17.2
Ezzelina	15.2	14.7	14.9
Isıde	16.8	14.2	15.5
La Torre	16.7	15.1	15.9
Osjecka 99	18.3	17.9	18.1
Prosementi	16.6	16.1	16.4
Queen	16.2	16.1	16.1
Riviera vicentina	15.2	12.3	13.8
Sabrina	15.2	15.3	15.3
Mean	**16.1^{ns}**	**15.4**	**15.8**

CV(%): 19.4%, ns: none significant

Regarding to previous studies in alfalfas stem number, Soya and Kavut [17] have determined between 12.1-12.4 in Bornova conditions, Kir ve Soya [11] have presented the between 11.3-18.5 in Izmir conditions, Mohammed [18] has found 10.6-25.8 in Ankara and Konya conditions, Demiroglu et al. [19] have found 11.3-11.9 in Bornova and Odemis conditions and Kavut et al. [7] have determined between 12.9-14.9 in Izmir conditions. In this study the average number of stems has obtained between 13.8-18.1 is similar to results that mentioned in above researches.

3.3. Stem Thickness (mm)

Two-year averages of stem thickness of foreign origin alfalfa cultivars and groupings of these averages have given in Table 3. As seen in Table 3, the difference between the stem thicknesses of alfalfa cultivars is significant in terms of year and cultivar (P≤0.01), in terms of year x cultivar interaction was determined to be insignificant.

Table 3. The stem thickness of alfalfa cultivars (mm)

Cultivars	2020	2021	Mean
Banat vs	2.76^{ns}	3.28	3.02 ab**
Basbag	1.98	2.52	2.25 c
Bilensoy 80	2.15	3.10	2.63 bc
Diane	2.55	3.08	2.82 abc
Elci	2.36	3.11	2.73 abc
Emiliana	3.34	3.28	3.31 a
Escorial	2.46	2.64	2.55 bc
Ezzelina	2.78	2.96	2.87 abc
Isıde	2.56	3.05	2.81 abc
La Torre	2.33	2.78	2.56 bc
Osjecka 99	2.60	3.53	3.06 ab
Prosementi	2.87	2.74	2.81 abc
Queen	2.67	2.74	2.70 abc
Riviera vicentina	3.13	3.14	3.13 ab
Sabrina	2.44	3.07	2.76 abc
Mean	2.60 B**	3.00 A	2.80

CV (%): 11.6%, **: P≤0.01, ns: none significant

In terms of cultivars, it has determined that the highest stem thickness was in Emiliana (3.31 mm), the lowest stem thickness was in Basbag (2.25 mm). Banat vs, Diane, Elci, Ezzelina, Iside, Osjecka 99, Queen, Riviera vicentina and Sabrina cultivars are also in the group with the highest value. In terms of years, it was determined that the 2.60 mm average stem thickness obtained in 2020 was statistically lower than the 3.00 mm average stem thickness obtained in 2021.

Regarding to previous studies on stem thickness in alfalfa; Seker [20] have found 2.78-2.89 mm in Erzurum ecological conditions, Soya and Kavut [17] have reported 2.78-2.90 mm in Bornova ecological conditions, Tongel and Ayan [21] reported that stem thickness varied between 2.93-3.27 mm on 19 alfalfa cultivars in Samsun ecological conditions, Dumlu et al. [22] reported that the stem thickness varies between 2.81-3.04 mm in Erzurum conditions. We found the stem thickness between 2.25-3.31 mm in this study that is similar to results that mentioned in above researches.

3.4. Green Forage Yield (kg da^{-1})

Two-year averages of forage yield of foreign origin alfalfa cultivars and groupings of these averages have given in Table 4. As seen in Table 4, the difference between the forage yields of alfalfa cultivars is significant in terms of year and cultivar (P≤0.05), in terms of year x cultivar interaction was determined to be insignificant. In terms of cultivars, it has seen that the highest forage yield cultivars was in Ezzelina cultivar (14069 kg). Banat vs, Bilensoy 80, Emiliana, Diane, Elci, Osjecka 99, Prosementi, Riviera vicentina, Iside and Queen cultivars are also in the highest value group. The lowest forage yield was determined in Basbag, Sabrina, La Torre and Escorial cultivars. In terms of years, it has seen that the average forage yield (11471 kg) in 2021 is higher than the forage yield (10565 kg) in 2020.

Table 4. The forage yield of alfalfa cultivars (kg da^{-1})

Cultivars Name	2020	2021	Mean
Banat vs	10150^{ns}	10337	10243 ab*
Basbag	10664	8748	9706 b
Bilensoy 80	10782	12014	11398 ab
Diane	11811	11673	11742 ab
Elci	10246	11977	11111 ab
Emiliana	10742	12052	11397 ab
Escorial	8761	10697	9729 b
Ezzelina	11878	16261	14069 a
Isıde	9033	11453	10243 ab
La Torre	9673	9574	9624 b
Osjecka 99	10373	11588	10981 ab
Prosementi	13187	11662	12424 ab
Queen	9972	12173	11072 ab
Riviera vicentina	11836	11563	11700 ab
Sabrina	9372	10298	9835 b
Mean	10565 B*	11471 A	11018

CV: 17.8%, *: P≤0.05, ns: none significant

The forage yield was obtained in the study is similar with forage yields of Kusvuran et al. [10] research that has obtained 10828 kg da^{-1} in Northern Cyprus ecological conditions. In addition, Gokalp et al. [23] have determined 11150-13905 kg da^{-1} in Tokat-Kazova conditions. However, the forage yield was obtained in the study higher than the Basbag et al. [24] results that is between 3672,13-6153,38 kg da^{-1} in irrigated conditions in Diyarbakir. Also Yılmaz et al. [25] have reported 1297-1771 kg da^{-1} in Kahramanmaras conditions. The yield obtained in alfalfa cultivation is largely related to the number of harvests. The number of harvests is higher in warm regions and less in cold regions. The difference in the number of harvests causes the forage yield obtained in alfalfa cultivation to be different. Therefore, different forage yields can obtained in different ecological regions.

3.5. Dry Matter Yield (kg da^{-1})

Two-year averages of dry matter yield of foreign origin alfalfa cultivars and groupings of these averages have given in Table 5. As seen in Table 5, the difference between the dry matter yields of alfalfa cultivars is significant only for cultivars (P≤0.05), in terms of year and year x cultivar interaction was determined to be insignificant. In terms of cultivars, it has seen that the highest dry matter yield has obtained from Ezzelina cultivar. Banat vs, Bilensoy 80, Emiliana, Diane, Elci, Osjecka 99, Prosementi, Riviera vicentina, Sabrina, Iside and Queen are also among the highest value

groups. The lowest dry matter yield was determined in Basbag, La Torre and Escorial cultivars.

Table 5. The dry matter yield of alfalfa cultivars (kg da^{-1})

Cultivars	2020	2021	Mean
Banat vs	3012^{ns}	3074	3043 ab *
Basbag	3076	2633	2855 b
Bilensoy 80	3180	3283	3232 ab
Diane	3327	3171	3249 ab
Elci	3143	3398	3270 ab
Emiliana	3194	3450	3322 ab
Escorial	2709	2974	2841 b
Ezzelina	3535	4376	3955 a
Iside	2954	3085	3020 ab
La Torre	3038	2854	2946 b
Osjecka 99	3260	3310	3285 ab
Prosementi	3857	3510	3684 ab
Queen	2913	3495	3204 ab
Riviera vicentina	3446	3501	3474 ab
Sabrina	3031	3063	3047 ab
Mean	**3178^{ns}**	**3279**	**3228**

CV: 15.1%, *: P≤0.05, ns: none significant

The dry matter yields have obtained in current study is similar to the dry matter yields in previous researches of alfalfa that have presented below. Altınok et al. [5] obtained 3.214 kg da^{-1} in Ankara conditions, Avci et al. [26] obtained 2094.0-2230.0 kg da^{-1} in Konya and Ankara conditions and Yüksel et al. [27] obtained 2845-3339 kg da^{-1} and 2032-2617 kg da^{-1} in Ankara and Isparta locations, respectively. However, the dry matter yields in the study have found to be higher than the dry matter yields of 1104.7-1333.5 kg da^{-1} in Erzurum ecological conditions [20], 2031-2710 kg da^{-1} in Odemis and Bornova conditions [7], 1143-2183 kg da^{-1} in the Goller [28] and 1122.7-1396.9 kg da^{-1} in Erzurum ecological conditions [22]. The dry matter yield has directly related to the forage yield obtained. In areas where forage yield is high, dry matter yield has generally also obtained higher.

4. CONCLUSIONS

The plant heights of alfalfa cultivars varied between 87.6-106.2 cm and the average was 97.6 cm, the number of stems varied between 13.8-18.1 and the average was 15.8, stem thickness varied between 2.25-3.31 mm and the average was 2.80 mm, the forage yield varied between 9706-14069 kg da^{-1} and the average was 11018 kg da^{-1}, the dry matter yield varied between 2841-3955 kg da^{-1} and the average was obtained as 3228 kg da^{-1}. Statistically, the highest plant height and stem thickness have obtained from Emiliana, while the highest forage yield and dry matter yield have obtained from Ezzelina. Emiliana and Ezzelina cultivars gave higher values than both standard and foreign cultivars. The number of stems of the cultivars did not differ statistically. In line with these parameters examined, it has concluded that Ezzelina and Emiliana cultivars showed superior characteristics in Bingöl province.

Acknowledgment

This study is a summary of Sanaz Yaryab's doctoral thesis and has supported by Bingöl University Scientific Research Projects Coordination Unit (Project No: BAP-GMYO-2020.00.002).

REFERENCES

[1] Açıkgöz E. Yem Bitkileri (3. Baskı). Uludağ üniversitesi güçlendirme vakfı. 2001.
[2] Soya H, Avcıoğlu R, Geren H. Yem bitkileri. Hasad Yayıncılık Ltd.1997.
[3] Kır B. kimi yonca çeşitlerinde tohum ve ot verimi ile kalite özellikleri üzerinde bir araştırma. Ege: Ege üniversites; 2006.
[4] Sevimay CS, Elçi Ş. Ankara koşullarında elçi yoncası klonlarında tohum teşekkülüne ve seçilen klonların ileriki döllerinde yem üretimine etki eden faktörler. Ankara: Ankara Üniversitesi; 1992.
[5] Altinok, S, Karakaya A. Forage yield of different alfalfa cultivars under Ankara conditions. Turk J Agric For. 2002; 26(1): 11-16.
[6] Çaçan E., Kökten K, Kaplan M. Determination of yield and quality characteristics of some alfalfa (*Medicago sativa* L.) cultivars in the East Anatolia Region of Turkey and correlation analysis between these properties. 2018.
[7] Kavut YT, Celen AE, Demiroğlu Topçu G, Kır B. Bazı yonca (*Medicago sativa* L.) genotiplerinin farklı lokasyonlardaki verim ve verim özellikleri üzerinde bir araştırma. Ege Üniversitesi Ziraat Fakültesi Dergisi. 2014 ; 51(1): 23-29.
[8] Gündel F D, Karadağ Y, Çinar S. Çukurova ekolojik koşullarında bazı sıcak mevsim baklagil yem bitkilerinin verim, kalite ve adaptasyonu üzerine bir araştırma. Gaziosmanpaşa Üniversitesi Ziraat Fakültesi Dergisi. 2014; 31(3): 10-19.
[9] Akbari N, Avcıoğlu R. Ege Bölgesine uygun bazı yonca (*Medicago sativa* L.) çeşitlerinin agronomik özellikleri ile yem kaliteleri üzerinde araştırma.1992.
[10] Kuşvuran A, Veyis T, Sağlamtimur T. KKTC Sulanan Koşullarinda Yonca (*Medicago Sativa* L.) ve Bazi Buğdaygil Yem Bitkilerinin Adaptasyon Kabiliyetlerinin Saptanmasi. Türkiye VI. Tarla Bitkileri Kongeresi. Antalya: 2005. p. 1181-1186.
[11] Kır B, Soya H. Kimi Yonca Çeşitlerinde Tohum ve ot Verimi İle Kalite özellikleri Üzerinde Bir Araştırma. Ege: Ege Üniversitesi; 2006.
[12] Kır H, karadağ Y. Tokat-kazova şartlarinda bazi yonca çeşitlerinin performanslarinin belirlenmesi. Tokat:Gaziosmanpaşa universitesi;2010.
[13] Mehmet Ö, Albayrak S. Batı Akdeniz sahil kuşağında yaygın yonca (Medicago sativa L.)

populasyonlarının toplanması ve morfolojik karekterizasyonu. Derim. 2014; 31(2): 79-88.
[14] Biçakçi E, Balabanli C. Çoklu melez parsellerinde yer alan yonca genotiplerinin tohum tutma özelliklerinin belirlenmesi. Süleyman Demirel Üniversitesi Fen Bilimleri Enstitüsü Dergisi. 2016; 20(3): 587-591.
[15] Engin B, Hanife M. Farklı yonca çeşitlerinin ot verimi ve bazı kalite özelliklerinin belirlenmesi. Yüzüncü Yıl Üniversitesi Tarım Bilimleri Dergisi. 2017; 27(2): 212-219.
[16] Çaçan E, Arslan İ. Bingöl Ovası'nda Yetiştiriciliği Yapılan Yoncaların (*Medicago sativa* L.) Verim ve Kalitelerinin Belirlenmesi. Türk Doğa ve Fen Dergisi, 2021;10(1):18-24.
[17] Soya H, Kavut Y, Avcıoğlu R. Bornova–İzmir Koşullarında Ekim Yonca (*Medicago sativa* L.) Çeşitlerinin Performansları Üzerinde Araştırmalar. Tarla Bitkileri Kongresi. 2005. p. 5-9.
[18] Suzan T. Mohammed A. Farklı lokasyonlarda bazı yonca çeşitlerinin yem verimleri ve bitkisel özellikleri, Ankara: Ankara Üniversitesi; 2007.
[19] [19] Demiroğlu G, Geren H, Avcioğlu R. Farklı yonca (*Medicago sativa* L.) genotiplerinin Ege Bölgesi koşullarına adaptasyonu. Ege Üniversitesi Ziraat Fakültesi Dergisi. 2008; 45(1): p. 1-10.
[20] Şeker H. Bazı Yeni Yonca Çeşitlerinin Erzurum Ekolojik Şartlarına Uyum ve Verim Denemesi/Adaptation and Yield Trial of Some New Alfalfa Cultivars to Erzurum Ecological Condition. Atatürk Üniversitesi Ziraat Fakültesi Dergisi. 2003; 34(3):217-221.
[21] Tongel MO, Ayan I. Nutritional contents and yield performances of Lucerne (*Medicago sativa* L.) cultivars in Southern Black Sea shores. Journal of Animal and Veterinary Advances. 2010;9(15): 2067-2073.
[22] Dumlu SE, Çakal Ş, Aksakal E, Uzun M, Özgöz MM, Terzioğlu K et al., Erzurum ekolojik koşullarında yonca (Medicago sativa L.) çeşit adayının performansının belirlenmesi. Alinteri Journal of Agriculture Science. 2017; 32(2): p. 55-61.
[23] Gökalp S, Yazici L , çankaya N, İspirli K , Bazı yonca (Medicago sativa L.) çeşitlerinin tokat-kazova ekolojik koşullarında ot verimi ve kalite performanslarının belirlenmesi. Gaziosmanpaşa Üniversitesi Ziraat Fakültesi Dergisi. 2017; 34(3): p. 114-127.
[24] Başbağ M, Gül İ, Saruhan V. Diyarbakır Sulu Koşullarında Yonca ve Üçgül Çeşit Verim ve Adaptasyonlarını Araştırma Projesi. TÜBİTAKTARP-2261 no'lu Proje Kesin Sonuç Raporu, Ankara, 2002.
[25] Yılmaz MF et al. Kahramanmaraş şartlarında farklı ekim sıklıklarının yoncada (*Medicago sativa* L.) ot ve tohum verimi üzerine etkileri in 11. Tarla Bitkileri Kongresi. 2015. p. 103-106.
[26] Avci MA, Özkose A, Tamkoc A. Determination of yield and quality characteristics of alfalfa (*Medicago sativa* L.) varieties grown in different locations. Journal of Animal and Veterinary Advances. 2013; 12(4): 487-490.
[27] Yüksel O, Albayrak S, Mevlut T, Sevimay C . Dry matter yields and some quality features of alfalfa (*Medicago sativa* L.) cultivars under two different locations of Turkey. Suleyman Demirel Universitesi Fen Bilimleri Enstitusu Dergisi.2016; 20(2).
[28] Açıkbas S, Albayrak S, Mevlut T. Doğal vejetasyondan toplanan bazı yonca (*Medicago sativa* L.) genotiplerinin ot verim ve kalitelerinin belirlenmesi. Türkiye Tarımsal Arastırmalar Dergisi. 2016; 4(2): 155-162.

Cilt 11, Sayı 1, Sayfa 136-141, 2022 Volume 11, Issue 1, Page 136-141, 2022

Araştırma Makalesi https://doi.org/10.46810/tdfd.1057096 Research Article

Türk Doğa ve Fen Dergisi
Turkish Journal of Nature and Science
www.dergipark.gov.tr/tdfd

Simulation of Disturbance Observer-Based Bone Tissue Change Prediction Approach for Orthopedic Drills

Yunis TORUN[1*]

[1] Sivas Cumhuriyet Üniversitesi, Mühendislik Fakültesi, Elektrik Elektronik Mühendisliği Bölümü, Sivas, Türkiye
Yunis TORUN ORCID No: 0000-0002-6187-0451

**Corresponding author: ytorun@cumhuriyet.edu.tr*

(Received: 12.01.2022, Accepted: 19.02.2022, Online Publication: 25.03.2022)

Keywords
Orthopedic Drill, Disturbance Observer, Bone Drilling

Abstract: Orthopedic drills are currently used for various operations in surgical fields such as orthopedics, ear, nose, and throat surgery. The path that orthopedic drills travel through the tissue is controlled manually by surgeons, and manual control leads to the risk of damaging areas such as nerves and tissues. In our study, an innovative approach is presented against existing drill designs and breakthrough detection problems. In the proposed model, the change in the load torque and the change in friction force caused by the tissue change in the drilling path are considered as a disturbance effect, and a disturbance observer has been developed that allows these disturbances to be observed. Observation of the disturbance effects allows the perception of the hardness of tissue change during drilling since it gives the change of load torque changes and friction coefficient, which cannot be measured under normal operation. The performance of the proposed approach has been proven by simulation study.

Ortopedik Matkaplar İçin Bozucu Gözlemci Tabanlı Kemik Doku Değişim Tahmin Yaklaşımı Benzetimi

Anahtar Kelimeler
Ortopedik Matkap, Bozucu Gözlemci, Kemik Delme

Öz: Günümüzde ortopedi, kulak burun boğaz gibi cerrahi alanlarda çeşitli operasyonlarda ortopedik matkaplar kullanılmaktadır. Ortopedik matkapların doku içerisindeki kat ettiği yol manuel olarak cerrahlar tarafından kontrol edilmektedir ve manuel kontrol sinir, doku gibi bölgelerde hasar oluşturma riskine yol açmaktadır. Çalışmamızda mevcut matkap tasarımlarına ve sorunlarına karşı yenilikçi bir model sunulmaktadır. Önerilen modelde yük momentindeki değişim ve matkap ucundaki doku değişikliğinden kaynaklanan sürtünme kuvveti değişimi bozucu etki olarak ele alınmış, bu bozucu etkilerin gözlemlenmesine olanak sağlayan bir bozucu gözlemci geliştirilmiştir. Bozucu etkilerinin gözlemlenmesi, normal şartlarda ölçülemeyen yük moment değişimlerinin ve sürtünme katsayısının değişimini verdiğinden dolayı, delme esnasında doku değişiminin algılanmasına olanak sağlamaktadır. Önerilen yöntemi başarımı benzetim çalışmaları ile kanıtlanmıştır.

1. INTRODUCTION

Bone drilling is used primarily in orthopedic surgery, but also in many surgical interventions such as thoracic surgery, plastic surgery, otolaryngology [1]. During surgery, implants such as screws, nails, wires and plates are used to fix the bone as a result of post-traumatic fractures in the body [2,3]. Cylindrical holes are drilled in the bone with the appropriate drill bit attached to orthopedic drills and implants are placed in these holes [1]. One of the risks in the usage of surgical drills is the potential of the drill bit to damage nerve, vessel and muscle tissues during the drilling process [4,5]. The rapidly rotating drill wraps around the surrounding tissues uncontrollably or the drill bit's inability to stop its movement immediately after exiting the second cortex of the bone is the reason for the potential of surgical drills to damage the tissues [4,6,7]. Breakthrough detection can be defined as the detection of the thrust force when the drill bit exits the second cortex [4,8]. During orthopedic surgical procedures, the force applied by the surgeon for the advancement of the drill bit varies since changing tissue hardness. The factors that affect the performance of the drilling process includes surgeon's dexterity, 'feel piercing' [9], phonological 'audible piercing' [10,11]. The drilling force perceived by the surgeon is a relative

concept. The drill bit penetration rate, the health/condition of the bone, and the drill type used in the operation affect the drilling force.

There are three types of approaches to detect the breakthrough in bone drilling in the literature. One of these approaches is the Computer Assisted Orthopedic Surgery approach in orthopedic surgery operations, which is based on the combination of medical imaging, skeletal-muscular system and the positioning of the surgical instrument in 3D space, and semi-robotic systems [12]. The second approach is the studies to integrate breakthrough detection sensors as force, vibration, acoustic, and torque sensors into the existing orthopedic drills [13–17]. Due to the cost-effectiveness of robotic and imaging systems, as well as the mounting and cost disadvantages of various sensors integrated into orthopedic drills, there has been a third approach for estimating tissue changes during drilling with real-time system dynamics analysis in recent years. In this approach, there are some studies to predict tissue change by analyzing the effects of changes in system dynamics on the closed-loop signal by using closed-loop signals used in drill control [4]. In orthopedic drills where direct current motors are used, the change of load torque and friction force indirectly causes a change in the closed-loop error signal, and this change allows the estimation of tissue change with a trained artificial intelligence-based breakthrough detection algorithm [4,7].

When the common literature was examined, no study was found to detect tissue change during a surgical drilling by estimating the disturbance with the disturbance observer. In this study, a new bone tissue change detection approach based on observing the change of the disturbance observer-based load torque and friction coefficient is presented. The mathematical model of the Brushless Direct Current Motor (BLDC) used in the orthopedic drill was constructed, then the quantitative value of the disturbance effect was observed with a closed-loop Proportional Integral Derivative (PID) controller, which will minimize the difference between the actual model and the model with disturbance applied. In the simulation studies, it has been proven that the change of the load torque and friction coefficient given to the system and whose waveforms are known, can be observed quantitatively with the developed disturbance observer.

2. MATERIAL AND METHOD

The disturbance observer-based torque and friction observer approach has been developed with the BLDC mathematical model, which is widely used in orthopedic drills. The change of load torque and friction gives meaningful information about the state of the drilling according to the hardness of the cortical and spongy bone types [4,13]. MATLAB/Simulink was preferred for simulation based on drill motor parameters [18], with the purpose of making real-time analysis, creating the mathematical model of the disturbance observer-based system.

2.1. Brushless Direct Current Motor and Its Mathematical Model

In the study, a brushless direct current motor (BLDC) was used due to its features such as high efficiency at low power, silent operation, low maintenance and low cost, absence of electrical arcs and minimum electrical losses. The following assumptions have been made in order to make the mathematical modeling of BLDC [19,20].

•All stator resistances and inductances are assumed to be equal and constant.
•The motor is not saturated.
•Eddy current and hysteresis effects in the magnetic materials of the machine have an insignificant effect on the rotational current.
•Semiconductors in the power switching circuit are ideal.
•All phases have the same Back-EMF waveform.
•Iron losses are negligible.

The flexibility of the rotor and shaft is assumed to be zero. A viscous friction model is used in the simulated model [21]. The relationship between the input voltage of a three-phase, star-connected BLDC and the phase currents and Back-EMF can be expressed mathematically as shown below.

$$V_{ab} = R(i_a - i_b) + L\frac{d}{dt}(i_a - i_b) + e_a + e_b \quad (1)$$

$$V_{bc} = R(i_b - i_c) + L\frac{d}{dt}(i_b - i_c) + e_b + e_c \quad (2)$$

$$V_{ca} = R(i_c - i_a) + L\frac{d}{dt}(i_c - i_a) + e_c + e_a \quad (3)$$

In the equations 1, 2 and 3, V represents the phase-to-phase voltage, R represents the resistance of each phase, L represents the inductance of each phase, and the Back-EMF voltages are represented as e_a, e_b, and e_c, respectively. Electromechanical behavior of the motor according to the law of motion can be stated as;

$$T_e = B\dot{\theta} + J\ddot{\theta} + T_L \quad (4)$$

In equation 4, T_e represents electrical torque, $\dot{\theta}$ represent mechanical speed, B represents viscous friction coefficient, J represents rotor inertia, T_L represents load torque. It is also expressed in the relations given in Equations 5 and 6 between voltages and currents:

$$V_{ab} + V_{bc} + V_{ca} = 0 \quad (5)$$

$$i_a + i_b + i_c = 0 \quad (6)$$

Based on Equations 5 and 6, only two voltage values are needed for modeling and when expressed as in Equations 7 and 8;

$$2V_{ab} + V_{bc} = 3Ri_a + 3L\frac{d}{dt}i_a + 2e_a - e_b - e_c \quad (7)$$

$$-V_{ab} + V_{bc} = 3Ri_b + 3L\frac{d}{dt}i_b + 2e_b - e_a - e_c \quad (8)$$

The produced electrical torque by the three-phase, star-connected BLDC is given in Equation 9.

$$T_e = (e_a i_a + e_b i_b + e_c i_c)/\dot{\theta}_m \quad (9)$$

The mathematical equations of trapezoidal Back-EMF voltages are expressed as in Equations 10, 11 and 12:

$$e_a = (k_e/2\dot{\theta}_m)Trapezoidal(\theta_e) \quad (10)$$

$$e_b = (k_e/2\dot{\theta}_m)Trapezoidal(\theta_e - 2\pi/3) \quad (11)$$

$$e_c = (k_e/2\dot{\theta}_m)Trapezoidal(\theta_e - 4\pi/3) \quad (12)$$

Here, k_e and θe represent the back-EMF constant and the electric angle, respectively. Also, P stands for the number of poles. Moreover, trapezoidal (θ_e) is a function defined as a trapezoidal wave, and a period of this function is as in Equation 13.

$$Trapezoidal(\theta_e) = \begin{cases} 1 & 0 \le \theta_e \le {}^{2\pi}/_{3} \\ 1 - \frac{6}{\pi(\theta_e - {}^{2\pi}/_{3})} & {}^{2\pi}/_{3} \le \theta_e \le \pi \\ -1 & \pi \le \theta_e \le {}^{5\pi}/_{3} \\ 1 - \frac{6}{\pi(\theta_e - {}^{5\pi}/_{3})} & {}^{5\pi}/_{3} \le \theta_e \le 2\pi \end{cases} \quad (13)$$

When equations 10, 11 and 12 are used in Equation 9, the expression of T_e is obtained as in Equation 14.

$$T_e = \frac{k_e}{2}\left[Trapezoidal(\theta_e)i_a + Trapezoidal(\theta_e - \frac{2\pi}{3})i_b + Trapezoidal(\theta_e - \frac{4\pi}{3})i_c\right] \quad (14)$$

When the electrical torque equation expressed as T_e in Equation 4 is arranged, the speed w of the rotor of the motor is given in equations 15b and 16.

$$T_e = J\frac{dw}{dt} + Bw + T_L \quad (15a)$$

$$T_e - T_L = J\frac{dw}{dt} + Bw \quad (15b)$$

$$w(s) = \frac{T_e - T_L}{Js + B} \quad (16)$$

The electrical and mechanical BLDC parameters which are used in the simulation study are given in Table 1 [18].

Table 1. Motor parameters used in the simulation study [18]

$R(\Omega)$	$L(H)$	K_{emf} $(V.s/rad)$	J (Nms^2/rad)	B (Nms/rad)
2.875	0.0085	175	0.0008	0.0001

2.2. Implementation of Disturbance Observer Design

The systems in which the effects of unknown or uncertain disturbance effects on the system can be observed without the use of external additional detectors are called disturbance observers [22,23]. Disturbance observers are used to observe immeasurable states and variables which are commonly used in force control applications, robotic manipulators, and many systems process control system [22,24,25].

There are several advantages of using an observer-based method for estimating state of the drilling in bone drilling operation. Observer is a system, which is used to reconstruct the states of a dynamic system by using input signal measurements. They are used in many applications such as feedback control, system stability monitoring and fault detection [26]. The disturbance observer was developed in the late 1980s as a new type of observer for the control of mechatronic systems, and they are used to predict the unknown inputs of the system, unlike state observers which are used to reconstruct the unknown states of a system [27]. Disturbance observers increase the stability and performance of the control system by predicting unknown disturbances affecting the control systems. Also, a disturbance observer can be used in a control system to reduce the number of costly detectors needed [28].

In this study, MATLAB/Simulink was preferred for simulation, in order to carry out real-time simulations, creating a mathematical model of the BLDC and disturbance observer-based system, and interpreting the simulations according to motor parameters. The block diagram of the simulated BLDC model is given in Figure1. The disturbance observer used for torque estimation in brushed direct current motors (DC), which was reported with research work by Lee and Ahn [27], has been adapted for BLDC and determined bone tissue changing in an orthopedic drill with observing the change in friction coefficient and load torque in the current study.

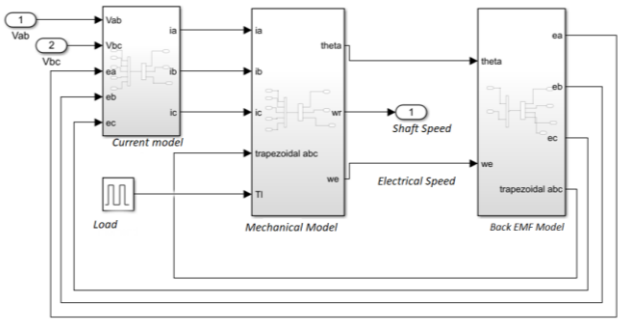

Figure 1. The simulation diagram of Brushless DC motor.

2.3. Detection of Changes in Load Torque and Friction Coefficient by Using Disturbance Observer

In this section, during the bone drilling process, the effect of the variation of the load torque and friction coefficient during the bicortical drilling path is modeled by using MATLAB/Simulink. While performing the simulation study, two models expressing the effects of either varying load torque or varying friction coefficient have been constructed. Considering the change in the load torque firstly; the effect of the electrical torque obtained from the mechanical model of the motor on the motor speed and position together with the load torque defined as T_e, T_L is taken as basis in the design of the disturbance observer. Simulink model of disturbance observer based load torque change detection is shown in Figure 2. A square waveform with 2Nm amplitude load torque, $T_{L,}$ has been applied to BLDC model to mimic the real drilling path. The variation of the friction coefficient has been assumed

zero for the first model as shown in Figure 3. The models mentioned in Figure 2 and Figure 3 consist of three sub-models in which the upper model represents the mathematical model without any disturbance, the middle model represents the model encountered with disturbance, the lower model represents the disturbance observer which produces the quantity of disturbance with the difference of ideal model output and disturbance applied model output. A PID controller that processes the rotor position difference at the outputs of the two models is used [27]. The coefficients of the PID controller determined by the MATLAB/Simulink PID Tuning Toolbox with the obtained transfer function were found as 0.0081, 0.0014 and 0.0044 for P, I and D, respectively. Secondly, the variation of the friction coefficient is determined for with friction observer. Depending on the amount of friction, the heat generated during the bone drilling process may cause thermal injuries around the hole drilled between the drill bit and the bone[29,30]. As shown in Figure 3, a friction pattern which mimics the friction of the drilling path has been applied as friction variation.

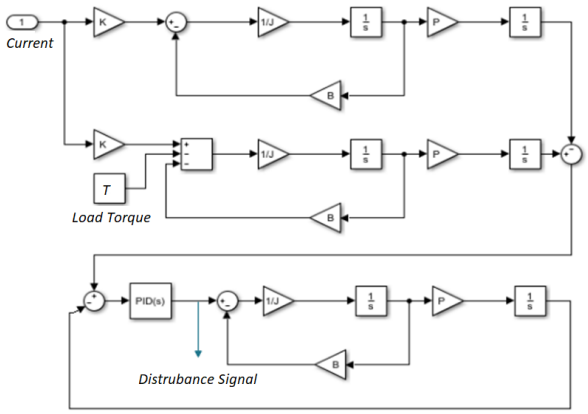

Figure 2. The model of disturbance observer based load torque change detection

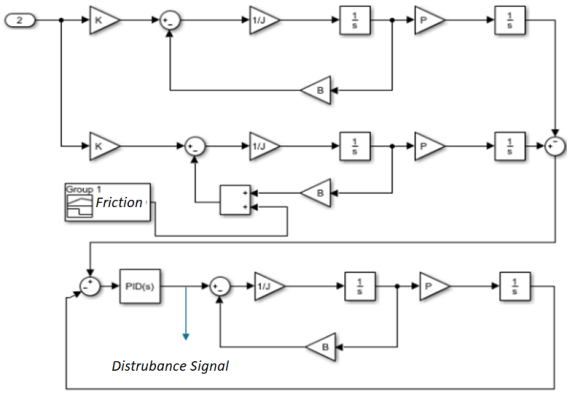

Figure 3. The model of disturbance observer-based friction coefficient variation detection

3. RESULTS AND DISCUSSIONS

The proposed models have been constructed in Simulink for simulation works. Since the hardness of a cortical bone changes according to the drilling path as mentioned in the work of Torun and Öztürk [4], we have simulated the change of load torque and friction coefficient as drilling one hole on bicortical bone. A detailed discussion about bicortical drilling path could be found with further reading of recent literature works[4,5,7,8,11,16,31]. For estimating the load torque, it is assumed that one-hole drilling is performed within 5 seconds. Drill bit contacts the first cortical layer at 1st second, then exits the first cortical layer and contacts the sponge layer at 2nd second, finally breakthrough occurs when drill bit exists the second cortical layer at 4th second. The actual load torque which was applied to model, and the observed value of the load torque are shown in Figure 4.

For estimating the friction coefficient between the drill bit and bone tissue a similar scenario has been assumed. Friction varies according to drill bit geometry, drill speed, and the hardness of drilled tissue as mentioned in [32,33]. In this work, it has been tried to form a synthetic friction coefficient waveform for the bicortical drilling path with knowledge of recent literature[4,6,31] which focuses on the changes in the dynamic of the drilling for bicortical bone. Drill bit contacts with the first cortical layer at zero instant. Friction increases as the drill bit travels through the first layer then decreases when it reaches the spongy bone. The friction value is lower in the sponge bone since the hardness of the sponge layer was lower than the cortical layer. The drill bit contacts the second cortical entry at the 1.5 second. Finally, breakthrough occurs as the drill bit exits the second cortical layer at 2.5 second. The synthetic wave form of friction coefficient and observed with disturbance observer have been shown in Figure 5.

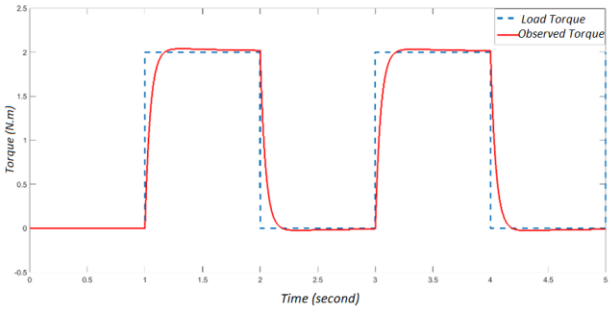

Figure 4. Applied synthetic load torque versus observed load torque with disturbance observer

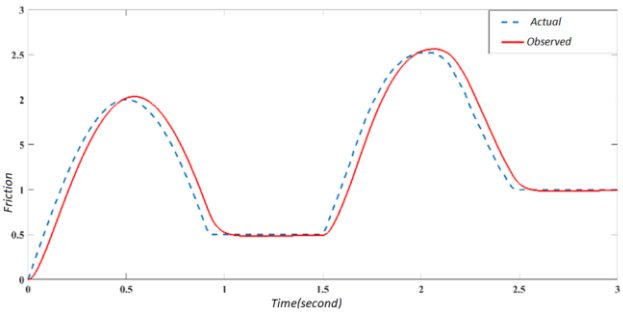

Figure 5. Applied synthetic friction versus observed friction with disturbance observer.

Observed load torque is close to the applied load torque at the steady-state, however, the sudden changes in the load torque cause the difference in the transient response of the disturbance observer. The rise time, delay time, and settling time have been measured as 140ms, 65 ms and

183 ms, respectively. The observed friction coefficient lags the synthetic friction coefficient with a 120 ms delay as shown in Figure 5. Since the objective of the study was to obtain the change of the tissue being drilled, it is important to observe the change of the load torque and friction with a reasonable time duration rather than obtaining the actual value of load torque and friction coefficient. Simulations show that change of load torque and friction could be obtained lower than 200ms later after the change of the drilled tissue. 200ms corresponds to the 0.2 mm drilling path with a drilling feed rate of 1mm/second (60mm/minutes) which is one of the nominal feed rate for bone drilling [33]. The 0.2 mm drilling path length can be regarded as a breakthrough error whose acceptable range lies within 1-2mm [34] to avoid damaging vital organs when drilling cortical bone.

As a result of the simulations, it was seen that the signals of the changing load torque value and the friction coefficient in the model were in a form that is similar to the signals at the observer output. This confirms that the orthopedic surgical drill, whose design will be developed in real-time, will be capable of detecting tissue changes in the transition through the bone layers during surgery and will be sufficiently sensitive and accurate for the detection of breakthrough.

4. CONCLUSION

In this study, disturbance observer, which observes the changes in load torque that is directly proportional to the thrust force generated during the bone drilling process and the change in viscous friction coefficient is designed in the Matlab/Simulink simulation environment. As a result of the simulations that have been carried out in the MATLAB/Simulink environment, it has been observed that the signals of the changing torque value and friction coefficient in the model are in a form that is similar to the signals at the observer output. This specifies that the orthopedic surgical drill is capable of detecting tissue changes as it passes through the layers of bone during surgery and has sufficient sensitivity and accuracy for breakthrough detection. Real-time implementation of the proposed approach on sheep-femur drilling with BLDC based drill will be performed in future works.

ACKNOWLEDGMENTS

This study was financially supported by Sivas Cumhuriyet University Scientific Research Grant Program (CUBAP) with M-737 project code and “Power Analysis and Optimization in Robotic Medical Drills” project name. The author would like to thank Dr. Ozhan PAZARCI and Ahmet OZTURK for their valuable comments based on their drilling experience.

REFERENCES

[1] Bertollo N, Robert W. Drilling of Bone: Practicality, Limitations and Complications Associated with Surgical Drill-Bits. Biomech. Appl., 2012. https://doi.org/10.5772/20931.

[2] Gönen E. Minimally invasive surgical techniques for the treatment of the shaft fractures of the long bones. Türk Ortop ve Travmatoloji Birliği Derneği Derg 2012;11:78–88. https://doi.org/10.5606/totbid.dergisi.2012.11.

[3] Farouk O, Krettek C, Miclau T, Schandelmaier P, Guy P, Tscherne H. Minimally invasive plate osteosynthesis: Does percutaneous plating disrupt femoral blood supply less than the traditional technique? J Orthop Trauma 1999. https://doi.org/10.1097/00005131-199908000-00002.

[4] Torun Y, Öztürk A. A New Breakthrough Detection Method for Bone Drilling in Robotic Orthopedic Surgery with Closed-Loop Control Approach. Ann Biomed Eng 2020;48. https://doi.org/10.1007/s10439-019-02444-5.

[5] Modi RA, Nayak RP. Detection of Breakthrough During Bone-Drilling in Orthopaedic Surgery 2014;1:794–8.

[6] Torun Y, Ozturk A, Hatipoglu N, Oztemur Z. Detection of Bone Excretion with Current Sensor in Robotic Surgery. UBMK 2018 - 3rd Int. Conf. Comput. Sci. Eng., 2018. https://doi.org/10.1109/UBMK.2018.8566443.

[7] Öztürk A. Robotik cerrahi matkaplarda güç analizi ile matkap ucu çıkış tespiti. Cumhuriyet Üniversitesi Fen Bilimleri Enstitüsü, 2019.

[8] Torun Y, Pazarci O, Ozturk A. Current Approaches to Bone-Drilling Procedures with Orthopedic Drills. Cyprus J Med Sci 2020;5:93–8. https://doi.org/10.5152/cjms.2020.1242.

[9] Augustin G, Zigman T, Davila S, Udilljak T, Staroveski T, Brezak D, et al. Cortical bone drilling and thermal osteonecrosis. Clin Biomech 2012;27. https://doi.org/10.1016/j.clinbiomech.2011.10.010.

[10] Praamsma M, Carnahan H, Backstein D, Veillette CJH, Gonzalez D, Dubrowski A. Drilling sounds are used by surgeons and intermediate residents, but not novice orthopedic trainees, to guide drilling motions. Can J Surg 2008.

[11] Ho D, Li T, Meng QH. Bone Drilling Breakthrough Detection via Energy-Based Signal. Proc. Annu. Int. Conf. IEEE Eng. Med. Biol. Soc. EMBS, vol. 2018-July, 2018. https://doi.org/10.1109/EMBC.2018.8512621.

[12] Zheng G, Nolte LP. Computer-Assisted Orthopedic Surgery: Current State and Future Perspective. Front Surg 2015;2. https://doi.org/10.3389/fsurg.2015.00066.

[13] Torun Y, Pazarci Ö. Parametric Power Spectral Density Estimation-Based Breakthrough Detection for Orthopedic Bone Drilling with Acoustic Emission Signal Analysis. Acoust Aust 2020;48. https://doi.org/10.1007/s40857-020-00182-6.

[14] Torun Y, Ozturk A, Hatipoglu N, Oztemur Z. Breakthrough detection for orthopedic bone drilling via power spectral density estimation of acoustic emission. 2018 Electr Electron Comput Sci Biomed Eng Meet EBBT 2018 2018:1–5. https://doi.org/10.1109/EBBT.2018.8391464.

[15] Ying Z, Shu L, Sugita N. Autonomous Penetration Perception for Bone Cutting during Laminectomy. 2020 8th IEEE RAS/EMBS Int. Conf. Biomed.

Robot. Biomechatronics, IEEE; 2020, p. 1043–8. https://doi.org/10.1109/BioRob49111.2020.9224375.

[16] Seibold M, Maurer S, Hoch A, Zingg P, Farshad M, Navab N, et al. Real-time acoustic sensing and artificial intelligence for error prevention in orthopedic surgery. Sci Rep 2021;11:3993. https://doi.org/10.1038/s41598-021-83506-4.

[17] Osa T, Abawi CF, Sugita N, Chikuda H, Sugita S, Tanaka T, et al. Hand-Held Bone Cutting Tool with Autonomous Penetration Detection for Spinal Surgery. IEEE/ASME Trans Mechatronics 2015;20:3018–27. https://doi.org/10.1109/TMECH.2015.2410287.

[18] Hingmire A, Pimple BB. Simulation and Analysis Studies of Speed Control of Brushless DC Motor Using Hall Sensors. 2018 Int. Conf. Smart Electr. Drives Power Syst., 2018, p. 384–7. https://doi.org/10.1109/ICSEDPS.2018.8536062.

[19] Safi SK. Analysis and simulation of the high-speed torque performance of brushless DC motor drives. IEE Proc - Electr Power Appl 1995;142. https://doi.org/10.1049/ip-epa:19951808.

[20] Aydoğdu Ö. Fırçasız doğru akım motorlarının genetik tabanlı bulanık denetleyici ile sensörsüz kontrolü. Selçuk Üniversitesi Fen Bilimleri Enstitüsü, 2006.

[21] Li X. Model-Based Design of Brushless Dc Motor Control and Motion Control Modelling for Robocup Ssl. 2015.

[22] Chen WH, Ballance DJ, Gawthrop PJ, O'Reilly J. A nonlinear disturbance observer for robotic manipulators. IEEE Trans Ind Electron 2000;47:932–8. https://doi.org/10.1109/41.857974.

[23] Alkaya A, Eker I. Luenberger observer-based sensor fault detection: Online application to DC motor. Turkish J Electr Eng Comput Sci 2014;22. https://doi.org/10.3906/elk-1203-84.

[24] Mohammadi A, Tavakoli M, Marquez HJ, Hashemzadeh F. Nonlinear disturbance observer design for robotic manipulators. Control Eng Pract 2013;21. https://doi.org/10.1016/j.conengprac.2012.10.008.

[25] Wen X. Enhanced disturbance-observer-based control for a class of time-delay system with uncertain sinusoidal disturbances. Math Probl Eng 2013;2013. https://doi.org/10.1155/2013/805687.

[26] Radke A, Gao Z. A survey of state and disturbance observers for practitioners. Proc. Am. Control Conf., vol. 2006, 2006. https://doi.org/10.1109/acc.2006.1657545.

[27] Lee SC, Ahn HS. Sensorless torque estimation using adaptive Kalman filter and disturbance estimator. Proc. 2010 IEEE/ASME Int. Conf. Mechatron. Embed. Syst. Appl. MESA 2010, 2010. https://doi.org/10.1109/MESA.2010.5552094.

[28] Kouhei O, Shibata M, Murakami T. Motion control for advanced mechatronics. IEEE/ASME Trans Mechatronics 1996;1. https://doi.org/10.1109/3516.491410.

[29] Eriksson AR, Albrektsson T, Albrektsson B. Heat caused by drilling cortical bone: Temperature measured in vivo in patients and animals. Acta Orthop 1984;55. https://doi.org/10.3109/17453678408992410.

[30] Bachus KN, Rondina MT, Hutchinson DT. The effects of drilling force on cortical temperatures and their duration: An in vitro study. Med Eng Phys 2000;22. https://doi.org/10.1016/S1350-4533(01)00016-9.

[31] Torun Y, Malatyalı S. Power Analysis of Robotic Medical Drill With Different Control Approaches. Cumhur Sci J 2020;41:527–33. https://doi.org/10.17776/csj.661666.

[32] Amewoui F, Le Coz G, Bonnet AS, Moufki A. Bone drilling: an identification of heat sources. Comput Methods Biomech Biomed Engin 2020;23. https://doi.org/10.1080/10255842.2020.1813418.

[33] Alam K, Piya S, Al-Ghaithi A, Silberschmidth V. Experimental investigation on the effect of drill quality on the performance of bone drilling. Biomed Tech 2020;65. https://doi.org/10.1515/bmt-2018-0184.

[34] Boiadjiev G, Chavdarov I, Delchev K, Boiadjiev T, Kastelov R, Zagurki K. Development of Hand-Held Surgical Robot ODRO-2 for Automatic Bone Drilling. J Theor Appl Mech 2017;47:12–22. https://doi.org/10.1515/jtam-2017-0017.

Cilt 11, Sayı 1, Sayfa 142-150, 2022 Volume 11, Issue 1, Page 142-150, 2022

Araştırma Makalesi https://doi.org/10.46810/tdfd.1060359 Research Article

Türk Doğa ve Fen Dergisi
Turkish Journal of Nature and Science
www.dergipark.gov.tr/tdfd

Structural Resistance of a Reinforced Concrete Building under Earthquake and Wind Loads in Isparta and Burdur Region

Nesibe UYSAL[1], Pınar USTA[2*], Özgür BOZDAĞ[3]

[1] Isparta University of Aplied Science, Graduate School of Education, Civil Engineering Departmant, Isparta, Turkey
[2] Isparta University of Aplied Science, Technology Faculty, Civil Engineering Departmant, Isparta, Turkey
[3] Dokuz Eylül University, Engineering Faculty, Civil Engineering Departmant, Izmir, Turkey
Nesibe UYSAL ORCID No: 0000-0003-3277-517X
Pınar USTA ORCID No: 0000-0001-9809-3855
Özgür BOZDAĞ ORCID No: 0000-0002-5389-5739

**Corresponding author: pinarusta@isparta.edu.tr*

(Received: 19.01.2022, Accepted: 04.03.2022, Online Publication: 25.03.2022)

Keywords
Irregularity, Earthquake, Wind

Abstract: It has been clearly seen from building experiences and studies that lateral load effects such as earthquake load and wind load make building irregularities more obvious. Hence, it is of great importance to evaluate the regularity of the structural systems in accordance with the conditions determined by the building regulations. In this paper, irregularity effects were investigated according to Turkish Building Earthquake Regulation (TBEC) 2018. A reference building which have vertical setback irregularity were analzed under earthquake and wind loads. Etabs software were used for structural analyses. Response spectrum method were used for the seismic analysis and TS498 for Wind load analysis. Effective relative storey drift, A1 –Torsional irregularity and B2 – Soft Storey Irregularity are comparatively investigated and Irregularity values were determined.

Isparta ve Burdur Bölgesi'ndeki Betonarme Binanın Deprem ve Rüzgar Yükleri Altındaki Yapısal Dayanımı

Anahtar Kelimeler
Düzensizlik, Deprem, Rüzgar

Öz: Deneyimler ve yapılan çalışmalar, deprem ve rüzgar yükleri gibi yanal yüklerin yapılarda bariz bir şekilde düzensizliğe neden olduğunu göstermektedir. Bu nedenle yapının düzensizlik açısından şartlara uygun olarak değerlendirilmesi büyük önem taşımaktadır. Bu çalışmada 2018 TBDY'ne (Türkiye Bina Deprem Yönetmeliği) göre yapıların düzensizlik etkileri araştırılmıştır. Düşey düzensizliğe sahip bir yapı deprem ve rüzgar yükü altında analiz edilmiştir. Sismik analiz için tepki spektrum metodu ve rüzgar yükü analizi için TS498 kullanılmıştır. Etkin göreli kat ötelemesi, A1-Burulma düzensizliği ve B2-Yumuşak kat düzensizliği karşılaştırmalı olarak incelenmiş ve düzensizlik değerleri belirlenmiştir.

1. INTRODUCTION

Wind and earthquakes, coupled with aging and vulnerable buildings, pose the potential for damage and loss of life and property. Both hazards can wreak catastrophic damage to buildings. Winds and earthquakes cause the majority of property loss in the world from all natural disasters. Although an seismic hazard may be more significant than the other, the rapid population growth, highrise buildings and irregularity buildings have greatly increased the potential of exposure to multiple hazards[1]. The effect of wind and earthquake on structures may vary depending on wind load and seismic activity of the region, location and distance from the sea [2].

Turkey, one of the most seismically active countries of the world in terms of its geological features, is situated on an active area surrounded by active faults [3]. In the last century, destructive earthquakes have occurred along the North Anatolian Fault Zone (NAFZ) and East Anatolian fault lines where there are two active faults [4]. Earthquakes can not be prevented by human activity, these events occur as a result of a natural ground movement. Earthquake is one of the natural disasters that has caused the most destruction and loss of life for centuries [5] [6].

Many earthquakes occur every day in our country, where is about 92% of areas and about 95% of the population is on the earthquake zone. Therefore, all structures must be constructed against earthquake [7]. Although most of these earthquakes are of small intensity, sometimes large earthquakes occur. Such earthquakes cause loss of life and property and damage to structures. Some of these damages are irreparable depending on the current condition of the building and the nature of the earthquake [8]. However, with the necessary precautions, some of the negative consequences caused by earthquakes can be prevented or reduced [5]. The earthquake map of Turkey and the studied area in the study are given in Figure 1.

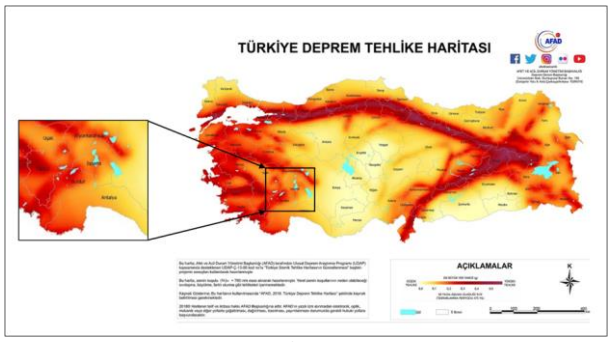

Figure 1. The earthquake map of Turkey and the studied area in the study [9]

Due to the shape formed by the fault lines in and around Isparta, this region is called the Isparta triangle or Isparta bend. The western edge of the Isparta Angle consists of the Fethiye–Burdur Fault Zone. The city of Isparta is located at the top of the triangle, below the point where the Burdur-Fethiye Zone intersects with the Akşehir Fault. Isparta and its surroundings are extremely sensitive against earthquakes. Isparta and its surroundings are extremely sensitive against earthquakes [8]. The earthquakes that occurred in Isparta and Burdur provinces are given in Table 1.

Table 1. The historical earthquakes that occurred in Isparta and Burdur [10]

Date	Region	Fault	M_s	I_0
End of 4th century BC	Dinar	?	?	?
88 BC	Dinar	?	?	IX-XI
AD 53	Dinar	?	?	VII-X
Beginning of 6th century AD	Isparta	?	?	VIII
Middle of 7th century AD	Isparta	?	?	IX-XI
AD 641–668	Isparta	?	?	VIII-X
1875	Dinar	Balkan Fault (20 km rupture)	?	IX-X
1889	Isparta	?	?	?
3 Oct. 1914	Burdur	Burdur Fault (23 km rupture)	7.1	IX
7 Aug. 1925	Dinar	Baklan Fault	6.0	VIII-IX
1933	Dinar	Baklan Fault	5.8	VIII
12 May 1971	Burdur	Burdur Fault	6.2	IX
1 Oct. 1995	Dinar	Dinar Fault (10 km rupture)	6.1	IX

Developments in structural materials and design technology in civil engineering have led to designs that satisfy strength requirements but are often flexible. This flexibility can cause unfavorable vibrations when the structure is subjected to wind or earthquake loads. These vibrations may lead to serious structural damage and affect the comfort of the occupants. Dynamics of buildings greatly depends on the characteristics of the external excitation as well as the physical properties of the building in terms of generalized masses, frequencies, and damping. Wind loads are characterized by low frequencies while earthquakes usually contain higher frequency load components [1].

On the other hand, besides the earthquake load, the wind load is also one of the important lateral loads that should be taken into account during the design phase of the building. Wind is a natural phenomenon that changes momentarily. Therefore, it is quite difficult to predict its properties such as intensity and direction. Analyzing how winds affect the structure dynamically and statically is a complex process [11].

In some cases, wind loads can be more critical to the carrier system and irreparable damage to the structure can occur if not taken into account during the design process. Wind load can cause serious damage especially in buildings which are high-rise and low cross-sectional areas [12]. With the increase in population, the number of high-rise buildings has increased considerably [13]. With the construction of high-rise buildings, the irregularity of the structure and its effects, which emerged as a result of wrong design, calculation, and application, started to become more evident.

Damages occurring in buildings after earthquake and wind loads may be caused by not taking into account irregularities such as A1 (Torsionally irregularity), A2 (Slab discontinuity), A3 (Existence of protrusions in the plan) and B1 (Strength irregularity between adjacent floors) and B2 (Soft story irregularity) during the design phase [9].

There have been many studies completed about seismic behavior of irregular structures. Demir et al. (2010) investigated horizontal seismic forces and torsional moments in different sites, the for the multiple storey structures [14]. Işık et al. (2018) examined the state of irregularity by the A3 plan in the TDBY of 2018[15]. Ilerisoy (2019) investigated vertical structural irregularities which are often inevitable due to building requirements and architectural imperatives, and having a major impact on building costs [16]. Ilgun et al. (2017) researched on A1 irregularity status in different spectral acceleration coefficients on reinforced concrete structures [17]. Keleş et al. (2021) and Uyan et al. (2021) investigated structural system safeties of 3, 5 and 7 storey existing reinforced concrete buildings having soft story irregularity according to TBEC-2018[18] [19]. Usta et al. (2022) analyzed regular and setback models of 5 storey, 9 storey, and 13 storey RC frames considered and the seismic risk effect over buildings that have vertical irregularity are investigated [20].

As seen, many studies have been conducted to investigate the effect of earthquake and wind. But there are less studies in which the structure is examined comparatively in terms of earthquake and wind load. In this study, it has been analyzed how earthquake and wind load that may occur in the Isparta and Burdur regions of Turkey will affect the performance of the structure which is located in these areas.

In the present context of study an reinforced concrete building is taken into consideration and the analysis is done as per the Turkish Standard. This building does not represent a particular real structure that has been built or proposed. However, the dimensions, general layout and other characteristics have been selected to be representative of a building for which the have vertical setback irregularity.

2. MATERIAL and METHOD

The aim in study is investigate the effects of earthquakes and wind loads. The building is considered to be located in Isparta and Burdur cities. For this purpose, a 12-storey reinforced concrete building was approached. The reinforced concrete building, having vertical setback irregularity. The building was dealt with the help of a ETABS software program [21]. Analysis and Irregularity controls of building were made under the earthquake and wind loads. The storey plans of the building are shown in Figure 2.a, Figure 2.b, Figure 2.c and Figure 2.d.

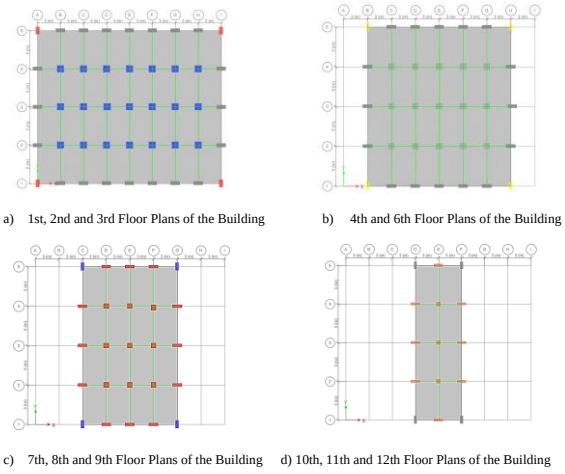

Figure 2. Floor plans of the building

The storey heights in the building are the same on each storey and are taken as 3 meter. Columns were designed in different sizes depending on the storey to catch optimum design and economy. Columns were chosen as 50x100 cm, 45x100 cm, 40x100 cm, 35x100 cm, 120x50 cm, 120x45 cm, 120x40 cm, 120x35 cm, 90x90 cm, 80x80 cm, 70x70 cm and 60x60 cm. Beams were chosen as 50x60 and 60x60. All slabs in the reinforced concrete building were formed with a thickness of 20 cm after analyzed according to TS 500/2000.

The dead load on the floors in the reinforced concrete building was G=3.5 kN (m2)-1 and the live load was taken as Q=2 kN (m2)-1. The dead load on the attic in the reinforced, concrete building was G=5 kN (m2)-1 and the live load was taken as Q = 1.5 kN (m2)-1 the modulus of elasticity was E=34000 MPa,

In order to represent other available buildings, the ground floor height was considered as 3 m. The building is unsymmetrical in Z direction. The distance between the axes of the building is designed 6 m intervals and the base-column joint area is defined as a fixed-support. The 3D view of the referenced building is given in Figure 3.

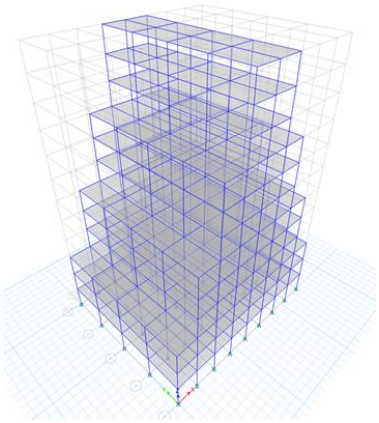

Figure 3. 3D View of the referenced building

The seismic design and examination of the structure was carried out according to TS 500. For this reason, the building importance coefficient, the structural system behavior coefficient, and the excess strength coefficient were taken as (I)=1, (R)=8, and (D)=3, respectively. Thus, the performance of a reinforced concrete structure with irregularity has been determined as a result of wind and earthquake load effects.

2.1. Earthquake Analysis and Definitions

Determining the earthquake behavior of the modeled reinforced concrete structure, the coordinates of the building were taken into consideration, and according the Turkey Building Earthquake Regulation 2018, the acceleration records were determined by selecting Central Düzce from the Disaster and Emergency Management Centre (DEMC) Earthquake Zones Map. Accordingly, the earthquake load coefficients used in the analyzes for the DD-2 (earthquake ground-motion level, probability of exceedance of which is 10% in 50 years) earthquake level Isparta and Burdur provinces are given in Table 2. In addition, the horizontal elastic design spectrum of Isparta and Burdur provinces defined in ETABS are given in figure 4 and figure 5, respectively.

Table 2. Earthquake Load Coefficients for Isparta and Burdur Provinces

	S_S	S_1	S_{DS}	S_{D1}	Soil Class
ISPARTA	0.612	0.148	0.551	0.118	ZB
BURDUR	0.980	0.226	0.882	0.181	ZB

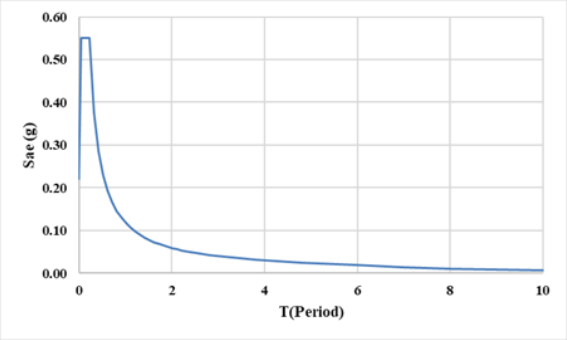

Figure 4. Horizontal elastic design spectrum of Isparta

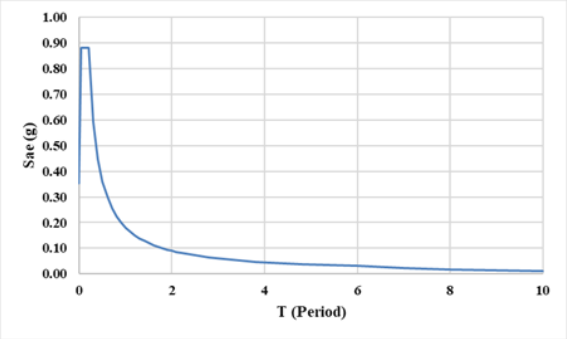

Figure 5. Horizontal elastic design spectrum of Burdur

In the 2018 Turkey Building Earthquake Regulation, there is a separate section for irregularity control of buildings. This section will be considered for irregularity checks as to the structure in the study.

To make a comparison between different cities, the analysis of building structure was performed by using ETABS software program for the elastic response of spectra data of Turkish standards codes. Natural vibration period for x and y direction is obtained from mode 1 and mode 2 respectively. The first mode (T1=0.975s) mode indicates the elastic state of the structure. The bending vibration is typical and parallel to the long span of the structure.

2.1.1. Effective relative storey drift

The Effective relative storey drift calculation is an important factor to control the stiffness of the structures during the design phase. An equation and a limit value are specified in the 2018 Turkish building earthquake code for the Effective relative storey drift control of the structures at the design stage. This equation and the limit value are shown in equation 1.

$$\lambda \frac{\delta_{imax}^{(x)}}{h_i} \leq 0.008\kappa \qquad (1)$$

For the Effective relative storey drift calculation, the fundamental vibration period of the building was determined for the provinces of Isparta and Burdur in the direction of the earthquake. The coefficients λx and λy were calculated for the fundamental period and then the effective relative storey drift ratios were found by using equation 1. Effective relative story drift analysis for earthquak load was made according to Equation 1. The results obtained are given in Figure 6.

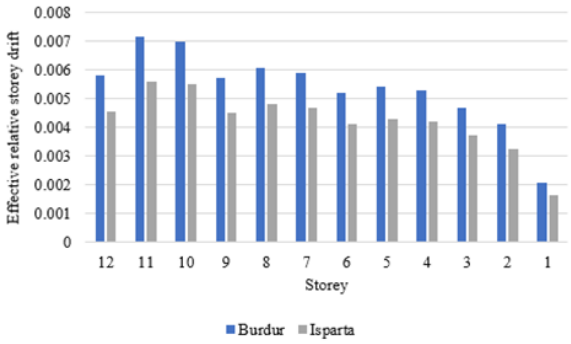

a) Effective relative storey drift for the X-direction

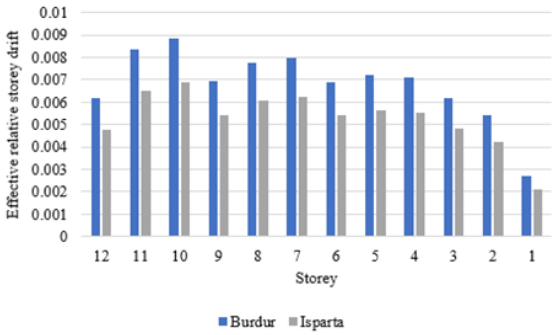

b) Effective relative storey drift for the Y-direction

Figure 6. Effective relative storey drift for the Isparta and Burdur according to earthquake load

As a result of the earthquake force applied in the X direction, the maximum effective relative storey drift ratio was observed at the 11th floor and its value was calculated as 0.005610 for the Isparta. For Burdur, the maximum effective relative storey drift ratio was observed at the same floor and its value was calculated as 0.007176. The maximum effective relative storey drift ratio in the Y direction for the province of Isparta was observed at the 10th floor and its value was calculated as 0.006858. The maximum effective relative storey drift ratio for the province of Burdur was calculated as 0.008794 at the same floor. Obtained findings were examined. As a result of the examination, it was determined that it was within acceptable limits in terms of TBEC 2018.

2.1.2. A1 –Torsional irregularity

A1-Torsional irregularity is seen frequently in structures. In order to control the torsional irregularity, the torsional irregularity coefficient must be calculated. Torsional irregularity is the ratio of maximum interstory drift value to the average interstory drift value at each story and given in equation 2. Torsional irregularity occurs when ηb value is between 1,20 and 2,00 in a structure.

$$\eta_{bi} = \frac{\Delta i_{max}}{\Delta i_{ort}} > 1.2 \qquad (2)$$

The Torsional irregularity values obtained from the calculations are given in the Figure 7 according to the cities and X and Y directions.

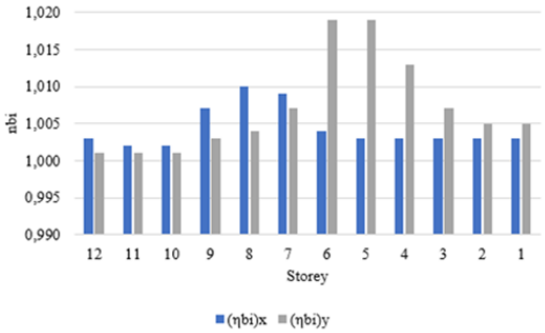

a) A1-Torsional irregularities for Isparta in the X -Y direction

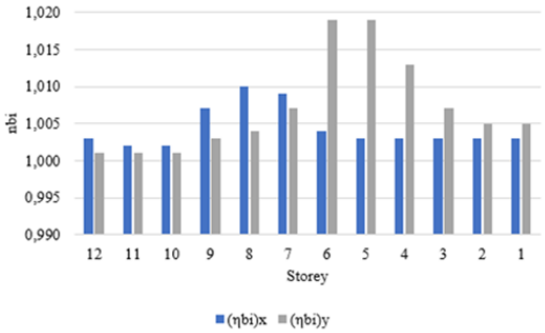

b)A1-Torsional irregularities for Burdur in the X -Y direction
Figure 7. A1-Torsional irregularity

As the figure 7 is examined, it is seen that the data obtained from the structure as a result of the analysis remain within the specified limit values in terms of A1-Torsion irregularities control.

It can be said that the model structure provides sufficient safety against torsional irregularity under the acceleration values in the study.

2.1.3. B2 – Soft storey irregularity

With respect to the TBEC 2018, the soft-storey irregularity plays an important role when choosing the seismic-analysis method different from the other moderncountries' codes. According to the regulation, if the average relative displacement rate of 5% horizontal force eccentricity on a floor is more than 2.0 value, B2-Soft Storey irregularity case occurs in the building. The soft-storey conditions from the TSC 2018 are expressed with Equations (3) and (4):

$$\eta_{ki} = \frac{(\boldsymbol{\Delta_i/H_i})_{ort}}{(\boldsymbol{\Delta_{i+1}/H_{i+1}})_{ort}} > 2.0 \quad (3)$$

$$\eta_{ki} = \frac{(\boldsymbol{\Delta_i/H_i})_{ort}}{(\boldsymbol{\Delta_{i-1}/H_{i-1}})_{ort}} > 2.0 \quad (4)$$

The soft storey irregularity values obtained from the calculations are given in the Table 3 according to the cities and X and Y directions.

Table 3. B2- Soft storey irregularity
a)B2- Soft Storey Irreularity for Isparta City in the X -Y direction

		X Direction				Y Direction			
Storey	H_i (m)	$(\Delta_i)_{ort}$ (m)	$(\Delta_i)_{ort}/H_i$	$\frac{(\boldsymbol{\Delta_i/H_i})_{ort}}{(\boldsymbol{\Delta_{i+1}/H_{i+1}})_{ort}}$	$\frac{(\boldsymbol{\Delta_i/H_i})_{ort}}{(\boldsymbol{\Delta_{i-1}/H_{i-1}})_{ort}}$	$(\Delta_i)_{ort}$ (m)	$(\Delta_i)_{ort}/H_i$	$\frac{(\boldsymbol{\Delta_i/H_i})_{ort}}{(\boldsymbol{\Delta_{i+1}/H_{i+1}})_{ort}}$	$\frac{(\boldsymbol{\Delta_i/H_i})_{ort}}{(\boldsymbol{\Delta_{i-1}/H_{i-1}})_{ort}}$
12	3	0.041	0.014	-	0.812	0.043	0.014	-	0.734
11	3	0.051	0.017	1.231	1.017	0.059	0.020	1.362	0.946
10	3	0.050	0.017	0.983	1.213	0.062	0.021	1.057	1.272
9	3	0.041	0.014	0.824	0.936	0.049	0.016	0.786	0.893
8	3	0.044	0.015	1.068	1.020	0.055	0.018	1.120	0.970
7	3	0.043	0.014	0.981	1.128	0.057	0.019	1.031	1.135
6	3	0.038	0.013	0.887	0.968	0.050	0.017	0.881	0.958
5	3	0.039	0.013	1.033	1.029	0.052	0.017	1.044	1.024
4	3	0.038	0.013	0.972	1.143	0.051	0.017	0.977	1.160
3	3	0.033	0.011	0.875	1.138	0.044	0.015	0.862	1.139
2	3	0.029	0.010	0.879	1.980	0.039	0.013	0.878	2.001
1	3	0.015	0.005	0.505	-	0.019	0.006	0.500	-

b) B2- Soft Storey Irreularity for Burdur City in the X -Y direction

		X Direction				Y Direction			
Storey	H_i (m)	$(\Delta_i)_{ort}$ (m)	$(\Delta_i)_{ort}/H_i$	$\frac{(\Delta_i/H_i)_{ort}}{(\Delta_{i+1}/H_{i+1})_{ort}}$	$\frac{(\Delta_i/H_i)_{ort}}{(\Delta_{i-1}/H_{i-1})_{ort}}$	$(\Delta_i)_{ort}$ (m)	$(\Delta_i)_{ort}/H_i$	$\frac{(\Delta_i/H_i)_{ort}}{(\Delta_{i+1}/H_{i+1})_{ort}}$	$\frac{(\Delta_i/H_i)_{ort}}{(\Delta_{i-1}/H_{i-1})_{ort}}$
12	3	0.064	0.021	-	0.815	0.067	0.022	-	0.737
11	3	0.078	0.026	1.228	1.022	0.091	0.030	1.357	0.950
10	3	0.077	0.026	0.978	1.219	0.096	0.032	1.053	1.274
9	3	0.063	0.021	0.820	0.937	0.075	0.025	0.785	0.892
8	3	0.067	0.022	1.068	1.020	0.084	0.028	1.122	0.971
7	3	0.066	0.022	0.980	1.129	0.087	0.029	1.030	1.135
6	3	0.058	0.019	0.886	0.970	0.076	0.025	0.881	0.958
5	3	0.060	0.020	1.031	1.030	0.080	0.027	1.044	1.026
4	3	0.058	0.019	0.971	1.141	0.078	0.026	0.975	1.161
3	3	0.051	0.017	0.876	1.134	0.067	0.022	0.862	1.137
2	3	0.045	0.015	0.882	1.977	0.059	0.020	0.880	1.998
1	3	0.023	0.008	0.506	-	0.030	0.010	0.501	-

As the table 3 is examined, it is seen that the data obtained from the model structure as a result of the analysis. It is seen that B2-Soft Storey irregularity was observed only in Isparta Y direction.

2.2. Wind Analysis and Definitions

As mentioned before, in cases where the wind load is not taken into account in the design of the structures, permanent and high damages may occur in the structures. For this reason, the behavior of the model structure under the influence of wind load, which is discussed in the article, is also examined. The design of wind load was calculated based on TS498. Although Eurocode is generally used in wind analysis, TS498 was chosen in this study. The ETABS software program is selected to perform analysis and Wind analysis was carried out for the model structure of Isparta and Burdur Cities. The wind speed was determined as 40 m/s and 50 m/s, respectively based on the Republic of Turkey Ministry of Environment and Urbanization Meteorology. The land regions in which the structures are located were selected as the 2nd region also based on TS498

2.2.1. Effective relative storey drift

Analyzes were made for the Isparta and Burdur model structures and the effective relative storey drift values were calculated according to the wind loads. Effective relative story drift analysis for wind load was made according to Equation 1. The results obtained are given in Figure 8.

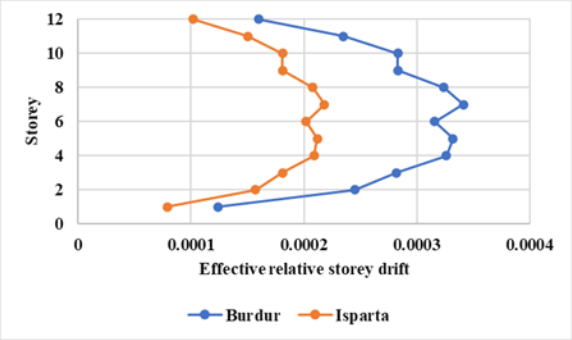

a) Effective relative storey drift ratio in the X direction

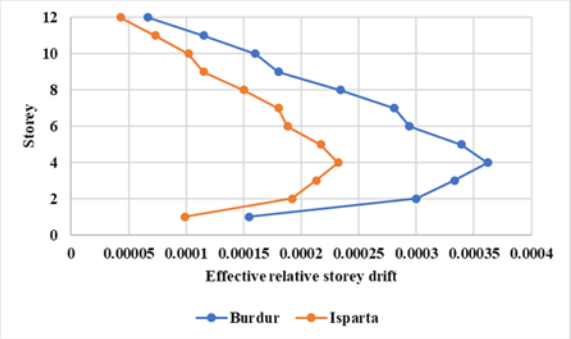

b) Effective relative storey drift ratio in the Y direction

Figure 8. Effective relative storey drift ratio in Isparta and Burdur provinces according to wind load

For Isparta X direction, the maximum effective relative story drift ratio was calculated as 0.000218 at the 7th storey, according to the wind load. For Burdur province, the maximum effective relative story drift ratio was calculated as 0.000341 at the 7th Storey. For Isparta Y direction, the maximum effective relative story drift ratio was calculated as 0.000232 at the 4th storey. The maximum effective relative story drift ratio for the province of Burdur was calculated as 0.000362 at the 4th storey. As the results of the analysis are evaluated in generally, it is seen that the effective relative storey drift for both cities is within the TBEC specified limits.

2.2.2. A1 – Torsional irregularity

Equation 2 was used to analyze the A1-torsion irregularity case in the Isparta and Burdur Cities according to the wind loads and the obtained values are given in Figure 9.

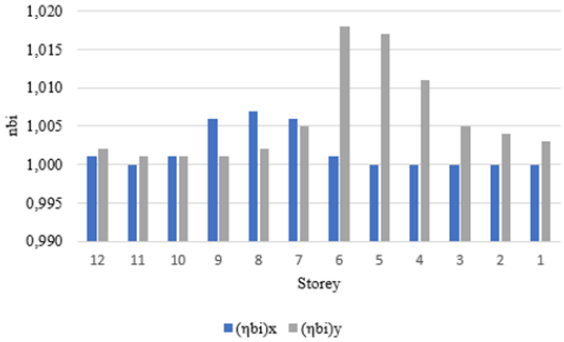

a) A1-Torsional irregularities for Isparta in the X -Y direction

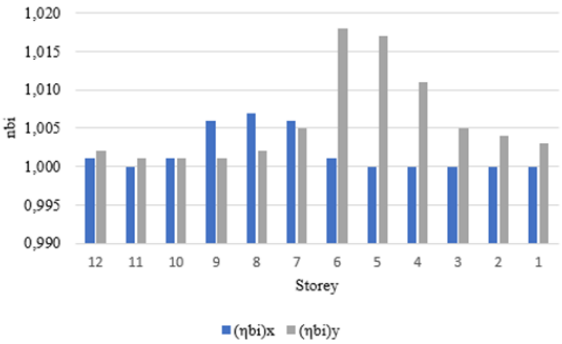

b) A1-Torsional irregularities for Burdur in the X -Y direction
Figure 9. A1-Torsional irregularity

As the figure 9 is examined, it is seen that the data obtained from the structure as a result of the analysis remain within the specified limit values in terms of A1-Torsion irregularities control. It can be said that the model structure provides sufficient security against torsional irregularity under the wind loads values in the study.

2.2.3. B2- Soft storey irregularity

Equation 3 and 4 were used to analyze the B2-Soft Storey irregularity case in the Isparta and Burdur Cities according to the wind loads and the obtained values are given in Table 4.

Table 4. B2-Soft Storey Irregularity
a) B2- Soft Storey Irreularity for Isparta City in the X -Y direction

		X Direction				Y Direction			
Storey	H_i (m)	$(\Delta_i)_{ort}$ (m)	$(\Delta_i)_{ort}/H_i$	$\frac{(\Delta_i/H_i)_{ort}}{(\Delta_{i+1}/H_{i+1})_{ort}}$	$\frac{(\Delta_i/H_i)_{ort}}{(\Delta_{i-1}/H_{i-1})_{ort}}$	$(\Delta_i)_{ort}$ (m)	$(\Delta_i)_{ort}/H_i$	$\frac{(\Delta_i/H_i)_{ort}}{(\Delta_{i+1}/H_{i+1})_{ort}}$	$\frac{(\Delta_i/H_i)_{ort}}{(\Delta_{i-1}/H_{i-1})_{ort}}$
12	3	0.003	0.001	-	0.678	0.001	0.0004	-	0.582
11	3	0.005	0.002	1.474	0.832	0.002	0.001	1.719	0.719
10	3	0.005	0.002	1.202	1.002	0.003	0.001	1.391	0.887
9	3	0.005	0.002	0.998	0.875	0.003	0.001	1.127	0.770
8	3	0.006	0.002	1.142	0.949	0.004	0.001	1.299	0.836
7	3	0.007	0.002	1.053	1.072	0.005	0.002	1.196	0.966
6	3	0.006	0.002	0.932	0.953	0.006	0.002	1.035	0.867
5	3	0.006	0.002	1.049	1.018	0.006	0.002	1.153	0.930
4	3	0.006	0.002	0.983	1.155	0.007	0.002	1.075	1.083
3	3	0.005	0.002	0.866	1.153	0.006	0.002	0.923	1.104
2	3	0.005	0.002	0.867	1.975	0.006	0.002	0.906	1.943
1	3	0.002	0.001	0.506	-	0.003	0.001	0.515	-

b) B2- Soft Storey Irreularity for Burdur City in the X -Y direction

		X Doğrultusu				Y Doğrultusu			
Kat	H_i (m)	$(\Delta_i)_{ort}$ (m)	$(\Delta_i)_{ort}/H_i$	$\frac{(\Delta_i/H_i)_{ort}}{(\Delta_{i+1}/H_{i+1})_{ort}}$	$\frac{(\Delta_i/H_i)_{ort}}{(\Delta_{i-1}/H_{i-1})_{ort}}$	$(\Delta_i)_{ort}$ (m)	$(\Delta_i)_{ort}/H_i$	$\frac{(\Delta_i/H_i)_{ort}}{(\Delta_{i+1}/H_{i+1})_{ort}}$	$\frac{(\Delta_i/H_i)_{ort}}{(\Delta_{i-1}/H_{i-1})_{ort}}$
12	3	0.005	0.002	-	0.678	0.002	0.001	-	0.581
11	3	0.007	0.002	1.475	0.832	0.003	0.001	1.720	0.718
10	3	0.008	0.003	1.201	1.002	0.005	0.002	1.392	0.890
9	3	0.008	0.003	0.998	0.875	0.005	0.002	1.123	0.769
8	3	0.010	0.003	1.143	0.951	0.007	0.002	1.301	0.835
7	3	0.010	0.003	1.052	1.072	0.008	0.003	1.197	0.965
6	3	0.009	0.003	0.933	0.952	0.009	0.003	1.036	0.867
5	3	0.010	0.003	1.051	1.018	0.010	0.003	1.153	0.930
4	3	0.010	0.003	0.982	1.156	0.011	0.004	1.075	1.084
3	3	0.008	0.003	0.865	1.153	0.010	0.003	0.923	1.106
2	3	0.007	0.002	0.868	1.978	0.009	0.003	0.904	1.940
1	3	0.004	0.001	0.505	-	0.005	0.002	0.516	-

As the table 4 is examined, it is seen that the data obtained from the model structure as a result of the analysis. It can be said that the model structure provides sufficient security against Soft Storey irregularity under the wind loads values in the study.

3. RESULTS

It is important to state that, even if the interstory drift ratios in buildings may be relatively small with no significant risk issues for the main force resisting system of the structure, nonstructural systems represent a high percentage of loss exposure of buildings to earthquakes [1]. Hence, all risk issues, all extra additioanal loads in structures must be carefully considered.

In this study, the vertical setback irregularity, formed because of the various design reasons was investigated.a reference building were compared in term of city, earthquake and wind load. The analyses were done using the ETABS structural analysis program. In this context, in a building model a vertical setback irregularity was deliberately formed.

It is stated in the 2018 TBEC that all structures to be built in earthquake zones should be designed by taking into account the irregularity conditions and evaluating within certain limits. In this paper, the building model with setback irregularity was discussed. The structure was examined according to the located in two different cities, Isparta and Burdur, and exposured to earthquake and wind loads. For this, ETABS structural analysis program has been used to evaluate the results by the referenced building. During examination of the result analyses, torsional irregularity, soft storey irregularity, and effective relative storey drift conditions occurring in the building were examined and compared.

According to the results obtained from the response spektrum analysis, it is seen that the effective relative storey drift and A1-torsion irregularity in both cities meet the regulation limit values. In B2-Soft Storey irregularity control, the value obtained in Isparta Y direction for the 2nd floor was found to be higher than the limit values of the regulation. In addition, it is seen that the effective relative storey drift values are higher in Burdur city than Isparta city. The reason for this is that the earthquake accelerations of Burdur city are higher compared to Isparta.

Besides the earthquake analysis, the results obtained from the wind load analysis, which is the second most important horizontal load acting on the structure, were compared in terms of torsional irregularity, soft story irregularity and effective relative story drift. According to the results obtained, it is seen that the effective relative storey drift, torsional irregularity and soft storey irregularity meet the regulation limit values for both cities according to the X and Y directions.

As the values obtained as a result of response spectrum and wind analysis were compared, the values obtained in the wind load analysis were lower than the values obtained from the earthquake analysis.

The acceleration values that change according to the location and coordinates of the cities and the annual wind average have been effective on this situation. For this reason, it is possible to obtain more critical results in studies to be carried out for different regions and different heights, unlike the results obtained from this study.

As a result, It seems that reinforced concrete buildings designed for earthquake and wind are safe under moderate earthquake loads. Nevertheless, it is important to, even if the interstory drift ratios in buildings may be relatively small with no significant apparent issues for the main force resisting system of the structure, nonstructural systems may represent a high percentage of loss exposure of buildings to earthquakes and winds. Hence, it is necessary to design by considering the wind load, especially in some regions in our country and appropriate regular design techniques are should recommended for the reduction under wind and earthquake loads.

REFERENCES

[1] Aly AM, Abburu S. On the Design of High-Rise Buildings for Multihazard: Fundamental Differences between Wind and Earthquake Demand. Shock and Vibration 2015;2015:1–22. https://doi.org/10.1155/2015/148681.

[2] Al-Soudani M, Abbas AN, Numan HA. Assessment of Reinforced Concrete Structures under Wind and Earthquake Using Different Design Methods. Journal of Engineering Research 2021. https://doi.org/10.36909/jer.10411.

[3] Atmaca B, Demir S, Murat Günaydin ;, Ahmet ;, Altunişik C, Hüsem M, et al. Field Investigation on the Performance of Mosques and Minarets during the Elazig-Sivrice Earthquake 2020;34(6). https://doi.org/10.1061/(ASCE)CF.1943.

[4] Bayraktar D. Antalya ve Çevresinde Tarihsel Dönem Depremlerinin Antik Yapılara Etkisinin Araştırılması. Düzce Üniversitesi Bilim ve Teknoloji Dergisi 2019;7:352–68. https://doi.org/10.29130/dubited.446563.

[5] Abbas M, Elbaz K, Shen S-L, Chen J. Earthquake effects on civil engineering structures and perspective mitigation solutions: a review. Arabian Journal of Geosciences 2021;14:1350. https://doi.org/10.1007/s12517-021-07664-5.

[6] Çimen İ, Hanbay S, Erdem S. Yüksek Katlı Düzensiz Geometrili Diagrid Yapıların Deprem Performansının Deneysel ve Nümerik Analizi. 4th International Symposium on Natural Hazardsand Disaster Management, vol. 3, 2020, p. 982–92. https://doi.org/10.33793/acperpro.03.02.38.

[7] Onat Ö, Usta P. 20 Katlı Betonarme Yapının Farklı Perde Duvar Yerleşimlerine Göre Deprem Analizi. European Journal of Science and Technology 2021;25:363–9. https://doi.org/10.31590/ejosat.912625.

[8] Satılmış S. Birinci El Kaynaklara Göre Isparta Depremleri (19. Yüzyılın İkinci Yarısı). Selçuk Üniversitesi Edebiyat Fakültesi Dergisi 2018:297–312. https://doi.org/10.21497/sefad.515374.

[9] Çavdar Ö, Yolcu A. Mevcut Bir Okul Binasının Türk Bina Deprem Yönetmeliği 2018'e Göre Yapısal Düzensizliklerinin İncelenmesi. Ordu University Journal of Science and Technology Ordu Üniv Bil Tek Derg 2018;8:153–64.

[10] Çarhoglu AI, Zabin P, Korkmaz KA. Investigation of Structural Behavior of Historical Churches under Effects: Isparta Hagia Banıya Church Case. International Civil Engineering & Architecture Symposium for Academicians, Antalya: 2014, p. 405–12.

[11] Çöğürcü MT, Uzun M. Prefabrike Yapıların Rüzgar Yükü Güvenliğinin Belirlenmesi. Selcuk University Journal of Engineering ,Science and Technology 2019;7:171–88. https://doi.org/10.15317/scitech.2019.191.

[12] Ümran M. Yüksek Yapılardaki Rüzgar Yüklerinin Hesabı. İnşaat Mühendisleri Odası 4. Ulusal Çelik Yapılar Sempozyumu. 2012, p. 27–38.

[13] Kushwaha D, Saleem H, Shrivastava LP. A Comparative Study on High Rise Building for various Geometrical Shapes Subjected to Wind Load of RCC & Composite Structure using ETABS. International Research Journal of Engineering and Technology 2019;6:1553–8.

[14] Demir A, Dönmez Demir D, Erdem RT, Bağcı M. Torsional Irregularıty Effects of Local Sıte Classes ın Multıple Storey Structures, IJREAS 2010;258-262

[15] Işık E, Özdemir M, Karaşin İB. Performance Analysis of Steel Structures with A3 Irregularities. International Journal of Steel Structures 2018;18(3):1083–94. https://doi.org/10.1007/s13296-018-0046-6.

[16] Yeşim İlerisoy Z. Vertical Structural Irregularities in Earthquake Codes within the Scope of Architectural Design. Online Journal of Art and Design. 2019;7(1):231-53

[17] İlgün A, Yorulmaz AM. Research on A1 Irregularity Status in Different Spectral Acceleration Coefficents on Reinforced Concrete Structures. Turkish Journal of Engineering. 2021;5(4):177-82. https://doi.org/10.31127/tuje.728820.

[18] Keleş Y, Kasap H, Yaman Z. Evaluating the effects of different slab types on static and dynamic characteristics of structures. Challenge Journal of Structural Mechanics 2021;7:71. https://doi.org/10.20528/cjsmec.2021.02.003.

[19] [19] Uyan B, Erdem RT. Düşeyde Düzensiz Mevcut Betonarme Binaların Deprem Performansının Araştırılması. ALKÜ Fen Bilimleri Dergisi. 2021;7(2):71-83. https://doi.org/10.46740/alku.1013881.

[20] Usta P, Bozdağ Ö, Onat Ö. Seismic Performance Evaluation of RC buildings using Irregularity based Indices. Tehnički Vjesnik 2022. https://doi.org/https://doi.org/10.17559/TV-20210720195034.

[21] ETABS Software Version 18, Computer and structures, Inc. Berkeley, California, USA

Cilt 11, Sayı 1, Sayfa 151-156, 2022 Volume 11, Issue 1, Page 151-156, 2022

Derleme https://doi.org/10.46810/tdfd.795053 Review

Türk Doğa ve Fen Dergisi
Turkish Journal of Nature and Science
www.dergipark.gov.tr/tdfd

Polymer-Based Transfection Agents Used in CRISPR-CAS9 System

Rizvan İMAMOĞLU[1*], Özlem KAPLAN[2], Mehmet Koray GÖK[3], İsa GÖKÇE[4]

[1] Bartın University, Faculty of Science, Department of Molecular Biology and Genetics, Bartın, Turkey
[2] Istanbul University, Faculty of Science, Department of Molecular Biology and Genetics, Istanbul, Turkey
[3] Istanbul University-Cerrahpasa, Faculty of Engineering, Department of Chemical Engineering, Istanbul, Turkey
[4] Gaziosmanpaşa University Faculty of Engineering and Architecture Department of Bioengineering, Tokat, Turkey
Rizvan İMAMOĞLU ORCID No: 0000-0002-6306-4760
Özlem KAPLAN ORCID No: 0000-0002-3052-4556
Mehmet Koray GÖK No: 0000-0003-2497-9359
İsa GÖKÇE ORCID No: 0000-0002-5023-9947

** Corresponding author: rimamoglu@bartin.edu.tr*

(Received: 16.09.2020, Accepted: 23.04.2021, Online Publication: 25.03.2022)

Keywords
CRISPR, *non-viral* transfection agent, polymeric carrier system,

Abstract: Genome editing is a method used to make desired changes in the target gene. Today, various methods are used for genome-editing studies; among them, one of the most widely used methods is the clustered, regularly interspaced short palindromic repeats (CRISPR). CRISPR-associated (Cas) genes and their corresponding CRISPR sequences constitute CRISPR-Cas systems. Due to its simplicity, it is likely that the CRISPR–Cas system could be used effectively in ex vivo gene therapy studies in humans. If this happens, the importance of CRISPR carrier systems will gradually increase. Viral and non-viral systems are used as delivery modalities in genome-editing studies. It has been proven that nanoparticles are the most promising tools for gene therapy due to their adjustable size, surface, shape, and biological behaviours. The polymeric carrier system has become the main non-viral substitute for gene delivery due to its reduced immunogenicity and pathogenicity. In this review, information about current studies related to polymeric carriers used in non-viral CRISPR delivery systems is presented.

CRISPR-CAS9 Sisteminde Kullanılan Polimer Bazlı Transfeksiyon Ajanları

Anahtar Kelimeler
CRISPR, Viral olmayan Transfeksiyon ajanları, Polimerik Trasnfeksiyon Ajanları,

Öz: Genom düzenleme, hedef gende istenilen değişiklikleri yapmak için kullanılan bir yöntemdir. Günümüzde genom düzenleme çalışmaları için çeşitli yöntemler kullanılmaktadır; bunlar arasında en yaygın kullanılan yöntemlerden biri kümelenmiş, düzenli aralıklarla yerleştirilmiş kısa palindromik tekrarlardır (CRISPR). CRISPR ile ilişkili (Cas) genleri ve bunlara karşılık gelen CRISPR dizileri, CRISPR-Cas sistemlerini oluşturur. Basitliği nedeniyle, CRISPR-Cas sisteminin insanlarda *ex vivo* gen terapisi çalışmalarında etkili bir şekilde kullanılmaya başlanmıştır ve CRISPR taşıyıcı sistemlerin önemi giderek artmaktadır. Genom düzenleme çalışmalarında dağıtım yöntemleri olarak viral ve viral olmayan sistemler kullanılmaktadır. Nanopartiküllerin ayarlanabilir boyutları, yüzeyleri, şekilleri ve biyolojik davranışları nedeniyle gen terapisi için en umut verici araçlar olduğu kanıtlanmıştır. Polimerik taşıyıcı sistem, azaltılmış immünojenisitesi ve patojenitesi nedeniyle gen aktarımı için viral olmayan ana ikame haline gelmiştir. Bu derlemede, viral olmayan CRISPR dağıtım sistemlerinde kullanılan polimerik taşıyıcılarla ilgili güncel çalışmalar hakkında bilgiler sunulmaktadır.

1. INTRODUCTION

The field of genome modification includes techniques used to obtain centered modifications inside an organism's DNA. Until today, the rapid transition of gene editing into clinical practice has occurred thanks to the emergence of programmable nucleases that allow scientists to perform gene editing in numerous cell types. Today, existing editing approaches include zinc finger nucleases (ZFNs), transcriptional activator-like effector nucleases (TALENs), and clustered, regularly interspaced short palindromic repeats (CRISPR)/CRISPR-associated

nuclease 9 (Cas9). ZFN is a targetable DNA fragmentation protein that can be used to cleave DNA sequences at any site. On the other hand, TALENs can cause a double-strand break in the target nucleotide sequence, which leads to genome modification by triggering the DNA damage response pathway [1]. From 2002 to 2011, respectively, ZFNs and TALENs have been mainly used in genome editing in animal and human cells and plants; however, during this time, they have also exhibited some disadvantages that prevent their usage in certain cases. For example, ZFNs show limited specificity and can cause off-target mutations [2]. In addition, vector design for ZFNs and TALENs takes time and effort to perform [3]. Table 1 presents a comparison of the TALEN, ZFN, and CRISPR-Cas9 genome editing techniques.

Table 1. Comparison of the TALEN, ZFN, and CRISPR–Cas9 genome editing techniques [4]

	CRISPR/Cas9	**ZFN**	**TALEN**
Molecular elements	Single-stranded gRNA+Cas9 endonuclease	ZFN protein+Fok1 endonuclease	RVD of the TALE protein sequenced repeat region+Fok1 endonuclease
Recognition site and specificity	• Usually 20 bp directory sequence + PAM sequence • Tolerate spatial/consecutive multiple mismatches	• Each ZFN protein recognizes 3 bp DNA • Tolerate a small number of positional mismatch	• Each TALE protein unit recognizes a single base pair of DNA. • Tolerate a small number of positional mismatch
Challenges and restrictions	• A PAM sequence must come before the targeted area. • Utilizing oligo synthesis and standard cloning procedures	• Difficult to target regions with poor G nucleotide content • Requires significant protein engineering	• 5′ targeted base should be one T nucleotide for each TALEN monomer • Difficult and complex cloning methods
Advantages	Targeting multiple genes	Small protein size and suitable for viral vector	High recognition specificity and no need to link between repeats
Transfection difficulties	The widely used SpCas9 is medium in size and may cause packaging issues for some viral vectors, but smaller orthologs are available	Since ZFN expression elements are small, they are simple to use in a variety of viral vectors.	Due to the large size of functional components, it is difficult.

Due to the reasons mentioned above, the use of CRISPR–Cas9 in genome editing has been widely preferred since 2013. The CRISPR–Cas9 method is an RNA-guided endonuclease that can specifically target DNA sequences through nucleotide base pairing. This system is highly specific, versatile, and simple. It has become a valuable tool in biological research for both gene function and gene editing because of these properties [5]. With the reporting of the first CRISP structure by Ishino in 1987, it has reached the present day as a mechanism used by many bacteria and archaea to protect them from virus invasion [6, 7]. In 2002, after observing the existence of several similar structures in different archaea and bacteria, Jansen proposed the acronym for CRISPR [8].

Finally, the approach was first applied to mammalian cells in 2013 and since then, the CRISPR–Cas system has occupied an important place in genome-editing research [9]. CRISPR–Cas structures are categorized from type I to type VI [10]. The type I system is characterized by the formation of Cas3, which is a protein with both DNase and helicase activities that can be used to degrade targets. The type II CRISPR–Cas system uses Cas1, Cas2, Cas9, and a fourth protein (either Csn2 or Cas4) [11]. The type III-A CRISPR–Cas system is an adaptive immune system guided by prokaryotic RNA, which uses Csm (a protein–RNA complex that can perform transcription-dependent immunity against foreign DNA) [12].

The type II CRISPR–Cas system is derived from *Streptococcus pyogenes* and consists of three parts: CRISPR RNA (crRNA), trans-activating crRNA (tracrRNA), and a Cas9 protein [13]. Cas9 is an enzyme that uses CRISPR sequences to recognize and separate specific DNA strands; thus, the Cas9 enzyme and CRISPR sequencing can be used together to edit genes in organisms and form the basis of CRISPR–Cas9 technology [14]. The regulation process has a huge range of applications, including the improvement of biotechnology products, basic organic studies, and disease treatment [15].

In general, Cas proteins obtained from bacteria have two nuclease domains and work together with single-guide RNA (sgRNA) to create a double-strand break in the target DNA sequence. sgRNA is the component that directs the Cas protein to the target DNA since it contains crRNA and tracrRNA and has a short sequence complementary to the target DNA sequence [9]. Another critical component is the protospacer adjacent motif (PAM), which is located in the target DNA sequence and guides the determination of the cut side of the Cas protein. This system has made it possible to perform applications such as mutation deletion, gene suppression and activation in the target region [14].

By applying this method in the field of genetic engineering, the structure of DNA can be changed precisely in areas where the genome is cut. Moreover, to recognize and repair damaged DNA, this method can be used in the field of genetic engineering by making use of the mechanism of cells. The successful application of the CRISPR–Cas9 system is based on the correction of the cut ends formed by the double-strand break in the DNA as a

result of the cutting created in the desired region of the genome/gene by non-homologous end-joining or a homologous recombination repair mechanism. By modifying the components of the system, the desired and designed genome/gene change can be realized. Also, through linking the engineered sgRNA sequence to the target DNA region by base pairing, the Cas protein recognizes the cleavage site and cuts both strands of the chain from three nucleotides near the PAM by way of nuclease activity, and subsequently, endogenous DNA repair is initiated. After this step, if the knockout of the target gene is aimed, the double-strand break is repaired by the non-homologous repair mechanism that is prone to error. Insertion mutations that occur during this time cause the loss of gene products.

1.1. CRISPR–Cas9 Carrier Systems

There are several obstacles to the practical application of the CRISPR–Cas9 Carrier Systems. These obstacles can be summarised as follows:

1. The stability of the CRISPR–Cas9 system against serum nucleases is very low.
2. The CRISPR–Cas9 system can stimulate the innate immune system.
3. This system may interact nonspecifically with non-target cells and serum proteins.
4. The CRISPR–Cas9 system can be easily cleaned by the kidney system.
5. It is difficult to enter target tissues through blood vessels
6. Degradation products of carriers can be toxic
7. Requires different approaches for different cell line [16-21].

To overcome these problems, new carrier systems have been introduced over time. Viral vectors (e.g., lentivirus, adeno-associated virus, and adenovirus) and physical strategies (e.g., microinjection, electroporation and osmocytosis-induced transduction, mechanical cell deformation, and hydrodynamic injection) are the most widely used delivery system strategies [22-25]. Viral vectors are widely used in CRISPR–Cas9 delivery, and viral carrier systems provide high efficiency in genome editing. However, viral carrier systems also show some basic limitations such as the risk of cancer development, the fact that it is a very long and difficult process to produce on a large scale and their propensity for immune-system stimulation [26, 27].

Physical carriers such as electroporation and microinjection have high degrees of transfection efficiency, but they are not suitable as methods to be adopted for *in vivo* purposes [28-30]. Instead, a hydrodynamic application strategy can be used for *in vivo* experiments; however, it causes various problems such as hepatomegaly, hypertension, and heart dysfunction [31, 32]. In recent years, many studies have been conducted on the development of nanoparticle systems to deliver the CRISPR–Cas9 system to target cells. By overcoming the aforementioned obstacles through the synthesis of advanced nanocarriers, the gene-delivery efficiency can be significantly increased [33-35]. Polymers exhibit significant potential due to their low carcinogenicity or immunogenicity, reduced restrictions with respect to load size, protection of cargo molecules, and creation of nanoformulations with the CRISPR–Cas9 system [36]. In addition, various modifications made on polymers can enhance their circulation time, the controlled release of cargo molecules and cell- or tissue-specific delivery capacities [37, 38]. This review focuses on polymeric nanocarrier systems used in the context of the CRISPR–Cas9 system.

1.2. CRISPR–Cas9 Polymeric Nanocarrier Systems

Polymeric nanoparticles are widely used for the transport of diverse types of nucleic acids [39]. Polymeric carriers can be synthesized from synthetic monomers [e.g., poly(lactic-co-glycolic) acid (PLGA) or polycaprolactone] or natural monomers (i.e., sugars such as chitosan) (Glass et al., 2018). Polymer can protect the cargo molecule from degradation and can increase specific release by functionalizing the cargo molecule with targeting moieties that will enable it to bind to surface receptors of the target cell [12]. However, there are few examples of polymeric carriers reported to date in the literature regarding the CRISPR–Cas9 delivery system. Nanoparticular systems can be used to transport all three forms of CRISPR–Cas9 components (i.e., Cas9 protein/sgRNA, Cas9 mRNA/sgRNA, and Cas9/sgRNA plasmid DNA) to desired cells.

In the literature, cationic polymers such as polyethyleneimine (PEI) have been studied for the transport of CRISPR–Cas9 systems. These polymers are highly positively charged, which can protect DNA from physical and chemical factors. In addition, it presents a high endosomal escape capability to liberate plasmid. So far, polymers such as PLGA, poly(amidoamine), PEI, and chitosan have been tested for delivery of the CRISPR–Cas9 plasmid to target cells, and they have demonstrated good genome-editing potential. They have high positive charges, can interact strongly with negatively charged nucleic acids, and can effectively escape from the endosome due to a strong proton-sponge effect; all of these ensure that it exhibits a high degree of gene-transfection efficiency [40]. In the research conducted by Ryu et al. [38], it was shown that commercial jet-PEI and 25-kDa branched PEI polymer-based DNA transfection reagent successfully delivered plasmid-encoding Cas9/sgRNA. However, the use of these nanocarriers has been restricted due to their high cytotoxicity [38]. Both the transfection and toxicity efficiency of PEI increase in parallel with its molecular weight. Therefore, low-molecular-weight PEI (LMWPEI) has been tested in CRISPR–Cas9 plasmid delivery since its low transfection efficiency is tolerable. Moreover, various modifications have been made to LMWPEI in order to improve its properties. Lino et al. [41] functionalized the LMWPEI polymer with polyethylene glycol (PEG) and cholesterol (CHOL) to obtain a lipopolymer. They showed notably that CHOL increased the permeability through the membrane and PEG increased the hemocompatibility and stability of the lipopolymer. This lipopolymer was then modified with specific aptamers for targeted delivery of

the CRISPR–Cas9 system [41]. Li et al. [34] developed a polymeric 'core-shell' complex with LMWPEI coated with RGD-R8-PEG-HA copolymer, which is a copolymer containing RGD-R8 peptide. In this arrangement, the peptide RGD-R8 had a significant effect on an integrin receptor that was overexpressed in tumours and tumour blood vessels and which gave the polymer tumour-targeting ability. In addition, Li et al. [42] showed that the anionic HA (hyaluronic acid) fragment reversed the cationic charge of the fluorinated LMWPEI and the PEG fragment made the complex more stable, thereby it reduced nonspecific interactions with the human body. In their research, Liu et al. [43] modified LMWPEI by fluorination. They revealed that the polymer subsequently became both hydrophilic and hydrophobic after fluorination, and nanopolymers with good resistance to the lipid bilayer were easily absorbed by cells, while escaping from endosomes also occurred [43]. Zhang et al. [44] assessed the in vitro transmission of the CRISPR–Cas9 system mediated by the cationic polymer PEI–cyclodextrin (PC) in HeLa cells. Their study showed that these nanocomplexes produced with Cas9/sgRNA plasmids were positively charged and could facilitate proper cell uptake and transfection. Ultimately, the efficient packaging and concentration of the plasmid encoding Cas9 and sgRNA in PC was realized. This study also emphasized that although it was similar to high-molecular-weight PEI in terms of structure, PC showed lower cytotoxicity, which allowed PC to function at high dose levels or repeated transfections [44]. Kang et al. [45], covalently linked conjugated branched PEI (bPEI) to the Cas9, then combined this grouping with sgRNA. This nanocomplex targeting the mecA gene was successfully transferred to *Staphylococcus aureus* despite the bacteria's thick cell wall. In addition, it was found that the efficiency of the polymer-conjugated Cas9 was relatively higher compared to the efficiency of genome editing of standard lipid-based formulations or natural Cas9 complexes [45].

PBAE has features such as low toxicity, high water solubility, good biocompatibility, pH sensitivity, and rapid drug release at acidic pH values [46]. A new nanostructure consisting of poly(β-amino ester) (PBAE) was designed by Zhu et al. [46] to transfer CRISPR/short-hairpin RNA (shRNA) to HPV16 transgenic mice. E6 and E7 human papillomavirus (HPV) are oncoproteins that play an essential role in the development of cervical cancer and drug resistance. Carboxylated branched poly(β-amino ester) nanoparticles produced by Rui et al.[45] ensured the efficient and rapid delivery of Cas9/sgRNA to the target cell cytoplasm and escaped from endosomes. This system demonstrated *in vitro* knockout and knockin efficiency results as 75% and 4%, respectively [47].

Xu et al. [48] showed a type of cationic CHOL-assisted PLGA nanoparticles (CLAN) consisting of PEG-PLGA and BHEM-CHOL (N,N-bis(2-hydroxyethyl)-N-methyl-N-(2-cholesteryloxycarbonyl aminoethyl) ammoniumbromide). While PEG was used to support the long-term circulation of the nanoparticles, cationic lipids were used to neutralize the negative charge of the polymer. These scholars also designed a CLAN library with different PEG densities and surface loads to produce the appropriate CLAN and then tested macrophage uptake *in vivo* to screen for the ideal option. Their results showed that nanoparticles with the highest surface loading and relatively low PEG density had the best uptake by macrophages [48]. PEGylation is widely used with the reticuloendothelial system to reduce opsonization and clearance. It can also be applied as a strategy for CRISPR–Cas9 delivery [49].

Chitosan is a positively charged, nontoxic and biodegradable polymer. Chitosan, as a widely used polymer for gene delivery systems, also exhibits potential for the delivery of the CRISPR/Cas9 system [43]. Zhang et al. [50] combined chitosan with mPEG for CRISPR–Cas9 delivery and showed that this nanocomplex protected DNA from nuclease nebulization and digestion.

2. CONCLUSION

Genome-editing studies are a field whose scope and importance are increasing with new and variable methods emerging. Especially given its simplicity and applicability, genome editing with CRISPR is likely to be a much more frequently used method in the future. The use of polymers is an increasingly common way by which the vectors used in genome editing are delivered. A wide range of nanocarriers has already been applied as non-viral delivery systems in human gene therapy. Advancements in materials science and nano-ecology allow the emergence of synthetic vectors with optimum physicochemical properties and tissue/cell targeting capabilities. Polymeric *non-viral* vectors have advantages such as the avoidance of potential toxicity and immunogenicity, good reproducibility, and adherence to good manufacturing practices.

New application strategies are being developed for the delivery of CRISPR–Cas9 components into the cell efficiently. Among these, cationic polymers are susceptible to modifications that allow targeting as well as basic properties such as low immunogenicity and carcinogenicity, and cargo protection. In conclusion, it can be said that the application of polymers in CRISPR–Cas9 delivery is an interesting area that warrants future research.

REFERENCES

[1] Gaj T, Gersbach CA, Barbas CF, 3rd. ZFN, TALEN, and CRISPR/Cas-based methods for genome engineering. Trends Biotechnol. 2013;31(7):397-405. Epub 2013/05/15. doi: 10.1016/j.tibtech.2013.04.004.

[2] Puchta H. Applying CRISPR/Cas for genome engineering in plants: the best is yet to come. Curr Opin Plant Biol. 2017;36:1-8. Epub 2016/12/04.

[3] Tang X, Lowder LG, Zhang T, Malzahn AA, Zheng X, Voytas DF, et al. A CRISPR-Cpf1 system for efficient genome editing and transcriptional repression in plants. Nat Plants. 2017;3:17018.

[4] Li H, Yang Y, Hong W, Huang M, Wu M, Zhao X. Applications of genome editing technology in the targeted therapy of human diseases: mechanisms, advances and prospects. Signal Transduct Target Ther. 2020;5(1):1.
[5] Doudna JA, Charpentier E. Genome editing. The new frontier of genome engineering with CRISPR-Cas9. Science. 2014;346(6213):1258096.
[6] Barrangou R, Fremaux C, Deveau H, Richards M, Boyaval P, Moineau S, et al. CRISPR provides acquired resistance against viruses in prokaryotes. Science. 2007;315(5819):1709-12.
[7] Ishino Y, Shinagawa H, Makino K, Amemura M, Nakata A. Nucleotide sequence of the iap gene, responsible for alkaline phosphatase isozyme conversion in Escherichia coli, and identification of the gene product. J Bacteriol. 1987;169(12):5429-33. Epub 1987/12/01. doi: 10.1128/jb.169.12.5429-5433.1987.
[8] Ishino Y, Krupovic M, Forterre P. History of CRISPR-Cas from Encounter with a Mysterious Repeated Sequence to Genome Editing Technology. J Bacteriol. 2018;200(7). Epub 2018/01/24.
[9] Mali P, Yang L, Esvelt KM, Aach J, Guell M, DiCarlo JE, et al. RNA-guided human genome engineering via Cas9. Science. 2013;339(6121):823-6.
[10] Makarova KS, Wolf YI, Alkhnbashi OS, Costa F, Shah SA, Saunders SJ, et al. An updated evolutionary classification of CRISPR-Cas systems. Nat Rev Microbiol. 2015;13(11):722-36..
[11] Rath D, Amlinger L, Rath A, Lundgren M. The CRISPR-Cas immune system: biology, mechanisms and applications. Biochimie. 2015;117:119-28.
[12] Liu TY, Liu JJ, Aditham AJ, Nogales E, Doudna JA. Target preference of Type III-A CRISPR-Cas complexes at the transcription bubble. Nat Commun. 2019;10(1):3001.
[13] Jinek M, Jiang F, Taylor DW, Sternberg SH, Kaya E, Ma E, et al. Structures of Cas9 endonucleases reveal RNA-mediated conformational activation. Science. 2014;343(6176):1247997.
[14] Zhang F, Wen Y, Guo X. CRISPR/Cas9 for genome editing: progress, implications and challenges. Hum Mol Genet. 2014;23(R1):R40-6.
[15] Hsu PD, Lander ES, Zhang F. Development and applications of CRISPR-Cas9 for genome engineering. Cell. 2014;157(6):1262-78.
[16] Cebrian-Serrano A, Davies B. CRISPR-Cas orthologues and variants: optimizing the repertoire, specificity and delivery of genome engineering tools. Mamm Genome. 2017;28(7-8):247-61.
[17] Dowdy SF. Overcoming cellular barriers for RNA therapeutics. Nat Biotechnol. 2017;35(3):222-9.
[18] Oude Blenke E, Evers MJ, Mastrobattista E, van der Oost J. CRISPR-Cas9 gene editing: Delivery aspects and therapeutic potential. J Control Release. 2016;244(Pt B):139-48..
[19] Timin AS, Muslimov AR, Lepik KV, Epifanovskaya OS, Shakirova AI, Mock U, et al. Efficient gene editing via non-viral delivery of CRISPR-Cas9 system using polymeric and hybrid microcarriers. Nanomedicine. 2018;14(1):97-108.
[20] Li L, He ZY, Wei XW, Gao GP, Wei YQ. Challenges in CRISPR/CAS9 Delivery: Potential Roles of Nonviral Vectors. Hum Gene Ther. 2015;26(7):452-62. Epub 2015/07/16. doi: 10.1089/hum.2015.069.
[21] Phillips AJ. The challenge of gene therapy and DNA delivery. J Pharm Pharmacol. 2001;53(9):1169-74. Epub 2001/10/02. doi: 10.1211/0022357011776603.
[22] Burks J, Nadella S, Mahmud A, Mankongpaisarnrung C, Wang J, Hahm JI, et al. Cholecystokinin Receptor-Targeted Polyplex Nanoparticle Inhibits Growth and Metastasis of Pancreatic Cancer. Cell Mol Gastroenterol Hepatol. 2018;6(1):17-32.
[23] Cheng R, Peng J, Yan Y, Cao P, Wang J, Qiu C, et al. Efficient gene editing in adult mouse livers via adenoviral delivery of CRISPR/Cas9. FEBS Lett. 2014;588(21):3954-8.
[24] Gori JL, Hsu PD, Maeder ML, Shen S, Welstead GG, Bumcrot D. Delivery and Specificity of CRISPR-Cas9 Genome Editing Technologies for Human Gene Therapy. Hum Gene Ther. 2015;26(7):443-51.
[25] Yin H, Song CQ, Dorkin JR, Zhu LJ, Li Y, Wu Q, et al. Therapeutic genome editing by combined viral and non-viral delivery of CRISPR system components in vivo. Nat Biotechnol. 2016;34(3):328-33.
[26] Hastie E, Samulski RJ. Adeno-associated virus at 50: a golden anniversary of discovery, research, and gene therapy success--a personal perspective. Hum Gene Ther. 2015;26(5):257-65.
[27] Kotterman MA, Chalberg TW, Schaffer DV. Viral Vectors for Gene Therapy: Translational and Clinical Outlook. Annu Rev Biomed Eng. 2015;17:63-89.
[28] Horii T, Arai Y, Yamazaki M, Morita S, Kimura M, Itoh M, et al. Validation of microinjection methods for generating knockout mice by CRISPR/Cas-mediated genome engineering. Sci Rep. 2014;4:4513.
[29] Remy S, Chenouard V, Tesson L, Usal C, Menoret S, Brusselle L, et al. Generation of gene-edited rats by delivery of CRISPR/Cas9 protein and donor DNA into intact zygotes using electroporation. Sci Rep. 2017;7(1):16554.
[30] Stewart MP, Sharei A, Ding X, Sahay G, Langer R, Jensen KF. In vitro and ex vivo strategies for intracellular delivery. Nature. 2016;538(7624):183-92.
[31] Hyland KA, Aronovich EL, Olson ER, Bell JB, Rusten MU, Gunther R, et al. Transgene Expression in Dogs After Liver-Directed Hydrodynamic Delivery of Sleeping Beauty Transposons Using Balloon Catheters. Hum Gene Ther. 2017;28(7):541-50.
[32] Yarmush ML, Golberg A, Sersa G, Kotnik T, Miklavcic D. Electroporation-based technologies for medicine: principles, applications, and challenges. Annu Rev Biomed Eng. 2014;16:295-320.
[33] Cunningham FJ, Goh NS, Demirer GS, Matos JL, Landry MP. Nanoparticle-Mediated Delivery

towards Advancing Plant Genetic Engineering. Trends Biotechnol. 2018;36(9):882-97.
[34] Liu C, Zhang L, Liu H, Cheng K. Delivery strategies of the CRISPR-Cas9 gene-editing system for therapeutic applications. J Control Release. 2017;266:17-26. Epub 2017/09/16.
[35] Su C, Liu Y, He Y, Gu J. Analytical methods for investigating in vivo fate of nanoliposomes: A review. J Pharm Anal. 2018;8(4):219-25.
[36] Hill AB, Chen M, Chen CK, Pfeifer BA, Jones CH. Overcoming Gene-Delivery Hurdles: Physiological Considerations for Nonviral Vectors. Trends Biotechnol. 2016;34(2):91-105.
[37] Lim J, You M, Li J, Li Z. Emerging bone tissue engineering via Polyhydroxyalkanoate (PHA)-based scaffolds. Mater Sci Eng C Mater Biol Appl. 2017;79:917-29.
[38] Ryu N, Kim MA, Park D, Lee B, Kim YR, Kim KH, et al. Effective PEI-mediated delivery of CRISPR-Cas9 complex for targeted gene therapy. Nanomedicine. 2018;14(7):2095-102.
[39] Aghamiri S, Mehrjardi KF, Shabani S, Keshavarz-Fathi M, Kargar S, Rezaei N. Nanoparticle-siRNA: a potential strategy for ovarian cancer therapy? Nanomedicine (Lond). 2019;14(15):2083-100.
[40] Chen K, Hong Y, Li Z, Wu YL, Wu C. Cationic polymeric nanoformulation: Recent advances in material design for CRISPR/Cas9 gene therapy. Progress in Natural Science: Materials International. 2019;29:617-627.
[41] Lino CA, Harper JC, Carney JP, Timlin JA. Delivering CRISPR: a review of the challenges and approaches. Drug Deliv. 2018;25(1):1234-57.
[42] Li L, Song L, Liu X, Yang X, Li X, He T, et al. Artificial Virus Delivers CRISPR-Cas9 System for Genome Editing of Cells in Mice. ACS Nano. 2017;11(1):95-111.
[43] Liu BY, He XY, Xu C, Xu L, Ai SL, Cheng SX, et al. A Dual-Targeting Delivery System for Effective Genome Editing and In Situ Detecting Related Protein Expression in Edited Cells. Biomacromolecules. 2018;19(7):2957-68.
[44] Zhang Z, Wan T, Chen Y, Chen Y, Sun H, Cao T, et al. Cationic Polymer-Mediated CRISPR/Cas9 Plasmid Delivery for Genome Editing. Macromol Rapid Commun. 2019;40(5):e1800068.
[45] Kang YK, Kwon K, Ryu JS, Lee HN, Park C, Chung HJ. Nonviral Genome Editing Based on a Polymer-Derivatized CRISPR Nanocomplex for Targeting Bacterial Pathogens and Antibiotic Resistance. Bioconjug Chem. 2017;28(4):957-67.
[46] Zhu D, Shen H, Tan S, Hu Z, Wang L, Yu L, et al. Nanoparticles Based on Poly (beta-Amino Ester) and HPV16-Targeting CRISPR/shRNA as Potential Drugs for HPV16-Related Cervical Malignancy. Mol Ther. 2018;26(10):2443-55.
[47] Rui Y, Wilson DR, Choi J, Varanasi M, Sanders K, Karlsson J, et al. Carboxylated branched poly(beta-amino ester) nanoparticles enable robust cytosolic protein delivery and CRISPR-Cas9 gene editing. Sci Adv. 2019;5(12):eaay3255.
[48] Xu C, Lu Z, Luo Y, Liu Y, Cao Z, Shen S, et al. Targeting of NLRP3 inflammasome with gene editing for the amelioration of inflammatory diseases. Nat Commun. 2018;9(1):4092.
[49] Turecek PL, Bossard MJ, Schoetens F, Ivens IA. PEGylation of Biopharmaceuticals: A Review of Chemistry and Nonclinical Safety Information of Approved Drugs. J Pharm Sci. 2016;105(2):460-75.
[50] Zhang H, Bahamondez-Canas TF, Zhang Y, Leal J, Smyth HDC. PEGylated Chitosan for Nonviral Aerosol and Mucosal Delivery of the CRISPR/Cas9 System in Vitro. Mol Pharm. 2018;15(11):4814-26.